Ultrasound Imaging in Reproductive Medicine

Advances in Infertility Work-up, Treatment and ART

Laurel A. Stadtmauer
Ilan Tur-Kaspa
Editors

Second Edition

Springer

EXTRAS ONLINE

Ultrasound Imaging in Reproductive Medicine

Laurel A. Stadtmauer • Ilan Tur-Kaspa
Editors

Ultrasound Imaging in Reproductive Medicine

Advances in Infertility Work-up, Treatment and ART

Second Edition

Springer

Editors
Laurel A. Stadtmauer, MD, PhD
The Jones Institute for Reproductive Medicine
Eastern Virginia Medical School
Norfolk, VA
USA

Ilan Tur-Kaspa, MD, FACOG
Institute for Human Reproduction
Chicago, IL
USA

ISBN 978-3-030-16698-4 ISBN 978-3-030-16699-1 (eBook)
https://doi.org/10.1007/978-3-030-16699-1

This Springer imprint is published by the registered company Springer Nature Switzerland AG.
The registered company address is: Gewerbestrasse 11, 6330 Cham, Switzerland

To my colleagues at the Jones Institute and Eastern Virginia Medical School who inspired me to become interested in 3D ultrasound, especially Dr. Alfred Abuhamad, and to my husband, Ivan, daughter, Alessandra, and mom and dad, who sacrificed and inspired me to follow my passions and dreams.

Laurel A. Stadtmauer

This book is dedicated to the love of my life, Hana Tur-Kaspa, and to our children, Leeron, Adi, and Tomer, for their continuous love, encouragement, and support, and to the living memories of my parents, Miriam and Chaim Tur-Kaspa, that their love, wisdom, and passion for education are an inspiration for us all.

Ilan Tur-Kaspa

Foreword

It is with great pleasure that I introduce this book, *Ultrasound Imaging in Reproductive Medicine: Advances in Infertility Work-up, Treatment, and ART, Second Edition*. The second edition, updated with current references and some new authors, reflects the demand for and interest in reproductive ultrasound, as the first edition has over 40,000 downloads of chapters. Ultrasound has proven to be essential in the care of the patient with infertility and in many aspects of reproductive medicine, and a high-quality book that encompasses what anyone in the field needs to know is a very valuable resource indeed.

This book is laid out in a very logical sequence. The first two sections present general information about ultrasound safety in reproductive medicine, technique for 3D ultrasound, and Doppler applications. The next three sections address the use of ultrasound in the infertility work-up, starting with ultrasound of the ovary, the uterus, and the fallopian tube, and male infertility. Each section addresses the normal changes followed by detailed chapters on specific abnormalities related to infertility. Part VI focuses on ultrasound in infertility and ART treatment, with detailed description of the role of ultrasound in follicle monitoring, oocyte retrieval, embryo transfer, and tubal patency and the new endometrial receptivity assay. The final section covers early pregnancy evaluation and ectopic pregnancy.

A formidable team of authors with international prominence was assembled to contribute various chapters in their specific areas of expertise. The book is written in a style that is easy to read and is replete with ultrasound images, illustrating various normal and abnormal conditions. The reader will learn about various aspects of ultrasound imaging in reproductive medicine in a systematic and comprehensive fashion from world authorities in the field. Various chapters reflect the current state of the science in pelvic imaging as it relates to the evaluation and management of the infertile couple.

Kudos to Dr. Laurel Stadtmauer and Dr. Ilan Tur-Kaspa, the book's editors, for their vision and hard work in accomplishing this masterpiece. Laurel is a gifted scientist, an actively practicing physician, and a superb gynecologic sonologist with tremendous expertise in advanced ultrasound imaging. Her skills and background present a special perspective as an editor that is evident throughout the book and translates into an evidence-based, practical approach to ultrasound imaging. Ilan is an internationally known expert in reproductive imaging, reproductive medicine, and infertility and gynecologic ultrasound and preimplantation genetic testing. They both have served as

Chair of the Reproductive Imaging Special Interest Group of the American Society for Reproductive Medicine (ASRM). Their skills and background present a special perspective as editors that is evident throughout the book and translates into an evidence-based, practical approach to ultrasound imaging in diagnosis and treatment of infertility.

This book belongs on the desk of any healthcare worker involved in the field of infertility. From my standpoint, this book will become the ultimate book on ultrasound in reproductive medicine.

Alfred Z. Abuhamad, MD
Department of Obstetrics and Gynecology
Eastern Virginia Medical School
Norfolk, VA, USA

Preface

Can one imagine infertility diagnosis and treatment today without imaging?

Since the start of IVF 40 years ago, the advancement of imaging with ultrasound has been remarkable. Ultrasound has revolutionized the practice of reproductive specialists worldwide and is used daily by the authors in all aspects of patient care in the field of reproductive medicine and obstetrics and gynecology. From the first encounter with patients who have been suffering from infertility and related diseases, ultrasound will be used for the evaluation of the uterus, ovaries, and fallopian tubes, to rule out abnormalities, evaluate the ovarian reserve, and maximize the success of obtaining a pregnancy and term delivery. Ultrasound will be part of the monitoring of a natural cycle, controlled ovarian hyperstimulation with oral agents and injectable gonadotropins with timing for intrauterine insemination, ART, and may assist in the decision to transfer the embryo in a fresh or frozen cycle. It then will be used to confirm intrauterine pregnancy, for the investigation of a pregnancy of unknown location, for evaluation and treatment of ectopic pregnancy, and for determination of the viability of the fetus or fetuses.

Therefore, it was natural for us, the coeditors, who have been involved in the field of advanced infertility work-up and treatment for over 25 years and have served as Chairs of the Reproductive Imaging Special Interest Group with the organization of multiple postgraduate courses at the American Society for Reproductive Medicine (ASRM), to compile the first edition of this book in 2014. Because of the success of the first edition, including about 40,000 downloads of chapters, and the technological advancements, we have been asked by the publisher to put together this second edition. We thank the international group of specialists who have contributed their expertise to make the book successful as well as the contributions of some new experts for this second edition.

This book will be used by infertility specialists, gynecologists, ultrasonographers, radiologists, nurses, and trainees who are involved in imaging and the diagnosis and treatment of the infertile couple. It is a practical book covering all normal findings and abnormalities in women of reproductive age. The book starts with ultrasound safety and principals of ultrasound and moves to the normal and abnormal uterus, ovaries, and fallopian tubes and the use in ART treatments and procedures. The advantages of 3D ultrasound are emphasized in the book. It concludes with the early pregnancy ultrasound. A new area of interest is endometrial receptivity, and this chapter has been included.

The authors have compiled many original ultrasound images with the chapters. All authors are internationally recognized specialists in reproductive medicine, as well as imaging, who have been involved with teaching, and their contributions provide unique comprehensive coverage of all aspects of this field and led to the success of the first edition. We hope you find the book helpful in improving the evaluation and treatment of your patients and an enjoyable resource.

See better; do ART better.

Norfolk, VA, USA — Laurel A. Stadtmauer, MD, PhD
Chicago, IL, USA — Ilan Tur-Kaspa, MD, FACOG

Acknowledgments

Today, one cannot imagine the practice of reproductive medicine and infertility without imaging. Over the last 25 years in practice, we have seen so many advances and improvements in ultrasound. These advances have established ultrasound as the preferred imaging technique for our specialty. It is an integral part of the examination of our patients and remains the safest and most cost-effective imaging modality for the diagnosis and treatment of infertility.

About 40,000 chapter downloads were done since the first edition of our book was published in 2014. We thank the readers who established this book as the primary textbook for ultrasound in reproductive medicine and hope to satisfy the unique demand with this new edition.

Special thanks to our coauthors, who have contributed their special experience and expertise to the field and made this second edition a fantastic book; our mentors over the years, who trained us in ultrasound; engineers, who have constantly been improving the quality of the ultrasound images; and our patients, whom we learn from daily.

Norfolk, VA, USA — Laurel A. Stadtmauer
Chicago, IL, USA — Ilan Tur-Kaspa

Contents

Contributors

Jacques S. Abramowicz, MD, FACOG, FAIUM Ultrasound Services, Fetal and Neonatal Care Center, University of Chicago, Department of Obstetrics and Gynecology, Chicago, IL, USA

Alfred Z. Abuhamad, MD Department of Obstetrics and Gynecology, Eastern Virginia Medical School, Norfolk, VA, USA

Gautam Nand Allahbadia, MD Reproductive Endocrinology & IVF, Millennium Medical Center IVF, Jumeirah, Dubai, UAE

Reproductive Endocrinology & IVF, Bourn Hall IVF, Jumeirah, Dubai, UAE

Reproductive Endocrinology & IVF, Orchid Fertility & Andrology Services, DHCC, Dubai, UAE

Reproductive Endocrinology & IVF, Dr. Amal Elias Fertility Center, Dubai, UAE

Reproductive Endocrinology & IVF, Canadian Specialist Hospital, Abu Hail, Dubai, UAE

Reproductive Endocrinology & IVF, Indo Nippon IVF, Mumbai, India

Rotunda – The Center For Human Reproduction, Mumbai, India

Medical Education & Research, ISRME, Mumbai, India

Medical Education & Research, Indira IVF, Udaipur, India

Jawaria Amir, MD Rosalind Franklin University of Medicine and Science, The Chicago Medical School, Chicago, IL, USA

Peter Aziz, MD Mount Sinai Hospital, Department of Obstetrics and Gynecology, Chicago, IL, USA

Juan Mariano Baronio, MD Department of Fertility, CEGYR, Buenos Aires, Argentina

Renato Bauman, MD, PhD Rotunda IVF, The National Fertility Centre, The Rotunda Hospital, Dublin, Ireland

Josef Blankstein, MD Rosalind Franklin University of Medicine and Science, Chicago, IL, USA

Mount Sinai Hospital, Department of Obstetrics and Gynecology, Chicago, IL, USA

Silvina M. Bocca, MD, PhD, HCLD The Jones Institute for Reproductive Medicine, Eastern Virginia Medical School, Department of Obsterics and Gynecology, Norfolk, VA, USA

Robert E. Brannigan, MD Northwestern Memorial Hospital, Department of Urology, Chicago, IL, USA

Carlos Capuñay, MD Department of Computed Tomography and Magnetic Resonance, Diagnóstico Maipú, Buenos Aires, Argentina

Patricia Carrascosa, MD, PhD, FSSCT Department of Computed Tomography and Magnetic Resonance, Diagnóstico Maipú, Buenos Aires, Argentina

David D. Casalino, MD Northwestern University School of Medicine, Department of Radiology, Chicago, IL, USA

David P. Cohen, MD, FACOG Institute for Human Reproduction, Chicago, IL, USA

Edmond Confino, MD Feinberg School of Medicine, Northwestern University, Chicago, IL, USA

Laura Detti, MD University of Tennessee Health Science Center, Department of Obstetrics and Gynecology, Memphis, TN, USA

Donald L. Fylstra, MD Department of Obstetrics and Gynecology, Medical University of South Carolina, Charleston, SC, USA

Gianluca Gennarelli, MD, PhD Sant'Anna Hospital, University of Turin, Department of Obstetrics and Gynecology, Turin, Italy

Tuhina Goel, MD, DNB All India Institute of Medical Sciences, New Delhi, India

Department of Obstetrics and Gynaecology, Saharanpur, Uttar Pradesh, India

Akanksha Allahbadia Gupta, MS Indira IVF, New Delhi, India

Jairo Hernández, PhD Centro de Asistencia a la Reproducción Humana de Canarias, San Cristobal de La Laguna, Spain

Bradley S. Hurst, MD Carolinas Medical Center, Department of Obstetrics and Gynecology, Reproductive Endocrinology and Infertility, Charlotte, NC, USA

Artemis Karkanaki, MD, MSc, PhD Third Department of Obstetrics and Gynecology, Hippokratio General Hospital of Thessaloniki, Thessaloniki, Greece

Aristotle University of Thessaloniki, Thessaloniki, Greece

Jennifer Fay Kawwass, MD Emory Reproductive Center, Atlanta, GA, USA

Emory University, Department of Reproductive Endocrinology and Infertility, Atlanta, GA, USA

Alessandra Kovac, MPH Center for Biostatistics in AIDS Research at Harvard T. H. Chan School of Public Health, Boston, MA, USA

Isaac Samuel Lam, BA Northwestern University Feinberg School of Medicine, Department of Urology, Chicago, IL, USA

A. H. Maham, MBBS Millennium Medical Center IVF, Dubai, UAE

Shumal Malepati, MD Trios Medical Group – Obstetrics & Gynecology, Kennewick, WA, USA

Audrey M. Marsidi, MD Emory University Hospital Midtown, Department of Gynecology and Obstetrics, Atlanta, GA, USA

Jose Miravet-Valenciano, MSc Igenomix, Valencia, Spain

Ana M. Monzo, MD, PhD La Fe University Hospital, University of Valencia, Human Reproduction Unit, Department of Obstetrics and Gynecology, Reproductive Medicine Research Group, Instituto de Investigación Sanitario La Fe, Valencia, Spain

Bijan Morshedi, BSc University of Virginia School of Medicine, Charlottesville, VA, USA

Ursula Res Muravec, MD, Msc Medical Center Dravlje, Department for Infertility, Ljubljana, Slovenia

Maximilian Murtinger, MD NEXTCLINIC IVF Zentren Prof. Zech, Bregenz, Austria

Alena D. Naumova, MD Monmouth Medical Center, Department of Obstetrics and Gynecology, Long Branch, NJ, USA

Ernest Hung Yu Ng, MBBS, MD Department of Obstetrics and Gynaecology, The University of Hong Kong, Hong Kong, SAR, China

Kamal Ojha, MD, FRCOG St. George's University Hospital, NHS Foundation Trust, Department of Obstetrics and Gynaecology, London, UK

Angela Palumbo, MD, PhD Centro de Asistencia a la Reproducción Humana de Canarias, San Cristobal de La Laguna, Spain

Callum Andrew Potts, BSc, MBBS Inova Fairfax Hospital, Women's and Children's Hospital, Falls Church, VA, USA

Nikolaos Prapas, MD, MSc, PhD Third Department of Obstetrics and Gynecology, Hippokratio General Hospital of Thessaloniki, Thessaloniki, Greece

Aristotle University of Thessaloniki, Thessaloniki, Greece

Beth W. Rackow, MD Columbia University Medical Center, Department of Obstetrics and Gynecology, New York, NY, USA

Alberto Revelli, MD PhD Sant'Anna Hospital, University of Turin, Department of Obstetrics and Gynecology, Turin, Italy

Adela Rodriguez-Fuentes, MD Universidad de La Laguna, Centro de Asistencia a la Reproducción Humana de Canarias, San Cristobal de La Laguna, Spain

Jean Paul Rouleau, MD Centro de Asistencia a la Reproducción Humana de Canarias, San Cristobal de La Laguna, Spain

Maria Ruiz-Alonso, MSc Igenomix, Valencia, Spain

Khaled Sakhel, MD Inova Fairfax Hospital, Department of Obstetrics and Gynecology, Falls Church, VA, USA

Maximilian Schuff, PhD NEXTCLINIC IVF Zentren Prof. Zech, Bregenz, Austria

Donna R. Session, MD Vanderbilt University Medical Center, Department of Obstetrics and Gynecology, Franklin, TN, USA

Carlos Simón, MD, PhD Valencia University, Valencia, Spain

Igenomix Academy and Igenomix, Valencia, Spain

Department of Obstetrics and Gynecology, Stanford University, Stanford, CA, USA

Department of Obstetrics and Gynecology, Baylor College of Medicine, Houston, TX, USA

Laura P. Smith, MD Reproductive Medicine and Surgery Center of Virginia, PLC, Charlottesville, VA, USA

Laurel A. Stadtmauer, MD, PhD The Jones Institute for Reproductive Medicine, Eastern Virginia Medical School, Norfolk, VA, USA

Carlos E. Sueldo, MD University of California San Francisco-Fresno, Department of Obstetrics and Gynecology, Fresno, CA, USA

Mette Toftager, MD, PhD Fertility Clinic, Rigshospitalet, Copenhagen University Hospital, Copenhagen, Denmark

Mai Tran, MD, MPH Fresno Department of Obstetrics and Gynecology, University of California, San Francisco, Fresno, CA, USA

Landon W. Trost, MD Mayo Clinic, Department of Urology, Rochester, MN, USA

Ilan Tur-Kaspa, MD, FACOG Institute for Human Reproduction, Chicago, IL, USA

Tomer Tur-Kaspa Wesleyan University, Middletown, CT, USA

Dimuthu Vinayagam, BSc, MD, MRCOG St. George's University Hospital, University of London, Cardiovascular Sciences Research Centre, London, UK

Part I

Safety in Ultrasound

1 Ultrasound in Reproductive Medicine: Is It Safe?

Jacques S. Abramowicz

Introduction

The first published description of the clinical use of ultrasound in obstetrics and gynecology (OB-GYN) dates from 1958 [1] and describes the value of this new technology for the diagnosis of abdominal masses, specifically ovarian cysts. Since then its use has increased exponentially and is ubiquitous in the daily practice of OB-GYN. Another OB-GYN specialty that has equally burgeoned is reproductive endocrinology and infertility (REI). These two disciplines are strongly interconnected, in part because of the major progress made in image quality and the introduction of new modalities, such as color and spectral Doppler or three-dimensional (3D) ultrasound, which has greatly facilitated diagnosis, interventions, and certain forms of therapy in fertility treatments and assisted reproductive technology. Because ultrasound is a waveform, with alternating positive and negative pressure, it has effects in tissues it traverses. These may be thermal and nonthermal (or mechanical). The question that bears asking is: can these effects be detrimental to the developing follicle, ovum, or early fetus? A publication describing premature ovulation in women whose ovaries were exposed to ultrasound is often quoted but dates from 1982 [2]. This chapter will briefly describe the physics of ultrasound and its interaction with live tissue, define bioeffects and on-screen indicators of potential risk, focus on ovarian scanning in ART, and discuss fetus susceptibility and safety measures. Bioeffects and safety of ultrasound in pregnancy, in general, and in later gestation, in particular, will not be addressed. The interested reader may consult various book chapters and reviews on this topic [3–11].

A Short Review of Ultrasound Physics

Ultrasound is a waveform, characterized by various parameters:

- *Frequency* is the number of cycles per second, measured in hertz (Hz). Human ears can discern sounds at approximately 20 Hz to 20,000 HZ. Diagnostic ultrasound is, generally, 2–15 million Hz (2–15 megahertz, MHz).
- *Wavelength* is the distance between two corresponding points on a particular wave. It is inversely proportional to the frequency (0.2–1.5 mm).
- *Resolution* (i.e., the shortest distance between two points which allows these two points to be displayed separately) depends on the wave-

J. S. Abramowicz (✉)
Ultrasound Services, Fetal and Neonatal Care Center, University of Chicago, Department of Obstetrics and Gynecology, Chicago, IL, USA
e-mail: jabramowicz@bsd.uchicago.edu

L. A. Stadtmauer, I. Tur-Kaspa (eds.), *Ultrasound Imaging in Reproductive Medicine*,
https://doi.org/10.1007/978-3-030-16699-1_1

length: the axial resolution ranges between 2 and 4 wavelengths. Therefore, the smaller the wavelength (which corresponds to the higher the frequency), the better the resolution (the distance between the two points is smaller) but the lower the penetration. This explains why endovaginal probes have better resolution (higher frequency) but lower penetration, hence the need to be closer to the organs being examined.

- Diagnostic ultrasound is not continuous but pulsed. There are pulses separated by silent intervals. The number of pulses occurring in 1 second is the *pulse repetition frequency* (PRF). The fraction of time that the pulsed ultrasound is on (duty factor) is very important from a potential bioeffect aspect. When the PRF increases, so does the duty factor. Since the ultrasound wave is sinusoidal, there are alternating periods of positive and negative pressure which allow the wave to propagate through tissues by means of particle motions. The speed of propagation is related both to the beam and several of the tissue properties. The average speed of sound propagation in biological tissues is estimated at 1540 m/sec.
- When pressure is exerted on the resisting insonated tissue, work is produced. The ability of the wave to do this is its *energy* (in joules), and the rate at which the energy is transformed from one form to another is the *power* (in watts, W, or milliwatts, mW).
- When the power is expressed as a function of area unit (in cm^2), this is *intensity* (generally in mW/cm^2). Bioeffects are conventionally related to the *acoustic intensity*. As stated above, pulses of energy are intermingled with periods where no energy is emitted. When describing an ultrasound wave, several parameters can be described in relation to time or space. By combining peak and average values in time and space, six intensities can be defined. The *spatial peak-temporal average intensity* (ISPTA) is the most practical and most commonly referred to and corresponds to the energy averaged over a period of time. The maximal permitted values based on various clinical applications being considered were first determined in 1976 by the US Food and Drug Administration (FDA) [12] but were modified in 1986 [13]. The most recent definition dates from 1992 [14]. These values (in mW/cm^2) are shown in Table 1.1 for the various applications (left column) as a function of the year they were implemented (modified from references [10–13]). The numbers in parentheses indicate the percentage increase, compared to the previously allowed intensity.

Table 1.1 Values of I_{SPTA} by modality and year of definition

	1976	1986	1992
Ophthalmic	17	17	17
Fetal imaging	46	94 (104%)	720 (667%)
Cardiac	430	430	720 (67%)
Peripheral vessel	720	720	720

It is interesting to observe from the table that, for fetal imaging, the ISPTA was allowed to increase by a factor of almost 16 from 1976 to the most recent values in 1992, yet, as will be described below, all known epidemiological information available regarding fetal effects predates 1992. A further remarkable fact is that intensity for ophthalmic examination has not changed from the original 17 mW/cm^2, a value approximately 42.5 times lower than the present allowed maximal value for fetal scanning. Furthermore, pelvic imaging (abdominal or transvaginal) is not specified in the above table, but one can assume that the ISPTA is the same as adult abdominal imaging, i.e., 720 mW/cm^2, also quite higher than that allowed for scanning of the eye.

Tissue Characteristics

When the ultrasound wave travels through a medium, its intensity diminishes with distance [15]. Biologic tissues are nonhomogeneous, and weakening (attenuation) of the signal results from *absorption* and *scattering*, as well as *reflection*. Absorption is the sound energy being converted to other forms of energy, and scattering is the sound being reflected in directions other than

its original direction of propagation. Since attenuation is proportional to the square of sound frequency, it becomes evident why higher frequency transducers have less penetration (but better resolution). Acoustic impedance can be described as the opposition to transmission of the ultrasound wave. It is proportional to the velocity of sound in the tissue (estimated at 1540 m/sec; see above) and to the tissue density.

Instrument Outputs

Publications of various instrument outputs are available [16]. From a clinical standpoint, there is no easy way to verify the actual output of the instrument in use. In addition, each attached transducer will generate a specific output, further complicated by which mode is being applied [17]. When comparing modes, the ISPTA increases from B-mode (34 mW/cm^2, average) to M-mode to color Doppler to spectral Doppler (1180 mW/cm^2). Average values of the temporal averaged intensity are 1 W/cm^2 in Doppler mode but can reach 10 W/cm^2 [18]. Therefore, precaution is needed when applying this mode. Most measurements are obtained from manufacturers' manuals, having been derived in laboratory conditions which may be different from real-life clinical conditions [19]. Furthermore, machine settings which are under the control of the clinician can alter the output. For instance, the degree of temperature elevation is proportional to the product of the amplitude of the sound wave by the pulse length and the PRF. Hence it is evident why any change (augmentation) in these properties can add to the risk of elevating the temperature, a potential mechanism for bioeffects. The three important parameters under end-user control are the *operating mode* (including choice of *transducer*), the *system setup/output control*, and the *dwell time*.

1. *Scanning mode*: as mentioned above, B-mode carries the lowest risk while spectral Doppler the highest (with M-mode and color Doppler in between). High pulse repetition frequencies are used in pulsed Doppler techniques, generating greater temporal average intensities and powers than B- or M-mode and hence greater heating potential. In spectral Doppler, the beam needs to be held in relatively constant position over the vessel of interest, which may add to the risk of a larger increase in temporal average intensity. Naturally, *transducer choice* is of great consequence since transducer frequency will determine penetration and resolution (vide supra) and field of view.
2. *System setup*: starting or default output power is very often high to allow better imaging, and end users will, generally, keep it as such, mostly out of lack of concern for bioeffects. Excellent, diagnostic images can be obtained at lower output powers, both in B-mode and spectral Doppler (Fig. 1.1). Recently major manufacturers have responded to requests from involved scientific organizations and are now offering a low output power in Doppler as their default. Only if needed can the end user increase the power. Fine-tuning performed by the examiner to optimize the image influences output but with no visible effect (except if one follows TI and/or MI displays; see below). Controls that regularize output include *focal depth* (usually with greatest power at deeper focus but, occasionally on some machines, with highest power in the near field), *increasing frame rate* and *limiting the field of view* (for instance, by high-resolution magnification or certain zooms). In Doppler mode, changing *sample volume* and/or *velocity range* (all done to optimize received signals) changes output. A very important control is receiver gain. It often has similar effects to the above controls on the recorded image but none on the output of the outgoing beam and is, therefore, completely safe to manipulate. In addition, over the years, as seen in the above table, output of instruments has increased [18].
3. *Dwell time* is directly under control of the examiner. It is the time during which the ultrasound beam remains at the same point in the tissue. Interestingly, dwell time is not taken into account in the calculation of the safety indices (TI and MI) nor, in general, until now,

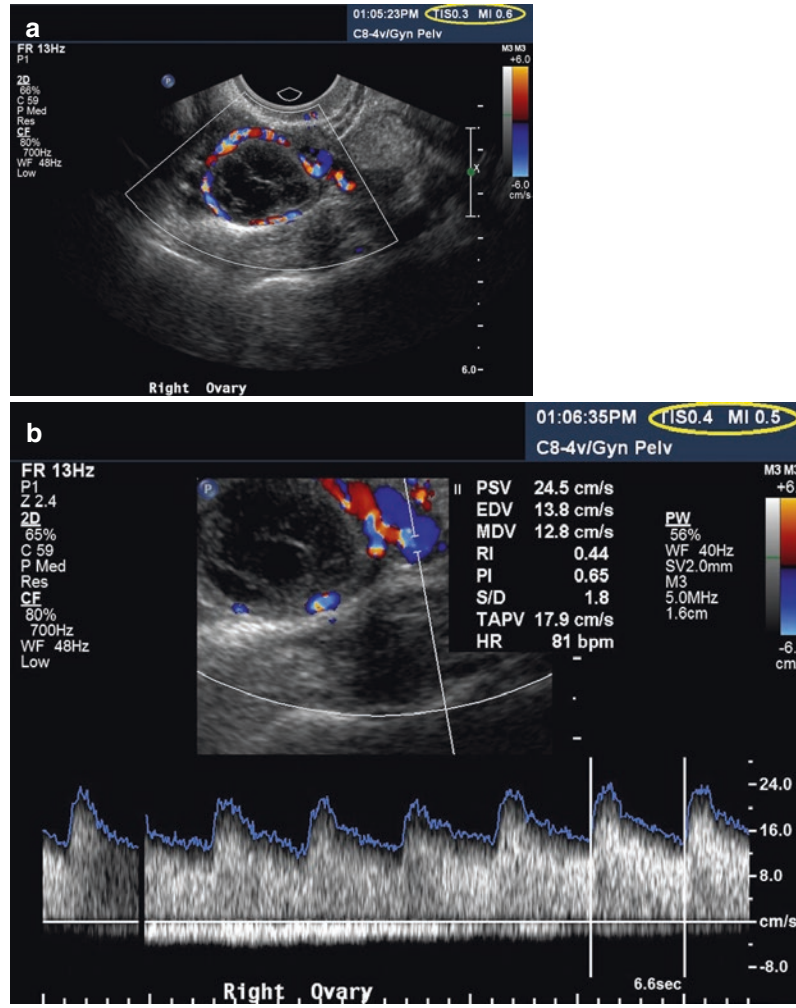

Fig. 1.1 Color (**a**) and spectral (**b**) Doppler of the corpus luteum. Please note the low TI (0.3 and 0.4, respectively) and MI (0.6 and 0.5, respectively) in both images

reported in clinical or experimental studies. Directly associated with dwell time is *examiner experience* in terms of knowledge of anatomy, bioeffects, instrument controls, and scanning techniques, since, presumably, the more experienced the examiner, the less scanning time is needed.

Ultrasound Bioeffects

Why is this even an issue? The average ultrasound professional (and the lay people) will state that ultrasound is obviously safe and that it's not X-rays [20]. Ultrasound, similarly to any sound, is a form of energy. The waveform has positive and negative pressures (see above). When such a waveform travels through *any* tissue, some of this energy is transformed into heat, an indirect effect (thermal effects), and some may directly cause movements of tissues or membranes as well as some more complex mechanical results (nonthermal or mechanical effects). Cavitation is one of these nonthermal effects. This refers to reaction of small gaseous bodies (bubbles) when exposed to an ultrasound field [21]. In inertial cavitation (formerly known as transient cavitation [22]), the bubble changes volume (expands under negative pressure and contracts under positive pressure) until the vibration amplitude of the bubble wall increases so much that the bubble implodes. This implosion generates highly localized shock

waves and is also associated with extremely high local temperatures, up to 10,000 K [23]. This is localized on a tiny area and for a very brief moment, and no heat is actually exchanged (adiabatic reaction). However, in addition to the temperature elevation, the implosion may result in the generation of free radicals such as hydroxyl radicals and hydrogen [24]. If the bubble does not collapse during the ultrasound exposure, the condition is referred to as stable cavitation with the bubble oscillating as the waveform progresses. Absence of cavitation foci (gas bubbles), as is the case in fetal lungs and bowels and, presumably, in the vicinity of the ovary and the developing follicle, renders this phenomenon extremely improbable.

These effects occur whenever a tissue is insonated, thus the designation bioeffects [25]. Many in vitro models, such as cells or tissue cultures, have been used to investigate ultrasound bioeffects and to gain a better understanding of the possible mechanisms of interaction between ultrasound and biologic tissue [26]. Studies on relatively simple nonmammalian organisms, such as insects, amphibians, and avians, are helpful in understanding the mechanisms of interaction between ultrasound and biologic systems [27]. However, from a clinical standpoint, bioeffect studies of mammalian species are of more relevance. Most of these studies were performed on small rodents, such as mice or rats. The extrapolation of experimental results to humans can be difficult, at best. A very comprehensive, albeit dated, review of the effects of ultrasound on mammalian development was prepared by Sikov [28]. He evaluated bioeffects depending on gestational age and thus attempted to extract information on the relation between exposure parameters and stage of development at exposure. Experimental studies indicate that intact mammalian systems (in vivo) do not show a significant rise in temperature when exposed to pulsed imaging equipment [28–30]. However, peripheral vessel pulsed and continuous-wave (CW) Doppler equipment, when used for a relatively long time (1–10 minutes), may be an exception [31, 32]. Therefore, Doppler should be used with care, especially during applications in which Doppler is used for the assessment of blood velocities in ovarian vessels in ART and studies of the first-trimester fetus [33]. Reports on the use of new technologies, such as three- and four-dimensional (3D/4D) ultrasound, are beginning to appear in the literature [34], but these do not appear to expose tissues to higher levels of acoustic energy [35].

The Output Indices

Because of the two main mechanisms (described above) involved in bioeffects of ultrasound, a Standard for Real-Time Display of Thermal and Mechanical Indices on Diagnostic Ultrasound Equipment, generally known as the output display standard or ODS, consisting of two indices – thermal (TI) and mechanical (MI) – was implemented in the USA around 1992–1994 [12, 14, 23]. Secondary to end users' desire for better imaging and as a result of discussions that involved the FDA, the AIUM, and the National Electrical Manufacturers Association (NEMA), in 1994, the FDA revised its guidance on diagnostic ultrasound 510(k) submissions to allow the use of the MI in place of the ISpPa in determining substantial equivalence of devices. This revision assumes that on-system displays of numerical indices, including MI and TI, will inform the user about the potential for either thermal or nonthermal bioeffects associated with the actual examination settings of the imaging system. This enables the clinician to increase acoustic power output beyond the existing FDA guidelines when clinically warranted (see Table 1.1). Before the 1994 FDA revision, such an increase was not possible. The maximum available acoustic output was limited by the manufacturer's software, which would not allow the output to exceed FDA guidelines for maximum exposure (for instance, 94 mW/cm^2 for fetal imaging). With the implementation of the ODS, diagnostic ultrasound systems can have a higher acoustic output (e.g., 720 mW/cm^2 for fetal imaging). With the higher limits comes the potential for increased risk to the patient. Therefore, the end user must make a careful risk/benefit analysis.

The purpose of the ODS is to help the clinician implement the ALARA (as low as reasonably achievable) principle and minimize the potential for bioeffects. A very important aspect of the implementation of the ODS, as explicitly emphasized in the original FDA recommendations for adoption, was education of the end users about bioeffects of ultrasound and safety-related issues. This particular goal appears to not have been very successful as indicated by the fact that 70–80% of end users worldwide know very little about bioeffects and the safety indices [36–39]. Furthermore, sonographers and OB-GYN residents and fellows in the USA seem to be similarly unfamiliar [40, 41].

The thermal index (TI) provides some indication of potential temperature increase, and the mechanical index (MI) provides indication of potential for nonthermal (i.e., mechanical) effects [23, 26, 42]. The TI is the ratio of instantaneous total acoustic power to the acoustic power estimated to be required to increase tissue temperature by a maximum of 1 °C. It is an estimate of the maximal temperature rise at a given exposure. *It is not a measurement of the actual or assumed temperature*. Some correlation exists with temperature rise in degrees Celsius but in no way does TI allow an estimate or a guess as to what that temperature change *actually* is in the tissue. There are three variants: TI for soft tissue (TIS), for early pregnancy when ossification is minimal; TI for bones (TIB), to be used when the ultrasound beam impinges on the bone, at or near the beam focus, such as late second and third trimesters of pregnancy; and TI for transcranial studies (TIC) when the transducer is essentially against the bone, mostly for examinations in adult patients. In ART, TIS is recommended. These indices were required to be displayed if equal to or over 0.4. There are several issues with TI, in particular the fact it does not take exposure time into account. Thus several authors have suggested modifications or frank changes in the way thermal effects can be assessed [43–45].

The MI has been developed as an on-screen indicator of the potential for nonthermal damage or cavitation-like phenomena related to B-mode operation. MI is inversely proportional to the center transducer frequency, i.e., the higher the frequency (as is used in ART), the lower the risk of mechanical effects. It is important to know that the MI is not based on actual in situ measurements. It is a theoretical formulation of the ratio of the pressure to the square root of the ultrasound frequency. Both the TI and MI can and should be followed as an indication of change in output during the clinical examination.

A complicating factor is uncertainties in TI (and MI) calculations. The error may be a factor of 2 or even 6. It is usual to consider a factor of 2 in risk evaluation. Hence a TI of 2 may indicate a potential raise of temperature from 1 °C (half of 2) to 4 °C (two times 2). This limits their usefulness but, at the moment, this remains the best tool we have.

Ovarian Scanning

Although the first described use of ultrasound in OB-GYN was for the diagnosis of an ovarian cyst [1], most research and publications have concentrated on obstetrics. This, however, changed with the recognition that ultrasound could be used to closely follow the ovarian cycle [46] and, subsequently, with the realization that this was a very helpful tool in induction of ovulation and many other ART procedures [47–49]. Questions regarding safety of the procedure were raised immediately with the rapid adaptation by clinicians [2, 50–52], with description of premature ovulation [2], reduced fertility in rats [50], reduction in pregnancy rates in ultrasound-monitored groups [51], and lower fertilization rate in women undergoing artificial insemination and who were monitored by ultrasound as compared with those who were not monitored by ultrasound. Furthermore, those who were monitored took significantly longer to become pregnant [52]. No mechanism for the findings is proposed in any of these publications, and no details on acoustic output or length of the examination (dwell time) are available. Later, Doppler assessment of ovarian vasculature was also introduced [53–57]. Intraovarian vessels can be interrogated by color and spectral Doppler to predict ovarian response [58]. The acoustic

outputs of these modalities are much higher than in conventional gray-scale B-mode, but excellent, diagnostic images may be obtained with low outputs as documented by low TI and MI, as can be seen in Fig. 1.1. Further novel technologies to investigate ovarian vasculature, described in various chapters in this book, include three-dimensional (3D) ultrasound [34, 59, 60] and the use of contrast agents [61, 62]. While 3D ultrasound appears safe [35], the injection of contrast agents into the body greatly increases the risks of harmful bioeffects by introducing cavitation foci (see above). Ovarian scanning carries specific worries. In transabdominal scanning, a lot of energy is absorbed by the (sometimes thick) subcutaneous layers. In endovaginal scanning, this "safety net" does not exist since the probe is relatively close to the organ of interest; thus less absorption occurs. Higher frequencies of the vaginal probes, however, are protective. Besides the direct effects of the ultrasound waveform, probe heating has to be considered. It is known that the surface of the probe can heat up by several degrees Celsius [63]. Most of this heat is dissipated by the abdominal wall tissues before reaching the ovary (or the fetus), but much less heat loss occurs with the endovaginal approach.

Ultrasound and the Ovum

As stated in the introduction, a study from 1982 demonstrated premature ovulation in women who underwent ultrasound examination of the ovaries (B-mode) in the late follicular phase 2. The authors compared patients in induced ovulation cycles and investigated timing of follicle rupture after the onset of LH surge or administration of hCG. Rupture never occurred before the 37th hour in control patients (no ultrasound in the follicular phase). However, ovulation (premature) was observed at 26–36 hours in about 50% cases in the study group (ultrasound during the previous 3 days or in the 36 hours immediately following the ovulatory stimulus). This study was very concerning but has never been reproduced. Since its description 30 years ago [48, 64], ultrasound-guided oocyte aspiration for in vitro fertilization and embryo transfer has now become a routine. There are only a few, relatively dated, studies aimed at determining the interaction between ultrasound exposure and successful fertilization. Most are, in fact, concerned with success or lack thereof of the procedure in terms of pregnancy rates and not possible bioeffects. This has not been studied with epidemiological methods but is, arguably, as important as analysis of embryonic/fetal effects. Some researchers have reported deleterious effects of ultrasound on the menstrual cycle, particularly decrease in ovulation rates in mice [65] and premature ovulation [2], as well as reduced cumulative pregnancy rates in mice [50] and in humans [51]. Others have demonstrated no effects on the ovulation process or egg quality, including DNA and RNA synthesis [66], nor on fertilization rate and embryonic development following in vitro fertilization and embryo transfer [67]. In general, the clinically available data on ultrasound exposure of oocytes during meiosis are confusing. Some researchers reported a deleterious effect on the fertility of patients undergoing artificial insemination with a reduction in the cumulative rate of pregnancy [51]. A study of ultrasound exposure of meiotically active, preovulatory oocytes showed no differences between rats exposed to ultrasound after the LH surge and controls in terms of pregnancy rate, number of corpora lutea, implantations, pups, and mean pup and placental weights at autopsy on day 22 of pregnancy [68]. Others have claimed an increase in the success rate, allowing ultrasound monitoring of follicular growth [69], although, evidently, this is not a direct effect of ultrasound but of improved timing. An attempt to clarify this was described by Mahadevan and colleagues [67]. They wanted to determine how oocytes obtained under ultrasound guidance affected the pregnancy rate. The results obtained with 3.5 MHz probes suggest that exposure of human oocytes to ultrasonic waves during the different phases of meiosis does not significantly influence the developmental potential of the in vitro fertilized embryos. Unfortunately, no researcher describes any of the relevant exposure parameters discussed earlier, except for ultrasound frequency.

Embryo/Fetus Susceptibility

The growing embryo/fetus is particularly sensitive to external influences. For instance, certain medications or drug of abuse taken by the pregnant woman, exposure to X-rays, and elevated temperature, secondary to infectious diseases, are all known teratological agents [70]. This is especially true in the first 10–12 weeks of gestation. Gestational age is thus a vital issue when dealing with possible bioeffects: milder exposure during the preimplantation period can have similar consequences to more severe exposures during embryonic and fetal development and can result in prenatal death and abortion or a wide range of structural and functional defects.

Several studies on the influence of ultrasound exposure in the preimplantation period are available. For instance, pregnant rats were exposed to a 2.5-MHz ultrasound field on the second and third day of gestation, at spatial average intensities of 150 mW/cm^2, comparable to human exposure [71]. No increase in prenatal mortality was found. Similarly, no increase in the rate of postnatal malformation was found after 20-minute exposures. In another experiment, pregnant mice were exposed to ultrasound in the first 3 days of gestation [72]. Spatial average intensity was determined to be 1 W/cm^2. A decreased uninterrupted pregnancy rate was noted after exposure for 5 minutes on the third day and after exposure for 200 seconds on day zero. In addition, a reduction in neonatal weight (after delivery) was observed at certain thresholds for exposure on day zero or one. In another series of studies by the same authors [73], ultrasound exposure led to damage of maternal tissue, as reflected in increased mortality, decreased weight gain, and paralysis of the pups. One of the major concerns is whether ultrasound can raise the temperature of the developing embryo/fetus. This concern stems from the fact that, under certain conditions, ultrasound may indeed cause a rise of temperature and, on the other hand, it is well known that hyperthermia is teratogenic. Most at risk is the fetal central nervous system (CNS) due to a lack of compensatory growth of damaged neuroblasts [74]. In experimental animals the most common defects are of the neural tube as well as microphthalmia, cataract, and microencephaly, with associated functional and behavioral problems [75]. More subtle effects are possible, such as abnormal neuronal migration with unclear potential results [76]. Other prominent defects are seen in craniofacial development (more specifically facial clefts), the skeleton, body wall, teeth, and heart [75]. Hyperthermia in utero (due to maternal influenza, for instance) has long been known to potentially induce structural anomalies in the fetus [77], but, relatively recently, it has been described as an environmental risk factor for psychological/behavioral disturbances [78] and, more particularly, schizophrenia [79]. It is stressed that these are *not ultrasound-induced* hyperthermia effects and that it is suggested that temperature elevation under 38.9 °C is probably not harmful. Yet, ultrasound has been shown to induce temperature increase in vivo [42], albeit not in humans. There is, however, a serious lack of data examining the effects of ultrasound while rigorously excluding other confounding factors. On the one hand, McClain and associates [80] exposed rats to 10 mW/cm^2 CW Doppler ultrasound for up to 2 hours at frequencies of 2.25 and 2.5 MHz. The fetuses were examined on day 20, and no consistent increase in mortality was observed, nor did the authors detect any other abnormalities. Evidence, however, of the possibility of ultrasonically produced embryolethal effects during organogenesis has been described [81]. Sikov and colleagues exposed an exteriorized rat uterus to various frequencies, some of them clinically relevant (0.8, 2, and 3.2 MHz), at day 9 and evaluated the offspring at day 20 [82]. The exposure was performed at different intensity levels, with exposure times at 5 or 15 minutes. No effect on fetal weight was observed, even at spatial average intensities as high as 30 W/cm^2, but prenatal mortality at 15–20 W/cm^2 (spatial average) clearly increased with increasing exposure time. The cause of this was ascribed to a thermal mechanism. A 2006 controversial study by Ang et al. looked at neuronal migration in rat pups after maternal exposure to ultrasound [76]. Neurons of the cerebral neocortex in many animals (including humans) are generated during fetal life in the brain proliferative zones and then migrate to their final destinations by following an

inside-to-outside sequence. In Ang's experiment, neurons generated at embryonic day 16 and destined for the superficial cortical layers were chemically labeled in over 335 rats. A small, but statistically significant, number of neurons failed to acquire their proper position and remained scattered within inappropriate cortical layers and/or in the subjacent white matter when exposed to ultrasound for a total of 30 minutes or longer during the period of their migration. The magnitude of dispersion of labeled neurons was variable but increased with duration of exposure to ultrasound (although not linearly, with the most extended exposure, unexpectedly, yielding less effect than the one immediately lower). It is not clear whether a relatively small misplacement in a relatively small number of cells that retain their origin cell class is of any clinical significance. It is also important to note that there are several major differences between the experimental setup of Ang et al. and the clinical use of ultrasound in humans [8]. Most noticeable was the exposure duration, up to 7 hours in Ang's setup, and the fact that scans were performed over a period of several days. Furthermore, embryos received "whole-brain" exposure to the beam, which is rare in humans, *except in very early gestation*. Brains of mice are much smaller than those in humans and develop over days. This should not completely deter from the study which encourages caution. Another study which demonstrates potential harmful effects of ultrasound (when spectral Doppler is used) showed that even relatively short insonation of chick embryos to clinically relevant Doppler resulted in short and medium memory loss and reduced ability to learn [83].

There are relatively few papers containing information which is pertinent from a human clinical standpoint and no epidemiological studies of ultrasound in early gestation. One scientific publication dating a few years indicated that fetal exposure was, most likely, within the upper limits recommended, at that time [84]. A landmark study in the field of ultrasound bioeffects correlated temperature with exposure time [85]. No thermal bioeffects were observed at temperature elevations of 39 °C, regardless of how long the ultrasound exposure lasts. However, for each increasing degree of temperature elevation, to stay within safety limits, the duration of ultrasound examination must be reduced by a factor of 4. More specifically, the review indicated that the maximum safe duration for a temperature of 43 °C is 1 minute, and for 42 °C it is 4 minutes. Similarly, at 41 °C, the exposure time may be increased to 16 minutes, and at 40 °C the duration of examination may be as long as 64 minutes. Based on the data available, the survey concluded that if the maximum temperature rise during the ultrasound exposure is kept less than 2 °C, any biologic effect (in an afebrile patient) is highly unlikely. As already addressed (see above), findings indicating that the ultrasound imaging transducer may act as a substantial heat source [63, 79] are of particular interest in ART and in the early stages of pregnancy because of the universal use of endovaginal scanning. The temperature at a clinically operated Doppler transducer was reported to increase by 10 °C when the Doppler was applied to the skin with a standard coupling gel [79]. Although tissue heating from the transducer is most likely limited to the tissue volume in the immediate vicinity of the transducer, this effect has to be kept in mind for ultrasound examinations in which an endocavity (e.g., endovaginal) transducer is used, although in experiments, the effects on the fetus seemed to be negligible after 2 cm penetration [79].

It must be emphasized, once more, that there are very few human studies, and those which have been performed do not preclude the possibility that adverse effects may be found under certain conditions. One of the rare studies in humans examined activation of various substances involved in the apoptotic cascade, after exposures to diagnostic endovaginal ultrasound [86]. Pregnant patients scheduled for interruption of pregnancy at 7–8 weeks were scanned with 5 MHz endovaginal probes for 0, 10, 20, and 30 minutes. Chorionic villi were obtained 4 hours later and analyzed for activation of caspase-3 and cytochrome release (believed to commit the cell to apoptosis). According to the authors, ISPTA was 13 mW/cm^2. Unfortunately, no indication on TI or MI is given. No or minimal activation of the above pathway was seen in controls (0 minute

exposure) or in those exposed for 10 minutes. The cleavage products of caspase-3 and cytochrome c were greatly increased after 20 and 30 minutes exposure, indicating a potential harmful effect of the ultrasound. Besides this study, all other published studies relate to scanning in the late first or second trimesters and not to ART or very early gestation. Epidemiological studies would be needed to clearly demonstrate an effect or lack thereof [10]. The very limited epidemiological data available indicate that no relation has been found between prenatal exposure to ultrasound and subsequent postnatal changes in children [87], but statistical considerations show that minor chemical and behavioral changes, long-term delayed effects, and certain genetic effects could easily escape detection [4].

As previously stated, it is very unlikely that diagnostic ultrasound causes fetal major structural anomalies. If the neonate, infant, or child manifests subtle, late effects, it is often very difficult, if not impossible, to find a cause-effect relationship between in utero exposure and such effects. There exists a well-documented significant increase in the likelihood of non-right-handedness in boys (and not in girls) exposed to diagnostic ultrasound in utero [88, 89]. This may be important since there is a higher prevalence of non-right-handedness in male infants with autism spectrum disorder (ASD). The prevalence of ASD has increased over the last 20 years as has the exposure to ultrasound. But so has exposure to cellular phones, television, microwaves, or any huge list of external influences. A mice study showed that male pups of mice exposed to ultrasound in utero were significantly less interested in social interaction and demonstrated significantly more activity compared to non-exposed pups in the presence of an unfamiliar mouse, thus indicating a change in social behavior [90]. A human study showed a possible relationship between the severity of ASD symptoms and in utero ultrasound exposure during the first trimester of pregnancy in fetuses with a genetic predisposition to ASD [91]. A very recent study [92] "found significantly greater mean depth of ultrasonographic penetration in the ASD group compared with the developmental delay group in the first trimester and compared with the typical development group in the first and second trimesters." While this sentence of the abstract seems very concerning, numerous responses were generated [93, 94], showing flaws in the study, particularly in the nonsensical conclusion that autism was associated with "deeper" ultrasound. The difference was 4 mm (12.9 cm vs. 12.5 cm). This has nothing to do with intensity or acoustic output and, in fact, proves nothing. Various scientific societies have published statements harshly critical of the study [95–97].

Thus, it appears that in vivo exposure to ultrasound at spatial average intensities *below 1 W/cm*^{2} (which is arguably the case in ART as well as early gestation) does not affect embryos/fetuses in the early stages of gestation. Limited data, however, suggest that levels of ultrasound of 1 W/cm^2 may lead to undesirable changes in maternal tissue. If one considers together the facts that hyperthermia is potentially harmful to the fetus and that ultrasound may, under certain circumstances, elevate tissue temperature, then precaution has to be recommended, particularly in early gestation and especially with modes known to emit higher acoustic energy levels (such as pulsed Doppler [98]). This recommendation is supported by experimental data. Further prospective studies on ultrasound safety in ART and pregnancy are highly recommended.

Safety Aspects of Ultrasound in Ovulation Induction and Early Gestation

There are many valid medical indications to perform ultrasound in early gestation [99]. These include, among others, bleeding, accurate gestation dating, confirmation of viability, and verification of number of fetuses. In addition, ultrasound is invaluable in ART. All these examinations are primarily performed with B-mode, a mode with relatively low acoustic output. However, more recently, screening for genetic abnormalities and early assessment of structural abnormalities are described in the literature in early (11–15 weeks) pregnancy. While most of

these are also performed with B-mode, Doppler is often used to detect blood vessels and/or to visualize and analyze cardiac valves, potentially exposing the fetus to much higher energy levels. One needs to keep in mind that, even with B-mode, dwell time is important since prolonged examination can result in higher exposure levels. Of particular importance is the reprehensible habit of having the parents (and the caregiver) "listen" to the fetal heartbeat with pulsed (spectral) Doppler. As explained above, the level of acoustic energy is much higher in Doppler mode than B-mode. Hence, the guidelines/recommendations of scientific bodies are to document fetal heartbeat only with M-mode [100]. Some leniency exists to allow, if judged necessary, only 4–5 beats to be recorded by Doppler while paying attention to keep the TI and MI below 1.

The evidence of ultrasonically induced bioeffects in humans is perhaps the most important information from the clinician's point of view. As pointed out by Ziskin and Petitti, "No matter how many laboratory experiments show a lack of effect from diagnostic ultrasound, it will always be necessary to study directly its effect in human populations before any definitive statement regarding risk can be made" [4]. Indeed, a lack of demonstrated effects is not equivalent to a factual lack of effects. All published epidemiological studies in humans have been performed with pre-1992 machines, a time when the maximal acoustic output of medical ultrasound instruments was allowed to greatly increased [101]. The words of Francis Duck in 1999 are still particularly valid: "No epidemiological or other evidence was then or is now available to support the assertion of safety at these higher exposures" [102].

Summary and Recommendations

Several statement and guidelines are available [103–108]. As already mentioned, based on various sources, it appears that acoustic output (as expressed by various intensities) can be much higher in Doppler mode: for instance, 34 mW/cm^2 for the ISPTA in B-mode versus 1180 mW/cm^2 for spectral Doppler and with color Doppler somewhat in between [109]. Concerns about the fact that outputs are much higher in Doppler applications were already expressed approximately 10 years ago in three editorials [102, 110, 111]. In one of these, the question was even raised whether research involving Doppler in the first trimester should even be considered for publication [111]. Despite this, as detailed above, ultrasound is routine in ART, and, in more recent years, there has been a recrudescence in the usage of Doppler in the first trimester and furthermore in the early stages of the first trimester. A very important recommendation, already mentioned, is to limit exposure to be as short as possible, compatible with an adequate diagnosis (as low as reasonably achievable [ALARA] principle). A very useful method to keep risk at a minimum is to use published guidelines in the USA [103] as well as BMUS-recommended.

- Perform a scan only when medically indicated.
- Know your machine and how controls change the output.
- Start at low output and increase only when necessary.
- Keep TI and MI below 1.
- Watch the clock, and keep the examination as brief as possible (but enough to obtain diagnostic accuracy).
- Be cautious when using Doppler.

Diagnostic ultrasound is an extremely powerful tool in the hands of experienced physicians, sonographers, nurses, and other users. The decision regarding the risks and benefits can be made only by the individual responsible for applying the ultrasound to the patient. This is a clinical responsibility but also an ethical and legal one. Education of end users is primordial in this regard.

References

1. Donald I, Macvicar J, Brown TG. Investigation of abdominal masses by pulsed ultrasound. Lancet. 1958;1:1188–95. 1958/06/07.
2. Testart J, Thebault A, Souderes E, Frydman R. Premature ovulation after ovarian ultrasonography. Br J Obstet Gynaecol. 1982;89:694–700.

3. Salvesen KA, Vatten LJ, Jacobsen G, Eik-Nes SH, Økland O, Molne K, et al. Routine ultrasonography in utero and subsequent vision and hearing at primary school age. Ultrasound Obstet Gynecol. 1992;2:243–4, 245–247.
4. Ziskin MC, Petitti DB. Epidemiology of human exposure to ultrasound: a critical review. Ultrasound Med Biol. 1988;14:91–6.
5. Nyborg WL. Biological effects of ultrasound: development of safety guidelines. Part II: general review. Ultrasound Med Biol. 2001;27:301–33.
6. Marinac-Dabic D, Krulewitch CJ, Moore RM Jr. The safety of prenatal ultrasound exposure in human studies. Epidemiology. 2002;13:S19–22.
7. Salvesen KA. EFSUMB: safety tutorial: epidemiology of diagnostic ultrasound exposure during pregnancy-European committee for medical ultrasound safety (ECMUS). Eur J Ultrasound. 2002;15:165–71.
8. Abramowicz JS. Prenatal exposure to ultrasound waves: is there a risk? Ultrasound Obstet Gynecol. 2007;29:363–7.
9. Church CC, Miller MW. Quantification of risk from fetal exposure to diagnostic ultrasound. Prog Biophys Mol Biol. 2007;93:331–53.
10. Abramowicz JS, Fowlkes JB, Stratmeyer ME, et al. Epidemiology of ultrasound bioeffects. In: Sheiner E, editor. Textbook of epidemiology in perinatology. New York: Nova Science Publishers, Inc.; 2010.
11. Sheiner E, Abramowicz JS. Ultrasound bioeffects and safety: what the practitioner should know. In: Fleischer AC, Abramowicz JS, Goncalves LF, et al., editors. Fleischer's sonography in obstetrics & gynecology. 8th ed. New York: McGraw-Hill Education/Medical; 2018.
12. FDA, Center for Devices and Radiological Health: 501(k) Guide for measuring and reporting acoustic output of diagnostic ultrasound medical devices. 1985.
13. US Food and Drug Administration (FDA): Diagnostic ultrasound guidance update. Rockville: Center for Devices and Radiological Health; 1987.
14. AIUM/NEMA. American Institute of Ultrasound in Medicine and the National Electrical Manufacturers' Association: Standard for real-time display of thermal and mechanical acoustic output indices on diagnostic ultrasound devices. Laurel/Rosslyn. 1992.
15. Insana MF. Sound attenuation in tissue. In: Goldman IW, Fowlkes JB, editors. Medical CT and ultrasound: current technology and applications. College Park: American Association of Physicists in Medicine; 1995.
16. Henderson J, Willson K, Jago JR, Whittingham TA. A survey of the acoustic outputs of diagnostic ultrasound equipment in current clinical use. Ultrasound Med Biol. 1995;21:699–705. Comparative Study 1995/01/01.
17. Martin K. The acoustic safety of new ultrasound technologies. Ultrasound. 2010;18:110–8.
18. Duck FA, Henderson J. Acoustic output of modern instruments: is it increasing? In: Barnett SB, Kossoff G, editors. Safety of diagnostic ultrasound. New York/London: The Parthenon Publishing Group; 1998.
19. Jago JR, Henderson J, Whittingham TA, Willson K. How reliable are manufacturer's reported acoustic output data? Ultrasound Med Biol. 1995;21:135–6. Letter 1995/01/01.
20. Zhu WH, Miller MW, Cox C. Lack of increase in cell transformation frequency of C3H cells after exposure to pulsed ultrasound. Ultrasonics. 1991;29:81–4. Research Support, U.S. Gov't, P.H.S. 1991/01/01.
21. Church CC. Spontaneous homogeneous nucleation, inertial cavitation and the safety of diagnostic ultrasound. Ultrasound Med Biol. 2002;28:1349–64. Research Support, U.S. Gov't, P.H.S. 2002/12/07.
22. Barnett SB, ter Haar GR, Ziskin MC, et al. Current status of research on biophysical effects of ultrasound. Ultrasound Med Biol. 1994;20:205–18.
23. Abbott JG. Rationale and derivation of MI and TI – a review. Ultrasound Med Biol. 1999;25:431–41.
24. Wu J, Nyborg WL. Ultrasound, cavitation bubbles and their interaction with cells. Adv Drug Deliv Rev. 2008;60:1103–16. Research Support, U.S. Gov't, Non-P.H.S. Review 2008/05/13. https://doi.org/10.1016/j.addr.2008.03.009.
25. O'Brien WD Jr. Ultrasound-biophysics mechanisms. Prog Biophys Mol Biol. 2007;93:212–55.
26. NCRP. (National Council on Radiation Protection and Measurements). Exposure criteria for medical diagnostic ultrasound: II. Criteria based on all known mechanisms. Report No. 140. Bethesda, MD. 2002.
27. Sikov MR. Effect of ultrasound on development. Part 1: Introduction and studies in inframammalian species. Report of the bioeffects committee of the American Institute of Ultrasound in Medicine. J Ultrasound Med. 1986;5:577–83.
28. Sikov MR. Effect of ultrasound on development. Part 2: Studies in mammalian species and overview. J Ultrasound Med. 1986;5:651–61.
29. Stratmeyer ME, Christman CL. Biological effects of ultrasound. Women Health. 1982;7:65–81.
30. Biological effects of ultrasound: mechanisms and clinical implications. Bethesda: National Council on Radiation Protection and Measurements; 1984.
31. Stratmeyer ME, Stewart HF. An overview of ultrasound: theory measurements, medical applications and biological effects. Rockville: U.S. Dept. of Health and Human Services, Public Health Service, Food and Drug Administration, Bureau of Radiological Health; 1982.
32. Thomenius KE, Lewin PA. Ultrasound bioeffects 1991. Ultrasound Q. 1991;9:111–37.
33. Dickey RP. Doppler ultrasound investigation of uterine and ovarian blood flow in infertility and early pregnancy. Hum Reprod Update. 1997;3:467–503. Review 1998/04/07.
34. Engels V, Sanfrutos L, Perez-Medina T, Alvarez P, Zapardiel I, Godoy-Tundidor S, et al. Periovulatory follicular volume and vascularization determined by 3D and power Doppler sonography as pregnancy predictors in intrauterine insemination cycles. J Clin

Ultrasound. 2011;39:243–7. 2011/04/19. https://doi.org/10.1002/jcu.20816.
35. Sheiner E, Hackmon R, Shoham-Vardi I, Pombar X, Hussey MJ, Strassner HT, et al. A comparison between acoustic output indices in 2D and 3D/4D ultrasound in obstetrics. Ultrasound Obstet Gynecol. 2007;29:326–8.
36. Marsal K. The output display standard: has it missed its target? Ultrasound Obstet Gynecol. 2005;25:211–4.
37. Sheiner E, Abramowicz JS. Clinical end users worldwide show poor knowledge regarding safety issues of ultrasound during pregnancy. J Ultrasound Med. 2008;27:499–501.
38. Akhtar W, Arain MA, Ali A, Manzar N, Sajjad Z, Memon M, et al. Ultrasound biosafety during pregnancy: what do operators know in the developing world?: national survey findings from Pakistan. J Ultrasound Med. 2011;30:981–5. 2011/06/28.
39. Sharon N, Shoham-Vardi I, Aricha-Tamir B, Abramowicz JS, Sheiner E. [What do ultrasound performers in Israel know regarding safety of ultrasound, in comparison to the end users in the United States?]. Harefuah. 2012;151:146–9, 190. 2012/04/24.
40. Bagley J, Thomas K, DiGiacinto D. Safety practices of sonographers and their knowledge of the biologic effects of sonography. J Diagn Med Sonogr. 2011;27:252–61.
41. Houston LE, Allsworth J, Macones GA. Ultrasound is safe... right?: resident and maternal-fetal medicine fellow knowledge regarding obstetric ultrasound safety. J Ultrasound Med. 2011;30:21–7. 2011/01/05
42. Nyborg WL. History of the American Institute of Ultrasound in Medicine's efforts to keep ultrasound safe. J Ultrasound Med. 2003;22:1293–300.
43. Karagoz I, Kartal MK. A new safety parameter for diagnostic ultrasound thermal bioeffects: safe use time. J Acoust Soc Am. 2009;125:3601–3610. 2009/06/11. https://doi.org/10.1121/1.3126525.
44. Ziskin MC. The thermal dose index. J Ultrasound Med. 2010;29:1475–9. 2010/09/30.
45. Bigelow TA, Church CC, Sandstrom K, Abbott JG, Ziskin MC, Edmonds PD, et al. The thermal index: its strengths, weaknesses, and proposed improvements. J Ultrasound Med. 2011;30:714–34. 2011/04/30
46. Queenan JT, O'Brien GD, Bains LM, Simpson J, Collins WP, Campbell S. Ultrasound scanning of ovaries to detect ovulation in women. Fertil Steril. 1980;34:99–105. 1980/08/01.
47. Vesper B, Schulte HR. [Ultrasonic follow-up check of overstimulation by gonadotrophin therapy (author's transl)]. Zentralblatt fur Gynakologie. 1980;102:791–6. 1980/01/01.
48. Lenz S, Lauritsen JG, Kjellow M. Collection of human oocytes for in vitro fertilisation by ultrasonically guided follicular puncture. Lancet. 1981;1:1163–4. Letter 1981/05/23.
49. Renaud R, Ehret C, Dervain I, Plas-Roser S, Aron C, Spira A. [Ovarian sonography: a new way of monitoring ovulation induction treatments]. Bull Acad Natl Med. 1981;165:353–8. 1981/03/01.
50. Bologne R, Demoulin A, Schaaps JP, Hustin J, Lambotte R. Influence of ultrasonics on the fecundity of female rats. C R Seances Soc Biol Fil. 1983;177:381–7. 1983/01/01.
51. Demoulin A, Bologne R, Hustin J, Lambotte R. Is ultrasound monitoring of follicular growth harmless? Ann N Y Acad Sci. 1985;442:146–52.
52. Quereux C, Mazili ML, Desroches A, Garnier R, Slaoui K, Bajolle F, et al. [Does ultrasound have an adverse effect on the fertility of women?]. J Gynecol Obstet Biol Reprod (Paris). 1986;15:159–64. 1986/01/01.
53. Feichtinger W, Putz M, Kemeter P. [Transvaginal Doppler sonography for measuring blood flow in the pelvis]. Ultraschall Medizin. 1988;9:30–6. 1988/02/01. https://doi.org/10.1055/s-2007-1011590.
54. Deutinger J, Reinthaller A, Bernaschek G. Transvaginal pulsed Doppler measurement of blood flow velocity in the ovarian arteries during cycle stimulation and after follicle puncture. Fertil Steril. 1989;51:466–70. 1989/03/01
55. Fleischer AC. Ultrasound imaging – 2000: assessment of utero-ovarian blood flow with transvaginal color Doppler sonography; potential clinical applications in infertility. Fertil Steril. 1991;55:684–91. Review 1991/04/01.
56. Campbell S, Bourne TH, Waterstone J, Reynolds KM, Crayford TJ, Jurkovic D, et al. Transvaginal color blood flow imaging of the periovulatory follicle. Fertil Steril. 1993;60:433–8. Research Support, Non-U.S. Gov't 1993/09/01.
57. Abramowicz JS, Jaffe R, Doppler PRTC. Assessment of uterine and ovarian blood flow during normal and abnormal cycles. In: Jaffe R, Pierson R, Abramowicz JS, editors. Imaging in infertility and reproductive endocrinology. Philadelphia: J.B. Lippincott; 1994.
58. Altundag M, Levi R, Adakan S, Goker EN, Killi R, Ozcakir HT, et al. Intraovarian stromal artery Doppler indices in predicting ovarian response. J Reprod Med. 2002;47:886–90. Evaluation Studies 2002/12/25.
59. Jarvela IY, Sladkevicius P, Kelly S, Ojha K, Campbell S, Nargund G. Quantification of ovarian power Doppler signal with three-dimensional ultrasonography to predict response during in vitro fertilization. Obstet Gynecol. 2003;102:816–22. Evaluation Studies Research Support, Non-U.S. Gov't 2003/10/11.
60. Merce LT, Gomez B, Engels V, Bau S, Bajo JM. Intraobserver and interobserver reproducibility of ovarian volume, antral follicle count, and vascularity indices obtained with transvaginal 3-dimensional ultrasonography, power Doppler angiography, and the virtual organ computer-aided analysis imaging program. J Ultrasound Med. 2005;24:1279–87. 2005/08/27.
61. Marret H, Brewer M, Giraudeau B, Tranquart F, Voelker K, Satterfield W. Ovine model to evaluate ovarian vascularization by using contrast-enhanced sonography. Comp Med. 2005;55:150–5. Evaluation Studies Research Support, Non-U.S. Gov't 2005/05/12.
62. Marret H, Brewer M, Giraudeau B, Tranquart F, Satterfield W. Assessment of cyclic changes

of microvessels in ovine ovaries using Sonovue contrast-enhanced ultrasound. Ultrasound Med Biol. 2006;32:163–9. Research Support, Non--U.S. Gov't 2006/02/09. https://doi.org/10.1016/j.ultrasmedbio.2005.10.004.
63. Duck FA, Starritt HC, ter Haar GR, Lunt MJ. Surface heating of diagnostic ultrasound transducers. Br J Radiol. 1989;62:1005–13.
64. Gleicher N, Friberg J, Fullan N, Giglia RV, Mayden K, Kesky T, et al. EGG retrieval for in vitro fertilisation by sonographically controlled vaginal culdocentesis. Lancet. 1983;2:508–9. Case Reports Letter Research Support, Non-U.S. Gov't 1983/08/27.
65. Heyner S, Abraham V, Wikarczuk ML, Ziskin MC. Effects of ultrasound on ovulation in the mouse. Gamete Res. 1989;22:333–8.
66. Heyner S, Abraham V, Wikarczuk ML, Ziskin MC. Effects of ultrasound on DNA and RNA synthesis in preimplantation mouse embryos. Mol Reprod Dev. 1990;25:209–14.
67. Mahadevan M, Chalder K, Wiseman D, Leader A, Taylor PJ. Evidence for an absence of deleterious effects of ultrasound on human oocytes. J In Vitro Fert Embryo Transf. 1987;4:277–80.
68. Williams SR, Rothchild I, Wesolowski D, Austin C, Speroff L. Does exposure of preovulatory oocytes to ultrasonic radiation affect reproductive performance? J In Vitro Fert Embryo Transf. 1988;5:18–21. 1988/02/01.
69. Kerin JF. Determination of the optimal timing of insemination in women. In: Richardson D, Joyce D, Symonds M, editors. Frozen human semen. London: Royal College of Obstetrics and Gynaecology; 1979. p. 105–32.
70. Brent RL, Beckman DA, Landel CP. Clinical teratology. Curr Opin Pediatr. 1993;5:201–11.
71. Takeuchi H, Nakazawa T, Kumakiri K, Kusano R. Experimental studies on ultrasonic Doppler method in obstetrics. Acta Obstet Gynaecol Jpn. 1970;17:11–16. 1970/01/01.
72. Stolzenberg SJ, Torbit CA, Edmonds PD, Taenzer JC. Effects of ultrasound on the mouse exposed at different stages of gestation: acute studies. Radiat Environ Biophys. 1980;17:245–70. Comparative Study 1980/01/01.
73. Stolzenberg SJ, Edmonds PD, Torbit CA, Sasmore DP. Toxic effects of ultrasound in mice: damage to central and autonomic nervous systems. Toxicol Appl Pharmacol. 1980;53:432–8. Research Support, U.S. Gov't, P.H.S. 1980/05/01.
74. Brodal P. Restitution of function after brain damage. In: Brodal P, editor. The central nervous system structure and function. 4th ed. New York: Oxford University Press; 2010. p. 147–56.
75. Edwards MJ, Saunders RD, Shiota K. Effects of heat on embryos and foetuses. Int J Hyperth. 2003;19:295–324.
76. Ang ES Jr, Gluncic V, Duque A, Schafer ME, Rakic P. Prenatal exposure to ultrasound waves impacts neuronal migration in mice. Proc Natl Acad Sci U S A. 2006;103:12903–10.
77. Graham JM Jr, Edwards MJ, Edwards MJ. Teratogen update: gestational effects of maternal hyperthermia due to febrile illnesses and resultant patterns of defects in humans. Teratology. 1998;58:209–21.
78. Stalberg K, Haglund B, Axelsson O, Cnattingius S, Pfeifer S, Kieler H. Prenatal ultrasound and the risk of childhood brain tumour and its subtypes. Br J Cancer. 2008;98:1285–7.
79. Calvert J, Duck F, Clift S, Azaime H. Surface heating by transvaginal transducers. Ultrasound Obstet Gynecol. 2007;29:427–32.
80. McClain RM, Hoar RM, Saltzman MB. Teratologic study of rats exposed to ultrasound. Am J Obstet Gynecol. 1972;114:39–42. 1972/09/01.
81. Sikov MR, Hildebrand BP. Embryotoxicity of ultrasound exposure at nine days of gestation in the rat. In: White D, Braun RE, editors. Ultrasound in medicine. New York: Plenum Press; 1977.
82. Sikov MR, Hildebrand BP. Effects of ultrasound on the prenatal development of the rat. Part 1. 3.2 MHz continuous wave at nine days of gestation. J Clin Ultrasound. 1976;4:357–63.
83. Schneider-Kolsky ME, Ayobi Z, Lombardo P, Brown D, Kedang B, Gibbs ME. Ultrasound exposure of the foetal chick brain: effects on learning and memory. Int J Dev Neurosci. 2009;27:677–83.
84. Hussain R, Kimme-Smith C, Tessler FN, Perrella RR, Grant EG, Sandstrom K. Fetal exposure from endovaginal ultrasound examinations in the first trimester. Ultrasound Med Biol. 1992;18:675–9. Comparative Study 1992/01/01.
85. Miller MW, Ziskin MC. Biological consequences of hyperthermia. Ultrasound Med Biol. 1989;15:707–22.
86. Zhang J, Zhou F, Song Y, Ying W, Zhang Y. Long dwell-time exposure of human chorionic villi to transvaginal ultrasound in the first trimester of pregnancy induces activation of caspase-3 and cytochrome C release. Biol Reprod. 2002;67:580–3. 2002/07/24.
87. Abramowicz JS, Fowlkes JB, Skelly AC, Stratmeyer ME, Ziskin MC. Conclusions regarding epidemiology for obstetric ultrasound. J Ultrasound Med. 2008;27:637–44.
88. Kieler H, Axelsson O, Haglund B, Nilsson S, Salvesen KA. Routine ultrasound screening in pregnancy and the children's subsequent handedness. Early Hum Dev. 1998;50:233–45. 1998/03/04.
89. Salvesen KA. Ultrasound in pregnancy and non-right handedness: meta-analysis of randomized trials. Ultrasound Obstet Gynecol. 2011;38:267–71. 2011/05/18. https://doi.org/10.1002/uog.9055.
90. McClintic AM, King BH, Webb SJ, Mourad PD. Mice exposed to diagnostic ultrasound in utero are less social and more active in social situations relative to controls. Autism Res. 2014;7:295–304. 2013/11/20. https://doi.org/10.1002/aur.1349.
91. Webb SJ, Garrison MM, Bernier R, McClintic AM, King BH, Mourad PD. Severity of ASD symptoms and their correlation with the presence of copy number variations and exposure to first trimester ultrasound. Autism Res. 2017;10:472–84. 2016/09/02. https://doi.org/10.1002/aur.1690.

92. Rosman NP, Vassar R, Doros G, DeRosa J, Froman A, DiMauro A, et al. Association of prenatal ultrasonography and autism spectrum disorder. JAMA Pediatr. 2018;172:336–344. 2018/02/13. https://doi.org/10.1001/jamapediatrics.2017.5634.
93. Somerset DA, Wilson RD. Prenatal ultrasonography and autism spectrum disorder. JAMA Pediatr. 2018. https://doi.org/10.1001/jamapediatrics.2018.1231.
94. Lees C. Prenatal ultrasonography and autism spectrum disorder. JAMA Pediatr. 2018. https://doi.org/10.1001/jamapediatrics.2018.1234.
95. AIUM. American Institute of Ultrasound in Medicine (AIUM) responds to autism study. http://www.aium.org/soundWaves/article.aspx?aId=965&iId=20160907. 2018. Accessed 30 July 2018.
96. ISUOG. International Society for Ultrasound in Obstetrics and Gynecology (ISUOG) statement on ultrasound exposure in the first trimester and autism spectrum disorders. http://www.isuog.org/NR/rdonlyres/57A3E1B7-5022-4D7F-BE0E93E1D239F29D/0/ISUOG_statement_on_ultrasound_exposure_in_the_first_trimester_and_autism_spectrum_disorders.pdf. 2018. Accessed 30 July 2018.
97. WFUMB. World Federation of Ultrasound in Medicine and Biology (WFUMB) statement on ultrasound exposure in the first trimester and autism spectrum. https://www.wfumb.org/safety-statements/c/0/i/22931999/new-wfumb-statement-ultrasound-exposure-first-trimester-and-autism-spectrum. 2018. Accessed 30 July 2018.
98. Sheiner E, Shoham-Vardi I, Pombar X, Hussey MJ, Strassner HT, Abramowicz JS. An increased thermal index can be achieved when performing Doppler studies in obstetric sonography. J Ultrasound Med. 2007;26:71–6.
99. AIUM. AIUM practice guideline for the performance of obstetric ultrasound examination. J Ultrasound Med. 2010;29:157–66.
100. AIUM. American Institute of Ultrasound in Medicine (AIUM) statement on measurement of fetal heart rate. https://www.aium.org/officialStatements/43. 2016. Accessed 30 July 2018.
101. Miller MW, Brayman AA, Abramowicz JS. Obstetric ultrasonography: a biophysical consideration of patient safety – the "rules" have changed. Am J Obstet Gynecol. 1998;179:241–54.
102. Duck FA. Is it safe to use diagnostic ultrasound during the first trimester? Ultrasound Obstet Gynecol. 1999;13:385–8.
103. Nelson TR, Fowlkes JB, Abramowicz JS, Church CC. Ultrasound biosafety considerations for the practicing sonographer and sonologist. J Ultrasound Med. 2009;28:139–50.
104. Safety Group of the British Medical Ultrasound Society (BMUS) Guidelines for the safe use of diagnostic ultrasound equipment. Ultrasound. 2010;18:52–9.
105. Abramowicz JS. Fetal Doppler: how to keep it safe? Clin Obstet Gynecol. 2010;53:842–50. Review 2010/11/05. https://doi.org/10.1097/GRF.0b013e3181fbae34.
106. AIUM. AIUM official statement: statement on the safe use of Doppler ultrasound during 11–14 week scans (or earlier in pregnancy). http://www.aium.org/publications/statements.aspx. 2011. Accessed 16 May 2012.
107. AIUM. AIUM Official Statement: prudent use in pregnancy. http://www.aium.org/publications/viewStatement.aspx?id=33. 2012. Accessed 16 May 2012.
108. AIUM. AIUM As Low As Reasonably Achievable (ALARA) principle. http://www.aium.org/publications/viewStatement.aspx?id=39. 2012.
109. BMUS (British Medical Ultrasound Society) Guidelines for the Safe Use of Diagnostic Ultrasound Equipment. http://www.bmus.org/ultras-safety/us-safety03.asp. 2000. Accessed 16 June 2012.
110. Chervenak FA, McCullough LB. Research on the fetus using Doppler ultrasound in the first trimester: guiding ethical considerations. Ultrasound Obstet Gynecol. 1999;14:161.
111. Campbell S, Platt L. The publishing of papers on first-trimester Doppler. Ultrasound Obstet Gynecol. 1999;14:159–60. 1999/11/07. https://doi.org/10.1046/j.1469-0705.1999.14030159.x.

Part II

Ultrasound Techniques

2 Basics of Three-Dimensional Ultrasound and Applications in Reproductive Medicine

Maximilian Murtinger and Maximilian Schuff

Introduction

Ultrasonography (US) plays a pivotal role in all major medical fields. This is due to the fact that US is a noninvasive, fast, and painless procedure without body exposure to ionizing radiation. The applied frequency for medical use ranges from 2 to 15 MHz, although frequencies up to 40 MHz may sometimes be used for special applications. US has an excellent safety profile as some thermal and mechanical effects on tissues are almost negligible, at the frequencies which are normally used in medical applications.

In fact, low invasivity is particularly needed in prenatal care, where even minor disturbances in embryogenesis and fetogenesis can have devastating effects. Moreover, the rapid technical innovations, notably the 3D imaging techniques, have made US a first-line diagnostic tool for the most varied medical applications, since it gives the clinician accurate anatomical images of the organs to be examined (width, height, and depth of images). This has also consequences in regard to more rapid diagnose findings and probably more distinct therapeutical approaches.

Three-dimensional US instruments still represent only a small portion of the overall medical imaging market; however their share has increased tremendously within the last years. Indubitably, their use will be further expanded, especially as regards applications in cardiology, oncology, obstetrics, and gynecology. Experts forecast that the compound annual growth rate for 3D US will be approximately 7% during the period 2017–2021, assuming that the global US market will expand from approximately 3 billion USD in 2015 to USD 9.5 billion by 2021 [1].

Three-dimensional US has one major advantage. While visualization with conventional two-dimensional (2D) ultrasound is limited to only sagittal and transverse planes (xz plane), 3D ultrasonography convinces by its accuracy in presenting the "true" volumes of analyzed objects. Therefore, measurement of distances is not restricted to certain planes but can be performed at any planes of the scanned volume. As a matter of fact, accuracy of diagnosis in two-dimensional sonography is often jeopardized by the fact that the physician has to imagine the three-dimensional structure on the basis of planar 2D images. In a 3D mode, the ability to choose the position of a 2D plane within the scanned volume allows an exact quantification of distinct areas.

In the recent years, 3D US technology has made rapid and remarkable progress and meanwhile has become an inherent part of many medical fields. The best example is the fetal ultrasound in first- and second-trimester screening within the scope of prenatal care. Although, in this par-

M. Murtinger (✉) · M. Schuff
NEXTCLINIC IVF Zentren Prof. Zech, Bregenz, Austria
e-mail: m.murtinger@ivf.at

L. A. Stadtmauer, I. Tur-Kaspa (eds.), *Ultrasound Imaging in Reproductive Medicine*,
https://doi.org/10.1007/978-3-030-16699-1_2

ticular field, the novel technique of 3D US was greeted with great skepticism, it is meanwhile considered to be an important and integral part of prenatal care with regard to detecting certain fetal anomalies including congenital heart defects, certain malformations of the neural tube, and anomalies of the surface anatomy. Although there are still some limitations regarding image quality, e.g., resulting from being influenced by the fetal position, the volume of amniotic fluid, or maternal obesity, 3D US is a relatively cheap and fast diagnostic tool compared to CT and MRI while offering a comparable level of accuracy. The routine use of 3D US is still not routinely recommended in the guidelines of international societies for first-trimester fetal US scans; however, most medical societies are well aware that these methods may be helpful in the evaluation of abnormalities [2]. Meanwhile, 3D US has also been implemented in the field of reproductive medicine. A vast number of articles on 3D US applications have been published on this topic.

The current chapter is aimed at (1) providing the readers with just basic information on this sophisticated technique, (2) giving a brief summary on the history of 3D US, (3) assessing the current applications within the context of infertility diagnosis and assisted reproduction, and (4) giving an outlook on possible forthcoming innovations.

Basics and Definitions

Ultrasound is characterized by longitudinal waves of pressure through a transmission medium with defined parameters: amplitudes, wavelength, propagation speed, and a frequency within a non-audible range of 20 kHz up to 500 MHz. One Hertz (Hz) is defined as one sound wave cycle or pulse occurring in 1 second. The generation of these US waves by transducers (probes) – the centerpiece of a US device – is based on the so-called piezoelectric effect, derived from the Greek words *ēlektron* (derived from amber, based on the observation that amber can acquire an electric charge by friction with certain other materials) and *piezein* (which means to squeeze or to press). This phenomenon was discovered in single-crystal quartz by Jacques and Pierre Curie in 1880 [3]. This discovery formed the basis for further research studies conducted by the physicist Paul Langevin, doctoral student of Pierre Curie – the inventor of the ultrasonic echography and later a professor at the Collège de France in Paris. Piezoelectric materials encompass solid substances, for instance, certain crystals such as quartz, ceramic, or ceramic perovskites, e.g., lead zirconate titanate, lead magnesium, or niobate–lead titanate. When electric currents with different potentials are applied to these piezoelectric materials, these currents induce rapid and rhythmical changes in the thickness of the material (Fig. 2.1). In consequence the mechanical energy is transformed into emitted sound waves. For each US pulse, a series of echoes are returned when the pulse is reflected from objects at greater or lesser distance. Vice versa the crystals can also absorb reflected sound waves and convert them into electric signals. Thus, US transducers always have dual functions (see Fig. 2.1). The US echoes are received by the transducer and converted into electronic signals that can be displayed on a monitor. The transducer probes may contain a single element or an ensemble of arranged individual single transducers. These are named as multiple-element probes (MEP) or transducer arrays. A schematic drawing of a US probe is given in Fig. 2.2. While single-element probes were used in the early days of US applications, they have gradually been replaced by MEPs from the early 1980s onward [4]. The most outstanding advantage of MEP is the possibility of beam steering. In MEPs each crystal has its own circuit; thus the US beam can be "steered" by changing the timing in which each element gets pulsed. Beam steering allows the multiple angle and/or multiple point inspection from a single probe and a single probe position (Fig. 2.3).

In general, for imaging tissues by US, two main types are used: pulsed and continuous waves. The wavelength (λ) is the spatial distance between consecutive cycles of sound and defines the resolution capacity. The greater λ, the less is the resolution (Fig. 2.4). The resolution is also determined by the frequency used as λ is defined by propagation speed or speed of sound (c)/fre-

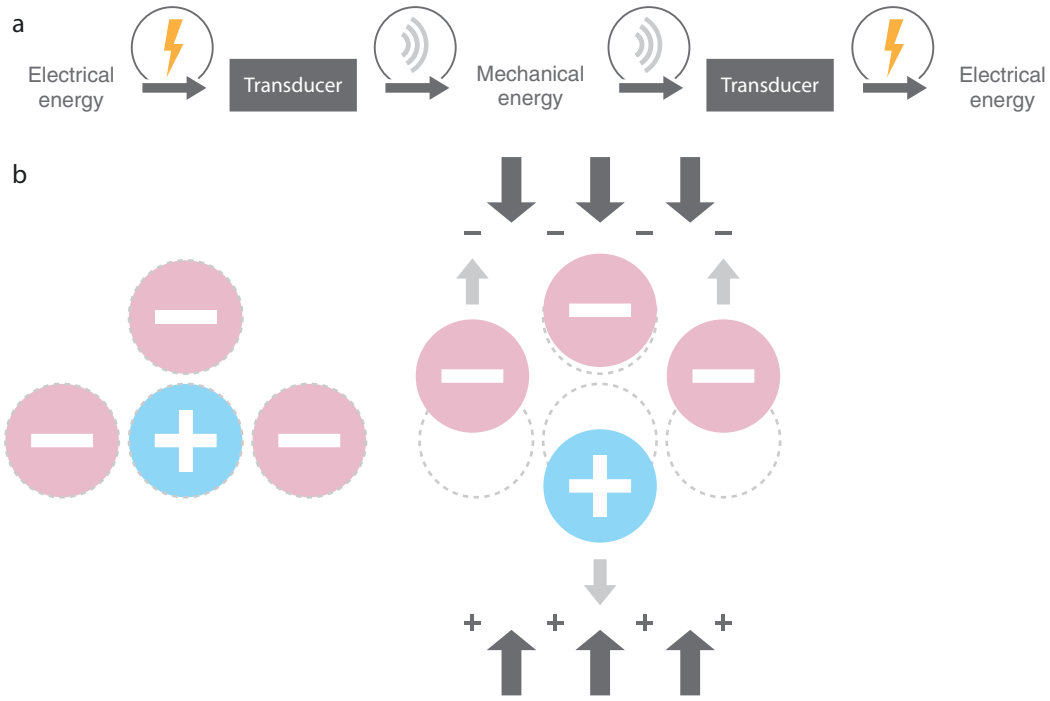

Fig. 2.1 (**a**, **b**) Principle of the piezoelectric effect. Schematic drawing of a transducer and the piezoelectric effect. Transducers containing the piezoelectric have a dual function. They can adsorb the electrical or mechanical energy and can transform it into each other (**a**). The piezoelectric materials such as quartz are assembled in a crystal lattice structure and contain different charged groups (in the case of quartz, positively charged silicon and negatively charged oxygen ions). Under mechanical stress, potential difference across its opposite faces is built

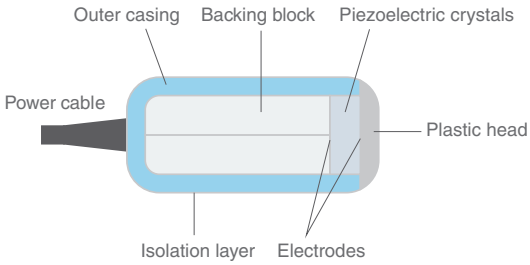

Fig. 2.2 Schematic drawing of a US probe

quency (*f*). Generally, propagation speed is the speed at which a sound wave travels through a medium or tissue. US waves can propagate in most biological tissues similar to those of water. Propagation speed varies, however, between different types of tissues depending on their density. A fourth important parameter is the penetration depth (PD). The PD is influenced by the absorption and dispersion of the analyzed tissue and has

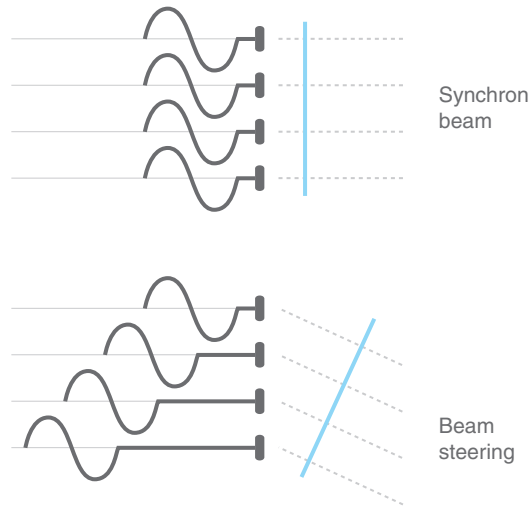

Fig. 2.3 Principle of beam steering. The multiple-element probes (MEP) allow beam steering. MEPs are selectively pulsed. The time delays of the pulses sent to the individual transducer elements are adjusted to steer the beam in one direction or the other, respectively

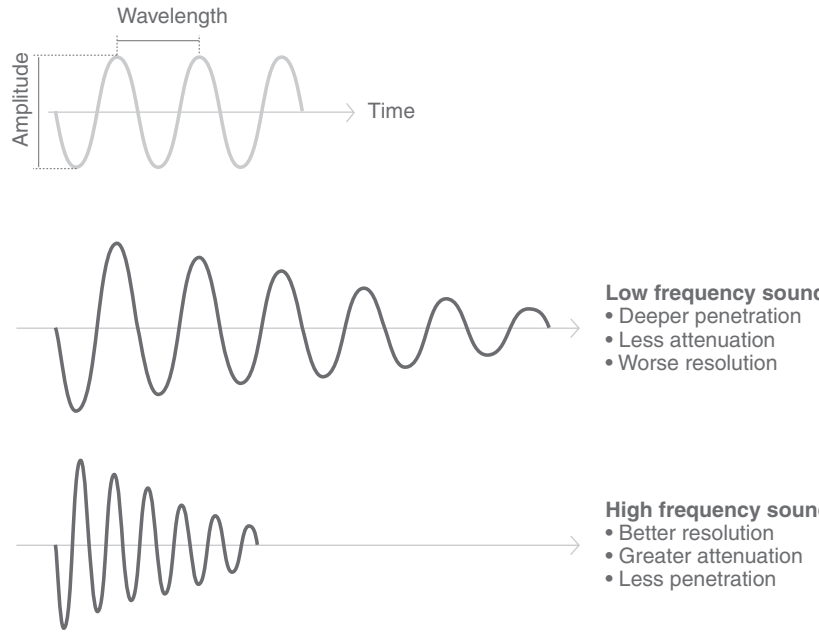

Fig. 2.4 Physical parameters of ultrasound. Representation of US waves with amplitude (maximum variation occurring in an acoustic variable) and wavelength (λ, length of space over which one cycle occurs). By passing through a medium, the amplitude decreases, while the frequency ($f = c/\lambda$) remains constant. High-frequency US enables better resolutions, but the amplitudes decrease much faster, which means in turn less penetration depth

a direct effect on the resolution (better resolution means less PD). Additionally, the acoustic impedance (z) is the fifth parameter that should be kept in mind. It describes the reflection of US waves on boundary surfaces – in other words the resistance of a US beam when it enters the target tissue. The impedance depends on the density (ρ) of the tissue and the speed (c) of the US wave ($z = \rho \times c$). When there is a large difference in z values between two tissues, the US beam is reflected. Some impedance values for different body tissues are listed in Table 2.1.

Sound power (P) is the rate at which the sound energy is emitted. This parameter is crucial for being able to exclude any risk of thermal and mechanical damages. P is given in Watt (1 W = 1 kg × m^2/s^3) and defined by sound intensity (I) and transmitted area of the US of $P = I \times A$. The intensity itself is defined by the sound pressure (p) and particle velocity (v) ($I = p \times$ v). The recommended safety limit for US sound power in pregnancy is usually below 100 mW/cm^2. According to the US Food and Drug Administration (FDA), the limit for obstetrical ultrasound is 94 mW/cm^2 for the spatial peak temporal average intensity and 190 W/cm^2 for spatial peak pulse average for fetal imaging [6].

Table 2.1 Propagation speed and impedances of US waves in different media and tissues

Media/tissue	Propagation speed [m/s]	Impedances
Air	340	0.0004×10^6
Water	1500	1.48×10^6
–		
Fat	1450	1.34×10^6
Soft tissue	1540	1.54×10^6
Liver	1549	1.65×10^6
Kidney	1561	1.63×10^6
Lung	1570	0.18×10^6
Muscles	1570	1.71×10^6
Bones	3600	7.8×10^6

Adapted from [5]. Acoustic impedances are given in Rayls [kg/m^2 × s]

Put into highly simplified terms, US image rendering can be done in basically two different modes: A-mode, which means the 1D presentation of the amplitude as a spike on the screen – thereby the intensity of the returned wave is correlated to – and B-Mode, where the intensity of the echo of the wave is recorded as a bright dot instead of a spike (the brightness is correlated to the intensity echoes; see Fig. 2.5). Each echo is represented as a dot in the image reflecting exactly the relevant position in the tissue sample analyzed. The aforementioned sequential activa-

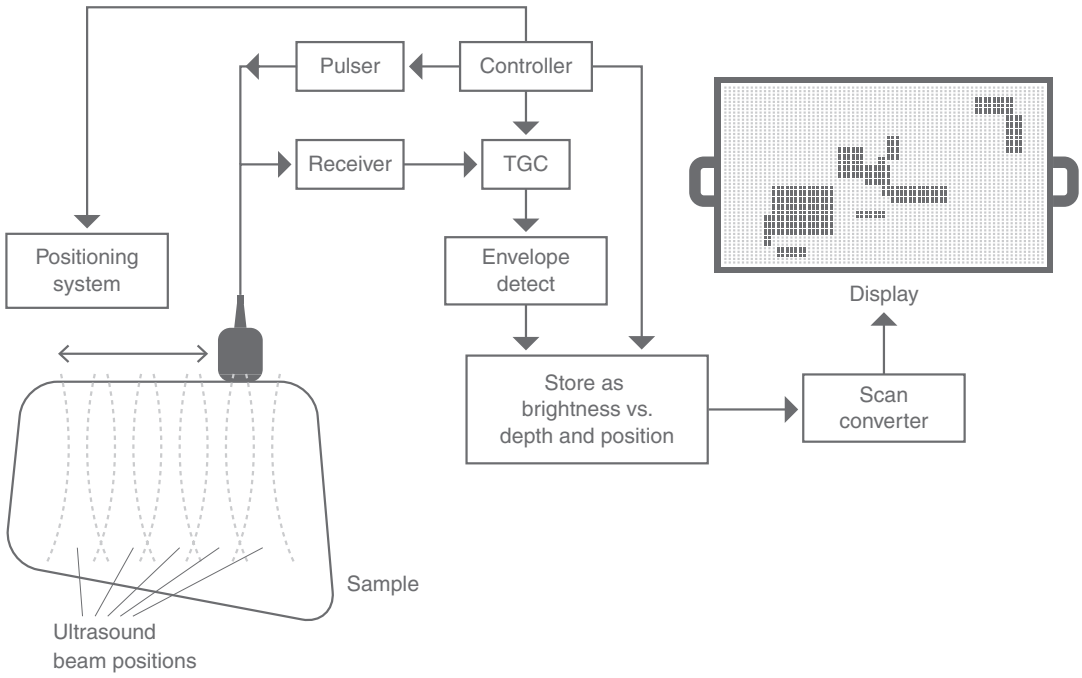

Fig. 2.5 Principle of B-mode imaging. In the B-mode (brightness-mode) system, a series of A-mode scans are used for 2D imaging. The system encompasses a pulser/receiver, which excites the transducer and amplifies echoes, the time gain compensator (TGC) in which signal gain is increased as time passes from the emitted wave pulse, the detection of the envelope of the signal, the scan converter for formatting the echoes for the display, and the display system. (Adapted from [7])

tion of MEPs allows the creation of multiple scan lines that can be assembled to obtain a 2D image.

Other imaging modes include M-mode or C-mode, to name but a few. M-mode means motion-mode. Therefore, a rapid sequence of A- or B-mode scans allows the rendering of tissue or organ motions. C-scan encompasses a series of A-scans in two orthogonal directions allowing the construction of an image at constant depth away from the transducer. The potential of C-mode imaging for medical application however has not been fully explored [8]. The duplex mode encompasses and combines the B-mode grayscale image and PW Doppler flow velocity measurements. The B-mode image provides the region of interest (ROI), where a Doppler sample volume is to be placed and where the flow velocity can be measured.

The terms used "2D," "3D," or "4D" refer to the dimension. Thus, 3D US refers specifically to the volume rendering of ultrasound data; 4D US scanning refers to the collection of several 3D volumes over a period of time; in other words it includes the time dimension.

In principle, the 3D mode is nothing else than a series of 2D scans used for building up a 3D structure. Three-dimensional sonography in medicine encompasses four steps: data acquisition, analysis and processing of volume, image animation and finalizing of the image, and data storage [9].

Additionally, Doppler US (sometimes also designated as D-mode) allows the measurement of velocity. This technique is based on the physical phenomenon of the Doppler shift, the observation of change in frequency or wavelength of a wave for an observer when either the source or the observer is moving. This effect was originally described by the Austrian physicist and mathematician Christian Doppler in 1842 [10]. Doppler shifts are usually in the range of 100 Hz to 11 kHz and are correlated to the velocity, the angle

between the transducer, and the direction of propagation as well as the operating frequency of the instrument. There are several US Doppler instruments available such as continuous-wave Doppler or pulsed-Doppler systems and 3D power Doppler. The latter plays an important role, inter alia, in prenatal diagnosis for quantification of blood flows in fetal organs [11]. Other fields of applications of 3D Doppler in gynecology include the assessment of uterine vascularization and blood flow as well as the characterization of gynecological tumors. However, the details of 3D Doppler US technology and application areas are not a subject of this chapter but are summarized in detail in the next chapter.

Theoretically, 3D US systems can be divided in different groups on the basis of the transducer used. Earlier 3D systems using conventional transducers are not able to directly assess the spatial volume, but 3D data is achieved by movement of the transducers. The 2D array transducers, which were launched on the market within the last decade, allow a direct volume scanning by electrical interrogation of ROI. They have a large number of elements in both the azimuth and elevation dimension. Therefore, 2D arrays can steer the acoustic beam in both dimensions and are capable of acquiring pyramidal volumetric data at high speed. This tremendous innovation achievement was able to significantly reduce motion artifacts while providing acceptable spatial resolution [12].

The types of transducers can also be classified according to their "acoustic window" – the location where the transducers contact the body to visualize the organs or tissues of interest. Thus, the probes are specifically formed to suit the intended application. This specially holds true for the intracavity (endo) probes. The intracavity probes allow a detailed examination of the uterus, the ovary, the bladder, the fallopian tubes, and the pouch of Douglas.

As a matter of fact, the success story of gynecological US and its related 3D applications is based on the development of intracavity probes, notably the development of transvaginal transducers by the companies Kretztechnik, Zipf, Austria, and Aloka Co., Tokyo, Japan, in the 1960s [13]. Although theoretically, gynecologic imaging could be performed with the transabdominal approach, endovaginal US yields much better results as it allows bringing the probe into the closest possible proximity to the ROI. Meanwhile, there is a multitude of transvaginal transducers with different features supporting different image formats (rectangular; 2D sector; 2D convex or curved where the maximum angular extent is the field of view; 2D trapezoidal; parallelepiped; 3D fan or broom shape; 3D truncated prism; 2D donut; or 3D tube) [4] as well as different sizes and shapes (footprints) available on the market and distributed by many companies, for instance, GE, Siemens, Philips, Hitachi, Toshiba, and many others. In gynecology, usually end-fire arrays are used which means that the arrays are located at the end of the probe. They are mostly convex or curved with a wide field of view.

The 3D probes used for acquisition of data can be divided into mechanical or electronical probes. The former are less expensive and represent an older innovation. They have a motor inside and cannot produce images in real time. A regular linear array transducer is motored to rotate, tilt, or translate within the probe under the computer control [14]. When rotating, the ultrasound transducer produces a 360° image. Multiple 2D images are acquired from the examined area when the motor is activated [15]. The electronical transducers are usually much faster. They encompass a fixed number of transducers that transmit signals via micro wires to the image processor. The US beam can be changed electrically, thus enabling much better images to be obtained.

In principle, 3D US examination consists of four steps (data acquisition, visualization, image processing, and storing of data), and there are four ways of 3D data acquisition:

1. Tracked freehand method: The transducer is swept over surface and the 3D image is built from a series of 2D images. Freehand 3D US allows intraoperative imaging of volumes of interest in a rapid and flexible manner [16]. This technique requires manual movement of the probe through the ROI. However, as a

prerequisite the exact angulation and position of the US transducers are needed which may be achieved by the use of position sensors.
2. Untracked freehand systems: With these systems, the operator moves the transducer in a regular motion, while the 2D images are performed. For a 3D image, a linear or angular spacing between the single images is assumed. The major disadvantage of this technique is that exact local positioning is not possible, and measurements, especially for volumes, are highly inaccurate.
3. A three-dimensional visualization can be intrinsically achieved by 2D transducer arrays: These arrays generate pyramidal pulses of the US, and the echoes are converted into 3D images. The advantage is that the transducer can remain stationary, and electronic scanning can be used to sweep a broad ultrasound beam over the entire volume under examination [17].
4. Mechanical assemblies: The transducer (probe) is moved either (1) linear, (2) tilted, or (3) in a rotational movement about its central axis by a mechanical assembly.

Visualization, Reconstruction, and Post-processing

To obtain a spatial image, a number of images must be converted into a 3D dataset for further processing. This process also involves the interpolation and improvement of data quality by filtering [18]. Thus, software programs for reconstruction (rendering) and imaging play a dominant role in 3D US. Several algorithms have been developed allowing for perfect visualization, manipulation, and processing of the received 3D images. It is apparent that the progress in software development was – and still is – the key to success for this technique. Currently, numerous visualization modalities are available:

1. Multi-planar view: This is probably the most commonly applied operating mode in gynecology. It was the first available visualization mode in 3D US. The display presents the three orthogonal planes simultaneously: the longitudinal, transverse, and coronal planes. The dataset can then be rotated or sliced in order to view the ROI. The multi-planar view displays the exact spatial relationships between the three planes. This mode is currently used in prenatal care of second-trimester screening to study the fetal profile, but it also assumes a major role in the assessment of congenital uterine anomalies [19, 20].
2. The tomographic ultrasound imaging (TUI) or multi-slice technique: TUI allows for a comprehensive sequential analysis of the desired organ (Fig. 2.6). The same imaging principle is employed in CT and MRI. For example, tomographic ultrasound imaging has been reported to greatly simplify pelvic floor assessment [21].
3. The static volume contrast imaging (VCI) mode: This mode allows for the receipt of information from adjacent slices in a volume. This imaging mode was especially developed to enhance the contrast between tissues and organs that would appear similar on conventional 2D US [22]. VCI is currently applied for detecting thoracic abnormalities [22] or imaging fetal pelvic anatomy [23]; it was found to be superior to 2D US in these studies [24]. VCI allows a better imaging of tissue interfaces. Thus, diffuse lesions such as those associated with adenomyosis could be better assessed [25].
4. Inversion mode: In inversion mode, volumes are displayed in their entirety as an echogenic area, while the grayscale portions of the image are rendered as transparent. Some IVF and obstetrical applications could benefit from this method [26]. For example, the examination of the fallopian tubes using this technique helps diagnose the presence of hydrosalpinges [27].
5. Transparency mode: The transparency mode (also known as maximum mode) images regions with high echo density in a glass-like mode. This mode is mostly used for imaging of cartilaginous structures. With this mode, high-echogenic voxels are higher valued.
6. The surface-rendering mode helps to detect and display the surface of the structures. It is most commonly used for the evaluation of

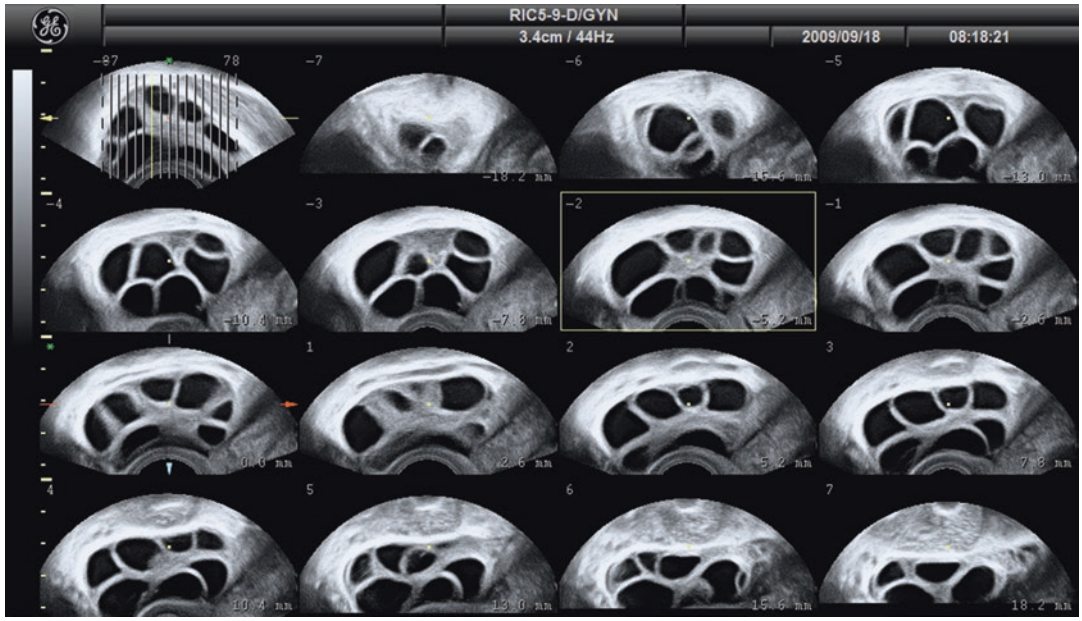

Fig. 2.6 Tomographic ultrasound image (TUI) of multiple follicles in a stimulated ovary

ovarian tumors [28, 29]. A smaller 3D dataset for rendering is extracted from the original 3D dataset to eliminate unnecessary parts adjacent to the object of interest [18]. This technique allows surface reconstruction of conspicuous parietal structures [28].

7. Glass-body rendering: Glass-body rendering (GBR) imaging is a combination of the transparency and color or power Doppler mode. It is very suitable for gynecologic applications; however, it is most useful for vessel imaging. In this mode the rendering algorithm is based on the simultaneous representation of gray and color Doppler scale [30].
8. Four-dimensional image techniques: The four-dimensional image techniques (such as the spatiotemporal image correlation (STIC)) allow for procedures such as echocardiography of the fetal heart [31, 32]. The received data is acquired by a single, automatic volume sweep; subsequently, the software analyzes the data according to their spatial and temporal domain and processes a 4D cine sequence. Prior to the launch of these 4D techniques, the examination of the fetal heart with conventional US was often difficult.
9. OmniView: OmniView (GE Medical Systems, Kretztechnik, Zipf, Austria) is a display technology for 3D and 4D US that allows integration of volume datasets and the simultaneous display of up to three independent (non-orthogonal) planes by manually drawing straight or curved lines from any direction or angle [32].

Although many 3D US display techniques have been employed (more than the ones described in this chapter), the two most commonly used are multi-planar reformatting and volume contrast imaging. Image quality has improved since the implementation of 3D US; nevertheless, the final quality still depends on the accuracy of the scanned volumes (also see next paragraph). Nevertheless, as previously mentioned, various software-based tools are currently available.

Post-processing is often done via the electronic scalpel (3D cutting) (Kretztechnik, Zipf, Austria), contrast and brightness regulation, or speckle reduction imaging (SRI). SRI was established on the Voluson platform in 2004 by GE Healthcare. The electronic scalpel allows

for the removal of pre-located obscuring structures in three steps: (1) rotation of the rendered image into a position where the obscuring structures can be cut; (2) the selection of the cutting mode; and (3) creation of the outline for the cut and activation of the cutting mode [33]. Speckles are recurrent problems in sonography due to interference of ultrasound echoes; they produce difficulties in differentiating anatomical structure. Many approaches have been attempted with the goal of reducing or even of eliminating speckles. Most significantly, the increased computer processing power and speed of calculation within recent years have allowed more complex image-processing techniques to reduce these artifacts without impairing image quality [34]. In addition, filtering is widely used for undesired echoes that are a recurrent phenomenon in sonography. Filtering allows the suppression of unwanted background noise or the enhancement of the desired information (suppressing and enhancing filters) [35].

Limitations

Three-dimensional US uses the same frequencies, applies to the same basics (as the 3D volume is reconstructed), and is thus falling under the same laws of physics. Therefore, the limitations are almost the same, and the prerequisite of high-quality 3D imaging is a good 2D US scan, and the best way to achieve a good 3D image is to optimize the image settings [20]. Improper calibration of the scanning assembly is the most common source of errors. This however holds true for both 2D and 3D techniques.

The original angle of the US beam at which the scan was performed will also impact on the quality of acquired planes. What definitely makes the difference between 3D and 2D is the "expert knowledge." Practitioners should be aware of the fact that they do not only need to learn the acquisition techniques but also need to get familiar with the software used. This might imply that even sonographers experienced in 2D techniques have to undergo a learning process in order to be able to handle the 3D US technique [36].

Additionally, the presence of artifacts might be a problem associated with 3D technique. Some of the artifacts may even be derived from 2D scan, such as shadowing effects. In a 3D volume, however, these artifacts might look completely different and are sometimes hard to recognize [37]. Other artifacts might be derived from volume rendering itself. One of the prominent artifacts associated with 3D imaging is well known from fetal imaging. Motion or vibration of the scanned target during the acquisition of a volume introduces an artifact into the volume which affects the overall volume quality and might lead to misdiagnosis [37]. According to our experience, all these shortcomings of this impressing technique can be handled by an experienced sonographer. Less experienced sonographers should be regularly supervised by experienced colleagues. In this way many of the apparent disadvantages can be compensated, e.g., the long time for post-processing.

History

Three-dimensional US meanwhile can look back on a long history of more than three decades. A 3D US system was first described by Kazunori Baba in 1984, who was also the first to obtain 3D images of a 19-week fetus by processing the raw 2D images on a minicomputer in 1986 [38, 39]. In 1987 Olaf T. von Ramm and Steven W. Smith patented "An acoustic pulse echo imaging system capable of producing an image of a three-dimensional object utilizing a two-dimensional display" [40].

Two years later, the first commercially available 3D US instrument the Combison 330 equipped with 7.5 MHz and integrated 3D system was presented at the French radiology congress in Paris in 1989 by the Austrian company Kretztechnik AG, Austria, and marketed in the same year [41]. The system used mechanical abdominal volume scan transducers with the mechanical swept-volume approach. Although the acquisition of the volume took only 1–2 seconds, the rendering process of the image took up to almost 20 min on an external computer. The

technical evolution of 3D US dovetailed with the evolution of fast and efficient computing systems. In fact, data processing and storage were one of the main limitations of the 3D US systems apart from problems intrinsic to US imaging: speckle, clutter, grating lobe, and other artifacts [42]. Thus, 3D US only prevailed from the 2000s onward.

Additionally, the rendering of this predecessor model was also limited in the ability to provide a set of orthogonal planes orientated images in strict relation to the axis of the probe. Another drawback was the special scan transducers that were needed for this prototype. They had to be held by their larger side, thus making them rather difficult to handle. For the majority of the more advanced US instruments, this problem could be solved by a 90° rotation of the 3D US device. The first translucent display using volume rendering was launched in 1991, and in the early 1990s alongside technical progress, there were 3D US images of embryos and early gestational-age fetuses and reported cases of fetal congenital malformations [43–46]. Since the mid-1990s, the number of publications on fetal 3D US imaging has increased dramatically. In 1997 the "First World Congress on 3D Ultrasound in Obstetrics and Gynecology" was launched in Mainz, Germany [47]. In 1999, the ISUOG 3D Focus group was founded to evaluate the role of 3D US and to make recommendations and to provide guidelines on the use of 3D US within the scope of obstetrics and gynecology [48]. At the end of the last millennium, offline reconstruction systems had become obsolete as imaging became available on the US instruments itself [49].

In 1998, the Voluson 530D 3D system implemented a technology that displayed not only the 3D sectional images but also processed the data of the entire volume in real time. With the commercial launch of this 3D instrument platform, 3D ultrasound technology competed with the higher-priced CT and MRI instruments; it allowed effective grayscale imaging, spectral Doppler, color Doppler, and Angio Color Imaging [50]. In the year 2000, the medical equipment manufacturer GE Healthcare introduced a new generation of clinical US systems, the Voluson 730, with real-time acquisition of volumes (16 volumes/s). In 2001, 4D US was first introduced by GE Medical Systems. Over the last decade, several US instruments were launched to the market encompassing supporting software for (semi-)automatic volume calculation such as SonoAVC (automatic volume calculation) or VOCAL (virtual organ computer-aided analysis).

Current Applications and Benefits of 3D US in Reproductive Medicine

This subchapter does not aim to give broad and specific information in regard to the different applications of 3D US in reproductive medicine as most of the applications are discussed in greater detail in the following chapters. However, this section offers a comprehensive overview and insight into the currently most important fields of application either prior to or during an ART therapy.

Prior to an IVF therapy, one of the most important 3D US applications consists of assessing potential uterine abnormalities as well as the endometrium, in detecting polyps, myoma, and cysts (Figs. 2.7, 2.8, and 2.9) and adnexal lesions, and, during IVF, in monitoring folliculogenesis in controlled ovarian stimulation (COS). A detailed overview of current applications in gynecology and ART is given in Table 2.2. As in 2D technique, the transvaginal approach (transvaginal US; TVUS) is the preferred examination method with 3D US within the scope of ART. Therefore, the transducer can be brought close to the ROI.

The sonographic assessment of the ovary is a key factor in the planning of assisted reproductive techniques, (i) basically to estimate the ovarian reserve and response of COS in a reliable manner and to decide the next steps of therapy, (ii) in suspicion of polycystic ovaries, and (iii) to estimate the risk of ovarian hyperstimulation syndrome (OHSS) due to hormonal stimulation and the administration of an ovulation trigger.

The sonographic calculation of antral follicles is the most reliable ovarian reserve test for

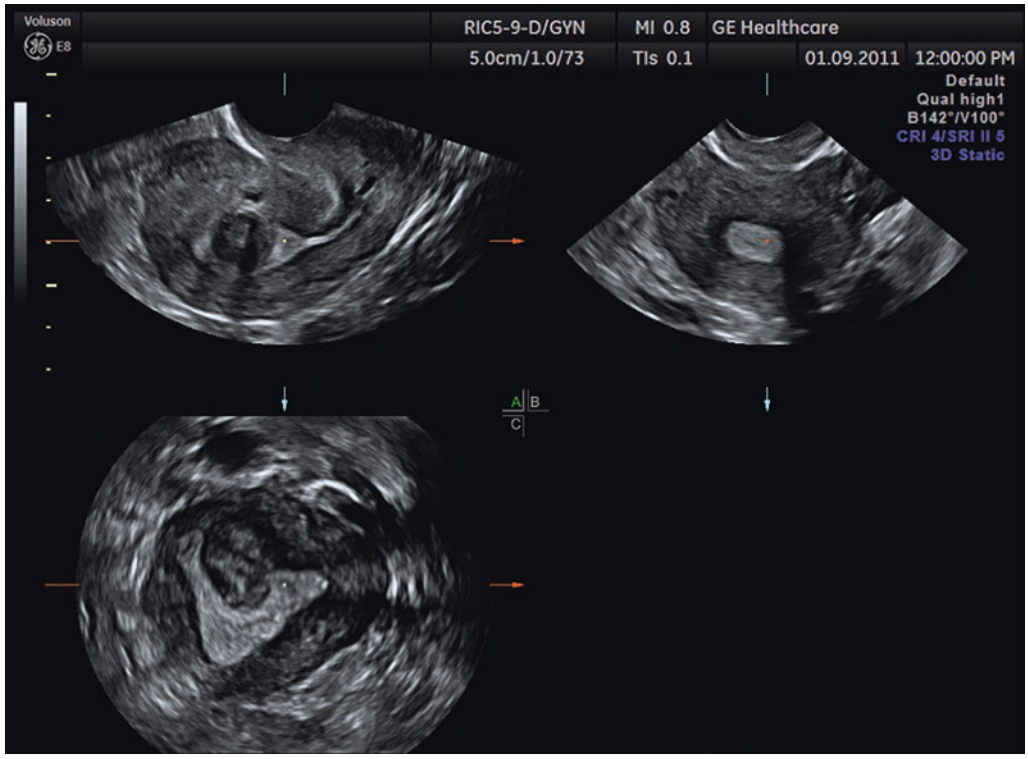

Fig. 2.7 3D US image of uterine myoma (Voluson E8)

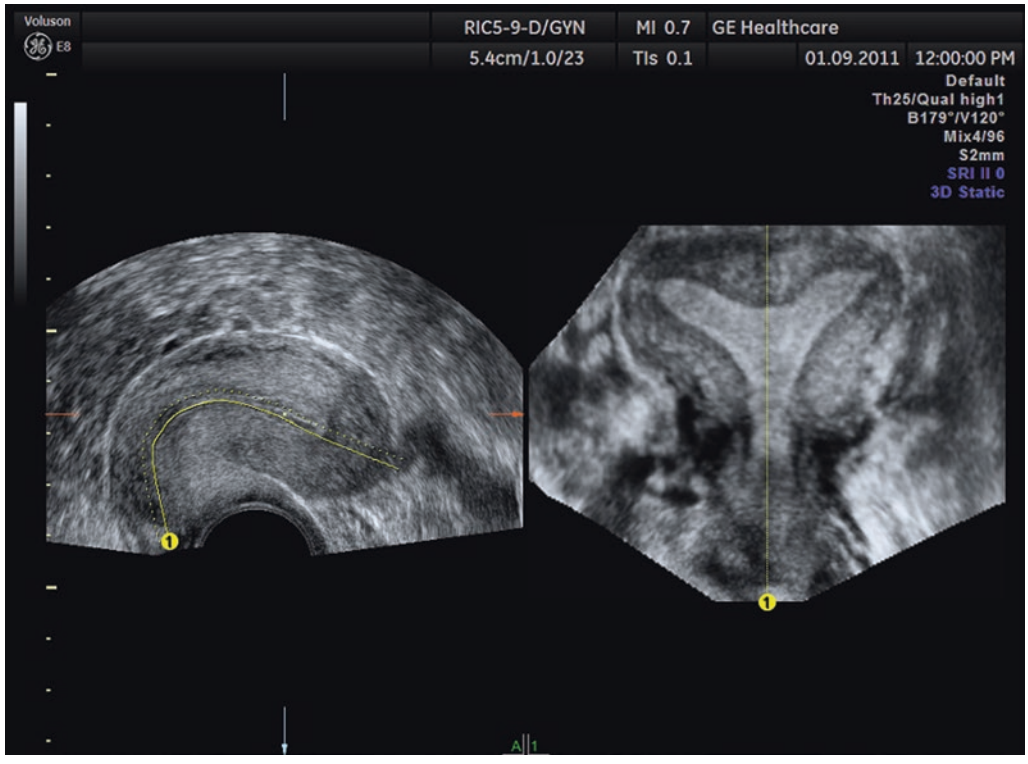

Fig. 2.8 3D US image of class U2a uterus (Voluson E8). Classification according to [51]

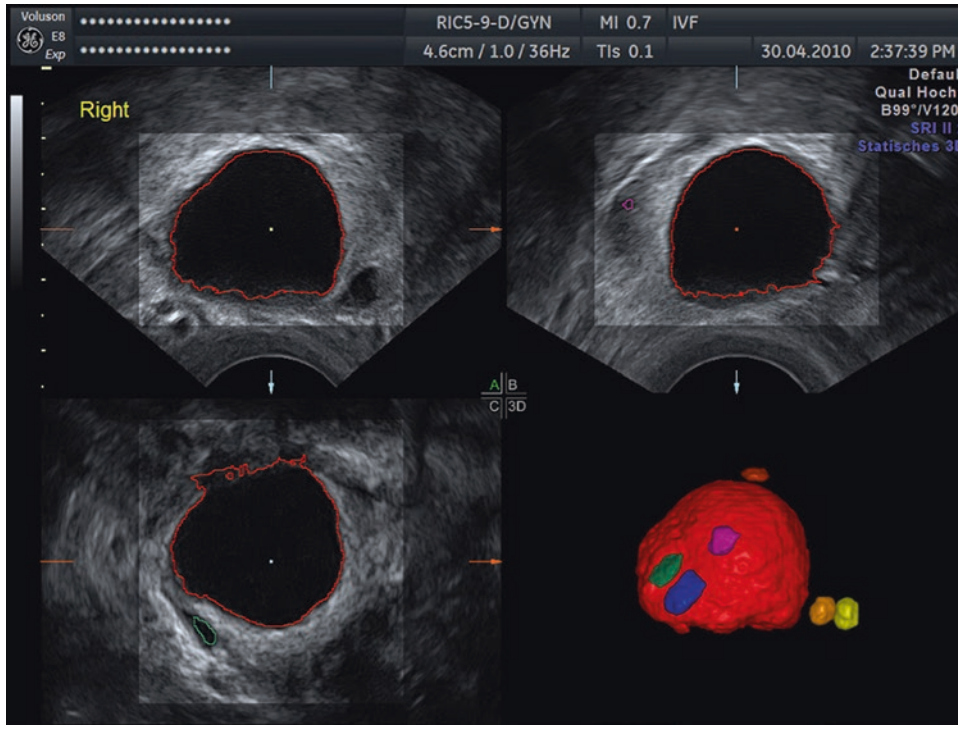

Fig. 2.9 Imaging of a cyst as a scan and in 3D reconstruction. US scans of a cyst performed with E8 Voluson and 3D imaging by SonoAVC software imaging by SonoAVC software

IVF. While the anti-Müllerian hormone (AMH) level can be obtained through a regular blood test and might be correlated to the antral follicle count (AFC) in a reliable manner, the US-based estimation of AFC captivates by the availability of quick results and the distinct depiction of the situation in each ovary (Fig. 2.10). To date, most studies have evaluated the AFC by 2D US. Thus, there is still little data on 3D US studies. In regard to AFC, there might be no groundbreaking advantages of 3D in a "normal" ovary, although 3D US techniques especially the semiautomated 3D US systems such as SonoAVC might be more suitable in regard to inter-observer reliability, given that the time needed for the examination is expected to be much shorter [52, 53]. The latter especially holds true for young women with a high AFC and patients with a polycystic ovary (PCO) situation where the semiautomatic 3D technique might be superior in assessing the true AFC and the exact ovarian volume [54, 55].

In fact, the US-based diagnostic Rotterdam criteria for polycystic ovary syndrome (PCOS) with either ≥12 follicles or an increased ovarian volume of >10 cm^3 are exclusively based on 2D US data [56]. As 3D US facilitates the quantitative measurement of total ovarian and stromal echogenicity as well as volume, 3D US techniques might be more reliable for investigation of this patient clientele. Therefore there might be a need to revise current US-based criteria for PCOS [57].

Three-dimensional ultrasonography might also play a more prominent role in the detection of pathologies of reproductive organs. While it may still play only a minor role in the detection of malignancies of the reproductive tract [58, 59], there is however a clear superiority of 3D imaging systems in other pathologies of the female reproductive tract, such as the investigation of congenital uterine malformations and certain benign conditions. 3D US permits optimal visualization and allows for a more accurate diagnosis when compared to other approaches for the screening of uterine malformations.

Congenital uterine malformations are estimated to have a prevalence of up to 30% in the

Table 2.2 Application of 3D US within the scope of reproductive medicine

Assessment		Advantages	Disadvantages
Ovary			
	Estimation of AFC	High reproducibility; high inter- and intra-observer reliability	Requires post-processing; probably no benefit in low AFC
	Folliculometry during COS	Accurately measures true follicle size: more accurate in the number of follicles, especially in good to high ovarian response; high inter- and intra-observer reliability; time-saving	Requires post-processing; the true value and consequences, e.g., for triggering still not fully evaluated
	Detection of pathologies of the ovary		Requires post-processing
Fallopian tube			
	Assessment of tubal pathologies	Good tool for detection of hydrosalpinges	Requires post-processing; only first-line diagnostic tool
Uterus			
	Investigation of uterine malformations	"Gold standard" –superior to all other imaging tools intended for this purpose	Requires post-processing
	Assessment of scar sections or adhesions	Accurate measurement of size	Requires post-processing
	Detection of pathologies	Accurate estimations of size and location	Requires post-processing; superficial lesions are difficult to detect; only first-line diagnostic tool
Endometrium			
	Detection of pathologies	Accurate estimations of size and location	Requires post-processing; only first-line diagnostic tool
	Evaluation of endometrial volume and structure	Accurate estimation of endometrial volume and elucidation of sub-endometrial vascularization	Data from 3D studies for predicting IVF outcome are controversial. Requires post-processing

population faced with recurrent miscarriages, compared to 1–10% in the general population [60]. Therefore uterine malformations might have a substantial impact on female fertility. Even though the most commonly occurring uterine malformations are suggested to be asymptomatic, some are assumed to be associated with implantation failure, pregnancy loss, or complications in the course of pregnancy and birth. Especially the septated uterus, one of the most common forms of uterine anomalies, is significantly associated with infertility and spontaneous abortion [61]. It has been also assumed that the prevalence of septated uteri is 3.5-fold higher among infertile patients compared to the general population [62]. In the case of uterine anomalies, 3D US has proofed to be an excellent predictive diagnostic tool, especially for the differentiation of certain anomalies. It offers similar specificity and sensitivity compared to MRI but is definitely cheaper and provides faster and easier handling. HSG was, besides the 2D US, the most frequently applied approach to analyze uterine malformations. However, this technique is invasive, and, most importantly, it cannot evaluate the external contour of the uterus [63]. Thus, HSG cannot be recommended as first-line diagnostic tool. Compared to the 2D US approach, the 3D US technique is, without doubt, superior when it comes to differentiating between different subtypes of uterine malformations. Since 2D US only provides information on the basis of axial and sagittal planes, it is limited in terms of accessibility required for the assessment of pathologies in the coronal (y) plane.

Compared to the 2D US approach, the 3D US technique is, without doubt, superior in regard to differentiate between different subtypes of uter-

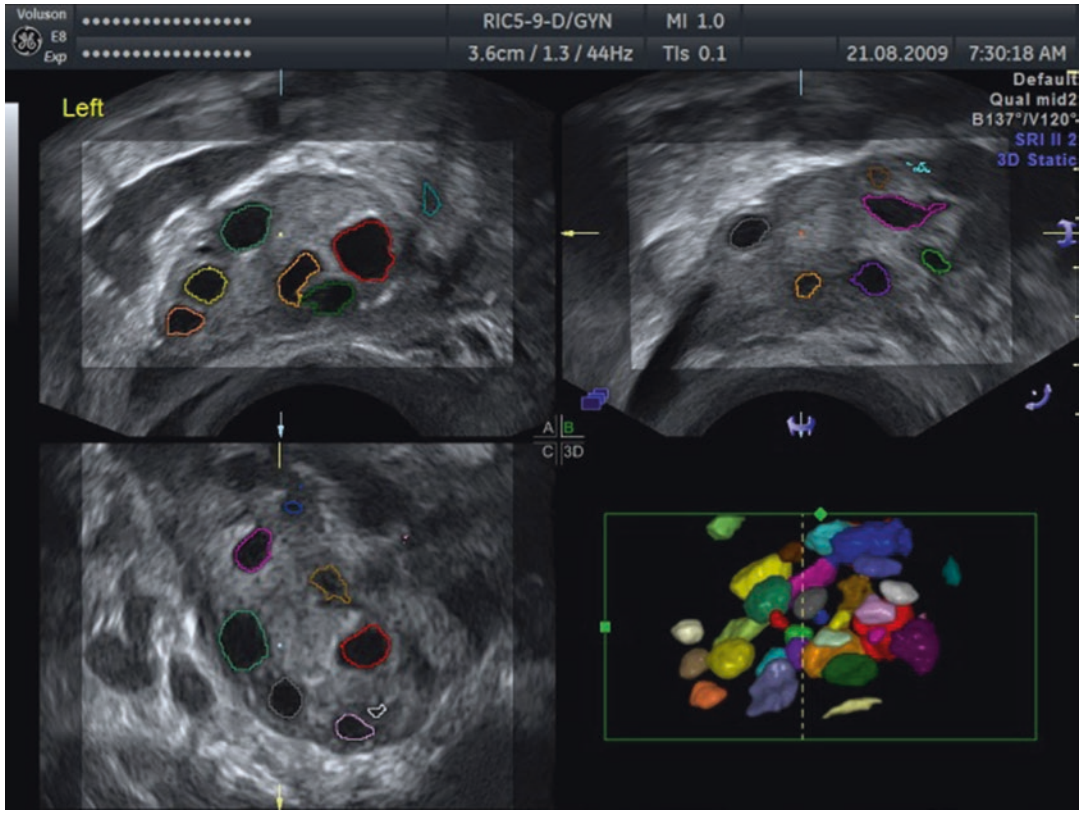

Fig. 2.10 Antral follicle count performed by 3D US SonoAVC. Automatically identified antral follicles by E8 Voluson in combination with SonoAVC software. Follicle boundaries are marked by different colors. Lower right: color-encoded three-dimensional reconstruction of follicles enables the accurate determination of the number of follicles

ine malformations. While 2D US provides only information through axial and sagittal planes, it is limited by accessibility to assess pathologies in the coronal (*y*) plane.

Thus, 3D US enables, for example, the detailed and accurate calculation of length and thickness of a diagnosed septum, which in turn provides important information for future therapy in order to be in a position to decide whether or not surgery would be recommended. Three-dimensional US allows for the calculation of uterine cavity volume and vascularization which might influence fertility prognosis [64]. Although not explicitly recommended, the European Society of Human Reproduction and Embryology (ESHRE) emphasized however the role of 3D US in the detection of uterine malformations in their recent guideline on recurrent pregnancy loss [65].

Moreover, 3D US plays also a pivotal role in the analysis of acquired uterine anomalies. Although hysteroscopy is undoubtedly still the gold standard in the diagnosis of Asherman's syndrome, 3D US may be the best first-line tool for the diagnosis of this pathology. Three-dimensional US is considered to be highly accurate in the depiction of adhesion and extent of cavity damage in Asherman patients, while, e.g., HSG often runs the risk of overestimating the severity of the disease compared to 3D US, a fact which is attributable to decreased clarity [66].

Some studies also suggest that 3D US guarantees high detection accuracy with respect to the site and position of adenomyosis in the uterine wall [67, 68]. It seems that this technique is also superior to the 2D technique, since 3D US allows a detailed visualization of the endo-myometrial junctional zone [68, 69].

While 3D US brings no advantage regarding the detection of fibroids and polyps, 3D US might be more accurate in the determination of their

specific locations. Especially when it comes to leiomyomas, 3D US might be helpful to identify their borders, thus differentiating between submucosal and intramural forms [63]. The application of 3D power Doppler could here provide additional supporting information about collateral vessels and can help the clinician make a decision as to whether or not consider embolization.

Furthermore, 3D US allows a precise estimation of endometrial morphology and volume with an excellent inter-observer and intra-observer reliability [70]. Endometrial thickness and subendometrial vascularity have been found to be predictive factors for IVF success. Nonoptimal endometrial build-up has a substantial impact on embryo implantation. In such cases, it might be recommended to opt for embryo cryopreservation, and a subsequent cryo-cycle might be recommended, in the hope that the endometrium built-up might be better [71].

Currently, most of the 3D US studies conducted in the course of an IVF therapy investigates the use of 3D US for follicle monitoring during controlled ovarian stimulation (COS). Meanwhile, this has become a wide-ranging topic, to which a separate chapter is devoted. Nevertheless, we should take this opportunity to mention some key points of 3D US. The US-based assessment of the size and volume of growing follicles has become an integral part in ART. The follicular growth rate depends on the ovarian response (which might be patient-specific), the stimulation protocol (mainly GnRH agonist long/short and GnRH antagonist) used, and the applied stimulation scheme (step-up/step-down). There is no doubt that oocyte maturity is linked with follicle size. However, it is worth mentioning that COS leads to the development of very heterogeneous cohorts of follicles at different sizes. In the early days of ART, the administration of the trigger for final oocyte maturation was based on E2 rise [72]. However, COS without US-based follicle monitoring and triggering is nowadays inconceivable in any fertility clinic. Accurate US monitoring is required for dose adjustment during stimulation (COS). At the same time, accurate monitoring is most critical for predicting oocyte competence and represents the best way to accurately time the trigger shot to induce final oocyte maturation in order to achieve the largest possible number of mature (MII) oocytes.

The aim of an IVF therapy should be to ensure the birth of a healthy child – if possible with as few stimulations cycles as possible in order to limit the inconveniences that might result from COS. This in turn means that a maximum number of mature and competent oocytes should be yielded during a COS cycle. The irregular growth of follicles, however, gives rise to some important questions: (1) when is the best moment to trigger final oocyte maturation; (2) what is the outcome with the smallest and the largest follicle pool; and (3) does it make sense to puncture the small follicle pool as this is a more elaborate process. Additionally, keeping in mind that an extended stimulation might rather result in follicular atresia than in a gain of surplus mature oocytes, it is of crucial importance to define the optimal timeframe for triggering. It almost goes without saying that a kind of standardization is needed in follicle monitoring and the provision of US instruments with a high accuracy.

To date, 2D US technique has been mostly used for follicle monitoring in COS cycles. With 2D TVUS only the two longest diameters of each growing follicle are measured, and the mean follicle diameter is calculated. The problem is that preconditions and course of COS differ completely from those of a natural cycle. Two-dimensional US accurately reflects the follicle volume if they have an almost round shape. In COS, however, in the presence of multifollicular growth, the follicles almost never exhibit such a spherical shape but rather an ellipsoid form. Thus, follicular size and volume may be underestimated for small follicles and often overestimated for the larger ones. In the past there were in fact controversial publications in regard to the outcome of different follicle pools and in recommendations when to trigger [73]. Besides different stimulation protocols, workflows, and different endpoints analyzed, one of the main reasons for discrepancies reported may be found in the lower accuracy in terms of determining the true follicular volume with 2D US systems since they neglect the third follicular diameter (*z*-diameter). In fact, several studies, for example, by Kyei-Mensah and colleagues, found discrep-

ancies in the follicular volume when comparing 2D and 3D US [74].

Although there are still some doubts, a large number of publications indicate that 3D US is more reliable than 2D US featuring a lower intra- and inter-observer variability [74–79].

To date, there is still no generally accepted consensus regarding the timing of the trigger shot for final oocyte maturation to yield the maximum possible number of mature and competent oocytes capable of being fertilized and resulting in good quality blastocysts after fertilization [73]. This issue along with the associated question which follicle cohort contains the most competent oocytes and whether smaller follicles are also worth to be punctured can only be solved using an accurate and reliable technique. Special user-friendly software solutions, such as automated volume count, SonoAVC (General Electric; GE), can identify follicles and automatically calculate their volumes and diameters in a rapid and reliable manner with easy application (Fig. 2.11). There is an urgent need for the implementation of the sophisticated 3D US instruments and the corresponding software in order to improve and personalize stimulation protocols and find a generally accepted consensus on the timing of the trigger shot.

Although there are currently some interesting approaches to evaluate follicular size in correlation to oocyte maturity and developmental competence, much more research is needed to bring light into this issue and to give recommendations on this issue [73–77, 80].

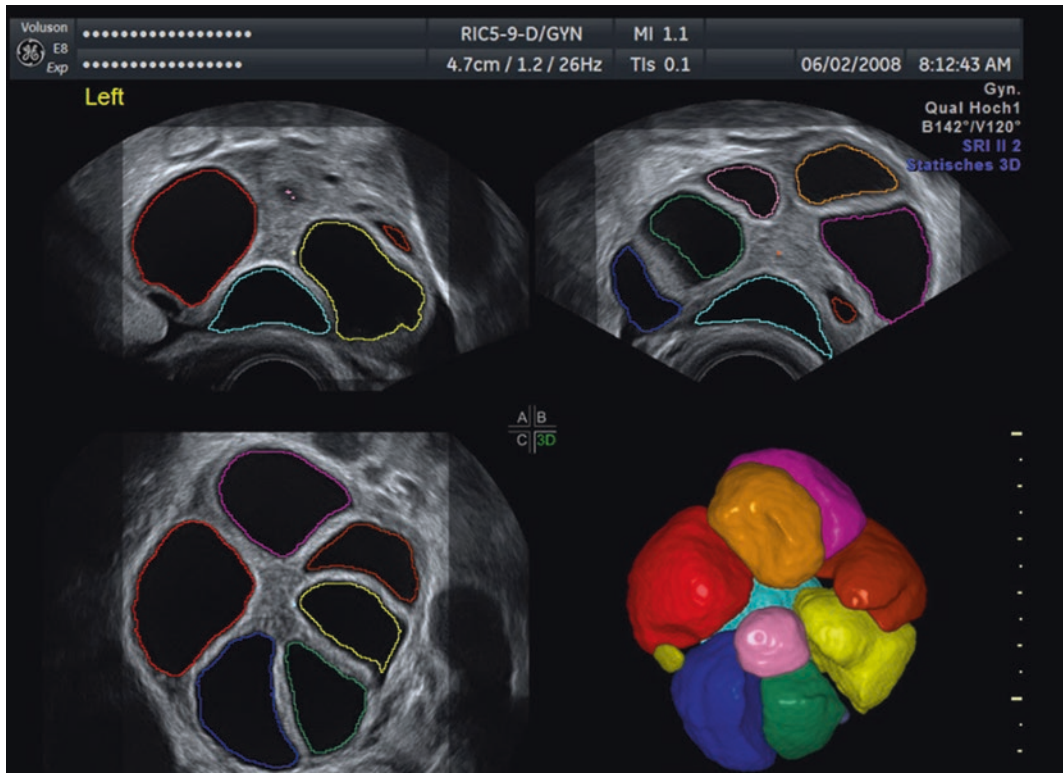

Fig. 2.11 Representation of a stimulated ovary generated via 3D TVUS scanning plus SonoAVC software 1 day before OPU. Follicle boundaries are marked by colors. Lower left: color-encoded three-dimensional reconstruction of follicles. Right: detailed SonoAVC report. Each colored line corresponds to a follicle. The lines are coded with the same colors as the corresponding follicles; dx, dy, and dz diameters; mean diameter; and volumes are automatically provided

Fig. 2.11 (continued)

Conclusions

Three-dimensional US opens up new clinical applications and facilitates many of the procedures originally performed with 2D US. Three-dimensional US offers some features not available with 2D US; this includes measurements in 3D space – including volume calculations – with high accuracy, even for non-regular shaped structures, display of an arbitrary section, and displaying a 3D image. Currently, in most fertility clinics, 3D US is not a diagnostic armamentarium, although it has become an indispensable tool in many specialty fields, such as prenatal diagnosis, neurology, or cardiology. However, we are witnessing a still growing interest in this stunning technique being implemented in many research settings within the scope of gynecology and reproductive medicine. Nowadays, within the scope of fertility therapy, 3D US has already become established as the preferred method for diagnosing uterine malformations. It may also play an increasingly important role in the near future when it comes to the accurate diagnosis of PCOS, in the assessment of ovarian reserve, and in estimating the risk of OHSS. Thus, 3D US will become one of the decision-making factors in choosing the optimal stimulation protocol and in monitoring follicular development, an area where 3D applications have the potential for optimizing the IVF process and setting benchmarks for standardization, i.e., in the process of COS.

When 3D US data is acquired, the information can be stored for documentation (which might be needed for future therapy planning and most important for legal reasons) or post-processing. It can be easily shared for an expert review, interdisciplinary consultation, teaching, and/or telemedicine. Additionally, data can be sent between IVF centers and the attending gynecologist,

which is most important for a patient-friendly therapy. Thereby, data can be transferred through a secured connection via a PACS server and virtual private network (VPN) tunneling, and the corresponding medical software allows seamless integration of all processes needed for an accurate and precise workflow [81].

Meanwhile, there are various post-processing modalities available. However, a lack of standardization, the time needed for post-processing, and operators who are often insufficiently trained are still obstacles to a broader application of 3D US and its use in a clinical setting. This last point is of particular importance, since the application of 3D techniques definitely needs extensive training and a learning curve [82]. There is a clear trend toward rapid increasing processing power, improved image quality, and more user-friendly instruments and software. However, manufactures should be encouraged to provide training modules and more user-friendly software for post-processing to allow a higher acceptance of 3D US techniques. Additionally, the implementation and usage of portable 3D US systems might possibly accelerate the application of 3D US. Thus, there is no doubt that new innovation will offer new application areas even within ART.

References

1. Ahirwar C. 3D/4D ultrasound equipment market to grow at a CAGR of 7.03% during the period 2017–2021. Red Newsire Global. Available from: https://www.rednewswire.com/global-3d-4d-ultrasound-equipment-market-to-grow-at-a-cagr-of-7-03-during-the-period-2017-2021/. Last Accessed on 18 May 2018.
2. Salomon LJ, Alfirevic Z, Bilardo CM, Chalouhi GE, Ghi T, Kagan KO, et al. SUOG practice guidelines: performance of first-trimester fetal ultrasound scan. Ultrasound Obstet Gynecol. 2013;41:102–13.
3. Curie P, Curie J. Dévelopment, par pression, de l'électricité polaire dans les cristaux hémièdres à faces inclinées. C R Hébd Séances Acad Sci. 1880;91:294–5.
4. Szabo TL, Lewin PA. Ultrasound transducer selection in clinical imaging practice. J Ultrasound Med. 2013;32:573–82.
5. Martin K, Ramnarine K. Physics. In: Hoskins PR, Martin K, Thrush A, editors. Diagnostic ultrasound: physics and equipment. 2nd ed. Cambridge, UK: Cambridge University Press; 2010.
6. Miller DL. Safety assurance in obstetrical ultrasound. Semin Ultrasound CT MR. 2008;29:156–64. Review.
7. Ultrasonic Systems. Radiology key. Available from: https://radiologykey.com/ultrasonic-systems/. Last Accessed on 30 May 2018.
8. Hua S, Yuchi M, Ding M. Computer Simulation for medical ultrasound c-mode imaging based on 2d array. Adv Mat Res. 2012;532(533):719–23. Available from: http://citeseerx.ist.psu.edu/viewdoc/download?doi=10.1.1.911.7989&rep=rep1&type=pdf. Last Accessed on 18 May 2018.
9. Merz E. 3D ultrasound in prenatal diagnosis. Curr Obstet Gynecol. 1999;9:93–100.
10. Doppler C. Ueber das farbige Licht der Doppelsterne und einiger anderer Gestirne des Himmels. Verlag der königl. böhm. Gesellschaft der Wissenschaften. 1903. Bd. 2, S. 465–482). Available from: http://digital.bib-bvb.de/view/bvbmets/viewer.0.6.2.jsp?folder_id=0&dvs=1528188779301~287&pid=5210835&locale=de&usePid1=true&usePid2=true#. Last Accessed on 30 May 2018.
11. Yamasato K, Zalud I. Three dimensional power Doppler of the placenta and its clinical applications. J Perinat Med. 2017;45:693–700. Review.
12. Gonçalves LF, Espinoza J, Kusanovic JP, Lee W, Nien JK, Santolaya-Forgas J, et al. Applications of 2-dimensional matrix array for 3- and 4-dimensional examination of the fetus: a pictorial essay. J Ultrasound Med. 2006;25:745–55.
13. Campbell S. A short history of sonography in obstetrics and gynaecology. Facts Views Vis Obgyn. 2013;5:213–29.
14. Prager RW, Ijaz UZ, Gee AH, Treece GM. Three-dimensional ultrasound imaging. Proceedings of the Institution of Mechanical Engineers, Part H: Journal of Engineering in Medicine. 2010;224:193–223.
15. Fenster A, Downey DB. 3-D ultrasound imaging: a review. IEEE Eng Med Biol Mag. 1996;15:41–51.
16. Zhang H, Banovac F, White A, Cleary K. Freehand 3D ultrasound calibration using an electromagnetically tracked needle. Available from: http://spie.org/Publications/Proceedings/Paper/10.1117/12.654906. Last Accessed on 20 May 2018.
17. Fenster A, Downey DB, Cardinal HN. Three-dimensional ultrasound imaging. Phys Med Biol. 2001;46:R67–99. Review.
18. Baba K. Development of 3D ultrasound. Donald Sch J Ultrasound Obstet Gynecol. 2010;4:205–15. Available from: https://www.dsjuog.com/doi/pdf/10.5005/jpjournals-10009-1144. Last Accessed on 02 May 2019.
19. De Jong-Pleij EA, Ribbert LS, Tromp E, Bilardo CM. Three-dimensional multiplanar ultrasound is a valuable tool in the study of the fetal profile in the second trimester of pregnancy. Ultrasound Obstet Gynecol. 2010;35:195–200.
20. Wong L, White N, Ramkrishna J, Araujo Júnior E, Meagher S, Costa Fda S. Three-dimensional imaging of the uterus: the value of the coronal plane. World J Radiol. 2015;7:484–93. Review.

21. Dietz HP, Shek KL. Tomographic ultrasound imaging of the pelvic floor: which levels matter most? Ultrasound Obstet Gynecol. 2009;33:698–703.
22. Ruano R. Recent advances in sonographic imaging of fetal thoracic structures. Expert Rev Med Devices. 2005;2:217–22. Review.
23. Jouannic JM, Rosenblatt J, Demaria F, Jacobs R, Aubry MC, Benifla JL. Contribution of three-dimensional volume contrast imaging to the sonographic assessment of the fetal uterus. Ultrasound Obstet Gynecol. 2005;26:567–70.
24. Principles of 3D Ultrasound. Radiology Key. Available from: https://radiologykey.com/principles-of-3d-ultrasound/. Last Accessed on 20 May 2018.
25. Alcázar JL. The use of three-dimensional ultrasound in gynecological patients. Donald Sch J Ultrasound Obstet Gynecol. 2008;2:10–6. Available from: https://pdfs.semanticscholar.org/8e47/f112875922a165e972af6f7d80df477046bb.pdf?_ga=2.166936311.817103330.1556788335-777804567.1540477073. Last Accessed on 02 May 2019.
26. Benacerraf BR. Inversion mode display of 3D sonography: applications in obstetric and gynecologic imaging. AJR Am J Roentgenol. 2006;187:965–71. Review.
27. Timor-Tritsch IE, Monteagudo A, Tsymbal T. Three-dimensional ultrasound inversion rendering technique facilitates the diagnosis of hydrosalpinx. J Clin Ultrasound. 2010;38:372–6.
28. Weber G, Merz E, Bahlmann F, Macchiella D. Ultrasound assessment of ovarian tumors–comparison between transvaginal 3D technique and conventional 2-dimensional vaginal ultrasonography. Ultraschall Med. 1997;18:26–30.
29. Campbell S. The potential diagnostic capabilities of three-dimensional surface rendering. Ultrasound Obstet Gynecol. 1999;14:148.
30. Turan S, Turan O, Baschat AA. Three- and four-dimensional fetal echocardiography. Fetal Diagn Ther. 2009;25:361–72. Review.
31. Adriaanse BM, Tromp CH, Simpson JM, Van Mieghem T, Kist WJ, Kuik DJ, et al. Interobserver agreement in detailed prenatal diagnosis of congenital heart disease by telemedicine using four-dimensional ultrasound with spatiotemporal image correlation. Ultrasound Obstet Gynecol. 2012;39:203–9.
32. Yeo L, Romero R, Jodicke C, Oggè G, Lee W, Kusanovic JP, et al. Four-chamber view and 'swing technique' (FAST) echo: a novel and simple algorithm to visualize standard fetal echocardiographic planes. Ultrasound Obstet Gynecol. 2011;37:423–31.
33. Merz E, Miric-Tesanic D, Welter C. Value of the electronic scalpel (cut mode) in the evaluation of the fetal face. Ultrasound Obstet Gynecol. 2000;16:564–8.
34. Powers J, Kremkau F. Medical ultrasound systems. Interface Focus. 2011;1:477–89.
35. Udupa JK. Three-dimensional visualization and analysis methodologies: a current perspective. Radiographics. 1999;19:783–806. Review.
36. Ong CL. The current status of three-dimensional ultrasonography in gynaecology. Ultrasonography. 2016;35:13–24. Review.
37. Zalud I, Rocha F. Artifacts, pitfalls and normal variants. Donald Sch J Ultrasound. 2012;6:1–8. Available from: https://www.dsjuog.com/doi/pdf/10.5005/jp-journals-10009-1221. Last Accessed on 02 May 2019.
38. Baba K, Satoh K. Development of a system for ultrasonic fetal three-dimensional reconstruction. Acta Obstet Gynaecol Jpn. 1986;38:1385.
39. Baba K, Satch K, Sakamoto S, Oka T, Shiego I. Development of an ultrasonic system for three-dimensional reconstruction of the fetus. J Perinat Med. 1989;17:19–24.
40. Von Ramm OT, Smith SW. Three-dimensional imaging system. 1987. United States Patent 4694434. Available from: http://www.freepatentsonline.com/4694434.html. Last accessed on 20 May 2018.
41. From Wired Frames to 3D. A short History of Kretztechnik AG, Zipf, Austria. Available from: http://www.ob-ultrasound.net/kretztechnik.html. Last accessed on 23 May 2018.
42. Lees W. Ultrasound imaging in three and four dimensions. Semin Ultrasound CT MR. 2001;22:85–105. Review.
43. Sohn C, Stolz W, Nuber B, Hesse A, Hornung B. Three-dimensional ultrasonic diagnosis in gynecology and obstetrics. Geburtshilfe Frauenheilkd. 1991;51:335–40.
44. Steiner H, Staudach A, Spitzer D, Graf AH, Wienerroither H. Does 3D sonography present new perspectives for gynecology and obstetrics? Geburtshilfe Frauenheilkd. 1993;53:779–82.
45. Steiner H, Spitzer D, Weiss-Wichert PH, Graf AH, Staudach A. Three-dimensional ultrasound in prenatal diagnosis of skeletal dysplasia. Prenat Diagn. 1995;15:373–7.
46. Bonilla-Musoles F, Raga F, Osborne NG, Blanes J. Use of three-dimensional ultrasonography for the study of normal and pathologic morphology of the human embryo and fetus: preliminary report. J Ultrasound Med. 1995;14:757–65.
47. Merz E, Pashaj S. Current role of 3D/4D sonography in obstetrics and gynecology. Donald School J Ultrasound Obstet Gynecol. 2013;7:400–8.
48. Woo J. A short History of the development of Ultrasound in Obstetrics and Gynecology. Available from: http://www.ob-ultrasound.net/isuog3dfocus.html. Last accessed on 23 May 2018.
49. Merton D. Diagnostic medical ultrasound technology: a brief historical review. J Diagn Med Sonography. 1997;13:10S–23S.
50. Brandl H, Gritzky A, Haizinger M. 3D ultrasound: a dedicated system. Eur Radiol. 1999;9:331–3. Review.
51. Grimbizis GF, Di Spiezio Sardo A, Saravelos SH, Gordts S, Exacoustos C, et al. The Thessaloniki

ESHRE/ESGE consensus on diagnosis of female genital anomalies. Hum Reprod. 2016;31:2–7.
52. Deb S, Campbell BK, Clewes JS, Raine-Fenning NJ. Quantitative analysis of antral follicle number and size: a comparison of two-dimensional and automated three-dimensional ultrasound techniques. Ultrasound Obstet Gynecol. 2010;35:354–60.
53. Coelho Neto MA, Ludwin A, Borrell A, Benacerraf B, Dewailly D, da Silva Costa F, et al. Counting ovarian antral follicles by ultrasound: a practical guide. Ultrasound Obstet Gynecol. 2018;51:10–20.
54. Nylander M, Frøssing S, Bjerre AH, Chabanova E, Clausen HV, Faber J, et al. Ovarian morphology in polycystic ovary syndrome: estimates from 2D and 3D ultrasound and magnetic resonance imaging and their correlation to anti-Müllerian hormone. Acta Radiol. 2017;58:997–1004.
55. Lam PM, Raine-Fenning N. The role of three-dimensional ultrasonography in polycystic ovary syndrome. Hum Reprod. 2006;21:2209–15.
56. Rotterdam ESHRE/ASRM-Sponsored PCOS consensus workshop group. Revised 2003 consensus on diagnostic criteria and long-term health risks related to polycystic ovary syndrome (PCOS). Hum Reprod. 2004;19:41–7.
57. Lam PM, Johnson IR, Raine-Fenning NJ. Three-dimensional ultrasound features of the polycystic ovary and the effect of different phenotypic expressions on these parameters. Hum Reprod. 2007;22:3116–23.
58. Alcázar JL, Jurado M. Three-dimensional ultrasound for assessing women with gynecological cancer: a systematic review. Gynecol Oncol. 2011;120:340–6.
59. Stachowiak G, Zając A, Pertynska-Marczewska M, Stetkiewicz T. 2D/3D ultrasonography for endometrial evaluation in a cohort of 118 postmenopausal women with abnormal uterine bleedings. Ginekol Pol. 2016;87:787–92.
60. Chan YY, Jayaprakasan K, Tan A, Thornton JG, Coomarasamy A, Raine-Fenning NJ. Reproductive outcomes in women with congenital uterine anomalies: a systematic review. Ultrasound Obstet Gynecol. 2011;38:371–82. Review.
61. Saravelos SH, Cocksedge KA, Li TC. Prevalence and diagnosis of congenital uterine anomalies in women with reproductive failure: a critical appraisal. Hum Reprod Update. 2008;14:415–29.
62. Hassan MA, Lavery SA, Trew GH. Congenital uterine anomalies and their impact on fertility. Womens Health (Lond). 2010;6:443–61. Review.
63. Turkgeldi E, Urman B, Ata B. Role of three-dimensional ultrasound in gynecology. J Obstet Gynaecol India. 2015;65:146–54. Review.
64. Bonilla-Musoles F, Martin N, Pepa Esquembre M, Caballero O. Uterine malformations: diagnosis with 3D/4D ultrasound. Donald School J Ultrasound Obstet Gynecol. 2015;9:123–48.
65. ESHRE Early Pregnancy Guideline Development Group. Recurrent pregnancy loss. Guideline of the European Society of Human Reproduction and Embryology, 2017. Available from: https://www.eshre.eu/Guidelines-and-Legal/Guidelines/Recurrent-pregnancy-loss.aspx. Last Accessed on 02 May 2019.
66. Kim MJ, Lee Y, Lee C, Chun S, Kim A, Kim HY, et al. Accuracy of three dimensional ultrasound and treatment outcomes of intrauterine adhesion in infertile women. Taiwan J Obstet Gynecol. 2015;54:737–41.
67. Luciano DE, Exacoustos C, Albrecht L, LaMonica R, Proffer A, Zupi E, et al. Three-dimensional ultrasound in diagnosis of adenomyosis: histologic correlation with ultrasound targeted biopsies of the uterus. J Minim Invasive Gynecol. 2013;20:803–10.
68. Exacoustos C, Brienza L, Di Giovanni A, Szabolcs B, Romanini ME, Zupi E, et al. Adenomyosis: three-dimensional sonographic findings of the junctional zone and correlation with histology. Ultrasound Obstet Gynecol. 2011;37:471–9.
69. Struble J, Reid S, Bedaiwy MA. Adenomyosis: a clinical review of a challenging gynecologic condition. J Minim Invasive Gynecol. 2016;23:164–85.
70. Yaman C, Sommergruber M, Ebner T, Pölz W, Moser M, Tews G. Reproducibility of transvaginal three-dimensional endometrial volume measurements during ovarian stimulation. Hum Reprod. 1999;14:2604–8.
71. Vanderzwalmen P, Zech NH, Ectors F, Stecher A, Lejeune B, Vanderzwalmen S, et al. Blastocyst transfer after aseptic vitrification of zygotes: an approach to overcome an impaired uterine environment. Reprod Biomed Online. 2012;25:591–9.
72. Quigley MM, Sokoloski JE, Richards SI. Timing human chorionic gonadotropin administration by days of estradiol rise. Fertil Steril. 1985;44:791–5.
73. Wirleitner B, Okhowat J, Vištejnová L, Králíčková M, Karlíková M, Vanderzwalmen P, et al. Relationship between follicular volume and oocyte competence, blastocyst development and live-birth rate: optimal follicle size for oocyte retrieval. Ultrasound Obstet Gynecol. 2018;51:118–25.
74. Kyei-Mensah A, Zaidi J, Pittrof R, Shaker A, Campbell S, Tan SL. Transvaginal three-dimensional ultrasound: accuracy of follicular volume measurements. Fertil Steril. 1996;65:371–6.
75. Hernández J, Rodríguez-Fuentes A, Puopolo M, Palumbo A. Follicular volume predicts oocyte maturity: a prospective cohort study using three-dimensional ultrasound and SonoAVC. Reprod Sci. 2016;23:1639–43.
76. Singh N, Usha BR, Malik N, Malhotra N, Pant S, Vanamail P. Three-dimensional sonography-based automated volume calculation (SonoAVC) versus two-dimensional manual follicular tracking in in vitro fertilization. Int J Gynaecol Obstet. 2015;13:166–9.
77. Vandekerckhove F, Bracke V, De Sutter P. The value of automated follicle volume measurements in IVF/ICSI. Front Surg. 2014;1:18. Review.
78. Murtinger M, Aburumieh A, Rubner P, Eichel V, Zech MH, Zech NH. Improved monitoring of ovarian stimulation using 3D transvaginal ultrasound plus

automated volume count. Reprod Biomed Online. 2009;19:695–9.
79. Revelli A, Martiny G, Delle Piane L, Benedetto C, Rinaudo P, Tur-Kaspa I. A critical review of bi-dimensional and three-dimensional ultrasound techniques to monitor follicle growth: do they help improving IVF outcome? Reprod Biol Endocrinol. 2014;12:107.
80. Martins WP, Vieira CV, Teixeira DM, Barbosa MA, Dassunção LA, Nastri CO. Ultrasound for monitoring controlled ovarian stimulation: a systematic review and meta-analysis of randomized controlled trials. Ultrasound Obstet Gynecol. 2014;43:25–33. Review.
81. Murtinger M, Zech MH, Spitzer D, Zech NH. Outpatient follicle monitoring: a plea for standardization in ultrasound based follicle monitoring and data transfer. J Reprod Infertil. 2014;15:105–8.
82. Rodriguez A, Guillén JJ, López MJ, Vassena R, Coll O, Vernaeve V. Learning curves in 3-dimensional sonographic follicle monitoring during controlled ovarian stimulation. J Ultrasound Med. 2014;33:649–55.

3 Two-Dimensional and Three-Dimensional Doppler in Reproductive Medicine

Ernest Hung Yu Ng

Introduction

In vitro fertilization-embryo transfer (IVF-ET) is an effective treatment for various causes of infertility and involves the development of multiple follicles, oocyte retrieval and embryo transfer after fertilization. Multiple embryos are still being replaced in order to compensate for their low implantation potential, which have remained steady at 30% for a long time. The development of multiple follicles in response to gonadotrophin stimulation is considered as the key factor leading to successful outcome. Successful implantation is dependent on interaction between a good quality embryo and a receptive endometrium.

Ultrasound examination is essential during IVF for predicting and monitoring the ovarian response to gonadotrophin, assessing the endometrium, guiding the transvaginal aspiration of oocytes and transferring embryos to the uterine cavity. Angiogenesis plays a critical role in various female reproductive processes such as the development of a dominant follicle, formation of a corpus luteum, growth of endometrium and implantation [1, 2]. This chapter covers the use of two dimensional (2D) and three dimensional (3D), in particular the role of endometrial and subendometrial blood flow determined by Doppler ultrasound in predicting the IVF success and the role of ovarian stromal blood flow determined by Doppler ultrasound in predicting ovarian response.

Endometrial Blood Flow

Ultrasound examination of the endometrium provides a noninvasive evaluation of the endometrium during IVF [3]. Ultrasound parameters of endometrial receptivity include endometrial thickness, endometrial pattern, endometrial volume and Doppler study of uterine arteries and the endometrium. Endometrial thickness and pattern have low positive predictive value and specificity for the IVF outcome [4, 5], whereas endometrial volume measured by 3D ultrasound is not predictive of pregnancy [6–9].

Assessment of endometrial blood flow adds a physiological dimension to the anatomical ultrasound parameters. A good blood flow towards the endometrium is usually considered as an essential requirement for successful implantation. Jinno et al. [10] measured endometrial tissue blood flow in infertile women by the intrauterine laser Doppler technique between days 4 and 6 of the luteal phase of a spontaneous cycle preceding IVF. The IVF pregnancy rate was significantly higher in women with endometrial tissue blood

E. H. Y. Ng (✉)
Department of Obstetrics and Gynaecology, The University of Hong Kong, Hong Kong, SAR, China
e-mail: nghye@hku.hk

L. A. Stadtmauer, I. Tur-Kaspa (eds.), *Ultrasound Imaging in Reproductive Medicine*,
https://doi.org/10.1007/978-3-030-16699-1_3

flow of at least 29 mL/min per 100 gm of tissue than in women with lower values (42% vs 15%, respectively, $P < 0.05$).

Endometrial blood flow starts from the radial artery, which divides after passing through the myometrial-endometrial junction to form the basal arteries that supply the basal portion of the endometrium and the spiral arteries that continue up towards the endometrium. Endometrial blood flow can be determined by colour and power Doppler ultrasound. Power Doppler imaging is more sensitive than colour Doppler imaging at detecting low velocity flow and hence improves the visualization of small vessels [11]. In combination with 3D ultrasound, power Doppler provides a unique tool with which to examine the blood flow of both endometrial and subendometrial regions.

Blood Flow of Uterine Vessels

Doppler study of uterine vessels reflecting downstream impedance to flow has been assumed to reflect the blood flow towards the endometrium. It is usually expressed as the pulsatility index (PI) and the resistance index (RI) (Fig. 3.1). PI is calculated as the peak systolic velocity (PSV) minus end-diastolic velocity divided by the mean, whereas RI is the ratio of PSV minus end-diastolic velocity divided by PSV.

Flow velocity waveforms are obtained from the ascending main branch of the uterine artery on the right and left side of the cervix in a longitudinal plane before it enters the uterus. The 'gate' of the Doppler is positioned when the vessel with good colour signals is identified on the screen. The PI and RI of the uterine arteries were calculated electronically when three similar, consecutive waveforms of good quality were obtained.

Good uterine blood flow as shown by low PI or RI is correlated with successful IVF outcomes [12, 13]. Steer et al. [12] classified PI measured on the day of ET as low, medium and high in the ranges of 0–1.99, 2.00–2.99 and ≥3.00, respectively, and reported a 35% implantation failure when PI was >3.0. Using a PI upper limit of 3.0 [12] or 3.3 [13], the uterine Doppler flow indices have a high negative predictive value and sensitivity (in the ranges of 88–100% and 96–100%, respectively) and a relatively higher range of positive predictive value and specificity (44–56% and 13–35%, respectively) when compared with endometrial thickness and pattern [5].

Uterine artery Doppler study may not reflect the actual blood flow to the endometrium as the major compartment of the uterus is the myometrium, and there is collateral circulation between uterine and ovarian vessels. I have shown that 2D Doppler study of uterine vessels is a poor reflection of subendometrial blood flow by 3D power Doppler in both stimulated and natural cycles as endometrial and subendometrial 3D Doppler flow indices were similar among patients with averaged uterine PI <2.0, 2.0–2.99 and ≥3.0 [14].

Endometrial and Subendometrial Blood Flow by 2D Doppler

Endometrial and subendometrial blood flow examined by colour (Table 3.1) and power Doppler (Table 3.2) were correlated with implantation or pregnancy rates of IVF. 2D Doppler flow indices of spiral arteries such as PI and PSV are not predictive of pregnancy [8, 15, 16], although Battaglia et al. [17] and Kupesic et al. [18] found significantly lower spiral artery PI in pregnant cycles than non-pregnant cycles.

Yang et al. [19] used a computer software to measure the area and intensity of colour signals present in the endometrium in a longitudinal axis, i.e. intraendometrial power Doppler area (EDPA). Significantly higher EDPA was found in pregnant cycles than non-pregnant cycles (8.8 mm^2 vs 5.8 mm^2, respectively). Patients with EDPA <5 mm^2 had significantly lower pregnancy rate (23.5% vs 47.5%; $P = 0.021$) and implantation rate (8.1% vs 20.2%; $P = 0.003$) than those with ≥5 mm^2. Contart et al. [20] graded endometrial blood flow by the visualization of power Doppler in the quadrants in the fundal region of the transverse plane but could not demonstrate any predictive value of such grading system.

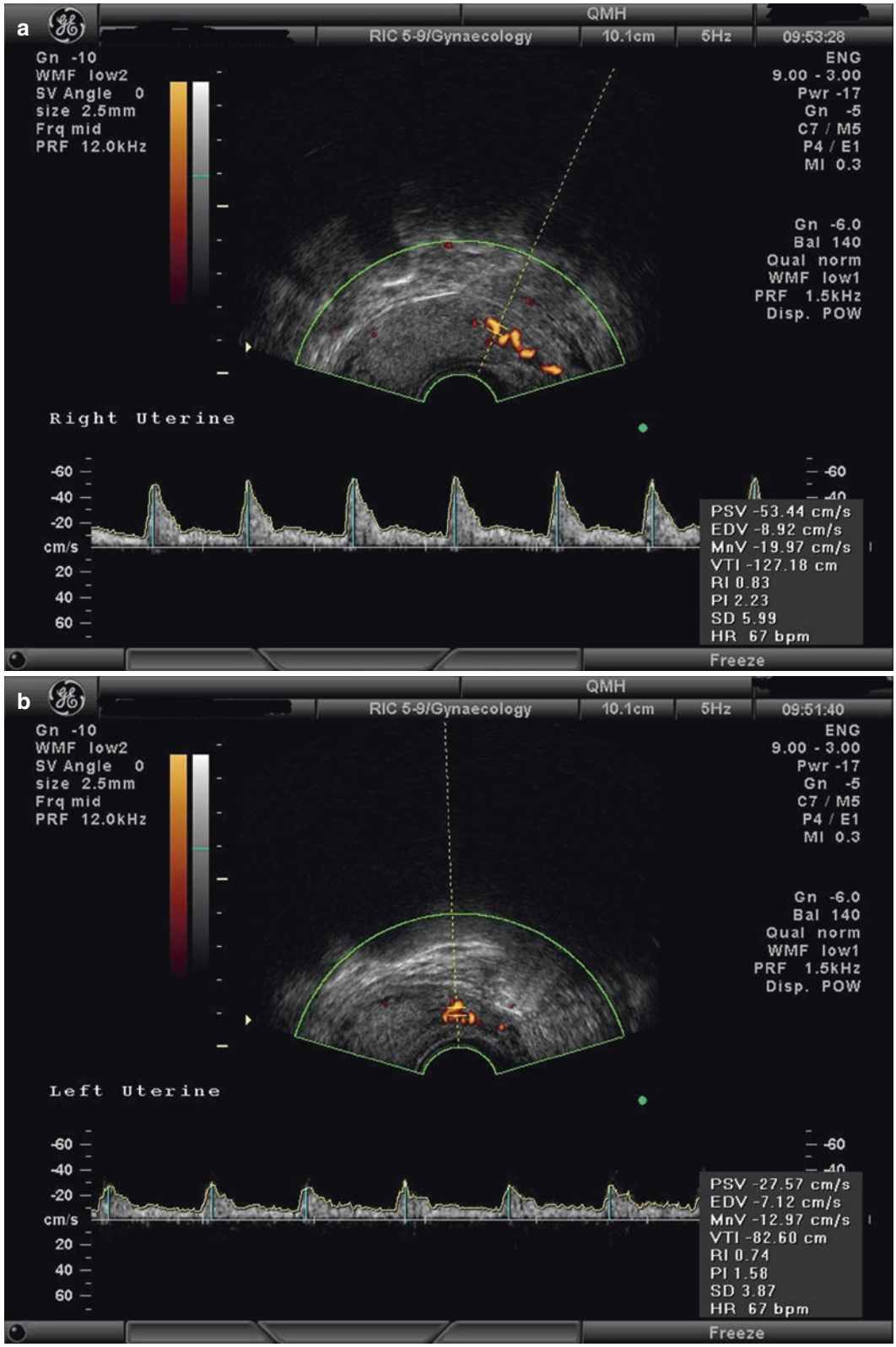

Fig. 3.1 (**a**, **b**) Uterine blood flow measured by 2D Doppler ultrasound

Table 3.1 Summary of studies of endometrial blood flow by 2D colour Doppler

Study	IVF cycles	USS parameters	USS day	Results
Zaidi et al. (1995) [15]	96 cycles using a long protocol	Spiral PI and PSV	hCG	No difference in subendometrial PI and PSV between pregnant and non-pregnant cycles
		Presence of endometrial and subendometrial flow		Absent subendometrial flow associated with no pregnancy
Battaglia et al. (1997) [17]	60 cycles	Uterine and spiral PI	OR	Uterine and spiral PI lower in pregnant than non-pregnant cycles
		Presence of endometrial blood flow		Absent subendometrial flow associated with no pregnancy
Chien et al. (2002) [21]	623 cycles using ultrashort and ultralong protocols	Uterine and spiral PI and RI	ET	Significantly lower implantation and pregnancy rates in patients without endometrial /subendometrial flow
		Presence of endometrial and subendometrial (<10 mm) blood flow		Presence of subendometrial flow 5.9 times to become pregnant than those with absent flow

USS ultrasound, *PI* pulsatility index, *PSV* peak systolic velocity, *OR* oocyte retrieval, *ET* embryo transfer

Table 3.2 Summary of studies of endometrial blood flow by 2D power Doppler

Study	IVF cycles	USS parameter	USS day	Results
Yang et al. (1999) [19]	95 cycles using long and short protocols	Intraendometrial power Doppler area (EDPA) $<5\ mm^2$; $\geq 5\ mm^2$	OR	Higher EDPA in pregnant cycles
	Endometrium ≥10 mm			Lower implantation and pregnancy rates when EDPA $<5\ mm^2$
Yuval et al. (1999) [16]	156 cycles using a long protocol	PI and RI	OR and ET	No difference in any USS parameters between pregnant and non-pregnant cycles
Contart et al. (2000) [20]	185 cycles using a long protocol	Fundal region along transverse plan Grades I, II, III and IV according to visualization of power Doppler in the quadrants	hCG	Implantation and pregnancy rates similar in all grades of endometrial vascularity
Schild et al. (2001) [26]	135 cycles using a long protocol; first cycle only	PI and PSV of vessels in endometrium and subendometrial area (<5 mm)	OR	No difference in spiral artery PI and PSV between pregnant and non-pregnant cycles
				Non-detectable spiral blood flow was not associated with a lower implantation rate
Maugey-Laulom et al. (2002) [22]	144 cycles using a long protocol	Presence of endometrial and subendometrial blood flow	ET	Absent endometrial and subendometrial flow associated with a lower pregnancy rate

USS ultrasound, *PI* pulsatility index, *PSV* peak systolic velocity, *OR* oocyte retrieval, *ET* embryo transfer

The presence of endometrial and subendometrial blood flow can be identified easily in 2D Doppler ultrasound. Absent endometrial and subendometrial blood flow has been shown to be associated with no pregnancy [15, 17] or a significantly lower pregnancy rate [21, 22].

Endometrial and Subendometrial Blood Flow by 3D Doppler

3D power Doppler ultrasound with the aid of the VOCAL® (virtual organ computer-aided analysis) imaging program for the 3D power Doppler

histogram has been used to measure endometrial volume and indices of blood flow within the endometrium (Fig. 3.2). Vascularization index (VI), which measures the ratio of the number of colour voxels to the number of all the voxels, is thought to represent the presence of blood vessels (vascularity) in the endometrium, and this was expressed as a percentage (%) of the endometrial volume. Flow index (FI), the mean power Doppler signal intensity inside the endometrium, is thought to express the average intensity of flow. Vascularization flow index (VFI) is a combination of vascularity and flow intensity [23].

The subendometrium can be examined through the application of 'shell-imaging' which allows the user to generate a variable contour that parallels the originally defined surface contour. The VI, FI and VFI of the subendometrial region are obtained accordingly (Fig. 3.3). The intra-observer and interobserver reliability of endometrial and subendometrial blood flow by 3D power Doppler have been confirmed to be high with all measurements obtaining an intra-class correlation of above 0.9 [24, 25].

Studies addressing the role of endometrial and subendometrial blood flow measured by 3D Doppler in IVF treatment are summarised in Table 3.3. Schild et al. [26] measured the subendometrial blood flow after pituitary downregulation but prior to ovarian stimulation and showed that subendometrial VI, FI and VFI were significantly lower in pregnant cycles than non-pregnant ones. Logistic regression analysis found that the subendometrial FI was the strongest predictive factor for the pregnancy outcome among other 3D Doppler flow indices.

Kupesic et al. [18] performed 3D ultrasound examination on the day of blastocyst transfer and found that subendometrial FI was significantly higher in pregnant cycles. Subendometrial VI and VFI were similar between pregnant and non-pregnant patients. Wu et al. [27] measured subendometrial blood flow on the day of hCG and demonstrated that subendometrial VFI was significantly higher in the pregnant group. Subendometrial VI and FI were also similar between pregnant and non-pregnant cycles. Subendometrial VFI was superior to subendometrial VI, subendometrial FI and endometrial volume in predicting the successful outcome in the receiver operating characteristics (ROC) curve analysis.

On the day of oocyte retrieval, Dorn et al. [28] compared the subendometrial blood flow before and after an intravenous administration of Levovist, which is a contrast agent and consists of 99.9% of D-galactose. All subendometrial 3D Doppler flow indices after the administration of the contrast agent were significantly higher than those without the contrast agent. However, all subendometrial 3D Doppler flow indices with and without the contrast agent were comparable between pregnant and non-pregnant cycles. The results of this study suggested that the use of 3D power Doppler ultrasound under a contrast agent during IVF treatment provided no additional advantage over the conventional 3D power Doppler ultrasound examination.

Järvelä et al. [29] determined endometrial and subendometrial VI after gonadotrophin stimulation but before hCG administration and again the day of oocyte retrieval. There were no differences between the pregnant and non-pregnant groups in endometrial and subendometrial VI on either day examined. I have published the largest study involving 451 transfer cycles [30]. Patients in the pregnant group had significantly lower uterine RI, endometrial VI and VFI than those in the non-pregnant group. Endometrial thickness, endometrial volume, endometrial pattern, uterine PI, endometrial FI and subendometrial VI, FI and VFI were similar between the non-pregnant and pregnant groups. The number of embryos replaced and endometrial VI were the only two predictive factors for pregnancy in a logistic multiple regression analysis. ROC curve analysis revealed that the area under the curve was around 0.5 for all ultrasound parameters for endometrial receptivity.

Implantation and pregnancy rates were comparable for patients with and without endometrial and subendometrial blood flow [30]. This finding is contradictory to those obtained by 2D Doppler ultrasound, which suggested that absent endometrial and subendometrial blood flows were associated with no pregnancy [15, 17] or much reduced pregnancy rate [21, 22].

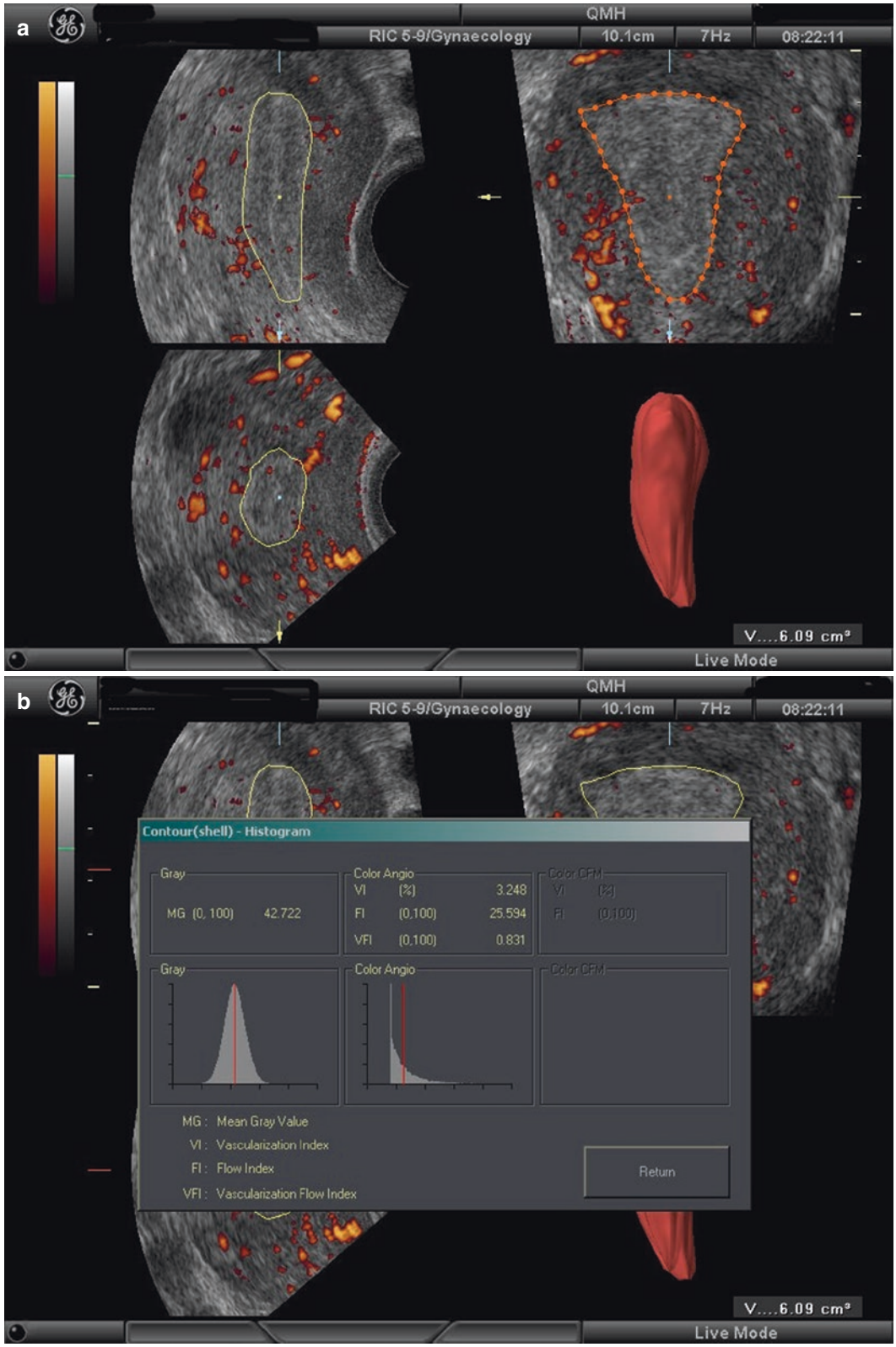

Fig. 3.2 (**a**, **b**) Endometrial volume and blood flow measured by 3D Doppler ultrasound

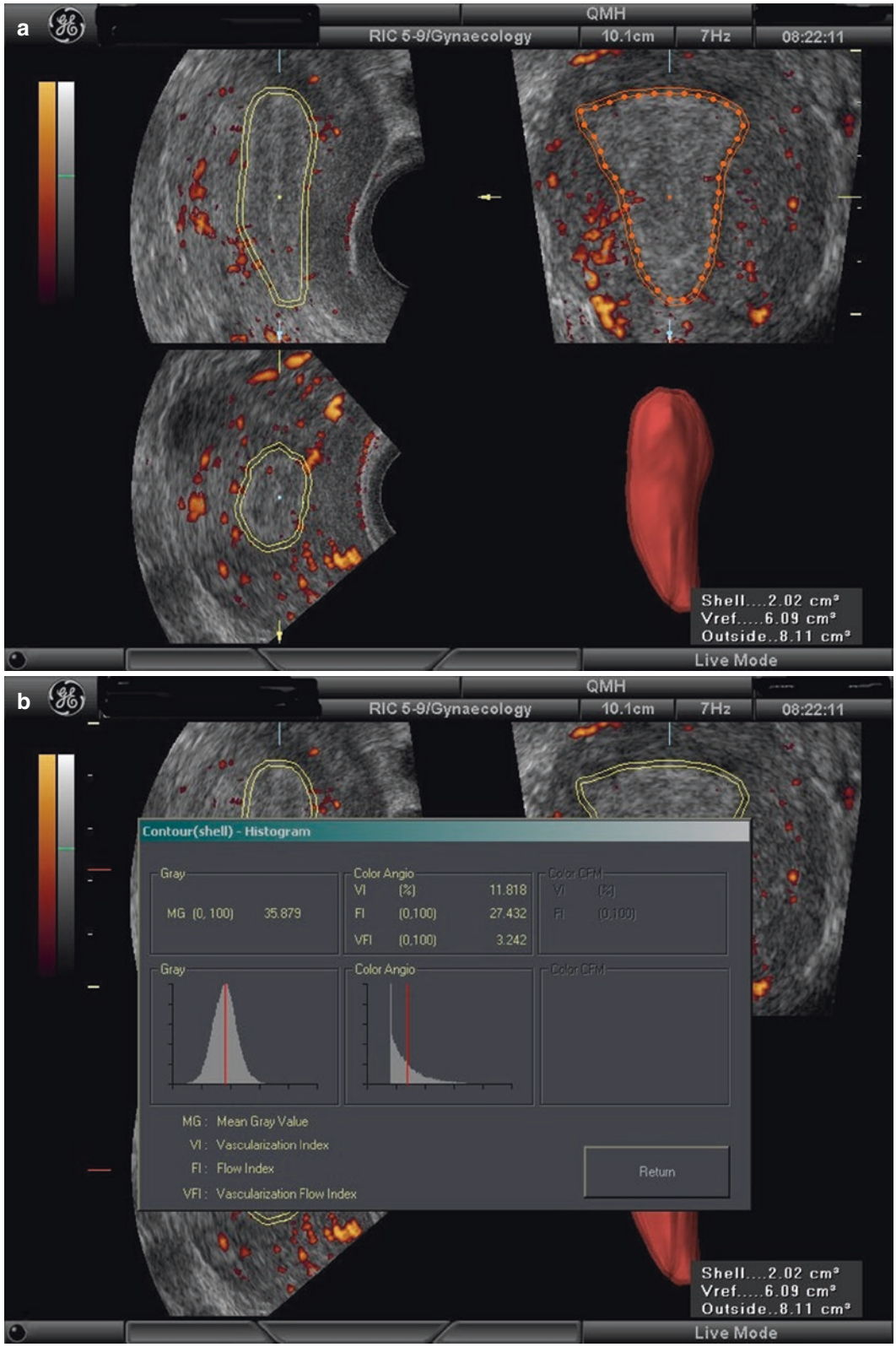

Fig. 3.3 (**a**, **b**) Subendometrial volume and blood flow measured by 3D Doppler ultrasound

Table 3.3 Summary of studies of endometrial and subendometrial blood flow by 3D power Doppler ultrasound

Study	IVF cycles	Inclusion/exclusion criteria	USS day	Results
Schild et al. (2000) [26]	75 cycles using a long protocol ET 2 days after TUGOR	Inclusion criteria Downregulation confirmed (endometrium <5 mm; no ovarian cyst of >2.5 cm; serum oestradiol <60 pg/ml)	Before stimulation	Subendometrial VI, FI and VFI lower in pregnant than non-pregnant cycles Subendometrial FI is the strongest predictive factor for IVF in logistic regression analysis
Kupesic et al. (2001) [18]	89 cycles using a long protocol Blastocyst transfer 5 days after TUGOR	Inclusion criteria Serum FSH < 10 IU/L No fibroid, ovarian cysts and ovarian endometriosis	ET (hCG +7)	Higher subendometrial FI in pregnant cycles
Wu et al. (2003) [27]	54 cycles; first cycles only (details of ovarian stimulation and ET not given)	Inclusion criteria Age < 38 years Normal uterine cavity Serum FSH <15 IU/L ≥2 good quality embryos	hCG	Subendometrial VFI higher in pregnant cycles
Dorn et al. (2004) [28]	42 cycles using a long protocol	Exclusion criteria Polycystic ovary syndrome Endometrium <6 mm Gynaecological surgery	OR	No difference in subendometrial VI, FI and VFI between pregnant and non-pregnant cycles
Järvelä et al. (2005) [29]	35 cycles using a long protocol ET 2 days after TUGOR	Exclusion criteria Uterine fibroids Endometriosis Single ovary Previous operation on the uterus or salpingectomy	After stimulation and OR	No difference in endometrial and subendometrial VI between pregnant and non-pregnant cycles on both days
Ng et al. (2006) [30]	451 cycles using a long protocol; first cycle only ET 2 days after TUGOR	Inclusion criteria Normal uterine cavity on scanning	OR	Endometrial VI and VFI lower in pregnant cycles
Ng et al. (2006) [33]	193 cycles Frozen-thawed embryo transfer cycles	Inclusion criteria Normal uterine cavity	LH + 1	No difference in endometrial and subendometrial 3D Doppler flow indices between pregnant and non-pregnant cycles
Mercè et al. (2008) [35]	80 cycles using a long protocol	Inclusion criteria First cycle Normal uterine cavity Serum FSH <10 IU/L Regular cycles Non-smokers	hCG	Higher endometrial VI, FI and VFI in pregnant cycles
Ng et al. (2009) [40]	293 cycles using a long protocol ET 2 days after OR	Inclusion criteria First cycle Normal uterine cavity	OR and ET	No difference in endometrial and subendometrial 3D Doppler flow indices on the 2 days and changes in these indices between pregnant and non-pregnant cycles

USS ultrasound, *VI* vascularization index, *FI* flow index, *VFI* vascularization flow index, *OR* oocyte retrieval, *ET* embryo transfer

The age of women, their smoking habits, their types of infertility and parity and causes of subfertility had no effect on all endometrial and subendometrial 3D Doppler flow indices [31]. Endometrial blood flow was negatively affected by serum oestradiol concentration on the day of hCG. Indeed, endometrial and subendometrial 3D Doppler flow indices in the stimulated cycles were significantly lower than those in the natural cycles of the same patients undergoing IVF treatment [32].

Uterine PI, uterine RI and endometrial and subendometrial 3D Doppler flow indices were comparable between the non-pregnant and pregnant groups in frozen-thawed embryo transfer cycles using natural or clomiphene-induced cycles [33]. On the other hand, endometrial and subendometrial blood flow was significantly higher in pregnant patients with livebirth following IVF and frozen-thawed embryo transfer treatment [34].

Mercè et al. [35] found that endometrial 3D power Doppler flow indices were statistically significantly higher in the pregnant group. The area under ROC curve was statistically significant for endometrial VI, FI and VFI when no grade 1 embryos or only one was transferred but not when two or three grade 1 embryos were transferred.

The pregnancy outcomes of women who had 3D power Doppler study of the endometrial and subendometrial regions on the day of oocyte retrieval in stimulated IVF cycles or on luteinizing hormone surge +1 day in frozen-thawed embryo transfer cycles were compared. Women in the pregnancy-induced hypertension (PIH) or small for gestational age (SGA) foetuses group had significantly lower endometrial VI (0.504 vs 1.051; $P = 0.023$) and VFI (0.121 vs 0.253; $P = 0.023$) than those in the non-PIH/SGA group [36]. The endometrial blood flow may have an impact on the placental development when pregnant and gives insight into a potential novel screening tool for assessing the risk of PIH or SGA in women undergoing IVF.

Changes in Endometrial and Subendometrial Blood Flow

Ultrasound examination was performed on the day of hCG [27, 35], oocyte retrieval [28–30] and blastocyst transfer [18]. There is no consensus when the ultrasound examination for assessing endometrial receptivity in IVF treatment should be done. The day of the ultrasound examination in these studies was chosen for logistic reasons.

Raine-Fenning et al. [37] showed that endometrial and subendometrial blood flow by 3D ultrasound increased during the proliferative phase, peaking around 3 days prior to ovulation before decreasing to a nadir 5 days post-ovulation. Hypoxia in the endometrium plays a beneficial role for implantation as the expression of vascular endothelial growth factor is upregulated by hypoxia [38], and relatively low oxygen tension was present around the blastocyst during the time of implantation [39].

Endometrial and subendometrial blood flow was measured on the days of hCG and ET [40]. Patients in non-pregnant and pregnant groups had comparable 3D Doppler flow indices of endometrial and subendometrial regions measured on either day. Percentage changes in endometrial and subendometrial 3D Doppler flow indices between these 2 days were also similar. Again, none of the ultrasound parameters was predictive of pregnancy in a multiple logistic regression analysis and the ROC curve analysis.

Prediction of Ovarian Response to Gonadotrophin

The development of multiple follicles in response to ovarian stimulation is the key factor leading to a successful outcome of IVF treatment. Poor ovarian response is associated with lower pregnancy rates, while exaggerated ovarian response leads to an increased risk of ovarian hyperstimulation syndrome. Prediction of ovarian responses prior to gonadotrophin stimulation is useful in counselling patients and helpful in tailoring the dosage of gonadotrophin to individual patients.

A number of ultrasound parameters have been examined to predict the ovarian response to gonadotrophins, including ovarian volume, antral follicle count (AFC) and ovarian stromal blood flow [15, 41–44].

Folliculogenesis in the human ovary is a complex process regulated by a variety of endocrine and paracrine signals [45]. It has been suggested that the availability of an adequate vascular supply to provide endocrine and paracrine signals may play a key role in the regulation of follicle growth [46]. Increased ovarian stromal blood flow may lead to a greater delivery of gonadotrophins to the granulosa cells of the developing follicles.

Ovarian Stromal Blood Flow by 2D Doppler

Ovarian stromal blood flow can be assessed by colour Doppler and power Doppler ultrasound. Power Doppler is better suited to the study of the ovarian stromal blood flow as it is more sensitive to lower velocities and essentially angle-independent [11, 47]. Flow velocity waveforms were obtained from stromal blood vessels away from the ovarian capsule, if present. The 'gate' of the Doppler was positioned when the vessel with good colour signals was identified on the screen. PI, RI and peak systolic blood flow velocity (PSV) of stromal vessels were calculated electronically when three similar, consecutive waveforms of good quality were obtained.

Zaidi et al. [48] showed that mean ovarian stromal PSV prior to pituitary downregulation was significantly correlated with the number of follicles, after controlling for patients' age. Patients with >6 follicles at retrieval had significantly higher velocity than those with <6 follicles (10.2 ± 5.8 cm/s vs 5.2 ± 4.2 cm/s). Similarly, Engmann et al. [41] demonstrated that ovarian stromal PSV after pituitary downregulation was the most important independent predictor of the number of oocytes obtained in patients with normal basal FSH concentration, when compared with age of women, basal FSH concentration, E2 concentration or FSH/LH ratio. Bassil et al. [49] reported that women with RI of ovarian blood flow >0.56 had a significantly longer stimulation and a significantly lower mean number of oocytes retrieved. Both BMI and AFC were not included in these three studies.

Popovic-Todorovic et al. [44] evaluated ovarian stromal blood by 2D power Doppler ultrasound, and a semi-quantitative score was allocated to each ovary according to the number and area of the power Doppler signals. Total Doppler score was the sum of scores for each ovary: score 1 for poor flow, score 2 for moderate flow and score 3 for good flow. The number of oocytes was predicted by AFC, total Doppler score, serum testosterone concentration and smoking status.

In a prospective study, 136 women aged <40 years with basal FSH concentration <10 IU/L received a standard regimen of ovarian stimulation in their first IVF cycle [50]. The ovarian stromal blood flow measured by 2D power Doppler was compared to age of women, body mass index, basal FSH concentration and AFC in the prediction of the ovarian response. Basal FSH concentration achieved the best predictive value in relation to the number of oocytes obtained, followed by AFC and BMI. AFC was the only predictive factor of serum oestradiol concentration on the day of HCG, while BMI was predictive of the gonadotrophin dosage. Ovarian stromal blood flow indices measured by power Doppler ultrasound had no predictive value for the ovarian response.

Ovarian Stromal Blood Flow by 3D Doppler

I further evaluated the role of ovarian stromal blood flow by 3D power Doppler. Age of women, BMI, basal FSH concentration, AFC and ovarian stromal vascularity indices measured by 3D power Doppler were compared in 111 women aged <40 years old with basal FSH concentration <10 IU/L in their first IVF cycle [51]. The results indicated that AFC achieved the best predictive value in relation to the number of oocytes obtained, followed by age of women and BMI. Basal FSH concentration was the only predictive factor for the duration and dosage of gonadotrophin used. Mean ovarian 3D power Doppler flow indices were not predictive of pregnancy in a multiple logistic regression analysis.

Therefore, ovarian stromal blood flow measured after pituitary downregulation by both 2D and 3D power Doppler was not predictive of the ovarian response in terms of the number of oocytes obtained, the duration and dose of FSH used and maximum serum E2 concentrations. These results were in line with those of previous studies assessing ovarian stromal blood flow in fertile Chinese women [52, 53]. There was no effect of age on mean PSV of ovarian stromal blood vessels determined by 2D colour Doppler

ultrasound. Using 3D Doppler ultrasound, ovarian stromal vascularity was significantly lower in fertile Chinese women aged ≥41 years, and the rate of decline of total ovarian vascularity index was only 0.18% per year [53]. These data strongly suggest that reduction in ovarian stromal blood flow with increasing age is a relatively late phenomenon and ovarian stromal blood flow is unlikely an early marker for ovarian response.

Conclusion

Ultrasound examination is a noninvasive method to evaluate the endometrium during IVF. Doppler flow of uterine vessels measured by 2D ultrasound has a high negative predictive value and sensitivity (in the ranges of 88–100% and 96–100%, respectively) and a relatively higher range of positive predictive value and specificity (44–56% and 13–35%, respectively) when compared with endometrial thickness and pattern. Doppler study of uterine arteries measured by 2D ultrasound does not reflect the blood flow to the endometrium measured by 3D ultrasound with power Doppler. Conflicting results are reported with regard to their role in the prediction of pregnancy in IVF.

Furthermore, endometrial and subendometrial blood flow measured by 3D ultrasound on the days of hCG and embryo transfer and the percentage change in these parameters between these 2 days were not predictive of pregnancy in IVF. On the other hand, the endometrial blood flow may give insight into a potential novel screening tool for assessing the risk of pregnancy induced hypertension or small for gestational age in women undergoing IVF. Ovarian stromal blood flow measured by 2D and 3D power Doppler ultrasound had no predictive value for the ovarian response during IVF.

References

1. Abulafia O, Sherer DM. Angiogenesis of the ovary. Am J Obstet Gynecol. 2000;182:240–6.
2. Smith SK. Regulation of angiogenesis in the endometrium. Trends Endocrinol Metab. 2001;12:147–51.
3. Ng EHY, Ho PC. The role of ultrasound parameters in the prediction of pregnancy during in vitro fertilization treatment. Expert Rev Obstet Gynaecol. 2008;3:503–14.
4. Turnbull LW, Lesny P, Killick SR. Assessment of uterine receptivity prior to embryo transfer: a review of currently available imaging modalities. Hum Reprod Update. 1995;1:505–14.
5. Friedler S, Schenker JG, Herman A, Lewin A. The role of ultrasonography in the evaluation of endometrial receptivity following assisted reproductive treatments: a critical review. Hum Reprod Update. 1996;2:323–35.
6. Raga R, Bonilla-Musoles F, Casan EM, Klein O, Bonilla F. Assessment of endometrial volume by three-dimensional ultrasound prior to embryo transfer: clues to endometrial receptivity. Hum Reprod. 1999;14:2851–4.
7. Yaman C, Ebner T, Sommergruber M, Polz W, Tews G. Role of three-dimensional ultrasonographic measurement of endometrium volume as a predictor of pregnancy outcome in an IVF-ET program. A preliminary study. Fertil Steril. 2000;74:797–801.
8. Schild RL, Knoblock C, Dorn C, Fimmers R, van der Ven H, Hansmann M. Endometrial receptivity in an in vitro fertilization program as assessed by spiral artery blood flow, endometrial thickness, endometrial volume, and uterine artery blood flow. Fertil Steril. 2001;75:361–6.
9. Ng EHY, Yeung WSB, Ho PC. Endometrial and subendometrial vascularity significantly lower in patients with endometrial volume ≤2.5ml. Reprod Biomed Online. 2009;18:262–8.
10. Jinno M, Ozaki T, Iwashita M, Nakamura Y, Kudo A, Hirano H. Measurement of endometrial tissue blood flow: a novel way to assess uterine receptivity for implantation. Fertil Steril. 2001;76:1168–74.
11. Guerriero S, Ajossa S, Lai MP, Risalvato A, Paoletti AM, Melis GB. Clinical applications of colour Doppler energy imaging in the female reproductive tract and pregnancy. Hum Reprod Update. 1999;5:515–29.
12. Steer CV, Campbell S, Tan SL, Crayford T, Mills C, Mason BA, Collins WP. The use of transvaginal color flow imaging after in vitro fertilization to identify optimum uterine conditions before embryo transfer. Fertil Steril. 1992;57:372–6.
13. Coulam CB, Bustillo M, Soenksen DM, Britten S. Ultrasonographic predictors of implantation after assisted reproduction. Fertil Steril. 1994;62:1004–10.
14. Ng EHY, Chan CCW, Tang OS, Yeung WSB, Ho PC. Relationship between uterine blood flow and endometrial and subendometrial blood flow during stimulated and natural cycles. Fertil Steril. 2006;85:721–7.
15. Zaidi J, Campbell S, Pittrof FR, Tan SL. Endometrial thickness morphology, vascular penetration and velocimetry in predicting implantation in an IVF program. Ultrasound Obstet Gynecol. 1995;6:191–8.

16. Yuval Y, Lipitz S, Dor J, Achiron R. The relationship between endometrial thickness, and blood flow and pregnancy rates in in-vitro fertilization. Hum Reprod. 1999;14:1067–71.
17. Battaglia C, Artini PG, Giulini S, Salvatori M, Maxia N, Petraglia F, Volpe A. Colour Doppler changes and thromboxane production after ovarian stimulation with gonadotrophin-releasing hormone agonist. Hum Reprod. 1997;12:2477–82.
18. Kupesic S, Bekavac I, Bjelos D, Kurjak A. Assessment of endometrial receptivity by transvaginal color Doppler and three-dimensional power Doppler ultrasonography in patients undergoing in vitro fertilization procedures. J Ultrasound Med. 2001;20:125–34.
19. Yang JH, Wu MY, Chen CD, Jiang MC, Ho HN, Yang YS. Association of endometrial blood flow as determined by a modified colour Doppler technique with subsequent outcome of in-vitro fertilization. Hum Reprod. 1999;14:1606–10.
20. Contart P, Baruffi RL, Coelho J, Mauri AL, Petersen C, Franco Junior JG. Power Doppler endometrial evaluation as a method for the prognosis of embryo implantation in an ICSI program. J Assist Reprod Genet. 2000;17:329–34.
21. Chien LW, Au HK, Chen PL, Xiao J, Tseng CR. Assessment of uterine receptivity by the endometrial-subendometrial blood flow distribution pattern in women undergoing in vitro fertilization-embryo transfer. Fertil Steril. 2002;78:245–51.
22. Maugey-Laulon B, Commenges-Ducos M, Jullien V, Papaxanthos-Roche A, Scotet V, Commenges D. Endometrial vascularity and ongoing pregnancy after IVF. Eur J Obstet Gynecol Reprod Biol. 2002;104:137–43.
23. Pairleitner H, Steiner H, Hasenoehrl G, Staudach A. Three-dimensional power Doppler sonography: imaging and quantifying blood flow and vascularization. Ultrasound Obstet Gynecol. 1999;14:139–43.
24. Raine-Fenning NJ, Campbell BK, Clewes JS, Kendall NR, Johnson IR. The reliability of virtual organ computer-aided analysis (VOCAL) for the semiquantification of ovarian, endometrial and subendometrial perfusion. Ultrasound Obstet Gynecol. 2003;22:633–9.
25. Raine-Fenning NJ, Campbell BK, Clewes JS, Kendall NR, Johnson IR. The interobserver reliability of three-dimensional power Doppler data acquisition within the female pelvis. Ultrasound Obstet Gynecol. 2004;23:501–8.
26. Schild RL, Holthanus S, Alquen JD, Fimmers R, Dorn C, van der Ven H, Hansmann M. Quantitative assessment of subendometrial blood flow by three-dimensional-ultrasound is an important predictive factor of implantation in an in-vitro fertilization programme. Hum Reprod. 2000;15:89–94.
27. Wu HM, Chiang CH, Huang HY, Chao AS, Wang HS, Soong YK. Detection of the subendometrial vascularization flow index by three-dimensional ultrasound may be useful for predicting the pregnancy rate for patients undergoing in vitro fertilization-embryo transfer. Fertil Steril. 2003;79:507–11.
28. Dorn C, Reinsberg J, Willeke C, Wendt A, van der Ven H, Schild RL. Three-dimensional power Doppler ultrasound of the subendometrial blood flow under the administration of a contrast agent (Levovist). Arch Gynecol Obstet. 2004;270:94–8.
29. Järvelä IY, Sladkevicius P, Kelly S, Ojha K, Campbell S, Nargund G. Evaluation of endometrial receptivity during in-vitro fertilization using three-dimensional power Doppler ultrasound. Ultrasound Obstet Gynecol. 2005;26:765–9.
30. Ng EHY, Chan CCW, Tang OS, Yeung WSB, Ho PC. The role of endometrial and subendometrial blood flow measured by three-dimensional power Doppler ultrasound in the prediction of pregnancy during in vitro fertilization treatment. Hum Reprod. 2006;21:164–70.
31. Ng EHY, Chan CCW, Tang OS, Yeung WSB, Ho PC. Factors affecting endometrial and subendometrial blood flow measured by three-dimensional power Doppler ultrasound during in vitro fertilization treatment. Hum Reprod. 2006;21:1062–9.
32. Ng EHY, Chan CCW, Tang OS, Yeung WSB, Ho PC. Comparison of endometrial and subendometrial blood flow measured by three-dimensional power Doppler ultrasound between stimulated and natural cycles in the same patients. Hum Reprod. 2004;19:2385–90.
33. Ng EHY, Chan CCW, Tang OS, Yeung WSB, Ho PC. The role of endometrial and subendometrial vascularity measured by three-dimensional power Doppler ultrasound in the prediction of pregnancy during frozen-thawed embryo transfer cycles. Hum Reprod. 2006;21:1612–7.
34. Ng EHY, Chan CCW, Tang OS, Yeung WSB, Ho PC. Endometrial and subendometrial vascularity is higher in pregnant patients with live birth following ART than in those who suffer a miscarriage. Hum Reprod. 2007;22:134–1141.
35. Mercè LT, Barco MJ, Bau S, Troyano J. Are endometrial parameters by three-dimensional ultrasound and power Doppler angiography related to in vitro fertilization/embryo transfer outcome? Fertil Steril. 2008;1:111–7.
36. Lai CW, Yung SS, Ng EH. Endometrial vascularity is lower in pregnancies with pregnancy-induced hypertension or small-for-gestational age in live birth after IVF. Ultrasound Obstet Gynecol. 2014;44:455–60.
37. Raine-Fenning NJ, Campbell BK, Kendall NR, Clewes JS, Johnson IR. Quantifying the changes in endometrial vascularity throughout the normal menstrual cycle with three-dimensional power Doppler angiography. Hum Reprod. 2004;19:330–8.
38. Sharkey AM, Day K, McPherson A, Malik S, Licence D, Smith SK, Charnock-Jones DS. Vascular endothelial growth factor expression in human endometrium is regulated by hypoxia. J Clin Endocrinol Metab. 2000;85:402–9.

39. Graham CH, Postovit LM, Park H, Canning MT, Fitzpatrick TE. Adriana and Luisa Castellucci award lecture 1999: role of oxygen in the regulation of trophoblast gene expression and invasion. Placenta. 2000;21:443–50.
40. Ng EHY, Chan CCW, Tang OS, Yeung WSB, Ho PC. Changes in endometrial and subendometrial blood flows in IVF. Reprod Biomed Online. 2009;18:269–75.
41. Engmann L, Sladkevicius P, Agrawal R, Bekir JS, Campbell S, Tan SL. Value of ovarian stromal blood flow velocity measurement after pituitary suppression in the prediction of ovarian responsiveness and outcome of in vitro fertilization treatment. Fertil Steril. 1999;71:22–9.
42. Kupesic S, Kurjak A. Predictors of IVF outcome by three-dimensional ultrasound. Hum Reprod. 2002;17:950–5.
43. Kupesic S, Kurjak A, Bjelos D, Vujisic S. Three-dimensional ultrasonographic ovarian measurements and in vitro fertilization outcome are related to age. Fertil Steril. 2003;79:190–7.
44. Popovic-Todorovic B, Loft A, Lindhard A, Bangsboll S, Andersson AM, Andersen AN. A prospective study of predictive factors of ovarian response in 'standard' IVF/ICSI patients treated with recombinant FSH. A suggestion for a recombinant FSH dosage normogram. Hum Reprod. 2003;18:781–7.
45. McGee EA, Hsueh AJ. Initial and cyclic recruitment of ovarian follicles. Endocr Rev. 2000;21:200–14.
46. Redmer D, Reynolds L. Angiogenesis in the ovary. Rev Reprod. 1996;1:182–92.
47. Rubin JM, Bude RO, Carson PL, Bree RL, Adler RS. Power Doppler US: a potentially useful alternative to mean frequency-based color Doppler US. Radiology. 1994;190:853–6.
48. Zaidi J, Barber J, Kyei-mensah A, Bekir J, Campbell S, Tan SL. Relationship of ovarian stromal blood flow at the baseline ultrasound scan to subsequent follicular response in an in vitro fertilization program. Obstet Gynecol. 1996;88:779–84.
49. Bassil S, Wyns C, Toussaint-Demylle D, Nisolle M, Gordts S, Donnez J. The relationship between ovarian vascularity and the duration of stimulation in in-vitro fertilization. Hum Reprod. 1997;12:1240–5.
50. Ng EHY, Tang OS, Chan CCW, Ho PC. Ovarian stromal blood flow in the prediction of ovarian response during in vitro fertilization treatment. Hum Reprod. 2005;20:3147–51.
51. Ng EHY, Chan CCW, Tang OS, Ho PC. Ovarian stromal vascularity is not predictive of ovarian response and pregnancy. Reprod BioMed Online. 2006;12:43–9.
52. Ng EHY, Fong DYT, Yeung WSB, Ho PC. Effects of age on hormonal and ultrasound markers of ovarian reserve in Chinese women with proven fertility. Hum Reprod. 2003;18:2169–74.
53. Ng EHY, Chan CCW, Yeung WSB, Ho PC. Effect of age on ovarian stromal flow measured by three-dimensional ultrasound with power Doppler in Chinese women with proven fertility. Hum Reprod. 2004;19:2132–7.

Part III

Ultrasound of the Ovary

The Normal Ovary: Changes in the Menstrual Cycle

4

Renato Bauman and Ursula Res Muravec

Transabdominal Ultrasound

The ovaries can be displayed along with the uterine body in transverse plane if they are not too distant from the uterus. According to the position of the ovaries that in normal circumstances can be variable, there is a real possibility that both ovaries could not be seen on the scan in the same time/image. In this situation in order to detect the second ovary, the examiner should move the probe cranially or caudally. If the ovary is located more cranially and near the pelvic wall, there is a realistic possibility that this ovary could be covered by the intestine, and so it could not be visualized and examined. The same is the situation with small postmenopausal ovaries that due to the size often cannot be distinguished from the intestines.

Full bowel loops can be misdiagnosed as an ovary, but if the examiner is patient enough to wait the peristaltic wave, it will solve the problem; otherwise the examiner has to verify the position of the iliac vessels in order to longitudinally find the position of the ovary.

R. Bauman (✉)
Rotunda IVF, The National Fertility Centre,
The Rotunda Hospital, Dublin, Ireland

U. R. Muravec
Medical Center Dravlje, Department for Infertility,
Ljubljana, Slovenia

Transvaginal Ultrasound

Alfred Kratochwil is considered to be the father of transvaginal ultrasound. He described in 1969 his experience with the new endovaginal sonography technique using the probe attached to the colposcope [1]. Due to the low quality of the obtained images, the technique was abandoned until the mid-1980s when the first endovaginal probe with the visible angle of 240° that allowed panoramic view of the genital organs was put in market. The first meeting about endovaginal ultrasound was organized in Hamburg, Germany, in 1985, by L. Popp [2]. First accepted with skepticism, the new technique was quickly adopted in the majority of sonography centers, first in Germany and then all over the world. Because of numerous advantages in pelvic sonography, the endovaginal technique today is essential for quality examination of the female pelvis.

Ovaries can be visualized with the probe moved laterally of the uterus toward the pelvic wall in the longitudinal or sagittal section. Ovaries have ellipsoid shape, with relatively hypoechogenic structure and homogenic echotexture, and often are positioned near the iliac blood vessels (Fig. 4.1). Using probes with the wide angle of insonation, it is possible to visualize in the same frontal section of both ovaries if they are positioned in the same plane. Regularly each ovary is visualized separately. In order to compare the ovaries, it is useful to divide the image in two parts and then visualize both ovaries (Fig. 4.2).

L. A. Stadtmauer, I. Tur-Kaspa (eds.), *Ultrasound Imaging in Reproductive Medicine*,
https://doi.org/10.1007/978-3-030-16699-1_4

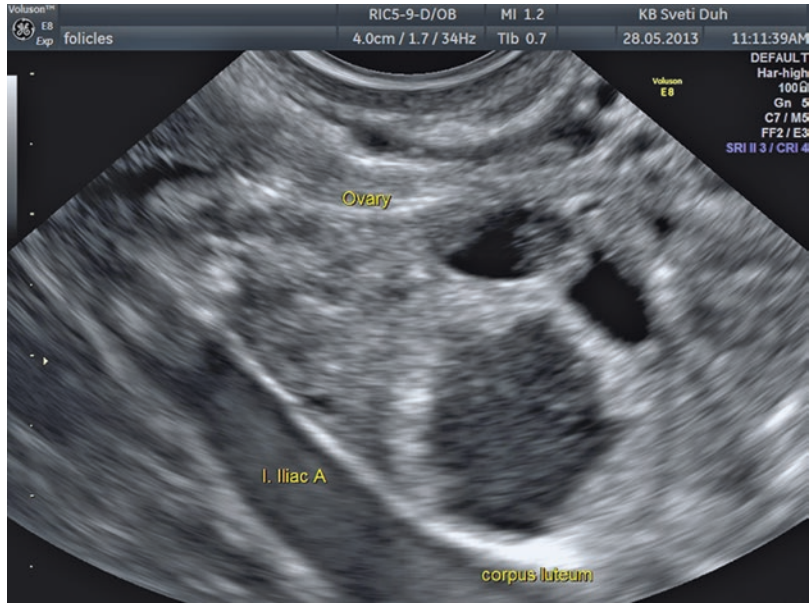

Fig. 4.1 Transvaginal image of the ovary with the corpus luteum; note the iliac vessels

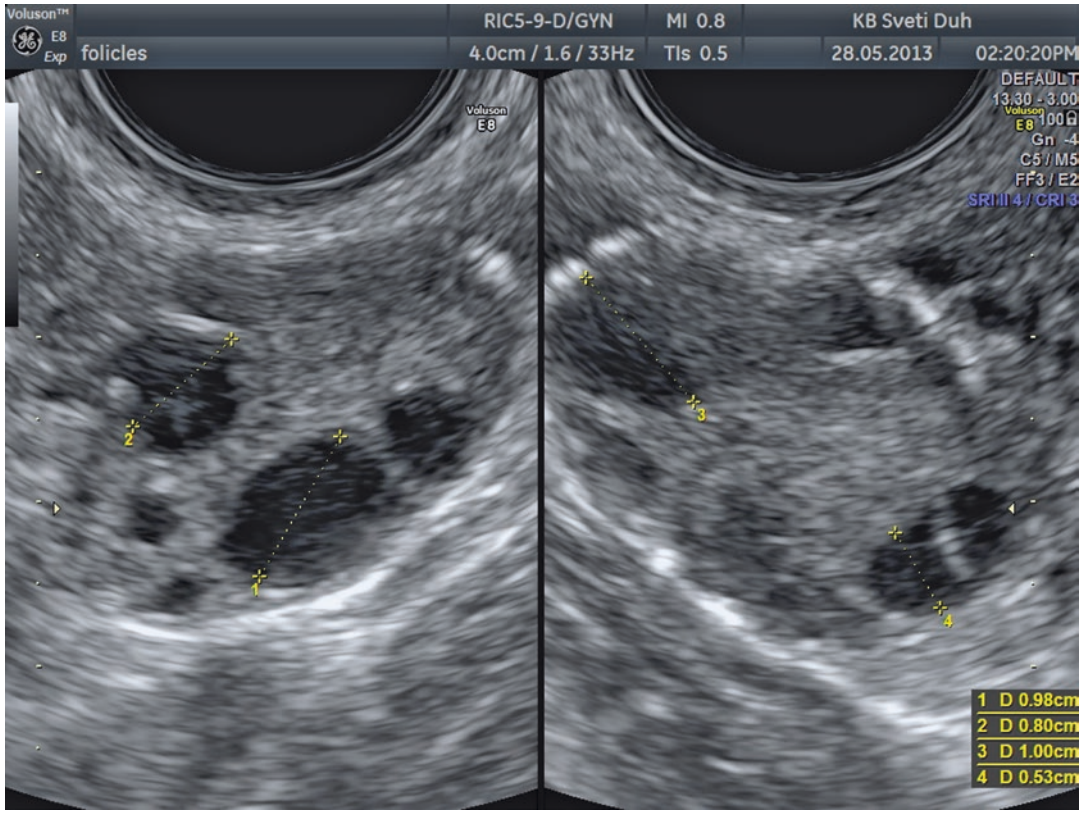

Fig. 4.2 Transvaginal image of both ovaries in early first phase

In fertile women ovaries are usually easily visualized because they are relatively big and have follicles and/or corpus luteum, structures that are easy to recognize using transvaginal ultrasound. The average size of the ovaries in premenopausal women is 3.5 × 2.5 × 1.5 cm (length × height × width) and in postmenopausal women is 2.0 × 1.5 × 1.0 cm. In order to measure, it is important to visualize the ovary in the frontal and sagittal plane. Three dimensions could be obtained, and the volume can be calculated using the ellipsoid formula ($V = 4/3 \times 3.14 \times (D1/2 \times D2/2 \times D3/2)$) [3] or the simplified ellipsoid formula ($V = 1/2 \times$ length × height × width). Difficulties in the visualization of normal ovaries can be caused by extreme cranial position of the ovary or in the case of severe adhesions in the pelvis. Transposed ovaries can be very difficult to find with abdominal ultrasound. Ovarian transposition is common in younger patients with pelvic malignancies (like cervical carcinoma). Transposed ovaries can be fixed anywhere up to the level of the lowest rib. Ovarian cysts that are common in this condition can help in detection of the ovarian position.

Postmenopausal Ovaries

Ovarian volume and diameter decrease with age, consequently making postmenopausal ovaries appear small hypoechoic structures. The absence of follicles results in difficult sonographic visualization and often may not be detected. Premenopausal ovaries can be visualized in 96% and postmenopausal in 62–65% of cases [3, 4].

Premenarchal Ovaries

Before, sexarche ovaries can be visualized by transabdominal ultrasound using the full-bladder technique or by transrectal approach using the transvaginal probe. The images obtained transrectally are quite similar to those obtained transvaginally. In children before 5 years of age, ovaries have a volume of less than 1 cm. Before puberty ovaries are small hypoechoic structures that measure less than 2 cm in diameter. Few years before menarche, small anechoic structures with sharp borders measuring 5–9 mm can be visualized, indicating the start of folliculogenesis.

In the years of adolescence, until the hypothalamus-hypophysis-ovary axis is not fully mature, ovaries are visualized with the variety of growing follicles of different sizes. Anovulation is common, and these large ovaries with a lot of follicles can often be misdiagnosed as polycystic ovaries.

Reproductive Age Ovaries

Changes in the morphological appearance of the ovary which can be detected by ultrasound come due to rhythmic changes in the secretion of female hormones FSH and LH. Ovaries pass through the menstrual cycle, in which we distinguish follicular phase, ovulation, and luteal phase. Ultrasound provides insight into the psychological changes during the ovarian cycle and allows accurate and reproducible investigations of follicular size, development, and growth during the follicular phase [5].

Newborn girl has 2 million follicles and before puberty 300,000 follicles are still present. For their development gonadotropins are not required. Since the mid-fetal life until menopause, there is a permanent reduction in the number of follicles, and only 400 (100–1000) follicles will achieve preovulatory maturation and ovulate until menopause.

The majority of primordial of follicles will go through the process of atresia.

In the first 5 days of the cycle, FSH levels are high in order to stimulate the development of a primary follicle in the ovary. A primary follicle measures 40 μm; it has one layer of granulosa cells and an oocyte. By further growth and multiplication of cells, a preantral follicle is developed. Preantral follicle has a diameter of only 150 μm, and it is not detectable by ultrasound.

Between the fifth and seventh days of the cycle, secondary antral follicles can be detected and are presented as anechoic spheroid zones inside the

ovary, approximately 2–3 mm in diameter. These are the first follicular structures that may be visualized by common ultrasound devices [5].

With further selection, one dominant follicle is being elected, while other follicles go into atresia. The dominant follicle can be detected between 8th and 12th day of the cycle when its size and growing pattern are clearly superior to other visualized follicles (Fig. 4.3). The remaining follicles can continue with their growth but just up to 14 mm in diameter. In up to 10% of maturely menstrual cycles, sonography can detect two dominant follicles [6].

The diameter is measured from one internal follicle wall to the other if the follicle is roundly shaped. If we are measuring an oval follicle, we have to measure three distances (the longest, the shortest, and the oblique) and then calculate the median: DF = (*D*1 + *D*2 + *D*3)/3. When measuring higher number of follicles during hormonal ovarian stimulation, it is usual to measure just two perpendicular distances (the longest and the shortest) and calculate the median: DF = *D*1 + *D*2/2.

The dominant follicle has a linear daily diameter growth of 2–3 mm per day, and at the moment of ovulation, the diameter of the dominant follicle is 18–27 mm [7].

This variety at the time of ovulation limits the use of follicle diameter for ovulation prediction.

In order to predict ovulation serial follicle, measurements have to be done in more than two menstrual cycles in each patient. In the majority of patients, a uniform pattern of morphologic sonographic changes prior to ovulation can be established, and the knowledge of follicle diameter and endometrial thickness and shape can help in infertility procedures during the natural cycle. Unfortunately not all patients have a uniform pattern and ovulate with different sizes of dominant follicles.

Besides follicle diameter, other sonographically visualized morphologic changes could help in the detection of ovulation. In more than 20% of follicles >18 mm, a cumulus oophorus can be visualized and is seen as a small anechoic part in the lumen of the dominant follicle that presents the detachment of granulosa cells containing the oocyte.

Twenty-four hours before the ovulation, a hypoechogenic line surrounding the preovulatory follicle can be visualized; it presents the separation of theca cells from internal granulosa cells. The theca cells are at that time hypervascularized and edematous, and these changes can be even better visualized using color Doppler (Fig. 4.4).

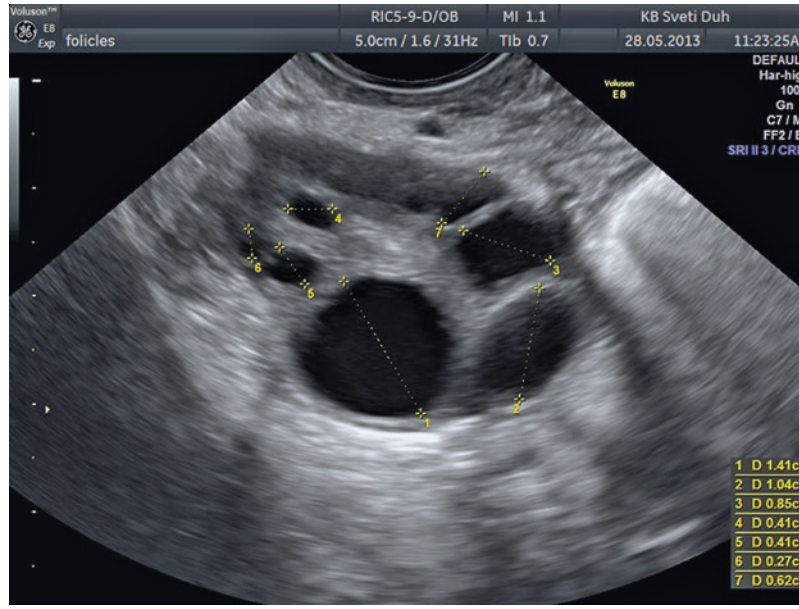

Fig. 4.3 Transvaginal image of a normal ovary in the first phase; note the dominant follicle

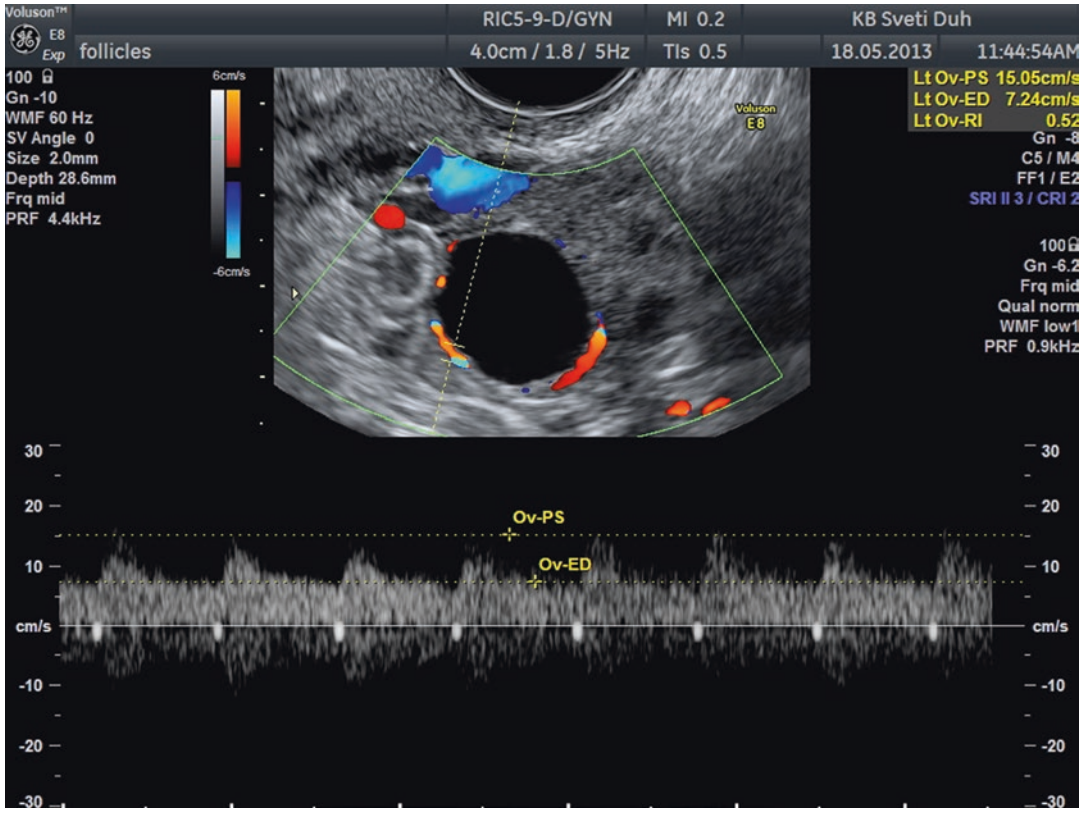

Fig. 4.4 Transvaginal color Doppler image of perifollicular vascularization of preovulatory follicle

Before ovulation the internal wall of the preovulatory follicle can be slightly hyperechoic with irregular internal borders. It is important to always check the endometrium because its thickness and shape correlate with the serum estradiol level, and endometrial findings can help in predicting the ovulation.

The key sonographic markers of ovulation are disappearance of or sudden decrease in follicle size (the most frequent sign of ovulation with the sensitivity of 84%), appearance of ultrasonic echoes in the follicle, irregularity of follicle wall and free fluid in the pouch of Douglas (in 77% of cases on the day of ovulation) [5, 8], and secretory changes of the endometrium.

After the ovulation, the follicle is transformed into corpus hemorrhagicum with internal echoes. The corpus luteum is afterward created with the vascularization and luteinization of granulosa cells. Sonographic appearance can be variable in size and shape [9]. The size is generally reduced and is visualized as a structure with thick hyperechogenic walls enclosing the hypoechoic center (see Fig. 4.1). It is well known that corpus luteum can also look like many pathologic changes of the ovary (endometriosis, cystic teratoma, and other benign or even malignant tumors), and sometimes it is absolutely necessary to perform an ultrasound examination after the menstruation in order to differentiate the possible pathology.

The corpus luteum vanishes before the start of next menstrual cycle, and the presence of vascularized corpus luteum 12 or more days after ovulation can be a first sign of pregnancy.

Color Doppler of the Normal Ovary

Transvaginal color Doppler (TVCD) plays an important role in better understanding the menstrual cycle physiology. This technique was intensively studied in the beginning of the 1990s,

and many studies proved the usefulness in detection of vascular changes in the uterus and the ovary [10–15].

The blood supply of the ovary has two sources: ovarian artery and the ovarian branch of the uterine artery that anastomoses and forms an arch in the ovarian hilus. Color Doppler signals of the uterine artery can be found on the lateral border of the ovary. The impedance indices found in the ovarian artery correlate with the menopausal status. Before menarche and after menopause, the ovarian artery is difficult to visualize because the ovaries are very poorly vascularized at that time. The resistance to blood flow is high and so are the flow indices (RI = resistance index, PI = pulsatility index). During the reproductive age, there is a difference in vascularization depending on which ovary has the dominant follicle. In the ovary with a dominant follicle, the resistance to blood flow is lower in comparison to the nondominant side. It is absolutely logic that a growing follicle or the corpus luteum needs more vascularization, so we register lower flow indices. As ovarian arteries are not easy to find, in order to perform objective measurements in practice, we estimate the intraovarian blood flow. Intraovarian blood flow changes during the cycle, and it is different pending age. Before puberty and after menopause, blood flow should not be detected in the ovaries using color Doppler. Any positive vascularization in that time of life in the ovaries has to raise suspicion about possible pathology of the vascularized ovary [11, 12].

TVCD in Preovulatory Phase

Perifollicular blood flow can be detected when a dominant follicle has a diameter of >10 mm. Few days prior to ovulation, the RI is around 0.54 ± 0.04. Two days before ovulation, the RI starts to decline, while at ovulation the RI is 0.44 ± 0.04. The flow velocity is increasing as the RI gets lower, and even if the RI is not changing, the peak systolic velocity rises on the onset of ovulation. Angiogenesis and dilatation of newly formed vessels between the theca and granulosa layer and changes in the follicular wall could be necessary for follicular rupture [13]. In the case of luteinized unruptured follicle, there is a failure of blood velocity to peak in the preovulatory period that proves that adequate vascularization is necessary for achieving ovulation [14].

The vascularization in the polycystic ovaries is detected in the hyperechoic stroma, and waveforms showed mean RI = 0.54 but without cyclic changes caused by hormonal steady state (anovulation). There are also no changes in the Doppler indices in the uterine artery that are usually found in regular menstrual cycles. The vascularization of the uterus and the ovary is hormonally dependent, and Doppler measurements reflect cyclic hormonal changes in the female genital organs.

The perifollicular vascularity is a constant challenge for clinicians and researchers. It is known that it correlates well with the level of follicular oxygenation. Oocytes from severe hypoxic follicles are associated with high frequency of abnormalities in the organization of the chromosomes. Color Doppler analysis of perifollicular blood may provide an indirect sign of the developmental competence of the oocyte [15]. In the stimulated cycles, there is a correlation of higher peak systolic velocity (PSV > 10 cm/s) in follicles with subsequent fertilized oocytes [16]. However, in the natural cycles, Doppler indices of perifollicular blood flow as predictors of oocyte quality are still of limited value [17]. Three-dimensional reconstruction of power Doppler perifollicular vascular network could be a better predictor for oocyte competence in natural cycles [18, 19].

TVCD is very reliable in confirming ovulation. A marked drop in blood flow indices and rise of blood flow velocities in the early luteal phase are signs of prominent vascularization and corpus luteum formation. Color Doppler findings added to ovarian morphology changes mentioned above accurately confirm ovulation.

TVCD and the Corpus Luteum

The formation of the corpus luteum is a key event in the reproductive life and also plays an important role in early pregnancy support. Immediately

after ovulation, blood vessels of the theca layer invade the cavity of the ruptured follicle (Fig. 4.5). There is a dramatic increase of the amount of blood flow with increased velocity and low impedance to blood flow. The RI is low (0.43 ± 0.04), remains at the same level for 4–5 days, and then gradually rises to a level of 0.49 ± 0.04, which is still lower than in the follicular phase (Fig. 4.6).

If the pregnancy is achieved, the corpus luteum has prominent blood flow with low Doppler indices (RI = 0.45 ± 0.04), and similar vascularization is detected during the first trimester. In the cases of threatened abortion ($p < 0.01$), missed abortion ($p < 0.01$), and incomplete abortion ($p < 0.01$), the resistance and pulsatility indices are significantly higher than in the normal pregnancy. There is a correlation between vascularization indices of the corpus luteum and hormonal levels of HCG, estradiol, and progesterone.

After the 23rd day of cycle, if there is no pregnancy, the corpus luteum starts its regression. The color flow signals are poor, and the Doppler indices are getting higher until menstruation and the start of the new cycle. At that time there is no color flow detected in the ovary.

Luteal phase defect could be assessed noninvasively by transvaginal color Doppler measurements of the blood flow in the corpus luteum. The mean RI in the defect luteal phase is significantly higher (RI = 0.56 ± 0.04; $p < 0.001$) compared to controls [20].

Three-Dimensional Ultrasound Visualization of the Normal Ovary

Volume of the Ovary

With the three-dimensional ultrasound (3D US), the image of the ovary could be obtained in all

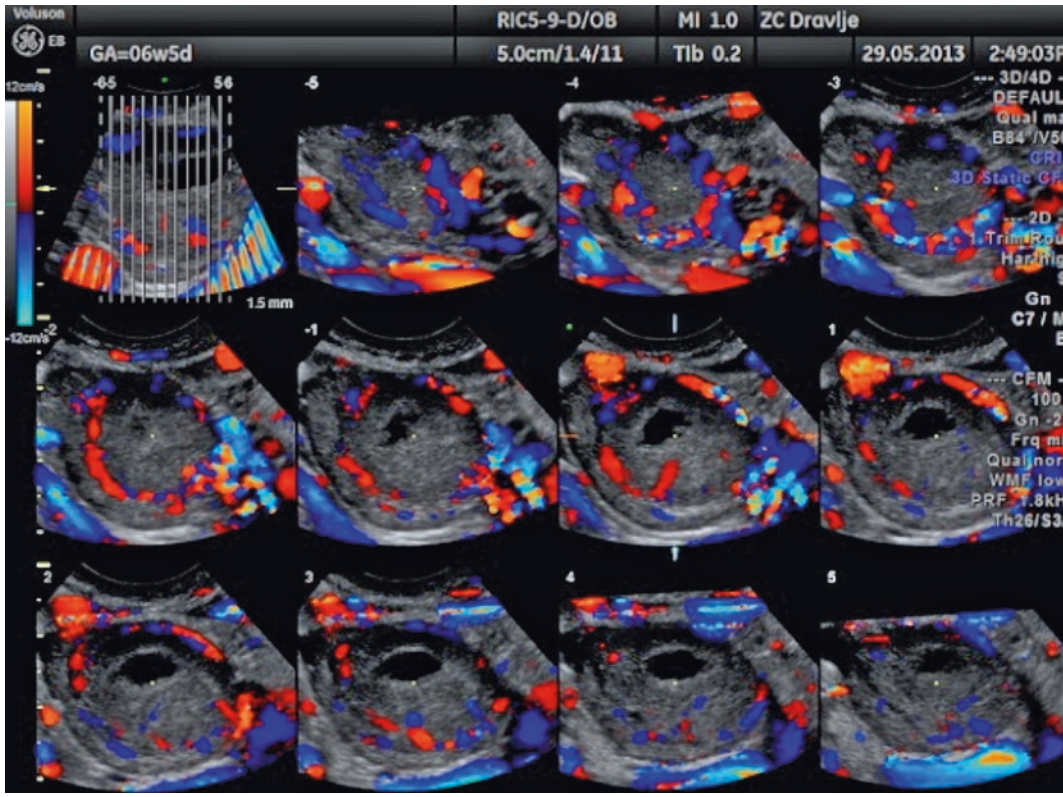

Fig. 4.5 Color Doppler image of vascularization of the corpus luteum

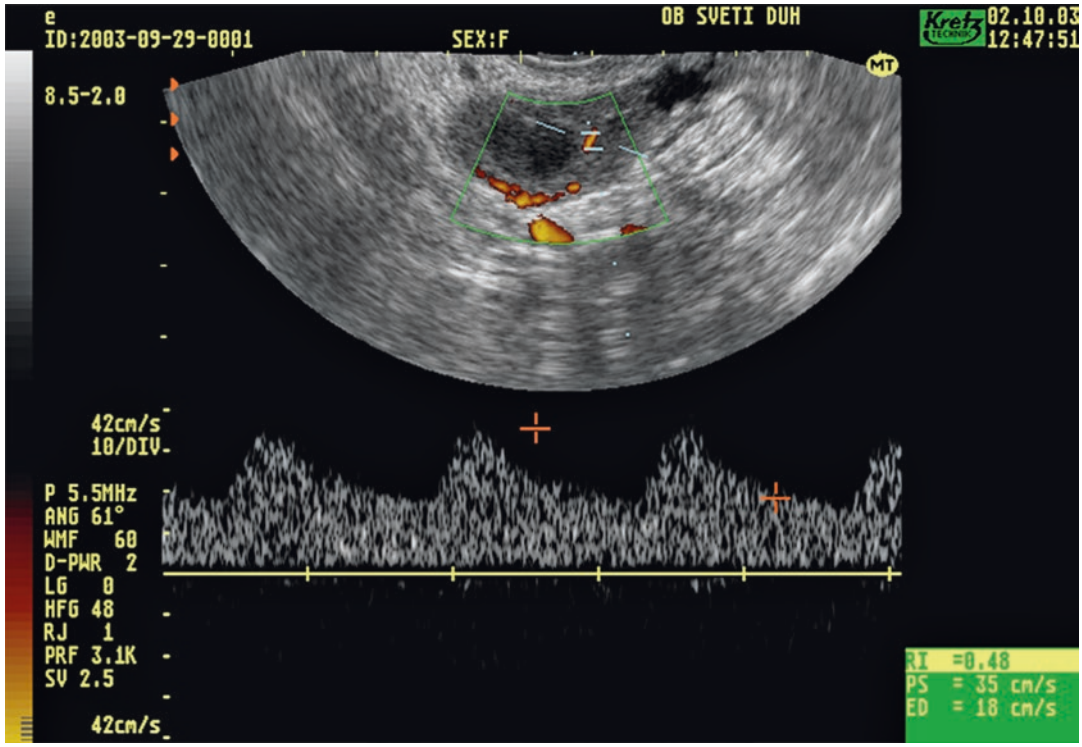

Fig. 4.6 Transvaginal color Doppler image of corpus luteum blood flow

three perpendicular dimensions. Storage capacities, reconstruction of the volume images, and simultaneous viewing of all three orthogonal planes are the main advantages of this method.

The volume of the ovary can be calculated using the simplified ellipsoid [3] formula ($V = 1/2 \times$ length $\times$ height $\times$ width) or sonographic formula (ovary = length $\times$ height $\times$ width $\times$ 0.5236).

Volume of the ovary can be measured even more precisely with semiautomatic VOCAL (virtual organ computer-aided analysis) technique (Fig. 4.7). VOCAL is a 3D software technology (General Electrics Healthcare, Kretz, Austria) program where the ovary is rotated around one axis from 6 to 30 times (every 30°, 15°, 9°, or 6° rotation angles), and in every step it is required to outline the ovarian borders. If the 30° step is chosen, the ovary is rotated six times. The software estimates the volume from these six planes of the ovary.

The ovarian volume in the reproductive age of women inversely correlates with age, and a statistically significant decrease in ovarian volume starts at 30 years of age [21, 22].

It is reported that average volume of the ovary by the age of 1 year is 0.26 cm^3 measured by transabdominal probe and increases steadily to an average of 1 cm^3 by 13 years of age [23]. The mean ovarian volume in nulliparous women in reproductive age is 7.8 cm^3 (2.6 SD), and it decreases to 3.4 cm^3 (1.3 SD) in the first 5 years of menopause. After 5 years of menopause, it shrinks to mean volume of 2.5 cm^3 (1.3 SD), and later in menopause it can become undetectable [3].

Measurement of ovarian volume to predict ovarian reserve and responsiveness to gonadotropins is limited, and it is useful only at the extremes of reproductive life. The novel ultrasound markers for the ovarian reserve, such as AFC (antral follicle count), AMH, and age, predict the ovarian reserve and responsiveness to gonadotropins much better [24, 25].

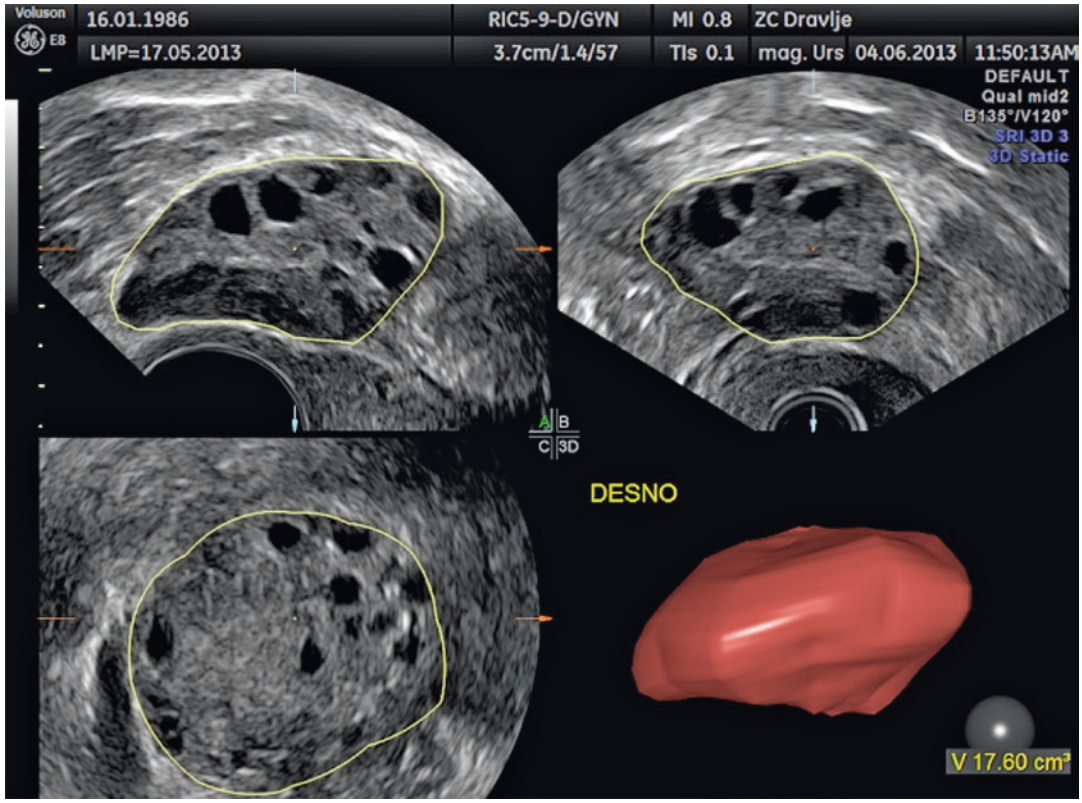

Fig. 4.7 3D volume measurement of the ovary with VOCAL techniques

Antral Follicle Count (AFC)

AFC is one of the markers of the ovarian reserve. Together with the AMH and age, it is considered as the best marker for ovarian reserve [26]. AFC is used to predict the response to the gonadotropin stimulation during assisted reproductive technology treatment.

AFC informs the clinician about quantitative and not the qualitative ovarian reserve. AFC correlates well with the number of oocytes retrieved after gonadotropin stimulation and not so good with the pregnancy results [26].

With advanced reproductive age, AFC decreases [27–31]. AFC declines progressively over time, with annual losses of 0.35–0.95 antral follicles per year [27, 31, 32]. The age-related nomograms in infertile women for the 3rd, 10th, 25th, 50th, 75th, 90th, and 97th percentiles for AMH and AFC were produced [31].

There is intra-cycle and inter-cycle variability, variability in the clinical definitions, and technical methods used to count and measure the volume of antral follicles. The practical recommendations for better standardization came out in 2010 [31]. It is recommended to count the cohort of 2–10 mm follicles between days 2 and 4 of menstrual cycle [31].

The technique used for AFC can be as follows:

- 2D scrolling through each ovary (manual counting of all antral follicles in the scroll)
- 2D counting of the antral follicles in one plane
- 3D SonoAVC (sonography-based automated volume count) (Fig. 4.8)

SonoAVC (General Electrics Healthcare, Kretz, Austria) is a novel ultrasound technique which can be used for the ultrasonographically

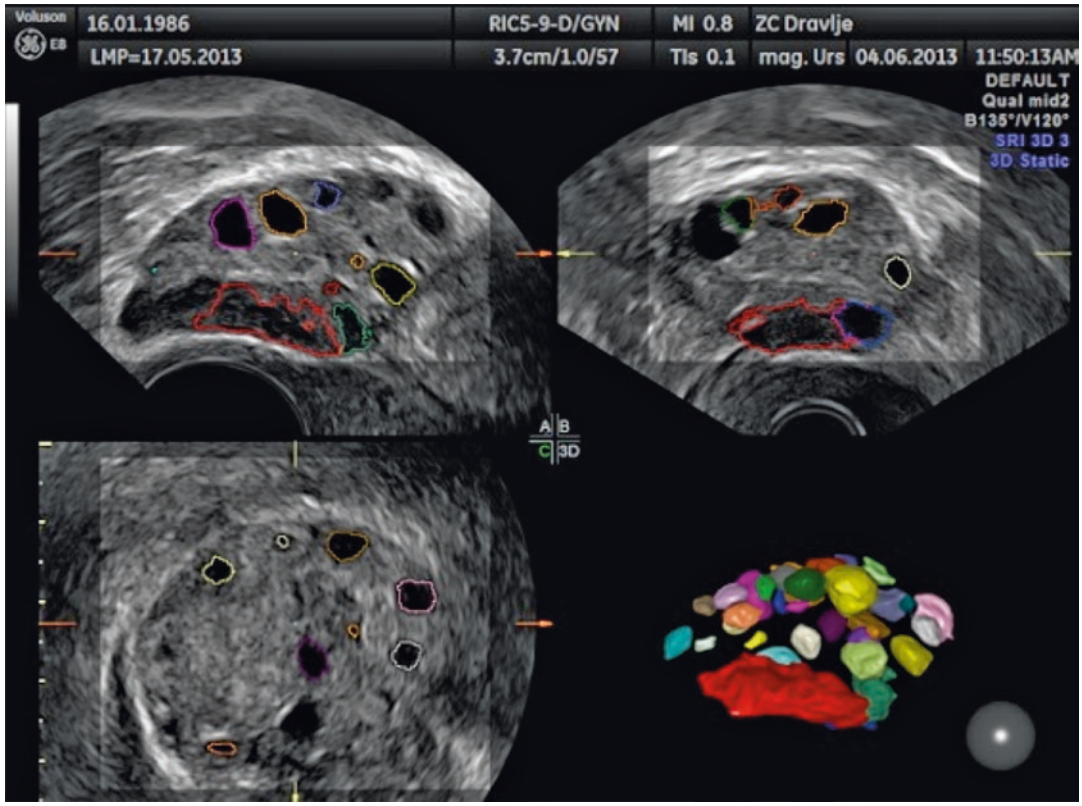

Fig. 4.8 Antral follicle count (AFC) measured by 3D US SonoAVC

hypoechogenic structures, such as the follicles. SonoAVC identifies hypoechogenic structures and their approximate shape in the selected 3D matrix and explorates the volume. It automatically recognizes the follicular borders in 3D and does a follicle volume assessment for each follicle in a selected volume box. The numbers and volumes of antral follicles are reported.

3D of the Dominant Follicle, Ovulation, and Formation of the Corpus Luteum

The majority of small growing follicles are round and can be easily measured by 2D US, either with one, two, or three perpendicular diameters. The dominant follicle usually changes the shape from round to oval before the ovulation. More precise measurement can be made with 3D ultrasound compared to 2D US measurements. 3D measurement of the dominant follicle can be obtained in three ways [33, 34]: first, classical with *x*, *y*, and *z* diameters as described before; second, with semimanual technique VOCAL described before; and third by automated technique SonoAVC (Fig. 4.9).

The measurements of VOCAL, SonoAVC, and actual volume of dominant follicle were comparable – the median actual volume of dominant follicle on the day of aspiration was 3.6 ml, with ranges from 2.9 to 8.0 ml [35]. SonoAVC is considered as a rapid and simple technique, with a good reproducibility and reliability [35].

On the basis of the dominant follicle volume measured with SonoAVC method, new criteria for timing hCG administration or planning the oocyte retrieval can be established [36]. Follicles with the measured volume ≥ 0.6 cm^3 on the day of hCG administration are associated with the finding of mature oocytes at the time of egg retrieval [36].

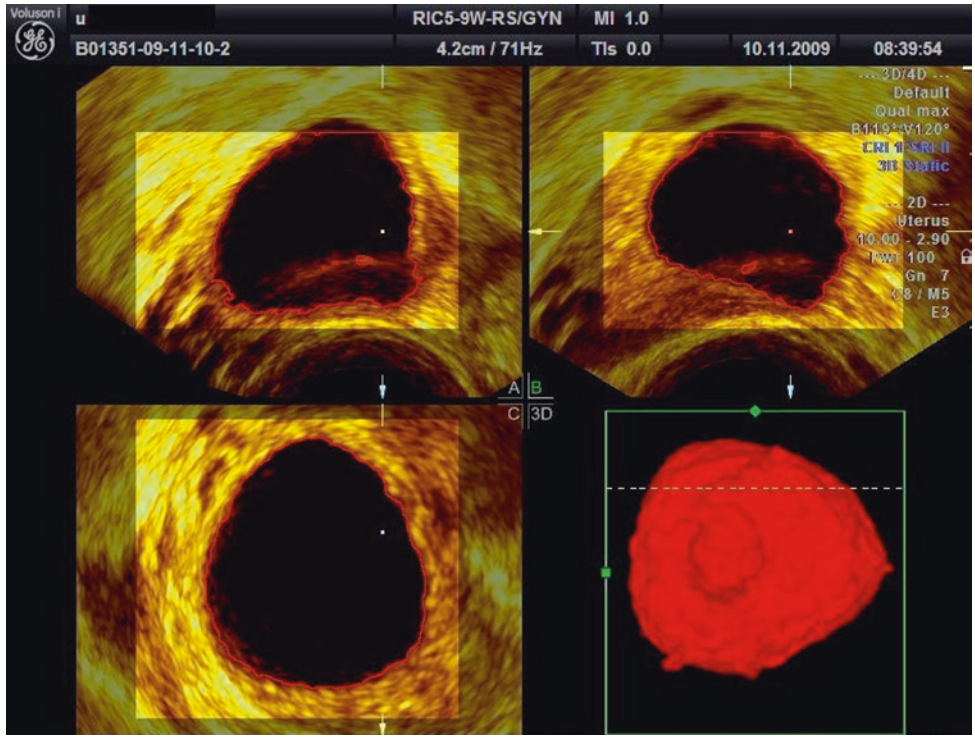

Fig. 4.9 3D measurement of the dominant follicle with SonoAVC

Additionally with 3D US, a cumulus oophorus can be visualized with the surface view, much better than with conventional 2D US (Fig. 4.10).

After ovulation the morphological changes in ruptured follicle can be even better observed with 3D US than with classical 2D ultrasound: decrease in follicle size can be measured with VOCAL or SonoAVC, appearance of ultrasonic echoes and irregularity of the follicular walls can be seen on 3D slices of the ruptured follicle, and volume of the free fluid in the cul-de-sac can be measured with SonoAVC [33, 34]. Currently there is not enough data that 3D US following of the natural cycle is superior to conventional 2D US.

3D Power Doppler of the Preovulatory Follicle and Corpus Luteum

As it is well known from 2D color Doppler US scanning, the vascularization in the ovary changes during the menstrual cycle. With the 2D US, the vascular indices (RI, PI) are measured just in one vessel selected very subjectively. 3D US vascularization gives schematical information about all vessels (sonographic angiogram) and additionally quantifying blood flow in the selected volume. 3D vascular indices can be measured: vascular index (VI), flow index (FI), and VFI (vascular flow index).

The vascularization index (VI) gives information in percent [%] about the amount of color values (vessels) in that volume of interest. The VI is calculated by dividing the figure of color values by the figure of total voxels minus the background voxels. Flow index (FI) measures the mean blood flow intensity. The figure ranges from 0 to 100. FI is calculated as the ratio of weighted color values (weighted by their amplitudes) to the number of the color values. The vascularization flow index (VFI) gives combined information of vascularization and mean blood flow intensity. The figure of the VFI is also

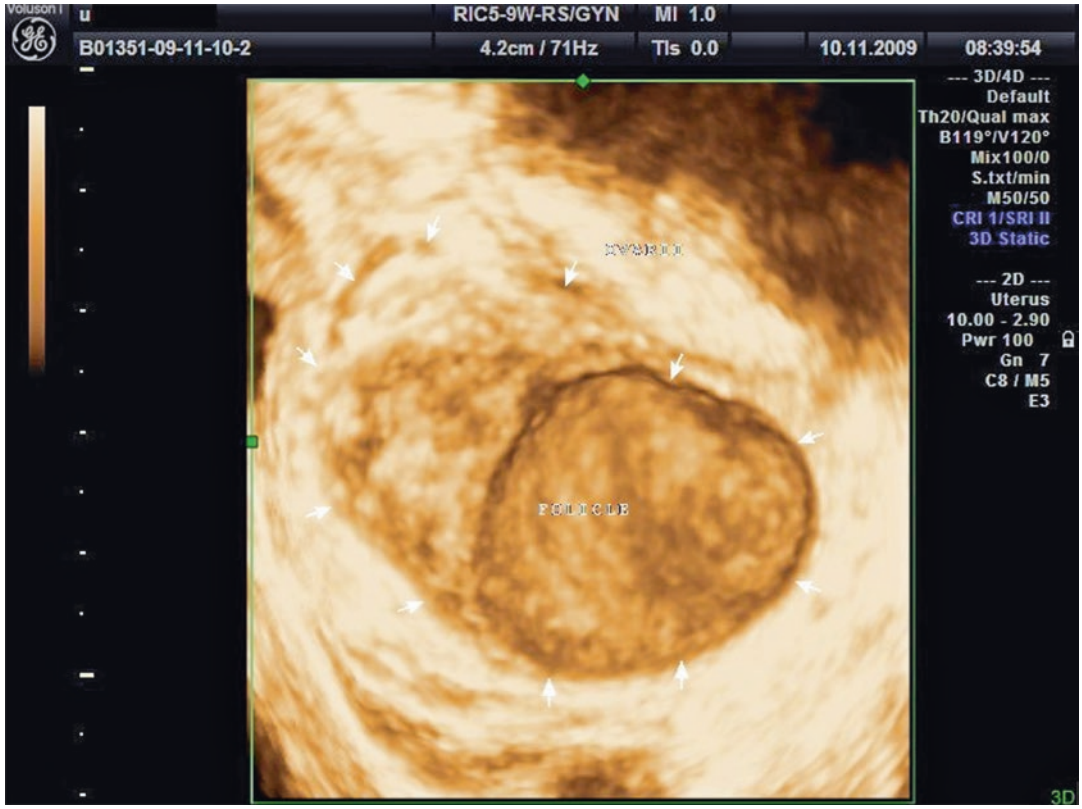

Fig. 4.10 3D surface view of the dominant follicle and cumulus oophorus (darker), with arrows marked the whole ovary

dimensionless and ranges from 0 to 100. It is calculated by dividing the weighted color values (weighted by their amplitudes) by the total voxels minus the background voxels.

3D vascular indices can be measured in the selected volume (ovary, dominant follicle, corpus luteum) in different phases of the menstrual cycle. In the follicular phase, the vascularization around the dominant follicle increases; the sonographic angiogram of the dominant follicle shows the angioarchitecture in the whole dominant follicle, as shown schematically with the color Doppler (Fig. 4.11). During the normal menstrual cycle, typical changes in vascular indices were noted [37–39]. Vascular indices (VI, FI, VFI) slowly increase during follicular phase in dominant follicle [35, 36]. In the late follicular phase, there is a short vascular depression in all indices. After ovulation very important vascular changes take place in the ruptured follicle. There is an increase vessel formation, and blood supply and increase in velocities are noted. In a ruptured follicle (Fig. 4.12), increase in vascular index (VI), flow index (FI), and VFI (vascular flow index) can be noted in the first 7 days after ovulation [37–39]. VFI in the corpus luteum 7 days after ovulation is on average 3.1 times higher than 1 day before the ovulation [37]. In the late luteal phase, the indices do not change significantly [37, 38].

The 3D sonographic angiogram is very useful because it is relatively easy to obtain and it gives a good impression on whole vascularization in selected volume. 3D vascularization indices are currently used mostly for research purposes, and broad clinical use is still limited due to technical problems, need for good equipment, and experience of the clinicians.

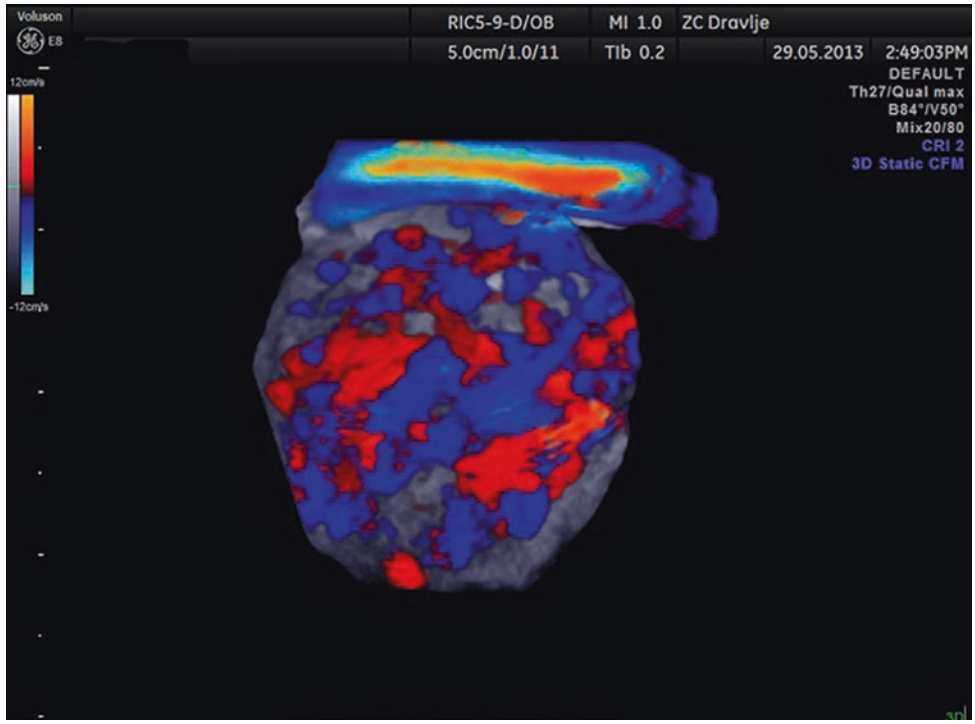

Fig. 4.11 3D color Doppler vascularization of dominant follicle before ovulation

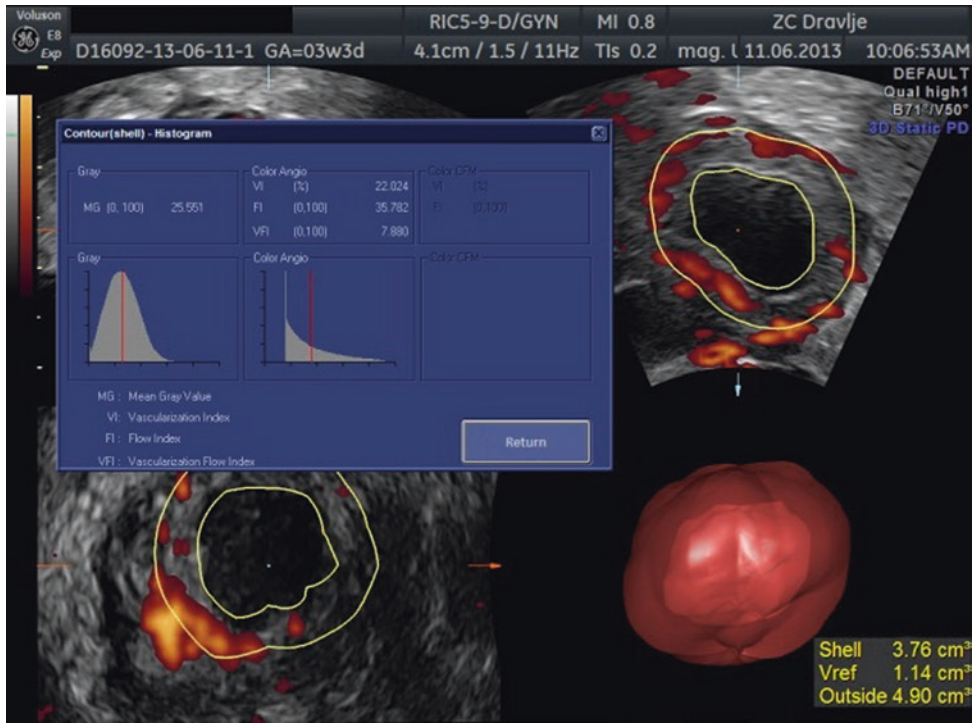

Fig. 4.12 3D vascularization of the corpus luteum with VI, FI, and VFI index

References

1. Kratochwill A. Ein neues vaginales schnittbildverfahren. Geburtshilfe Frauenheilkd. 1969;29:379–85.
2. Popp LW. Gynaekologische endosonographie. Quickborn: Klemke; 1986.
3. Merz E, Miric-Tesanic D, Weber G, Bahlmann F. Sonographic size of the uterus and ovaries in pre- and postmenopausal women. Ultrasound Obstet Gynecol. 1996;7:1–5.
4. Sladkevicius P, Valentin L, Marsal K. Transvaginal grey-scale and Doppler ultrasound examinations of the uterus and ovaries in healthy postmenopausal women. Ultrasound Obstet Gynecol. 1995;6:81–90.
5. Vlaisavljevic V. Echographic evidence of follicle development and maturation. Donald Sch J Ultrasound Obstet Gynecol. 2011;5(3):267–72.
6. Picker RH, Smith DH, Tucker MH, Saunders DM. Ultrasonic signs of imminent ovulation. J Clin Ultrasound. 1983;11:1–2.
7. Matijevic R, Grgic O. Predictive values of ultrasound monitoring of the menstrual cycle. Curr Opin Obstet Gynecol. 2005;17:405–10.
8. Jarvela IY, Sladkevicius P, Kelly S, Ojha K, Nargund G, Campbell S. Three dimensional sonographic and power Doppler characterization of ovaries in late follicular phase. Ultrasound Obstet Gynecol. 2003;22(5):520–6.
9. Deichert U, Daume E. Zyklische veranderungen am ovar. In: Deichert U, Ducla V, Schlief R, editors. Funktionelle sonographie in gynakologie und reproduktionsmedizin. Berlin: Springer; 1993. p. 71–132.
10. Collins WP, Jurkovic D, Waterstone J, Campbell S. Ovarian morphology, endocrine function and intrafollicular blood flow during periovulatory period. Hum Reprod. 1991;6:319–24.
11. Kurjak A, Schulman H, Sosic A, Zalud I, Shalan H. Transvaginal ultrasound, color flow and Doppler waveform of the postmenopausal adnexal mass. Obstet Gynecol. 1992;80:917–21.
12. Kurjak A, Kupesic S. Ovarian senescence and its significance on uterine and ovarian perfusion. Fertil Steril. 1995;64:532–7.
13. Bourne T, Jurkovic D, Waterstone J, Campbell S, Collins WP. Intrafollicular blood flow during human ovulation. Ultrasound Obstet Gynecol. 1991;1:53–9.
14. Kupesic S, Kurjak A. Uterine and ovarian perfusion during the periovulatory period assessed by transvaginal color Doppler. Fertil Steril. 1993;3:439–43.
15. Van Blerkom J, Antczak M, Schrader R. The developmental potential of the human oocyte is related to the dissolved oxygen content of follicular fluid: association with vascular endothelial growth factor levels and perifollicular blood flow characteristics. Hum Reprod. 1997;12:1047–55.
16. Nargund G, Doyle PE, Bourne TH, Parsons JH, Cheng WC, Campbell S, et al. Ultrasound derived indices of follicular blood flow before hCG administration and the prediction of oocyte recovery and preimplantation embryo quality. Hum Reprod. 1996;11:2512–7.
17. Lovrec VG, Vlaisavljevic V, Reljic M. Dependence of the in-vitro fertilization capacity of the oocyte on perifollicular flow in the preovulatory period of unstimulated cycles. Wien Klin Wochenschr. 2001;113(Suppl 3):21–6.
18. Vlaisavljevic V, Reljic M, Lovrec VG, Zazula D, Sergent N. Measurement of perifollicular blood flow of the dominant preovulatory follicle using three-dimensional power Doppler. Ultrasound Obstet Gynecol. 2003;22:520–6.
19. Vlaisavljevic V, Borko E, Radakovic B, Zazula D, Dosen M. Changes in perifollicular vascularity after administration oh human chorionic gonadotropin measured by quantitative three-dimensional power Doppler ultrasound. Wien Klin Wochenschr. 2010;122(Suppl 2):85–90.
20. Kupesic S, Kurjak A, Vujisic S, Petrovic M. Luteal phase defect: comparison between Doppler velocimetry, histological and hormonal markers. Ultrasound Obstet Gynecol. 1997;9:105–12.
21. Pavlik EJ, DePriest PD, Gallion HH, Ueland FR, Reedy MB, Kryscio RJ, et al. Ovarian volume related to age. Gynecol Oncol. 2000;77:410–2.
22. Kupesic S, Kurjak A, Bjelos D, Vujisic S. Three-dimensional ultrasonographic ovarian measurements and in vitro fertilization outcome are related to age. Fertil Steril. 2003;79:190–7.
23. Bernaschek G, Lubec G, Schaller A. Sonographische untersushungen uber das wachstum von uterus und ovarien zwischen dem 1.-14. Lebensjahr. Geburtshilfe Frauenheilkd. 1984;44:727–30.
24. Jayaprakasan K, Campbell B, Hopkisson J, Johnson I, Reine-Fenning N. A prospective, comparative analysis of anti-mullerian hormone, inhibin-B, and three-dimensional ultrasound determinants of ovarian reserve in the prediction of poor response to control ovarian stimulation. Fertil Steril. 2010;3:855–64.
25. Henriks DJ, Kwee WS, Mol BW, te Velde ER, Broekmans FJ. Ultrasonography as a tool for the prediction of outcome in IVF patients: a comparative meta-analysis of ovarian volume and antral follicle count. Fertil Steril. 2007;87:764–75.
26. Broekmans F, de Zieger D, Howles C, Gougeon A, Trew G, Olivennes F. The antral follicle count: practical recommendations for better standardization. Fertil Steril. 2010;94(3):1044–51.
27. Ruess ML, Kline J, Santos R, Levin B, Timor-Tritsch I. Age and the ovarian follicle pool assessed with transvaginal ultrasonography. Am J Obstet Gynecol. 1996;174:624–7.
28. Scheffer GJ, Broekmans FJ, Looman CW, Blankenstein M, Fauser BCJM, de Jong FH, et al. The number of antral follicles in normal women with proven fertility is the best reflection of the reproductive age. Hum Reprod. 2003;18:700–6.
29. Chang MW, Chiang CH, Hsieh TT, Soong YK, Hsu KH. Use of antral follicle count to predict the out-

come of assisted reproductive technologies. Fertil Steril. 1998;69:505–10.
30. Kline J, Kinney A, Kelly A, Reuss ML, Levin B. Prediction of antral follicle count during reproductive years. Hum Reprod. 2005;20:2179–89.
31. Almog B, Shehata F, Suissa S, Holzer H, Shalom-Paz E, La Marca A. Age-related nomograms of serum antimullerian hormone levels in a population of infertile women: a multicenter study. Fertil Steril. 2011;7:2359–63.
32. Ng EH, Yeung WS, Fong DY, Ho PC. Effects of age on hormonal and ultrasound markers of ovarian reserve in Chinese women with proven fertility. Hum Reprod. 2003;18:2169–74.
33. Res Muravec U. Ultrazvuk u asistiranoj reprodukciji. In: Hajder E, Hajder M, editors. Neplodnost i reproduktivna endokrinologija. Tuzla: Nacionalna i univerzitetska biblioteka BIH; 2011. p. 185–203.
34. Res Muravec U. Ultrazvuk u diagnostici PCOS. In: Sindrom policističnih jajnika, M Hajder, E Hajder, E Hajder, Tuzla: Off-set, 2016:119–28.
35. Salama S, Arbo E, Lamazou F, Levaillant JM, Frydman R, Fanchin R. Reproducibility and reliability of automated volumetric measurement of single preovulatory follicles using SonoAVC. Fertil Steril. 2010;93:2069–73.
36. Rodriguez-Fuentes A, Hernandez J, Garcia-Guzman R, Chinea E, Iaconianni L, Palumbo A. Prospective evaluation of automated follicle monitoring in 58 in vitro fertilization cycles: follicular volume as a indicator of oocyte maturity. Fertil Steril. 2010;93:616–20.
37. Jokubkiene L, Sladkevicius P, Rovas L, Valentin L. Assessment of changes in volume and vascularity of the ovaries during the normal menstrual cycle using three-dimensional power Doppler ultrasound. Hum Reprod. 2006;10:2661–8.
38. Hope JM, Long K, Kudla M, Arslan A, Tsymbal T, Strok I, et al. Three-dimensional power Doppler angiography of cyclic ovarian blood flow. J Ultrasound Med. 2009;8:1043–52.
39. Engels V, Sanfrutos L, Perey-Medina T, Alvarez P, Zapardiel I, Godoy-Tunidor S, et al. Periovulation follicular volume and vascularization determined by 3D and power Doppler sonography as pregnancy predictors in intrauterine insemination cycles. J Clin Ultrasound. 2011;5:243–7.

Ultrasound and Ovarian Reserve

5

Laurel A. Stadtmauer, Mai Tran, Alessandra Kovac, and Ilan Tur-Kaspa

Definition of Ovarian Reserve

Ovarian reserve is a term that reflects the number of oocytes that are available for procreation. There are biochemical and morphological markers correlating with ovarian reserve indirectly. The most common ultrasound morphological markers are antral follicle counts in two or three dimensions, ovarian volume, and ovarian blood flow to the stoma.

The ovaries contain several subtypes of follicles: the primordial follicles (≤0.05 mm diameter), primary follicles, secondary follicles, pre-antral follicles, and antral follicles (>2 mm diameter). Primordial follicles consist of the oocyte with a thin layer of granulosa and stromal cells, too small to be seen on ultrasound. The gonadotropin-dependent stage (antral follicles) can be visualized on ultrasound as small cysts. As a follicle grows, it develops follicular fluid, which can be seen on ultrasound. Antral follicles are visible, measure from 2 to 10 mm, and represent the pool of follicles recruited in the follicular phase for ovulation. The antral follicle count (AFC) is the total number of follicles counted in 2D or 3D per ovary and correlates well with the number of recruitable mature oocytes for IVF. The recruitment process occurs over 3–4 months.

Before initiating ovarian stimulation, the baseline day 3D US is a prerequisite for planning the IVF therapy in detail; it can estimate the ovarian reserve. The AFC in the early follicular phase can determine whether a patient will be a hyper, normal, or poor responder and whether there are any ovarian cysts. If the patient has a low AFC as defined by <5 follicles total, it is recommended to choose a no suppression protocol with either a micro-flare Lupron protocol or mild stimulation, and only a few oocytes are anticipated. The AFC and AMH are the most accurate in determining the anticipated number of oocytes [1].

Female reproductive aging is a process that will reduce fecundity (the ability to have a viable embryo implanted). The process of aging involves decrease in both the quantity and quality of the oocytes within the follicles. At 4 months of fetal life, the germ cells are surrounded by the somatic cells forming the primordial follicles, containing

L. A. Stadtmauer (✉)
The Jones Institute for Reproductive Medicine, Eastern Virginia Medical School, Norfolk, VA, USA
e-mail: stadtmla@evms.edu

M. Tran
Fresno Department of Obstetrics and Gynecology, University of California, San Francisco, Fresno, CA, USA

A. Kovac
Center for Biostatistics in AIDS Research at Harvard T. H. Chan School of Public Health, Boston, MA, USA

I. Tur-Kaspa
Institute for Human Reproduction, Chicago, IL, USA

L. A. Stadtmauer, I. Tur-Kaspa (eds.), *Ultrasound Imaging in Reproductive Medicine*,
https://doi.org/10.1007/978-3-030-16699-1_5

the peak number of oocytes at 6–7 million. At birth, there are 1 million oocytes, with loss by atresia [2]. It further decreases to 300,000 to 500,000 follicles at puberty. Throughout life, follicles leave the primordial pool and enter the growing recruitable pool taking about 85 days or three menstrual cycles to reach ovulation. Most follicles undergo atresia, until rescued by the FSH at puberty by the activation of the pituitary-gonadal axis. The rate of decline of follicles during the reproductive years is steady at approximately 1000 follicles per month. The rate of decline rapidly increases after 37 years of age. The loss in the quality is due to increased rate of meiotic nondisjunction leading to increased rate of aneuploidy in early embryos at older female ages. At menopause, average age of 51, the number of follicles remaining will be less than 1000 [3].

The first noticeable sign of reproductive aging is shortening of the cycle by 2–3 days due to decrease in the follicular phase by early selection and maturation of the dominant follicle. These signs occur relatively late, much after the changes in the quantity and quality of the oocytes have occurred. Other biochemical changes include a gradual increase in circulating levels of FSH and deceases in serum anti-Mullerian hormone (AMH). The ovarian reserve is primarily composed of the resting primordial follicles in dormant-arrested state. AMH is involved in the regulation of the number of these primordial follicles that advance to a gonadotropin-dependent phase to progress to early antral follicles. As the follicles become more FSH dependent, there is less AMH within the follicles [4]. The follicles that grow to produce the mature oocytes in IVF are the antral follicles. The importance of measuring the antral follicle count is to be able to predict whether a woman will respond poorly or excessively to the exogenous gonadotropins given in IVF stimulation. There are large variations that exist in women at the same age [5].

Antral Follicle Count and Ovarian Reserve

The estimation of antral follicle count and antral follicle size performed by TVUS is currently the most reliable method and gives the best correlation with retrieved oocytes [6–8]; moreover, it is easy to perform and is noninvasive. The definition of AFC is the number of follicles in both ovaries between 2 and 10 mm, added up, that can be recruited with the threshold dose of gonadotropins for each patient. Therefore, the AFC determined by ultrasound on day 2 or 3 of the cycle, notably by 2D or 3D techniques, is the best predictor for poor ovarian response, ovarian hyperstimulation syndrome (OHSS), oocytes collected, and live birth rates [2, 6–11]. Recent evidence shows that it can be done at any point in the cycle [12] and that 3D ultrasound can more reliably count the small follicles [7]. Ovaries with decreased AFC and with increased AFC are shown in Fig. 5.1. Only a small number of ovarian follicles are highly responsive to FSH during an IVF stimulation. The number of these antral follicles represents the "recruitable or selectable follicles." The antral follicle count (AFC) reflects the ovarian reserve and is predictive of the IVF outcome with regard to the number of yielded oocytes in response to hormonal stimulation. Frattarelli and colleagues correlated the AFC with the number of mature follicles ($r = 0.52$) and the number of oocytes ($r = 0.38$) and found that AFC < 4 was associated with a high cancellation rate and poor pregnancy rates [13]. For the high responders, the cutoff level of >14 antral follicles has the best combination of sensitivity and specificity for predicting a hyperresponse with values close to 90%. It is important in the selection of the protocol and gonadotropin dosage in an attempt to decrease OHSS and cancelled cycles. The accurate assessment of the ovarian reserve is a way to individualize optimal therapy. The ovarian volume also correlates with the AFC and can be measured by TVUS [13, 14].

Standard AFC assessment is performed primarily with 2D US imaging. Although this modality might be sufficient in some cases, there might be some uncertainties and disadvantages.

Three-dimensional AFC is more reproducible and accurate, but the method is less standardized, and 3D technology may not be freely available for all reproductive endocrinologists. Figure 5.2 shows the 3D antral follicle count in inverse

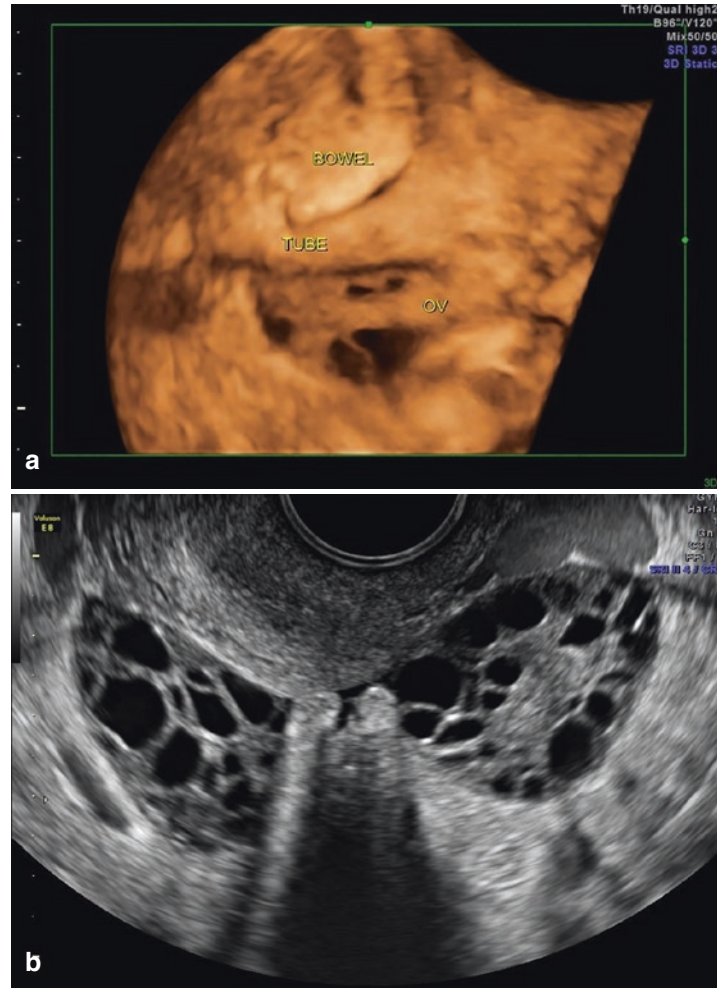

Fig. 5.1 (**a**) Decreased ovarian reserve with antral follicle count (AFC) less than 5. (**b**) Increased ovarian reserve with AFC greater than 15 per ovary

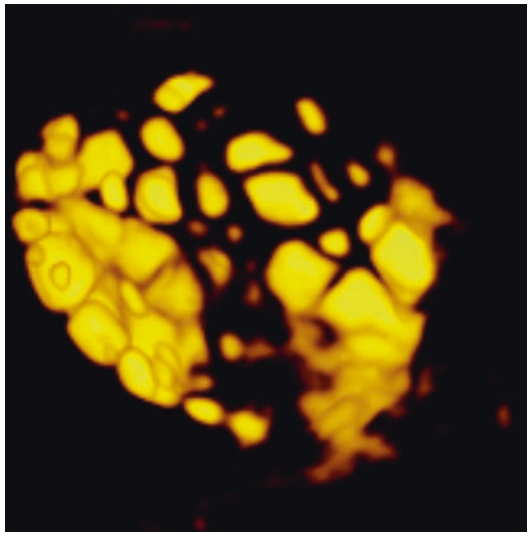

Fig. 5.2 3D antral follicle count in inverse mode

mode. On the baseline scan, it is imperative to distinguish between the total antral follicle count (TAFC), including follicles >6 mm in diameter; however, the number of small antral follicles is more predictive of the number of oocytes retrieved. The size of the follicles after stimulation correlates with the maturity of the oocytes obtained. Akbariasbagh et al. found that the fertility rate of oocytes aspirated from small (diameter <12 mm; volume ≤1 mm^3) follicles (55%) was significantly lower than the fertility rate of oocytes aspirated from follicles >12 mm and volume >1 mm^3 [15]. However, they found that the oocytes obtained from small follicles continue to cleave and develop into embryos with not significantly different quality from those derived from larger follicles. AFC is also a predictor of pregnancy loss, and low AFC correlates with four

times increase in early miscarriages [16]. However, the data on prediction of pregnancy and live birth rates are poor [11, 17] although the oocyte yield is a predictor of live births.

Endocrine Markers of Ovarian Reserve

Endocrine markers of ovarian reserve, anti-Mullerian hormone (AMH), and inhibin B are direct markers of quantity and follicular cohort numbers. AMH correlates with the pre- and early antral follicles. Indirect markers are basal day 3 FSH, and estradiol (E2) levels and high levels indicate fewer small antral follicles. Both AFC and AMH predict similarly the response to treatment with higher precision than day 3 FSH, but ultrasound is the only method so far that allows a direct assessment of each ovary separately, and the presence of ovarian cysts can underestimate the ovarian reserve. Identification of participants who are likely to respond poorly during IVF treatment is clinically relevant as the couple can be counselled regarding cycle cancellation and lower chance of success. Pretreatment AFC and AMH measured on day 3 of the preceding cycle were found to be the most significant predictors of the number of oocytes retrieved especially for low and high responders in multiple studies including a meta-analysis by Hendricks et al. [6, 18–23]. These studies showed AFC and AMH demonstrated similar predictive power based on ROC area under the curve (AUC) analysis and correlated with oocyte number better than other parameters such as FSH or age. However, as with AFC, AMH is a good predictor ovarian response but correlates less well with pregnancy outcomes, which is more important outcome for the patient than oocyte number [24]. The results are inconsistent with some studies showing an association with AMH and live births [25] and others do not [26, 27]. The validity of AFC for ovarian reserve comes from studies showing a direct correlation with the number of nongrowing follicles viewed on histologic sections [23]. On the other hand, ovarian volume, vascularity, and perfusion had no significant value in predicting poor ovarian response, and all are inferior to AFC [28]. The hypothesis that aneuploidy is negatively associated with the quantity of oocytes in the ovary is supported by studies showing decrease AFC in women with spontaneous abortions after IVF. The conclusions are not supported by all studies possibly because some lack power and it may depend on the mechanism of diminished ovarian reserve. In many women with low AFC, especially at a young age, there is a decrease in quantity but not in quality of the oocytes.

According to the ASRM [29], AFC is a predictor of ovarian response, but not the sole criteria. AFC may vary depending on the quality of the machine and the use of 3D and needs standardization.

3D Ultrasound and Ovarian Volume

Ovarian volume can be calculated by measuring each ovary manually in three perpendicular directions and applying the formula of the ellipsoid ($D1 \times D2 \times D3 \times \pi/6$). Ovarian volume can also be automatically calculated using the software called "virtual organ computer-aided analysis" or VOCAL (Fig. 5.3). This imaging program calculates organ volume from the areas of the three orthogonal sections, sagittal, transverse, and coronal views, and allows very precise calculation of ovarian volumes. However, ovarian volume can be affected by ovarian cysts. Ovarian volume and antral follicle volume can now be automated. Three-dimensional US is an excellent technique for calculating ovarian volume very precisely using the VOCAL program and observing the ovary with rotating angles. Low ovarian reserve and poor response to controlled ovarian hyperstimulation in ART are associated with volumes <3 cm^3 as seen by Lass and colleagues with increased cancellation rates [30]. Polycystic ovaries are associated with volumes >6.6 cm^3 for polycystic ovarian morphology (PCOM), and for the diagnosis of polycystic ovary syndrome (PCOS), the ovarian volume is ≥ 10 cm^3. Ovarian hyperstimulation syndrome (OHSS) is associated with increased ovarian volume [31, 32]. However, the total volume of the ovaries detected by trans-

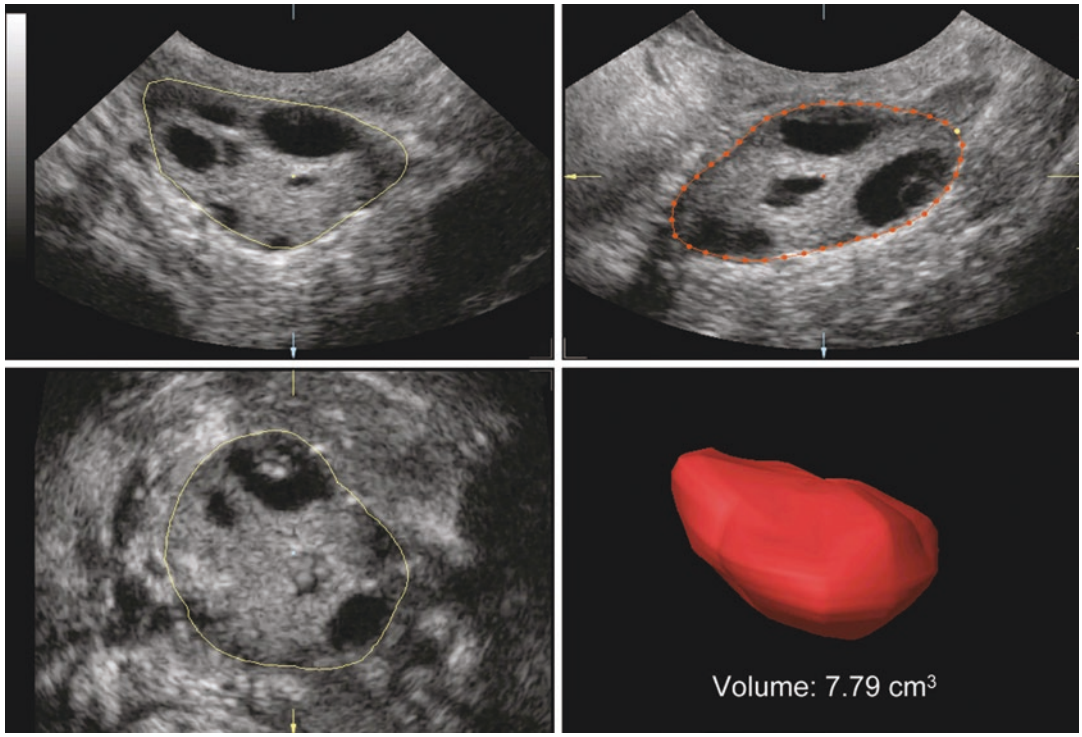

Fig. 5.3 3D ovarian volume

vaginal ultrasound is not better than the AFC in predicting risk parameters.

The studies of IVF patients have demonstrated that 3D ultrasound volume measurements for follicles correlate better with the volume of aspirated follicular fluid than 2D ultrasound measurements [32]. One of the most frequently employed applications is the sonography-based automated volume calculation (SonoAVC; GE Medical Systems, Zipf, Austria). The application of SonoAVC for IVF shown in Fig. 5.4 was first described by Raine-Fenning et al. [33] and will be discussed in detail in a later chapter. Studies with SonoAVC have not shown a clear benefit in improving IVF outcomes [34, 35]. In a study by Wertheimer et al., the authors evaluated the effect of follicle trafficking with SonoAVC follicular volume measurements on treatment outcomes in GnRH antagonist IVF cycles and found that it did not attain better fertility outcomes than standard 2D ultrasound [35]. However, it is interesting to note that in a small study by Hernandez et al., the authors found that under a standard protocol for hCG administration, a multivariate model including follicular volume as measured by SonoAVC can predict the count of mature oocytes [36]. Even if there is no clinical benefit, the advantages of SonoAVC may be a decrease in scanning time as the ovarian volumes are saved in the machine and can be calculated later after the patient is off the table. This may lead to less discomfort for the patients. However, the time required for manual assessment of the 3D data should be added to the time in scanning, and there is a learning curve to be reproducible. Rodriguez Fuentes analyzed the impact of SonoAVC on time and the clinical outcome of IVF treatment. They found a time reduction of 4 minutes per case after including the post-processing time [34]. Their study has shown that SonoAVC provides different results from those of 2D ultrasound imaging when the size of the follicle is considered. Furthermore, SonoAVC provides a mean to standardize follicle measurement, especially when imaging is done by different sonographers.

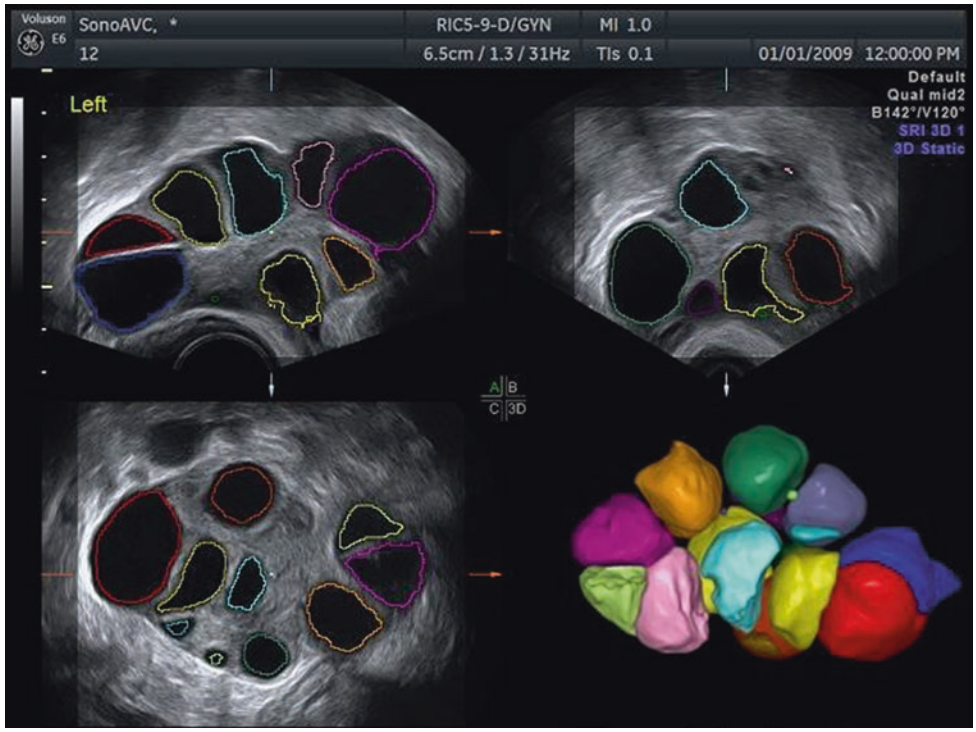

Fig. 5.4 SonoAVC of a stimulated ovary

Evaluation of Ovarian Stroma Flow and Perifollicular Blood Flow with 3D Ultrasound

It is possible that poor ovarian vascularization impairs access of gonadotropins to the ovarian follicles. Power Doppler US in combination with 3D US and VOCAL is a very good approach for correlating the ovarian vascular network with the ovarian response to ART. The significance of ovarian stromal blood flow with ovarian reserve was studied [37]. Variability some studies showed correlation of undetectable basal ovarian stromal blood flow with poor response and others did not. Studies on ovarian stromal blood flow and vascularization in PCOS have shown conflicting results, and the topic will be covered in another chapter.

The recognition and selection of high-quality oocytes is important to the success of the IVF cycles. During an IVF stimulation with gonadotropins, the largest follicles reach a diameter of 17–24 mm prior to human chorionic gonadotropin (hCG) trigger. During the growth of the follicles, there is an increased vascularization and an increase development of the capillary network that helps transport the hormones and oxygen and other nutrients to area [38]. VEGF is an important factor in follicle development. The retrieval of many good-quality oocytes increases the likelihood of a high fertilization rate and an adequate number of high-quality embryos. Perifollicular blood flow has been studied as a predictor of the quality of oocytes and embryos and pregnancy outcomes. The way perifollicular blood flow is measured is by power Doppler around the time of the hCG trigger or before oocyte retrieval. The power Doppler can qualitatively measure the flow into the vessels with a high sensitivity [39, 40] (Broini et al. 2004). The Chiu grading system is dependent on the percentage of follicular circumference with flow. Indices for Doppler flow into the follicles include PI, RI, and SD ratios. A recent meta- analysis of PFBF in predicting IVF success showed that although the studies were heterogeneous and conflicting, there was a positive correlation with oocyte quality and pregnancy rates. However, large randomized trials are lacking [41].

Ovarian Cysts

Ovarian cysts are important to diagnose by ultrasound in the infertile patient and can affect the ovarian volume. The most common ovarian cysts seen in infertility patients are simple functional cysts, hemorrhagic cysts, endometriomas, and dermoid cysts. Functional cysts are the most common cystic masses seen on ultrasound in the reproductive age group. These cysts tend to stay less than 10 cm and regress after one to two cycles and are either follicular cysts or luteal cysts. If they are small (<3 cm) and not hormonally active, they do not need to be treated before ART. However, patients with large simple ovarian cysts may have lower response to stimulation, and ovarian cyst aspiration immediately prior to ovarian stimulation has been shown to be beneficial [42]. A hemorrhagic cyst will show no flow into the cyst, will jiggle with the ultrasound probe, and will resolve spontaneously (Fig. 5.5a).

An endometrioma is also a very common finding in the infertile patient and is a sign of the presence of endometriosis in other areas [43, 44]. The typical endometrioma is a unilocular cyst with homogeneous low-level internal echogenicity (ground glass echogenicity) of the cyst fluid (Fig. 5.5b). With respect to endometrioma, a

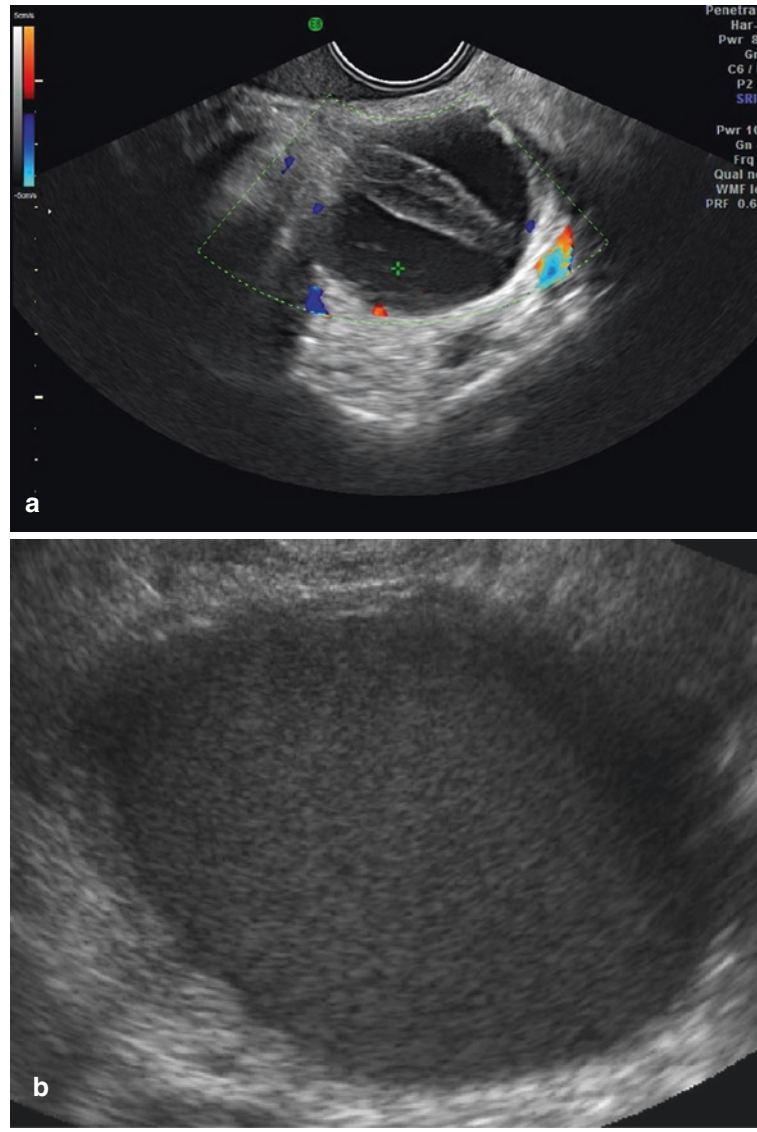

Fig. 5.5 (**a**) Hemorrhagic cyst. (**b**) Endometrioma with ground glass appearance. (**c**) Dermoid cyst 3D with hair. (**d**) Dermoid cyst 2D sebaceous material and hair. (**e**) Malignant ovarian cyst with blood flow into the cyst

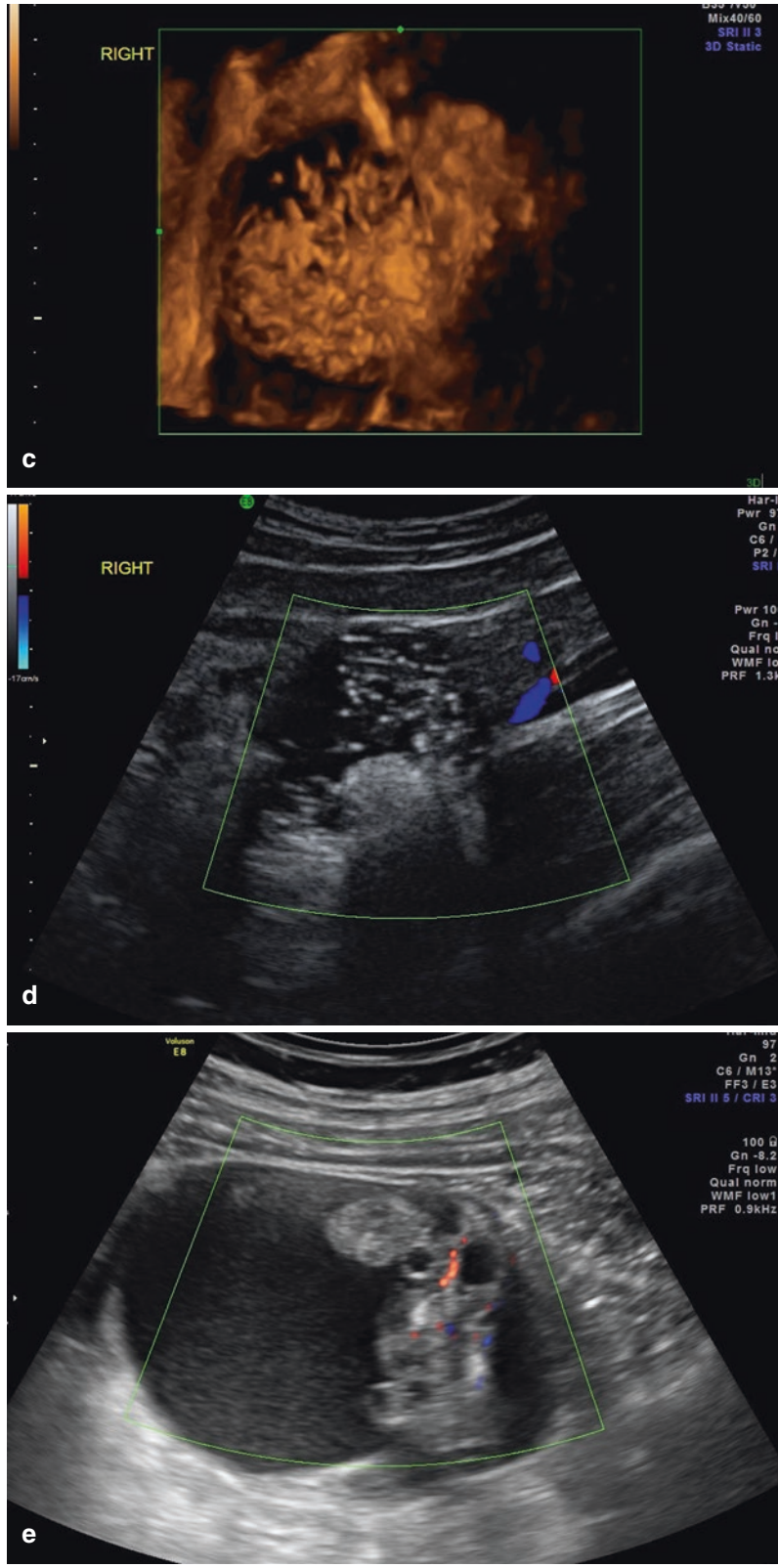

Fig. 5.5 (continued)

correct diagnosis is important for infertility with possible need for ART. Transvaginal ultrasonography is the imaging of choice to differentiate ovarian endometriomas from other adnexal masses [45, 46]. Studies show that an endometrioma is associated with lower response to ovarian stimulation. However, removing the endometrioma can also affect ovarian response and may significantly diminished ovarian reserve as the base of the ovary is usually burned and the cyst wall is stripped with damage to the follicles [47]. Dermoid cysts can present as solid hyperechoic heterogeneous masses with a mixed pattern of solid and cystic areas (Fig. 5.5c, d). They may contain calcifications, fat, and hair. Dermoids should be removed prior to IVF if they are causing pain or if there is a question of malignancy. Puncture during oocyte retrieval should be avoided due to high risk of peritonitis.

Although malignancy is rare in women of reproductive age, a suspicious ovarian mass may be seen on an initial infertility scan. Differentiating benign from malignant tumors is done with a combination of morphological evaluation and Doppler ultrasound [48]. The sensitivity and specificity for a combination of US findings and color Doppler in predicting benign from malignant were 0.93 and 0.85 in this study. Figure 5.5e shows an ovarian mass highly suspicious of a malignancy, a complex mass with papillary projections, and blood flow into the cyst.

Ultrasound and Polycystic Ovary

Polycystic ovary syndrome (PCOS) is one of the most common endocrine disorders impairing female fertility; it has been reported to occur in about 20% of the general female population and in up to 50% of women undergoing IVF therapy [49–51]. This topic is covered in detail in another chapter but will be discussed briefly here. Ultrasound is one of the criteria for the diagnosis of PCOS. Current data suggest that polycystic ovaries detected by transvaginal ultrasonography may be found in approximately 75% of women with a clinical diagnosis of PCOS [52, 53]. However, it is not a rule that all women with polycystic ovaries will demonstrate the clinical and biochemical features of PCOS such as oligomenorrhea and/or hyperandrogenism. Polycystic ovaries per se, even without PCOS, constitute a risk factor for the development of ovarian hyperstimulation syndrome (OHSS), and the stimulation protocol chosen should reflect this.

Transvaginal ultrasound is a highly sensitive method for identification of polycystic ovaries. The most commonly used criteria today are those proposed by Dewailly and colleagues with a string of pearls pattern [54, 55] where the antral follicles are arranged peripherally with a dense core of ovarian stroma (Fig. 5.6). This was reaffirmed in the Rotterdam 2003 consensus which proposed that the transvaginal threshold for PCOM is based on the presence of an ovarian volume $\geq$10 cm^3 (milliliters) or $\geq$12 small follicles in a single ovary [56]. The use of 3D ultrasound and of color and pulsed Doppler ultrasound showing increased ovarian blood flow may further enable the identification of polycystic ovaries but is not mandatory for the diagnosis [57]. However, it is important to note that results of studies on ovarian stromal blood flow and vascularization in PCOS have demonstrated conflicting results [58].

With advancement in ultrasound technology and concern that polycystic ovarian morphology (PCOM) may be overdiagnosed using the Rotterdam follicle number per ovary (FNPO) ($\geq$12 small follicles in a single ovary), the Androgen Excess Society and Polycystic Ovary Syndrome Society (AEPS) 2013 guidelines recommend using the follicle number per ovary $\geq$25 as the ultrasound threshold for PCOS when using newer technology that has maximal resolution of ovarian follicles (i.e., transducer frequency >8 MHz) [59]. The AEPS task force found that studies investigating women from the general population and studies analyzing control and PCOS populations with appropriate statistics suggest setting the criteria for increased FNPO at $\geq$25 follicles in women aged 18–35 years but maintaining the criteria for increased ovarian volume at $\geq$10 cm^3. They also noted that ovarian volume had less diagnostic potential for PCOM than FNPO. However, if such technology is not available, AEPS recommends using ovarian volume $\geq$10 cm^3 as the ultrasound threshold for rou-

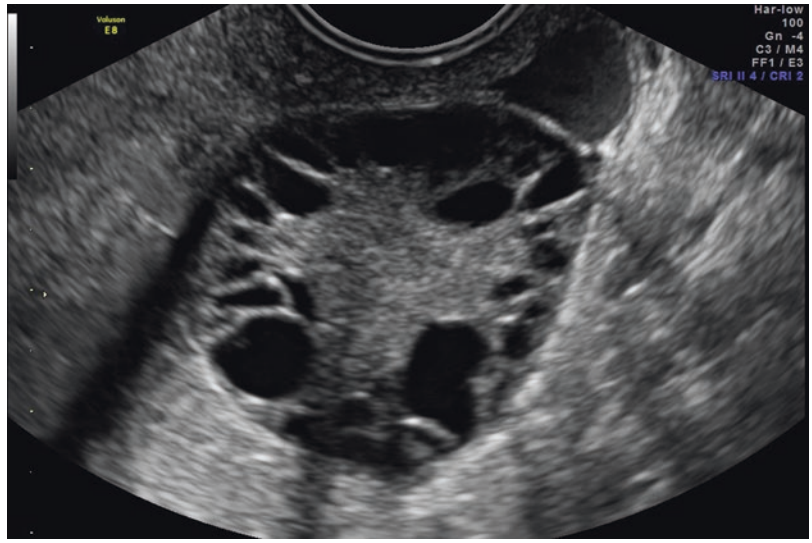

Fig. 5.6 Polycystic-appearing ovary

tine daily practice but not for research inquiries that necessitate the exact and complete characterization of patients.

Comparisons between transabdominal and transvaginal ultrasound do not find significant differences in the detection rate of polycystic ovaries. However, transabdominal sonography is not suitable for acquiring an exact follicle count but may reliably be used to quantify ovarian volume especially in circumstances where it is the only method to evaluate ovarian morphology. The automated 3D US techniques facilitate the exclusion of a false-positive PCOS diagnosis and reflect pathophysiological changes in these patients in a more accurate manner. It provides novel means to calculate follicle count and assess for ovarian volume and stromal vascularity. Due to the elevated risk for OHSS, an early detection of PCOS is highly recommended for women undergoing IVF treatment. No other imaging modality, such as magnetic resonance imaging (MRI) for the visualization of the ovaries, is needed for the diagnosis of PCOS.

At present, a few studies have evaluated the use of 3D US in PCOS patients [60–69], and a smaller amount has addressed automated 3D US (SonoAVC) [33, 57, 58, 70, 71]. Only one study had postulated a 3D US follicle threshold for PCOM using 3D volume-based software [57]. In this retrospective cohort study, Allemand et al. analyzed 29 normoandrogenic, ovulatory women with tubal or male factor infertility and 10 PCOS women with chronic anovulation and clinical or biochemical hyperandrogenism. Mean FNPO and the maximal number of follicles in a single sonographic plane (FSSP) were determined by 3D TVUS, and the ovarian volume was determined by 2D TVUS simultaneously. The authors posited a higher threshold of antral follicles (20 or more) for PCOS patients, which is considerably higher than that of the Rotterdam criteria. The authors explained this discrepancy by the identification of more follicles by 3D US. Moreover, the authors found the agreement level between the observers was 0.82. However, the weaknesses of this study are the small number of patients, missing direct comparison to 2D US, and low sensitivity (true positive rate) using receiver-operating characteristics (ROCs). Two studies comparing the follicle count between 3D and 2D methodology in polycystic ovaries had conflicting results. While Battaglia et al. [64] found no significant difference in the mean number of follicles between 2D and 3D US calculations in females with polycystic ovaries, Nylander et al. [72] found that 3D US counted more follicles than 2D US. The authors also found that ovarian volume measurements by 2D TVUS was 1.48 mL smaller than from 3D TVUS. In addition, there is increased stromal blood flow mea-

sured by Doppler and decrease in RI into the ovary. This may be part of the enhancement of production of androgens.

According to the AEPS, the literature suggests that 3D ultrasonography holds promise in the assessment of PCOM but states that more studies are needed before AEPS can recommend its routine use.

According to most publications dealing with 3D US in PCOS patients, there is a broad agreement about increased ovarian volume of polycystic ovaries [64, 66]. According to AEPS, the mean ovarian volume ranges from 10.6 and 16.7 mL in female with polycystic ovaries compare to 5.2 to 8.7 mL in healthy female of reproductive age [59]. Pascual et al [63] and Battaglia et al. [64] found strong correlation in ovarian volume calculations between 3D and 2D ultrasonography; however, AEPS stated that the discrepancy in overall ovarian size between the two studies (3D US measurements: 12.6 vs 13.2 $P < 0.05$, respectively) was significant, suggesting technical and interobserver variability. Despite this observation, AEPS did not recommend against using 3D US in determining ovarian volume for the diagnosis of PCOS. Conclusively, AEPS highly recommends the use of in-house reference normal ovarian volume values but recommends the existing ovarian volume $\geq$10 cm^3 criteria determine by either 2D or 3D US if in-house reference normal values are unavailable.

Nevertheless, there is still disagreement regarding ovarian vascularity, stromal changes, and cutoff values for antral follicles. More about PCOS is discussed in Chap. 6.

Antral Follicle Count and SonoAVC

The antral follicle count in 2D and 3D are generally similar although 3D ultrasound is superior for the high antral follicle population. In the inversion mode, follicles will appear white and can be counted easily. Image or volume rotation using the cine-loop facilitates the process (see Fig. 5.2a). Assisted reproductive techniques including in vitro fertilization (IVF) and ovulation induction require close monitoring of follicular development. Follicular development is commonly assessed with transvaginal ultrasounds during which each follicle is measured in two or three dimensions. As there are often more than 10–20 follicles, this is very time-consuming. In addition, follicular borders are irregular, and hence, this method has poor reproducibility and is often an inaccurate assessment of follicular volume. A software program called the automated follicular assessment using segmental topology or FAST program was developed to automate the follicular measurements. Therefore, our objective was to determine the accuracy, reproducibility, and efficiency of this novel program. This will be discussed further in another chapter.

One disadvantage of 2D ultrasonography for antral follicle counts involves inter- and intraobserver reproducibility. Of note, only a handful of studies compare the accuracy of ultrasound in regard to AFC and inter-/intraobserver reliability. Scheffer et al. [73] described the value of AFC determined by AVC needed for the improvement of standardization. They compared healthy volunteers with proven fertility to patients visiting an infertility clinic. For each patient, 2D or 3D TVUS was conducted for AFC (2–10 mm), and interobserver reliability was calculated. Both techniques were adequate when only a few follicles were present; however, when higher AFCs occurred, the reproducibility decreased with the 2D technique. In addition to this report, studies by the group of Raine-Fenning [33, 70, 71] demonstrated an improvement of interobserver/intraobserver reliability by the application of 3D methods (by automated systems, such as SonoAVC).

Research has been conducted to evaluate if AFCs vary at different point in the menstrual cycle and if ultrasonographic markers of ovarian reserve differ between the left and right ovary. Interestingly, Deb et al. found that small antral follicles ($\leq$6.0 mm) calculated using 3D US displayed little intra-cycle variation, while large AFC (>6.0 mm) and ovarian volume revealed significant intra-cycle variation [12]. Though some studies found there was no significant difference in AFC between the right and left ovary

[74, 75], most studies, especially those with larger sample sizes and utilizing 3D US, found that AFC was higher in the right ovary than the left [76, 77]. For instance, in a study of 1423 female of reproductive age, Korsholm et al. found that the right ovarian volume was larger than the left, AFC was higher in the right in those with higher AMH, and almost half of those with polycystic ovarian morphology in one ovary, more so in the right ovary than the left [78]. When measured with 3D US, Deb et al. also found that there is a significant difference in ovarian volume, total AFC of each ovary, and antral follicles >6.0 mm between the right and left ovary within an individual [79]. These studies stress the importance of performing a full characterization of both ovaries when scanning patients.

The SonoAVC software is especially designed for the automatic detection of multifollicular growth and to overcome the aforementioned problems of follicle observation by 2D US [32, 34, 70, 80–86]. This software allows not only the display of single follicles in 3D but also automatically calculates the number and volume of hypoechoic structures in a 3D echo-derived data set; furthermore, it provides estimations regarding the absolute dimensions of follicles. The only necessary requirement is adjustment of the ROI box over the entire ovary to include only the information which is needed for calculation and to check during post-processing. Measurements are based on calculation of the largest diameters in three orthogonal planes: the mean follicle diameter, the follicular volume, and the volume-based diameter of the follicle. Thus, the volume is calculated via the voxel count within hypoechoic structures. The true volume can be measured, and SonoAVC calculates the follicle diameter by rendering the follicle as a perfect sphere. This results in the visualization of sono-anatomic details, which could not previously be recognized. A major advantage of this sono-anatomic rendering is that individual structures are color-coded (see Fig. 5.4) allowing the exact count, which is needed for the determination of factors such as ovarian reserve. More about SonoAVC is discussed in Chap. 17.

AFC, AMH, and Oocyte Cryopreservation

Oocyte or embryo preservation after ovarian stimulation, ovarian tissue cryopreservation, in vitro maturation (IVM) of cumulo-oocyte complexes, and downregulation of ovaries with gonadotropin-releasing hormone analogue during chemotherapy are methods that have been attempted to preserve fertility in the female oncological patient. Though some of these options are controversial or experimental, others are more established for fertility preservation. The American Society of Clinical Oncology and the American Society for Reproductive Medicine state that ovarian stimulation for embryo or mature oocyte cryopreservation is the most established strategy to result in a future pregnancy [87, 88]. In those with estrogen-sensitive tumors or those who cannot delay cancer therapy, transvaginal retrieval of immature oocytes within IVM of oocytes may be considered. In this method, immature oocytes are retrieved from unstimulated postpubertal ovaries and subsequently matured in the laboratory for mature oocyte or embryo cryopreservation [88]. In a study by Sonigo et al., the researcher found that 20 antral follicles and 3.7 ng/ml AMH were the thresholds for cryopreservation of at least 10 meiosis II oocytes after IVM, while having ≤19 follicles or ≤3.0 ng/ml AMH was associated with a risk of cryopreservation of ≤2 mature oocytes [89]. However, due to limited studies on the safety and efficacy of this approach in the oncological patient, this technique is still considered investigational [88]. More studies need to be done to assess the efficacy and safety of this method and the potential of these oocytes after cryopreservation in patients with malignancies.

Conclusion

AFC is highly predictive for the ovarian reserve reflected by the number of oocytes retrieved on stimulation and strongly associated with the serum AMH level. This is helpful for counselling the patient and determining the stimulation protocol. The estimation of the ovarian response by US is simple and noninvasive; thus, it is an advis-

able procedure. The reliability of this method is increased with 3D instruments. There are several advantages of the new 3D US techniques. Software systems such as SonoAVC allow decreased inter- and intrapersonal variability in the processing, readout, and interpretation of ultrasound scans. While manual post-processing of US scans is required, this can be performed later once the patient is off the table. The ultrasound definition of PCOS may need modification to incorporate the 3D automated technology. More studies need to be done to evaluate the potential of cryopreservation of ovarian tissue or immature oocytes in the oncological patient.

References

1. Fleming R, Seifer D, Frattarelli JR, Ruman J. Assessing ovarian response: antral follicle count versus anti-Müllerian hormone. Reprod Biomed Online. 2015;31:486–96.
2. Nelson SM. Biomarkers of ovarian response: current and future applications. Fertil Steril. 2013;99:963–9.
3. Faddy MJ, Gosden RG, Gougeon A, Richardson SJ, Nelson JF. Accelerated disappearance of ovarian follicles in mid-life: implications for forecasting menopause. Hum Reprod. 1992;7:1342–6.
4. Robertson DM, Lee CH, Baerwald A. Interrelationships among reproductive hormones and antral follicle count in human menstrual cycles. Endocr Connect. 2016;6:98–107.
5. La Marca A, Argento C, Sighinolfi G, Grisendi V, Carbone M, D'Ippolito G, et al. Possibilities and limits of ovarian reserve testing in ART. Curr Pharm Biotechnol. 2012;13:398–408.
6. Hendriks DI, Mol BW, Bancsi LF, Te Velde ER, Broekmans FI. Antral follicle count in the prediction of poor ovarian reserve and IVF outcome after in vitro fertilization: a meta-analysis and comparison with basal FSH level. Fertil Steril. 2005;83:291–310.
7. Broekmans FJ, de Ziegler D, Howles CM, Gougeon A, Trew G, Olivennes F. The antral follicle count: practical recommendations for better standardization. Fertil Steril. 2010;94:1044–51.
8. Muttukrishna S, McGarrigle H, Wakim R, Khadum I, Ranieri DM, Sethal P. Antral follicle count, antimullerian hormone and inhibin B: predictors of ovarian response in assisted reproductive technology? BJOG. 2005;112:1384–90.
9. Johnson NP, Bagrie EM, Coomarasamy A, Bhattacharya S, Shelling AN, Jessop S, et al. Ovarian reserve tests for predicting fertility outcomes for assisted reproductive technology: the International Systematic Collaboration of Ovarian Reserve Evaluation protocol for a systematic review of ovarian reserve test accuracy. BJOG. 2006;113:1472–80.
10. Jayaprakasan K, Deb S, Batcha M, Hopkisson J, Johnson I, Campbell B, et al. The cohort of antral follicles measuring 2-6 mm reflects the quantitative status of ovarian reserve as assessed by serum levels of anti-Mullerian hormone and response to controlled ovarian stimulation. Fertil Steril. 2010;94:1775–81.
11. Jayaprakasan K, Chan Y, Islam R, Haoula Z, Hopkisson J, Coomarasamy A, et al. Prediction of in vitro fertilization outcome at different antral follicle count thresholds in a prospective cohort of 1,012 women. Fertil Steril. 2012;98:657–63.
12. Deb S, Campbell BK, Clewes JS, Pincott-Allen C, Raine-Fenning NJ. Intracycle variation in number of antral follicles stratified by size and in endocrine markers of ovarian reserve in women with normal ovulatory menstrual cycles. Ultrasound Obstet Gynecol. 2013;41:216–22.
13. Fratterelli JL, Lauria-Costab DF, Miller BT, Bergh PA, Scott RT. Basal antral follicle number and mean ovarian diameter predict cycle cancellation and ovarian responsiveness in assisted reproductive technology cycles. Fertil Steril. 2000;7:512–7.
14. Danninger B, Brunner M, Obruca A, Feichtinger W. Prediction of ovarian hyperstimulation syndrome by ultrasound volumetric assessment [corrected] of baseline ovarian volume prior to stimulation. Hum Reprod. 1996;11:1597–9.
15. Akbariasbagh F, Lorzadeh N, Azmoodeh A, Ghaseminejad A, Mohamadpoor J, Kazemirad S. Association among diameter and volume of follicles, oocyte maturity, and competence in intracytoplasmic sperm injection cycles. Minerva Ginecol. 2015;87(5):397–403.
16. Jayaprakasan K, Hilwah N, Kendall NR, Hopkisson JF, Campbell BK, Johnson IR, et al. Does 3D ultrasound offer any advantage in the pretreatment assessment of ovarian reserve and prediction of outcome after assisted reproduction treatment? Hum Reprod. 2007;22:1932–41.
17. Hsu A, Arny M, Knee AB, Bell C, Cook E, Novak AL, et al. Antral follicle count in clinical practice: analyzing clinical relevance. Fertil Steril. 2011;95:474–9.
18. van der Stege JG, van der Linden PJ. Useful predictors of ovarian stimulation response in women undergoing in vitro fertilization. Gynecol Obstet Investig. 2001;52:43–6.
19. Karande VC. Managing and predicting low response to standard in vitro fertilization therapy: a review of the options. Treat Endocrinol. 2003;2:257–72.
20. Broekmans FJ, Knauff EA, te Velde ER, Macklon NS, Fausser BC. Female reproductive ageing: current knowledge and future trends. Trends Endocrinol Metab. 2007;18:58–65.
21. Broer SL, Mol BWJ, Hendriks D, Broekmans FJM. The role of antimullerian hormone in prediction of outcome after IVF: comparison with the antral follicle count. Fertil Steril. 2009;91:705–14.
22. Riggs RM, Duran EH, Baker MW, Kimble TD, Hobeika E, Yin L, et al. Assessment of ovarian reserve with antimullerian hormone: a comparison of the predictive value of antimullerian hormone, follicle-

stimulating hormone, inhibin B and age. Am J Obstet Gynecol. 2008;199:202e1–8.
23. Hansen KR, Hodnett GM, Knowlton N, Craig LB. Correlation of ovarian reserve tests with histologically determined primordial follicle number. Fertil Steril. 2011;95:855–64.
24. Iliodromiti S, Kelsey TW, Wu O, Anderson RA, Nelson SM. The predictive accuracy of anti-Mullerian hormone for live birth after assisted conception: a systematic review and meta-analysis of the literature. Hum Reprod Update. 2015;20:560–57.
25. Brodin T, Hadziosmanovic N, Berglund L, Oloysson M, Holte J. Comparing four ovarian reserve markers-associations with ovarian response and live births after assisted reproduction. Acta Obstet Gynecol Scand. 2015 Oct;94(10):1056–63. https://doi.org/10.1111/aogs.12710.
26. Kedem A, Haas J, Geva LL, Yerushalmi G, Gilboa Y, Kanety H, et al. Ongoing pregnancy rates in women with low and extremely low AMH levels. A multivariate analysis of 769 cycles. PLoS One. 2013;8:e81629.
27. Reichman DE, Goldschlag D, Rosenwaks Z. Value of antimullerian hormone as a prognostic indicator of in vitro fertilization outcome. Fertil Steril. 2014;101:1012–8.
28. Jayaprakasan K, Al-Hasie H, Jayaprakasan R, Campbell B, Hopkisson J, Johnson I, et al. The three-dimensional ultrasonographic ovarian vascularity of women developing poor ovarian response during assisted reproduction treatment and its predictive value. Fertil Steril. 2009 Dec;92(6):1862–9.
29. ASRM Practice Guidelines. Testing and interpreting measures of ovarian reserve: a committee opinion. Fertil Steril. 2015;103(3):e9–e17.
30. Lass A, Brinsden P. The role of ovarian volume in reproductive medicine. Hum Reprod Update. 1999;5:256–66.
31. McDougall MJ, Tan SL, Jacobs HS. IVF and the ovarian hyperstimulation syndrome. Hum Reprod. 1992;5:597–600.
32. Ata B, Tulandi T. Ultrasound automated volume calculation in reproduction and in pregnancy. Fertil Steril. 2011;95:2163–70.
33. Raine-Fenning N, Jayaprakasan K, Clewes J, Joergner I, Bonaki SD, Chamberlain S, et al. SonoAVC: a novel method of automatic volume calculation. Ultrasound Obstet Gynecol. 2008;31:691–6.
34. Rodriguez-Fuentes A, Hernandez J, Garcia-Guzman R, Chinea E, Iaconianni L, Palumbo A. Prospective evaluation of automated follicle monitoring in 58 in vitro fertilization cycles: follicular volume as a new indicator of oocyte maturity. Fertil Steril. 2010;93:616–20.
35. Wertheimer A, Nagar R, Oron G, Meizner I, Fisch B, Ben-Haroush A. Fertility treatment outcomes after follicle tracking with standard 2-dimensional sonography versus 3-dimensional sonography-based automated volume count: prospective study. J Ultrasound Med. 2017; https://doi.org/10.1002/jum.14421.
36. Hernández J, Rodríguez-Fuentes A, Puopolo M, Palumbo A. Follicular Volume Predicts Oocyte Maturity: A Prospective Cohort Study Using Three-Dimensional Ultrasound and SonoAVC. Reprod Sci. 2016;23(12):1639–43.
37. Jadaon JE, Ben-Ami M, Haddad S, Radin O, Bar-Ami S, Younis JS. Prospective evaluation of early follicular ovarian stromal blood flow in infertile women undergoing IVF-ET treatment. Gynecol Endocrinol. 2012;28(5):356–9. https://doi.org/10.3109/09513590.2011.633659.
38. Vural F, Vural B, Doger E, Çakıroğlu Y, Çekmen M. Perifollicular blood flow and its relationship with endometrial vascularity, follicular fluid EG-VEGF, IGF-1, and inhibin-a levels and IVF outcomes. J Assist Reprod Genet. 2016;33:1355–62.
39. Chui DK, Pugh ND, Walker SM, Gregory L, Shaw RW. Follicular vascularity--the predictive value of transvaginal power Doppler ultrasonography in an in-vitro fertilization programme: a preliminary study. Hum Reprod. 1997;12:191–6.
40. Borini A, Tallarini A, Maccolini A, et al. Perifollicular vascularity monitoring and scoring: a clinical tool for selecting the best oocyte. Eur J Obstet Gynecol Reprod Biol. 2004;115:102–5.
41. Huyghe S, Verest A, Thijssen A, Ombelet W. The prognostic value of perifollicular blood flow in the outcome after assisted reproduction: a systematic review. Facts Views Vis Obgyn. 2017;9(3):153–6.. Review
42. Firouzabadi RD, Sekhavat L, Javedani M. The effect of ovarian cyst aspiration on IVF treatment with GnRH. Arch Gynecol Obstet. 2010 Mar;281(3):545–9.
43. Okaro E, Condous G, Khalid A, Timmerman D, Ameye L, Van Huffel S, et al. The use of ultrasound-based 'soft markers' for the prediction of pelvic pathology in women with chronic pelvic pain, can we reduce the need for laparoscopy? BJOG. 2006;113:251–6.
44. Raine-Fenning N, Jayaprakasan K, Deb S. Three-dimensional ultrasonographic characteristics of endometriomata. Ultrasound Obstet Gynecol. 2008;31:718–24.
45. Asch E, Levine D. Variations in appearance of endometriomas. J Ultrasound Med. 2007;26:993–1002.
46. Kumfer MC, Schwimer SR, Lebovic J. Transvaginal sonographic appearance of endometriomas: spectrum of findings. J Ultrasound Med. 1992;11:129–33.
47. Somigliana E, Vercellini P, Viganó P, Ragni G, Crosignani PG. Should endometriomas be treated before IVF-ICSI cycles? Hum Reprod Update. 2006;12:57–64.
48. Liu Z, Yang F, Zhang Y, Yu H, Zhu H, Yang R, Fan L. Conventional, Doppler and contrast-enhanced ultrasonography in differential diagnosis of ovarian masses. Cell Physiol Biochem. 2016;39(6):2398–408.
49. Balen A, Michelmore K. What is polycystic ovary syndrome? Are national views important? Hum Reprod. 2002;17:2219–27.
50. Polson DW, Adams J, Wadsworth J, Franks S. Polycystic ovaries--a common finding in normal women. Lancet. 1988;1:870–2.
51. Alborzi S, Khodaee R, Parsanejad ME. Ovarian size and response to laparoscopic ovarian electro-

cauterization in polycystic ovarian disease. Int J Gynaecol Obstet. 2001;74:269–74.
52. Amer SA, Li TC, Bygrave C, Sprigg A, Saravelos H, Cooke ID. An evaluation of the inter-observer and intra-observer variability of the ultrasound diagnosis of polycystic ovaries. Hum Reprod. 2002;17:1616–22; Jacobs HS. Polycystic ovaries and polycystic ovary syndrome. Gynecol Endocrinol 1987;1:113–31. Review.
53. Kousta E, White DM, Cela E, McCarthy MI, Franks S. The prevalence of polycystic ovaries in women with infertility. Hum Reprod. 1999;14:2720–3.
54. Dewailly D, Gronier H, Poncelet E, Robin G, Leroy M, Pigny P, et al. Diagnosis of polycystic ovary syndrome (PCOS): revisiting the threshold values of follicle count on ultrasound and of the serum AMH level for the definition of polycystic ovaries. Hum Reprod. 2011;26(11):3123–9. https://doi.org/10.1093/humrep/der297.. Epub 16 Sep 2011
55. Dewailly D, Lujan ME, Carmina E, Cedars MI, Laven J, Norman RJ, et al. Definition and significance of polycystic ovarian morphology: a task force report from the Androgen Excess and Polycystic Ovary Syndrome Society. Hum Reprod Update. 2013;20(3):334–52. https://doi.org/10.1093/humupd/dmt061.
56. Rotterdam ESHRE/ASRM-Sponsored PCOS Consensus Workshop Group. Revised 2003 consensus on diagnostic criteria and long-term health risks related to polycystic ovary syndrome. Fertil Steril. 2004;81:19–25.
57. Allemand MC, Tummon IS, Phy JL, Foong SC, Dumesic DA, Session DR. Diagnosis of polycystic ovaries by three-dimensional transvaginal ultrasound. Fertil Steril. 2006;85:214–9.
58. He LR, Zhou LX, Pan RK, Zhang X. Clinical significance of counting follicles in diagnosis of polycystic ovary syndrome by the three-dimensional ultrasound imaging with sonography based automated volume calculation method. Zhonghua Fu Chan Ke Za Zhi. 2011;46:350–4.
59. Goodman NF, Cobin RH, Futterweit W, Glueck JS, Legro RS, Carmina E, American Association of Clinical Endocrinologists (AACE); American College of Endocrinology (ACE); Androgen Excess and PCOS Society (AES). American Association of Clinical Endocrinologists, American College of Endocrinology, and Androgen Excess and PCOS Society Disease State Clinical Review: guide to the best practices in the evaluation and treatment of polycystic ovary syndrome--part 1. Endocr Pract. 2015 Nov;21(11):1291–300.
60. Lam PM, Johnson IR, Raine-Fenning NJ. Three-dimensional ultrasound features of the polycystic ovary and the effect of different phenotypic expressions on these parameters. Hum Reprod. 2007;22(12):3116–23. https://doi.org/10.1093/humrep/dem218.
61. Lam P, Raine-Fenning N, Cheung L, Haines C. Three-dimensional ultrasound features of the polycystic ovary in Chinese women. Ultrasound Obstet Gynecol. 2009;34(2):196–200. https://doi.org/10.1002/uog.6442.
62. Sun L, Fu Q. Three-dimensional transrectal ultrasonography in adolescent patients with polycystic ovarian syndrome. Int J Gynecol Obstet. 2007;98(1):34–8. https://doi.org/10.1016/j.ijgo.2007.02.024.
63. Pascual MA, Graupera B, Hereter L, Tresserra F, Rodriguez I, Alcázar JL. Assessment of ovarian vascularization in the polycystic ovary by three-dimensional power Doppler ultrasonography. Gynecol Endocrinol. 2008;24(11):631–6. https://doi.org/10.1080/09513590802308099.
64. Battaglia C, Battaglia B, Morotti E, Paradisi R, Zanetti I, Meriggiola MC, et al. Two- and three-dimensional sonographic and color Doppler techniques for diagnosis of polycystic ovary syndrome. J Ultrasound Med. 2012;31(7):1015–24. https://doi.org/10.7863/jum.2012.31.7.1015.
65. Peres Fagundes PA, Chapon R, Olsen PR, Schuster AK, Mattia MM, Cunha-Filho JS. Evaluation of three-dimensional SonoAVC ultrasound for antral follicle count in infertile women: Its agreement with conventional two-dimensional ultrasound and serum levels of anti-Müllerian hormone. Reprod Biol Endocrinol. 2017;15(1):1–7.
66. Järvelä IY, Mason HD, Sladkevicius P, Kelly S, Ojha K, Campbell S, et al. Characterization of normal and polycystic ovaries using three-dimensional power Doppler ultrasonography. J Assist Reprod Genet. 2002;19:582–90.
67. Pan HA, Wu MH, Cheng YC, Li CH, Chang FM. Quantification of Doppler signal in polycystic ovary syndrome using three-dimensional power Doppler ultrasonography: a possible new marker for diagnosis. Hum Reprod. 2002;17:201–6.
68. Jokubkiene L, Sladkevicius P, Valentin L. Number of antral follicles, ovarian volume, and vascular indices in asymptomatic women 20 to 39 years old as assessed by 3-Dimensional sonography. J Ultrasound Med. 2012;31(10):1635–49. https://doi.org/10.7863/jum.2012.31.10.1635.
69. Scheffer GJ, Broekmans FJ, Bancsi LF, Habbema JD, Looman CW, Te Velde ER. Quantitative transvaginal two- and three-dimensional sonography of the ovaries: reproducibility of antral follicle counts. Ultrasound Obstet Gynecol. 2002;20:270–5.
70. Raine-Fenning N, Jayaprakasan K, Chamberlain S, Devlin L, Priddle H, Johnson I, et al. Automated measurements of follicle diameter: a chance to standardize? Fertil Steril. 2009;91:1469–72.
71. Raine-Fenning N, Jayaprakasan K, Deb S, Clewes J, Joergner I, Dehghani Bonaki S, Johnson I. Automated follicle tracking improves measurement reliability in patients undergoing ovarian stimulation. Reprod Biomed Online. 2009;18(5):658–63.
72. Nylander M, Frøssing S, Bjerre AH, Chabanova E, Clausen HV, Faber J, et al. Ovarian morphology in polycystic ovary syndrome: estimates from 2D and 3D ultrasound and magnetic resonance imaging and

their correlation to anti-Müllerian hormone. Acta Radiol. 2017 Aug;58(8):997–1004.
73. Scheffer GJ, Broekmans FJ, Dorland M, Habbema JD, Looman CW, Velde ER. Antral follicle counts by transvaginal ultrasonography are related to age in women with proven natural fertility. Fertil Steril. 1999;72(5):845–51.
74. Baerwald AR, Adams GP, Pierson RA. A new model for ovarian follicular development during the human menstrual cycle. Fertil Steril. 2003;80(1):116–22. https://doi.org/10.1016/s0015-0282(03)00544-2.
75. Jokubkiene L, Sladkevicius P, Valentin L. Number of antral follicles, ovarian volume, and vascular indices in asymptomatic women 20 to 39 years old as assessed by 3-Dimensional sonography: A prospective cross-sectional study. J Ultrasound Med. 2012;31(10):1635–49. https://doi.org/10.7863/jum.2012.31.10.1635.
76. Alserri A, Kuriya A, Holzer H, Tulandi T. Lateralization of ovarian follicles. Gynecol Obstet Investig. 2014;77(2):117–20. https://doi.org/10.1159/000358395.
77. Köninger A, Koch L, Edimiris P, Nießen S, Kasimir-Bauer S, Kimmig R, et al. Intraindividual right–left comparison of sonographic features in polycystic ovary syndrome (PCOS) diagnosis. Eur J Obstet Gynecol Reproduct Biol. 2014;181:124–9.
78. Korsholm AS, Hvidman HW, Bentzen JG, Nyboe Andersen A, Birch PK. Left-right differences in ovarian volume and antral follicle count in 1423 women of reproductive age. Gynecol Endocrinol. 2017;33(4):320–3. https://doi.org/10.1080/09513590.2016.1259406.
79. Deb S, Kannamannadiar J, Campbell BK, Clewes JS, Raine-Fenning NJ. The interovarian variation in three-dimensional ultrasound markers of ovarian reserve in women undergoing baseline investigation for subfertility. Fertil Steril. 2011;95(2):667–72.
80. Deutch TD, Joergner I, Matson DO, Oehninger S, Bocca S, Hoenigmann D, et al. Automated assessment of ovarian follicles using a novel three-dimensional ultrasound software. Fertil Steril. 2009 Nov;92(5):1562–8.
81. Raine-Fenning N, Deb S, Jayaprakasan K, Clewes J, Hopkisson J, Campbell B. Timing of oocyte maturation and egg collection during controlled ovarian stimulation: a randomized controlled trial evaluating manual and automated measurements of follicle diameter. Fertil Steril. 2010;94:184–8.
82. Ben-Haroush A, Farhi J, Zahalka Y, Sapir O, Meizner I, Fisch B. Small antral follicle count (2-5 mm) and ovarian volume for prediction of pregnancy in in vitro fertilization cycles. Gynecol Endocrinol. 2012:28(6)432–5.
83. Deb S, Jayaprakasan K, Campbell BK, Clewes JS, Johnson IR, Raine-Fenning NJ. Intraobserver and interobserver reliability of automated antral follicle counts made using three-dimensional ultrasound and SonoAVC. Ultrasound Obstet Gynecol. 2009;33:477–83.
84. Deb S, Campbell BK, Clewes JS, Raine-Fenning NJ. Quantitative analysis of antral follicle number and size: a comparison of two-dimensional and automated three-dimensional ultrasound techniques. Ultrasound Obstet Gynecol. 2010;35:354–60.
85. Jayaprakasan K, Campbell BK, Clewes JS, Johnson IR, Raine-Fenning NJ. Three-dimensional ultrasound improves the interobserver reliability of antral follicle counts and facilitates increased clinical work flow. Ultrasound Obstet Gynecol. 2008;31:439–44.
86. Forman RG, Robinson J, Yudkin P, Egan D, Reynolds K, Barlow DH. What is the true follicular diameter: an assessment of the reproducibility of transvaginal ultrasound monitoring in stimulated cycles. Fertil Steril. 1991;56:89–92.
87. Loren AW, Mangu PB, Beck LN, Brennan L, Magdalinski AJ, Partridge A, et al. Fertility preservation for patients with cancer: American Society of Clinical Oncology clinical practice guideline update. J Clin Oncol. 2013;31(19):2500–10. https://doi.org/10.1200/jco.2013.49.2678.
88. Practice Committee of American Society for Reproductive Medicine. Fertility preservation in patients undergoing gonadotoxic therapy or gonadectomy: a committee opinion. Fertil Steril. 2013;100(5):1214–23.
89. Sonigo C, Simon C, Boubaya M, Benoit A, Sifer C, Sermondade N, et al. What threshold values of antral follicle count and serum AMH levels should be considered for oocyte cryopreservation after in vitro maturation? Hum Reprod. 2016;31(7):1493–500.

PCOS

6

Ana M. Monzo, Nikolaos Prapas, and Artemis Karkanaki

The Definition of Polycystic Ovary Syndrome

Polycystic ovary syndrome (PCOS) is the most commonly diagnosed endocrine disorder, affecting up to 10% of women of reproductive age with highly heterogeneous presentation [1, 2]. PCOS is associated with metabolic adverse outcomes and reproductive dysfunction [3]. Until 2003, when the presence of polycystic ovarian morphology (PCOM) was included, the diagnosis of PCOS was based on the presence of clinical or laboratory evidence of hyperandrogenemia and chronic oligo- or anovulation [4]. Despite the name of this syndrome, polycystic ovarian morphology (PCOM) was not considered for the diagnosis until the consensus workshop held in Rotterdam in 2003 [5, 6]. Thereafter, the sonographic evidence of polycystic morphology was recognized as an equal diagnostic criterion of the syndrome and was further defined and simplified into the existence of either 12 or more follicles of 2–9 mm diameter or an increased ovarian volume of more than 10 cm^3 on both or even one ovary. Thus, the current diagnosis of PCOS requires the presence of two of the following three findings: hyperandrogenism, chronic ovulatory dysfunction, and PCOM. Importantly, PCOM should not be confused with the syndrome, since the diagnosis of PCOS presupposes the existence of one more diagnostic criterion at least. Nevertheless, the prevalence of PCOS varies according to the diagnostic criteria used, with estimates ranging from 9% in women of reproductive age, according to NIH (National Institutes of Health) criteria, up to 18%, with the Rotterdam criteria) [3, 7, 8].

It should be emphasized that the diagnosis is posed after the exclusion of secondary causes that mimics the clinical expression of PCOS, as thyroid dysfunction, hyperprolactinemia, congenital adrenal hyperplasia (including nonclassical), Cushing's syndrome, androgen-secreting tumors, and idiopathic hirsutism. Thus, four distinct clinical phenotypes of PCOS are recognized, according to the combination of manifestations [9]. The distinct phenotypes are seen in Table 6.1. The first two phenotypes, already diagnosed by the old criteria of NIH of 1990 [4], are widely characterized as the "classic PCOS." The last two groups, "newer PCOS,"

A. M. Monzo (✉)
La Fe University Hospital, University of Valencia, Human Reproduction Unit, Department of Obstetrics and Gynecology, Reproductive Medicine Research Group, Instituto de Investigación Sanitario La Fe, Valencia, Spain
e-mail: monzo_ana@gva.es

N. Prapas · A. Karkanaki
Third Department of Obstetrics and Gynecology, Hippokratio General Hospital of Thessaloniki, Thessaloniki, Greece

Aristotle University of Thessaloniki, Thessaloniki, Greece

L. A. Stadtmauer, I. Tur-Kaspa (eds.), *Ultrasound Imaging in Reproductive Medicine*,
https://doi.org/10.1007/978-3-030-16699-1_6

Table 6.1 Classification of PCOS phenotypes

Phenotypes	A	B	C	D
Hyperandrogenism	+	+	+	–
Ovarian Dysfunction	+	+	–	+
PCOM	+	–	+	+
	Classic PCOS		Newer PCOS	

Hyperandrogenism (clinical or biochemical), ovarian dysfunction (oligo-amenorrhea or chronic anovulation)
PCOM polycystic ovarian morphology

comprise additional phenotypes that aroused after the new diagnostic criteria of Rotterdam [5, 6], and both include the polycystic ovarian morphology as a feature in contrast to the classic PCOS phenotypes. However, despite the consented criteria, there is still uncertainty concerning the importance of each syndrome feature and the severity of the metabolic and reproductive dysfunction every phenotype implies [9, 10].

The unstable and relatively common finding (20–25%) of PCOM in the general population [11, 12] triggered the opposition of the Androgen Excess Society which stated that PCOS is a primarily androgen excess disorder, and this feature should be a prerequisite for the diagnosis of the syndrome. Subsequently, according to the Androgen Excess Society, one of the two newer phenotypes with polycystic ovarian morphology and anovulation could not be defined as PCOS [13]. However, this opinion is not widely accepted and is currently under investigation.

Importantly, none of the current criteria take into account the normal changes in ovarian volume and follicle number with the age in women with PCOS. The adult diagnostic criteria for PCOS include normal physiological events that occur during puberty, and there may be an amelioration of clinical features of PCOS during the menopausal transition. In fact, acne, changes in hair growth, and menstrual irregularities are normal physiological events that develop during puberty and may represent clinical evidence of elevated androgen levels if they are severe and persisting during puberty. Some features of polycystic ovarian morphology on ultrasound can be normal in healthy pubertal girls [14]. In addition, there is a trend toward more regular cycles and improvement on hirsutism with aging, ovarian volume decreases, and morphology may be less evident in PCOS during menopausal transition. For these reasons, PCOS diagnosis should be carefully assessed at these specific moments in order to not increase or decrease artificially the prevalence of PCOS, and age-based ultrasound criteria for polycystic ovary morphology should be defined.

The Polycystic Ovarian Morphology (PCOM)

The polycystic ovarian morphology (PCOM), as defined in Rotterdam, is conditioned by two elements, the presence of 12 or more follicles (2–9 mm diameter) and/or ovarian volume more than 10 cm^3, in a single or both ovaries. This definition leaves no margin for subjective assessments regarding the diagnosis which can be set even with polycystic morphology in a single ovary. Women taking an oral contraceptive pill cannot be diagnosed as the pill reduces the ovarian volume despite the possible persistence of PCOM [5, 6, 15]. In the case of a dominant follicle (>10 mm) or a corpus luteum, the ultrasonography should be repeated in the next cycle, while an abnormal cyst or ovarian asymmetry requires further investigation [5, 6, 16].

Furthermore, the transvaginal approach, whenever possible, and especially in obese women, is highly recommended. Importantly, the scan should be performed during the early follicular phase (days 3–5) of a spontaneous cycle in women with regular cycles and of a progesterone-induced bleeding episode or randomly in women with irregular cycles [5, 6]. The time of the day is meaningful only if Doppler examination is performed due to the diurnal variation in uterine and ovarian blood flow [17, 18].

The current definition of PCOM does not taken into account the distribution of the follicles, the stromal brightness (echogenicity), and its volume; finally, there is not reference to the blood flow characteristics through the uterine and ovarian arteries, including the intraovarian stromal blood flow.

The typical polycystic ovary was initially described by Adams et al. as an enlarged ovary

with highly vascular and hyperechogenic stroma, compared to the cortex, and with many small follicles arranged in the periphery [19]. Interestingly, the cohort of small follicles of 2–5 mm diameter seems to be a better indicator of the ovarian reserve [20] and is negatively determined by the age [21]. This agrees with the hypothesis that the excess of AMH production and/or of 2–5 mm follicles, resulting from hyperandrogenism, is involved in the follicular arrest of PCOS, and its role on follicular growth lasts up to the stage of 2–5 mm and then declines [59]. In PCOS patients, there is a strong negative correlation between the numbers of follicles sized 2–5 and 6–9 mm, and it is not linked to metabolic parameters [22].

On the other hand, the term multifollicular ovary refers to an ovary with many small follicles of variable size, scattered through an increased amount of stroma, but not in the classic type of "necklace" as in the polycystic ovary. Multicystic ovary may represent a milder disturbance of the ovary where normal folliculogenesis happens to some degree [23]. Multicystic ovaries are common in early adolescence and in the majority regress without evolving to PCOS [24].

Asymptomatic women with only PCOM are commonly found in the general population up to 32% of women [25]. These women may conceal some mild abnormalities of androgen secretion, insulin sensitivity, and glucose metabolism [26–28], though the data are still contradictory [26]. It has been named latent PCOS [29]. The sole presence of polycystic ovarian morphology seems to recede with age and especially after the age of 35 years [25, 30]. However, when women with PCOM are subjected to controlled ovarian stimulation and ovulation, as an infertility treatment, they behave like women with PCOS and are faced with an increased risk of hyperstimulation and ovarian hyperstimulation syndrome (OHSS) [31–33]. Indeed, Swanton et al. found that the rates of severe OHSS were similar between women with PCOM and PCOS and significantly higher compared to controls [31]. In spite of significantly lower doses of FSH, women with both PCOM and PCOS responded with higher estradiol level numbers of retrieved oocytes to controlled ovarian stimulation [32, 34, 35].

Furthermore, serum, basal anti-Müllerian hormone (AMH) levels of women with PCOM were found intermediate between controls and women with PCOS, despite the low androgen levels, suggesting a granulosa cell abnormality [36]. Likewise, AMH concentrations and follicle numbers, after controlled ovarian stimulation, were shown higher in women with PCOM compared to controls and lower compared to PCOS patients with PCOM and hyperandrogenism [37].

Regardless of the response and the possibility of OHSS, there was no difference in fertilization, implantation, clinical pregnancy, and live birth rates among women with PCOM and PCOS and controls [31, 32, 38]. Importantly, women with PCOM had similar oocyte and embryo quality with women with PCOS but significantly lower miscarriage rates [34].

In conclusion, the ultrasound assessment of PCOM is very useful for the diagnosis of PCOS and possibly its severity and prognosis, the surveillance of the controlled ovarian stimulation in such patients, the prediction of outcome following fertility treatments, the diagnosis of OHSS, the decision of turning to in vitro oocyte maturation or freeze-all embryos in these women, and the diagnosis of other genital tract anomalies and even endometrial hyperplasia that are often overlooked [5, 6, 31, 39, 40]. A point to consider during every ultrasound scanning is that the diagnosis of polycystic ovarian morphology does not exclude other underlying causes of infertility as well as internal genitalia malformations.

Follicle Number and Size

The antral follicle count (AFC) is a direct quantitative marker of ovarian reserve and responsiveness to ovarian stimulation [41]. The follicular number shows an annual loss of 0.35–0.95 antral follicles per year following the reproductive aging of women [42]. There is a high correlation between AFC and reproductive age which is widely applicable in assisted reproduction treatments [43, 44]. The visible follicle by ultrasound means is the result of a sophisticated journey of an oocyte through the reproductive life of a

female. A follicle is an oocyte surrounded by granulosa cells. The follicle grows by a small increase in the oocyte volume, a significant proliferation of the surrounding granulosa cells, and an expansion of the antral cavity. There are three stages of follicles: primordial, early growing, and antral [45, 46].

Primordial follicles have a very small size of less than 0.05 mm and are not visible [47]. Early growing follicles are less than 2 mm and comprise of large primary, secondary, preantral, early antral, and small antral follicles [45]. Several months are required for a new growing follicle to reach the preantral stage (0.15 mm) and 70 additional days to reach the size of 2 mm. Early growing follicle growth is unaffected by cyclic hormonal fluctuations and is regulated by subtle interactions between FSH and local factors produced by theca and granulosa cells, as well as the oocyte [48].

Only a small number of preantral follicles progress to antral stage which are more than 2 mm and become selectable during the late follicular phase [49]. From the time they enter the selectable stage during the late luteal phase, follicles become sensitive to cyclic changes of FSH in terms of granulosa cell proliferation. These are the follicles that contribute to the hormonal cyclic profile depicted in the classic diagram of the menstrual cycle. Indeed, as the follicle develops, its responsiveness to gonadotropins progressively increases under the control of local factors acting in an autocrine/paracrine fashion [48].

The number of these selectable follicles, especially the small antral (2–5 mm), is believed to reflect the number of remaining primordial follicles and, thus, the ovarian reserve [50]. The larger follicles >6 mm are totally gonadotropin dependent, and one of them will evolve to dominant during the next follicular phase, while the rest will become atretic. So, in this phase, all other healthy follicles with granulosa cell activity tend not to exceed 6 mm, suggesting that all larger follicles are possibly atretic and do not reflect the actual reproductive capability of the woman [51, 52]. In agreement with this hypothesis, serum AMH levels are also strongly correlated to the count of small antral follicle (2–5 mm) [53] but not to the 6–9 mm follicle pool in normo-ovulatory and PCOS patients [22]. Moreover, in vitro studies show that AMH levels are low or undetectables in follicles larger than 9 mm [54].

In PCOS, the balance between androgens, anti-Müllerian hormone (AMH), and FSH is disrupted leading to follicular arrest [55]. Abundant LH drives the theca cells to produce androgens, but FSH concentrations and conversion of androgens to estradiol are insufficient, resulting in failure to select a dominant follicle, thus chronic anovulation [56]. AMH, secreted by granulosa cells, plays a major role in governing this balance because it inhibits transition from primordial to primary follicles. Hence, PCOS is characterized by increased growth of small follicles (2–5 mm) [20] and subsequent growth arrest leading to the typical polycystic morphology. AMH may have a role in suppressing FSH action contributing to anovulation. Still, the 6–9 mm follicles also appear to be affected by the unfavorable environment of the syndrome [58]. Although the pool of growing primary and secondary follicles in PCOS women is two- to threefold that of normal ovaries, the pool of primordial follicles is normal [57].

The follicle number, using two-dimensional (2D) ultrasound, is estimated both in longitudinal and anteroposterior cross sections of the ovaries, as the performer slowly moves the transducer from one side of the ovary to the other. After the identification of the ovary, a scout sweep is performed in the two planes, and the largest follicle is localized. Then the counting is performed starting from the outer ovarian margin to the opposite. The procedure is repeated with the contralateral ovary [45]. It has been observed that the number of follicles counted by 2D is overestimated compared to oocytes retrieved and even more in ovaries with many follicles as the polycystic when they are stimulated, possibly because of double counting (repetitions) and inclusion of atretic follicles [45, 59].

The size of follicles in 2D ultrasonography is expressed as the mean of the diameters measured on the two aforementioned sections [5, 6]. However, in clinical practice, three techniques are applied [60]. The first includes a single measurement of the maximal diameter in the lon-

gitudinal plane; the second includes an additional measurement of a diameter at 90° to the first; and the third is expanded to the measurement of a perpendicular to the previous two diameters in the transverse plane, after manual rotation of the transducer. In the latter two cases, the diameter is the mean of the two or three diameters, respectively.

Nevertheless, with more sensitive ultrasound probes and the vaginal route, well-trained operators can visualize and count small follicles of less than 2 mm nowadays. Therefore, the consequence of the improved ovarian imaging is the reevaluation of the current follicle number threshold. In this direction, the Androgen Excess and PCOS Society [61] recommends setting the threshold at 25 or more follicles per ovary, only when using newer technology that affords maximal resolution (devices with maximum probe frequencies >8 MHz), and also per age classes to better define PCOS [62, 81].

None of the ultrasound criteria take into account the normal decrease in ovarian volume and follicle number with age. As suggested by Kim and coworkers [63], age-specific cutoffs for defining ultrasound PCOM are needed for PCOS women.

However, even with the most advanced ultrasonography devices, evaluation of PCOM for diagnosis of PCOS has high variability, and it can be difficult to count antral follicles transabdominally in obese or virgin patients. In these cases, there is a need for more objective parameters, and the serum AMH level could be useful for diagnosis of PCOS [64] with a cutoff of 4.7 ng/dl, although AMH does not appear to be helpful in all phenotypes [65, 66].

Alternatively, the size of a follicle could be defined by its volume. For optimal in vitro fertilization (IVF) outcome, the follicular fluid volume should be more than 1 and up to 7 mL, which corresponds to a spheroid follicle diameter of 12–24 mm [67]. The follicular volume can be calculated by 2D ultrasound from the mean diameter using the formula of a sphere: $4/3 \times \pi \times$ diameter [68]. When the mean diameter is estimated by the three follicular diameters, as described above, it is more accurate [60]. Follicles scarcely have the shape of a sphere; they usually are more elliptical, and therefore, the formula of a sphere does not provide an accurate estimation of the volume [69].

This matter has been addressed by the three-dimensional (3D) calculation of follicular volume which can be assessed by two ways: manually and automatically. The manual measurement is performed more often by the program virtual organ computer-aided analysis (VOCAL®). Initially, the data is acquired by an automatic mechanical sweep of the region ensuring that the entire ovary is included. The process is repeated for the contralateral ovary, and the data are saved. The data are then processed using VOCAL. Each follicle is delineated manually by tracing around its perimeter, and the volume of interest is calculated automatically.

The automatic technique is performed by the program automatic volume calculation (SonoAVC®). The data are captured as described above and then processed by SonoAVC after right positioning. This program identifies every single follicle with a specific color and then automatically calculates the mean diameter (relaxed sphere diameter), the maximum dimensions (x, y, z), and the follicle volume (Fig. 6.1). This later method is highly valid and provides more accurate values than those estimated from 2D measurements and automated measurements of follicular diameter as well as calculated using VOCAL [59, 60, 70].

AFC can also be performed by 3D ultrasound. Data are acquired as described above. There are three ways to count the follicles. In the first, the observer counts manually the follicles in a multiplanar view that is using all three perpendicular planes simultaneously in order to enhance the spatial awareness. In the second way, the ovary is defined by VOCAL, inversion mode is applied, the follicles are displayed without the surrounding ovarian tissue, and, finally, the counting is performed in multiplanar view (Figs. 6.2 and 6.3). In the last way, SonoAVC displays every single follicle in a specific color in an inversion mode, again without the ovarian tissue (see Fig. 6.1). SonoAVC can distinguish follicles of 1–2 mm diameter and provides the option of post-procession where manually the observer picks any missed follicles or excludes any that

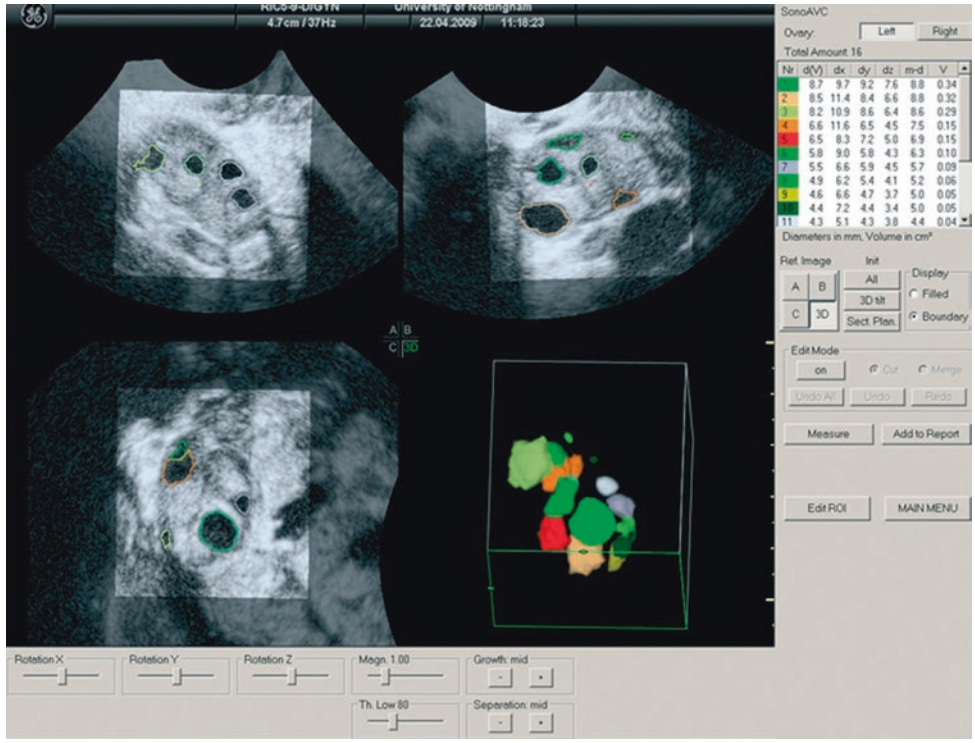

Fig. 6.1 Multiplanar display of an ovarian three-dimensional ultrasound dataset by SonoAVC. Each follicle has a specific color, and its measurements are displayed on the right side. (Reprinted from Deb et al. [52]. With permission from John Wiley & Sons, Inc.)

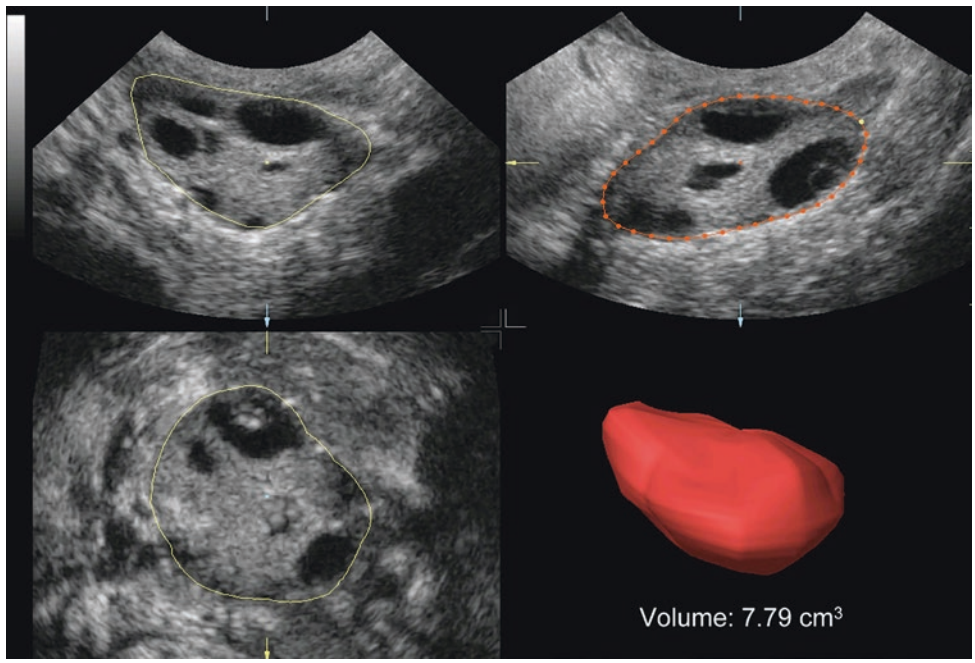

Fig. 6.2 Ovarian volume calculation using VOCAL before the application of inversion mode. (Reprinted from Jayaprakasan et al. [71], by permission of Oxford University)

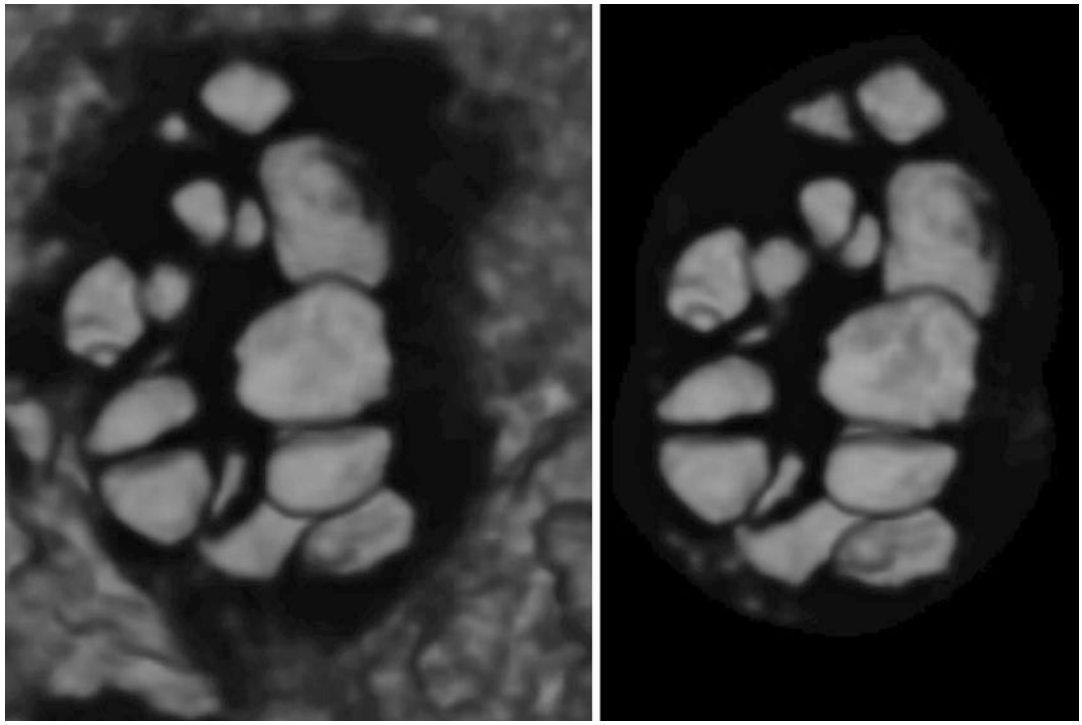

Fig. 6.3 Ovarian volume calculation using VOCAL after application of inversion mode. (Reprinted from Jayaprakasan et al. [71], by permission of Oxford University)

has been included incorrectly. Post-procession seems necessary since SonoAVC misses follicles of random sizes that are easily recognized in the multiplanar view due to their specific color [72].

Although only a few studies have compared follicle counts with 3D and 2D ultrasonography in PCOS, and the data suggest that 3D methodology holds promise in the evaluation, further studies are required before its routine use can be recommended [61]. One recent study has demonstrated that AFC with 2D transvaginal ultrasound was significantly lower than estimates from 3D and magnetic resonance imaging (MRI) in overweigth PCOS patients. Moreover, serum AMH correlated strongest with antral follicular count from 3D when compared to 2D and MRI [73].

Ovarian Volume

Women with PCOS have a larger ovarian volume [16, 19, 20, 74, 75]. The ovarian volume (OV) declines with age as the follicle both in women with PCOS and controls, but this decline does not correlate so well with age as the follicle number does [42, 76, 77]. The pattern of the OV falling in women with PCOS is different because it declines less markedly than of controls despite the similar decline in follicle number. This fact suggests that the stroma plays a significant role [77, 78] and also the size of the follicles, because the decrease with age affects mainly the number of small follicles (2–6 mm) but not of bigger follicles (7–10 mm) in women with PCOS [79]. Alsamarai et al. demonstrated a linear decline in OV and concluded that age-dependent criteria for the diagnosis of PCOS are necessary [77]. This point could be of value in assisted reproduction field as the patients are very often more than 40 years old but still in danger for OHSS.

The calculation of the OV is performed either using the formula for a prolate ellipsoid (0.5233 × length × width × thickness) [5, 6] or automatically by the software of the ultrasound

equipment just outlining the ovary. The simplified formula, 0.5 × length × width × thickness, is practical and easy to use. The polycystic ovarian morphology is diagnosed when the OV exceeds 10 cm^3 [5, 6]. This consensus definition was based on the findings of studies that investigated the sensitivity and specificity of a diagnostic cut-off level [20, 74, 75]. Lower volume thresholds have been proposed subsequently ranging to 6.4 to 7 cm^3 [80, 81].

However, the use of OV rather than follicle count for the diagnosis of PCOS has not been adequately validated and may have a relatively low sensitivity for discriminating between patients with PCOS and controls [61]. Again 3D ultrasound provides a more reliable, accurate, and reproducible assessment of OV than the 2D-based methods, with better spatial information and the ability to correct any shape irregularities [67, 82–84]. Three-dimensional ultrasound also confirmed the greater OV of women with PCOS [85–88]. There are two ways to calculate the OV: the conventional full planar technique and the VOCAL program. During the conventional method, the observer scrolls through one plane of the multiplanar display and simultaneously delineates the ovary in a different plane [84, 88]. With VOCAL program, the observer manually defines the contour of the ovary, while the dataset is rotated through 180° [88] (Fig. 6.4). Raine-Fenning et al. compared the two techniques and found that measurements with VOCAL program are superior to conventional, though comparable [88, 90].

Recently, a cross-sectional study including 313 PCOS women has concluded that OV > 10 cc was two times more likely than those with OV ≤ 10 cc to exhibit biochemical markers of

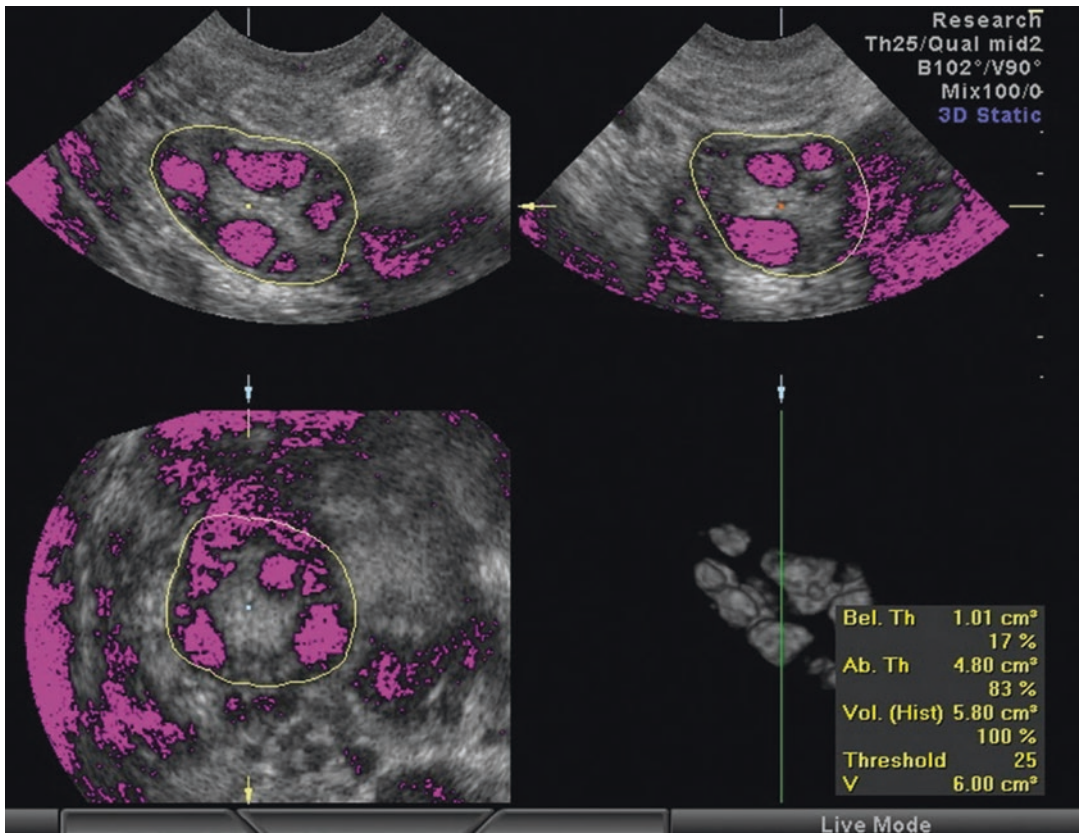

Fig. 6.4 Calculation of stromal volume determining the stromal and follicular area by setting a threshold of voxels. (Reprinted from Lam et al. [89], by permission of Oxford University)

insulin resistance, suggesting that OV is an important factor associated with metabolic risk in women with PCOS [91].

Stromal Area, Volume, and Echogenicity

Despite the fact that increased stromal area and echogenicity are not included to the diagnostic criteria of PCOS, they are still characteristic ultrasonographic features of the syndrome [75, 91]. Patients with PCOS present higher stromal area and volume [75, 78, 89, 91–95] with the exception of a Chinese PCOS population [85]. Stromal hypertrophy is a common and specific indicator of ovarian hyperandrogenism [91]. The hypertrophic theca cells in the stroma of women with PCOS produce higher amounts of androgens [93]. Indeed, ovarian stromal area was found to correlate with androgen levels and free androgen index (FAI) [78, 91, 96]. In clinical practice, the measurement of ovarian volume is a good surrogate for the stromal volume, because increased stromal volume is the main cause of ovarian enlargement in PCOS, except for patients taking contraceptive pills [5, 6, 16, 91].

Another marker of stromal hypertrophy is the stromal area to total ovarian area ratio (S/A). S/A is the stromal area defined by the periphery of the hyperechoic stroma divided by the total ovarian area defined by the perimeter of the ovary in the maximum plane section [97, 98]. Women with PCOS have a higher S/A value when compared to women with polycystic ovarian morphology or controls, whereas the last two groups do not differ significantly [95]. Furthermore, S/A ratio in women with PCOS correlates well with androstenedione,testosterone17α-hydroxyprogesterone, FAI, and insulin levels [91, 95, 96, 98, 99]. S/A ratio could be the most efficient ultrasound performance for hyperandrogenism [40, 98]. In this line, a cutoff value of S/A of 0.32 is the best predictor of elevated androstenedione and testosterone levels. This cutoff value could be used in everyday clinical practice and even included in the diagnostic criteria of the syndrome [98, 99].

Two different PCOM profiles in PCOS patients, attending to S/A ratio (cutoff 0.34), percentage of 5–9 mm or 2–4 mm follicles, and "necklace" sign, have been defined. Interestingly, PCOM showing S/A ratio < 0.34, >50% follicles measuring 2–4 mm, and no "necklace" sign with ubiquitously distributed follicles identified insulin-resistant PCOS patients instead of hyperandrogenic non-insulin-resistant PCOS patients with 88% of sensitivity, 78% of specificity, negative likelihood ratio 4.01, negative likelihood ratio 0.16, positive predictive value 84%, and negative predictive value 83%. On the contrary, a pattern of S/A ratio > 0.34, >50% follicles measuring 5–9 mm, and "necklace" sign was seen in 78% of hyperandrogenic non-insulin-resistant PCOS patients [100]. This different ovarian profiles support the concept that two physiopathogenetic pathways, one characterized by hyperandrogenism and the other by insulin resistance, could induce the same effects, namely, they could interfere with selection mechanisms of the dominant follicle and also induce atresia of secondary follicles. This hypothesis may have important implications for the management of patients, since insulin-resistant pattern seems to significantly influence ovarian response to gonadotropin administration [101], ovarian drilling success [102], and increased risk of ovarian hyperstimulation syndrome [97].

Two-dimensional ultrasound measurement of the stromal area can be performed by two ways: the manual and the semiautomatic. In the first method, the area is calculated using the formula of an ellipse: $\pi/4 \times \text{length} \times \text{width}$ ($0.78 \times \text{length} \times \text{width}$ or simplified to $0.8 \times \text{length} \times \text{width}$). In the second method, the stromal area is defined by delineating its perimeter and is then calculated automatically by the ultrasound machine [16]. Three-dimensional measurement of stromal volume is achieved either after the calculation and subtraction of the total follicular volume from the total ovarian volume [78, 93] (these 3D techniques have already been described in the previous paragraphs) or using VOCAL program and by determining a limit area (number of voxels) which determines the stromal and follicular area (see Fig. 6.4). Thus, the stromal and the follicular area are

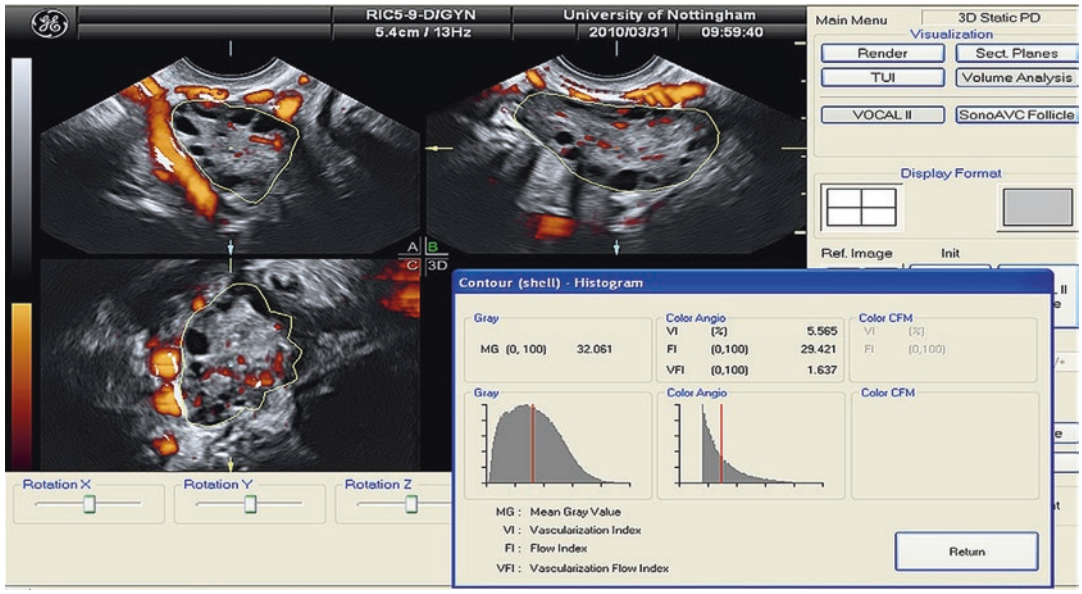

Fig. 6.5 Mean gray value (MG) and 3D power Doppler indices within the ovarian volume delineated using VOCAL. (Reprinted from Deb et al. [108], Copyright 2011, with permission from Elsevier)

calculated above and below of the limit area with the VOCAL program, respectively [93].

Stromal echogenicity had been a key feature for many years [75, 103, 104] until the first more objective assessments showed that there was no significant difference in stromal echogenicity between women with PCOS and controls [92, 105]. 2D ultrasound measurement of stromal echogenicity can be either a subjective operator assessment [75, 103, 104] or an objective calculation derived by the intensity level of the ultrasound pixels within the stroma displayed on the sonographic image [97]. The difference found with the first subjective measurements was attributed to increased volume of ovarian stroma in relation to the lower mean echodensity of the ovary due to the higher number of follicles [92]. Another marker of echogenicity is the stromal index which is the ratio of the mean stromal echogenicity to the mean ovarian (total) echogenicity [105]. Stromal index was found to be higher in PCOS [92], but this was not confirmed [105].

Three-dimensional ultrasound assessments of stromal echogenicity were in accordance with the 2D objective calculations which showed no difference between women with PCOS and controls [93, 94, 106, 107]. The 3D assessment of echogenicity is performed by the mean gray (MG) value that is calculated automatically by the VOCAL program (Fig. 6.5). The MG value represents the mean tissue density of a defined area and is calculated by the mean signal intensity of the grayscale voxels [93, 106, 107]. Three-dimensional ultrasound is considered more appropriate for the quantification of the stromal echogenicity especially for research purposes [87].

Ovarian Stromal Blood Flow

The ovarian stromal blood flow was traditionally believed to be higher in women with PCOS compared to controls [16, 86, 109–114] until the publication of some contradictory studies [93, 94, 115, 116]. The higher blood flow was explained by the reduced resistance and pulsatility indices in the ovarian and stromal vessels found by some investigators [111, 112]. Interestingly, a negative correlation between ovarian volumes and ovarian stromal resistance index in PCOS has been shown [117]. The results of both 2D and 3D ultrasound examinations are conflicting. The controversy in

literature could be explained by the different study designs, selection of controls, criteria used for the definition of PCOS, the lack of hormonal assessments, the variety in ultrasound equipment and settings, and, finally, the arbitrary selection of vessels in 2D ultrasound [93, 116].

2D ultrasound assessment of blood flow could be subjective through color Doppler maps that are no longer used or objective by measuring flow velocity and resistance with pulsed-wave Doppler (PWD). PWD is used to depict the flow velocity waveform from the vessel of interest. Angle correction is applied whenever necessary to fit the incident beam. The waveforms are then analyzed manually (at least three optimal waveforms in a row) or automatically to calculate peak systolic velocity (PSV), end-diastolic velocity (EDV), resistance index (RI), pulsatility index (PI), and, lately, capacitance index (CI), which is the area under the curve for the diastolic part of the waveform, and S/D ratio that is the ratio of the PSV divided by the EDV [93, 116]. A strong correlation was reported between stromal PI and LH/FSH [118].

Three-dimensional ultrasound assessment of blood flow is easy to perform. When the power Doppler signal is optimal, the 3D volume box is opened, and a 3D sweep scan is performed. Then the VOCAL program quantifies the information using the histogram facility, and the blood flow indices are calculated automatically (see Fig. 6.5). Vascularization index (VI) represents the ratio of color voxels within the total dataset relative to both color and gray information, providing, thus, an indication of the number and/or size of the vessels lying in the area of interest and, therefore, the degree of vascularity. VI is expressed as a percentage of the ovarian volume. Flow index (FI) is the mean power Doppler intensity, and as the intensity of the signal is dependent on the number of erythrocytes within a given volume at any time, this index is considered reflective of the average intensity of flow inside the ovary. Vascularization flow index (VFI) represents the ratio of the weighted color voxels to total voxels. VFI is calculated by multiplying VI and FI and gives a unified value for both vascularity and volume flow reflecting the tissue perfusion [119].

These indices are all significantly affected by volume flow, attenuation, vessel number, and erythrocyte density, but in different ways. The VI and VFI seem to have a more predictable relationship, whereas the FI often demonstrates a more complex cubic relationship that is not always logical. Further work is required before a better understanding of 3D power Doppler ultrasound imaging is achieved [120]. However, the findings are controversial even with 3D power Doppler.

Some studies showed increased vascularity and blood flow in the ovaries of women with PCOS [107, 121–123] explained possibly by the higher vascular endothelial growth factor (VEGF), while others did not report any significant difference [85, 93, 94, 106, 107]. Higher ovarian VFI was correlated with lower BMI, hyperandrogenism, greater LH/FSH values, ovarian volumes, and follicle numbers [93, 94, 123]. The 3D ultrasound approach is preferable because it provides the possibility to examine the blood flow and vascularization in the whole ovary, avoiding the arbitrary selection of a single vessel, or even to define a region and calculate separately the flow within and around this region [87, 124].

The basal stromal flow measurement is considered to have no predictive value in PCOS with regard to pregnancy, since the flow indices between conception and non-conception cycles in women with PCOS undergoing IVF are similar [116, 149]. Nevertheless, the stromal blood perfusion has been proven the most relevant predictor of ovarian response to controlled ovarian stimulation compared to ovarian or stromal volume [92, 149]. Jarvela et al. compared the vascularization per follicle between women with PCOS and controls, after pituitary suppression during IVF. Women with PCOS had lower ovarian vascularization per follicle and demanded lower doses of FSH to achieve a similar level of vascularization after stimulation with FSH and hCG administration [106]. Moreover, there was a significant positive correlation between the number of retrieved oocytes and vascularized ovarian volume after stimulation. Still, the calculation of ovarian vascularization per follicle was ambiguous, and there was no report to clinical outcome.

Role of Ultrasound in Monitoring the Effects of Laparoscopic Ovarian Drilling

Laparoscopic ovarian drilling (LOD) is an effective, although interventional, therapy of anovulatory infertility in women with PCOS. LOD is considered by the ESHRE/ASRM PCOS consensus workshop the second-line intervention in the clomiphene citrate-resistant PCOS patients [125]. Usually, ovarian cortex is drilled in three to six points per ovary with a bipolar electrosurgical probe, unipolar needle electrode, or laser [126–129].

The success of LOD could be estimated with ultrasound given that the ovarian volume reduces 3 weeks after intervention [147] and also the stromal blood flow in the early follicular phase of the first postoperative cycle or 3 months after drilling [121, 122, 148]. The 3D Doppler assessment showed significantly higher ovarian stromal VI, FI, and VFI coexisting with higher AMH levels in PCOS compared to controls before drilling and decreased ovarian blood flow, AFC, and AMH concentrations after drilling [121, 122, 130]. The same results were observed after a 6-month follow-up of PCOS patients undergoing ovarian drilling by transvaginal hydrolaparoscopy [128]. There was no difference in stromal blood perfusion between responders (spontaneous ovulation after LOD) and nonresponders with PCOS [122] and any clinical outcome report. However, decreased AMH levels and AFC after LOD may indicate a possible diminished ovarian reserve, and this surgical treatment must be carefully indicated [160].

Uterine Size and Perfusion

Literature references upon uterine ultrasound characteristics in PCOS are scarce. The uterine volume has been found either smaller [131, 132] or bigger [19, 133] in women with PCOS and lower in 40% of adolescent with the syndrome [134] and also in correlation with LH [133]. In few studies, a new criterion was suggested, the ratio of ovarian to uterine volume with an upper limit of 1.0 which was doubted and abandoned [132, 135]. Endometrial thickness was diverse in women and adolescents with PCOS [134, 136, 137] without correlation with the time interval since the last period [134]. Nevertheless, in a more recent study, there was no difference in endometrial thickness and volume between women with PCOS and controls [138].

The uterine and endometrial blood flow was found lower in women with PCOS [110, 111, 123, 134, 139–143] with the exemption of one study [138]. The lower uterine and endometrial blood perfusion is reflected in higher values of Doppler indices as PI and RI in PCOS and is correlated with obesity and hyperandrogenemia (higher levels of androstenedione, DHEAS, and LH/FSH) [110, 111, 142, 143]. Furthermore, uterine perfusion increases with exogenous estrogen and progesterone as well as antiandrogen administration [139, 144], while there is a significant negative correlation between estrogens and uterine PI [145]. This impaired uterine perfusion was associated with metabolic disorders and risk factors for cardiovascular events [140, 141]. The only study to investigate the endometrial blood flow with 3D Doppler did not reveal any significant difference between PCOS and controls in 2D pulsed-wave (uterine arteries) and 3D power Doppler (endometrial and subendometrial blood flow) indices, apart from significantly disturbed endometrial perfusion in women with PCOS and clinical signs of hyperandrogenemia diagnosed only by 3D Doppler [138]. On the other hand, 6 months of metformin treatment in obese PCOS women showed a significant increase in the endometrial thickness, endometrial volume, and endometrial and subendometrial vascularity indices (VI, FI, VFI). No change in the RI and PI of the uterine artery in both periovulatory and midluteal phases was seen. Measures were also performed using 3D Doppler sonography. These results suggest that metabolic, endocrine, vascular, and anti-inflammatory effects of metformin improve markers of endometrial receptivity [146].

PCOS is also associated with recurrent miscarriages [150]. Likewise, hyperandrogenemia has been reported as a serious etiology of recurrent pregnancy loss, regardless of PCOS, possibly due

to lower endometrial and subendometrial blood perfusion secondary to elevated uterine arterial resistance [151–158]. Altogether, higher uterine resistance and lower ovarian stromal resistance, as reported in women with PCOS due to hyperandrogenemia and unopposed estrogens, are indicative of failure of conception in IVF and recurrent miscarriage. Recent evidence conclude that PCOS according to the Rotterdam Criteria increase the risk of miscarriage in lean women undergoing pre-implantation genetic diagnosis, and transfer of a single euploid blastocyst transfer [159]. Thus, further research and maybe threshold value establishment, especially, in 3D power Doppler could contribute to a prognosis algorithm of failed implantation and miscarriage in women with PCOS undergoing assisted reproduction.

Future Points

PCOS is a persistent challenge to the clinician, as the phenotype of the syndrome can vary widely from puberty to postmenopause, and diagnostic criteria must be assessed taking into account the broad and heterogeneous spectrum, even in the same patient throughout her life. Ultrasound examination has an outstanding position in the diagnosis and management of women with PCOS. However, there is still place for improvement and many matters that should be addressed. The research regarding the ultrasound evaluation and the diagnostic and prognostic markers of PCOS is insufficient. The methodology and mainly the diagnostic criteria applied in existing studies are not unanimous and widely accepted. The heterogenous phenotypic spectrum of the syndrome renders necessary the clustered investigation both of clinical and ultrasound indices as well as the correlation of hormonal findings with the clinical practice. Finally, the application of 3D ultrasound seems promising, at least in research level, as it provides better spatial awareness, more objective volumetric and vascularization assessment, reduced scanning time, and better intra- and interobserver variability, despite the higher cost and training requirements. Nevertheless, 3D ultrasound does not seem to add much in clinical practice for the present.

References

1. Franks S. Polycystic ovary syndrome. N Engl J Med. 1995;333:853–61. Erratum in: N Engl J Med. 1995;333:1435.
2. Diamanti-Kandarakis E, Kouli CR, Bergiele AT, Filandra FA, Tsianateli TC, Spina GG, Zapanti ED, Bartzis MI. A survey of the polycystic ovary syndrome in the Greek island of Lesbos: hormonal and metabolic profile. J Clin Endocrinol Metab. 1999;84:4006–11.
3. Azziz R, Woods KS, Reyna R, Key TJ, Knochenhauer ES, Yildiz BO. The prevalence and features of the polycystic ovary syndrome in an unselected population. J Clin Endocrinol Metab. 2004;89:2745–9.
4. Zawadzki JA, Dunaif A. Diagnostic criteria for polycystic ovary syndrome: towards a rational approach. In: Dunaif A, Givens JR, Haseltine FP, Merriam GR, editors. Polycystic ovary syndrome. Boston: Blackwell Scientific; 1992. p. 377–84.
5. The Rotterdam ESHRE/ASRM-Sponsored PCOS Consensus Workshop Group. Revised 2003 consensus on diagnostic criteria and long-term health risks related to polycystic ovary syndrome (PCOS). Hum Reprod. 2004;19:41–7.
6. The Rotterdam ESHRE/ASRM-Sponsored PCOS Consensus Workshop Group. Revised 2003 consensus on diagnostic criteria and long-term health risks related to polycystic ovary syndrome (PCOS). Fertil Steril. 2004;81:19–25.
7. Asuncion M, Calvo RM, San Millan JL, Sancho J, Avila S, Escobar-Morreale HF. A prospective study of the prevalence of the polycystic ovary syndrome in unselected Caucasian women from Spain. J Clin Endocrinol Metab. 2000;85:2434–8.
8. March WA, Moore VM, Willson KJ, Phillips DI, Norman RJ, Davies MJ. The prevalence of polycystic ovary syndrome in a community sample assessed under contrasting diagnostic criteria. Hum Reprod. 2010;25:544–51.
9. Karkanaki A, Piouka A, Katsikis I, Farmakiotis D, Macut D, Panidis D. Adiponectin levels reflect the different phenotypes of polycystic ovary syndrome: study in normal weight, normoinsulinemic patients. Fertil Steril. 2009;92:2078–81.
10. Diamanti-Kandarakis E, Panidis D. Unraveling the phenotyping map of polycystic ovary syndrome (PCOS): a prospective study of 634 women with PCOS. Clin Endocrinol. 2007;67:735–42.
11. Polson DW, Adams J, Wadsworth J, Franks S. Polycystic ovaries-a common finding in normal women. Lancet. 1988;1:870–2.
12. Clayton RN, Ogden V, Hodgkinson J, Worswick L, Rodin DA, Dyer S, et al. How common are polycystic ovaries in normal women and what is their significance for the fertility of the population? Clin Endocrinol. 1992;37:127–34.
13. Azziz R, Carmina E, Dewailly D, Diamanti-Kandarakis E, Escobar-Morreale HF, Futterweit W, Janssen OE, Legro RS, Norman RJ, Taylor AE, Witchel SF. Androgen Excess Society. Positions statement: criteria for defining polycystic ovary syndrome

as a predominantly hyperandrogenic syndrome: an Androgen Excess Society guideline. J Clin Endocrinol Metab. 2006;91:4237–45.
14. Peña AS, Metz M. What is adolescent polycystic ovary syndrome? J Paediartr Child Health. 2017;27. https://doi.org/10.1111/jpc.13821.
15. Christensen JT, Boldsoen J, Westergaard JG. Ovarian volume in gynecologically healthy women using contraception or using IUD. Acta Obstet Gynecol Scand. 1997;76:784–9.
16. Balen AH, Laven JSE, Tan SL, Dewailly D. Ultrasound assessment of the polycystic ovary: international consensus definitions. Hum Reprod. 2003;9:505–14.
17. Zaidi J, Jurkovic D, Campbell S, Pitroff R, McGregor A, Tan SL. Description of circadian rhythm in uterine artery blood flow indices during the peri-ovulatory period. Hum Reprod. 1995;10:1642–6.
18. Zaidi J, Tan SL, Pitroff R, Campbell S, Collins W. Blood flow changes in the intra-ovarian arteries during the peri-ovulatory period-relationship to the time of day. Ultrasound Obstet Gynecol. 1996;7:135–40.
19. Adams J, Franks S, Polson DW, Mason HD, Abdulwahid N, Tucker M, Morris DV, Price J, Jacobs HS. Multifollicular ovaries: clinical and endocrine features and response to pulsatile gonadotropin releasing hormone. Lancet. 1985;2:1375–9.
20. Jonard S, Robert Y, Cortet-Rudelli C, Pigny P, Decanter C, Dewailly D. Ultrasound examination of polycystic ovaries: is it worth counting the follicles? Hum Reprod. 2003;18:598–603.
21. Jonard S, Dewailly D, Pigny P, Robert Y, Decanter C. What are the determinants of the antral follicle number at ovarian ultrasonography (U/S) in PCOS? ESHRE Congress, Madrid, 29 June to 3 July 2003, oral communication, 0–119. Hum Reprod. 2003;18 Suppl 1:42.
22. Peigné M, Catteau-Jonard S, Robin G, Dumont A, Pigny P, Dewailly D. The numbers of 2–5 and 6–9 mm ovarian follicles are inversely correlated in both normal women and polycystic ovary syndrome patients: what is the missing ling? Hum Reprod. 2018; https://doi.org/10.1093/humrep/dey017.
23. Raine-Fenning N. What's in a number? The polycystic ovary revisited. Hum Reprod. 2011;11:3118–22.
24. Balen AH, Dunger D. Pubertal maturation of the internal genitalia. Ultrasound Obstet Gynecol. 1995;6:164–5.
25. Johnstone EB, Rosen MP, Neril R, Trevithick D, Sternfeld B, Murphy R, Addauan-Andersen C, McConnell D, Pera RR, Cedars MI. The polycystic ovary post-rotterdam: a common, age-dependent finding in ovulatory women without metabolic significance. J Clin Endocrinol Metab. 2010;95:4965–72.
26. Azziz R, Carmina E, Dewailly D, Diamanti-Kandarakis E, Escobar-Morreale HF, Futterweit W, Janssen OE, Legro RS, Norman RJ, Taylor AE, Witchel SF. Task Force on the Phenotype of the Polycystic Ovary Syndrome of The Androgen Excess and PCOS Society. The Androgen Excess and PCOS Society criteria for the polycystic ovary syndrome: the complete task force report. Fertil Steril. 2009;91:456–88.
27. Adams JM, Taylor AE, Crowley WF Jr, Hall JE. Polycystic ovarian morphology with regular ovulatory cycles: insights into the pathophysiology of polycystic ovarian syndrome. J Clin Endocrinol Metab. 2004;89:4343–50.
28. Kousta E, Cela E, Lawrence N, Penny A, Millauer B, White D, et al. The prevalence of polycystic ovaries in women with a history of gestational diabetes. Clin Endocrinol. 2000;53:501–7.
29. Dewailly D. Diagnostic criteria for PCOS: Is there a need for a rethink? Best Practice & Research Clinical Obstetrics and Gynaecology. 2016;37:5–11.
30. Koivunen R, Laatikainen T, Tomas C, Huhtaniemi I, Tapanainen J, Martikainen H. The prevalence of polycystic ovaries in healthy women. Acta Obstet Gynecol Scand. 1999;78:137–41.
31. Swanton A, Storey L, McVeigh E, Child T. IVF outcome in women with PCOS, PCO and normal ovarian morphology. Eur J Obstet Gynecol Reprod Biol. 2010;149:68–71.
32. Esinler I, Bayar U, Bozdag G, Yarali H. Outcome of intracytoplasmic sperm injection in patients with polycystic ovary syndrome or isolated polycystic ovaries. Fertil Steril. 2005;84:932–7.
33. McDougall MJ, Tan SL, Jacobs HS. IVF and the ovarian hyperstimulation syndrome. Hum Reprod. 1992;5:597–600.
34. Sahu B, Ozturk O, Ranierri M, Serhal P. Comparison of oocyte quality and intracytoplasmic sperm injection outcome in women with isolated polycystic ovaries or polycystic ovarian syndrome. Arch Gynecol Obstet. 2008;277:239–44.
35. Elting MW, Kwee J, Schats R, Rekers-Mombarg LT, Schoemaker J. The rise of estradiol and inhibin B after acute stimulation with follicle-stimulating hormone predict the follicle cohort size in women with polycystic ovary syndrome, regularly menstruating women with polycystic ovaries, and regularly menstruating women with normal ovaries. J Clin Endocrinol Metab. 2001;86:1589–95.
36. Catteau-Jonard S, Bancquart J, Poncelet E, Lefebvre-Maunoury C, Robin G, Dewailly D. Polycystic ovaries at ultrasound: normal variant or silent Polycystic Ovary Syndrome? Ultrasound Obstet Gynecol. 2012;40(2):223–9. https://doi.org/10.1002/uog.11202.
37. Eldar-Geva T, Margalioth EJ, Gal M, Ben-Chetrit A, Algur N, Zylber-Haran E, Brooks B, Huerta M, Spitz IM. Serum anti-Mullerian hormone levels during controlled ovarian hyperstimulation in women with polycystic ovaries with and without hyperandrogenism. Hum Reprod. 2005;20:1814–9.
38. Engmann L, DiLuigi A, Schmidt D, Nulsen J, Maier D, Benadiva C. The use of gonadotropin-releasing hormone (GnRH) agonist to induce oocyte maturation after cotreatment with GnRH antagonist in high-risk patients undergoing in vitro fertilization prevents the risk of ovarian hyperstimulation syndrome: a pro-

spective randomized controlled study. Fertil Steril. 2008;89:84–91.
39. Son WY, Tan SL. Laboratory and embryological aspects of hCG-primed in vitro maturation cycles for patients with polycystic ovaries. Hum Reprod Update. 2010;16:675–89.
40. Nardo LG, Gelbaya TA. Evidence-based approach for the use of ultrasound in the management of polycystic ovary syndrome. Minerva Ginecol. 2008;60:83–9.
41. Broekmans FJ, Kwee J, Hendriks DJ, Mol BW, Lambalk CB. A systematic review of tests predicting ovarian reserve and IVF outcome. Hum Reprod Update. 2006;12:685–718.
42. Scheffer GJ, Broekmans FJ, Dorland M, Habbema JD, Looman CW, te Velde ER. Antral follicle counts by transvaginal ultrasonography are related to age in women with proven natural fertility. Fertil Steril. 1999;72:845–51.
43. Kline J, Kinney A, Kelly A, Reuss ML, Levin B. Predictors of antral follicle count during the reproductive years. Hum Reprod. 2005;20:2179–89.
44. Broer SL, Mol BW, Hendriks D, Broekmans FJ. The role of antimüllerian hormone in prediction of outcome after IVF: comparison with the antral follicle count. Fertil Steril. 2009;91:705–14.
45. Broekmans FJM, de Ziegler D, Howles CM, Gougeon A, Trew G, Olivennes F. The antral follicle count: practical recommendations for better standardization. Fertil Steril. 2010;94:1044–51.
46. Craig J, Orisaka M, Wang H, Orisaka S, Thompson W, Zhu C, et al. Gonadotropin and intra-ovarian signals regulating follicle development and atresia: the delicate balance between life and death. Front Biosci. 2007;12:3628–39.
47. Charleston JS, Hansen KR, Thyer AC, Charleston LB, Gougeon A, Siebert JR, et al. Estimating human ovarian non-growing follicle number: the application of modern stereology techniques to an old problem. Hum Reprod. 2007;22:2103–10.
48. Gougeon A. Human ovarian follicular development: from activation of resting follicles to preovulatory maturation. Ann Endocrinol (Paris). 2010;71:132–43.
49. Gougeon A. Regulation of ovarian follicular development in primates: facts and hypotheses. Endocr Rev. 1996;17:121–55.
50. Broekmans FJ, Faddy MJ, Scheffer G, te Velde ER. Antral follicle counts are related to age at natural fertility loss and age at menopause. Menopause. 2004;11:607–14.
51. Gougeon A. Ovarian follicular growth in humans: ovarian ageing and population of growing follicles. Maturitas. 1998;30:137–42.
52. Deb S, Campbell BK, Clewes JS, Raine-Fenning NJ. Quantitative analysis of antral follicle number and size: a comparison of two-dimension and automated three-dimension ultrasound techniques. Ultrasound Obstet Gynecol. 2010;35:354–60.
53. Dewailly D, Andersen CY, Balen A, Broekmans F, Dilaver N, Fanchin R, Griesinger G, Kelsey TW, La Marca A, Lambalk C, et al. The physiology and clinical utility of anti-Mullerian hormone in women. Hum Reprod Update. 2014;20:370–85.
54. Pellatt L, Hanna L, Brincat M, Galea R, Brain H, Whitehead S, et al. Granulosa cell production of anti-Mullerian hormone is increased in polycystic ovaries. J Clin Endocrinol Metab. 2007;92:240–5.
55. Franks S, Stark J, Hardy K. Follicle dynamics and anovulation in polycystic ovary syndrome. Hum Reprod Update. 2008;14:367–78.
56. Lebbe M, Woodruff TK. Involvement of androgens in ovarian health and disease. Mol Hum Reprod. 2013;19:828–37.
57. Webber LJ, Stubbs S, Stark J, Trew GH, Margara R, Hardy K, Franks S. Formation and early development of follicles in the polycystic ovary. Lancet. 2003;362:1017–21.
58. Dewailly D, Catteau-Jonard S, Reyss AC, Maunoury-Lefebvre C, Poncelet E, Pigny P. The excess in 2–5 mm follicles seen at ovarian ultrasonography is tightly associated to the follicular arrest of the polycystic ovary syndrome. Hum Reprod. 2007;22:1562–6.
59. Raine-Fenning N, Jayaprakasan K, Clewes J. Automated follicle tracking facilitates standardization and may improve work flow. Ultrasound Obstet Gynecol. 2007;30:1015–8.
60. Raine-Fenning N, Jayaprakasan K, Clewes J, Joergner I, Bonaki SD, Chamberlain S, Devlin L, Priddle H, Johnson I. SonoAVC: a novel method of automatic volume calculation. Ultrasound Obstet Gynecol. 2008;31:691–6.
61. Dewailly D, Lujan ME, Carmina E, Cedars MI, Laven J, Norman RJ, Escobar-Morreale HF. Definition and significance of polycystic ovarian morphology: a task force report from the Androgen Excess and Polycystic Ovary Syndrome Society. Hum Reprod Update. 2014;20:334–52.
62. Lujan ME, Jarrett BY, Brooks ED, Reines JK, Peppin AK, Muhn N, et al. Updated ultrasound criteria for polycystic ovary syndrome: reliable thresholds for elevated follicle population and ovarian volume. Hum Reprod. 2013;28:1361–8.
63. Kim HJ, Adams JM, Gudmundsson JA, Arason G, Pau CT, Welt CK. Polycystic ovary morphology: age-based ultrasound criteria. Fertil Steril. 2017;108:548–53.
64. Christiansen SC, Eilertsen TB, Vanky E, Carlsen SM. Does AMH reflect follicle number similarly in women with and without PCOS? PLoS One. 2016; https://doi.org/10.1371/journal.pone.0146739.
65. Iliodromiti S, Kelsey TW, Anderson RA, Nelson SM. Can anti-Mullerian hormone predict the diagnosis of polycystic ovary syndrome? A systematic review and meta-analysis of extracted data. J Clin Endocrinol Metab. 2013;98:3332–40.
66. Carmina E, Campagna AM, Fruzzetti F, Lobo RA. AMH measurement versus ovarian ultrasound in the diagnosis of polycystic ovary syndrome in different phenotypes. Endocr Pract. 2016;22:287–93.

67. Wittmaack FM, Kreger DO, Blasco L, Tureck RW, Mastroianni L Jr, Lessey BA. Effect of follicular size on oocyte retrieval, fertilization, cleavage, and embryo quality in in vitro fertilization cycles: a 6-year data collection. Fertil Steril. 1994;62:1205–10.
68. Amer A, Hammadeh ME, Kolkailah M, Ghandour AA. Three-dimensional versus two-dimensional ultrasound measurement of follicular volume: are they comparable? Arch Gynecol Obstet. 2003;268:155–7.
69. Penzias AS, Emmi AM, Dubey AK, Layman LC, DeCherney AH, Reindollar RH. Ultrasound prediction of follicle volume: is the mean diameter reflective? Fertil Steril. 1994;62:1274–6.
70. Ata B, Tulandi T. Ultrasound automated volume calculation in reproduction and in pregnancy. Fertil Steril. 2011;95:2163–70.
71. Jayaprakasan K, Hilwah N, Kendall NR, Hopkisson JF, Campbell BK, Johnson IR, Raine-Fenning NJ. Does 3D ultrasound offer any advantage in the pretreatment assessment of ovarian reserve and prediction of outcome after assisted reproduction treatment? Hum Reprod. 2007;22:1932–41.
72. Deb S, Jayaprakasan K, Campbell BK, Clewes JS, Johnson IR, Raine-Fenning NJ. Intraobserver and interobserver reliability of automated antral follicle counts made using three-dimensional ultrasound and SonoAVC. Ultrasound Obstet Gynecol. 2009;33:477–83.
73. Nylander M, Frøssing S, Bjerre AH, Chabanova E, Clausen HV, Faber J, Skouby SO. Ovarian morphology in polycystic ovary syndrome: estimates from 2D and 3D ultrasound and magnetic resonance imaging and their correlation to anti-Müllerian hormone. Acta Radiol. 2017;58:997–1004.
74. Van Santbrink EJ, Hop WC, Fauser BC. Classification of normogonadotropin infertility: polycystic ovaries diagnosed by ultrasound versus endocrine characteristics of PCOS. Fertil Steril. 1997;67:452–8.
75. Pache TD, Hop WC, Wladimiroff JW, Schipper J, Fauser BC. How to discriminate between normal and polycystic ovaries. Radiology. 1992;17:589–93.
76. Erdem A, Erdem M, Biberoglu K, Hayit O, Arslan M, Gursoy R. Age-related changes in ovarian volume, antral follicle counts and basal FSH in women with normal reproductive health. J Reprod Med. 2002;47:835–9.
77. Alsamarai S, Adams JM, Murphy MK, Post MD, Hayden DL, Hall JE, Welt CK. Criteria for polycystic ovarian morphology in polycystic ovary syndrome as a function of age. J Clin Endocrinol Metab. 2009;94:4961–70.
78. Kyei-Mensah A, Tan SL, Zaidi J, Jacobs HS. Relationship of ovarian stromal volume to serum androgen concentrations in patients with polycystic ovary syndrome. Hum Reprod. 1998;13:1437–41.
79. Haadsma ML, Bukman A, Groen H, Roeloffzen EM, Groenewoud ER, Heineman MJ, et al. The number of small antral follicles (2-6mm) determines the outcome of endocrine ovarian reserve tests in a subfertile population. Hum Reprod. 2007;22:1925–31.
80. Allemand MC, Tummon IS, Phy JL, Foong SC, Dumesic DA, Session DR. Diagnosis of polycystic ovaries by three-dimensional transvaginal ultrasound. Fertil Steril. 2006;85:214–9.
81. Dewailly D, Gronier H, Poncelet E, Robin G, Leroy M, Pigny P, Duhamel A, Catteau-Jonard S. Diagnosis of polycystic ovary syndrome (PCOS): revisiting the threshold values of follicle count on ultrasound and of the serum AMH level for the definition of polycystic ovaries. Hum Reprod. 2011;26:3123–9.
82. Jayaprakasan K, Campbell BK, Clewes JS, Johnson IR, Raine-Fenning NJ. Three-dimensional ultrasound improves the interobserver reliability of antral follicle counts and facilitates increased clinical work flow. Ultrasound Obstet Gynecol. 2008;31:439–44.
83. Raine-Fenning NJ, Campbell BK, Clewes JS, Johnson IR. The interobserver reliability of ovarian volume measurement is improved with three-dimensional ultrasound, but dependent upon technique. Ultrasound Med Biol. 2003;29:1685–90.
84. Kyei-Mensah A, Maconochie N, Zaidi J, Pittrof R, Campbell S, Tan SL. Transvaginal three-dimensional ultrasound: accuracy of ovarian follicular volume measurements. Fertil Steril. 1996;65:371–6.
85. Ng EH, Chan CC, Yeung WS, Ho PC. Comparison of ovarian stromal blood flow between fertile women with normal ovaries and infertile women with polycystic ovary syndrome. Hum Reprod. 2005;20:1881–6.
86. Pan HA, Wu MH, Cheng YC, Li CH, Chang FM. Quantification of Doppler signal in polycystic ovarian syndrome using 3D power Doppler ultrasonography. Hum Reprod. 2002;17:2484–8.
87. Lam PM, Raine-Fenning NJ. The role of three-dimensional ultrasonography in polycystic ovary syndrome. Hum Reprod. 2006;21:2209–15.
88. Raine-Fenning NJ, Clewes JS, Kendall NR, Bunkheila AK, Campbell BK, Johnson IR. The interobserver reliability and validity of volume calculation from three-dimensional ultrasound datasets in the in vitro setting. Ultrasound Obstet Gynecol. 2003;21:283–91.
89. Lam PM, Johnson IR, Raine-Fenning NJ. Three-dimensional ultrasound features of the polycystic ovary and the effect of different phenotypic expressions on these parameters. Hum Reprod. 2007;22:3116–23.
90. Dewailly D, Robert Y, Helin I, Ardaens Y, Thomas-Desrousseaux P, Lemaitre L, Fossati P. Ovarian stromal hypertrophy in hyperandrogenic women. Clin Endocrinol. 1994;41:557–62.
91. Buckett WM, Bouzayen R, Watkin KL, Tulandi T, Tan SL. Ovarian stromal echogenicity in women with normal and polycystic ovaries. Hum Reprod. 1999;14:618–21.
92. Yoo RY, Sirlin CB, Gottschalk M, Chang RJ. Ovarian imaging by magnetic resonance in obese adolescent girls with polycystic ovary syndrome: a pilot study. Fertil Steril. 2005;84:985–95.
93. Lam P, Raine-Fenning NJ, Cheung L, Haines C. Three-dimensional ultrasound features of the

polycystic ovary in Chinese women. Ultrasound Obstet Gynecol. 2009;34:196–200.
94. Fulghesu AM, Ciampelli M, Belosi C, Apa R, Pavone V, Lanzone A. A new ultrasound criterion for the diagnosis of polycystic ovary syndrome: the ovarian stroma/total area ratio. Fertil Steril. 2001;76:326–31.
95. Pache TD, de Jong FH, Hop WC, Fauser BCJM. Association between ovarian changes assessed by transvaginal sonography and clinical and endocrine signs of the polycystic ovary syndrome. Fertil Steril. 1993;59:544–9.
96. Lam PM, Raine-Fenning N. Polycystic ovarian syndrome: a misnomer for an enigmatic disease. Ultrasound Obstet Gynecol. 2009;33:621–7.
97. Fulghesu A, Angioni S, Frau E, Belosi C, Apa R, Mioni R, Xamin N, Capobianco GP, Dessole S, Fruzzetti F, Lazzarini V, Minerba L, Melis GB, Lanzone A. Ultrasound in polycystic ovary syndrome-the measuring of ovarian stroma and relationship with circulating androgens: results of a multicentric study. Hum Reprod. 2007;22:2501–8.
98. Belosi C, Selvaggi L, Apa R, Guido M, Romualdi D, Fulghesu AM, Lanzone A. Is the PCOS diagnosis solved by ESHRE/ASRM 2003 consensus or could it include ultrasound examination of the ovarian stroma? Hum Reprod. 2006;21:3108–15.
99. Ardaens Y, Robert Y, Lemaitre L, Fossati P, Dewailly D. Polycystic ovarian disease: contribution of vaginal endosonography and reassessment of ultrasonic diagnosis. Fertil Steril. 1991;55:1062–8.
100. Alviggi C, Conforti A, De Rosa P, Strina I, Palomba S, Vallone R, et al. The Distribution of stroma and antral Follicles Differs between insulin-resistance and hyperandrogenism-related Polycystic Ovarian syndrome. Front Endocrinol. 2017; https://doi.org/10.3389/fendo.2017.00117.
101. Fedorcsak P, Dale PO, Storeng R, Tambo T, Abyholm T. The impact of obesity and insulin resistance on the outcome of IVF or ICSI in women with polycystic ovarian syndrome. Hum Reprod. 2001;16:1086–91.
102. Amer S, Li TC, Samuelson C, Ledger W. The impact of insulin resistance on the outcome of laparoscopic ovarian diathermy in women with polycystic ovarian syndrome. Acta Obstet Gynecol Scand. 2011;9(0):338–43.
103. Pache TD, Hop WC, Wladimiroff JW, Schipper J, Fauser BCJM. Transvaginal sonography and abnormal ovarian appearance in menstrual cycle disturbances. Ultrasound Med Biol. 1991;17:589–93.
104. Al-Took S, Watkin K, Tulandi T, Tan SL. Ovarian stromal echogenicity in women with clomiphene citrate-sensitive and clomiphene citrate-resistant polycystic ovary syndrome. Fertil Steril. 1999;71:952–4.
105. Jarvela IY, Mason HD, Sladkevicius P, Kelly S, Ojha K, Campbell S, Nargund G. Characterization of normal and polycystic ovaries using three-dimensional power Doppler ultrasonography. J Assist Reprod Genet. 2002;19:582–90.
106. Pascual MA, Graupera B, Hereter L, Tresserra F, Rodriguez I, Alcazar JL. Assessment of ovarian vascularization in the polycystic ovary by three-dimensional power Doppler ultrasonography. Gynecol Endocrinol. 2008;24:631–6.
107. Agrawal R, Sladkevicius P, Engmann L, Conway GS, Payne NN, Bekis J, Tan SL, Campbell S, Jacobs HS. Serum vascular endothelial growth factor concentrations and ovarian stromal blood flow are increased in women with polycystic ovaries. Hum Reprod. 1998;13:651–5.
108. Deb S, Jayaprakasan K, Campbell BK, Clewes JS, Raine-Fenning NJ. The interovarian variation in three-dimensional ultrasound markers of ovarian reserve in women undergoing baseline investigation for subfertility. Fertil Steril. 2011;95:667–72.
109. Aleem FA, Predanic M. Transvaginal color Doppler determination of the ovarian and uterine blood flow characteristics in polycystic ovary disease. Fertil Steril. 1996;65:510–6.
110. Ozkan S, Vural B, Caliskan E, Bodur H, Turkoz E, Vural F. Color Doppler sonographic analysis of uterine and ovarian artery blood flow in women with polycystic ovary syndrome. J Clin Ultrasound. 2007;35:305–13.
111. Loverro G, Vicino M, Lorusso F, Vimercati A, Greco P, Selvaggi L. Polycystic ovary syndrome: relationship between insulin sensitivity, sex hormone levels and ovarian stromal blood flow. Gynecol Endocrinol. 2001;15:142–9.
112. Zaidi J, Campbell S, Pittrof R, Kyei-Mensah A, Shaker A, Jacobs HS, Tan SL. Ovarian stromal blood flow in women with polycystic ovaries-a possible new marker for diagnosis? Hum Reprod. 1995;10:1992–6.
113. Dolz M, Osborne NG, Blanes J, Raga F, Abad-Velasco L, Villalobos A, Pellicer A, Bonilla-Musoles F. Polycystic ovarian syndrome: assessment with color Doppler angiography and three-dimensional ultrasonography. J Ultrasound Med. 1999;18:303–13.
114. Tugrul S, Oral O, Guclu M, Kutlu T, Uslu H, Pekin O. Significance of Doppler ultrasonography in the diagnosis of polycystic ovary syndrome. Clin Exp Obstet Gynecol. 2006;33:154–8.
115. Younis JS, Jadaon JE, Haddad S, Izhaki I, Ben-Ami M. Prospective evaluation of basal stromal Doppler studies in women with good ovarian reserve and infertility undergoing in vitro fertilization-embryo transfer treatment: patients with polycystic ovary syndrome versus ovulatory patients. Fertil Steril. 2011;95:1754–8.
116. Battaglia C, Genazzani AD, Salvatori M, Giulini S, Artini PG, Genazzani AR, Volpe A. Doppler, ultrasonographic and endocrinological environment with regard to the number of small subcapsular follicles in polycystic ovary syndrome. Gynecol Endocrinol. 1999;13:123–9.
117. Ozdemir O, Sari ME, Kalkan D, Koc EM, Ozdemir S, Atalay CR. Comprasion of ovarian stromal blood

flow measured by color Doppler ultrasonography in polycystic ovary syndrome patients and healthy women with ultrasonographic evidence of polycystic. Gynecol Endocrinol. 2015;3:322–6.
118. Pairleitner H, Steiner H, Hasenoehrl G, Staudach A. Three dimensional power Doppler sonography: imaging and quantifying blood flow and vascularization. Ultrasound Obstet Gynecol. 1999;14:139–43.
119. Raine-Fenning NJ, Nordin NM, Ramnarine KV, Campbell BK, Clewes JS, Perkins A, Johnson IR. Determining the relationship between three-dimensional power Doppler data and true blood flow characteristics: an in-vitro flow phantom experiment. Ultrasound Obstet Gynecol. 2008;32:540–50.
120. El Behery MM, Diab AE, Mowafy H, Ebrahiem MA, Shehata AE. Effect of laparoscopic ovarian drilling on vascular endothelial growth factor and ovarian stromal blood flow using 3-dimensional power Doppler. Int J Gynaecol Obstet. 2011;112:119–21.
121. Elmashad AI. Impact of laparoscopic ovarian drilling on anti-Mullerian hormone levels and ovarian stromal blood flow using three-dimensional power Doppler in women with anovulatory polycystic ovary syndrome. Fertil Steril. 2011;95:2342–6.
122. Mala YM, Ghosh SB, Tripathi R. Three-dimensional power Doppler imaging in the diagnosis of polycystic ovary syndrome. Int J Gynaecol Obstet. 2009;105:36–8.
123. Raine-Fenning NJ, Campbell BK, Clewes JS, Kendall NR, Johnson IR. The interobserver reliability of three-dimensional power Doppler data acquisition within the female pelvis. Ultrasound Obstet Gynecol. 2004;23:501–8.
124. Hann LE, Hall DA, McArdle CR, Seibel M. Polycystic ovarian disease: sonographic spectrum. Radiology. 1984;150:531–4.
125. ESHRE/ASRM-Sponsored PCOS Consensus Workshop Group. Consensus on infertility treatment related to polycystic ovary syndrome. Fertil Steril. 2008;89:505.
126. Farquhar C, Brown J, Marjoribanks J. Laparoscopic drilling by diathermy or laser for ovulation induction in anovulatory polycystic ovary syndrome. Cochrane Database Syst Rev. 2012;(6):CD001122.
127. Hendriks ML, König T, Korsen T, Melgers I, Dekker J, Mijatovic V, et al. Short-term changes in hormonal profiles after laparoscopic ovarian laser evaporation compared with diagnostic laparoscopy for PCOS. Hum Reprod. 2014;29:2544–52.
128. Giampaolino P, Morra I, De Rosa N, Cagnacci A, Pellicano M, Di Carlo C, et al. Impact of transvaginal hydrolaparoscopy ovarian drilling on ovarian stromal blood flow and ovarian volume in clomiphene citrate-resistant PCOS patients: a case-control study. Gynecol Endocrinol. 2017;33(9):690–3.
129. Seyam EM, Hefzi E. Laparoscopic ovarian drilling versus GnRH antagonist combined with cabergoline as a prophylaxis against the re-development of ovarian hyperstimulation syndrome. Ginecol Endocrinol. 2018;15:1–7.
130. Seyam EM, Mohamed TG, Hasan MM, Abd Al Mawgood MH. Evaluation of ultrasonographic and Anti-Mullerian Hormone (AMH) changes as predictors for ovarian reserve after laparoscopic ovarian drilling for women with polycystic ovarian síndrome. Middle East Fertility Society Journal. 2014;19:314–23.
131. Orsini LF, Venturoli S, Lorusso R, Pluchinotta V, Paradisi R, Bovicelli L. Ultrasonic findings in polycystic ovarian disease. Fertil Steril. 1985;43:709–14.
132. Balen AH, Conway GS, Kaltsas G, Techatrasak K, Manning PJ, West C, Jacobs HS. Polycystic ovary syndrome: the spectrum of the disorder in 1741 patients. Hum Reprod. 1995;10:2107–11.
133. Shah B, Parnell L, Milla S, Kessler M, David R. Endometrial thickness, uterine, and ovarian ultrasonographic features in adolescents with polycystic ovarian syndrome. J Pediatr Adolesc Gynecol. 2010;23:146–52.
134. Parisi L, Tramonti M, Casciano S, Zurli A, Gazzarini O. The role of ultrasound in the study of polycystic ovarian disease. J Clin Ultrasound. 1982;10:167–72.
135. Peri N, Levine D. Sonographic evaluation of the endometrium in patients with a history or an appearance of polycystic ovarian syndrome. J Ultrasound Med. 2007;26:55–9.
136. Vanky E, Kjøtrød S, Salvesen KA, Romundstad P, Moen MH, Carlsen SM. Clinical, biochemical and ultrasonographic characteristics of Scandinavian women with PCOS. Acta Obstet Gynecol Scand. 2004;83:482–6.
137. Lam P, Johnson I, Raine-Fenning N. Endometrial blood flow is impaired in women with polycystic ovarian syndrome who are clinically hyperandrogenic. Ultrasound Obstet Gynecol. 2009;34:326–34.
138. Ajossa S, Guerriero S, Paoletti AM, Orrù M, Melis GB. The antiandrogenic effect of flutamide improves uterine perfusion in women with polycystic ovary syndrome. Fertil Steril. 2002;77:1136–40.
139. Ajossa S, Guerriero S, Paoletti AM, Orrù M, Melis GB. Hyperinsulinemia and uterine perfusion in patients with polycystic ovary syndrome. Ultrasound Obstet Gynecol. 2002;20:276–80.
140. Chekir C, Nakatsuka M, Kamada Y, Noguchi S, Sasaki A, Hiramatsu Y. Impaired uterine perfusion associated with metabolic disorders in women with polycystic ovary syndrome. Acta Obstet Gynecol Scand. 2005;84:189–95.
141. Battaglia C, Artini PG, Genazzani AD, Sgherzi MR, Salvatori M, Giulini S, Volpe A. Color Doppler analysis in lean and obese women with polycystic ovary syndrome. Ultrasound Obstet Gynecol. 1996;7:342–6.
142. Battaglia C, Artini PG, D'Ambrogio G, Genazzani AD, Genazzani AR. The role of color Doppler imaging in the diagnosis of polycystic ovary syndrome. Am J Obstet Gynecol. 1995;172:108–13.
143. de Ziegler D, Bessis R, Frydman R. Vascular resistance of uterine arteries: physiological effects of estradiol and progesterone. Fertil Steril. 1991;55:775–9.

144. Killam AP, Rosenfeld CR, Battaglia FC, Makowski EL, Meschia G. Effect of estrogens on the uterine blood flow of oophorectomized ewes. Am J Obstet Gynecol. 1973;115:1045–52.
145. Tulandi T, Watkin K, Tan SL. Reproductive performance and three dimensional ultrasound volume determination of polycystic ovaries following laparoscopic ovarian drilling. Int J Fertil Womens Med. 1997;42:436–40.
146. Mohsen IA, Elkattan E, Nabil H, Khattab S. Effects of metformin treatment on endometrial vascular índices in anovulatory obese/overweight women with polycystic ovarian síndrome using three-dimensional power Doppler ultrasonography. Clin Ultrasound. 2013;41:275–82.
147. Wu MH, Huang MF, Tsai SJ, Pan HA, Cheng YC, Lin YS. Effects of laparoscopic ovarian drilling on young adult women with polycystic ovarian syndrome. J Am Assoc Gynecol Laparosc. 2004;11:184–90.
148. Engmann L, Sladkevicius P, Agrawal R, Bekir JS, Campbell S, Tan SL. Value of ovarian stromal blood flow velocity measurement after pituitary suppression in the prediction of ovarian responsiveness and outcome of in vitro fertilization treatment. Fertil Steril. 1999;71:22–9.
149. Cocksedge KA, Li TC, Saravelos SH, Metwally M. A reappraisal of the role of polycystic ovary syndrome in recurrent miscarriage. Reprod Biomed Online. 2008;17:151–60.
150. Okon MA, Laird SM, Tuckerman EM, Li TC. Serum androgen levels in women who have recurrent miscarriages and their correlation with markers of endometrial function. Fertil Steril. 1998;69:682–90.
151. Li TC, Spuijbroek MD, Tuckerman E, Anstie B, Loxley M, Laird S. Endocrinological and endometrial factors in recurrent miscarriage. BJOG. 2000;107:1471–9.
152. Cocksedge KA, Saravelos SH, Wang Q, Tuckerman E, Laird SM, Li TC. Does free androgen index predict subsequent pregnancy outcome in women with recurrent miscarriage? Hum Reprod. 2008;23:797–802.
153. Ferreira AM, Pires CR, Moron AF, Araujo Júnior E, Traina E, Mattar R. Doppler assessment of uterine blood flow in recurrent pregnancy loss. Int J Gynaecol Obstet. 2007;98:115–9.
154. Nakatsuka M, Habara T, Noguchi S, Konishi H, Kudo T. Impaired uterine arterial blood flow in pregnant women with recurrent pregnancy loss. J Ultrasound Med. 2003;22:27–31.
155. Habara T, Nakatsuka M, Konishi H, Asagiri K, Noguchi S, Kudo T. Elevated blood flow resistance in uterine arteries of women with unexplained recurrent pregnancy loss. Hum Reprod. 2002;17:190–4.
156. Ng EH, Chan CC, Tang OS, Yeung WS, Ho PC. Endometrial and subendometrial vascularity is higher in pregnant patients with livebirth following ART than in those who suffer a miscarriage. Hum Reprod. 2007;22:1134–41.
157. Mercé LT, Barco MJ, Bau S, Troyano J. Are endometrial parameters by three-dimensional ultrasound and power Doppler angiography related to in vitro fertilization/embryo transfer outcome? Fertil Steril. 2008;89:111–7.
158. Zohav E, Orvieto R, Anteby EY, Segal O, Meltcer S, Tur-Kaspa I. Low endometrial volume may predict early pregnancy loss in women undergoing in vitro fertilization. J Assist Reprod Genet. 2007;24:259–61.
159. Luo L, Gu F, Jie H, Ding C, Zhao Q, Wang Q, Zhou C. Early miscarriage rate in lean polycystic ovary syndrome women after euploid embryo transfer – a matched-pair study. Reprod Biomed Online. 2017;35:576–82.
160. Amer SA, Shamy TTE, James C, Yosef AH, Mohamed AA. The impact of laparoscopic ovarian drilling on AMH and ovarian reserve: a meta-analysis. Reproduction. 2017;154:R13–21.

Part IV

Ultrasound of the Uterus

The Normal Uterus

7

Khaled Sakhel, Alfred Z. Abuhamad, and Callum Andrew Potts

Uterus

The uterus is a muscular organ whose purpose is to provide the implantation site and nutrients to the developing fetus. It is located in the true pelvis and lies between the urinary bladder anteriorly and the rectosigmoid colon posteriorly. The space between the uterus and the rectosigmoid is the posterior cul-de-sac, which is the most dependent area in the peritoneal cavity and where fluid tends to accumulate.

There are three main anatomic components of the uterus: the upper part or fundus that lies superior to the fallopian tube ostia, the main body or corpus, and the cervix. The lower segment of the corpus is sometimes termed the isthmus. The corpus is made up of the muscular myometrium and the endometrium. The endometrium is hormonally responsive and undergoes changes in response to ovarian hormones during a menstrual cycle. These changes prepare for implantation of the fertilized ovum. The myometrium does not undergo significant anatomic changes in response to the menstrual cycle.

This chapter discusses and illustrates the sonography of a normal uterus, including the uterine myometrium and endometrium. It also highlights the changes that occur during a normal menstrual cycle.

The uterus can be evaluated by transabdominal (transvesical) sonography (TAS) and transvaginal sonography (TVS). Two other techniques including the transrectal and translabial approach are seldom used and are usually reserved in patients where neither TAS nor TVS are feasible.

The advantage of TAS is the ability to assess the upper pelvis especially in patients with larger uteri that are greater than 12 weeks in size. Disadvantages of the TAS approach include the requirement of a full bladder and a limited image resolution especially in patients with large BMI as well as in patients with lower abdominal scars from prior surgery.

The TVS approach is clearly superior in imaging quality due to the use of higher frequency probes and is by far the most commonly used method for imaging of the pelvis. It is limited, however, by depth of penetration of the transvaginal ultrasound probe and therefore can only assess structures in the true pelvis which is adequate in most cases. For TVS the patient is asked to empty her bladder and lie supine in the lithotomy position with the legs flexed. The uterus can

K. Sakhel (✉)
Inova Fairfax Hospital, Department of Obstetrics and Gynecology, Falls Church, VA, USA

A. Z. Abuhamad
Department of Obstetrics and Gynecology, Eastern Virginia Medical School, Norfolk, VA, USA

C. A. Potts
Inova Fairfax Hospital, Women's and Children's Hospital, Falls Church, VA, USA

L. A. Stadtmauer, I. Tur-Kaspa (eds.), *Ultrasound Imaging in Reproductive Medicine*,
https://doi.org/10.1007/978-3-030-16699-1_7

be evaluated using the traditional two-dimensional (2D) probe which portrays the image in the sagittal and transverse planes. It can also be evaluated using a three-dimensional (3D) probe which can portray a reconstructed coronal image of the uterus. Ultrasound is considered the imaging modality of choice for assessing the uterus. Compared with other modalities including computed tomography (CT) and magnetic resonance imaging (MRI), ultrasound is less expensive, faster, better tolerated, and does not expose the patient to radiation. With the increasing use of 3D image reconstruction, sonography typically provides at least as much information as MRI [1].

The American Institute for Ultrasound in Medicine (AIUM) has put forth practice guidelines for the "Performance of Ultrasound of the Female Pelvis," "Ultrasound Examinations in Reproductive Medicine and Infertility," and "Focused Reproductive Endocrinology and Infertility Scan." These are helpful in establishing indications and reporting requirements [2–4].

Sonography of the uterus includes examination for size, shape, contour, orientation, and appearance of the myometrium, endometrium, and cervix. Unless the fallopian tubes are distended with fluid, they are not usually apparent during routine pelvic sonography. In addition, the cul-de-sac is routinely evaluated for scar tissue, fluid, and masses [2–4].

The uterus is first imaged in its long axis on the midsagittal plane which is obtained by optimizing the long axis of the echogenic endometrium. The midsagittal plane allows the visualization of a cross section of the myometrium, endometrium, cervix, cul-de-sac, rectum, and bladder (Fig. 7.1). In this plane, the angle between the cervix and uterus can be measured. The midtransverse plane is perpendicular to the midsagittal plane and can be obtained by rotating the probe 90° clockwise or counterclockwise. It allows visualization of a cross section of the uterine structures at different levels from fundus to outer cervical os (Fig. 7.2). The 3D ultrasound probe, when available, can acquire a volume of the uterus, and the software will use the data to generate and display a coronal image (Fig. 7.3). The coronal plane is that plane that bisects the uterus parallel to the plane of the ultrasound bed and the supine body. This has been shown to be especially helpful in detecting Mullerian anomalies and for IUD localization [1]. The Z-technique is a simple technique that describes the steps required for the display of the mid-coronal plane out of a 3D volume of the uterus [5].

As images obtained during 2D ultrasound are used to construct the 3D image, initial 2D image quality is important for diagnostic accuracy [6]. Limitations of 2D imaging, including obesity, prior surgery, and shadowing or enhancing artifacts, may be compounded with 3D reconstruction and may mimic pathology. Hence it is important to review of the original 2D acquisition planes in conjunction with the 3D reconstruction.

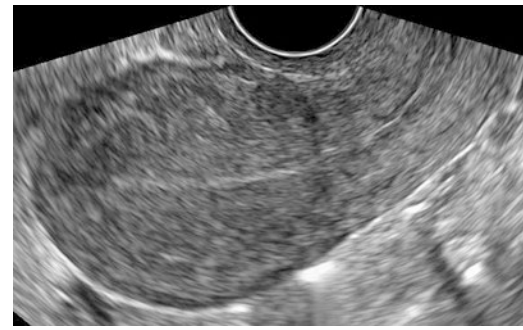

Fig. 7.1 Midsagittal plane showing an immediate postmenstrual cycle thin endometrium (Type A) with an anteverted uterus

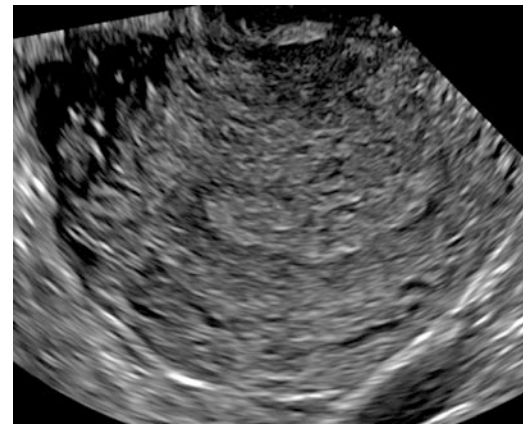

Fig. 7.2 Midtransverse plane of the uterus

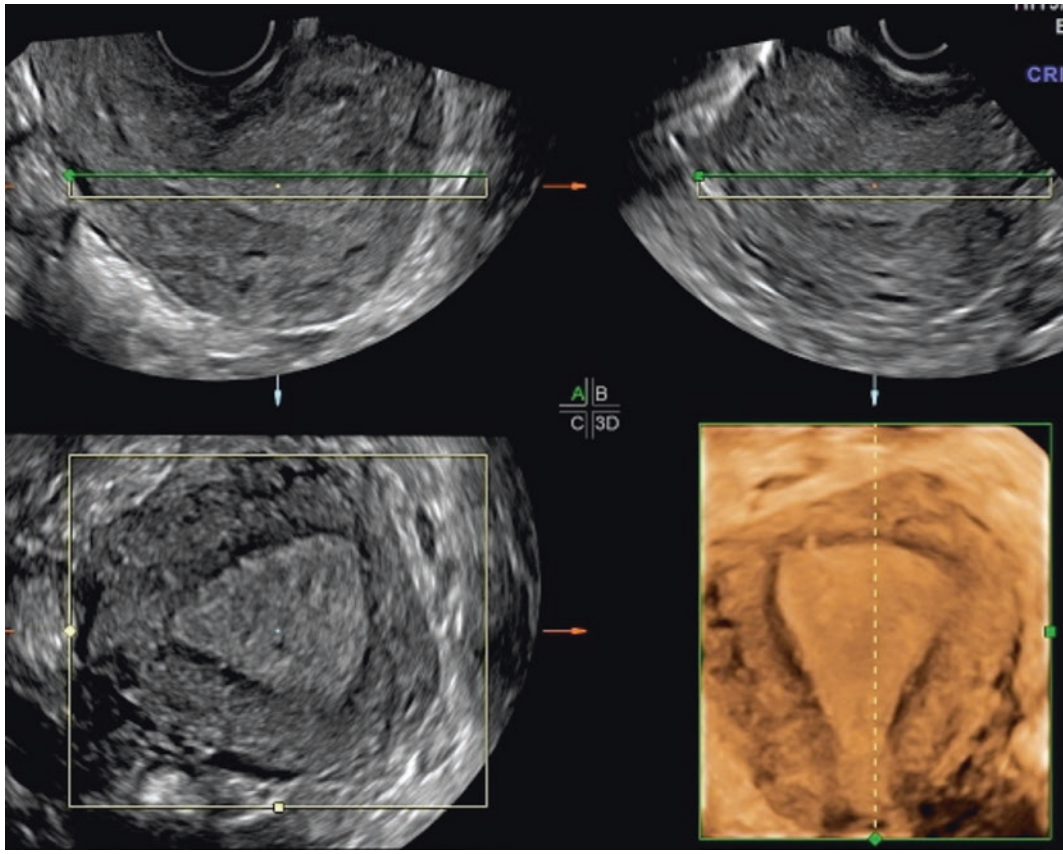

Fig. 7.3 The three orthogonal planes, sagittal, transverse, and coronal planes, as well as the rendered image. The coronal image also portrays the hypoechoic junctional zone of the myometrium

Measurements of the uterus include the length, height, and width. The length and height are measured in the midsagittal plane, whereas the width is measured in the transverse plane [7, 8]. The length is measured from outer serosal surface of the fundus to the external os of the cervix. If volume assessment of the uterus is required, then the cervical length should be excluded from the height measurement. Uterine volume may be calculated using the following formula: volume = length × width × height × 0.52. The length of a normal nulliparous uterus is 6–8.5 cm, and in multiparous women it is 8–10.5 cm. The height is measured from anterior to posterior serosal surfaces and perpendicular to the long axis of the uterus. The height of the normal uterus in nulliparous women is 2–4 cm, and in multiparous women it is 4–6 cm. The width of the corpus is taken at the widest region of the uterus on a transverse plane. The width of a nulliparous uterus is 3–5 cm and 4–6 cm in multiparous women.

The orientation of the uterus is described in the anteroposterior and right-left dimensions in relation to the supine body. The orientation is noted once the optimum midsagittal image is obtained using the echogenic endometrium for guidance. The direction of the ultrasound probe can provide the right to left orientation. The orientation in the anteroposterior dimension is described in terms of version and flexion which require image processing. The uterus is said to be flexed or angled across the isthmus when there is an angle between the cervix and the corpus of the uterus (Fig. 7.4). The anteroflexed and retroflexed uteri can pose a challenge to procedures that require access to the endometrial cavity. If there

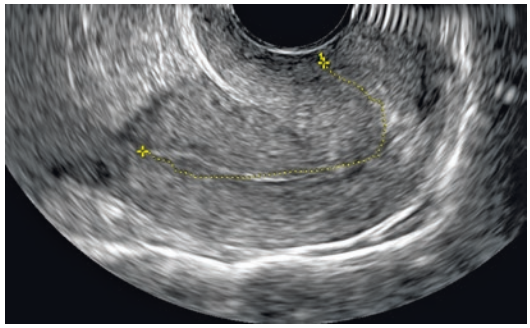

Fig. 7.4 Anteroflexed uterus with the traced line showing the sharp angle between the cervix and the endometrial cavity

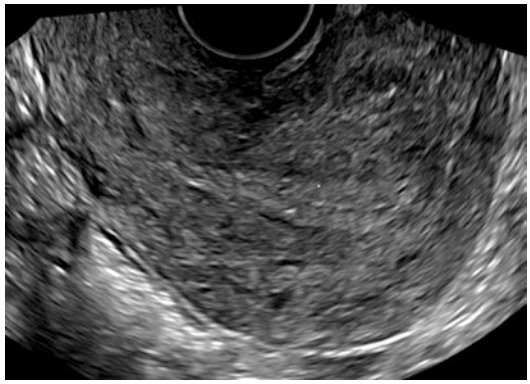

Fig. 7.5 Retroverted uterus with minimal angulation between the cervix and the endometrial cavity

is no angulation between the cervix and the corpus, the uterus is described in terms of version (Figs. 7.1 and 7.5). It is important to describe and report the orientation of the uterus as part of the ultrasound examination. This information is helpful if uterine instrumentation is required.

Myometrium

The uterine myometrium is made of a homogeneous layer of smooth muscle and blood vessels. The uterine arteries reach the uterus at the level of the cardinal ligaments and divide into ascending and descending branches that travel within the layers of the broad ligament along the lateral wall. Sonographically the normal myometrium has a medium echogenicity, less than the endometrium, with a granular echotexture. The myometrium can be divided into three layers. The inner or junctional myometrium, which abuts the endometrium, is thin and hypoechoic compared to the thicker homogeneous middle layer (see Fig. 7.3) [8, 9]. Thickening of this layer has been shown to be associated with adenomyosis [10]. The arcuate vessels separate the middle and outer layer which is also thin and slightly less echogenic than the middle layer. The myometrium does not appear to change sonographically during the course of the menstrual cycle.

Endometrium

The uterine endometrium is the site of dynamic changes in response to ovarian hormones during the menstrual cycle. It can be divided into the inner functional layer that sloughs during menses and the outer basal layer which abuts the myometrial junctional layer. The changes that occur during the menstrual cycle can be seen sonographically, and periodic assessment at different stages of the menstrual cycle may provide important information about endometrial function and receptivity [8, 9, 11–18].

The immediate postmenstrual endometrium is a thin echogenic line (Type A) at that intersection of anterior and posterior uterine walls and normally measures 3–8 mm (see Fig. 7.1). Assessing the endometrial thickness in patients presenting with postmenopausal bleeding is an important step in the overall evaluation process. It is important to know that a thin endometrium in that setting, typically at less than 5 mm, has been correlated in multiple studies with absence of endometrial cancer. When measuring endometrial thickness on ultrasound, it is critical to ensure that the uterus is in a midsagittal plane, the whole endometrial stripe is seen from the fundus to the endocervix, the thickest portion is measured, and the image is clear and magnified. Under the influence of increasing estradiol hormone levels secreted by the growing ovarian follicles, endometrial proliferation occurs. Sonographically this is seen as thickening of the lining into the so-called trilaminar layer (Type B)

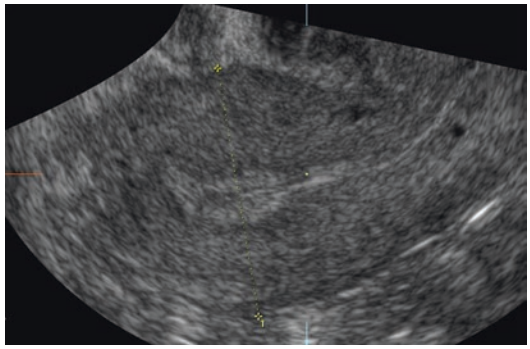

Fig. 7.6 Trilaminar endometrium (Type B) pattern begins to develop under the influence of increasing estradiol in the early proliferative phase

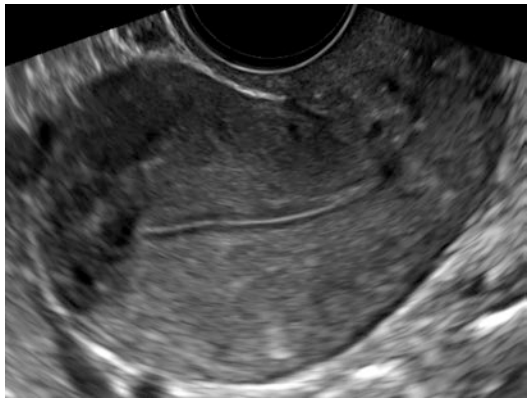

Fig. 7.7 Late proliferative phase endometrium with an accentuated trilaminar pattern (Type C)

with an anterior and posterior hypoechoic layer separated in the midline by a hyperechogenic central line (Fig. 7.6). During the late proliferative period and near the time of ovulation, endometrial lining is 8–12 mm in thickness with an accentuated trilaminar appearance (Type C, Fig. 7.7).The postovulatory endometrial lining, under the influence of progesterone hormone secreted by the corpus luteum, is characterized by loss of the trilaminar appearance and the development of a uniformly hyperechoic stripe (Type D, Fig. 7.8).

The implantation, pregnancy, and live birth rates following in vitro fertilization (IVF) are affected by the midcycle endometrial thickness [15, 19–25]. Studies have shown that a midcycle endometrial thickness less than 8 mm was associated with poor IVF outcome as compared to at least 9-mm thickness. There is conflicting evidence as to the detrimental effect of increased endometrial thickness beyond 12 mm. Cases of successful pregnancies in patients with endometrial thickness as low as 4 mm have also been reported [26].

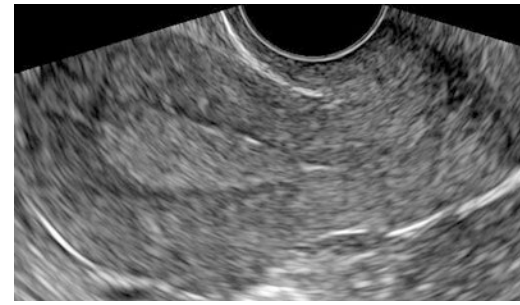

Fig. 7.8 Luteal phase endometrium showing a homogenously thickened hyperechoic stripe (Type D)

Cervix

The cervix can be divided into the portio vaginalis or ectocervix, the endocervix, and the endocervical canal. It is amenable to imaging using TAS, TVS, and translabial sonography.

Clinically the presence of endocervical mucus has been used in the assessment of the presence of increasing estradiol levels and the lead follicle. Scoring methods of the cervical mucus including the Insler and Moghissi that looked at the amount, consistency, spinnbarkeit, and ferning were introduced [27, 28]. However these often needed to be performed repeatedly which is not practical and uncomfortable for the patient. Ultrasound assessment of the cervix, in conjunction with the pelvic sonography being performed, has been introduced to look at the changes associated with the menstrual cycle [29].

Sonographically the cervical stroma is usually of the same consistency as the myometrium. The endocervical canal is normally spindle shaped and begins at the bottleneck where the endometrium tapers off. The presence of anechoic pockets within the cervix represents Nabothian cysts and is a normal finding. The cervical stroma is not

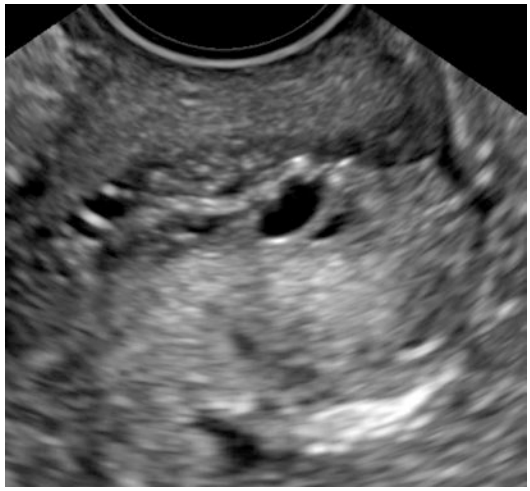

Fig. 7.9 Cervix with Nabothian cysts and blood during menses

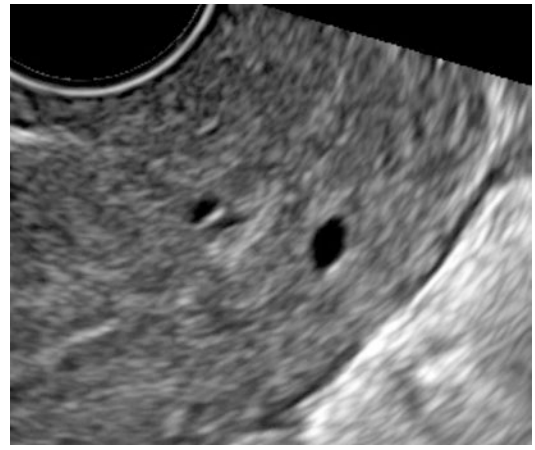

Fig. 7.11 Cervix in mid-proliferative phase showing a thicker and hyperechoic endocervix and presence of Nabothian cysts

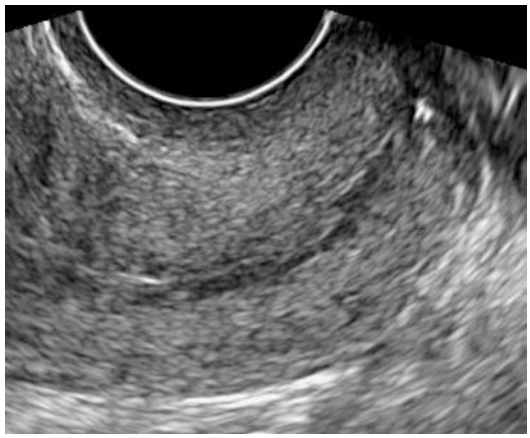

Fig. 7.10 Cervix in early proliferative phase after menses showing a thin endocervix

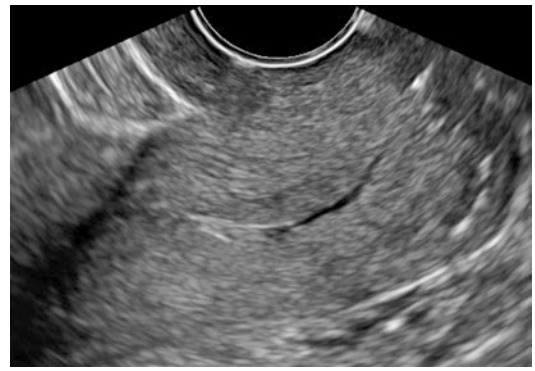

Fig. 7.12 Cervix at day 13 of cycle showing mucus in the endocervix under the effect of increasing estradiol

affected by the hormonal changes. The changes are limited to the endocervix and the appearance of cervical mucus. The endocervix during menses is noted to contain complex fluid with blood and mucus (Fig. 7.9). After the cessation of menses, the endocervix is noted to be thin and relatively hypoechogenic (Fig. 7.10). The endocervix is noted to increase in echodensity starting on cycle day 7 or when the leading follicle is 11 mm, endometrial thickness of 5.8 mm, and estradiol levels of around 289 pmol/l (Fig. 7.11). In addition, cervical mucus can be observed within the endocervical canal as of cycle day 13 or when the lead follicle is 16.8 mm and endometrial thickness is 7.5 mm or when estradiol level exceeds 500 pmol/l (Fig. 7.12) [29].

References

1. Sakhel K, Benson CB, Platt LD, Goldstein SR, Benacerraf BR. Begin with the basics: role of 3-dimensional sonography as a first-line imaging technique in the cost-effective evaluation of gynecologic pelvic disease. J Ultrasound Med. 2013;32(3):381–8.

2. American College of Nurse-Midwives (ACNM); American College of Obstetricians and Gynecologists (ACOG); American College of Osteopathic Obstetricians and Gynecologists (ACOOG); American Society for Reproductive Medicine–Society for Reproductive Endocrinology and Infertility (ASRM-SREI); Association of Women's Health, Obstetric and Neonatal Nurses (AWHONN). AIUM practice guideline for the performance of a focused reproductive endocrinology and infertility scan. J Ultrasound Med. 2012;31(11):1865–74.
3. American Institute of Ultrasound in Medicine (AIUM); American College of Radiology (ACR); American Congress of Obstetricians and Gynecologists (ACOG); Society for Pediatric Radiology (SPR); Society of Radiologists in Ultrasound (SRU). AIUM practice guideline for the performance of ultrasound of the female pelvis. J Ultrasound Med. 2014;33(6):1122–30.
4. AIUM practice Guideline for ultrasonography in Reproductive Medicine. American Institute of Ultrasound in Medicine, Society for Reproductive Endocrinology and Infertility, American Society of Reproductive Medicine. J Ultrasound Med. 2009;28(1):128–37.
5. Abuhamad AZ, Singleton S, Zhao Y, Bocca S. The Z technique: an easy approach to the display of the mid-coronal plane of the uterus in volume sonography. J Ultrasound Med. 2006;25(5):607–12.
6. Andreotti RF, Fleischer AC. Practical applications of 3D sonography in gynecologic imaging. Radiol Clin N Am. 2014;52(6):1201–13.
7. Merz E, Miric-Tesanic D, Bahlmann F, Weber G, Wellek S. Sonographic size of uterus and ovaries in pre- and postmenopausal women. Ultrasound Obstet Gynecol. 1996;7(1):38–42.
8. Poder L. Ultrasound evaluation of the uterus. In: Callen PW, editor. Ultrasonography in obstetrics and gynecology. 5th ed. Philadelphia: Saunders Elsevier; 2008. p. 919–41.
9. Mitchell DG, Schonholz L, Hilpert PL, Pennell RG, Blum L, Rifkin MD. Zones of the uterus: discrepancy between US and MR images. Radiology. 1990;174(3. Pt 1):827–31.
10. Sakhel K, Abuhamad A. Sonography of adenomyosis. Ultrasound Med. 2012;31(5):805–8.
11. Fleischer AC, Kalemeris GC, Entman SS. Sonographic depiction of the endometrium during normal cycles. Ultrasound Med Biol. 1986;12(4):271–7.
12. Fleischer AC, Pittaway DE, Beard LA, Thieme GA, Bundy AL, James AE Jr, Wentz AC. Sonographic depiction of endometrial changes occurring with ovulation induction. J Ultrasound Med. 1984;3(8):341–6.
13. Randall JM, Fisk NM, McTavish A, Templeton AA. Transvaginal ultrasonic assessment of endometrial growth in spontaneous and hyperstimulated menstrual cycles. Br J Obstet Gynaecol. 1989;96(8):954–9.
14. Randall JM, Templeton A. Transvaginal sonographic assessment of follicular and endometrial growth in spontaneous and clomiphene citrate cycles. Fertil Steril. 1991 Aug;56(2):208–12.
15. Gonen Y, Casper RF, Jacobson W, Blankier J. Endometrial thickness and growth during ovarian stimulation: a possible predictor of implantation in in vitro fertilization. Fertil Steril. 1989;52(3):446–50.
16. Lenz S, Lindenberg S. Ultrasonic evaluation of endometrial growth in women with normal cycles during spontaneous and stimulated cycles. Hum Reprod. 1990;5(4):377–81.
17. Santolaya-Forgas J. Physiology of the menstrual cycle by ultrasonography. J Ultrasound Med. 1992;11(4):139–42.
18. Bakos O, Lundkvist O, Bergh T. Transvaginal sonographic evaluation of endometrial growth and texture in spontaneous ovulatory cycles-a descriptive study. Hum Reprod. 1993;8(6):799–806.
19. Barker MA, Boehnlein LM, Kovacs P, Lindheim SR. Follicular and luteal phase endometrial thickness and echogenic pattern and pregnancy outcome in oocyte donation cycles. J Assist Reprod Genet. 2009;26:243–9.
20. McWilliams GD, Frattarelli JL. Changes in measured endometrial thickness predict in vitro fertilization success. Fertil Steril. 2007;88:74–81.
21. Amir W, Micha B, Ariel H, Liat LG, Jehoshua D, Adrian S. Predicting factors for endometrial thickness during treatment with assisted reproductive technology. Fertil Steril. 2007;87:799–804.
22. Richter KS, Bugge KR, Bromer JG, Levy MJ. Relationship between endometrial thickness and embryo implantation, based on 1,294 cycles of in vitro fertilization with transfer of two blastocyst-stage embryos. Fertil Steril. 2007;87:53–9.
23. Kovacs P, Matyas S, Boda K, Kaali SG. The effect of endometrial thickness on IVF/ICSI outcome. Hum Reprod. 2003;18:2337–41.
24. Noyes N, Hampton BS, Berkeley A, Licciardi F, Grifo J, Krey L. Factors useful in predicting the success of oocyte donation: a 3-year retrospective analysis. Fertil Steril. 2001;76:92–7.
25. Gonen Y, Casper RF, Jacobson W, Blankier J. Endometrial thickness and growth during ovarian stimulation: a possible predictor of implantation in in vitro fertilization. Fertil Steril. 1989;52:446–50.
26. Sundstrom P. Establishment of a successful pregnancy following in-vitro fertilization with an endometrial thickness of on more than 4 mm. Hum Reprod. 1998;13:1550–2.
27. Insler V, Melmed H, Eichenbrenner I, Serr DM, Lunenfeld B. The cervical score, a simple semiquantitative method for monitoring of the menstrual cycle. Int J Gynaecol Obstet. 1972;10:223–8.
28. Moghissi KS. Postcoital test: physiologic basis, technique, and interpretation. Fertil Steril. 1976;27:117–29.
29. Duijkers IJ, Klipping C. Ultrasonographic assessment of endocervix and cervical mucus in ovulatory menstrual cycles. Eur J Obstet Gynecol Reprod Biol. 2000;93(1):13–7.

Congenital Uterine Anomalies

8

Beth W. Rackow

Introduction

Congenital anomalies of the female reproductive tract, or Müllerian anomalies (MA), may involve the uterus, cervix, fallopian tubes, or vagina. Of the Müllerian anomalies, uterine anomalies are the most common; prevalence rates range from 3% to 8% of fertile and infertile women [1–5]. The true incidence of uterine anomalies in the general population, cited as 0.5% [6], is hard to determine because reproduction is not always affected; thus, some individuals are asymptomatic and unidentified, and accurate assessment and diagnosis has not always occurred [4, 5, 7]. The etiology of MA is poorly understood; the majority of MA are infrequent and sporadic, although some familial clustering occurs, and MA are generally attributed to polygenic and multifactorial causes [8, 9]. This chapter will review the embryologic development of the female reproductive tract, classification of congenital uterine anomalies, gynecologic and obstetric presentations of congenital uterine anomalies, imaging techniques, and management options for uterine anomalies.

B. W. Rackow (✉)
Columbia University Medical Center, Department of Obstetrics and Gynecology, New York, NY, USA
e-mail: bwr2113@cumc.columbia.edu

Embryology of the Female Reproductive Tract

While genetic sex is determined at the time of fertilization, male or female phenotype is not defined until after the sixth week of development. Early in embryologic development, both the Wolffian (mesonephric) and Müllerian (paramesonephric) ducts are present. The paired Wolffian ducts connect the embryologic kidney (mesonephros) to the cloaca between 5 and 10 weeks of gestation; development of the functional kidney (metanephros) is stimulated by an outgrowth of the Wolffian duct, the ureteric bud. Müllerian duct development occurs concomitant with the development of the urinary tract, and kidney and ureteral anomalies are associated with MA. The spectrum of renal anomalies includes agenesis, ectopic location, or abnormal anatomy [10]. Although gonadal development begins at the same time as Müllerian duct development, at 6 weeks of gestation, the two processes are separate and distinct; females with MA usually have normal ovaries and steroid hormone production.

Normal development of the female tract involves a complex series of events, and failure of any part of this process can result in a Müllerian anomaly. Paired Müllerian ducts arise from coelomic epithelium along the lateral walls of the urogenital ridge, and these solid ducts are present by week 6 of development. In the absence of Müllerian-inhibiting substance released from the

L. A. Stadtmauer, I. Tur-Kaspa (eds.), *Ultrasound Imaging in Reproductive Medicine*,
https://doi.org/10.1007/978-3-030-16699-1_8

male gonad, the Müllerian ducts proliferate while the Wolffian ducts regress. The Müllerian ducts elongate caudally and cross the Wolffian ducts medially, and midline fusion of the ducts forms the primitive uterovaginal structure. By week 10 of development, fusion occurs between the caudal end of the joined Müllerian ducts and the urogenital sinus. Subsequently, the unified Müllerian ducts undergo internal canalization which results in two lumens divided by a midline septum. Resorption of the septum commonly occurs in a caudal-to-cranial direction. The fused caudal portion of the Müllerian ducts becomes the uterus, cervix, and upper vagina, and the unfused cranial portion becomes the fallopian tubes. Uterine development is completed by week 20 of development.

The lower vagina has a separate embryologic origin. At week 10, when the fused Müllerian ducts connect with the urogenital sinus, the sinovaginal bulbs develop and proliferate toward the caudal end of the uterovaginal canal, forming a solid vaginal plate that elongates with time. The central cells of the vaginal plate degenerate in a caudal-to-cranial direction, forming a hollow structure. Vaginal development is also complete by week 20 of development. The hymenal membrane originates from the sinus tubercle and separates the vaginal lumen from the urogenital sinus. The central epithelial cells usually degenerate prior to birth, achieving a patent structure with a thin fold of mucus membrane at the introitus.

Although the caudal-to-cranial direction of Müllerian duct fusion and septal resorption is the traditional theory of female reproductive tract development, unusual MA have been documented that are exceptions to this order of progression. Examples include a complete septate uterus with a double cervix and vaginal septum and a normal uterus and cervix with an isolated longitudinal vaginal septum [11–14]. Hence, midline fusion of the Müllerian ducts and septal resorption may not be a unidirectional process as theorized but may be bidirectional [15]. Other constellations of Müllerian anomalies have been described that further defy the traditional concept of Müllerian duct development [16].

Classification of Müllerian Anomalies

Müllerian anomalies are commonly classified into three categories: agenesis and hypoplasia, lateral fusion defects, and vertical fusion defects. Reproductive tract abnormalities due to in utero exposure to diethylstilbestrol (DES) comprise a fourth group of anomalies. *Agenesis and hypoplasia* can occur for a portion of or an entire Müllerian duct, or for both ducts, affecting one or multiple Müllerian structures. *Lateral fusion defects* are the most common category of Müllerian defects and originate due to failure of migration of the ducts, midline fusion of the ducts, or absorption of the midline septum between the ducts. A range of anomalies can occur including symmetric or asymmetric and nonobstructed or obstructed Müllerian structures. *Vertical fusion defects* occur due to disordered fusion of the Müllerian ducts with the urogenital sinus or abnormal vaginal canalization and may present with menstrual flow obstruction.

Although there is no universally accepted standard classification for Müllerian anomalies, the American Society of Reproductive Medicine (ASRM) classification system from 1988 is commonly utilized and provides a standardized nomenclature to describe anomalies (Fig. 8.1) [4, 17]. This classification system focuses on the major categories of uterine anomalies and describes them based on their embryologic etiology. Hypoplasia/agenesis (category I) and unicornuate (category II) denote anomalies with developmental failure of one or both Müllerian ducts; didelphys (category III) and bicornuate (category IV) describe anomalies involving a varying degree of failure of midline fusion; septate (category V) and arcuate (category VI) identify anomalies with some degree of failure of resorption of the midline septum. DES drug-related anomalies (category VII) are a separate category of anomalies and will not be discussed in this chapter. With this classification system, associated anomalies of the vagina, cervix, fallopian tubes, and urinary system must be documented separately. Two additional issues with this classification system are the inability to fully

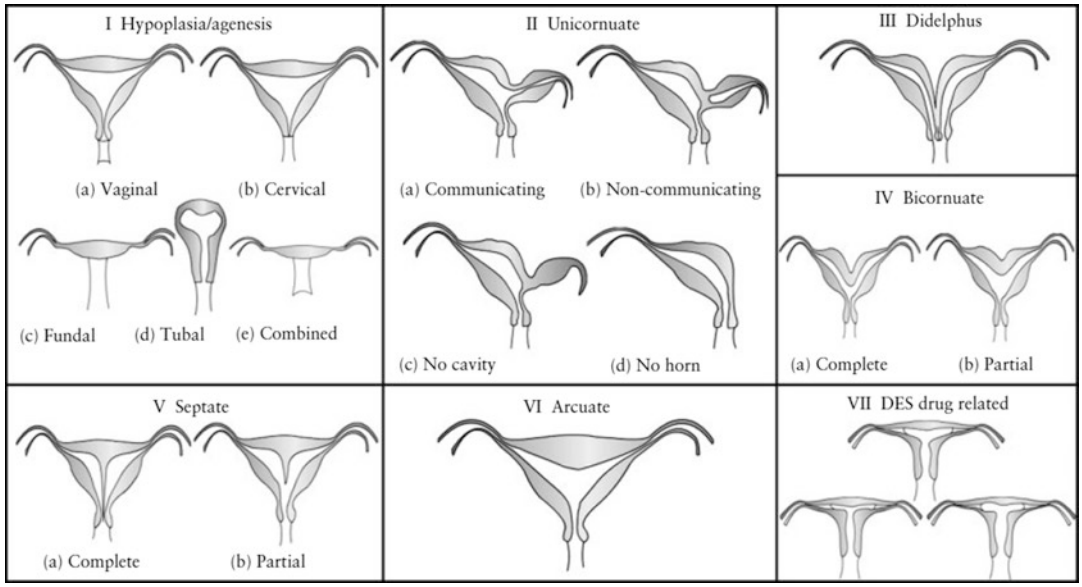

Fig. 8.1 Classification of uterine anomalies according to the American Society of Reproductive Medicine [17]. DES, diethylstilbestrol. (Reprinted from Bermejo et al. [18]. With permission from John Wiley & Sons, Inc.)

describe a uterine anomaly when multiple abnormalities are present (i.e., septate uterus with duplicated cervix) and the lack of specific diagnostic criteria to enable differentiation between bicornuate, septate, and arcuate uteri [4, 11, 19, 20]. Hence, complex anomalies need to be described according to the component parts.

Overview of the Uterine Anomalies

Müllerian Agenesis

The most extreme of the Müllerian anomalies is Müllerian agenesis, otherwise known as Mayer-Rokitansky-Küster-Hauser (MRKH) syndrome, which occurs due to agenesis or hypoplasia of the Müllerian ducts and affects approximately 1 in 5000 females [21]. Müllerian agenesis involves congenital absence of the vagina and variable uterine development that ranges from agenesis to hypoplastic and rudimentary structures. One study demonstrated that in females with MRKH, 87% had Müllerian remnants, 26% of the remnants were cavitated and contained endometrial tissue, 7% had a Müllerian remnant measuring >4 cm, and 30% had anomalies of the urinary tract [22]. Along with urologic anomalies, Müllerian agenesis is associated with other extragenital anomalies involving skeletal, cardiac, and auditory systems and digits and palate [23, 24].

Unicornuate Uterus

The unicornuate uterus arises due to agenesis or hypoplasia of one of the two Müllerian ducts. The unicornuate uterus is a functional uterus with a normal-appearing cervix and a single fallopian tube, and the contralateral side may have a variety of configurations: agenesis or a rudimentary horn in 74% [6]. The rudimentary horn can be noncommunicating (70–90%) or communicating with the unicornuate uterus and may contain functional endometrium [25]. Women with a rudimentary uterine horn containing functional endometrium may present with cyclic or chronic pain, endometriosis, or a horn gestation [25]. Nonfunctional rudimentary horns are usually asymptomatic. Lastly, the unicornuate uterus is associated with a 40% incidence of renal anomalies, usually ipsilateral to the anomalous side [25–27].

Uterus Didelphys

The uterus didelphys results from complete failure of lateral fusion of the two Müllerian ducts; duplication of the Müllerian structures is the result. Anatomically, these women have two unicornuate uteri, two separate endometrial cavities, and two cervices. In the majority of women with a uterus didelphys, vaginal duplication also occurs, and a longitudinal vaginal septum is present. Additionally, this uterine anomaly can present with an *o*bstructed *h*emi*v*agina and associated *i*psilateral *r*enal *a*nomaly, termed OHVIRA syndrome [28, 29].

Bicornuate Uterus

Incomplete lateral fusion of the Müllerian ducts at the fundus results in a bicornuate uterus. Commonly, a single cervix and two endometrial cavities are present. Variability exists in the extent of separation between the two cavities, with maximal separation extending down to the internal cervical os (complete bicornuate). A fundal indentation of at least 1 cm is commonly used to differentiate a bicornuate from a septate uterus [11, 30–33]. Although a normal vagina is commonly present, a longitudinal vaginal septum can occur with the bicornuate uterus [14].

Septate Uterus

The septate uterus occurs due to a defect in resorption of the midline division between the two fused Müllerian ducts, and a fibromuscular septum remains. The degree of septation can vary from complete, extending from the uterine fundus through the cervix, to partial, in which a portion of the caudal aspect of the septum is resorbed. Since the Müllerian ducts are completely fused, a normal external fundal contour is present despite a complete or partial division of the endometrial cavity. A longitudinal vaginal septum is a common finding with a complete septate uterus and can also occur with a partial septate uterus [14]. Endometriosis is also associated with septate uteri and has been documented in 30% of fertile and infertile women with septate uteri [34, 35].

Arcuate Uterus

The arcuate uterus demonstrates a slight, rounded midline septum with a broad fundus and sometimes has a small indentation at the fundus. It has been characterized as a variant of normal uterine anatomy or a uterus with a small partial septum [17]. Appropriate imaging to define uterine anatomy is essential so as not to misclassify a uterus as arcuate instead of partial septate or bicornuate, which have different reproductive implications.

Clinical Presentation of Congenital Uterine Anomalies

Although many females with congenital uterine anomalies are asymptomatic and a late diagnosis may occur during evaluation of infertility [36, 37], it is important to recognize several gynecologic and obstetric signs and symptoms that may indicate a uterine disorder (Table 8.1). Müllerian agenesis presents with primary amenorrhea. Women with an obstructive anomaly may report cyclic or noncyclic pelvic pain, and dysmenorrhea if they menstruate, and these symptoms can begin several months after menarche or into adulthood. Obstructive uterine anomalies are associated with hematometra, retrograde menstruation,

Table 8.1 Clinical presentation of uterine anomalies

Gynecology	Obstetrics
Pelvic pain, cyclic or noncyclic	Pregnancy loss: first and second trimester
Dysmenorrhea	Cervical incompetence
Primary amenorrhea with pain	Preterm labor and delivery
Primary amenorrhea without pain	Intrauterine growth restriction
Hematometra	Placental abruption
Abnormal uterine bleeding	Intrauterine fetal demise
Dyspareunia	Malpresentation
	Cesarean delivery
	Pregnancy-induced hypertension (related to renal abnormalities)
	Pregnancy in rudimentary uterine horn

and endometriosis [26, 38]. Endometriosis is a common finding in women with obstructive and nonobstructive Müllerian anomalies and is a known etiology of infertility [34, 38]. Abnormal bleeding can occur with uterine anomalies and has been associated with septate uteri [34] and can be due to vaginal anomalies: a partial or microperforate vaginal obstruction or a longitudinal vaginal septum. A nonobstructive vaginal anomaly such as a longitudinal vaginal septum, which is commonly found with septate and didelphys uteri, may be the first hint that a uterine anomaly is present; associated symptoms include difficulty with tampon insertion, bleeding around one tampon (two are required), and dyspareunia. Hence, if a vaginal anomaly is identified, then uterine imaging is warranted [14].

In obstetrics, congenital uterine anomalies are associated with a higher rate of poor obstetric outcomes: recurrent pregnancy loss (RPL), first and second trimester pregnancy loss, intrauterine growth restriction, preterm labor and preterm birth, placental abruption, malpresentation, and intrauterine fetal demise [1, 7, 26, 39–41]. Among women with RPL, the incidence of uterine anomalies is highly variable and ranges from 6% to 38%, but based on meta-analyses it is likely closer to 12–16% and as high as 25% in women with second trimester pregnancy loss [3–5, 42]. Uterine dysfunction may occur due to diminished cavity size, insufficient musculature, impaired ability to distend, abnormal myometrial and cervical function, inadequate vascularity, or abnormal endometrial development [1, 3, 8, 27, 43–48]. Due to higher rates of malpresentation, an increased rate of cesarean delivery can be seen with uterine anomalies [41]. Additional obstetric complications such as cervical incompetence [49], pregnancy-induced hypertension (due to renal anomalies), and antepartum and postpartum bleeding are also associated with congenital uterine anomalies. Lastly, pregnancy may occur in an obstructed or rudimentary uterine horn. These pregnancies are surgical emergencies due to an 89% rate of rupture and the related morbidity and mortality [25].

Imaging of Congenital Uterine Anomalies

Initial testing to evaluate pelvic anatomy, especially in infertile women, may include hysterosalpingography (HSG) and two-dimensional ultrasonography (2DUS). While these modalities are useful for the initial assessment of uterine anomalies, additional testing may be warranted such as saline infusion ultrasonography (SIS), magnetic resonance imaging (MRI), and the increasingly common technique of three-dimensional ultrasonography (3DUS). The benefit of 3DUS and MRI is the ability to simultaneously assess the uterine fundus and cavity [18]. However, there are inherent strengths and limitations to each imaging technique; thus, a combination of several techniques may be necessary to evaluate a uterine anomaly. Although surgical evaluation (i.e., laparoscopy, hysteroscopy, laparotomy) has been considered the gold standard for evaluation of complex Müllerian anomalies [19, 43], with readily available diagnostic imaging, surgery is infrequently necessary to diagnose an anomaly. Surgical intervention with hysteroscopy and/or laparoscopy may only be necessary when the uterine anomaly is amenable to surgery and the intervention is clinically necessary [4, 50, 51]. This discussion will review all available imaging techniques and will focus on the technique of 3D ultrasonography.

Hysterosalpingography

A common procedure for evaluation of tubal patency in women with infertility, HSG also provides information about the contour of the uterine cavity. In a woman with a uterine anomaly, the HSG may identify patent canals and any complex communications, but is unable to adequately evaluate the external uterine contour and, hence, cannot reliably differentiate between uterine anomalies [4, 11, 36]. When a uterine anomaly is identified, assessment of the external uterine contour can be achieved with 2DUS, 3DUS, and/or SIS. In one study, HSG correctly diagnosed 55%

of septate and bicornuate uteri, and the addition of ultrasonography improved this result to 90% [52]. Since the HSG involves exposure to ionizing radiation, in young women with desired fertility, this test should only be ordered when clinically indicated.

Two-Dimensional Ultrasonography

Two-dimensional transabdominal or transvaginal ultrasonography is a common technique for assessing pelvic structures and is the appropriate initial imaging modality for asymptomatic women [53]. It effectively visualizes the uterine structure and endometrial contour, can detect a pelvic mass or hematometra, confirms the presence of ovaries, and can be used to evaluate the kidneys. When 2DUS is performed in the secretory phase of the menstrual cycle, better visualization of the endometrium and internal uterine contour can be achieved [54, 55]. A compilation of 2DUS studies for uterine anomalies noted a pattern of low sensitivity and high specificity; although 2DUS can only identify about half of the uterine anomalies present, the diagnosis of an anomaly is highly likely to be correct [4]. When indicated, *saline infusion sonography* can be employed to further assess the internal and external uterine contours and can accurately diagnose uterine anomalies as well as identify other intracavitary abnormalities such as polyps, myomas, or adhesions [4, 51, 56].

Pelvic Magnetic Resonance Imaging

Pelvic MRI is a sensitive and specific imaging modality for evaluating Müllerian anomalies [11, 57]. MRI provides detailed delineation of internal and external uterine contours, can differentiate between a myometrial and fibrous uterine division, can differentiate between a septate cervix and duplicated cervix, can diagnose vaginal anomalies, and can identify if a rudimentary uterine horn contains functional endometrium [11, 18]. Furthermore, MRI can also assess renal morphology and location. Although costly, this non-invasive imaging modality is less expensive than surgery [19]. Pelvic MRI may not be necessary for every patient with a uterine anomaly and may be best utilized for the evaluation of complex Müllerian anomalies [18, 37, 53].

A number of studies have evaluated the efficacy of MRI to assess surgically confirmed uterine anomalies [19, 58–61]. A range of sensitivity (29–100%) and specificity (33–100%) and positive predictive value (83–100%) and negative predictive value (25–100%) was identified. The ability of MRI to detect and correctly diagnose a uterine anomaly can be limited by the availability of technically adequate images which may be influenced by the MRI machine and software utilized and requires image interpretation by a practitioner with experience in the diagnosis of uterine anomalies [19, 51].

Three-Dimensional Ultrasonography

Three-dimensional ultrasonography (3DUS) is a newer imaging technique that provides detailed and highly accurate views of pelvic anatomy; it constructs three-dimensional volumes from a series of two-dimensional images [19, 32]. After the volume is created, it can be stored and any section of a structure can be examined. With uterine anomalies, the ability to visualize the coronal section of the uterus is invaluable for assessing the architecture of the endometrial cavity and the uterine fundus (Fig. 8.2) [18, 32, 50, 62, 63]. Therefore, by evaluating the internal and external uterine contours, 3DUS is able to reliably differentiate between various uterine anomalies and can assess the often subtle differences between septate and bicornuate uteri [18, 19, 32, 33, 62, 64]. However, distortion by leiomyomas may make uterine assessment more challenging [7, 19, 62]. This modality is less expensive and less time-consuming than surgery or pelvic MRI, is less invasive than surgery, and may be better tolerated and thus is ideal for evaluating symptomatic women and those at high risk of uterine anomalies [18, 19, 53, 55]. Although the ASRM classification for uterine anomalies (see Fig. 8.1) does not provide dimensions or measurements to enable differenti-

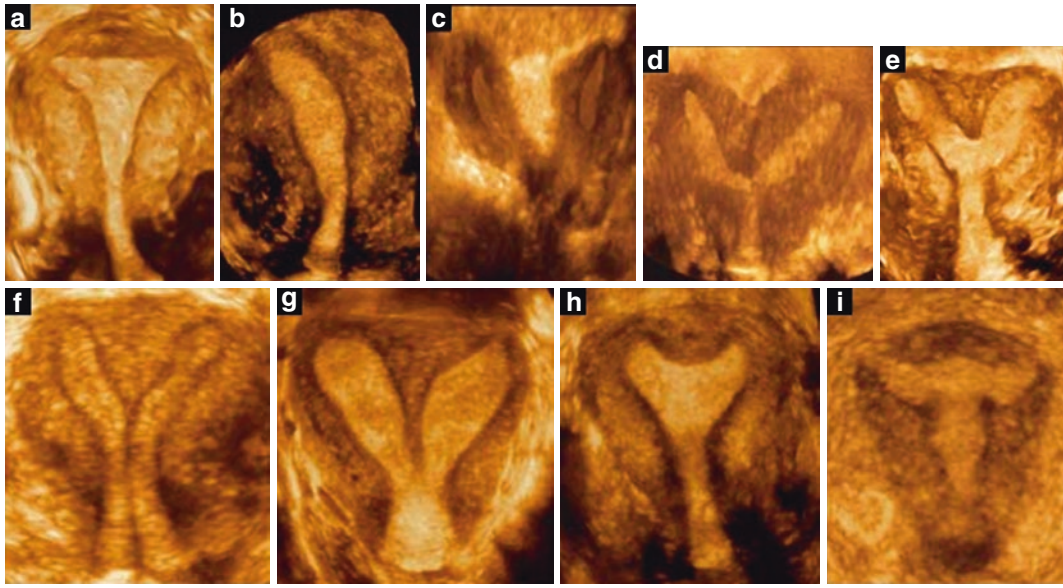

Fig. 8.2 Three-dimensional rendered coronal ultrasound images demonstrating different uterine anomalies using the American Fertility Society classification [17]: (**a**) normal uterus; (**b**) unicornuate uterus; (**c**) didelphic uterus; (**d**) complete bicornuate uterus; (**e**) partial bicornuate uterus; (**f**) complete septate uterus; (**g**) partial septate uterus; (**h**) arcuate uterus; (**i**) uterus with diethylstilbestrol (DES) drug-related malformations. (Reprinted from Bermejo et al. [18]. With permission from John Wiley & Sons, Inc.)

Table 8.2 Three-dimensional ultrasound criteria for classification of congenital uterine anomalies

Uterine morphology	Fundal contour	External contour
Normal	Straight or convex	Uniformly convex or with indentation <10 mm
Arcuate	Concave fundal indentation with central point of indentation at obtuse angle (>90°)	Uniformly convex or with indentation <10 mm
Partial septate	Presence of septum (does not extend to cervix) with central point of septum at an acute angle (<90%)	Uniformly convex or with indentation <10 mm
Complete septate	Presence of septum that completely divides cavity from fundus to cervix	Uniformly convex or with indentation <10 mm
Bicornuate	Two well-formed uterine cornua	Fundal indentation >10 mm dividing the two cornua
Unicornuate uterus	Single well-formed uterine cavity with a single interstitial portion of fallopian tube and concave fundal contour	Fundal indentation >10 mm dividing the two cornua if a rudimentary horn is present

Adapted from [20, 64]

ation of uterine anomalies based on ultrasound findings, a modification of the ASRM criteria based on 3DUS landmarks has been utilized to facilitate the diagnosis of uterine anomalies (Table 8.2, Fig. 8.3) [11, 17, 19, 20, 50, 64].

When compared to HSG and 2DUS, 3DUS demonstrates high sensitivity and specificity for the identification of a normal uterus (98% and 100%), arcuate uterus (100% and 100%), or major uterine anomaly (100% and 100%) [62]. In comparison, 2DUS has lower sensitivity and specificity for the diagnosis of a normal uterus (88% and 94%) or arcuate uterus (67% and 94%) but is similarly accurate with major uterine anomalies (100% and 95%). Hence, 2DUS may be best utilized as a screening test for uterine

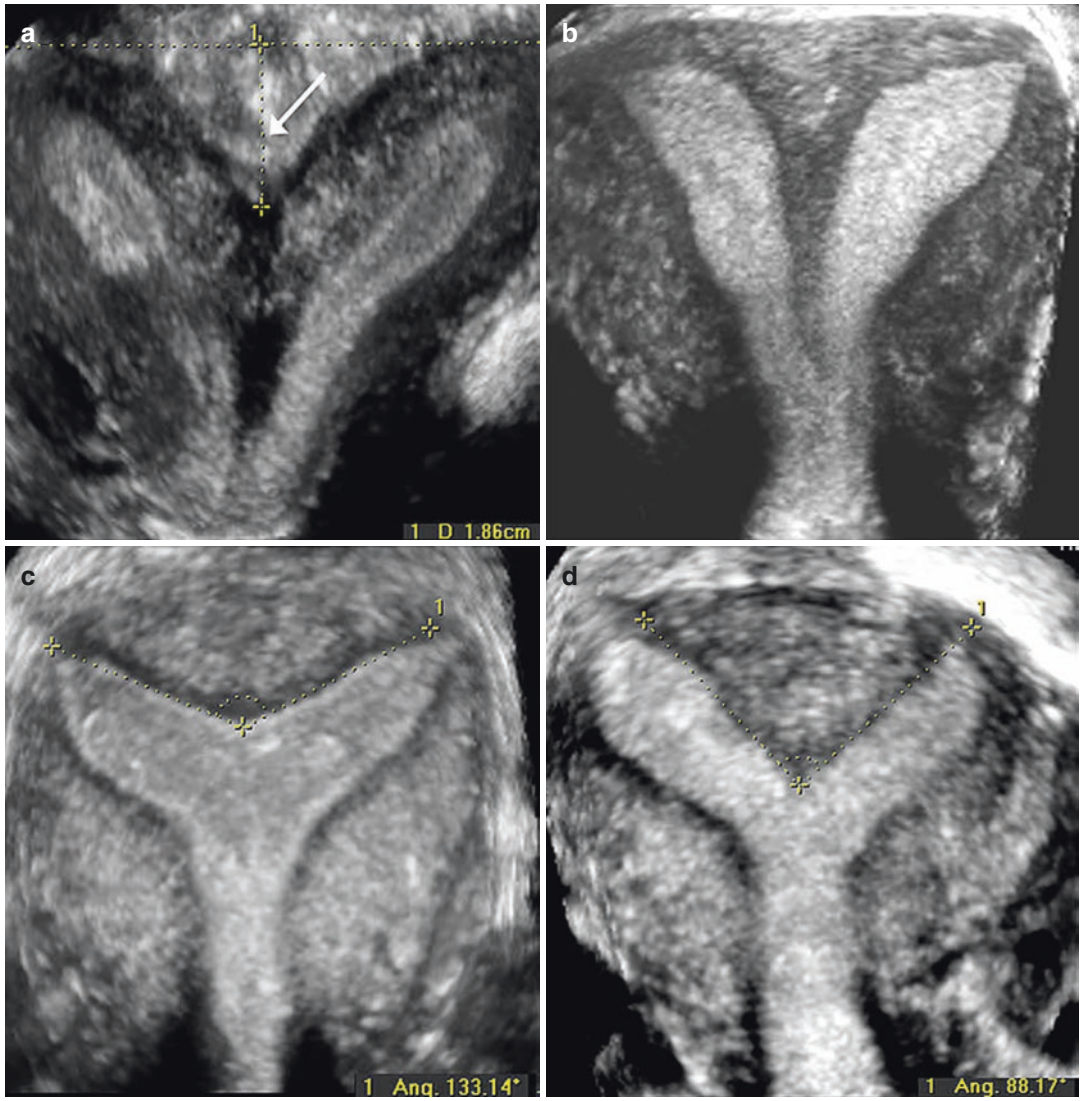

Fig. 8.3 Three-dimensional rendered coronal ultrasound images demonstrating ultrasound criteria for classification of congenital uterine anomalies. (**a**) Bicornuate uterus: two divergent cornua are noted, divided by a sagittal cleft >10 mm (*arrow*). (**b**) Complete septate uterus: a normal external uterine contour is present, and a septum divides the endometrial cavity and extends to the cervix. (**c**) Arcuate uterus: a normal external uterine contour is identified with a concave fundal indentation of the endometrial cavity at an obtuse angle. (**d**) Partial septate uterus: a normal external uterine contour is present, the septum does not extend to the cervix, and the central point of the fundal indentation demonstrates an acute angle. (Reprinted from Ghi et al. [50], Copyright 2009, with permission from Elsevier)

anomalies, with 3DUS as the definitive diagnostic test [62].

Several studies investigated the accuracy of 3DUS for the evaluation and diagnosis of uterine anomalies and confirmed the radiologic findings at surgery (laparoscopy and/or hysteroscopy). In one study, 3DUS assessment of the uterine fundus correlated 91.6% with laparoscopic findings, and evaluation of the uterine cavity correlated 100% with hysterosalpingography [65]. Wu et al. compared 3DUS with laparoscopy for the detection of uterine anomalies, and 3DUS demon-

strated 100% sensitivity and specificity and correctly diagnosed 92% (11/12) of septate uteri and 100% (3/3) of bicornuate uteri [33]. A study of 3850 infertile women who underwent uterine evaluation with 3DUS and hysteroscopy identified 689 (17.9%) with septate uteri, and 3DUS demonstrated 99.27% sensitivity and 100% specificity for diagnosing a septate uterus [7]. Another recent study investigated 254 nulliparous women with recurrent pregnancy loss, and 3DUS findings were confirmed by office hysteroscopy (for normal uteri) or laparoscopy/hysteroscopy if a uterine anomaly was identified [50]. Fifty-four subjects (19%) were diagnosed with a uterine anomaly, and 3DUS correctly identified 52 (92.3%) of the anomalies; two partial septate uteri were misclassified as bicornuate and arcuate. When 3DUS and 2DUS were compared for the diagnosis of uterine anomalies during different phases of the menstrual cycle, both modalities had higher sensitivity and specificity during the luteal phase, but 3DUS demonstrated greater sensitivity and specificity in both the follicular and luteal phases, and the diagnostic accuracy of 3DUS was comparable to HSG, hysteroscopy, and laparoscopy [55]. Lastly, the reproducibility of the interpretation of 3DUS volumes to diagnose uterine anomalies has been established [64].

Few studies have compared the diagnosis of uterine anomalies by 3DUS versus pelvic MRI. Bermejo et al. determined that in women with uterine anomalies, 3DUS and MRI demonstrate a high degree of concordance, with a kappa index of 0.880 (95% CI, 0.77–0.99) [18]. Discrepancies occurred in the diagnosis of 4 of 65 anomalies; 3DUS misclassified 1 bicornuate uterus as uterus didelphys and 3 septate uteri as bicornuate uteri. In a recent similar study, Graupera et al. determined that 3DUS was highly accurate in the diagnosis of uterine anomalies with a high level of agreement with pelvic MRI (kappa value between 0.9 and 1.0 for each anomaly, $p < 0.001$) [66]. In contrast, Faivre et al. investigated women with suspected septate and bicornuate uteri; all 31 uterine anomalies were confirmed by hysteroscopy and/or laparoscopy [51]. 3DUS correctly identified 31/31 uterine anomalies, and pelvic MRI correctly identified 24/31 uterine anomalies; 5 septate uteri were misclassified as bicornuate uteri and 2 partial septate uteri as complete septate uteri. These discrepancies were attributed to the lack of a coronal uterine image and lack of familiarity with the evaluation of uterine anomalies.

A recent retrospective study compared 3DUS and MRI diagnosis in surgically proven Müllerian duct anomaly cases; all patients also underwent hysteroscopy and laparoscopy [67]. 3DUS identified 28 of 29 (96%) anomalies correctly; one patient was diagnosed by 3DUS with a uterine septum but had an arcuate uterus. In contrast, MRI correctly identified 23 of 29 (79%) anomalies correctly. The authors concluded that with experienced providers, 3DUS can have a higher diagnostic accuracy level than MRI for evaluation of Müllerian anomalies. However, since the MRI studies were not obtained with a specific MA protocol, this may have had a negative impact on the ability to correctly diagnose the MA; therefore, this study may best show that 3DUS has diagnostic accuracy for MA comparable to that of laparoscopy and hysteroscopy.

A recent consensus publication investigated the accuracy of imaging techniques in diagnosing Müllerian anomalies [53]. A pooled analysis of 38 studies demonstrated that the imaging techniques with highest overall diagnostic accuracy were, in decreasing order, 3DUS (97.6%), SIS (96.5%), 2DUS (86.6%), and HSG (86.9%). MRI correctly subclassified 85.8% of the anomalies, and the authors stated that this implies that MRI correctly identifies the presence of an anomaly in >90% of cases. Overall, 3DUS was found to be at least as accurate as MRI, and possibly more accurate, for subclassifying Müllerian anomalies.

Thus, 3DUS has been demonstrated to be at least as accurate as pelvic MRI for diagnosing uterine anomalies. However, 3DUS is not a widely available imaging modality and requires a high level of practitioner skill and experience to achieve high diagnostic accuracy [18, 19, 60]. Although these studies have promising results, it must be emphasized that they were performed by practitioners with expertise in the performance and interpretation of 3DUS and in the diagnosis of uterine anomalies.

Urinary Tract Imaging

Lastly, since urinary tract anomalies are associated with Müllerian anomalies, imaging of the urinary tract should be considered when a uterine anomaly is identified. Upper urinary tract anomalies include renal agenesis, horseshoe or pelvic kidney, duplication of the collecting system, or an ectopic ureter [10]. Renal anomalies most commonly occur with unicornuate and didelphic uteri and with Müllerian agenesis and are infrequently identified with bicornuate, septate, and arcuate uteri [68]. If an obstructive Müllerian anomaly is identified such as a unicornuate uterus with a rudimentary uterine horn or uterus didelphys with an obstructed hemivagina, renal anomalies including renal agenesis are commonly identified ipsilateral to the obstruction. In more than 50% of cases, renal agenesis is predictive of an obstructive Müllerian anomaly [25].

Options for urinary tract imaging include renal ultrasound, intravenous pyelogram, computed tomography (CT) scan, or magnetic resonance (MR) urogram. Due to a higher risk of urinary tract anomalies, more detailed imaging is warranted in females with complex uterine and/or vaginal anomalies involving a unilateral obstruction such as a unicornuate or uterus didelphys or Müllerian agenesis [68]. In other women diagnosed with a Müllerian anomaly, consideration should be given to renal evaluation with ultrasonography based on symptoms and the extent of the malformation [10]. However, some experts state that imaging of the urinary tract in females with Müllerian anomalies is recommended as mandatory [53].

Reproductive Outcomes with Uterine Anomalies

Challenges with maintenance of pregnancy, not conception, are commonly associated with uterine anomalies; uterine anomalies do not prevent conception, and normal reproductive outcomes are possible. Infertile women have a 3.4–8% mean prevalence of uterine anomalies which is comparable to that of the fertile population [3–5]. A higher prevalence of uterine anomalies (12.6–16.7%) is seen in women with RPL [3–5]. These data suggest that uterine anomalies have a negligible effect on fertility, and maintenance of pregnancy is the larger issue [3, 34]. Furthermore, women with uterine anomalies who undergo assisted reproductive technologies have comparable pregnancy rates to infertile women with normal uteri but a higher rate of pregnancy loss and preterm delivery [69]. These adverse reproductive outcomes are attributed to deficient musculature and reduced cavity size, abnormal vascularity, and cervical insufficiency [68].

Depending on the population studied and the accuracy of the imaging modalities in diagnosing uterine anomalies, the arcuate [4, 5] or septate uterus [3, 11, 70] is the most common uterine anomaly. Saravelos et al. report that the arcuate uterus is the most common uterine anomaly in the general (2.4%) and recurrent miscarriage (12.0%) populations, but the septate uterus is most common in the infertile population (3.9%) [4]. A more recent meta-analysis identified that the arcuate uterus is the most common anomaly (3.9%) in the general population and its prevalence is not increased in groups at high risk for poor reproductive outcomes, while the septate uterus is the most common anomaly (3.0–15.4%) in high-risk populations (women with infertility and a history of miscarriage) [5]. These data highlight the reproductive dysfunction associated with the septate uterus and raise questions about a possible relationship between the septate uterus and infertility.

The septate uterus contains a hypovascular fibromuscular septum, and this structural abnormality as well as abnormalities in the endometrium overlying the septum may predispose this anomaly to the worst reproductive outcomes [44, 48, 71]. A compilation of studies investigating pregnancy outcome in women with an untreated septate uterus identified a 44% abortion rate (range 23–67%), 22% preterm delivery rate (range 8.6–33%), 33% term delivery rate (range 0–68%), and 50% live birth rate (range 28–68.5%) (Table 8.3) [3]. Another study compared women with septate uteri to the general population and identified an increased rate of early abortion

Table 8.3 Reproductive outcomes in women with congenital uterine anomalies

Uterine anomaly	Number of studies	Number of patients	Number of pregnancies	Abortion rate	Preterm birth rate	Term delivery rate	Live birth rate
Unicornuate	11	151	250	36.5	16.2	44.6	54.2
Didelphys	8	114	152	32.2	28.3	36.2	55.9
Bicornuate	4	261	627	36	23	40.6	55.2
Septate	4	198	499	44.3	22.4	33.1	50.1
Arcuate	3	102	241	25.7	7.5	62.7	66

Based on data from [3]
Rates are averaged and presented as a percentage

(41.1% versus 12.1%) and late abortion and preterm delivery (12.6% versus 6.9%) [7]. Due to variability in the pregnancy outcomes reported in the included studies, these data may overstate the degree of reproductive compromise seen with this anomaly and represent a "worst-case scenario" [20]. Regardless, it is clear that the septate uterus may significantly impact reproductive outcomes. Fortunately, it is the most treatable uterine anomaly and can be corrected with hysteroscopy, a minimally invasive procedure.

Unicornuate, didelphys, and bicornuate uteri are implicated in adverse reproductive outcomes; live birth rates for women with these uterine anomalies are at least 50–55%, and miscarriage rates are approximately 35% (see Table 8.3) [3, 68]. These rates are somewhat better than those associated with the septate uterus and, again, may represent a less optimistic statement of reproductive outcomes. A 2009 review of pregnancy outcomes with a unicornuate uterus identified similar reproductive outcomes: 24.3% first trimester loss, 9.7% second trimester loss, preterm delivery 20.1%, term delivery 44.0%, and total live birth rate 49.9% [72]. Additionally, overall obstetrical outcomes may be somewhat better with the bicornuate uterus due to variability in the degree of cavity division; the rate of preterm delivery differs between partial (29%) and complete (66%) bicornuate uteri [73].

By definition, the arcuate uterus deviates minimally from normal uterine anatomy and thus is traditionally considered benign and not associated with an increased risk of adverse pregnancy outcomes [17, 32]. However, the arcuate uterus has been associated with a range of reproductive outcomes: live birth rates range from 48% to 82.7% [1, 3, 39]. One concern is that when less accurate imaging techniques are utilized, a bicornuate or partial septate uterus may be misclassified as an arcuate uterus and mistakenly associated with worse reproductive outcomes [32]. Based on what is known about arcuate uterine anatomy, the more optimistic reproductive data are more believable, and surgical intervention is likely not warranted unless poor reproductive outcomes occur.

Indications for Surgical Intervention

Historically, surgery was considered the gold standard for the evaluation and diagnosis of Müllerian anomalies. However, due to the availability of advanced imaging techniques that can assess the uterine fundal contour and endometrial cavity architecture, diagnostic surgical procedures such as an exam under anesthesia, vaginoscopy, hysteroscopy, and laparoscopy are infrequently necessary when diagnosing uterine anomalies.

Surgical intervention is indicated for women with obstructive anomalies, pelvic pain, endometriosis, and poor obstetric outcomes such as RPL, second trimester loss, or preterm delivery. In women with RPL and preterm delivery, it is important to rule out extrauterine causes of these obstetric issues [8, 26]. Although certain uterine anomalies such as the septate uterus are amenable to surgical correction, the unicornuate uterus is never considered operable (although rudimentary horns may warrant surgical intervention), and bicornuate and didelphys uteri are considered

operable in select circumstances [26, 68, 70, 74]. Abdominal metroplasty can be performed to unify a bicornuate uterus or uterus didelphys but is only performed in select patients with poor obstetric outcomes [26, 70, 74]. The goals of surgery include treatment of pelvic pain and endometriosis, restoration of pelvic anatomy, and preservation of fertility.

Hysteroscopic metroplasty to correct a partial or complete septate uterus can improve reproductive outcomes and is indicated in women with prior pregnancy loss or poor obstetrical outcomes [3, 43, 75, 76]. After the hysteroscopic procedure, the risk of pregnancy loss or other adverse perinatal outcomes is dramatically decreased; in observational studies, live birth and miscarriage rates are improved to approximately 80% and 15%, respectively [3, 7, 34, 43, 75]. For surgical treatment of a uterine septum, the hysteroscopic approach is preferred due to its safety, simplicity, and excellent postoperative results [43, 70]. Although laparoscopy can be utilized along with hysteroscopy to assess the fundal contour and guide the extent of septum resection, it is not mandatory, and transabdominal ultrasonography may provide equivalent visualization with less risk [34, 43, 76].

While hysteroscopic metroplasty for women with RPL significantly improves the live birth rate, in women with unexplained infertility, surgery achieves modest improvements in pregnancy and live birth rates [43, 70, 77, 78]. Furthermore, an observational study identified that women with unexplained infertility and a septate uterus who underwent hysteroscopic metroplasty had significantly improved rates of conception (38.6% vs. 20.4%) and live birth (34.1% vs. 18.9%) compared to women with unexplained infertility and a normal uterus [79]. These data lend support to the concern about implantation issues with a septate uterus. The risks of pregnancy loss and possible infertility are of concern when a septate uterus is identified in a woman with infertility or in a woman of advanced reproductive age with desired fertility. In these women, prophylactic metroplasty may prevent miscarriage or other obstetric complications and may improve fertility. Surgical intervention is commonly recommended to optimize pregnancy outcomes in women with prolonged infertility, in women over age 35, and in women pursuing infertility treatment with assisted reproductive technologies [1, 26, 34, 45, 70, 79–82]. However, surgical intervention for a septate uterus identified in an asymptomatic woman warrants a thorough discussion of the potential benefits and risks of prophylactic intervention [76].

In women with a unicornuate uterus, excision of a communicating or noncommunicating functional rudimentary uterine horn and the attached fallopian tube is recommended to prevent a horn or tubal gestation [25, 70]. Due to the high risk of pregnancy complications with a functional uterine horn, surgical excision is recommended even in asymptomatic women. Additionally, this intervention treats pelvic pain associated with hematometra, hematosalpinx, retrograde menstruation, and endometriosis [25, 70]. If the uterine horn does not contain endometrium and the woman is asymptomatic, surgical excision is not required.

Lastly, the benefit of surgical correction for an arcuate uterus is unclear. This uterine configuration is considered a variant of normal, and reproductive outcomes are generally good [76]. As discussed above, previous studies describing poor reproductive outcomes with an arcuate uterus may have misclassified the uterine anomaly. Thus in the setting of recurrent pregnancy loss or poor obstetric outcomes, uterine anatomy should be carefully assessed to determine if an anomaly is present, and counseling about the option of surgical intervention should occur as appropriate.

Conclusion

Maintaining a high suspicion for uterine anomalies is important because they affect 3–8% of fertile and infertile women and 12–16% of women with recurrent miscarriage and have a variety of presentations in gynecology and obstetrics. It is critical to obtain detailed uterine assessment during office 2DUS and to know when further imaging is warranted. Although a range of imaging modalities is available, 2DUS is a reasonable

"screening test" for uterine anomalies, and 3DUS is the appropriate "diagnostic test." 3DUS is a non-invasive imaging technique that can screen low-risk and high-risk women with desired fertility and accurately identify those with uterine anomalies that may impact pregnancy outcomes [32, 53]. However, complex Müllerian anomalies beyond uterine anomalies may require additional imaging such as pelvic MRI to better define the anomaly. The availability of diagnostic imaging that accurately and reliably differentiates and diagnoses uterine anomalies enables the identification of women at risk of pregnancy complications, allows timely and appropriate surgical intervention, and helps guide future pregnancy management [32, 63]. To optimize patient outcomes, accurate diagnosis of uterine anomalies is essential.

References

1. Raga F, Bauset C, Remohi J, Bonilla-Musoles F, Simon C, Pellicer A. Reproductive impact of congenital Müllerian anomalies. Hum Reprod. 1997;12:2277–81.
2. Simon C, Martinez L, Pardo F, Tortajada M, Pellicer A. Müllerian defects in women with normal reproductive outcome. Fertil Steril. 1991;56:1192–3.
3. Grimbizis GF, Camus M, Tarlatzis BC, Bontis JN, Devroey P. Clinical implications of uterine malformations and hysteroscopic treatment results. Hum Reprod Update. 2001;7:161–74.
4. Saravelos SH, Cocksedge KA, Li TC. Prevalence and diagnosis of congenital uterine anomalies in women with reproductive failure: a critical appraisal. Hum Reprod Update. 2008;14:415–29.
5. Chan YY, Jayaprakasan K, Zamora J, Thornton JG, Raine-Fenning N, Coomarasamy A. The prevalence of congenital uterine anomalies in unselected and high-risk populations: a systematic review. Hum Reprod Update. 2011;17:761–71.
6. Nahum GG. Uterine anomalies: how common are they, and what is their distribution among subtypes? J Reprod Med. 1998;43:877–87.
7. Kupesic S, Kurjac A, Skenderovic S, Bjelos D. Screening for uterine abnormalities by three-dimensional ultrasound improves perinatal outcomes. J Perinat Med. 2002;30:9–17.
8. Propst AM, Hill JA. Anatomic factors associated with recurrent pregnancy loss. Semin Reprod Med. 2000;18:341–50.
9. Hammoud AO, Gibson M, Mathew Peterson C, Kerber RA, Mineau GP, Hatasaka H. Quantification of the familial contribution to Müllerian anomalies. Obstet Gynecol. 2008;111:378–84.
10. Oppelt P, von Have M, Paulsen M, Strissel PL, Strick R, Brucker S, et al. Female genital malformations and their associated abnormalities. Fertil Steril. 2007;87:335–42.
11. Troiano RN, McCarthy SM. Müllerian duct anomalies: imaging and clinical issues. Radiology. 2004;233:19–34.
12. Chang AS, Siegel CL, Moley KH, Ratts VS, Odem RR. Septate uterus with cervical duplication and longitudinal vaginal septum: a report of five new cases. Fertil Steril. 2004;81:1133–6.
13. Pavone ME, King JA, Vlahos N. Septate uterus with cervical duplication and a longitudinal vaginal septum: a Müllerian anomaly without a classification. Fertil Steril. 2006;85:e9–10.
14. Haddad B, Louis-Sylvestre C, Poitout P, Paniel BJ. Longitudinal vaginal septum: a retrospective study of 202 cases. Eur J Obstet Gynecol Reprod Biol. 1997;74:197–9.
15. Ergun A, Pabuccu R, Atay V, Kücük T, Duru NK, Güngör S. Three sisters with septate uteri: another reference to bidirectional theory. Hum Reprod. 1997;12:140–2.
16. Acien P, Acien M, Sanchez-Ferrer ML. Mullerian anomalies "without a classification": from the didelphys-unicollis uterus to the bicervical uterus with or without septate vagina. Fertil Steril. 2009;91:2369–75.
17. Buttram VC Jr, Gomel V, Siegler A, DeCherney A, Gibbons W, March C. The American Fertility Society classification of adnexal adhesions, distal tubal occlusion, tubal occlusion secondary to tubal ligation, tubal pregnancies, Müllerian anomalies and intrauterine adhesions. Fertil Steril. 1988;49:944–55.
18. Bermejo C, Ten Martinez P, Cantarero R, Diaz D, Perez Pedregosa J, Barron E, et al. Three-dimensional ultrasound in the diagnosis of Müllerian duct anomalies and concordance with magnetic resonance imaging. Ultrasound Obstet Gynecol. 2010;35:593–601.
19. Deutch TD, Abuhamad AZ. The role of 3-dimensional ultrasonography and magnetic resonance imaging in the diagnosis of Müllerian duct anomalies: a review of the literature. J Ultrasound Med. 2008;27:413–23.
20. Woelfer B, Salim R, Banerjee S, Elson J, Regan L, Jurkovic D. Reproductive outcomes in women with congenital uterine anomalies detected by three-dimensional ultrasound screening. Obstet Gynecol. 2001;98:1099–103.
21. Evans TN, Poland ML, Boving RL. Vaginal malformations. Am J Obstet Gynecol. 1981;141:910–20.
22. Fedele L, Bianchi S, Frontino G, Ciappina N, Fontana E, Borruto F. Laparoscopic findings and pelvic anatomy in Mayer-Rokitansky-Küster-Hauser syndrome. Obstet Gynecol. 2007;109:1111–5.
23. Oppelt P, Renner SP, Kellermann A, Brucker S, Hauser GA, Ludwig KS, et al. Clinical aspects of Mayer-Rokitansky-Küster-Hauser syndrome: recommendations for clinical diagnosis and staging. Hum Reprod. 2006;21:792–7.

24. Pittock ST, Babovic-Vuksanovic D, Lteif A. Mayer-Rokitansky-Küster-Hauser anomaly and its associated malformations. Am J Med Genet. 2005;135A:314–6.
25. Jayasinghe Y, Rane A, Stalewski H, Grover S. The presentation and early diagnosis of the rudimentary uterine horn. Obstet Gynecol. 2005;105:1456–67.
26. Lin PC, Bhatnagar KP, Nettleton GS, Nakajima ST. Female genital anomalies affecting reproduction. Fertil Steril. 2002;78:899–915.
27. Fedele L, Zamberletti D, Vercellini P, Dorta M, Candiani GB. Reproductive performance of women with unicornuate uterus. Fertil Steril. 1987;47:416–9.
28. Vercellini P, Daguati R, Somigliana E, Vigano P, Lanzani A, Fedele L. Asymmetric lateral distribution of obstructed hemivagina and renal agenesis in women with uterus didelphys: institutional case series and a systematic literature review. Fertil Steril. 2007;87:719–24.
29. Smith NA, Laufer MR. Obstructed hemivagina and ipsilateral renal anomaly (OHVIRA) syndrome: management and follow-up. Fertil Steril. 2007;87:918–22.
30. Fedele L, Ferrazzi E, Dorta M, Vercellini P, Candiani GB. Ultrasonography in the differential diagnosis of 'double' uteri. Fertil Steril. 1988;50:361–4.
31. Candiani GB, Ferrazzi E, Fedele L, Vercellini P, Dorta M. Sonographic evaluation of uterine morphology: a new scanning technique. Acta Eur Fertil. 1986;17:345–8.
32. Salim R, Jurkovic D. Assessing congenital uterine anomalies: the role of three-dimensional ultrasonography. Best Pract Res Clin Obstet Gynaecol. 2004;18:29–36.
33. Wu MH, Hsu CC, Huang KE. Detection of congenital Müllerian duct anomalies using three-dimensional ultrasound. J Clin Ultrasound. 1997;25:487–92.
34. Fedele L, Bianchi S, Frontino G. Septums and synechiae: approaches to surgical correction. Clin Obstet Gynecol. 2006;49:767–88.
35. Nawroth F, Rahimi G, Nawroth C, Foth D, Ludwig M, Schmidt T. Is there an association between septate uterus and endometriosis? Hum Reprod. 2006;21:542–4.
36. Braun P, Grau FV, Pons RM, Enguix DP. Is hysterosalpingography able to diagnose all uterine malformations correctly? A retrospective study. Eur J Radiol. 2005;53:274–9.
37. Mazouni C, Girard G, Deter R, Haumonte JB, Blanc B, Bretelle F. Diagnosis of Müllerian anomalies in adults: evaluation of practice. Fertil Steril. 2008;89:219–22.
38. Sanfilippo JS, Wakim NG, Schikler KN, Yussman MA. Endometriosis in association with uterine anomaly. Am J Obstet Gynecol. 1986;154:39–43.
39. Acien P. Reproductive performance of women with uterine malformations. Hum Reprod. 1993;8:122–6.
40. Ludmir J, Samuels P, Brooks S, Mennuti MT. Pregnancy outcome of patients with uncorrected uterine anomalies managed in a high-risk obstetric setting. Obstet Gynecol. 1990;75:906–10.
41. Hua M, Odibo AO, Longman RE, Macones GA, Roehl KA, Cahill AG. Congenital uterine anomalies and adverse pregnancy outcomes. Am J Obstet Gynecol. 2011;205:558 e1–5.
42. Acien P. Incidence of Müllerian defects in fertile and infertile women. Hum Reprod. 1997;12:1372–6.
43. Homer HA, Li TC, Cooke ID. The septate uterus: a review of management and reproductive outcome. Fertil Steril. 2000;73:1–14.
44. Fedele L, Bianchi S, Marchini M, Franchi D, Tozzi L, Dorta M. Ultrastructural aspects of endometrium in infertile women with septate uterus. Fertil Steril. 1996;65:750–2.
45. Fedele L, Bianchi S. Hysteroscopic metroplasty for septate uterus. Obstet Gynecol Clin N Am. 1995;22:473–89.
46. Andrews MC, Jones HW Jr. Impaired reproductive performance of the unicornuate uterus: intrauterine growth retardation, infertility, and recurrent abortion in five cases. Am J Obstet Gynecol. 1982;144:173–6.
47. Moutos DM, Damewood MD, Schlaff WD, Rock JA. A comparison of the reproductive outcome between women with a unicornuate uterus and women with a didelphic uterus. Fertil Steril. 1992;58:88–93.
48. Candiani GB, Fedele L, Zamberletti D, De Virgiliis D, Carinelli S. Endometrial patterns in malformed uteri. Acta Eur Fertil. 1983;14:311–8.
49. Golan A, Langer R, Wexler S, Segev E, Niv D, David MP. Cervical cerclage: its role in the pregnant anomalous uterus. Int J Fertil. 1990;35:164–70.
50. Ghi T, Casadio P, Kuleva M, Perrone AM, Savelli L, Giunchi S, et al. Accuracy of three-dimensional ultrasound in diagnosis and classification of congenital uterine anomalies. Fertil Steril. 2009;92:808–13.
51. Faivre E, Fernandez H, Deffieux X, Gerviase A, Frydman R, Levaillant JM. Accuracy of three-dimensional ultrasonography in differential diagnosis of septate and bicornuate uterus compared with office hysteroscopy and pelvic magnetic resonance imaging. J Minim Invasive Gynecol. 2012;19:101–6.
52. Reuter KL, Daly DC, Cohen SM. Septate versus bicornuate uteri: errors in imaging diagnosis. Radiology. 1989;172:749–52.
53. Grimbizis GF, DiSpezio Sardo A, Saravelos SH, Gordts S, Exacoustos C, Van Schoubroeck D, et al. The Thessaloniki ESHRE/ESGE consensus on diagnosis of female genital anomalies. Hum Reprod. 2016;31:2–7.
54. Nicolini U, Bellotti M, Bonazzi B, Zamberletti D, Candiani GB. Can ultrasound be used to screen uterine malformations? Fertil Steril. 1987;47:89–93.
55. Caliskan E, Ozkan S, Cakiroglu Y, Sarisoy HT, Corakci A, Ozeren S. Diagnostic accuracy of real-time 3D sonography in the diagnosis of congenital Müllerian anomalies in high-risk patients with respect to the phase of the menstrual cycle. J Clin Ultrasound. 2010;38:123–7.
56. Goldberg JM, Falcone T, Attaran M. Sonohysterographic evaluation of uterine abnor-

malities noted on hysterosalpingography. Hum Reprod. 1997;12:2151–3.
57. Troiano RN. Magnetic resonance imaging of Müllerian duct anomalies of the uterus. Top Magn Reson Imaging. 2003;14:269–79.
58. Pellerito JS, McCarthy SM, Doyle MB, Glickman MG, DeCherney AH. Diagnosis of uterine anomalies: relative accuracy of MR imaging, endovaginal sonography, and hysterosalpingography. Radiology. 1992;183:795–800.
59. Letterie GS, Haggerty M, Lindee G. A comparison of pelvic ultrasound and magnetic resonance imaging as diagnostic studies for Müllerian tract abnormalities. Int J Fertil Menopausal Stud. 1995;40:34–8.
60. Fedele L, Dorta M, Brioschi D, Massari C, Candiani GB. Magnetic resonance evaluation of double uteri. Obstet Gynecol. 1989;74:844–7.
61. Carrington BM, Hricak H, Nuruddin RN, Secaf E, Laros RK Jr, Hill EC. Müllerian duct anomalies: MR imaging evaluation. Radiology. 1990;176:715–20.
62. Jurkovic D, Geipel A, Gruboeck K, Jauniaux E, Natucci M, Campbell S. Three-dimensional ultrasound for the assessment of uterine anatomy and detection of congenital anomalies: a comparison with hysterosalpingography and two-dimensional sonography. Ultrasound Obstet Gynecol. 1995;5:233–7.
63. Raine-Fenning N, Fleischer AC. Clarifying the role of three-dimensional transvaginal sonography in reproductive medicine: an evidence-based appraisal. J Exp Clin Assist Reprod. 2005;2:10.
64. Salim R, Woelfer B, Backow M, Regan L, Jurkovic D. Reproducibility of three-dimensional ultrasound diagnosis of congenital uterine anomalies. Ultrasound Obstet Gynecol. 2003;21:578–82.
65. Raga F, Bonilla-Musoles F, Blanes J, Osborne NG. Congenital Müllerian anomalies: diagnostic accuracy of three-dimensional ultrasound. Fertil Steril. 1996;65:523–8.
66. Graupera B, Pascual MA, Hereter L, Browne JL, Ubeda B, Rodriguez I, et al. Accuracy of three-dimensional ultrasound compared with magnetic resonance imaging in diagnosis of Mullerian duct anomalies using ESHRE-ESGE consensus on the classification of the female genital tract. Ultrasound Obstet Gynecol. 2015;46:616–22.
67. Ergenoglu AM, Sahin C, Simsek D, Akdemir A, Yeniel AO, Yerli H, et al. Comparison of three-dimensional ultrasound and magnetic resonance imaging diagnosis in surgically proven Mullerian duct anomaly cases. Eur J Obstet Gynecol Reprod Biol. 2016;197:22–6.
68. Reichman DE, Laufer MR. Congenital uterine anomalies affecting reproduction. Best Pract Res Clin Obstet Gynaecol. 2010;24:193–208.
69. Marcus S, al-Shawaf T, Brinsden P. The obstetric outcome of in vitro fertilization and embryo transfer in women with congenital uterine malformation. Am J Obstet Gynecol. 1996;175:85–9.
70. Taylor E, Gomel V. The uterus and fertility. Fertil Steril. 2008;89:1–16.
71. Dabirashrafi H, Bahadori M, Mohammad K, Alavi M, Moghadami-Tabrizi N, Zandinejad K, et al. Septate uterus: new idea on the histologic features of the septum in this abnormal uterus. Am J Obstet Gynecol. 1995;172:105–7.
72. Reichman D, Laufer MR, Robinson BK. Pregnancy outcomes in unicornuate uteri: a review. Fertil Steril. 2009;91:1886–94.
73. Heinonen PK, Saarikoski S, Pystynen P. Reproductive performance of women with uterine anomalies: an evaluation of 182 cases. Acta Obstet Gynecol Scand. 1982;61:157–62.
74. Jacobsen LJ, DeCherney A. Results of conventional and hysteroscopic surgery. Hum Reprod. 1997;12:1376–81.
75. Tomazevic T, Ban-Frangez H, Ribic-Pucelj M, Premru-Srsen T, Verdenik I. Small uterine septum is an important risk variable for preterm birth. Eur J Obstet Gynecol Reprod Biol. 2007;135:154–7.
76. Practice Committee of the American Society of Reproductive Medicine. Uterine septum: a guideline. Fertil Steril. 2016;106:530–40.
77. Pabuccu R, Gomel V. Reproductive outcome after hysteroscopic metroplasty in women with septate uterus and otherwise unexplained infertility. Fertil Steril. 2004;81:1675–8.
78. Fedele L, Arcaini L, Parazzini F, Vercellini P, Di Nola G. Reproductive prognosis after hysteroscopic metroplasty in 102 women: life-table analysis. Fertil Steril. 1993;59:768–72.
79. Mollo A, De Franciscis P, Colacurci N, Cobellis L, Perino A, Venezia R, et al. Hysteroscopic resection of the septum improves the pregnancy rate of women with unexplained infertility: a prospective controlled trial. Fertil Steril. 2009;91:2628–31.
80. Rackow BW, Arici A. Reproductive performance of women with Müllerian anomalies. Curr Opin Obstet Gynecol. 2007;19:229–37.
81. Choe JK, Baggish MS. Hysteroscopic treatment of septate uterus with neodymium-YAG laser. Fertil Steril. 1992;57:81–4.
82. Daly DC, Maier D, Soto-Albors C. Hysteroscopic metroplasty: six years' experience. Obstet Gynecol. 1989;73:201–5.

Uterine Fibroids

9

Bradley S. Hurst

Background

The identification of uterine fibroids during evaluation for infertility or in preparation for assisted reproductive technology can present a perplexing problem for patients and their providers, especially when fibroids are asymptomatic. The concern is well-deserved, since unnecessary surgery for fibroids exposes the patient to risks, has a high potential to result in adhesion formation, may require future cesarean delivery, and may reduce fertility if adhesions compromise the tubo-ovarian relationship or distort the uterine cavity. However, failure to treat fibroids could impair spontaneous conception, compromise outcomes of fertility treatments, or increase the risk of miscarriage and pregnancy-related complications. The goal of this chapter will be to provide rational treatment options for women with uterine fibroids, based on the best available data.

A uterine fibroid is a monoclonal growth of fibrovascular cells that arise from the myometrium. Estrogen and progesterone receptors are present in fibroids, and both hormones stimulate fibroid proliferation. Fibroids are surrounded by a dense vascular pseudocapsule, and larger masses usually have a greater vascular supply [1]. Factors within the pseudocapsule stimulate fibroid growth, including a local overexpression of aromatase, which converts androgens to estrogens [2]. Estrogen stimulates growth factors in the pseudocapsule, including EGF, IGF-1, bFGF, GH, TGF-β, PDGF, endothelin A, and VEGF [3]. Vitamin D deficiency appears to stimulate fibroid growth [4].

The prevalence of fibroids peaks during the fourth decade because of the cumulative effects of estrogen, progesterone, and growth factors on myoma growth during the reproductive years [5]. Fibroids are more numerous and larger in African-Americans. Ultrasound studies have found a cumulative incidence of fibroids in approximately 80% of African-American women by age 50 [6]. However, fibroids are common in all ethnicities, including a cumulative incidence of 70% in Caucasian women. There is great interest in identifying dietary and environmental factors that contribute to fibroid growth. There is increasing evidence that hypertension, a family history of fibroids, time since last birth, food additives, and soybean milk consumption increase the risk of uterine fibroids [7]. Oral contraceptives, depot medroxyprogesterone acetate, smoking, and increased parity reduce the risk of fibroids.

The fibroid deforms the surrounding tissues as it grows. A fibroid that develops in the myometrial wall is considered an "intramural" myoma (Fig. 9.1). A fibroid that protrudes into the

B. S. Hurst (✉)
Carolinas Medical Center, Department of Obstetrics and Gynecology, Reproductive Endocrinology and Infertility, Charlotte, NC, USA
e-mail: brad.hurst@atriumhealth.com

L. A. Stadtmauer, I. Tur-Kaspa (eds.), *Ultrasound Imaging in Reproductive Medicine*,
https://doi.org/10.1007/978-3-030-16699-1_9

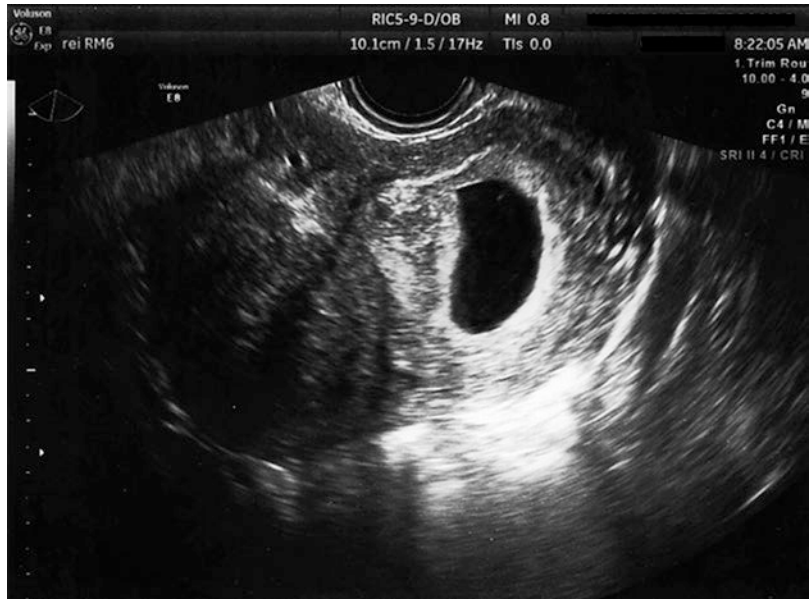

Fig. 9.1 Saline infusion sonohysterography with intramural fibroid

endometrial mucosa is a "submucous" myoma. Fibroids that protrude the serosal surface of the uterus are called "subserosal" myomas (Fig. 9.2). Other terms sometimes used to describe the location of fibroids include "sessile," a type of submucous myoma that is located in the myometrium but also distorts the endometrium (Fig. 9.3). A "pedunculated" fibroid is located primarily outside of the uterus, connected to the uterus by a fibrovascular stalk (Fig. 9.4). In this chapter, the terms fibroid, myoma, and leiomyoma are used interchangeably.

In 2011, the International Federation of Gynecology and Obstetrics (FIGO) published a classification system further describing the location of fibroids [8], and clinical studies often refer to this classification. There are eight fibroid types. Submucous fibroids are divided into Type 0 (completely intracavitary), Type 1 (>50% intracavitary), and Type 2 (≥ 50% intramural) (Fig. 9.5). A Type 3 fibroid is intramural but contacts the endometrium, Type 4 is intramural and entirely within the endometrium, and Type 5 is intramural and distorts the serosa but is ≤50% subserosal. A Type 6 fibroid is partly intramural but >50% subserosal, and a Type 7 fibroid is subserosal pedunculated. A Type 8 fibroid is not attached to the uterus and may include other locations such as the cervix or could be a parasitic fibroid. Finally, a "Hybrid 2–5" fibroid distorts

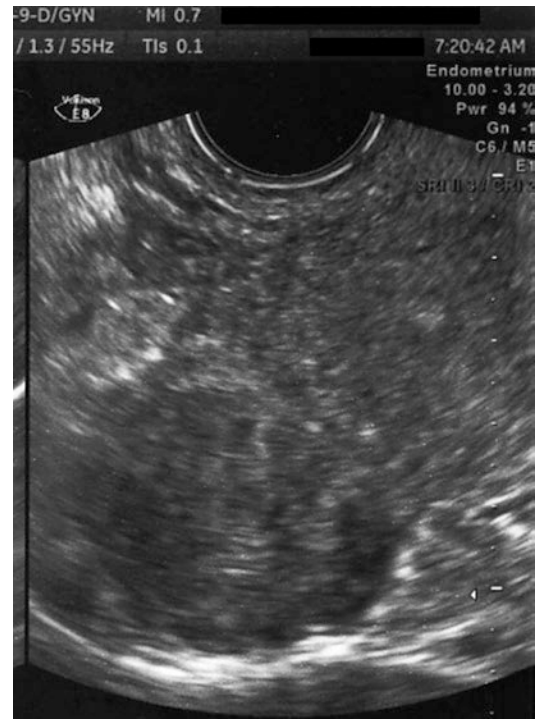

Fig. 9.2 Transvaginal ultrasound demonstrating subserosal fibroid

the endometrium and the serosa but is <50% submucosal and <50% subserosal.

Symptoms attributed to fibroids are determined by the size and the location of the

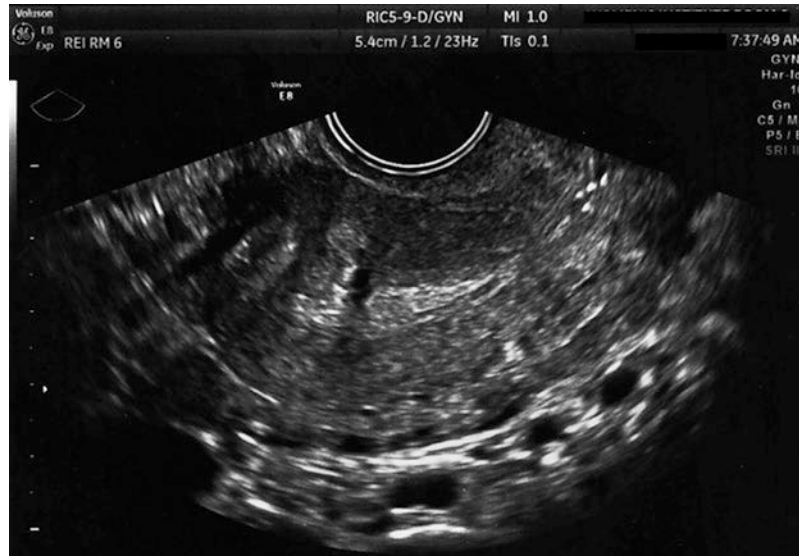

Fig. 9.3 Transvaginal ultrasound demonstrating several uterine fibroids, including one submucous myoma with deflection of the endometrial cavity

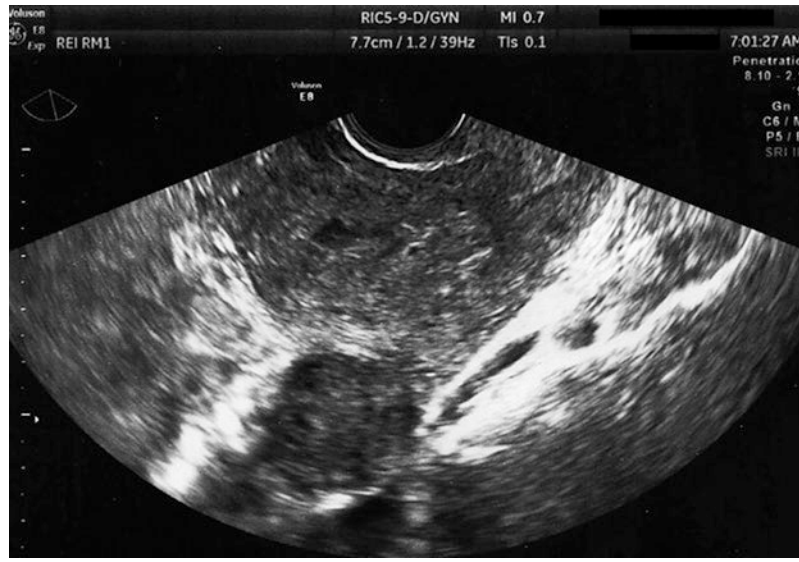

Fig. 9.4 Transvaginal ultrasound demonstrating pedunculated fibroid

masses. Most intramural, subserosal, and pedunculated fibroids are asymptomatic. However, large fibroids may cause bulk symptoms such as abdominal pressure, bloating, or distention. A myoma that presses against the bladder may cause urinary frequency, urgency, or nocturia. A fibroid that compresses the rectum may cause constipation, diarrhea, or alternating symptoms. Infarction of a fibroid may cause severe acute pain, and the inflammation caused by degenerating myoma may cause adhesions. Fibroids located in the posterior cul-de-sac may cause dyspareunia. Occasionally, fibroids are associated with chronic, intermittent, or cyclic pain.

Submucous myomas often cause abnormal uterine bleeding (Fig. 9.6). Symptoms of submucous fibroids include menorrhagia, dysmenorrhea, clotting, and intermenstrual bleeding [9]. When bleeding is severe, anemia may occur. With the high prevalence of fibroids and the multitude of symptoms that may be attributed to fibroids, it is not surprising that fibroids are the leading indication for hysterectomy. However,

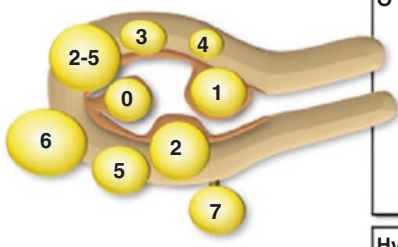

SM - Submucosal	0	Pedunculated intracavitary
	1	<50% intramural
	2	≥50% intramural
O - Other	3	Contacts endometrium; 100% intramural
	4	Intramural
	5	Subserosal ≥ 50% intramural
	6	Subserosal <50% intramural
	7	Subserosal pedunculated
	8	Other (specify e.g. cervical, parasitic)

Hybrid leiomyomas (impact both endometrium and serosa)	Two numbers are listed separated by a hyphen. By convention, the first refers to the relationship with the endometrium while the second refers to the relationship to the serosa. One example is below	
	2–5	Submucosal and subserosal, each with less than half the diameter in the endometrial and peritoneal cavities, respectively.

Fig. 9.5 International Federation of Gynecology and Obstetrics (FIGO) published a classification system further describing the location of fibroids [8]. (Reprinted with permission from Munro et al. [8])

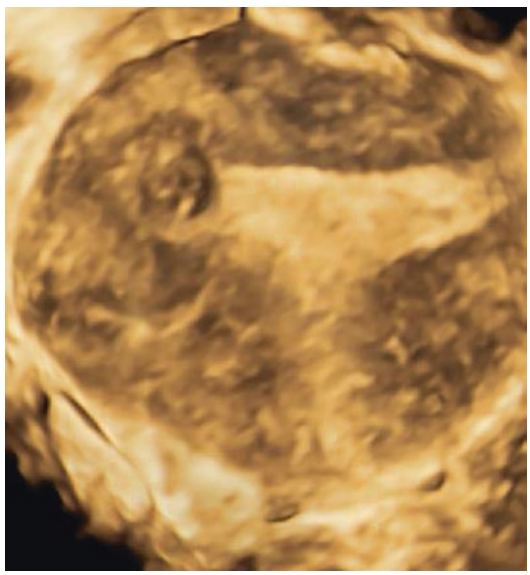

Fig. 9.6 Three-dimensional mapping of a submucosal fibroid

other treatment options must be considered for women who are interested in childbearing.

Fibroids and Fertility

It is difficult to determine the direct impact of fibroids on fertility, since the incidence of uterine fibroids increases with age, fertility declines with age, and many women with fibroids conceive spontaneously.

The location of fibroids is important in determining the impact on fertility. In some circumstances, fibroids impair fertility by mechanically distorting the uterine cavity, altering the endometrium and impairing embryo implantation and growth. Other obvious causes of fibroid-related infertility may include mechanical obstruction of the tubal ostia.

Submucous myomas directly impair fertility and cause adverse reproductive outcomes by several potential mechanisms [9]. These fibroids alter the vascular supply and development of the endometrium with intramural myomas or alter growth factors and inflammatory substances that may impair implantation or fetal growth. The mechanical distortion of the endometrial cavity almost certainly has a direct effect on fertility. In general, greater endometrial distortion more clearly results in compromised fertility. Myomectomy improves fertility in these cases.

Intramural fibroids reduce fertility when they are 4 cm or larger, and myomectomy appears to restore fertility [10]. Additionally, FIGO Type 3 intramural fibroids 2 cm or larger that touch the endometrium impair fertility [11]. Another study found that fertility was reduced in women who

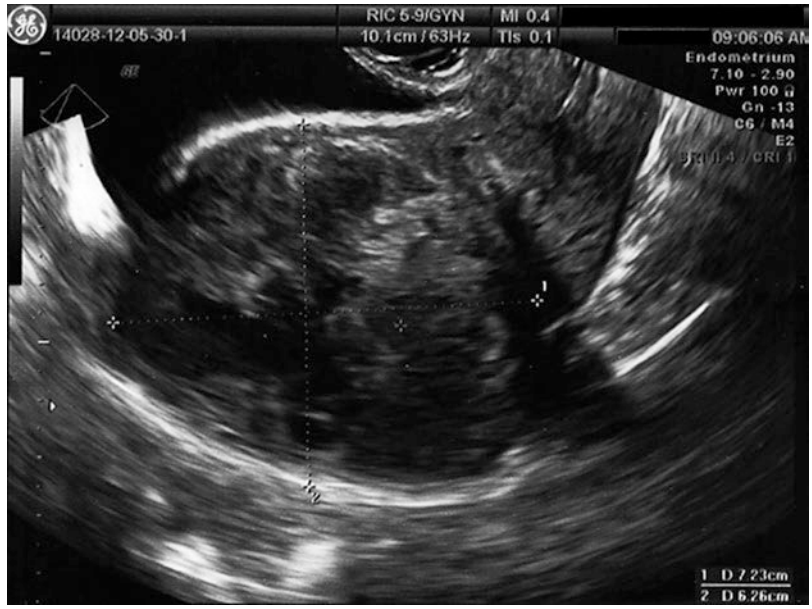

Fig. 9.7 Transvaginal ultrasound demonstrating multiple intramural fibroids; the entire endometrium is difficult to visualize

had two or more intramural fibroids, or for intramural fibroids that are 3 cm or larger [12]. However, there is no clear evidence that myomectomy enhances fertility in women with intramural myomas [13, 14]. Subserosal fibroids do not impair fertility [15].

Many women have multiple fibroids, and the different size, location, number, and relative relationship to the endometrium increase the difficulty in establishing the effect of fibroids on fertility, as no two individuals are directly comparable (Fig. 9.7). As such, the relative usefulness of myomectomy in these situations cannot be established with certainty.

Fibroids and IVF

Studies of the impact of fibroids in IVF cycles are helpful to establish the impact, since many factors impacting fertility are either controlled, such as male infertility, or directly evaluated, such as the impact of age on cycle outcome. Submucosal fibroids have long been recognized to reduce IVF pregnancy and birth rates [16, 17]. Furthermore, hysteroscopic myomectomy improves pregnancy rates, with outcomes comparable to women with a normal uterine cavity [18].

The effect of medium and large intramural myomas on IVF outcomes is unclear, and some studies have shown little clinical effect. When IVF outcomes are generally poor, IVF live birth rates were not improved by myomectomy in one small retrospective study: IVF "ongoing" pregnancy rates were 17% after myomectomy (n = 47), 21% with untreated fibroids (n = 11), and 19% in normal controls [17]. However, 50% of women with fibroids experienced a spontaneous abortion, compared to 34% after myomectomy, suggesting that fibroids compromise pregnancy outcomes. A study of 46 IVF cases with intramural and subserosal fibroids showed that outcomes were similar to controls, but fibroid size was not assessed [19]. Other investigators found that myomas, 73% of which were subserosal, had no effect on conception in 39 women [20]. A study of 119 women with asymptomatic intramural or subserosal fibroid found that myomas smaller than 5 cm did not compromise IVF pregnancy or birth rates when matched to controls [21]. The outcome was not changed when the group was limited to those with intramural myomas.

Contrary to these reports, increasing evidence suggests that some intramural fibroids are associated with lower ART live birth rates. A retrospec-

tive study found a significant decrease in IVF live birth rates in women under age 40 years with intramural fibroids (49% and 58%, respectively) [22]. In 2005, a meta-analysis showed a significantly lower implantation rate with intramural fibroids compared to controls, 16.4 vs. 27.7%, respectively (OR 0.62, 0.48–0.8), and a significantly lower birth rate per embryo transfer with fibroids compared to controls, 31.2% and 40.9% (OR 0.69, 0.50–0.95) [23]. In a retrospective study of 91 IVF cycles in women with intramural or subserosal fibroids, Stovall et al. found a significantly lower pregnancy rate with fibroids (37%) compared to matched controls (53%) [24]. The fibroids size ranged from 8 to 54 mm, with a mean diameter of 29 mm, and 95% were intramural. The implantation rate was 14% with fibroids, significantly lower than the 20% implantation rate in controls without fibroids. Another study found that women with intramural fibroids had significantly lower pregnancy rates compared to women without fibroids, 16% and 34%, respectively, $p < 0.05$ [16]. Implantation rates were more than 50% lower with intramural fibroids compared to the controls ($p < 0.005$), even though the mean diameter of the fibroids was 24 mm. A meta-analysis assessed 19 observational studies comprising 6087 IVF cycles and found a significantly lower IVF live birth (RR = 0.79, 95% CI 0.70–0.88, $p < 0.0001$) and clinical pregnancy rate (RR = 0.85, 95% CI 0.77–0.94, $p = 0.002$) in women with intramural fibroids compared to those without fibroids [25]. The authors concluded that non-cavity-distorting intramural fibroids are associated with adverse pregnancy outcomes in women undergoing IVF. Oliveira et al. found a significantly lower pregnancy rate with IVF only when intramural fibroids were 4 cm or larger [10].

Recent studies have identified characteristics that impair ART live birth rates. A case-control study of 151 women with FIGO Type 3 intramural fibroids found that fibroids 2 cm or larger that touch the endometrium impair IVF pregnancy and live birth rates, but smaller fibroids do not compromise outcomes [11]. Finally, one case-controlled study women undergoing IVF found that the live birth rate was reduced in women who had two or more intramural fibroids (OR 0.47; 95% CI 0.26–0.83) or if intramural fibroids that are 3 cm or larger (OR 0.41; 95% CI 0.19–0.89) [12]. There was no difference in pregnancy outcomes in those with one intramural fibroid <3 cm. Subserosal fibroids do not impair fertility [15].

Egg donation provides an opportunity to study the effect of implantation while minimizing the effect of confounding factors of maternal age and male fertility. There is evidence that egg donation outcomes are lower in African-American women compared to other populations, although the populations are too small to conclude that fibroids are the primary explanation for this effect [26]. It is possible that uterine fibroids could provide a possible explanation for this observation.

Uterine fibroids may increase the difficulty of the oocyte retrieval or embryo transfer and either may lower IVF outcomes. A fibroid may raise the ovary out of the pelvis, especially large masses. If this occurs, it may be necessary to perform laparoscopic oocyte retrieval or ultrasound-directed transabdominal retrieval. A fibroid may increase the difficulty of the embryo transfer in one of several ways: distorting the position of the cervix in a way that it is difficult or impossible to expose the cervix with a speculum, by markedly altering the endocervical course or causing endocervical stenosis (Fig. 9.8). Finally, a large fibroid may make visualization of embryo transfer difficult or impossible when an abdominal ultrasound-guided procedure is performed. This can be critical since increasing difficulty or tortuosity of the endocervix makes it difficult to visualize the transfer catheter to confirm optimal placement.

Myomas and Obstetrical Outcomes

While the impact of fibroids on fertility is still debated, obstetrical outcomes appear to be compromised by uterine fibroids in some [9] but not all studies. A population-based retrospective study by Sheiner et al. [27] found that women with fibroids had a 3.5-fold increased incidence of intrauterine growth restriction (6.8% vs. 1.9%), a 4-fold increase in placental abruption (2.8% vs. 0.7%), a 5-fold higher incidence of

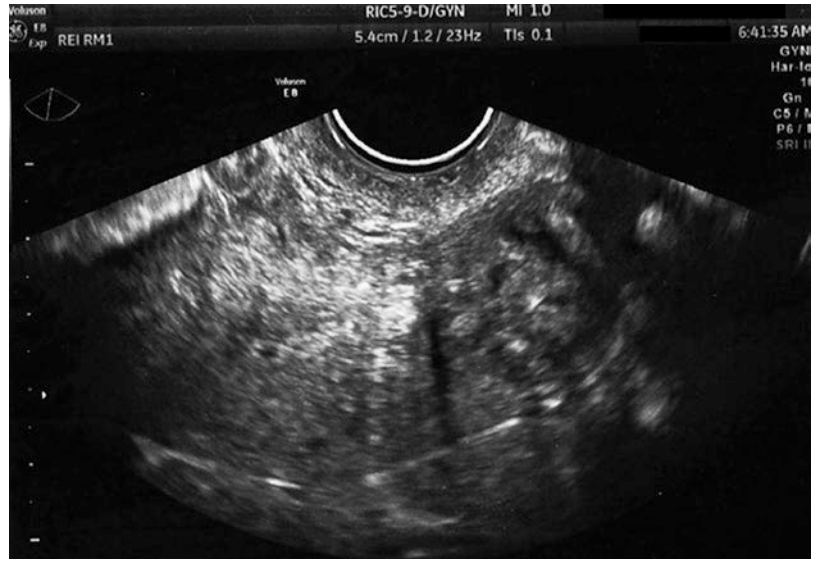

Fig. 9.8 Transvaginal ultrasound demonstrating large fibroid in the lower uterus and cervix

transverse lie or breech presentation (16.9% vs. 2.4%), a 5 times higher cesarean section rate (57.7% vs. 10.8%), 70% higher risk of premature rupture of membranes (9.6% vs. 5.5%), and were 3 times more likely to receive transfusion (4.2% vs. 1.4%). All of these outcomes were significant, with $p < 0.001$. Adjusting for maternal age, parity, gestational age, and malpresentation, pregnancies with fibroids still had a 6.7 times higher risk of cesarean delivery, with 95% CI 5.5–8.1, $p < 0.01$). Placental abruption and preterm deliveries remained significantly more common with fibroids. The size and locations of the fibroids were not assessed in this study, but other investigators have found that fibroids adjacent to the placenta increase the risk of bleeding and premature rupture of membranes [28].

A retrospective study in 2012 supports the hypothesis that fibroids have a detrimental impact on pregnancy, especially when the fibroids are large [29]. The mean gestation age at delivery for women with fibroids larger than 5 cm was 36.5 weeks, significantly earlier than women with smaller fibroids or no fibroids. Other significant effects included shortened cervix, premature preterm rupture of membranes, preterm delivery, blood loss during delivery, and the need for postpartum transfusion. Considering these and other publications, authors of a literature review concluded that pregnancy outcomes are compromised in women who have intramural fibroids [30].

Uterine fibroids tend to enlarge during pregnancy, regardless of size and maternal age [31]. Although the growth or degeneration of a fibroid is not linear throughout the course of pregnancy, there is remarkable growth during the early pregnancy. This was demonstrated in a prospective case-controlled study of women with fibroids undergoing IVF, in which fibroids were serially measured by ultrasound in 25 women who conceived and in 25 who failed to become pregnant [32]. A significant 34% increase in the mean diameter of fibroids was found in early pregnancy, compared to a 2% increase in those who failed to conceive. There was no correlation between ovarian response to stimulation and fibroid growth. Therefore, the growth was attributed solely to pregnancy-associated factors. The observation that fibroids grow in diameter by approximately 30–35% during the early pregnancy is concerning, as it is possible that an asymptomatic or seemingly "innocent" fibroid near the endometrium could enlarge and lead to unexpected problems during pregnancy. Approximately 70% of fibroids grow by a volume of 10% or more between the first and second and second and third trimesters [31]. However, there is limited evidence that treatment improves outcomes.

Myomectomy could be justified in some circumstances to reduce the risk of adverse pregnancy outcomes [33]. Unfortunately, the benefit of myomectomy for intramural fibroids has not been definitively proven. The most compelling evidence for intramural myomas appears to be cases with large fibroids, 4 cm or larger, and tumors close to the uterine cavity. It is important to clarify this issue since myomectomy for intramural fibroids has a risk of morbidity and adhesion formation, and surgery should not be considered unless the benefits outweigh the risks.

Some studies have questioned the relationship between uterine fibroids and miscarriage and poor pregnancy outcomes. A study of over 500 women with uterine fibroids found no increase in risk of miscarriage after adjusting for confounding factors (adjusted hazard ratio = 0.83, 95% confidence interval: 0.63, 1.08) [34]. Furthermore, a meta-analysis that utilized five studies that included 1394 women with fibroids and 20,435 without found no increase in risk of spontaneous abortion (risk ratio 0.83, 95% CI 0.68–0.98) [35]. No characteristic of fibroids was associated with risk in these studies.

Despite the contradictory literature, myoma size, location, and number are key factors when considering treatments such as myomectomy. However, size, location, and number are not separable for an individual patient, and the provider must weigh the cumulative impact of all three factors when deciding if how and when to treat an infertile woman with uterine fibroids.

Diagnosis of Uterine Fibroids

A focused history and physical examination may provide suspicion of uterine fibroids. Symptoms related to fibroids may include menorrhagia, dysmenorrhea, menstrual clotting, intermenstrual bleeding, pelvic pain, pressure, progressive constipation or alternating constipation and diarrhea, abdominal distention, or urinary frequency. However, other conditions can cause any of these symptoms, and fibroids are often asymptomatic. On examination, the uterus is often enlarged and irregular with uterine fibroids due to the distortion from the individual masses. A rectovaginal examination may be helpful to identify posterior fibroids. However, other conditions, such as adenomyosis, can cause uterine enlargement, and a clinically significant fibroid may be present, even if the examination is normal. Diagnostic testing with ultrasound is appropriate for any women with infertility and is considered an important component of the infertility evaluation.

Ultrasound

Transvaginal ultrasound provides better image quality than abdominal ultrasound, but both methods might be necessary if the uterus is markedly enlarged with uterine fibroids. Since overlying bowel may limit the visualization of the uterus, abdominal ultrasound is performed with the bladder full enough to provide a "window" for the uterus. Vaginal ultrasound studies are performed with an empty bladder for patient comfort.

Careful examination of the endometrium and myometrium is needed to assess anatomic abnormalities. A submucous myoma is easily identified when the endometrium has a preovulatory "triple stripe" pattern. If there is no endometrial distortion, or deflection of trilaminar endometrium, a submucous fibroid is unlikely. In the early follicular phase and after ovulation, when the endometrium is more homogeneous, endometrial distortion is more difficult to assess, and saline infusion sonohysterography should be performed if a submucous fibroid is suspected [33].

Uterine fibroids have several variations in ultrasound appearance, depending on the characteristics of the mass. For example, a calcified myoma has a bright echogenic pattern and distortion or "artifact" beyond the mass (see Fig. 9.7). Although calcified fibroids are easily identified, distortion that occurs beyond the mass may "hide" the endometrium or other fibroids. Uterine fibroids are sometimes visible as "hypoechogenic" oval masses in the myometrium. Less often, a fibroid may have the same echogenic pattern as the surrounding myometrium and be identified by finding a deflection of the endometrial or the serosal surface of the uterus. Subtle or uncer-

tain findings should be cautiously interpreted, since normal physiologic contractions of the myometrium can be confused with an intramural fibroid. If an uncertain abnormality is suspected, the sonographer should reassess the area of interest after a few minutes to allow a contracted area to change. Another method that may be helpful is the use of color Doppler. Since the fibroid is surrounded by a rich vascular supply, a myoma will usually demonstrate a "ring of fire" [36]. In some cases, 3-D ultrasound may also provide additional anatomic insight regarding the position of the myoma (see Fig. 9.6).

Fibroids must be differentiated from adenomyosis, especially when surgery is considered, since resection of adenomyosis and repair of the defect can be difficult [33]. Adenomyosis may have several appearances by ultrasound, making the diagnosis uncertain in some cases. To add to the confusion, hormonal changes might cause variations in the appearance of an area of adenomyosis throughout the cycle, since the response of adenomyosis is similar to the normal endometrial response. Adenomyosis may appear hyperechoic, hypoechoic, or the signal may be mixed. Adenomyosis can enlarge or shrink in throughout a menstrual cycle, depending on the hormonal response. In some cases, adenomyosis forms a nodular myometrial mass which is readily identified by ultrasound. Adenomyosis can also be a diffuse condition affecting a large segment of the myometrium, with the only ultrasound finding being a subtle uterine enlargement. Sometimes, adenomyosis and uterine fibroids have a remarkably similar appearance with ultrasound, and some women have both conditions. Color Doppler studies are helpful to distinguish uterine fibroids from adenomyosis, since vascular flow is peripheral with fibroids and more homogeneously affects adenomyosis lesions.

Saline Infusion Sonohysterography

Saline infusion sonohysterography (SIS) is a routine procedure performed in preparation for IVF in many centers. SIS is also helpful when a submucous or sessile myoma is suspected based on clinical history or ultrasound examination.

Saline infusion sonography is performed by filling the uterus with saline while assessing the uterine cavity by transvaginal ultrasound. If evaluation of tubal patency is needed, a foam or bubble/saline infusion system may be beneficial [37].

Magnetic Resonance Imaging

Magnetic resonance imaging (MRI) is a highly sensitive method to define the size, number, and location of fibroids. While the expense of the test limits the widespread utilization, in some circumstances when myomectomy is planned, MRI can help determine whether abdominal or laparoscopic myomectomy is the more appropriate route. MRI can also be useful to visualize an extremely large uterus, whereas the field of visualization is limited with ultrasound. MRI is beneficial to visualize the uterus when calcifications make adequate assessment difficult with transvaginal or abdominal ultrasound. Finally, MRI can help differentiate fibroids and adenomyosis [38].

Management of Uterine Fibroids

Observation

Observation is reasonable for infertile women who are asymptomatic, especially with intramural fibroids smaller than 3 cm, especially those that do not contact the endometrium. Furthermore, observation is appropriate for symptomatic infertile women with subserosal or pedunculated fibroids, as long as the severity of symptoms does not warrant surgery.

Medical Therapies

Newer treatments are becoming available for the medical treatment of uterine fibroids, primarily gonadotropin-releasing hormone agonists and antagonists (GnRHa) and selective progesterone receptor antagonists. There is limited evidence of benefit for older hormonal treatments used for fibroids such as combined oral contraceptive pills

or continuous progestin pills [39]. At best, oral contraceptives and progestins may be considered as temporizing measures. Injectable GnRH agonists and now oral GnRH antagonists such as elagolix may be used to decrease menorrhagia, especially in preparation for surgery to allow for recovery of anemia or thin the endometrial lining to facilitate hysteroscopic resection of a submucous fibroid. GnRHa reduces the diameter and volume of fibroids, while the patient is hypoestrogenic, but rapid regrowth of fibroids occurs when the medication is discontinued. GnRHa use before myomectomy can make the procedure more difficult and increases the likelihood of persistent or recurrent fibroids [40]. Cost and side effects of these medications limit their long term.

Ulipristal acetate is a selective progesterone receptor modulator approved to treat symptomatic uterine fibroids in Europe and Canada. Approximately 62 and 73% of women become amenorrheic during treatment, and bleeding is controlled in over 80% of women with abnormal bleeding due to fibroids [41]. Menstruation resumes after each treatment course and is diminished compared with the baseline. Since repeated courses may reduce the need for surgery for some women with fibroids, conception without further intervention may occur.

Pregnancy outcome data is limited after treatment with ulipristal. One study reported that 15 of 21 women who attempted to conceive were successful after participating in one of the ulipristal clinical trials [42]. Among the 18 reported pregnancies, 12 resulted in births of a healthy baby and 6 ended in early miscarriage. While this early observation is encouraging, it is too soon to determine if selective progesterone receptor agonists will be a good option for infertile women with symptomatic fibroids who wish to avoid surgery.

Myomectomy

Indications for myomectomy for infertile women with uterine fibroids include (1) abnormal uterine bleeding not responding to conservative treatments; (2) high level of suspicion of pelvic malignancy; (3) growth after menopause; (4) infertility when there is distortion of the endometrial cavity or tubal obstruction; (5) recurrent pregnancy loss (with distortion of the endometrial cavity); (6) pain or pressure symptoms that interfere with quality of life; (7) urinary tract symptoms (frequency and/or obstruction); and (8) iron deficiency anemia secondary to chronic blood loss [43]. Myomectomy women with otherwise unexplained infertility myomectomy may improve pregnancy outcomes [40, 44]. Surgery should be considered for infertile women with submucous myomas, Type 3 fibroids that abut the endometrium that are 2 cm or larger, multiple intramural fibroids, or a myoma 4 cm or larger in women with otherwise unexplained infertility when appropriate fertility treatments have been unsuccessful.

Myomectomy is usually the best option for young women who desire preservation of the uterus. The type of myomectomy, hysteroscopic, open, or laparoscopic, is chosen based on patient symptoms; location, size, and number of fibroids; and the skill and experience of the surgeon. Considerations to the rout of surgery must include selection of the approach that provides greatest improvement in the prognosis, a high safety profile. The decision should be made with the knowledge of the length of patient recovery and cost of the procedure, but these should not be the deciding factors for choosing the surgical route.

An appropriate preoperative evaluation is essential to prepare for surgery. In many cases, ultrasound establishes the fibroid size and location. SIS is beneficial to determine the relationship of a submucous myoma to the myometrium for women with a submucosal myoma. MRI should be considered if an atypical ultrasound appearance is identified, if the ultrasound is not conclusive, or if adenomyosis is suspected.

Hysteroscopic Myomectomy

Hysteroscopic myomectomy is the most appropriate approach when a submucous myoma has been identified, before initiating fertility treatment. Hysteroscopic myomectomy is appropriate for symptomatic submucous myomas and for infertile women with asymptomatic submucous myomas.

Reproductive outcomes appear to improve after hysteroscopic myomectomy [9]. Hysteroscopic myomectomy lowers the incidence of first trimester losses and improves the term live birth rate [45]. However, the evidence for improved outcome comes primarily from low-quality studies. A 2015 Cochrane review of the subject concluded that "A large benefit with the hysteroscopic removal of submucous fibroids for improving the chance of clinical pregnancy in women with otherwise unexplained subfertility cannot be excluded" [46].

For optimal visualization during hysteroscopy, the procedure is either performed in the follicular phase of the cycle to ensure a thin endometrial lining or after pretreatment with a GNRH agonist or hormonal contraception for 1 or 2 months before surgery. Hysteroscopic myomectomy can be performed concurrently with abdominal or laparoscopic myomectomy to reduce bulk symptoms.

During hysteroscopic myomectomy, the uterine cavity is filled with distention media, and the fibroid is resected with monopolar or bipolar cautery with the resectoscope. A bipolar instrument allows the use of saline for distention. It is important to closely monitor fluid deficits during any hysteroscopic procedure as dangerous electrolyte imbalances can occur, especially with use of a monopolar resectoscope and glycine as a distention medium [47].

The hysteroscopic morcellator cuts intrauterine myoma into small chips and evacuates the fragments into a tissue trap. A meta-analysis found that successful removal of all endometrial lesions was more frequent with hysteroscopic morcellation than conventional resection (odds ratio 4.49, 95% confidence interval [CI] 1.94–10.41; $p < 0.001$), operative time was approximately 5 minutes shorter with morcellation (95% CI −7.20 to −2.68; $p < 0.001$), and no difference in complications was found [48]. To minimize bleeding during hysteroscopic myomectomy, the myoma base may be injected with dilute vasopressin.

During hysteroscopic myomectomy of a sessile myoma located partially within the myometrial wall, there tends to be progressive herniation of the intramural component of the myoma into the uterine cavity [49]. Movement of the fibroid into the cavity may allow for more complete resection of the fibroid than would be expected based on the percentage of the fibroid in the cavity as seen during SIS. However, continued resection into the myometrium may result in uterine perforation and could cause injury to structures adjacent to the uterus, including bowel and bladder. The use of concurrent abdominal ultrasound can provide additional safety during complex hysteroscopic procedures, allowing for better identification of the relationship of the surgical site and the myometrium [33].

Abdominal Myomectomy

Although Washington Atlee reported his experience performing successful abdominal myomectomies in 1845 [50], the mortality rates were high until Victor Bonney mastered the techniques of this procedure, after being inspired by his childless wife's emotionally devastating hysterectomy for a submucous leiomyoma in 1908. Bonney introduced many surgical techniques still used today, including uterine artery compression with his "Bonney clamp" to reduce bleeding and elevation of the uterus to improve exposure during myomectomy. He described an approach to obliterate the dead space from the myoma bed by under-sewing the deeper tissue layers. In this career, Bonney performed more than 700 myomectomies. His mortality rate was 1.1%, remarkably low in an era before blood transfusions and antibiotics. By the 1930s, Bonney advocated myomectomy for any woman wishing to have children under the age of 41.

Abdominal myomectomy is typically performed through a Pfannenstiel incision, although a Maylard incision or vertical incision may be helpful for women with massive fibroids. The fibroid pseudocapsule is injected with an agent to reduce intraoperative bleeding. A Cochrane review found moderate-quality evidence that preoperative use of vaginal misoprostol may reduce bleeding during myomectomy; low-quality evidence that bupivacaine plus epinephrine, tranexamic acid, gelatin-thrombin matrix, a pericervical tourniquet, ascorbic acid, dinoprostone,

loop ligation, and a fibrin sealant patch may reduce bleeding during myomectomy; and no evidence that oxytocin, morcellation, and temporary clipping of the uterine artery reduces blood loss [51]. The surgeon should use a systematic approach and remove as many fibroids as possible through a single incision, with careful dissection of the fibroid from the surrounding pseudocapsule [1]. Morbidity of abdominal myomectomy is comparable to abdominal hysterectomy, at least for a uterus up to 18-week size [52].

Long-term abdominal myomectomy outcomes are usually good, and patient satisfaction is high [53, 54], but adhesions or recurrent fibroids may compromise the results in some individuals. Myomectomy often reduces menorrhagia and improves fertility in women with excessive bleeding or infertility primarily caused by endometrial distortion from submucous myomas or large intramural myomas. Slightly more than 50% of women conceive after open myomectomy [55]. Adhesions form in more than 90% of abdominal myomectomies, with the incidence highest (94%) with posterior incisions and lower (56%) with fundal or anterior uterine incisions [56]. When severe, adhesions can result in bowel obstruction and require additional intervention. Although adhesion barriers may be recommended to minimize the extent of adhesions, a Cochrane review found no evidence that barrier agents improved pain or fertility outcomes and low-quality evidence that oxidized regenerated cellulose, expanded polytetrafluoroethylene, and sodium hyaluronate with carboxymethylcellulose may all be more effective than no treatment in reducing adhesion formation following pelvic surgery [57]. Growth of new fibroids is not uncommon after myomectomy, but additional surgery is required in a minority of patients.

Laparoscopic Myomectomy

Laparoscopic myomectomy provides several advantages compared to laparotomy. Reduced postoperative pain, shorter recovery time, less common postoperative febrile morbidity, reduced intraoperative blood loss, and less adhesion formation with laparoscopic myomectomy are the clear advantages seen in the minimally invasive approach. Recurrence risks and pregnancy outcomes are comparable after resection of myomas from abdominal versus laparoscopic route [40].

Appropriate patient selection is important when considering laparoscopic myomectomy. Optimal candidates have less than four fibroids and fibroid diameters less than 8–10 cm. Skilled surgeons may sometimes exceed these arbitrary limits, although operating time are longer with more extensive procedures [58].

The pregnancy and obstetrical outcomes of laparoscopic myomectomy are good when optimal surgical techniques are used to perform the procedure. The importance of gentle dissection of the fibroid from the pseudocapsule, with preservation of the pseudocapsule, has been demonstrated, as 74% of infertile women who underwent intracapsular subserous and intramural myomectomy preserving the myoma pseudocapsule eventually conceived [36]. Many of these women were allowed to deliver vaginally, and there were no cases of uterine dehiscence.

Although many techniques of laparoscopic myomectomy have been described, we use modifications of techniques described in 2005 [40]. Four ports are used. In cases with large fibroids, the laparoscope is placed in the left upper quadrant at “Palmer’s point,” a 5-mm port is placed to the right of the umbilicus and another in the right lower quadrant, and an 11 mm port is placed in the left lower quadrant to prevent instrument collision. Injection of the pseudocapsule with a dilute solution of vasopressin limits intraoperative blood loss (Fig. 9.9). When a small fibroid near the endometrial cavity cannot be visualized directly by laparoscopy, intracorporeal or transvaginal ultrasound may be helpful to identify and remove the mass. A harmonic scalpel hook provides the ability to cut into the uterus to expose the fibroid and the pseudocapsule and limit bleeding (Fig. 9.10). The fibroid is removed based on the principles of traction and countertraction, with care taken to preserve the pseudocapsule (Fig. 9.11). The myomectomy site must be closed to avoid dead space, and a barbed running suture placed in layers is effective to prevent

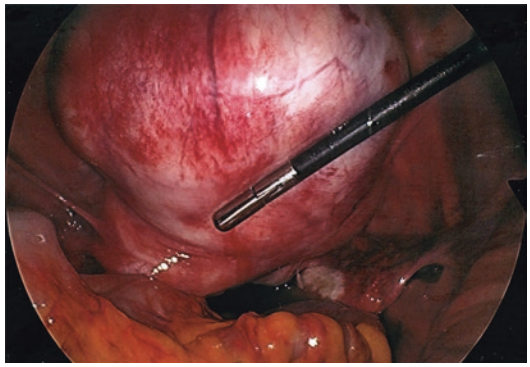

Fig. 9.9 Large fibroid demonstrated during laparoscopy with prominent vessels

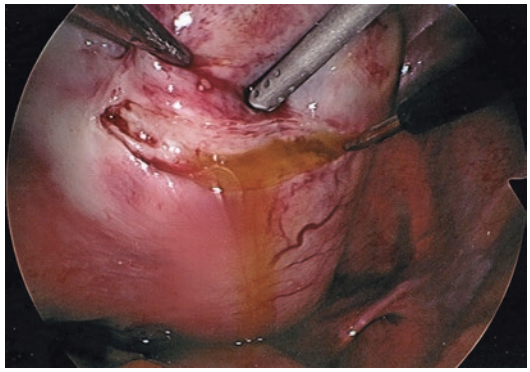

Fig. 9.10 Incision into the same fibroid showing degenerative changes and liquefaction during laparoscopic myomectomy

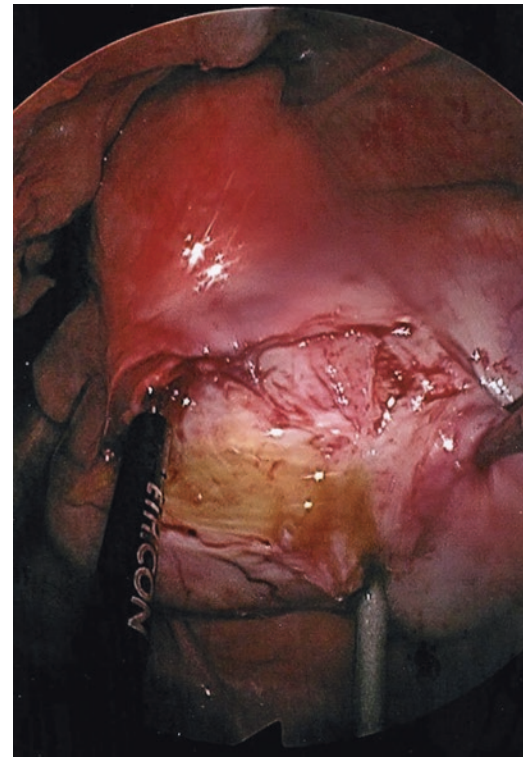

Fig. 9.11 Fibroid enucleation of the same fibroid from its surrounding pseudocapsule

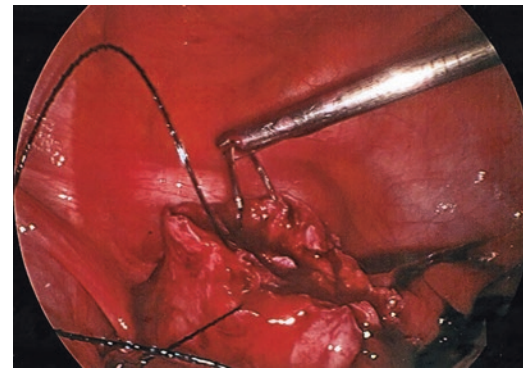

Fig. 9.12 Repair of myomectomy site from same procedure as Figs. 9.7, 9.8, and 9.9 with barbed suture

slippage and loosening of suture during repair (Fig. 9.12) [59]. An absorbable adhesion barrier is used to limit adhesion formation at the incision sites. We now extend the left lower abdominal incision to approximately 3 cm, place the enucleated fibroids in a bag, and use an "apple-peeling" technique to remove the surgical specimens instead of using a mechanical morcellator.

While there is a steep learning curve associated with complex laparoscopic myomectomy, robotic-assisted laparoscopy may allow for laparoscopic myomectomy to be more widely utilized. Robotic-laparoscopic myomectomy has a shorter learning curve and does not increase morbidity. Advantages of robotic surgery include improved dexterity and three-dimensional view. A meta-analysis found robotic myomectomy was associated with fewer complications, less blood loss, fewer surgical conversions, and less postoperative bleeding compared with laparoscopic and abdominal myomectomy [60]. Disadvantages of robotic surgery include the loss of tactile sensation during surgery and increased cost [61]. Alternately, laparoscopic myomectomy with the use of single-port

surgery presents a steep learning curve but has proposed benefits such as fewer surgical scars and comparable outcomes when performed by surgeons skilled in this technique [62].

It is important to note that myomectomy increases the risk of uterine rupture during pregnancy or labor [63]. While this risk is small, approximately 0.5–0.7%, uterine rupture is an obstetrical emergency and can have catastrophic consequences for the mother and fetus [39]. For this reason, cesarean delivery is often recommended for women who conceive after myomectomy. In order to allow for uterine healing, a 3-month interval between myomectomy and attempts to conceive is often recommended.

Uterine Artery Embolization

Uterine artery embolization (UAE) is a reasonable alternative to hysterectomy with improved bleeding, pain, and improved quality of life [53]. However, myomectomy is preferred when future fertility is desired. In 1 study, 31 women tried to conceive after UAE, but only 1 became pregnant, and she experienced a miscarriage [64]. This finding is logical, since fibroids are smaller but persist after UAE, and UAE alters uterine perfusion. However, the same investigators found that when fibroids were the only cause for infertility in 15 women with a mean age of 34.8, 9 conceived in the year following UAE, 5 experienced a live birth, and 8 experienced a live birth after a mean of 43 months [65].

MRgFUS

Magnetic resonance-guided focused ultrasound surgery (MRgFUS) is a noninvasive treatment for fibroids that uses MRI to deliver focused ultrasound energy to heat target tissue. MRgFUS was approved by the FDA in 2004 after studies showed significant improvement in quality of life scores [66]. In one prospective randomized study, the mean fibroid volume was reduced by 18%, and quality of life scores were higher after MRgFUS than women who underwent a sham procedure [67]. MRgFUS-related complications include skin and sciatic nerve injury, and there is a small risk of bowel and bladder injury.

Less than half of women are eligible for MRgFUS, due to excessive fibroid size, high cost of the procedure, and exclusion of women who desire fertility [68]. The procedure requires several hours of dedicated MRI time [69]. MRgFUS is not recommended when future pregnancy is desired, but by 2010, there were 54 pregnancies reported in 51 women MRgFUS, resulting in a 41% live birth rate, 20% ongoing pregnancies, a 28% spontaneous abortion rate, and an 11% pregnancy termination rate [66]. One center reported a high rate of pregnancy and live birth in infertile women who underwent MRgFUS [70]. While these data are encouraging, more studies are needed to determine the safety and efficacy of MRgFUS to treat uterine fibroids in infertile women. The ExAblate system is available in only a limited number of centers, which makes this approach inaccessible or impractical for many women [71].

Conclusion

As women delay childbearing, uterine fibroids are increasingly identified during an infertility evaluation. Identification of the size, number, and location of fibroids is determined by ultrasound. Submucosal fibroids reduce fertility and compromise pregnancy, and outcomes are improved after hysteroscopic myomectomy. Women with untreated intramural fibroids have a higher incidence of maternal and fetal pregnancy-related complications, and there is increasing evidence that fertility and pregnancy outcomes are improved following myomectomy. Laparoscopic or abdominal myomectomy is appropriate for women with symptomatic fibroids who desire fertility. Intracorporeal ultrasound may be useful when a fibroid deviates the endometrial cavity but cannot be identified by visual inspection of the uterus during myomectomy. Approximately 50% of women conceive after myomectomy, and IVF outcomes may improve. When fibroids are too extensive to perform myomectomy, or when a

hysterectomy is required, preservation of the ovaries may allow consideration of a gestational carrier pregnancy.

References

1. Tinelli A, Malvasi A, Rahimi S, Negro R, Cavallotti C, Vergara D, et al. Myoma pseudocapsule: a distinct endocrino-anatomical entity in gynecological surgery. Gynecol Endocrinol. 2009;25:661–7.
2. Ishikawa H, Reierstad S, Demura M, Rademaker AW, Kasai T, Inoue M, et al. High aromatase expression in uterine leiomyoma tissues of African-American women. J Clin Endocrinol Metab. 2009;94:1752–6.
3. Islam MS, Ciavattini A, Petraglia F, Castellucci M, Ciarmela P. Extracellular matrix in uterine leiomyoma pathogenesis: a potential target for future therapeutics. Hum Reprod Update. 2018;24:59–85.
4. Ciebiera M, Włodarczyk M, Słabuszewska-Jóźwiak A, Nowicka G, Jakiel G. Influence of vitamin D and transforming growth factor β3 serum concentrations, obesity, and family history on the risk for uterine fibroids. Fertil Steril. 2016;106:1787–92.
5. Practice Committee of American Society for Reproductive Medicine in collaboration with Society of Reproductive Surgeons. Myomas and reproductive function. Fertil Steril. 2008;90:S125–30.
6. Baird DD, Dunson DB, Hill MC, Cousins D, Schectman JM. High cumulative incidence of uterine leiomyoma in black and white women: ultrasound evidence. Am J Obstet Gynecol. 2003;188:100–7.
7. Stewart EA, Cookson CL, Gandolfo RA, Schulze-Rath R. Epidemiology of uterine fibroids: a systematic review. BJOG. 2017;124:1501–12.
8. Munro MG, Critchley HO, Broder MS, Fraser IS. FIGO Working Group on menstrual disorders. FIGO classification system (PALM-COEIN) for causes of abnormal uterine bleeding in nongravid women of reproductive age. Int J Gynaecol Obstet. 2011;113:3–13.
9. American Association of Gynecologic Laparoscopists (AAGL): Advancing Minimally Invasive Gynecology Worldwide. AAGL practice report: practice guidelines for the diagnosis and management of submucous leiomyomas. J Minim Invasive Gynecol. 2012;19:152–71.
10. Oliveira FG, Abdelmassih VG, Diamond MP, Dozortsev D, Melo NR, Abdelmassih R. Impact of subserosal and intramural uterine fibroids that do not distort the endometrial cavity on the outcome of in vitro fertilization-intracytoplasmic sperm injection. Fertil Steril. 2004;81:582–7.
11. Yan L, Yu Q, Zhang YN, Guo Z, Li Z, Niu J, et al. Effect of type 3 intramural fibroids on in vitro fertilization-intracytoplasmic sperm injection outcomes: a retrospective cohort study. Fertil Steril. 2018;109:817–22.
12. Christopoulos G, Vlismas A, Salim R, Islam R, Trew G, Lavery S. Fibroids that do not distort the uterine cavity and IVF success rates: an observational study using extensive matching criteria. BJOG. 2017;124:615–21.
13. Olive DL. The surgical treatment of fibroids for infertility. Semin Reprod Med. 2011;29:113–23.
14. Pritts EA, Parker WH, Olive DL. Fibroids and infertility: an updated systematic review of the evidence. Fertil Steril. 2009;91:1215–23.
15. Kroon B, Johnson N, Chapman M, Yazdani A, Hart R. Australasian CREI Consensus Expert Panel on Trial evidence (ACCEPT) group. Australasian CREI Consensus Expert Panel on Trial evidence. Aust NZ J Obstet Gynaecol. 2011;51:289–95.
16. Eldar-Geva T, Meagher S, Healy DL, MacLachlan V, Breheny S, Wood C. Effect of intramural, subserosal, and submucosal uterine fibroids on the outcome of assisted reproductive technology treatment. Fertil Steril. 1998;70:687–91.
17. Seoud MA, Patterson R, Muasher SJ, Coddington CC 3rd. Effects of myomas or prior myomectomy on in vitro fertilization (IVF) performance. J Assist Reprod Genet. 1992;9:217–21.
18. Narayan R, Goswamy RK. Treatment of submucous fibroids, and outcome of assisted conception. J Am Assoc Gynecol Laparosc. 1994;1:307–11.
19. Farhi J, Ashkenazi J, Feldberg D, Dicker D, Orvieto R, Ben Rafael Z. Effect of uterine leiomyomata on the results of in-vitro fertilization treatment. Hum Reprod. 1995;10:2576–8.
20. Ramzy AM, Sattar M, Amin Y, Mansour RT, Serour GI, Aboulghar MA. Uterine myomata and outcome of assisted reproduction. Hum Reprod. 1998;13:198–202.
21. Somigliana E, De Benedictis S, Vercellini P, Nicolosi AE, Benaglia L, Scarduelli C, et al. Fibroids not encroaching the endometrial cavity and IVF success rate: a prospective study. Hum Reprod. 2011;26:834–9.
22. Surrey ES, Lietz AK, Schoolcraft WB. Impact of intramural leiomyomata in patients with a normal endometrial cavity on in vitro fertilization-embryo transfer cycle outcome. Fertil Steril. 2001;75:405–10.
23. Benecke C, Kruger TF, Siebert TI, Van der Merwe JP, Steyn DW. Effect of fibroids on fertility in patients undergoing assisted reproduction. A structured literature review. Gynecol Obstet Invest. 2005;59:225–30.
24. Stovall DW, Parrish SB, Van Voorhis BJ, Hahn SJ, Sparks AE, Syrop CH. Uterine leiomyomas reduce the efficacy of assisted reproduction cycles: results of a matched follow-up study. Hum Reprod. 1998;13:192–7.
25. Sunkara SK, Khairy M, El-Toukhy T, Khalaf Y, Coomarasamy A. The effect of intramural fibroids without uterine cavity involvement on the outcome of IVF treatment: a systematic review and meta-analysis. Hum Reprod. 2010;25:418–29.
26. Bodri D, Guillen JJ, Lopez M, Vernaeve V, Coll O. Racial disparity in oocyte donation outcome: a

multiethnic, matched cohort study. Hum Reprod. 2010;25:436–42.
27. Sheiner E, Bashiri A, Levy A, Hershkovitz R, Katz M, Mazor M. Obstetric characteristics and perinatal outcome of pregnancies with uterine leiomyomas. J Reprod Med. 2004;49:182–6.
28. Muram D, Gillieson M, Walters JH. Myomas of the uterus in pregnancy: ultrasonographic follow-up. Am J Obstet Gynecol. 1980;138:16–9.
29. Shavell VI, Thakur M, Sawant A, Kruger ML, Jones TB, Singh M, et al. Adverse obstetric outcomes associated with sonographically identified large uterine fibroids. Fertil Steril. 2012;97:107–10.
30. Klatsky PC, Tran ND, Caughey AB, Fujimoto VY. Fibroids and reproductive outcomes: a systematic literature review from conception to delivery. Am J Obstet Gynecol. 2008;198:357–66.
31. De Vivo A, Mancuso A, Giacobbe A, Savasta LM, De Dominici R, Dugo N, et al. Uterine myomas during pregnancy: a longitudinal sonographic study. Ultrasound Obstet Gynecol. 2011;37:361–5.
32. Benaglia L, Cardellicchio L, Filippi F, Paffoni A, Vercellini P, Somigliana E, et al. The rapid growth of fibroids during early pregnancy. PLoS One. 2014;9:e85933.
33. Hurst BS. Anatomic abnormal uterine bleeding due to anatomic causes. In: Marshburn PB, Hurst BS, editors. Disorders of menstruation. West Sussex: Wiley-Blackwell; 2011. p. 86–107.
34. Hartmann KE, Velez Edwards DR, Savitz DA, Jonsson-Funk ML, Wu P, Sundermann AC, Baird DD. Prospective cohort study of uterine fibroids and miscarriage risk. Am J Epidemiol. 2017;186:1140–8.
35. Sundermann AC, Velez Edwards DR, Bray MJ, Jones SH, Latham SM, Hartmann KE. Leiomyomas in pregnancy and spontaneous abortion: a systematic review and meta-analysis. Obstet Gynecol. 2017;130:1065–72.
36. Tinelli A, Malvasi A, Hurst BS, Tsin DA, Davila F, Dominguez G, et al. Surgical management of neurovascular bundle in uterine fibroid pseudocapsule. JSLS. 2012;16:119–29.
37. Ludwin I, Ludwin A, Wiechec M, Nocun A, Banas T, Basta P, et al. Accuracy of hysterosalpingo-foam sonography in comparison to hysterosalpingo-contrast sonography with air/saline and to laparoscopy with dye. Hum Reprod. 2017;32:758–69.
38. Shwayder J, Sakhel K. Imaging for uterine myomas and adenomyosis. J Minim Invasive Gynecol. 2014;21:362–76.
39. Hurst BS, Tinelli A, Malvasi A, Parker WH. Fibroid complications in pregnancy. In: Malvasi A, Tinelli A, Di Renzo GC, editors. Management and therapy of early pregnancy complications first and second trimesters. Cham: Springer International Publishing; 2016. p. 135–60.
40. Hurst BS, Matthews ML, Marshburn PB. Laparoscopic myomectomy for symptomatic uterine myomas. Fertil Steril. 2005;83:1–23.
41. Donnez J, Hudecek R, Donnez O, Matule D, Arhendt HJ, Zatik J, et al. Loumaye. Efficacy and safety of repeated use of ulipristal acetate in uterine fibroids. Fertil Steril. 2015;103:519–27.
42. Luyckx M, Squifflet JL, Jadoul P, Votino R, Dolmans MM, Donnez J. First series of 18 pregnancies after ulipristal acetate treatment for uterine fibroids. Fertil Steril. 2014;102:1404–9.
43. Wallach EE, Vlahos NF. Uterine myomas: an overview of development, clinical features, and management. Obstet Gynecol. 2004;104:393–406.
44. Kundu S, Iwanuk C, Staboulidou I, Garcia-Rocha GJ, Soergel P, Hertel H, et al. Morbidity, fertility and pregnancy outcomes after myoma enucleation by laparoscopy versus laparotomy. Arch Gynecol Obstet. 2018;297:969–76.
45. Roy KK, Singla S, Baruah J, Sharma JB, Kumar S, Singh N. Reproductive outcome following hysteroscopic myomectomy in patients with infertility and recurrent abortions. Arch Gynecol Obstet. 2010;282:553–60.
46. Bosteels J, Kasius J, Weyers S, Broekmans FJ, Mol BW, D'Hooghe TM. Hysteroscopy for treating subfertility associated with suspected major uterine cavity abnormalities. Cochrane Database Syst Rev. 2015;21:CD009461.
47. Litta P, Leggieri C, Conte L, Dalla Toffola A, Multinu F, Angioni S. Monopolar versus bipolar device: safety, feasibility, limits and perioperative complications in performing hysteroscopic myomectomy. Clin Exp Obstet Gynecol. 2014;41:335–8.
48. Li C, Dai Z, Gong Y, Xie B, Wang B. A systematic review and meta-analysis of randomized controlled trials comparing hysteroscopic morcellation with resectoscopy for patients with endometrial lesions. Int J Gynaecol Obstet. 2017;136:6–12.
49. Casadio P, Youssef AM, Spagnolo E, Rizzo MA, Talamo MR, De Angelis D, et al. Should the myometrial free margin still be considered a limiting factor for hysteroscopic resection of submucous fibroids? A possible answer to an old question. Fertil Steril. 2011;95:1764–8.
50. Chamberlain G. The master of myomectomy. J Royal Soc Med. 2003;96:302–4.
51. Kongnyuy EJ, Wiysonge CS. Interventions to reduce haemorrhage during myomectomy for fibroids. Cochrane Database Syst Rev. 2014;15:CD005355.
52. Pundir J, Walawalkar R, Seshadri S, Khalaf Y, El-Toukhy T. Perioperative morbidity associated with abdominal myomectomy compared with total abdominal hysterectomy for uterine fibroids. J Obstet Gynaecol. 2013;33:655–62.
53. Manyonda IT, Bratby M, Horst JS, Banu N, Gorti M, Belli AM. Uterine artery embolization versus myomectomy: impact on quality of life--results of the FUME (Fibroids of the Uterus: Myomectomy versus Embolization) Trial. Cardiovasc Intervent Radiol. 2012;35:530–6.
54. Dilek S, Ertunc D, Tok EC, Cimen R, Doruk A. The effect of myomectomy on health-related quality of

life of women with myoma uteri. J Obstet Gynaecol Res. 2010;36:364–9.
55. Malzoni M, Tinelli R, Cosentino F, Iuzzolino D, Surico D, Reich H. Laparoscopy versus minilaparotomy in women with symptomatic uterine myomas: short-term and fertility results. Fertil Steril. 2010;93:2368–73.
56. Anonymous. An expanded polytetrafluoroethylene barrier (Gore-Tex Surgical Membrane) reduces post-myomectomy adhesion formation. The Myomectomy Adhesion Multicenter Study Group. Fertil Steril. 1995;63:491–3.
57. Ahmad G, O'Flynn H, Hindocha A, Watson A. Barrier agents for adhesion prevention after gynaecological surgery. Cochrane Database Syst Rev. 2015;30(4):CD000475.
58. Sizzi O, Rossetti A, Malzoni M, Minelli L, La Grotta F, Soranna L, et al. Italian multicenter study on complications of laparoscopic myomectomy. J Minim Invasive Gynecol. 2007;14:453–62.
59. Modi R. Laparoscopic myomectomy with aquadissection and barbed sutures. J Gynecol Endosc Surg. 2011;2:47–52.
60. Wang T, Tang H, Xie Z, Deng S. Robotic-assisted vs. laparoscopic and abdominal myomectomy for treatment of uterine fibroids: a meta-analysis. Minim Invasive Ther Allied Technol. 2018;28:1–16.
61. Nezhat C, Lavie O, Hsu S, Watson J, Barnett O, Lemyre M. Robotic-assisted laparoscopic myomectomy compared with standard laparoscopic myomectomy--a retrospective matched control study. Fertil Steril. 2009;91:556–9.
62. Jeong JH, Kim YR, Hong KP, Ha JE, Kim EJ, Hong DK, et al. Clinical experience with single-port access laparoscopic cystectomy and myomectomy. Clin Exp Reprod Med. 2016;43:44–50.
63. Chao AS, Chang YL, Yang LY, Chao A, Chang WY, Su SY, et al. Laparoscopic uterine surgery as a risk factor for uterine rupture during pregnancy. PLoS One. 2018;13:e0197307.
64. Torre A, Paillusson B, Fain V, Labauge P, Pelage JP, Fauconnier A. Uterine artery embolization for severe symptomatic fibroids: effects on fertility and symptoms. Hum Reprod. 2014;29:490–501.
65. Torre A, Fauconnier A, Kahn V, Limot O, Bussierres L, Pelage JP. Fertility after uterine artery embolization for symptomatic multiple fibroids with no other infertility factors. Eur Radiol. 2017;27:2850–9.
66. Rabinovici J, David M, Fukunishi H, Morita Y, Gostout BS, Stewart EA, MRgFUS Study Group. Pregnancy outcome after magnetic resonance-guided focused ultrasound surgery (MRgFUS) for conservative treatment of uterine fibroids. Fertil Steril. 2010;93:199–209.
67. Jacoby VL, Kohi MP, Poder L, Jacoby A, Lager J, Schembri M, et al. PROMISe trial: a pilot, randomized, placebo-controlled trial of magnetic resonance guided focused ultrasound for uterine fibroids. Fertil Steril. 2016;105:773–80.
68. Behera MA, Leong M, Johnson L, Brown H. Eligibility and accessibility of magnetic resonance-guided focused ultrasound (MRgFUS) for the treatment of uterine leiomyomas. Fertil Steril. 2010;94:1864–8.
69. Hesley GK, Gorny KR, Henrichsen TL, Woodrum DA, Brown DL. A clinical review of focused ultrasound ablation with magnetic resonance guidance: an option for treating uterine fibroids. Ultrasound Q. 2008;24:131–9.
70. Zou M, Chen L, Wu C, Hu C, Xiong Y. Pregnancy outcomes in patients with uterine fibroids treated with ultrasound-guided high-intensity focused ultrasound. BJOG. 2017;124 Suppl 3:30–5.
71. Sridhar D, Kohi MP. Updates on MR-guided focused ultrasound for symptomatic uterine fibroids. Semin Intervent Radiol. 2018;35:17–22.

Uterine Polyps

10

Silvina M. Bocca, Bijan Morshedi,
and Alena D. Naumova

Endometrial Polyps

Endometrial polyps are localized overgrowths of endometrium that protrude into the uterine cavity causing different degrees of distortion and may be a factor in female infertility by physical interference with gamete transport, alteration of the endometrial milieu, and unresponsiveness to the cyclical global endometrial changes. As such polyps remain mostly asymptomatic, their diagnosis is often incidental during routine investigations prior to embarking on assisted reproductive treatment (ART), but there are certain high-risk groups that deserve special attention and closer monitoring.

Polyps contain a variable amount of glands, stroma, and blood vessels, the relative amounts of which influence their visual appearance. They may be soft and cystic (Fig. 10.1a) or firm and fibrous; sessile (Fig. 10.1b) or pedunculated (Fig. 10.1c); hyperplastic, atrophic, or functional (undergo cyclical changes); single or multiple polyps (Fig. 10.2); range from a few millimeters to several centimeters in size; and may originate from the uterine fundus (Fig. 10.3), mid-wall (see Figs 10.1b and 10.2b), cornua (Fig. 10.4), or cervix (Fig. 10.5).

The prevalence of polyps can range from 10% to 15% in asymptomatic premenopausal women by TV US [1], 6–11% in asymptomatic infertile women [2], 13% in asymptomatic postmenopausal women undergoing TVUS [3], and 8–36% in postmenopausal women on tamoxifen therapy [4]. The natural history of endometrial polyps is variable with spontaneous regression reported between 6.3% [5] and 27% [6] after 12–22.5 months of follow-up and recurrence rates as high as 42% [7] depending on association with risk factors such as higher number of endometrial polyps and longer follow-up, concomitant endometriosis [8], having hyperplasia without atypia [9], or being on tamoxifen [10]. The majority of uterine polyps are benign. A systematic review of observational studies reported endometrial hyperplasia without atypia rates between 0.2% and 23.8% in polyps [11], premalignant atypical endometrial hyperplasia ranging from 1% to 3% [12, 13], and endometrial polyp cancer within the range 0.5–3% [12, 14, 15].

S. M. Bocca (✉)
The Jones Institute for Reproductive Medicine, Eastern Virginia Medical School, Department of Obsterics and Gynecology, Norfolk, VA, USA
e-mail: boccas@evms.edu

B. Morshedi
University of Virginia School of Medicine, Charlottesville, VA, USA

A. D. Naumova
Monmouth Medical Center, Department of Obstetrics and Gynecology, Long Branch, NJ, USA

L. A. Stadtmauer, I. Tur-Kaspa (eds.), *Ultrasound Imaging in Reproductive Medicine*,
https://doi.org/10.1007/978-3-030-16699-1_10

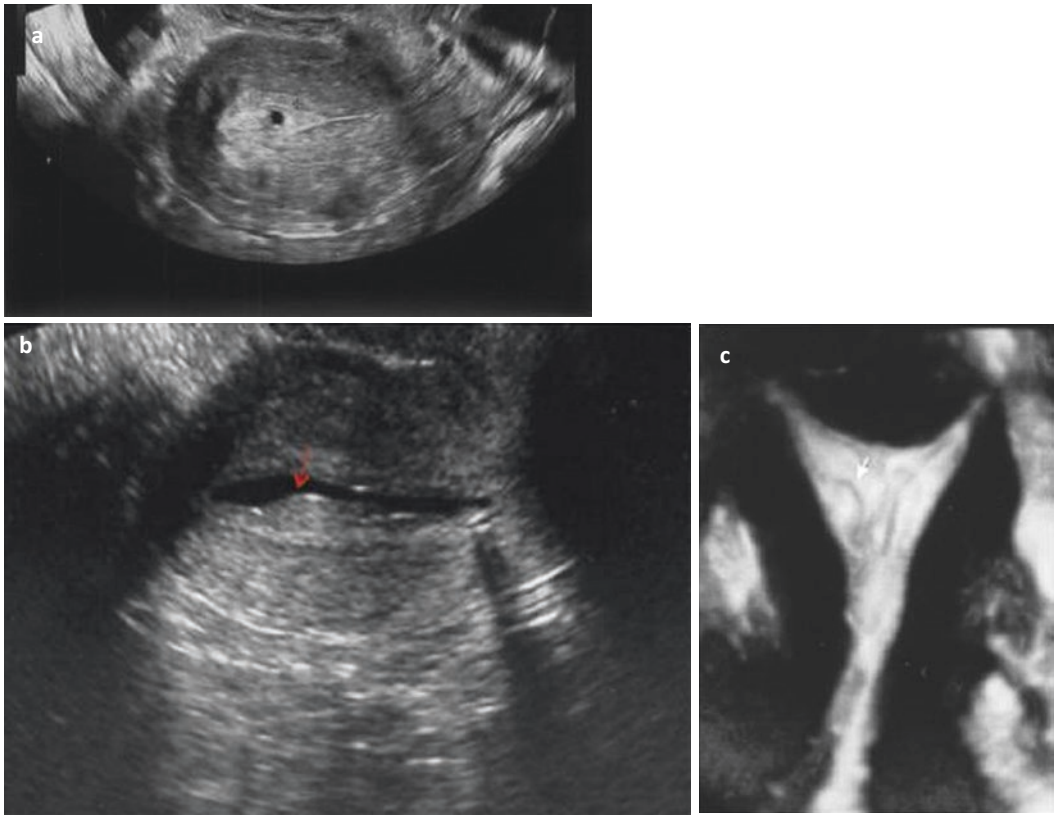

Fig. 10.1 (**a**) Cystic polyp shown in longitudinal 2D view of the uterus. (**b**) Sessile polyps (*arrow*) shown in a transverse 2D view of the uterus distended by saline infusion. (**c**) Coronal view (3D) of the uterus showing a pedunculated polyp (*arrow*)

Two- and Three-Dimensional Transvaginal Ultrasound

The American College of Obstetrics and Gynecology [16] recommends transvaginal ultrasound (TVUS) as the primary imaging test of the uterus for the evaluation of abnormal uterine bleeding (AUB), followed by sonohysterography (SHG) or hysteroscopy and lastly magnetic resonance imaging (MRI) if images are not adequate or further evaluation of the cavity is necessary. Similarly, The American Association of Gynecologic Laparoscopists' (AAGL) guidelines for the diagnosis of endometrial polyps [17] state that TVUS provides reliable information for the detection of endometrial polyps and should be the investigation of choice where available, the addition of color or power Doppler increases the capacity of TVUS to diagnose endometrial polyps, adding intrauterine contrast to sonography (with or without 3D imaging) improves the diagnostic capacity for endometrial polyps, and blind dilation and curettage or biopsy should not be used for diagnosis of endometrial polyps.

Clark et al. [18] reported that the criteria for diagnosis of uterine polyps vary according to the test used, but optimal testing and standardized definitions are lacking. On US polyps appear as nonspecific endometrial thickening (Fig. 10.6b) or a focal mass identified as an echogenic lesion (see Figs 10.2a, 10.3a, 10.6a and 10.10a), which disturbs the midline endo-

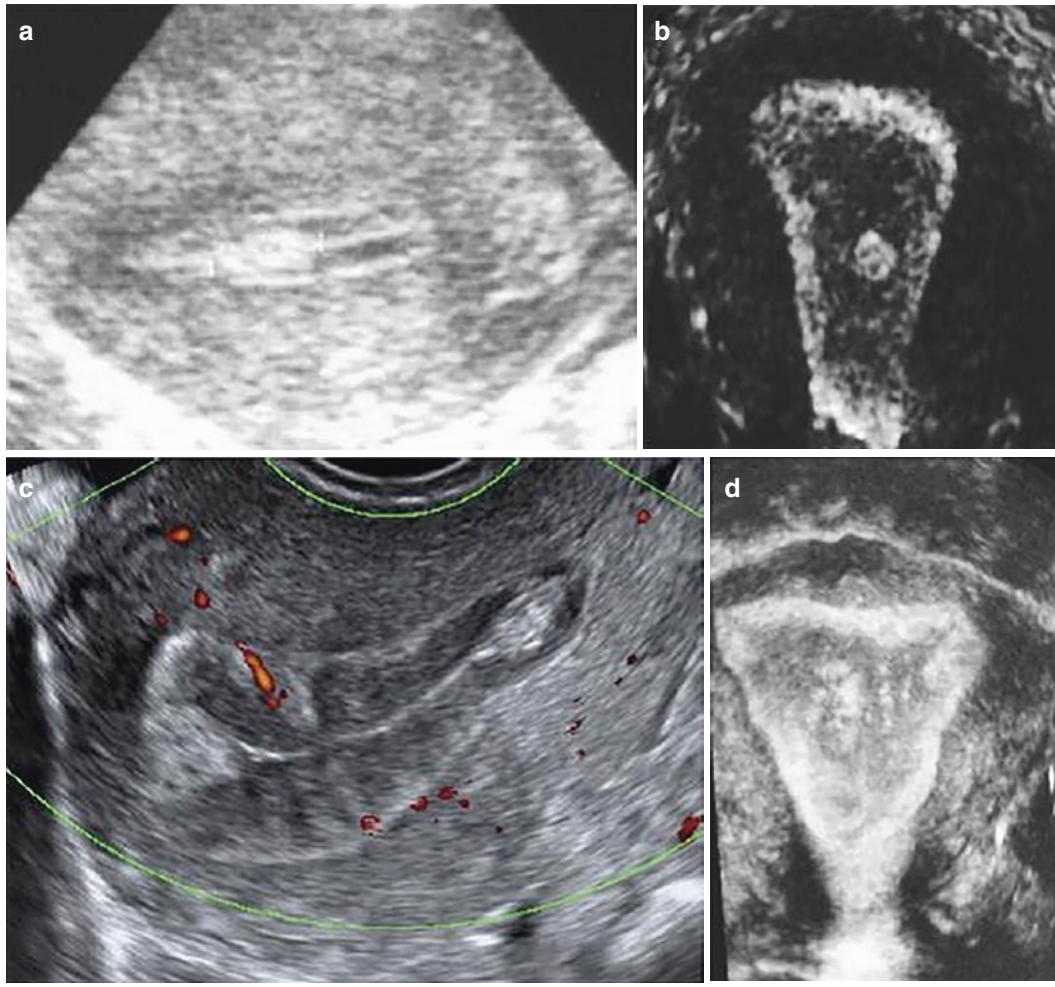

Fig. 10.2 Endometrial polyps. A single polyp located in a lateral wall at midcorpus, shown in two-dimensional transvaginal ultrasonographic view (**a**) and in 3D imaging (**b**). Multiple polyps and submucosal fibroids (by Pathology) shown by 2D US (**c**) and 3D US (**d**)

metrial echo but does not disrupt the interface between the myometrium and endometrium. The lesion is usually oval shaped with a homogeneous texture, although hypoechoic cystic spaces may be seen. Blood flow may be identified within a feeding vessel extending to the polyp on color-flow Doppler imaging (see Figs 10.2c and 10.6b). Saline infusion sonography (SIS) and three-dimensional US (3D US) help delineate the borders of the intracavity lesion (see Figs 10.1b and 10.7). None of these findings can reliably distinguish among polyps, submucosal fibroids, adenomyosis, and neoplastic change. In premenopausal women, the TVUS examination should be performed early in the proliferative phase when the endometrium is at its thinnest (4–8 mm) [19, 20] to minimize false-positive and false-negative findings [21]. In a retrospective review of multiple studies, Salim and his group [22] reported that for TVUS, the sensitivity varies between 19 and 96%, specificity of 53 and 100%, positive pre-

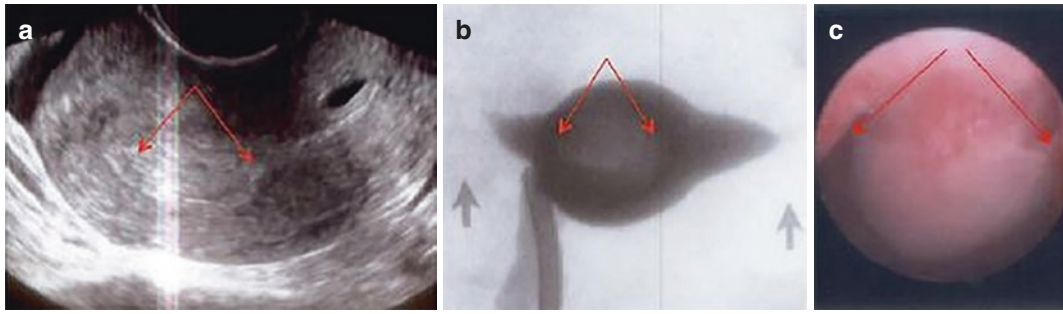

Fig. 10.3 Large polyp (*arrows*) occupying the entire fundal area shown in a sagittal 2D view (**a**), in an HSG view (**b**) giving a globular appearance of the uterus, and in a hysteroscopic view (**c**)

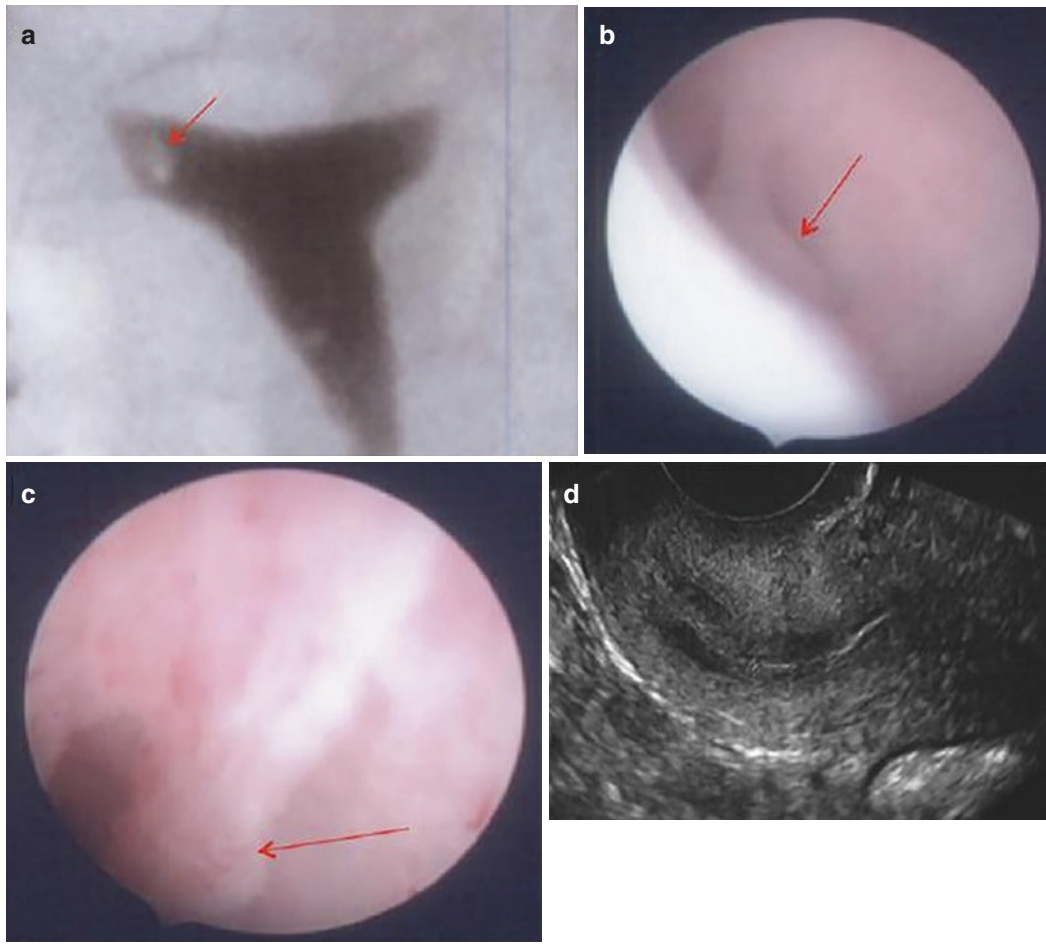

Fig. 10.4 Cornual polyps (*arrows*) clearly seen in HSG (**a**) and hysteroscopy (**b**, **c**) but not visualized in 2D US (**d**)

dictive value (PPV) of 75 and 100%, and negative predictive value (NPV) of 87 and 9%, when compared with hysteroscopy with guided biopsy [23, 24, 25]. The ranges were tighter in a single-large prospective study evaluating the causes of menorrhagia: 86% sensitivity, 94% specificity, 91% PPV, and 90% NPV [26]. In general, TVUS appears to have a good degree of

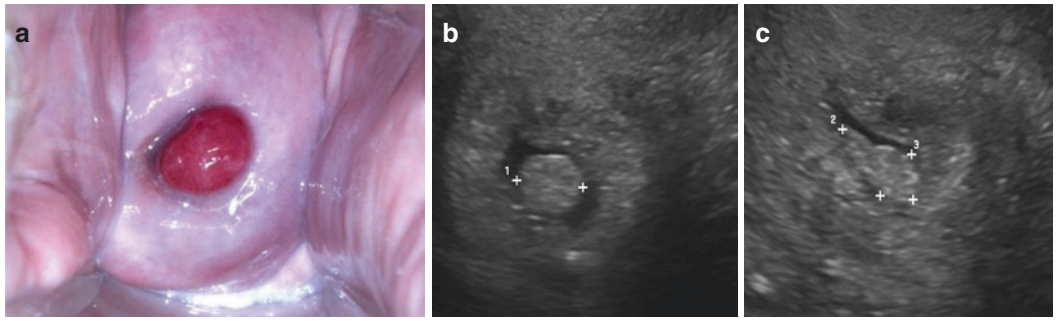

Fig. 10.5 Cervical polyp protruding from the external os (**a**) under speculum visualization. Polyp outlined by fluid in the endocervical canal visualized by TV US in coronal (**b**) and in sagittal (**c**) views

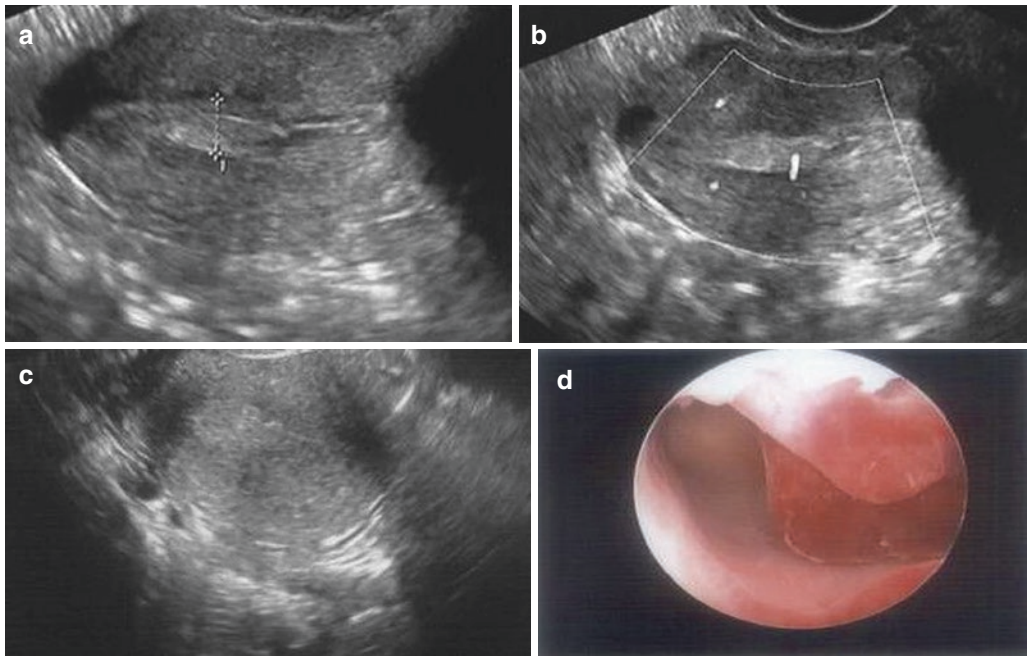

Fig. 10.6 Transvaginal ultrasonographic view of an endometrial polyp (**a**, *cursor*) appearing as an echogenic ovoid structure containing a feeding vessel visualized by Doppler (**b**) or as a nonspecific endometrial thickening (**c**. 2D TV US, **d**. hysteroscopy)

accuracy when performed with high-resolution equipment by proficient practitioners.

Three-dimensional US is a noninvasive imaging technique with the ability to generate multiplanar reconstructed images (Fig. 10.8) through the uterus and its external contours. Coronal views of the uterus allow more accurate visualization between the endometrium and myometrium at the fundus and cornual angles, providing superior diagnostic accuracy in detecting endometrial polyps compared to 2D TVUS. We demonstrated that physicians who learn the Z technique [27] are able to retrieve the mid-coronal plane of the uterus faster and improve its image quality in volume sonography. In a prospective blinded study to evaluate the costs, accuracy, risks, and benefits of 3D TV sonography compared to hysterosalpingography [28], we concluded that 3D TV sonography provides visualization and evaluation of the uterine cavity with similar or better accuracy than standard hysterosalpingography (HSG) in the office setting, without radiation exposure, with

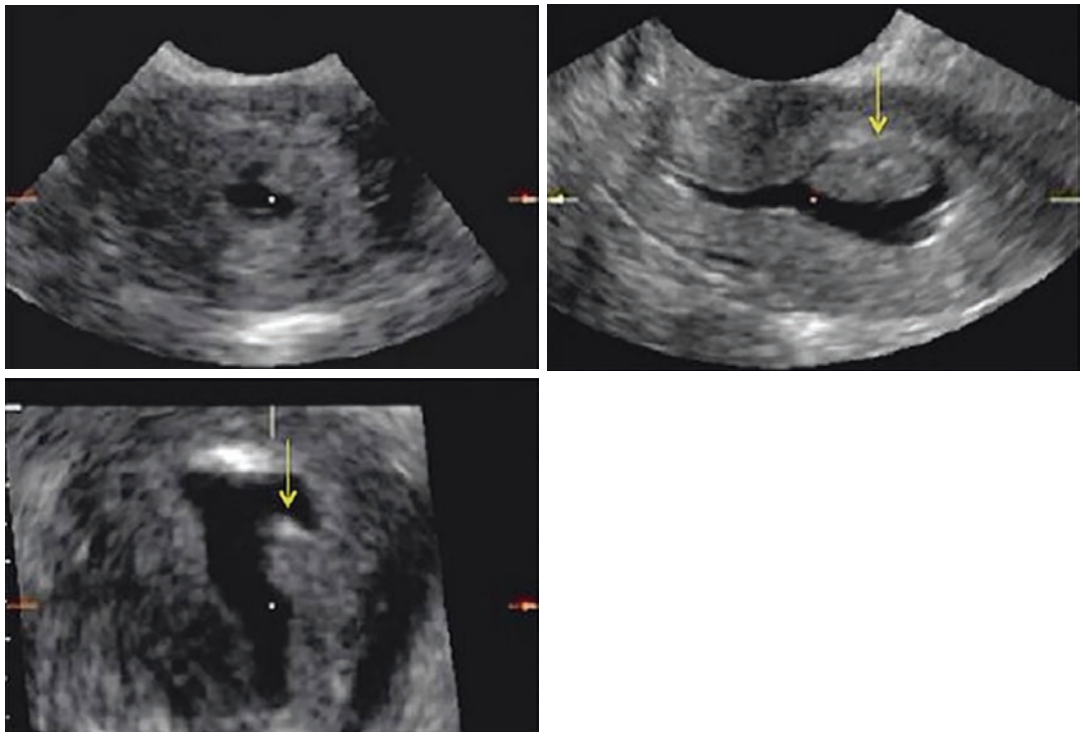

Fig. 10.7 3D-rendered view of the uterus during sonohysterography. The *arrow* points to an endometrial polyp in the left midcorpus

lower cost and morbidity. Studies with non-contrast 3D TVUS show limited improvement to diagnosing endometrial polyps when compared to hysteroscopy with biopsy, reporting 3D US to have sensitivity of 100%, specificity of 71–99%, PPV of 89–99%, and NPV of 100% [29, 30, 31]. Addition of saline solution contrast to 3D sonography results in slightly higher specificity (88–99%) and PPV (97–100%) for endometrial polyps than those of 3D US, with reasonably high sensitivity of 92–95% and NPV of 97% [30]. Despite the multiple advantages of performing 3D US, including having diagnostic accuracy comparable to MRI or combined laparoscopy and hysteroscopy, it is still not widely available and accepted as a diagnostic tool, and multiple insurance carriers deny its reimbursement.

Radiographic Indices: Polyp Morphology, Endometrial Thickness and Polyp Size, Color Doppler and Pedicle Artery, Interrupted Mucosal Sign, Combination

Polyp Morphology and Endometrial Thickness

The AAGL practice guidelines [17] describe that, on TVUS, polyps typically appear as a hyperechoic lesion with regular contours within the uterine lumen, surrounded by a thin hyperechoic halo, occasionally with cystic within, or the polyp may appear as a nonspecific endometrial thickening or focal mass within the endometrial cavity. These sonographic findings are not specific and may be found with other diseases such as myomas [32].

Polyp size should be assessed at the time of US as this can provide useful information in aiding management. An increase in polyp diameter appears to correlate with risk of malignancy [33], with smaller polyps being more likely to resolve spontaneously. Ultrasonographic measurement of endometrial thickness is of limited value in detecting benign abnormalities in the premenopausal woman due to physiologic menstrual changes as compared with its ability to exclude malignancy in the postmenopausal woman [34, 35]. Endometrial thickening (see Fig. 10.6) is a nonspecific finding of endometrial hyperplasia (Fig. 10.9b) as well as other causes such as polyp, endometrial cancer, trophoblastic disease (Fig. 10.9d), retained products of conception (Fig. 10.9c), or submucosal leiomyoma (Fig. 10.10) [36]. Song et al. [37] reported that, although TV US is poor at detecting them, its diagnostic value for endometrial polyps in infertile women could be improved by adding the measurement of endometrial thickness to the variables that are routinely assessed. The main use of endometrial thickness measured on TV US

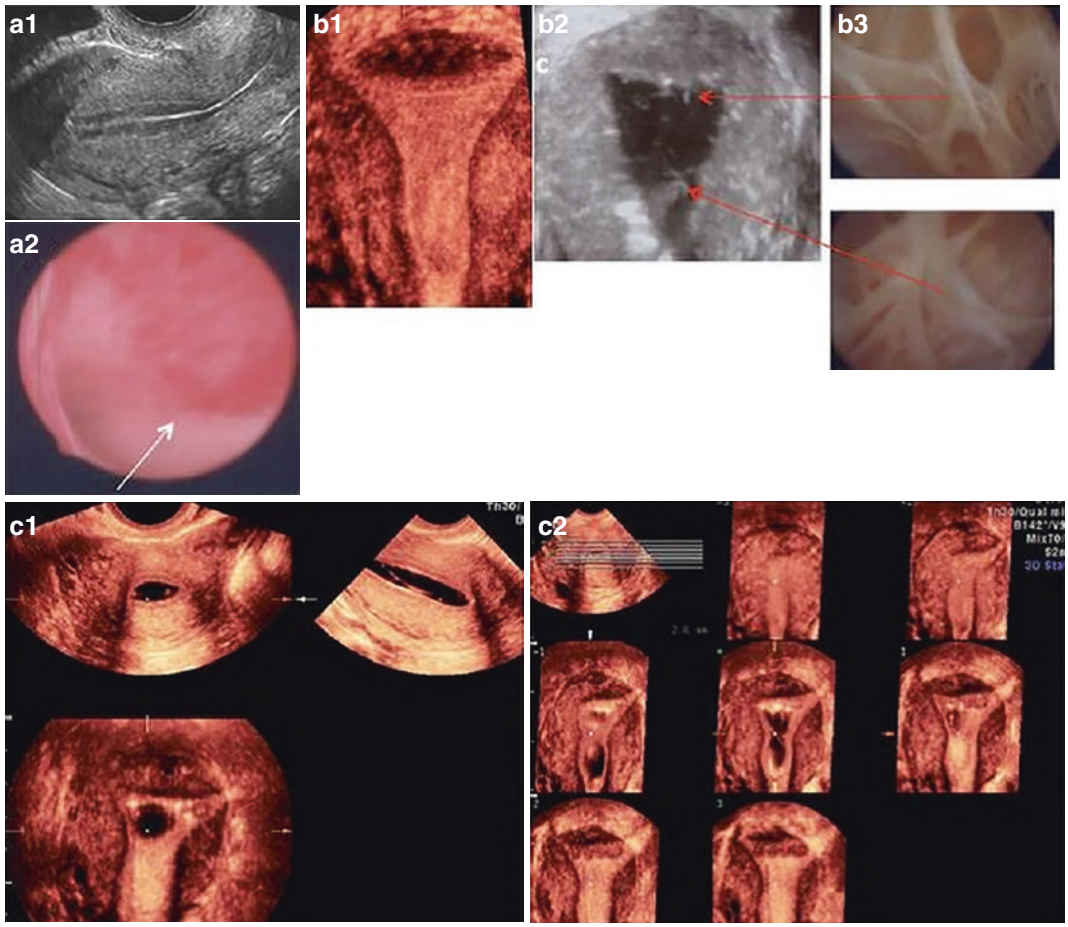

Fig. 10.8 Intrauterine lesions that may not be easily detected by TVUS. (**a1**) Apparently normal 2D sagittal view of the uterus. (**a2**) Same uterus as in (**a1**), containing flat hyperemic lesions visualized directly by hysteroscopy (benign polyp on pathology). (**b1**) Apparently normal 3D coronal view of the uterus. (**b2**) Multiple thin bands of synechiae seen on 3D SIS and hysteroscopy (**b3**). (**c1**) Synechiae not clearly visualized on 3D-SIS but more clearly identified upon evaluation of the multiplanar views (**c2**) of the uterus

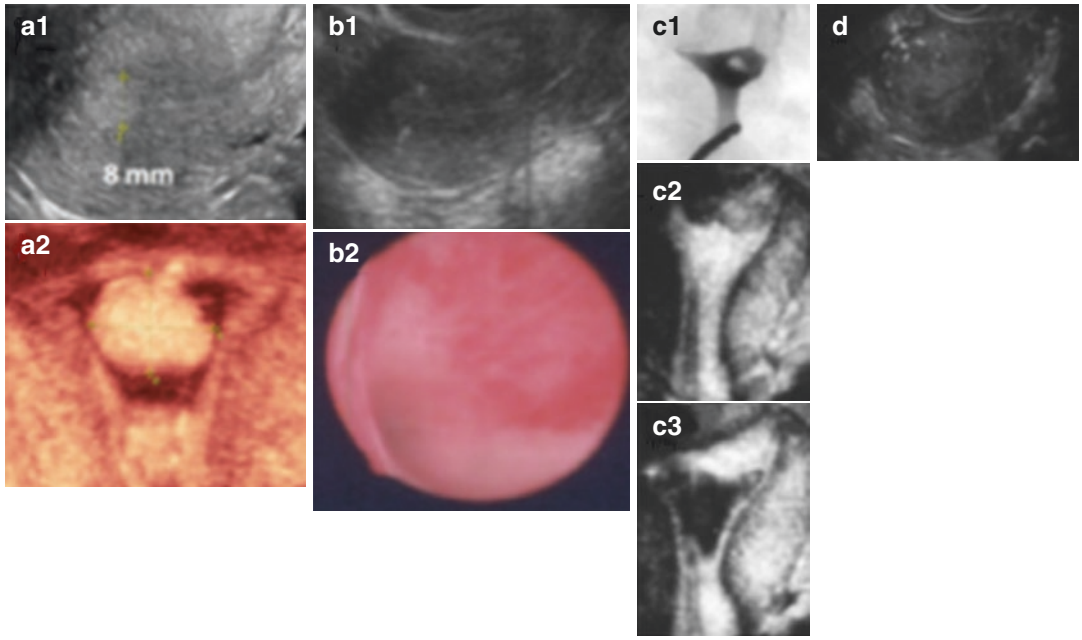

Fig. 10.9 Examples of different endometrial pathologies presenting as endometrial thickening in TV US. (**a**) Endometrial polyp (**a1** 2D US, **a2** 3D SIS); (**b**) complex hyperplasia without atypia (**b1** 2D US, **b2** flat lesions in hysteroscopy); (**c**) retained products of conception (**c1** HSG, **c2** 3D US, **c3** 3D SIS); (**d**) trophoblastic disease (multivessel signal)

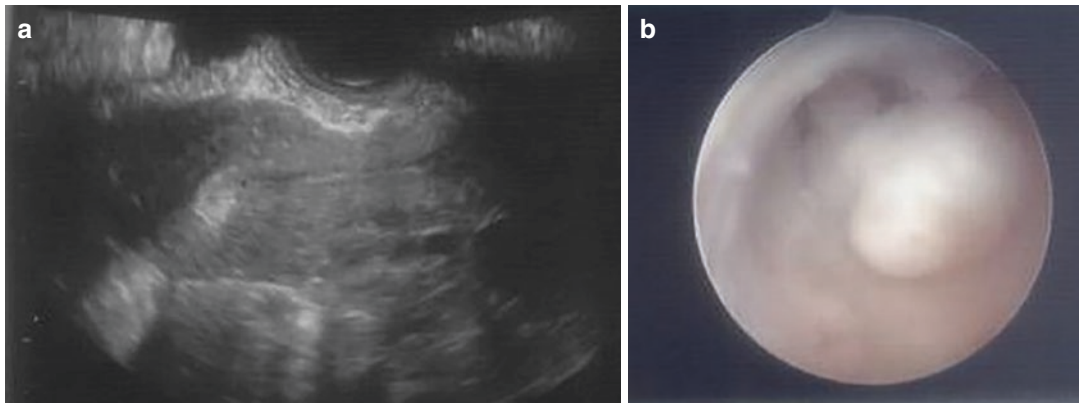

Fig. 10.10 Echogenic mass on 2D US (**a**) cannot be differentiated from a 2 cm fibroid resected hysteroscopically (**b**)

is the high negative predictive value of a thin distinct echo [16]. In women with postmenopausal bleeding, endometrial thickness less than 4 mm has a risk of malignancy of 1 in 917 and does not require endometrial sampling. In premenopausal patients with AUB, an endometrial echo less than 5 mm early in the cycle excludes significant pathology. Cavkaytar S [38]. assessed the role of sonographic endometrial thickness and hysteroscopic polyp size in predicting premalignant and malignant polyps in 328 postmenopausal women with AUB and thickened endometrium. Premalignant and malignant polyps were identified in 26 (7.9%) of cases. Sonographic measurement showed a greater endometrial thickness in cases of premalignant and malignant polyps

when compared to benign polyps. Endometrial thickness demonstrated a sensitivity of 53.8%, specificity of 85.8%, PPV of 24.6%, and NPV of 95.6% at a cutoff limit of 11.5 mm with diagnostic accuracy of 83.2%. Polyp size has a diagnostic accuracy of 94.8% with a sensitivity of 92.3%, specificity of 95.0%, PPV of 61.5%, and NPV of 99.3% at a cutoff point of 19.5 mm.

Color Doppler and Pedicle Artery

The addition of color-flow or power Doppler may improve the diagnostic capability of TVUS [17]. Color-flow Doppler may demonstrate the single feeding vessel typical of endometrial polyps. Power Doppler is reported to increase sensitivity to 91% and 97% in patients with and without symptoms, respectively [39]. Specificity and NPV may be increased to 95% and 94%, respectively, when color-flow Doppler is added to gray-scale TVUS to identify the feeding vessel (see Figs. 10.2c and 10.6b) [40]. There are limited data to support color-flow or power Doppler aiding in the differentiation of hyperplasia and malignancy in polyps [41, 42, 43], with no difference in the histologic grading of polyps on the basis of their resistive index, pulsatility index, or size [20]. Power Doppler has been reported to be more accurate than color flow for demonstrating vascular networks in one study assessing postmenopausal women with abnormal bleeding and thickened endometrium on baseline US [39]. Cogendez et al. [44] studied the role of TV power Doppler US in the differential diagnosis of benign intrauterine focal lesions in 480 premenopausal women with AUB. Three different vascular flow patterns were defined: single-vessel pattern, multiple-vessel pattern, and circular flow pattern. Histopathological results after hysteroscopy were as follows: endometrial polyp, 69%, and submucous myoma, 31%. Of the cases with endometrial polyps, 80% demonstrated a single-vessel pattern, 7.5% a multiple-vessel pattern, and 0% a circular pattern. Vascularization was not observed in 12.5% of patients with polyps. Of the cases with submucosal myomas, 72.2% demonstrated a circular flow pattern and 27.8% a multiple-vessel pattern, and none of them showed a single-vessel pattern. The sensitivity, specificity, and positive and negative predictive values of the single-vessel pattern in diagnosing endometrial polyps were 80, 100, 100, and 69.2%, respectively; and for the circular pattern in diagnosing submucous myoma, these were 72.2, 100, 100, and 88.9%, respectively. Power Doppler blood flow mapping is a useful, practical, and noninvasive diagnostic method for the differential diagnosis of benign intrauterine focal lesions. The combination of SHG with feeding artery visualization was reported to increase polyp detection by Anioł et al. [45]. Sonography detection of endometrial polyp based on feeding artery visualization had a 40% sensitivity, whereas SHG polyp detection had a sensitivity of 75% and a specificity of 100%. The PPV and NPVs of SHG in diagnosing endometrial polyps were estimated at 75% and 72% (95% CI, 52–86%), respectively. The combination of SHG and feeding artery imaging in TV US was 84% sensitive and 95% specific in detecting endometrial polyps. The positive and negative predictive values were PPV = 96% and NPV = 89%. These authors concluded that SHG with feeding artery visualization may become a standard method in the diagnostics of endometrial polyps in perimenopausal women. The diagnostic utility of saline infusion Doppler (SIS-D) in endometrial mass lesions was also evaluated by Ogutcuoglu et al. [46] demonstrating that, according to SIS-D, 92.2% of the lesions that had single-vessel feeding patterns were endometrial polyps ($p < 0.0001$) and 57.1% of the lesions that had multiple-vessel feeding patterns were submucous myomas ($p < 0.0001$). At this time, sonographic examination either with or without color-flow or power Doppler sonography is not a substitute for pathologic evaluation after surgical removal.

Interrupted Mucosa Sign

The most widely accepted and commonly used sonographic features of a polyp are an echogenic endometrial lesion with a single feeding vessel. Although these findings are extremely helpful, they are not always sonographically evident, and visualization may depend on body habitus or timing of imaging during the phase of menstrual cycle. Kamaya et al. [47] reports that in their

clinical practice, the additional sonographic finding of the interrupted mucosa sign (see Fig. 10.2a) helps in the diagnosis of endometrial polyps. The interrupted mucosa sign is identified when the highly echogenic linear interface where opposing endometrial mucosal surfaces coapt can be followed to a point at which it is focally interrupted (typically by an endometrial polyp). This sign may also be helpful during the latter half of the menstrual cycle, when polyps may be isoechoic to the endometrium and their borders indistinct. A single feeding vessel was visualized in 62.07%, whereas the interrupted mucosa sign was visualized in 58.62% of patients with polyps. The presence of a feeding vessel, the interrupted mucosa sign, or both detected 82.76% of the polyps. In the multivariate analysis, only the interrupted mucosa sign was a statistically significant predictor of pathologic diagnosis of a polyp ($p = 0.035$), with an odds ratio of 3.83 (95% confidence interval, 1.10–13.29). Other sonographic findings were not independent predictors of a polyp: mass ($p = 0.35$), single feeding vessel ($p = 0.31$), endometrial thickness ($p = 0.88$), and endometrial echogenicity ($p = 0.45$). The sensitivity, specificity, and positive predictive value of the interrupted mucosa sign were 59%, 75%, and 85%, respectively. The interrupted mucosa sign is a promising sonographic sign for identification of endometrial polyps, with greater predictive power than previously described signs.

Sonoelastography (SE)

Ultrasound elastography or sonoelastography (SE) has been recently developed to display similar information on tissue stiffness as an image [48]. It demonstrates the displacement and elasticity of the tissue that has developed secondary to pressure. With this method, it is possible to measure the differences in parenchymal strain and the amount of compression by using the color spectrum (elastographic scoring) technique, as well as obtaining the strain rates as numerical values by the help of the technical properties of the device. With an increasing number of studies, it has been used to detect lesions that are overlooked due to similar echogenicity in B-mode imaging and to differentiate benign and malignant masses in superficial tissues. Czuczwar et al. [49] designed a study to assess whether SE may be used to visualize the different stiffness of endometrial polyps and submucosal fibroids. Due to their histologic structure, authors assumed that on strain elastography, endometrial polyps should appear as soft lesions, whereas submucosal fibroids should appear as hard lesions. The diagnostic accuracy rates for B-mode sonography, power Doppler imaging, and SE in distinguishing endometrial polyps and submucosal fibroids were 70.2%, 65.9%, and 89.4%, respectively. The proportion of correct findings was significantly higher for strain elastography than for B-mode sonography ($p = 0.0265$) and power Doppler imaging ($p = 0.0153$). They concluded that SE complements sonography in differentiating intrauterine lesions and it may be used to visualize the different stiffness of endometrial polyps and submucosal fibroids.

Combination of Radiographic Indices

Fang et al. [50] evaluated the usefulness of combined radiographic indices for diagnosis of endometrial polyps and concluded that a combination of endometrial echogenicity, thickness, and volume on sonography may be better than a single indicator for predicting endometrial polyps in infertility. However, the endometrial or subendometrial vascularization index, flow index, and vascularization flow index were not useful for prediction. Bhaduri et al. [51] studied the likelihood ratio (LR) of SHG findings for discriminating endometrial polyps from submucosal fibroids. The LR of 13.4 was achieved for polyps when there was a combination of an intact endometrial-myometrial interface, a single vessel, an acute angle, and homogeneous echogenicity. The highest LR of 27.8 was achieved for submucosal fibroids when the combination of sonographic features included an absent endometrial-myometrial interface, an arborized/multiple vascular pattern, an obtuse angle, and heterogeneous echogenicity. A combination of sonographic findings may provide high LRs for discriminating endometrial polyps from submucosal fibroids.

Sonohysterography

Indications for SHG (also called saline infusion sonography (SIS) or hydrosonogram) include, but are not limited to, evaluation of abnormal uterine bleeding; uterine cavity especially with regard to uterine myomas, polyps, and synechiae; and abnormalities detected on endovaginal sonography, including focal or diffuse endometrial or intracavitary abnormalities [52]. This technique which involves injection of sterile saline into the endometrial cavity followed by a TVUS increases sonographic contrast of the endometrial cavity, enabling delineation of the size, number, and location of polyps that could have been missed on grayscale TVUS, and is likely to improve diagnostic accuracy [53, 54]. With SIS, polyps appear as echogenic, smooth, intracavitary masses with either broad bases or thin stalks outlined by fluid [55]. Differentiating endometrial polyps from submucosal fibroids can be difficult (see Fig. 10.10), but examination of lesion echotexture and identification of overlying echogenic endometrium are useful features to distinguish the two [56]. Jokubkiene et al. [57] studied the appearance of the endometrium at SHG in the luteal phase of the menstrual cycle and concluded that one should avoid performing SHG in the luteal phase, not only because there may be a fertilized ovum in the genital tract but also because endometrial folds are common in this phase and may lead to over diagnosis of focal endometrial pathology, such as polyps. Advantages of SIS include assessment of both the uterine cavity and other uterine and pelvic structures [58] and the potential to assess tubal patency in patients with infertility. Disadvantages of SIS include an inability to determine final endometrial disease, a slower learning curve compared with non-contrast TVUS [59], and patient discomfort caused by fluid leakage or pain during examination [60]. Several studies report SHG to be significantly more accurate than TVUS alone in making a diagnosis of intracavitary leiomyomas or polyps [61, 62], with a higher sensitivity (93% versus 65%) and specificity (94% versus 76%) than TVUS. Only SHG can distinguish between focal and uniform thickening of the endometrium and structural abnormalities.

Some studies comparing the accuracy of several diagnostic modalities show SHG to be as effective as hysteroscopy in detecting structural versus histopathologic abnormalities [63, 64]. When compared with hysteroscopy with guided biopsy, SIS has a sensitivity of 58–100%, specificity of 35–100%, PPV of 70–100%, and NPV of 83–100% [17]. A number of level II studies report no significant difference between SIS and diagnostic hysteroscopy in diagnosing endometrial polyps [64, 65]. Interestingly, the risk of malignancy was increased sevenfold (odds ratio, 7.3; 95% confidence interval, 1.9–27.8) in women with distension difficulties at saline contrast SHG, and two-thirds of the women with a poorly distensible uterine cavity had a malignant diagnosis. To the contrary, a systematic accuracy review using hysteroscopy with or without biopsy or hysterectomy as reference standards found that the accuracy of SIS in the diagnosis of endometrial polyps was lower than that for diagnosis of other uterine cavity abnormalities such as submucous fibroids. The pooled sensitivity was 0.86 (95% CI 0.81–0.91), the pooled specificity was 0.81 (95% CI 0.72–0.88), and the likelihood ratios (LRs) were 5.23 (95% CI 3.98–6.90) and 0.12 (95% CI 0.08–0.17), respectively, consistent with a moderately accurate test for detecting and excluding polyps [66].

A meta-analysis conducted by Nieuwenhuis et al. [67] to compare 3D SHG to 2D SHG for the diagnosis of focal intracavitary lesions found no statistically significant differences between these modalities. Inoue et al. [68] compared 3D SHG to preoperative MRI for the detection of endometrial polyps and for accurate identification of the site of attachment within the uterine cavity. Endometrial polyps could only be identified in 37.5% of women using MRI but could be identified in all women using 3D SHG. The accuracy rate of the attachment site of endometrial polyps was 87.5% on 3D-SISH and 18.8% (in all patients) or 50.0% (in polyp-detected patients) on MRI, indicating a higher accuracy rate using 3D

SHG. SHG is a reliable, cost-effective, and safe diagnostic tool in the evaluation of the uterine cavity prior to ART [69] showing high agreement with hysteroscopy combined with histopathological examination [70, 71, 72].

Special Groups: Infertility, Concomitant Benign Gynecological Disorders, High Risk for Malignancy Groups

Even though the literature is unclear as to when evaluation with imaging is indicated and how often to reevaluate different populations, there are certain groups that deserve closer monitoring such as infertile women of increasing age, obese or hypertensive patients, women on tamoxifen, and possibly some with other concomitant benign gynecological conditions such as fibroids, cervical polyps, and endometriosis.

Impact of Polyps on Infertility

Endometrial polyps are frequently seen in subfertile women (Fig. 10.11), and there is some evidence suggesting a detrimental effect on fertility due to mechanical interference with sperm and embryo transport, embryo implantation, or through intrauterine inflammation or altered production of endometrial receptivity factors. Regardless of the mechanism of endometrial disturbance, uterine polyps have been associated with decreased pregnancy rates both in natural conceptions [73, 74, 75] and in intrauterine insemination (IUI) cycles [76]. Transvaginal US provides an excellent technique to diagnose the size and the anatomic location of endometrial polyps [77], but, since their recurrence rate after resection in these groups is unknown, it is difficult to design monitoring protocols.

Perez-Medina et al. [76] reported that polyps were detected in 452 of 2800 (16.1%) consecutive patients scheduled for IUI and that, after hysteroscopic polypectomy, both spontaneous pregnancy rates and those associated with ART increased, with a 63% cumulative pregnancy rate compared with 28% in the control group (RR 2.3, 95% CI 1.6–3.2). Increased cumulative pregnancy rates of 76% [78] and of 78% [74] were also reported after hysteroscopic polypectomy in cases of female infertility. Stamatellos et al. [79] reported on 83 subjects with endometrial polyps and no other cause for their infertility subjected to hysteroscopic polypectomy. Spontaneous abortion rate in the first trimester of pregnancy was 6%, and there was no statistical difference between patients with small (≤1 cm) or bigger (>1 cm)/multiple polyps. They concluded that hysteroscopic polypectomy appeared to improve fertility and increase pregnancy rates in previous infertile women with no other reason to explain their infertility, irrespective of the size or number of the polyps.

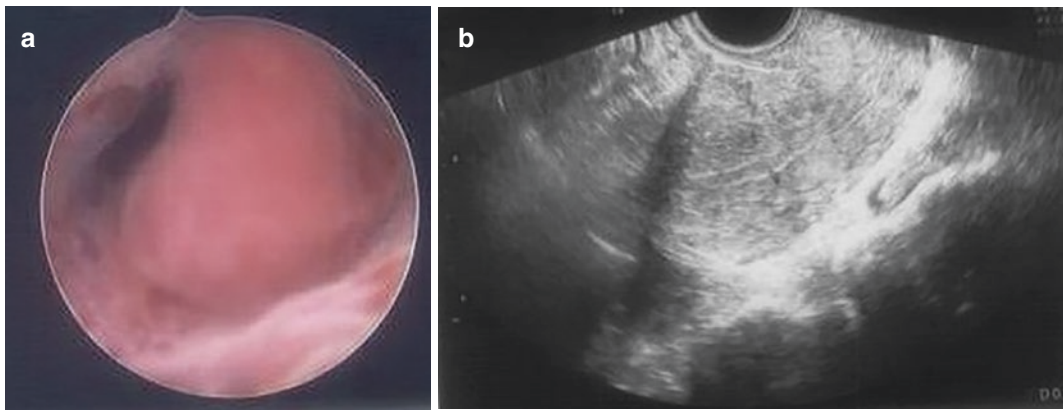

Fig. 10.11 Incidental polyp found during hysteroscopy (**a**) in a patient who failed three cycles of intrauterine insemination for unexplained infertility with normal TV US (**b**)

Polyps located at the fundal and tubocornual regions (see Fig. 10.4), regardless of their size [80, 81, 82], mechanically affect fertility and disturb normal cellular function due to chronic inflammation. Their hysteroscopic resection is advisable with many cases of spontaneous conception [83] and with significantly higher pregnancy rates than that of polyps resected from other locations [80]. These two different mechanisms could explain the differences in conception rates after hysteroscopic removal of polyps in different locations.

The incidental finding of polyps during controlled ovarian hyperstimulation (COH) for IVF poses a very challenging situation, and the diversity of management options can be confusing: cycle cancelation, embryo freezing, ignoring the polyp and continuing treatment, and, lastly, hysteroscopic polypectomy during the IVF cycle before oocyte retrieval without cycle cancelation [84, 85] (Madani et al.) [85]. There is conflict surrounding the size of polyp needed to be removed to achieve an improvement in ART. Some authors [86, 87] reported that removal of polyps <2 cm has no impact on the outcome of fertility treatment, while others [78] suggested that restoration of fertility was not dependent on the size of lesion removed or that there was no significant difference in the reproductive outcome for patients with polyps ≤2.5 or > 2.5 cm. Even though Lass et al. [88] and Check et al. [89] reported no effect of endometrial polyps <2 cm discovered before or during IVF on implantation rates, they also noted an increase, but not statistically significant, in miscarriage rates, making the recommendations for hysteroscopic polypectomy immediately following oocyte retrieval and freezing all embryos for embryo transfer in a subsequent cycle. Bulent Tiras' group [90] presented probably the largest retrospective study on the impact of endometrial polyps on pregnancy rates in 8359 ICSI patients between 2005 and 2009. Localization of the polyp (upper, middle, or lower third of the uterine cavity) or polyp size (4–14 mm) did not seem to affect pregnancy rates, miscarriage rates, and live birth rates in ICSI cycles and that patients with an endometrial polyp detected before ICSI treatment and resected by hysteroscopy had similar pregnancy rates compared with patients with no endometrial polyps. These incidental polyps have a twofold increased odds of biochemical pregnancy (18.3% vs 0.6%, p = 0.01, OR 2.12; 95% CI 1.09–4.12) compared with the non-polyp group [91]. To address this, some authors have proposed performing an US-guided endometrial polypectomy on the oocyte retrieval day or the first day of ovarian stimulation in IVF cycles in patients with a large (≥10 mm) polyp [92] as more patient-friendly option for patients with a large endometrial polyp undergoing IVF. In conclusion, further studies are required to identify the most appropriate management of endometrial polyps found during IVF stimulation.

Intrauterine Lesions in Patients with Recurrent Implantation Failure (RIF) and Recurrent Pregnancy Loss (RPL)

Bozdag G [93]. emphasizes that RIF may be due to unrecognized uterine pathology which varies, based on hysteroscopic findings, between 18–50% and 40–43% in patients undergoing IVF with or without RIF, respectively, and that endometrial polyps may be associated with increased miscarriage rate. Doldi et al. [94] found 40% of patients scheduled to undergo IVF, with normal HSG within the previous year and normal US within the previous 2 months, had subtle intracavitary uterine pathologies: endometrial polyps in 65%, endometrial hyperplasia in 17%, endometrial hypotrophia in 13%, and others (endometritis, adhesions in 5%). In a prospective observational study [95], hysteroscopic findings in 55 patients undergoing IVF who repeatedly failed to conceive despite transfer of two good-quality embryos were assessed. All patients had a normal uterine cavity on HSG performed within 1 year. In 45% an abnormality was noted at hysteroscopy: polyps (n = 10), endometritis (n = 7), adhesions (n = 6), and submucous fibroid (n = 2). Significantly higher pregnancy (50% versus 20%) and implantation (19% versus 6%) rates were obtained after hysteroscopic surgical correction of the abnormality.

Several authors have reported on the reproductive benefits of hysteroscopic polypectomy prior to IUI or IVF, since endometrial polyps were present in 8.5% of 200 women with RPL at the time of hysteroscopy [96] and up to 43.3% in patients with normal TV US [97]. Moreover, Mouhayar et al. [98] concluded that office or operative hysteroscopic polypectomy is cost-effective when performed prior to both IUI and IVF over a range of plausible pregnancy rates and procedural costs. In summary, due to the high incidence of pathologic findings in infertile patients and the improvement in pregnancy rates after treatment, it seems prudent to perform a diagnostic hysteroscopy before the first embryo transfer in all patients, thereby reducing the failures and then the cost of IVF.

Polyps and Concomitant Benign Gynecological Conditions

Regardless of the anatomical location, some benign gynecological disorders may lead to implantation failure [99], and their surgical correction may improve pregnancy outcomes [100, 101]. Increased polyp occurrence has been reported in association with endometriosis, chronic endometritis, fibroids, and synechiae (Fig. 10.12). Zheng et al. [102] reported that the risk of polyp is increased in women with endometriosis compared with those without (pooled RR, 2.81; 95% CI, 2.48–3.18) suggesting the importance of performing a hysteroscopy to look for these polyps in patients with endometriosis. Functional polyps and chronic endometritis are among the most common abnormalities seen in the endometrium of patients with implantation failure and RPL. Carvalho et al. [103] evaluated morphological vascular changes in endometrial samples from asymptomatic infertile patients and found signs of endometritis, vascular changes, and polyps in 176 (40.5%), 168 (38.6%), and 102 (23.4%) cases, respectively. Polyps were associated with endometritis in 27.4% cases and with other vascular changes besides the vascular stalk in 13.7%. The authors suggest that these alterations may be etiologically related placing functional polyps among the spectrum of inflammatory endometrial diseases. Kitaya et al. [104] reported that endometrial micropolyps (Fig. 10.13) coexist at a high rate with chronic endometritis. Compared with the non-polypoid endometrium, macropolypoid endometrium contained a lower density of pan-leukocytes, pan-T cells, and NK cells, whereas micropolypoid endometrium had a higher density of pan-leukocytes and B cells, along with a lower density of NK cells. The prevalence of endometrial polyps in hysterectomies for uterine fibroids was found to be 20.1% ($n = 155$) [105]. Age ≥45 years, hypertension, endometrial hyperplasia, cervical polyps, and number of fibroids (≥2) were positively correlated with the coexistence of these two pathologies.

High-Risk Groups: Sonographic Parameters of Malignancy

Infertility specialists are treating an increasing number of women of advanced maternal age, postmenopausal status, and women with cancer or at increased risk for malignancy and should be vigilant on monitoring these high-risk groups. Risk factors for endometrial malignancy include advanced age, menopausal status, size of the lesion, hypertension, obesity, presence of postmenopausal bleeding [33, 106], and tamoxifen use [107]. Kuribayashi et al. [108] reported 0.97% incidence of incidental asymptomatic endometrial cancer and atypical hyperplasia in infertile women ages 19–44 years undergoing hysteroscopy, so they recommended that hysteroscopic polypectomy should be performed when endometrial polyps are detected on investigational screening and surgical specimens should be checked for the presence of malignancy. The prevalence of endometrial polyps in postmenopausal women can be as high as 35%, and it has been steadily increasing with the wide dissemination of ultrasound in the routine gynecological practice [107, 109]. A systematic review of 17 observational studies including over 10,000 women reported that the incidence of malignant or premalignant polyps was significantly higher in postmenopausal compared with premenopausal women (5.4 versus 1.7%; RR 3.86; 95% CI 2.9–5.1) and those with bleeding compared to those without bleeding (4.2% versus 2.2%, RR 2.0; 95% CI 1.2–3.1) [107] and polyp size does not seem to be a reliable parameter for malignancy detection.

The incidence of endometrial cancer is reported to be approximately 2 per 1000 women taking tamoxifen compared with 0.2 per 1000 patient years among control patients taking a pla-

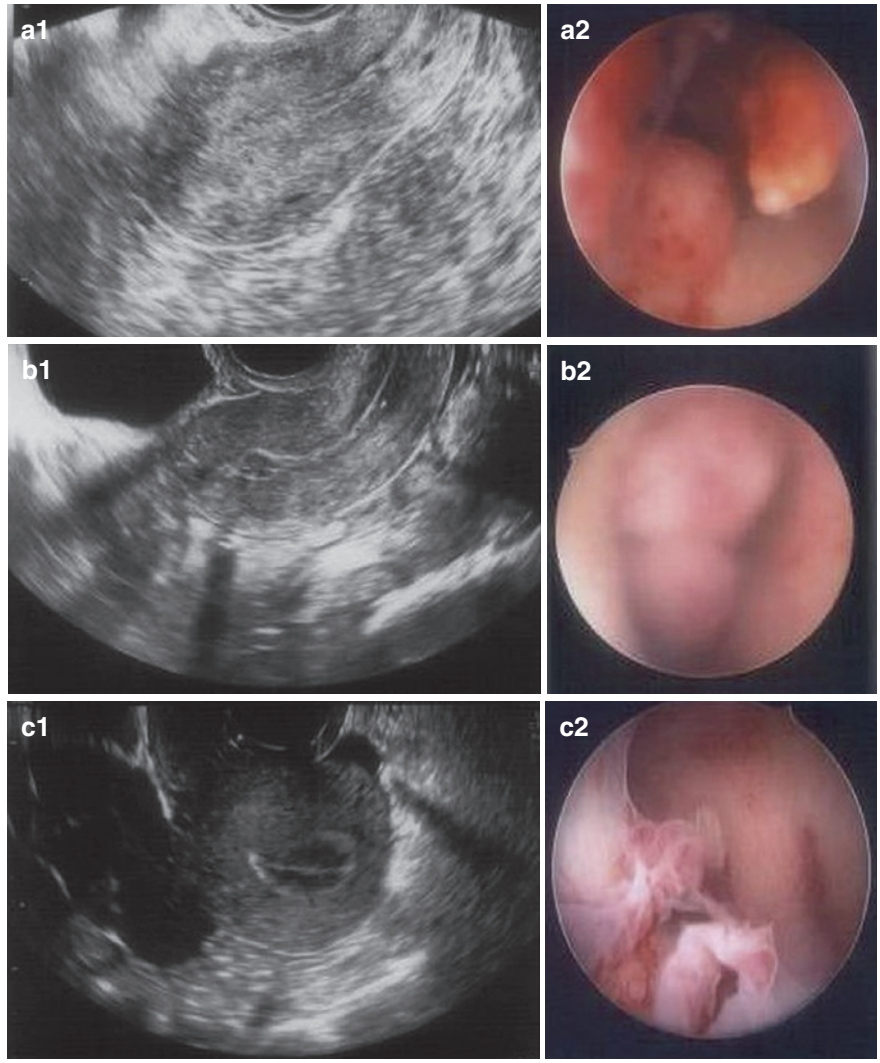

Fig. 10.12 Endometrial polyps coexisting with other benign gynecological diseases such as chronic endometritis (**a**), submucosal fibroids (**b**), and synechiae (**c**). 1. TVUS images; 2. hysteroscopic images

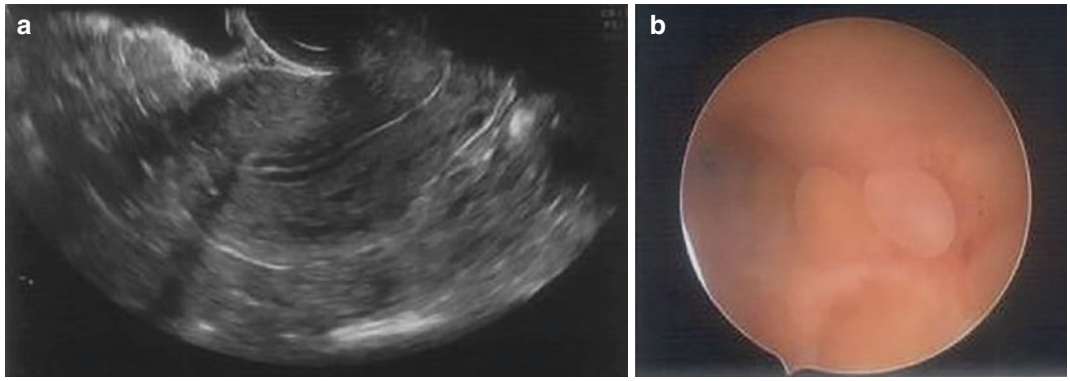

Fig. 10.13 Micropolyps measuring 1–2 mm in diameter could not be seen in 2D US imaging (**a**) but could be detected during hysteroscopy (**b**)

cebo [110]. Premenopausal women treated with tamoxifen have no known increased risk of uterine cancer and require no additional monitoring beyond routine gynecologic care. Routine endometrial surveillance has not proven to be effective in increasing the early detection of endometrial cancer in women using tamoxifen and is not recommended because of the significant false-positive findings due to tamoxifen's endometrial changes such as enlargement of the subendometrial glands, resulting in increased endometrial thickness, irregular echoes, and cystic changes that do not correlate with malignant histology [111]. Asymptomatic women with breast cancer have a high prevalence of baseline subclinical endometrial polyps, and it is very high in obese postmenopausal patients with estrogen receptor-positive breast cancer [112]. Therefore, there may be a future role for baseline pre-tamoxifen screening of some sort for the obese asymptomatic postmenopausal patient, especially if they are elderly and estrogen receptor positive. Another high-risk group is women with hereditary cancer syndromes [113]. Patients with Lynch syndrome accounts for most cases of hereditary uterine cancer with a lifetime risk of 25–60% for developing endometrial cancer. Patients with Cowden syndrome carry a high lifetime risk of breast cancer (25–50%) and endometrial cancer (5–10%). Patients with BRCA mutations also carry other cancer risks (albeit smaller than their risk of breast and ovarian cancer), including prostate cancer, pancreatic cancer, melanoma, and potentially uterine cancer [114].

Determining what US parameters are reassuring or worrisome will assist in identifying patients who will benefit from a follow-up strategy instead of an unnecessary surgical intervention. ACOG Committee Opinion [115] states that when endometrial thickness is <4 mm on TV US in postmenopausal women with bleeding, endometrial sampling is not required unless the uteri could not be easily visualized or there is endometrial heterogeneity (Fig. 10.14) [116]. Even though polyp size >15 mm [117] or ≥19.5 mm [116] seems to have a great

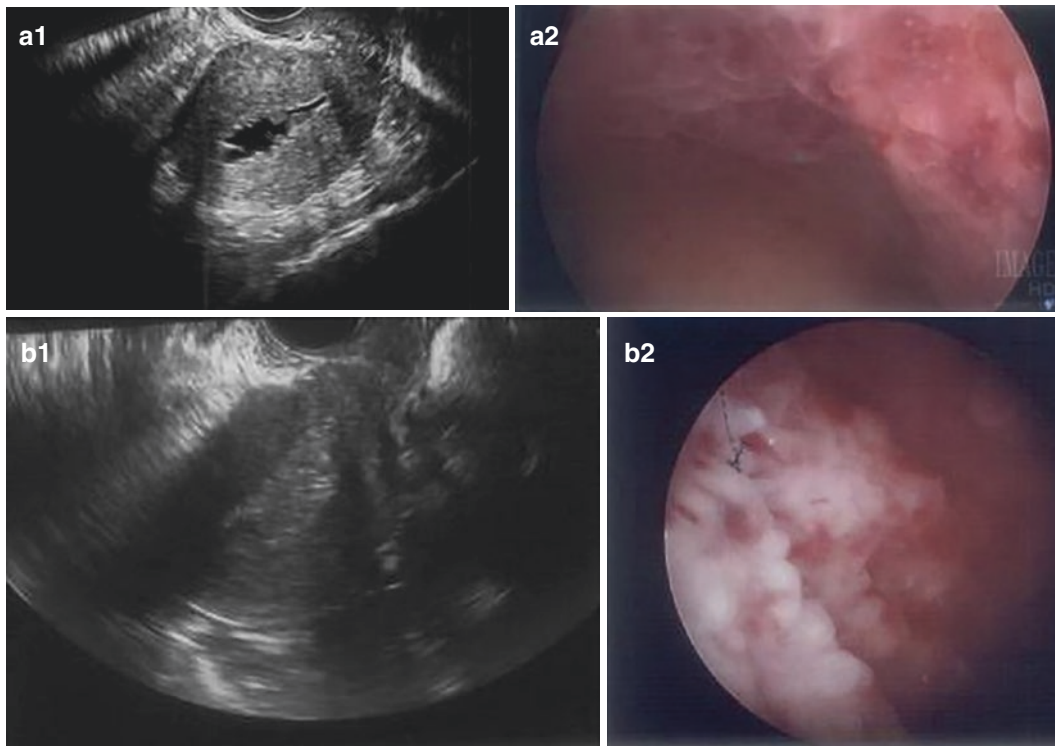

Fig. 10.14 Endometrial irregularities in a premenopausal woman diagnosed with a benign endometrial polyp (**a**) and in a postmenopausal woman (**b**) diagnosed with complex hyperplasia with atypia. 1. 2D TVUS; 2. hysteroscopic views

accuracy for predicting premalignancy and malignancy, histologic evaluation is still necessary. Goldberg et al. [118] studied a combination of 2D sonographic endometrial parameters that are predictors of malignancy. Five sonographic parameters were evaluated: heterogeneous or complex echogenicity of the lesion, presence of a "bright edge sign," regular endometrial-myometrial junction, the presence of a normal endometrium adjacent to the lesion, and detection of small intralesional cysts. The sonographic appearance of numerous small intralesional cysts (cystic formation) was highly related to benign polyp; the presence of a lesion with heterogeneous echogenicity had sensitivity and specificity for malignancy of 63.5 and 88.5%, respectively. They showed that asymptomatic endometrial lesions, which are homogenous, have bright edges, and small intralesional cysts are likely to be benign. By identifying individuals at risk, physicians are able to offer screening and prevention strategies to reduce morbidity and mortality.

Cervical Polyps

Polyps of the lower reproductive tract are found in 7.8–50% of women [83]. Cervical polyps (see Fig. 10.5) found in 2–5% of cases are of low clinical significance and can cause postcoital, intermenstrual, or postmenopausal bleeding, heavy and/or irregular bleeding, or vaginal discharge, as well as difficulty with IUI and embryo transfer. Malignancy or dysplasia can occur in 0.2–1.5% of cases [79, 119–121] and is most common in the perimenopausal age group [122]. Others [123] reported a higher rate of clinically significant histologic findings in cervical polyps (14 of 369 cases, 3.7%) in patients ages 18–87 years (mean 46.5 years), suggesting that removal of all cervical polyps with subsequent histologic review is warranted. In addition, as many as 25% of patients who have a cervical polyp have a coexisting endometrial polyp [79] making hysteroscopy a worthwhile process for their treatment, in contrast to insufficient D&C or blind endometrial biopsies. This information has significant implications as physicians plan appropriate counseling and management for the common diagnosis of cervical polyps.

Wildenberg et al. [124] reported that cervical disease, both benign and malignant, originating in the cervix or in the fundus, may be frequently overlooked or misdiagnosed during US imaging. This group proposed a cervical US scanning protocol that includes both transabdominal and endocervical techniques. In their protocol, grayscale US of the cervix is performed with both long-axis (sagittal) and short-axis (labeled "coronal" endovaginal or "transverse" transabdominal) views. They also routinely perform color Doppler US of the cervix to evaluate for abnormal vascularity, which may permit detection of subtle lesions. SIS also can be used to aid in detection and characterization of intracavitary and endocervical lesions [125]. Experimental US techniques for evaluation of the cervix include use of intracervical transducers [126] and elastography [127]. At grayscale US, endocervical polyps typically appear slightly hyperechoic compared with the normal mucosa and may be mobile at dynamic imaging with use of transducer pressure. Color and spectral Doppler US may reveal a vascular stalk arising from the endocervical mucosa and extending into the polyp, confirming the endocervical origin. Endocervical polyps may undergo cystic change and may be confused with nabothian cysts if the vascular pedicle is not visualized. It is important to visualize if the lesion arises from the uterine body and extends into the endocervical canal, particularly a prolapsed intracavitary leiomyoma or endometrial polyp. Visualization of the origin of an endocervical mass can sometimes be aided by hysterosonography [128] or MR imaging [129] if necessary. The most common diagnostic pitfalls encountered include failure to recognize the presence of a cervical lesion, failure to appreciate the malignant potential of a lesion, misinterpretation of a pseudolesion as a pathologic condition, and misidentification of the origin of a lesion [124]. The presence of a large amount of endometrial fluid should raise concern for a mass lesion obstructing the

endocervical canal (see Fig. 10.5) and should prompt more thorough US of the cervix and lower endometrium for malignancy, including use of color Doppler US.

The finding of cervical polyps in pregnancy poses a difficult management dilemma. Symptomatic women may present with vaginal bleeding, postcoital bleeding, vaginal discharge, cervical infection, or even with symptoms mimicking threatened preterm labor. The degree of symptoms is not related to the length or the volume of the polyp. Tokunaka et al. [130] evaluated obstetrical outcomes of women who underwent polypectomy of cervical polyps during pregnancy and delivered singleton infants between 2005 and 2011. The removed polyps were classified into decidual ($n = 41$) polyps and endocervical ($n = 42$) polyps. No malignant polyps were found. The removal of decidual polyps during pregnancy carried a higher risk of spontaneous abortion (12.2% versus 0%, $p = 0.026$) and preterm delivery (34.2% versus 4.8%, $p = 0.001$) than that of endocervical polyps. Authors concluded that it might be safer not to remove cervical polyps during pregnancy, except in cases in which the polyps are suspected to be malignant.

False-Positive, False-Negative, and Artifacts

There is not a single imaging technique that can accurately diagnose all possible intrauterine pathologies. Ultrasonography may not distinguish very small polyps, flat endometrial anomalies (Fig. 10.15), cornual polyps (see Fig. 10.4), or thin bands of synechiae (see Fig. 10.15) even when combined with SIS [131]. To the contrary, there could be transient endometrial changes detected by US as a possible structural defect, such as an intrauterine blood clot (Fig. 10.16a) or presence of mucus especially in hyperestrogenic states such as during COH for IVF (Fig. 10.16b) that may spontaneously resolve. Our group [132] reported up to 20% transient early postoperative intrauterine changes by 3D US in patients undergoing hysteroscopic correction of various uterine anomalies that spontaneously resolve in the second postoperative month and did not interfere with embryo implantation. The transient changes consisted of intrauterine cystic loculations (Fig. 10.16c) and endometrial irregularities/possible mucus accumulations that were sometimes larger and even more complex in appearance than the original lesions

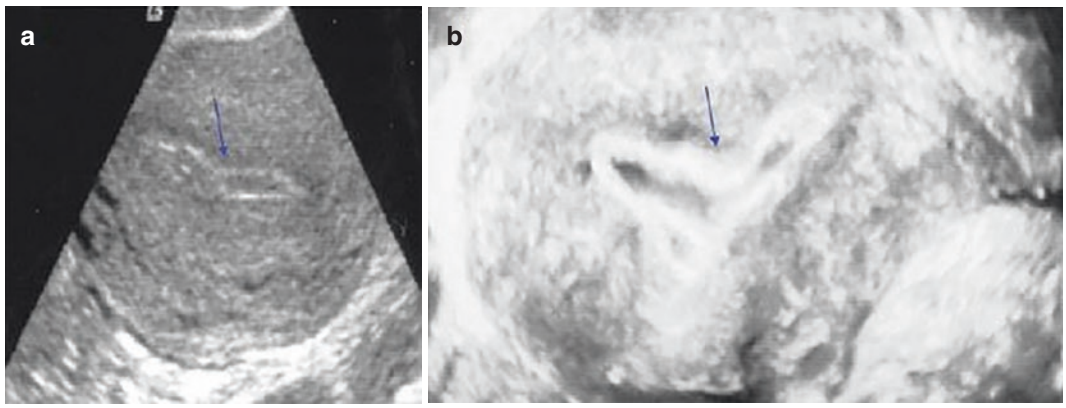

Fig. 10.15 Nonspecific endometrial US findings. An area of endometrial constrictions is shown by 2D US (**a**), 3D SIS (**b**), and HSG (**c**). *Arrows* point to the area of narrowing representing synechiae. A flat endometrial polyp was not observed on 2D TVUS (**d**) but was resected during hysteroscopy (**e**)

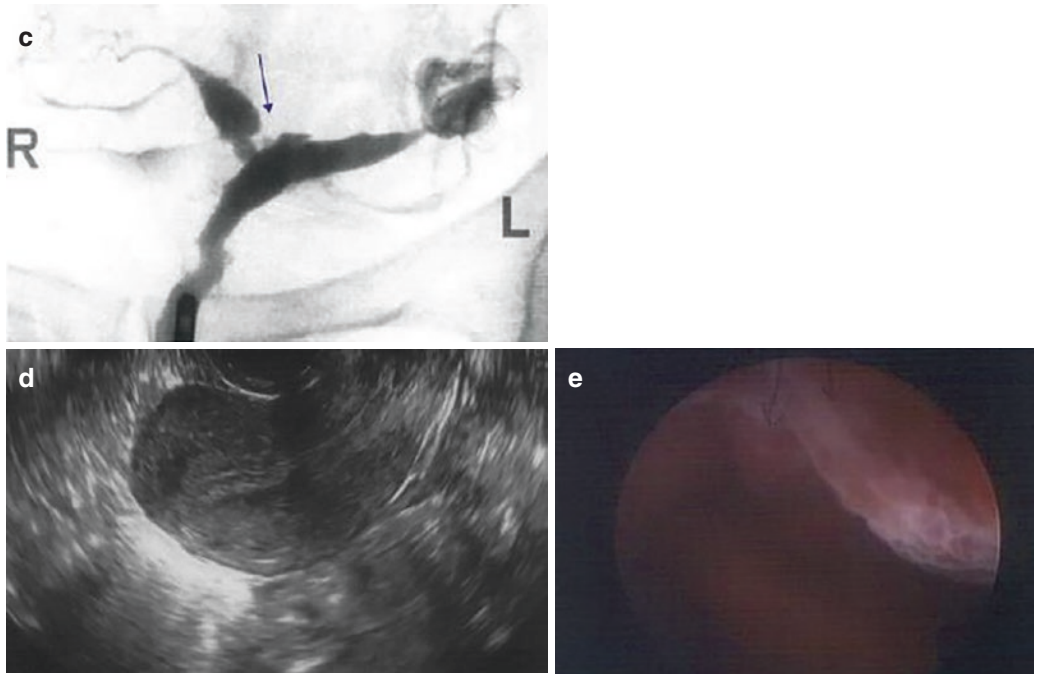

Fig. 10.15 (continued)

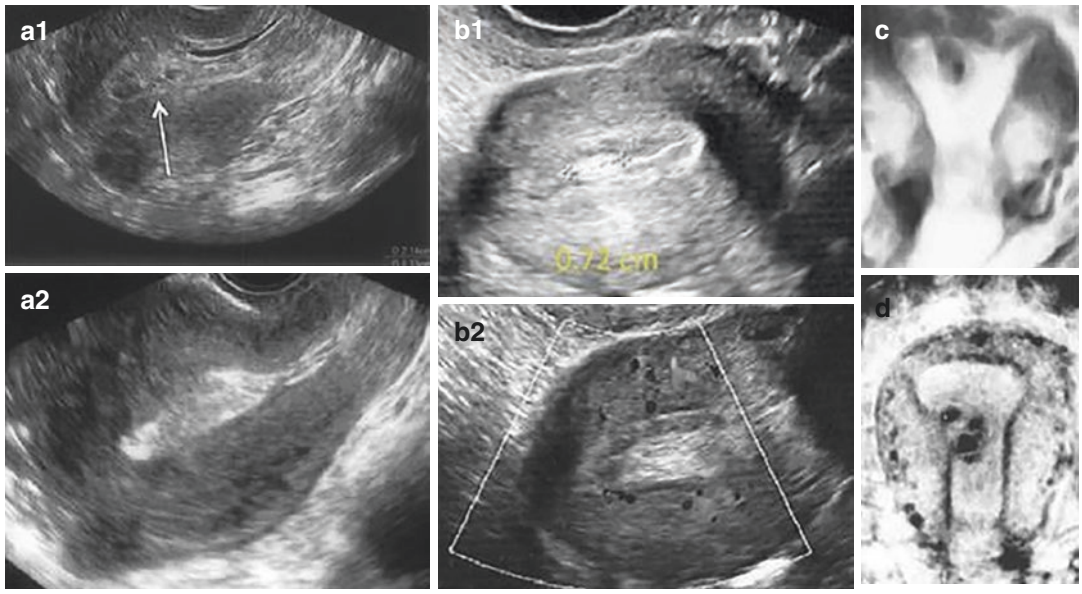

Fig. 10.16 Transient endometrial changes detected as morphological anomalies by US. Endometrial clots and fluid seen on menstrual day 4 (**a1**) that spontaneously disappeared 1 day later (**a2**). Endometrial mucus seen during ovarian stimulation for IVF (**b1**). Notice lack of internal blood flow in the hyperechoic mucus accumulation (**b2**). Monoloculated (**c**) and multiloculated (**d**) cystic lesions observed by 3D US a few weeks after hysteroscopy that spontaneously resolved within 2 months post op

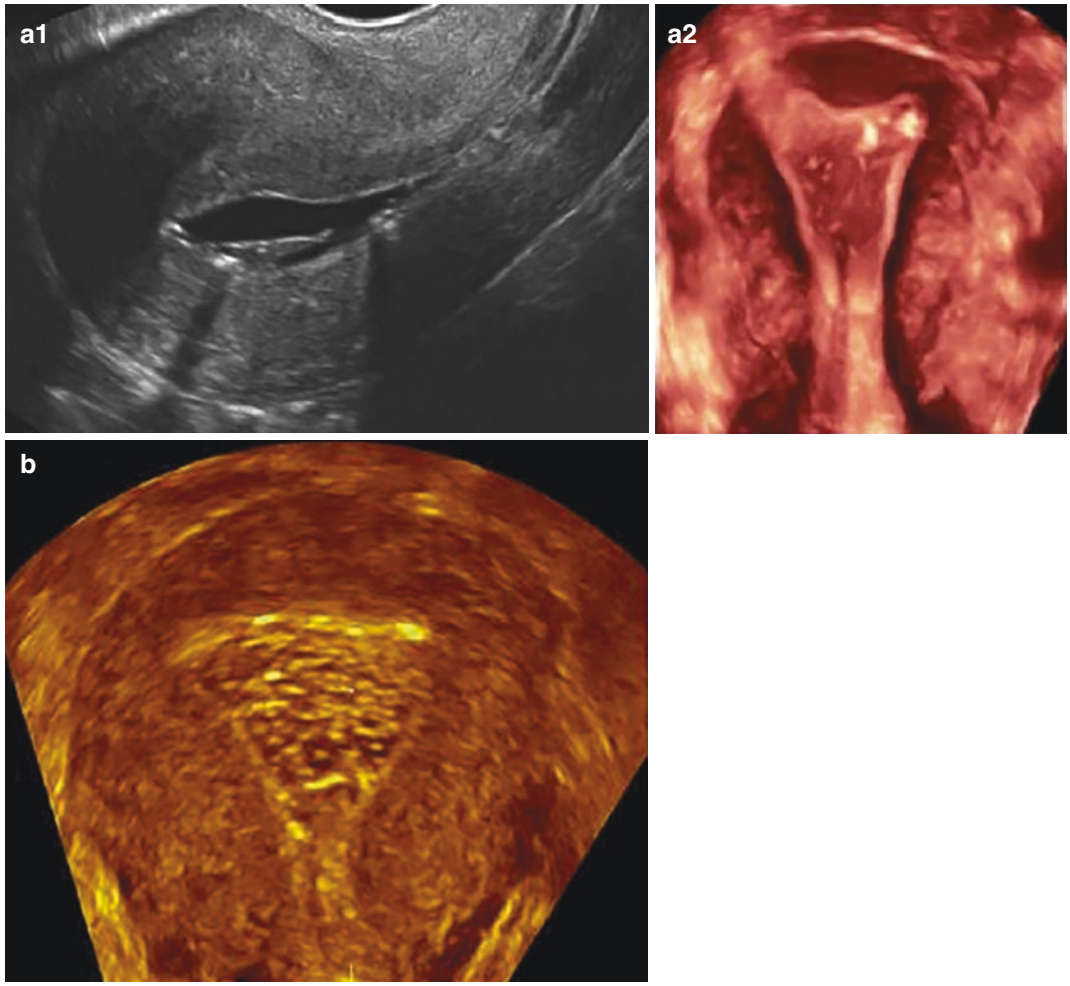

Fig. 10.17 Artifacts created during SIS giving the false impression of intracavitary pathology. Endometrial tunneling created by the catheter used resembling a polyp in a 2D sagittal view (**a1**) and in a 3D coronal view (**a2**). Air bubbles injected during SIS may resemble trophoblastic disease (**b**, 3D coronal view)

and always coincided with the resection site. Grimbizis et al. [133] reported that diagnostic hysteroscopy, on the other hand, can misdiagnose normal endometrium for small endometrial polyps or, to the contrary, can misdiagnosed a case of endometrial cancer as an endometrial polyp. Also, some artifacts can be unintentionally created during SIS that could mimic intrauterine pathology such as catheter tunneling of the endometrium which could be mistaken for a polyp (Fig. 10.17a) or injection of air bubbles which could be mistaken for a trophoblastic disease (Fig. 10.17b).

References

1. Clark TJ, Gupta JK. Handbook of outpatient hysteroscopy: a complete guide to diagnosis and therapy. Boca Raton: CRC Press; 2005.
2. Fatemi HM, Kasius JC, Timmermans A, van Disseldorp J, Fauser BC, Devroey P, et al. Prevalence of unsuspected uterine cavity abnormalities diagnosed by office hysteroscopy prior to in vitro fertilization. Hum Reprod. 2010;25:1959e65.
3. Dreisler E, Stampe Sorensen S, Ibsen PH, Lose G. Prevalence of endometrial polyps and abnormal uterine bleeding in a Danish population aged 20-74 years. Ultrasound Obstet Gynecol. 2009;33(1):102–8.

4. Cohen I. Endometrial pathologies associated with postmenopausal tamoxifen treatment. Gynecol Oncol. 2004;94:256–66.
5. Wong M, Crnobrnja B, Liberale V, Dharmarajah K, Widschwendter M, Jurkovic D. The natural history of endometrial polyps. Hum Reprod. 2017;32(2):340–5. https://doi.org/10.1093/humrep/dew307. Epub 2016 Dec 18.
6. DeWaay DJ, Syrop CH, Nygaard IE, Davis WA, Van Voorhis BJ. Natural history of uterine polyps and leiomyomata. Obstet Gynecol. 2002;100:3–7.
7. Yang JH, Chen CD, Chen SU, Yang YS, Chen MJ. Factors influencing the recurrence potential of benign endometrial polyps after hysteroscopic polypectomy. PLoS One. 2015;10(12):e0144857. https://doi.org/10.1371/journal.pone.0144857. eCollection 2015.
8. Wang N, Zhang Y, Liu B. Demographic and clinical features of endometrial polyps in patients with endometriosis. Biomed Res Int. 2016;2016:1460793. https://doi.org/10.1155/2016/1460793. Epub 2016 May 3.
9. Paradisi R, Rossi S, Scifo MC, Dall'O' F, Battaglia C, Venturoli S. Recurrence of endometrial polyps. Gynecol Obstet Investig. 2014;78(1):26–32. https://doi.org/10.1159/000362646. Epub 2014 May 23.
10. Gao W, Zhang L, Li W, Li J, Wang W, Zhao W, Feng L. Three-year follow-up results of polypectomy with endometrial ablation in the management of endometrial polyps associated with tamoxifen in Chinese women. Eur J Obstet Gynecol Reprod Biol. 2012;161(1):62–5. https://doi.org/10.1016/j.ejogrb.2011.10.014. Epub 2012 Feb 4.
11. Lieng M, Istre O, Qvigstad E. Treatment of endometrial polyps: a systematic review. Acta Obstet Gynecol Scand. 2010;89:992–1002.
12. Antunes A Jr, Costa-Paiva L, Arthuso M, Costa JV, Pinto-Neto AM. Endometrial polyps in pre- and postmenopausal women: factors associated with malignancy. Maturitas. 2007;57:415–21.
13. Ferrazzi E, Zupi E, Leone FP, Savelli L, Omodei U, Moscarini M, et al. How often are endometrial polyps malignant in asymptomatic postmenopausal women? A multicenter study. Am J Obstet Gynecol. 2009;200:235.e1–6.
14. Wang JH, Zhao J, Lin J. Opportunities and risk factors for premalignant and malignant transformation of endometrial polyps: management strategies. J Minim Invasive Gynecol. 2010;17:53–8.
15. Orvieto R, Bar-Hava I, Dicker D, Bar J, Ben-Rafael Z, Neri A. Endometrial polyps during menopause: characterization and significance. Acta Obstet Gynecol Scand. 1999;78:883–6.
16. Committee on Practice Bulletins—Gynecology. ACOG practice bulletin no. 128: diagnosis of abnormal uterine bleeding in reproductive-aged women. Obstet Gynecol. 2012;120(1):197–206. https://doi.org/10.1097/AOG.0b013e318262e320.
17. American Association of Gynecologic Laparoscopists practice report. Practice guidelines for the diagnosis and management of endometrial polyps. J Minim Invasive Gynecol. 2012;19(1):3–10. https://doi.org/10.1016/j.jmig.2011.09.003.
18. Clark TJ, Stevenson H. Endometrial Polyps and Abnormal Uterine Bleeding (AUB-P): what is the relationship, how are they diagnosed and how are they treated? Best Pract Res Clin Obstet Gynaecol. 2017;40:89–104. https://doi.org/10.1016/j.bpobgyn.2016.09.005. Epub 2016 Oct 1.
19. Goldstein SR, Zeltser I, Horan CK, Snyder JR, Schwartz LB. Ultrasonography-based triage for perimenopausal patients with abnormal uterine bleeding. Am J Obstet Gynecol. 1997;177:102–8.
20. Goldstein SR, Monteagudo A, Popiolek D, Mayberry P, Timor-Tritsch I. Evaluation of endometrial polyps. Am J Obstet Gynecol. 2002;186:669–74.
21. Nalaboff KM, Pellerito JS, Ben-Levi E. Imaging the endometrium: disease and normal variants. Radiographics. 2001;17:145–9.
22. Salim S, Won H, Nesbitt-Hawes E, Campbell N, Abbott J. Diagnosis and management of endometrial polyps: a critical review of the literature. J Minim Invasive Gynecol. 2011;18(5):569–81.
23. Oldani S, Moschetta M, De Giorgi O, et al. The role of transvaginal ultrasonography and outpatient diagnostic hysteroscopy in the evaluation of patients with menorrhagia. Hum Reprod. 1997;12:1768–71.
24. Ragni G, Diaferia D, Vegetti W, Colombo M, Arnoldi M, Crosignani PG. Effectiveness of sonohysterography in infertile patient work-up: a comparison with transvaginal ultrasonography and hysteroscopy. Gynecol Obstet Investig. 2005;59:184–8.
25. Valenzano MM, Lijoi D, Mistrangelo E, Fortunato T, Costantini S, Ragni N. The value of sonohysterography in detecting intracavitary benign abnormalities. Arch Gynecol Obstet. 2005;272:265–8.
26. Vercellini P, Cortesi I, Oldani S, Moschetta M, De Giorgi O, Crosignani PG. The role of transvaginal ultrasonography and outpatient diagnostic hysteroscopy in the evaluation of patients with menorrhagia. Hum Reprod. 1997;12:1768–71.
27. Abuhamad AZ, Singleton S, Zhao Y, Bocca S. The Z technique: an easy approach to the display of the mid-coronal plane of the uterus in volume sonography. J Ultrasound Med. 2006;25(5):607–12.
28. Bocca SM, Oehninger S, Stadtmauer L, Agard J, Duran EH, Sarhan A, et al. A study of the cost, accuracy, and benefits of 3-dimensional sonography compared with hysterosalpingography in women with uterine abnormalities. J Ultrasound Med. 2012;31(1):81–5.
29. Kupesic S, Kurjak A, Skenderovic S, Bjelos D. Screening for uterine abnormalities by three-dimensional ultrasound improves perinatal outcome. J Perinat Med. 2002;30:9–17.
30. La Torre R, De Felice C, De Angelis C, Coacci F, Mastrone M, Cosmi EV. Transvaginal sonographic

evaluation of endometrial polyps: a comparison with two dimensional and three dimensional contrast sonography. Clin Exp Obstet Gynecol. 1999;26:171–3.
31. Makris N, Skartados N, Kalmanatis K, Mantzaris G, Papadimitriou A, Antsaklis AN. Evaluation of abnormal uterine bleeding by transvaginal 3-D hysterosonography and diagnostic hysteroscopy. Eur J Gynaecol Oncol. 2007;28:39–42.
32. Bernard JP, Rizk E, Camatte S, Robin F, Taurelle R, Lecuru F. Saline contrast sonohysterography in the preoperative assessment of benign intrauterine disorders. Ultrasound Obstet Gynecol. 2001;17:145–9.
33. Ben-Arie A, Goldchmit C, Laviv Y, Levy R, Caspi B, Huszar M, et al. The malignant potential of endometrial polyps. Eur J Obstet Gynecol Reprod Biol. 2004;115:206–10.
34. Dijkhuizen FP, Brolmann HA, Potters AE, Bongers MY, Heinz AP. The accuracy of transvaginal ultrasonography in the diagnosis of endometrial abnormalities. Obstet Gynecol. 1996;87:345–9.
35. Breitkopf DM, Fredrickson RA, Snyder RR. Detection of benign endometrial masses by endometrial stripe measurement in premenopausal women. Obstet Gynecol. 2004;104:120–5.
36. Griffin Y, Sudigali V, Jacques A. Radiology of benign disorders of menstruation. Semin Ultrasound CT MR. 2010;31(5):414–32.
37. Song Y, Shen LC, Huang W, Lei HK, Wang QS, Zhu HL. Diagnostic value of endometrial thickness determined by transvaginal sonography in infertile women with endometrial polyps. Chin Med J. 2012;125(13):2279–83.
38. Cavkaytar S, Kokanali MK, Ceran U, Topcu HO, Sirvan L, Doganay M. Roles of sonography and hysteroscopy in the detection of premalignant and malignant polyps in women presenting with postmenopausal bleeding and thickened endometrium. Asian Pac J Cancer Prev. 2014;15(13):5355–8.
39. Jakab A, Ovári L, Juhász B, Birinyi L, Bacskó G, Tóth Z. Detection of feeding artery improves the ultrasound diagnosis of endometrial polyps in asymptomatic patients. Eur J Obstet Gynecol Reprod Biol. 2005;119:103–7.
40. Timmerman D, Verguts J, Konstantinovic ML, Moerman P, Van Schoubroeck D, Deprest J, et al. The pedicle artery sign based on sonography with color Doppler imaging can replace second-stage tests in women with abnormal vaginal bleeding. Ultrasound Obstet Gynecol. 2003;22:166–71.
41. Alcazar JL, Castillo G, Mínguez JA, Galán MJ. Endometrial blood flow mapping using transvaginal power Doppler sonography in women with postmenopausal bleeding and thickened endometrium. Ultrasound Obstet Gynecol. 2003;21:583–8.
42. Vuento MH, Pirhonen JP, Mäkinen JI, Tyrkkö JE, Laippala PJ, Grönroos M, et al. Screening for endometrial cancer in asymptomatic postmenopausal women with conventional and colour Doppler sonography. Br J Obstet Gynaecol. 1999;106:14–20.
43. de Kroon C, Hiemstra E, Trimbos JB, Jansen FW. Power Doppler area in the diagnosis of endometrial cancer. Int J Gynecol Cancer. 2010;20:1160–5.
44. Cogendez E, Eken MK, Bakal N, Gun I, Kaygusuz EI, Karateke A. The role of transvaginal power Doppler ultrasound in the differential diagnosis of benign intrauterine focal lesions. J Med Ultrason (2001). 2015;42(4):533–40. https://doi.org/10.1007/s10396-015-0628-2. Epub 2015 Apr 8.
45. Anioł M, Dec G, Wojda K, Sieroszewski P. Usefulness of saline infusion sonohysterography and feeding artery imaging in endometrial polyp diagnosis. Ginekol Pol. 2017;88(6):285–8. https://doi.org/10.5603/GP.a2017.0054.
46. Ogutcuoglu B, Karadag C, Inan C, Dolgun ZN, Yoldemir AT, Aslanova L. Diagnostic utility of saline infusion doppler sonohysterography in endometrial mass lesions. Pak J Med Sci. 2016;32(2):284–8. https://doi.org/10.12669/pjms.322.9452.
47. Kamaya A, Yu PC, Lloyd CR, Chen BH, Desser TS, Maturen KE. Sonographic evaluation for endometrial polyps: the interrupted mucosa sign. J Ultrasound Med. 2016;35(11):2381–7. Epub 2016 Sep 14.
48. Dietrich CF, Barr RG, Farrokh A, Dighe M, Hocke M, Jenssen C, Dong Y, et al. Strain elastography - how to do it? Ultrasound Int Open. 2017;3(4):E137–49. . Published online 2017 Dec 7. https://doi.org/10.1055/s-0043-119412.
49. Czuczwar P, Wozniak S, Szkodziak P, Kudla MJ, Pyra K, Paszkowski T. Elastography improves the diagnostic accuracy of sonography in differentiating endometrial polyps and submucosal fibroids. J Ultrasound Med. 2016;35(11):2389–95. Epub 2016 Sep 14.
50. Fang L, Su Y, Guo Y, Sun Y. Value of 3-dimensional and power Doppler sonography for diagnosis of endometrial polyps. J Ultrasound Med. 2013;32(2):247–55.
51. Bhaduri M, Tomlinson G, Glanc P. Likelihood ratio of sonohysterographic findings for discriminating endometrial polyps from submucosal fibroids. J Ultrasound Med. 2014;33(1):149–54. https://doi.org/10.7863/ultra.33.1.149.
52. AIUM. Practice guideline for the performance of sonohysterography. J Ultrasound Med. 2015;34(8):1–6. https://doi.org/10.7863/ultra.34.8.15.13.0005.
53. Jansen FW, de Kroon CD, van Dongen H, Grooters C, Louwe L, Trimbos-Kemper T. Diagnostic hysteroscopy and saline infusion sonography: prediction of intrauterine polyps and myomas. J Minim Invasive Gynecol. 2006;13:320–4.
54. Schwarzler P, Concin H, Bosch H, Berlinger A, Wohlgenannt K, Collins WP, et al. An evaluation of sono-hysterography and diagnostic hysteroscopy for the assessment of intrauterine pathology. Ultrasound Obstet Gynecol. 1998;11:337–42.

55. Schorge J, Schaffer J, Halvorson L, Hoffman B, Bradshaw K, Cunningham F. Abnormal uterine bleeding. In: Schorge JO, Schaffer JI, Halvorson LM, Hoffman BL, Bradshaw KD, Cunningham FG, editors. Williams gynecology. New York: McGraw-Hill Professional; 2008. p. 174–96.
56. Richenberg J. Ultrasound of the uterus. In: Callen O, editor. Ultrasonography in obstetrics and gynecology. Philadelphia: WB Saunders; 2000. p. 837.
57. Jokubkiene L, Sladkevicius P, Valentin L. Appearance of the endometrium at saline contrast sonohysterography in the luteal phase of the menstrual cycle: a prospective observational study. Ultrasound Obstet Gynecol. 2015;45(3):339–45. https://doi.org/10.1002/uog.13458. Epub 2015 Jan 28.
58. Widrich T, Bradley LD, Mitchinson AR, Collins RL. Comparison of saline infusion sonography with office hysteroscopy for the evaluation of the endometrium. Am J Obstet Gynecol. 1996;174:1327–34.
59. Syrop CH, Sahakian V. Transvaginal sonographic detection of endometrial polyps with fluid contrast augmentation. Obstet Gynecol. 1992;79:1041–3.
60. Exalto N, Stappers C, van Raamsdonk LAM, Emanuel MH. Gel instillation sonohysterography: first experience with a new technique. Fertil Steril. 2007;87:152–5.
61. Bingol B, Gunenc Z, Gedikbasi A, Guner H, Tasdemir S, TIras B. Comparison of diagnostic accuracy of saline infusion sonohysterography, transvaginal sonography and hysteroscopy. J Obstet Gynaecol. 2011;31(1):54–8.
62. Kamel HS, Darwish AM, Mohamed SA. Comparison of transvaginal ultrasonography and vaginal sonohysterography in the detection of endometrial polyps. Acta Obstet Gynecol Scand. 2000;79:60–4.
63. Kelekci S, Kaya E, Alan M, Alan Y, Bilge U, Mollamahmutoglu L. Comparison of transvaginal sonography, saline infusion sonography, and office hysteroscopy in reproductive-aged women with or without abnormal uterine bleeding. Fertil Steril. 2005;84:682–6.
64. Epstein E, Ramirez A, Skoog L, Valentin L. Transvaginal sonography, saline contrast sonohysterography and hysteroscopy for the investigation of women with postmenopausal bleeding and endometrium > 5 mm. Ultrasound Obstet Gynecol. 2001;18(2):157–62.
65. Schwärzler P, Concin H, Bösch H, Berlinger A, Wohlgenannt K, Collins WP, et al. An evaluation of sonohysterography and diagnostic hysteroscopy for the assessment of intrauterine pathology. Ultrasound Obstet Gynecol. 1998;11:337–42.
66. De Kroon CD, de Bock GH, Dieben SW, Jansen FW. Saline contrast hysterosonography in abnormal uterine bleeding: a systematic review and meta-analysis. BJOG. 2003;110:938–47.
67. Nieuwenhuis LL, Hermans FJ, de Vaate AJM B, Leeflang MM, Brölmann HA, Hehenkamp WJ, et al. Three-dimensional saline infusion sonography compared to two-dimensional saline infusion sonography for the diagnosis of focal intracavitary lesions. Cochrane Database Syst Rev. 2017;5:CD011126. https://doi.org/10.1002/14651858.CD011126.pub2.
68. Inoue T, Kitajima M, Taniguchi K, Masuzaki H. Three-dimensional saline-infusion sonohysterography is useful for the identification of endometrial polyp. J Obstet Gynaecol Res. 2016;42(7):855–9. https://doi.org/10.1111/jog.12994. Epub 2016 Apr 14.
69. Obajimi G, Ogunkinle B. Routine saline infusion sonohysterography prior to asissted conception: a review of our initial experience. Ann Ib Postgrad Med. 2016;14(2):99–102.
70. Lopes VM, Barguil JP, Lacerda TS, Souza ALM, Rocha Filho AMD, Roller MF, et al. An overview of the results of hysterosonography prior to in vitro fertilization. JBRA Assist Reprod. 2017;21(4):302–5. https://doi.org/10.5935/1518-0557.20170051.
71. Radwan P, Radwan M, Kozarzewski M, Polac I, Wilczyński J. Evaluation of sonohysterography in detecting endometrial polyps - 241 cases followed with office hysteroscopies combined with histopathological examination. Wideochir Inne Tech Maloinwazyjne. 2014;9(3):344–50. https://doi.org/10.5114/wiitm.2014.43024. Epub 2014 May 26.
72. Ahmadi F, Rashidy Z, Haghighi H, Akhoond M, Niknejadi M, Hemat M, et al. Uterine cavity assessment in infertile women: sensitivity and specificity of three-dimensional hysterosonography versus hysteroscopy. Iran J Reprod Med. 2013;11(12):977–82.
73. Valle RF. Therapeutic hysteroscopy in infertility. Int J Fertil. 1984;29:143–8.
74. Varasteh NN, Neuwirth RS, Levin B, Keltz MD. Pregnancy rates after hysteroscopic polypectomy and myomectomy in infertile women. Obstet Gynecol. 1999;94:168–71.
75. Wang Y, Han M, Li C, Sun A, Guo X, Zhang Y. The value of hysteroscopy in the diagnosis of infertility and habitual abortion. Chin Med Sci J. 1992;7:226–9.
76. Perez-Medina T, Bajo-Arenas J, Salazar F, Redondo T, Sanfrutos L, Alvarez P, et al. Endometrial polyps and their implication in the pregnancy rates of patients undergoing intrauterine insemination: a prospective, randomized study. Hum Reprod. 2005;20:1632–5.
77. Zhu Y, Du M, Yi L, Liu Z, Gong G, Tang X. CD4+ T cell imbalance is associated with recurrent endometrial polyps. Clin Exp Pharmacol Physiol. 2018. https://doi.org/10.1111/1440-1681.12913. [Epub ahead of print].
78. Spiewankiewicz B, Stelmachow J, Sawicki W, Cendrowski K, Wypych P, Swiderska K. The effectiveness of hysteroscopic polypectomy in cases of female infertility. Clin Exp Obstet Gynecol. 2003;30:23–5.
79. Stamatellos I, Stamatopoulos P, Bontis J. The role of hysteroscopy in the current management

of the cervical polyps. Arch Gynecol Obstet. 2007;276(4):299–303.
80. Yanaihara A, Yorimitsu T, Motoyama H, Watanabe H, Kawamura T. Location of endometrial polyp and pregnancy rate in infertility patients. Fertil Steril. 2008;90:180–2.
81. Shokeir TA, Shalan HM, El-Shafei MM. Significance of endometrial polyps detected hysteroscopically in eumenorrheic infertile women. J Obstet Gynaecol Res. 2004;30:84–9.
82. Lee A, Ying YK, Novy MJ. Hysteroscopy, hysterosalpingography and tubal ostial polyps in infertility patients. J Reprod Med Obstet Gynecol. 1997;42:337–41.
83. Tanos V, Berry KE, Seikkula J, Abi Raad E, Stavroulis A, Sleiman Z, et al. The management of polyps in female reproductive organs. Int J Surg. 2017;43:7–16. https://doi.org/10.1016/j.ijsu.2017.05.012. Epub 2017 May 5.
84. Batioglu S, Kaymak O. Does hysteroscopic polypectomy without cycle cancellation affect IVF? Reprod Biomed Online. 2005;10:767–9.
85. Madani T, Ghaffari F, Kiani K, Hosseini F. Hysteroscopic polypectomy without cycle cancellation in IVF cycles. Reprod Biomed Online. 2009;18:412–5.
86. Hereter L, Carreras O, Pasciial M. Repercusion de la presencia de polipos endometriales en un ciclo de FIV [Spanish]. Prog Obstet Ginecol. 1998;41:5–7.
87. Isikoglu M, Berkkanoglu M, Senturk Z, Coetzee K, Ozgur K. Endometrial polyps smaller than 1.5 cm do not affect ICSI outcome. Reprod Biomed Online. 2006;12:199–204.
88. Lass A, Williams G, Abusheikha N, Brinsden P. The effect of endometrial polyps on outcomes of in vitro fertilization (IVF) cycles. J Assist Reprod Genet. 1999;16:410–5.
89. Check JH, Bostick-Smith CA, Choe JK, Amui J, Brasile D. Matched controlled study to evaluate the effect of endometrial polyps on pregnancy and implantation rates following in vitro fertilization-embryo transfer (IVF-ET). Clin Exp Obstet Gynecol. 2011;38:206–8.
90. Tiras B, Korucuoglu U, Polat M, Zeyneloglu H, Saltik A, Yarali H. Management of endometrial polyps diagnosed before or during ICSI cycles. Reprod Biomed Online. 2012;24:123–8.
91. Elias RT, Pereira N, Karipcin FS, Rosenwaks Z, Spandorfer SD. Impact of newly diagnosed endometrial polyps during controlled ovarian hyperstimulation on in vitro fertilization outcomes. J Minim Invasive Gynecol. 2015;22(4):590–4. https://doi.org/10.1016/j.jmig.2014.12.170. Epub 2015 Jan 8.
92. Moon JW, Kim CH, Park SY, Kim SH, Chae HD, Kang BM. Comparison of ultrasound-guided endometrial polypectomy carried out on the oocyte retrieval day and the first day of ovarian stimulation in IVF-ICSI cycles. Reprod Biomed Online. 2016;33(3):376–80. https://doi.org/10.1016/j.rbmo.2016.06.008. Epub 2016 Jun 27.
93. Bozdag G. What is the role of office hysteroscopy in women with failed IVF cycles? Reprod Biomed Online. 2008;17:410–5.
94. Doldi N, Persico P, Di Sebastiano F, Marsiglio E, De Santis L, Rabellotti E, et al. Pathologic findings in hysteroscopy before IVF-ET. Gynecol Endocrinol. 2005;21:235–7.
95. Oliveira FG, Abdelmassih VB, Diamond MP, Dozortsev D, Nagy ZP, Abdelmassih R. Uterine cavity findings and hysteroscopic interventions in patients undergoing in-vitro fertilization-embryo transfer who repeatedly cannot conceive. Fertil Steril. 2003;80:1371–5.
96. Elsokkary M, Elshourbagy M, Labib K, Mamdouh A, El-Shahawy Y, Nossair WS, et al. Assessment of hysteroscopic role in management of women with recurrent pregnancy loss. J Matern Fetal Neonatal Med. 2017;2:1–11. https://doi.org/10.1080/14767058.2017.1319925. [Epub ahead of print].
97. Elsetohy KA, Askalany AH, Hassan M, Dawood Z. Routine office hysteroscopy prior to ICSI vs. ICSI alone in patients with normal transvaginal ultrasound: a randomized controlled trial. Arch Gynecol Obstet. 2015;291(1):193–9. https://doi.org/10.1007/s00404-014-3397-z. Epub 2014 Aug 1.
98. Mouhayar Y, Yin O, Mumford SL, Segars JH. Hysteroscopic polypectomy prior to infertility treatment: a cost analysis and systematic review. Eur J Obstet Gynecol Reprod Biol. 2017;213:107–15. https://doi.org/10.1016/j.ejogrb.2017.04.025. Epub 2017 Apr 13.
99. Fox C, Morin S, Jeong JW, Scott RT Jr, Lessey BA. Local and systemic factors and implantation: what is the evidence? Fertil Steril. 2016;105(4):873–84. https://doi.org/10.1016/j.fertnstert.2016.02.018. Epub 2016 Mar 3.
100. Bosteels J, Weyers S, Puttemans P, Panayotidis C, Van Herendael B, Gomel V, et al. The effectiveness of hysteroscopy in improving pregnancy rates in subfertile women without other gynaecological symptoms: a systematic review. Hum Reprod Update. 2010;16:1–11.
101. Dawood A, Al-Talib A, Tulandi T. Predisposing factors and treatment outcome of different stages of intrauterine adhesions. J Obstet Gynaecol Can. 2010;33:767–70.
102. Zheng QM, Mao HI, Zhao YJ, Zhao J, Wei X, Liu PS. Risk of endometrial polyps in women with endometriosis: a meta-analysis. Reprod Biol Endocrinol. 2015;13:103. https://doi.org/10.1186/s12958-015-0092-2.
103. Carvalho FM, Aguiar FN, Tomioka R, de Oliveira RM, Frantz N, Ueno J. Functional endometrial polyps in infertile asymptomatic patients: a possible evolution of vascular changes secondary to endometritis. Eur J Obstet Gynecol Reprod Biol. 2013;170(1):152–6. https://doi.org/10.1016/j.ejogrb.2013.05.012. Epub 2013 Jun 14.
104. Kitaya K, Tada Y, Taguchi S, Funabiki M, Hayashi T, Nakamura Y. Local mononuclear cell infiltrates in infertile patients with endometrial macropolyps versus micropol-

yps. Hum Reprod. 2012;27(12):3474–80. https://doi.org/10.1093/humrep/des323. Epub 2012 Sep 5.
105. Kınay T, Öztürk Başarır Z, Fırtına Tuncer S, Akpınar F, Kayıkçıoğlu F, Koç S. Prevalence of endometrial polyps coexisting with uterine fibroids and associated factors. Turk J Obstet Gynecol. 2016;13(1):31–6. https://doi.org/10.4274/tjod.36043. Epub 2016 Mar 10.
106. Costa-Paiva L, Godoy CE Jr, Antunes A Jr, Caseiro JD, Arthuso M, Pinto-Neto AM. Risk of malignancy in endometrial polyps in premenopausal and postmenopausal women according to clinicopathologic characteristics. Menopause. 2011;18(12):1278–82.
107. Lee SC, Kaunitz AM, Sanchez-Ramos L, Rhatigan RM. The oncogenic potential of endometrial polyps: a systematic review and meta-analysis. Obstet Gynecol. 2010;116(5):1197–205.
108. Kuribayashi Y, Nakagawa K, Sugiyama R, Motoyama H, Sugiyama R. Frequency of endometrial cancer and atypical hyperplasia in infertile women undergoing hysteroscopic polypectomy. J Obstet Gynaecol Res. 2017;43(9):1465–71. https://doi.org/10.1111/jog.13408. Epub 2017 Jul 14.
109. Troncon JK, Zani AC, Candido-Dos-Reis FJ, Rosa-E-Silva JC. Endometrial polyps - when should Hysteroscopic resection be performed? Rev Bras Ginecol Obstet. 2016;38(7):315–6. https://doi.org/10.1055/s-0036-1586488. Epub 2016 Jul 29.
110. Fisher B, Costantino JP, Redmond CK, Fisher ER, Wickerham DL, Cronin WM. Endometrial cancer in tamoxifen-treated breast cancer patients: findings from the National Surgical Adjuvant Breast and bowel project (NSABP) B-14. J Natl Cancer Inst. 1994;86:527–37.
111. ACOG 601 June 2014 (reaffirmed 2016) Committee Opinion. Tamoxifen and uterine cancer. Obstet Gynecol. 2014;123(6):1394–7. https://doi.org/10.1097/01.AOG.0000450757.18294.cf.
112. Lubián López DM, Orihuela López F, García-Berbel Molina L, Boza Novo P, Pozuelo Solís E, Menor Almagro D, et al. Endometrial polyps in obese asymptomatic pre and postmenopausal patients with breast cancer: is screening necessary? Gynecol Oncol. 2014;133(1):56–62. https://doi.org/10.1016/j.ygyno.2013.12.029.
113. ACOG practice bulletin no. 634: hereditary cancer syndromes and risk assessment. Obstet Gynecol. 2015;125(6):1538–43. https://doi.org/10.1097/01.AOG.0000466373.71146.51.
114. Committee on Practice Bulletins–Gynecology, Committee on Genetics, Society of Gynecologic Oncology. ACOG practice bulletin no. 182: hereditary breast and ovarian cancer syndrome. Obstet Gynecol. 2017;130(3):e110–26. https://doi.org/10.1097/AOG.0000000000002296.
115. Committee on Practice Bulletins-Gynecology. ACOG practice bulletin no. 126: management of gynecologic issues in women with breast cancer. Obstet Gynecol. 2012;119(3):666–82. https://doi.org/10.1097/AOG.0b013e31824e12ce.
116. Litta P, Di Giuseppe J, Moriconi L, Delli Carpini G, Piermartiri MG, Ciavattini A. Predictors of malignancy in endometrial polyps: a multi-institutional cohort study. Eur J Gynaecol Oncol. 2014;35(4):382–6.
117. Lasmar BP, Lasmar RB. Endometrial polyp size and polyp hyperplasia. Int J Gynaecol Obstet. 2013;123(3):236–9. https://doi.org/10.1016/j.ijgo.2013.06.027. Epub 2013 Sep 3.
118. Goldberg Y, Lavie O, Mandel R, Kaufman Y, Segev Y, Auslender R. Two-dimensional sonographic evaluation of endometrial polyps - parameters that are reassuring. Gynecol Obstet Investig. 2016;81(4):359–62. https://doi.org/10.1159/000441779. Epub 2016 Jun 4.
119. Esim Buyukbayrak E, Karageyim Karsidag AY, Kars B, Sakin O, Ozyapi Alper AG, Pirimoglu M, et al. Cervical polyps: evaluation of routine removal and need for accompanying D&C. Arch Gynecol Obstet. 2011;283(3):581–4.
120. Younis MT, Iram S, Anwar B, Ewies AA. Women with asymptomatic cervical polyps may not need to see a gynaecologist or have them removed: an observational retrospective study of 1126 cases. Eur J Obstet Gynecol Reprod Biol. 2010;150(2):190–4. https://doi.org/10.1016/j.ejogrb.2010.02.020. Epub 2010 Mar 4.
121. Nelson AL, Papa RR, Ritchie JJ. Asymptomatic cervical polyps: can we just let them be? Womens Health (Lond). 2015;11(2):121–6. https://doi.org/10.2217/whe.14.86.
122. Schnatz PF, Ricci S, O'Sullivan DM. Cervical polyps in postmenopausal women: is there a difference in risk? Menopause. 2009;16(3):524–8.
123. Levy RA, Kumarapeli AR, Spencer HJ, Quick CM. Cervical polyps: is histologic evaluation necessary? Pathol Res Pract. 2016;212(9):800–3. https://doi.org/10.1016/j.prp.2016.06.010. Epub 2016 Jun 25.
124. Wildenberg JC, Yam BL, Langer JE, Jones LP. US of the nongravid cervix with multimodality imaging correlation: Normal appearance, pathologic conditions, and diagnostic pitfalls. Radiographics. 2016;36(2):596–617. https://doi.org/10.1148/rg.2016150155.
125. Davis PC, O'Neill MJ, Yoder IC, Lee SI, Mueller PR. Sonohysterographic findings of endometrial and subendometrial conditions. Radiographics. 2002;22(4):803–16.
126. Dubinsky TJ, Reed SD, Grieco V, Richardson ML. Intracervical sonographic-pathologic correlation: preliminary results. J Ultrasound Med. 2003;22(1):61–7.
127. Thomas A, Kümmel S, Gemeinhardt O, Fischer T. Real-time sonoelastography of the cervix: tissue elasticity of the normal and abnormal cervix. Acad Radiol. 2007;14(2):193–200.
128. Rezvani M, Shaaban A. Imaging of cervical pathology. Top Magn Reson Imaging. 2010;21(4):261–71.

129. Kozawa E, Takahashi M, Meguro S, Yasuda M, Iwasa N, Fujiwara K, et al. Benign and malignant tumor of the uterine body with broccoli sign: MR imaging features for differential diagnosis. Jpn J Radiol. 2013;31(7):437–43.
130. Tokunaka M, Hasegawa J, Oba T, Nakamura M, Matsuoka R, Ichizuka K, et al. Decidual polyps are associated with preterm delivery in cases of attempted uterine cervical polypectomy during the first and second trimester. J Matern Fetal Neonatal Med. 2015;28(9):1061–3. https://doi.org/10.3109/14767058.2014.942633. Epub 2014 Jul 30.
131. Markovitch O, Tepper R, Aviram R, Fishman A, Shapira J, Cohen I. The value of sonohysterography in the prediction of endometrial pathologies in asymptomatic postmenopausal breast cancer tamoxifen-treated patients. Gynecol Oncol. 2004;94:754–9.
132. Bocca SM, Oehninger S, Abuhamad AZ. Detection of transient postoperative changes in the endometrial cavity by 3-dimensional ultrasonography after hysteroscopic correction of various uterine anomalies. J Ultrasound Med. 2008;27(3):461–5.
133. Grimbizis G, Tsolakidis D, Mikos T, Anagnostou E, Asimakopoulos E, Stamatopoulos P, et al. A prospective comparison of transvaginal ultrasound, saline infusion sonohysterography, and diagnostic hysteroscopy in the evaluation of endometrial pathology. Fertil Steril. 2010;94:2720–5.

Intrauterine Adhesions

11

Gautam Nand Allahbadia,
Akanksha Allahbadia Gupta, and A. H. Maham

Introduction

Ever since the first description of intrauterine adhesions (IUAs) by Joseph Asherman in 1948, this intrauterine pathology has been recognized as a significant gynecological complication, diagnosed with increased frequency [1, 2]. Commonly referred to as Asherman's syndrome and intrauterine synechiae, these lesions cover a spectrum that ranges from minor and insignificant to severe cohesive adhesions that affect menstrual function and fertility [3]. Pathology shows fibrous connective tissue bands with or without glandular tissue, although this may range from filmy to dense [1]. Adhesions may be classified into grades I to IV depending on the consistency and severity. Seven classification systems are described, with no universal acceptance of any one system and no validation of any of them [4].

Incidence

Intrauterine adhesions are the most frequent complications after hysteroscopic surgery in women of reproductive age, the prevalence of IUA after hysteroscopic surgery being correlated with intrauterine pathology (myoma, polyp, or adhesions) [5]. The true incidence of IUA is unknown, with most cases occurring within close temporal proximity to a pregnancy, usually within 4 months and, usually, while the woman is in a hypoestrogenized state [1]. Westendorp et al. [6] reported intrauterine adhesions in 40% of patients at ambulatory hysteroscopy, performed 3 months after secondary removal of placental remnants more than 24 hours after delivery or a repeat curettage for incomplete abortions [6]. Salzani et al. [7] reported IUA on hysteroscopy performed 3–12 months after curettage following abortion in

G. N. Allahbadia (✉)
Reproductive Endocrinology & IVF, Millennium Medical Center IVF, Jumeirah, Dubai, UAE

Reproductive Endocrinology & IVF, Bourn Hall IVF, Jumeirah, Dubai, UAE

Reproductive Endocrinology & IVF, Orchid Fertility & Andrology Services, DHCC, Dubai, UAE

Reproductive Endocrinology & IVF, Dr. Amal Elias Fertility Center, Dubai, UAE

Reproductive Endocrinology & IVF, Canadian Specialist Hospital, Abu Hail, Dubai, UAE

Reproductive Endocrinology & IVF, Indo Nippon IVF, Mumbai, India

Rotunda – The Center For Human Reproduction, Mumbai, India

Medical Education & Research, ISRME, Mumbai, India

Medical Education & Research, Indira IVF, Udaipur, India

A. A. Gupta
Indira IVF, New Delhi, India

A. H. Maham
Millennium Medical Center IVF, Dubai, UAE

L. A. Stadtmauer, I. Tur-Kaspa (eds.), *Ultrasound Imaging in Reproductive Medicine*,
https://doi.org/10.1007/978-3-030-16699-1_11

37.6% of the women, which were mostly mucous and grade I (56.1%) [7]. Khanna and Agrawal [8] reported intrauterine adhesions in 34.8% of the women at hysteroscopy, of whom 68.8% were positive for tubercular bacilli [8]. The number of previous abortions and curettage procedures did not correlate with the presence of IUA [7].

Manifestation

Intrauterine adhesions may be manifested by amenorrhea accompanied with cyclic pelvic pain caused by outflow obstruction or hypomenorrhea, with up to a fourth of the patients having painless menses of normal flow and duration [1, 2], frequently associated with infertility [1].

Causes

Intrauterine adhesions or synechiae evolve after trauma to the endometrium from surgical procedures usually secondary to curettage of a recently pregnant uterus in the context of missed abortion or pregnancy-related hemorrhage [1–3], following hysteroscopic myomectomy (10%) and transmural myomectomies, especially when combined with uterine ischemia [9]. Previous curettage on a gravid uterus has been reported as the possible cause of Asherman's syndrome in the majority (64%) of patients [10]. In a prospective, randomized, controlled trial in 82 women, Tam et al. [11] reported that conservative management and medical evacuation for spontaneous abortion are both acceptable alternatives to standard surgical evacuation, which resulted in a prevalence of 7.7% filmy IUA at hysteroscopic diagnosis of IUA, 6 months after initial treatment [11].

Dawood et al. [12] evaluated the predisposing factors and treatment outcomes of different stages of intrauterine adhesions over a 7-year period in 65 patients. They identified stage I intrauterine adhesions in 36.9%, stage II in 46.2%, and stage III in 16.9% of patients, the main reasons for referral being infertility (stage I 75%, stage II 73.3%, stage III 27.3%) and amenorrhea (stage I 25%, stage II 23.3%, stage III 72.7%). The main predisposing factor was dilatation and curettage, with 40 patients reporting IUA related to early pregnancy curettage; 45% had stage I adhesions, 42.5% had stage II, and 12.5% had stage III in contrast with 10 patients who had peripartum curettage, in whom 60% developed stage III adhesions ($p = 0.004$) [12].

Genital tuberculosis has been reported as an important and common cause of Asherman's syndrome in India, causing oligomenorrhea or amenorrhea with infertility. Sharma et al. [13] studied 28 women with positive evidence of genital tuberculosis on endometrial biopsy (histopathology or culture) or positive polymerase chain reaction (PCR) on endometrial aspirate or positive findings of tuberculosis on laparoscopy or hysteroscopy who underwent hysteroscopy with or without laparoscopy for suspected Asherman's syndrome. They reported various grades of adhesions (grade I in 17.8%, grade II in 28.5%, grade III in 28.5%, and grade IV in 17.5%) at hysteroscopy in all women, bilateral (28.5%) or unilateral (21.3%) blocked ostia, or inability to see the ostia (28.5%). Only four women (14.3%) had open ostia. On laparoscopy performed on 18 women, there were varying grades of adhesions in 16 (88.8%) women, with beading (33.3%), tubercles (33.3%), caseation (11.1%), and tubo-ovarian masses (11.1%) [13].

Risk Factors

In women with menstrual disorders, a statistically significant 12-fold increased risk for Asherman's syndrome grades I–IV was found, previous abortion, as well as infection during surgery being associated with a mildly but nonsignificant increased risk [6]. Myomectomy for multiple, apposing fibroids is reported to have a higher incidence of IUA [9]. Uterine arteries embolization also carries a risk of intracavitary adhesions. Poujade et al. [14] reported a significant risk of uterine synechiae after placement of uterine compression sutures [(Hackethal technique) that transverse the uterine cavity for controlling postpartum hemorrhage (PPH)], with the development of uterine synechiae on explorative hysteroscopy or HSG in 26.7% of women [14].

Effects

In addition to abnormal menses, infertility and recurrent spontaneous abortion are common complaints of IUA, and the accompanying retrograde menstruation may lead to endometriosis [2, 15]. Adhesions are a significant source of impaired organ functioning, decreased fertility, bowel obstruction, difficult reoperation, and, possibly, pain with consequent financial sequelae [16].

Diagnosis

History and a high index of suspicion contribute significantly to the diagnosis of IUA. Several confirmatory tests, such as hysteroscopy, ultrasound-guided techniques (3D hysterosonography [3D HS], two-dimensional [2D] and three-dimensional [3D] transvaginal ultrasonography [TVS], hydrosonography, minimal invasive saline contrast hysterosonography [SCHS], saline infusion hysterography [SIS], sonohysterosalpingography), radiographic techniques (hysterosalpingography [HSG]), and rarely magnetic resonance imaging, have been used for the diagnosis of IUA. However, hysteroscopy has been documented as the gold standard for the diagnosis and treatment of IUA, and the several comparative studies evaluating these techniques have used hysteroscopy as the reference standard to evaluate the efficiency of a particular technique against the other. Hysteroscopy may be recommended in patients who develop menstrual disorders, either after secondary intervention for placental remnants after delivery or after a repeat curettage [6].

The Role of Ultrasound in the Diagnosis

Several ultrasound techniques, such as transvaginal color Doppler sonography (TCDS), sonohysterosalpingography (SHSG), and three-dimensional sonography (3DS), are capable of providing diagnostic information that, in some cases, is equivalent to the information afforded by established techniques that require exposure to radiation, such as hysterosalpingography (HSG), or that are more invasive, such as hysteroscopy or diagnostic laparoscopy [17], tissue biopsies, and dilation and curettage (D&C). The role of ultrasonography for the diagnosis of IUA has been studied by several authors with mixed opinions, and all these studies used hysteroscopy as the most reliable reference standard.

El-Mazny et al. [18] reported abnormal hysteroscopic findings, including IUA, in 33.1% of patients with reported normal uterine findings on HSG who were scheduled for assisted reproductive techniques (ART) (in vitro fertilization [IVF]/intracytoplasmic sperm injection [ICSI] investigations) [1].

Transvaginal sonography (TVS) has been reported to be specific (100%), but not sensitive (41.7%) compared with outpatient hysteroscopy, which leads the authors to suggest that outpatient hysteroscopy should be part of the infertility workup before ART even in patients with normal HSG and/or TVS and especially in patients with prior failed ART cycles who reported a significantly higher incidence of abnormal hysteroscopic findings. The procedure was acceptable in almost all patients with no reported complications [18].

Fedele et al. [19] performed transvaginal US before hysteroscopy as part of the routine diagnostic workup in 77 women who had repeated spontaneous abortions. They were able to correctly identify uterine adhesions (minimal in ten instances and moderate in one) with TVS in 90.0% (10/11) of the women in whom this finding was subsequently confirmed at hysteroscopy. The sensitivity, specificity, PPV, and NPV of transvaginal US were 91, 100, 100, and 98.5%, respectively. Hysteroscopic findings were considered the reference. They concluded that TVS, which is a noninvasive and relatively inexpensive procedure, seems to be effective in screening for uterine adhesions in a population at risk [19].

Narayan and Goswamy [20] correlated preoperative TVS (performed on days 7, 14, and 21 in spontaneous ovulatory cycles) with hysteroscopic findings (performed in the subsequent cycle) in 200 patients being investigated for infertility. A total of 182 patients were diagnosed

correctly to have an abnormality by TVS giving a false-positive rate of 5.5%. The sensitivity and PPV of TVS in detecting endometrial pathology were 98.9 and 94.3%, respectively, with a PPV of 98.5% for the detection of intrauterine adhesions and a strong correlation between findings from transvaginal sonography and hysteroscopy. The authors concluded that TVS may be used to detect intrauterine pathology and identify patients in whom hysteroscopy and hysteroscopic surgery are indicated [20]. With further advance in ultrasound technology, Knopman and Copperman [21] assessed the value of three-dimensional (3D) ultrasound in the management of patients with suspected Asherman's syndrome in a case series of 54 infertile patients who presented with suspected Asherman's syndrome. Intrauterine adhesions (IUAs) were demonstrated on 3D ultrasound and HSG in all cases and confirmed by hysteroscopy. They reported 100% sensitivity with 3D ultrasound for correctly grading the extent of IUAs compared to only 66.7% for HSG. In 61.1% of cases in which HSG results were inconsistent with hysteroscopy, lower uterine segment outflow obstruction was present, and HSG misclassified findings as severe Asherman's with complete cavity obstruction. With a postoperative conception rate of 90%, the authors concluded that 3D ultrasound provides a more accurate depiction of adhesions and extent of cavity damage than HSG in patients with suspected Asherman's syndrome, particularly when differentiating severe IUAs from lower uterine segment outflow obstruction. Therefore, grading systems utilizing HSG to classify severity of disease should be revised to include 3D ultrasound findings [21].

Sonohysterography, a simple ultrasound (US) procedure technique, involves placement of a 5-F catheter into the endometrial canal with subsequent instillation of sterile saline solution under US guidance. Saline infusion offers a good contrast, enabling improved visualization and distinction between diffuse and focal abnormalities. Sonohysterography has been shown to be a safe, simple, and cost-effective outpatient method for evaluating the potentially abnormal endometrium using transvaginal ultrasound (US) in an outpatient setting and to plan the next step in case management [22]. Besides the cost-related issues, it has been indicated as a well-tolerated technique with a short learning curve in the diagnosis of abnormal uterine bleeding (premenopausal and postmenopausal), bleeding while using tamoxifen, suspected congenital uterine abnormality, and Asherman's syndrome [23]. According to Badu-Peprah et al. [24], sonohysterography is an affordable and feasible diagnostic modality in developing nations for evaluating the endometrial cavity that should be used more often where equipment and skill permit [24], thereby obviating the need for laparoscopy and hysteroscopy in the majority of cases [25]. In a very recent study, Kowalczyk et al. [26] reported real-time 3D sonohysterography (SIS 3D) to be a minimally invasive advance to conventional 2D sonohysterography (sensitivity 72% and specificity 96%) that enables a three-dimensional image of the uterine cavity and enables examination of endometrial lesions with a sensitivity and specificity of 83 and 99%, respectively, and a diagnostic precision similar to the results achieved by hysteroscopy [26].

In a prospective study on 65 infertile women 19–43 years of age, Soares et al. [27] compared the diagnostic accuracy of sonohysterography (SHG) in uterine cavity diseases in infertile patients with that of HSG and TVS, using hysteroscopy as the gold standard. Sonohysterography and HSG had a sensitivity of 75% in the detection of intrauterine adhesions and respective PPVs of 42.9 and 50%, while TVS showed a sensitivity and PPV of 0% for this diagnosis. The authors concluded that while sonohysterography was in general the most accurate test with a markedly superior diagnostic accuracy for polypoid lesions and endometrial hyperplasia (EH), with total agreement with the gold standard, however, in diagnosis of intrauterine adhesions, SHG had limited accuracy, similar to that obtained by HSG, with a high false-positive diagnosis rate [27]. Makris et al. [28] compared 3D hysterosonography (3D HS) and diagnostic hysteroscopy in 242 women with abnormal uterine bleeding. They reported a similar specificity (99.4%) but a higher sensitivity for hysteroscopy

compared to 3D HS (98.7% vs. 93.5%, respectively). The PPV and NPV of 3D HS were 98.6 and 97%, respectively, compared to 98.7 and 99.4% for hysteroscopy, respectively. The 2 techniques were in agreement for 8 cases of adhesions and in 165 cases of normal endometrium [28].

de Kroon et al. [23] evaluated the accuracy of minimal invasive saline contrast hysterosonography (SCHS) in the diagnosis of uterine pathology. They reported that this technique can detect intracavity abnormalities (with a prevalence of 54%) with a sensitivity, specificity, PPV, and NPV of 94, 89, 91, and 92%, respectively, and in combination with endometrial sampling, whenever indicated, it might be able to replace diagnostic hysteroscopy as the gold standard in the evaluation of the uterine cavity in 84% of the diagnostic hysteroscopies as SCHS is two to nine times cheaper than diagnostic hysteroscopy. However, SCHS fails more frequently in postmenopausal women than premenopausal women (12.5% vs. 4.7%; $p = 0.03$), and the chance of a non-conclusive SCHS is 7.6%, being higher if the uterine volume is greater than 600 cm^3 (relative risk, 2.63; 95%-CI, 1.05–6.60) and if two or more myomas are present: (RR, 2.65; 95%-CI, 1.16–6.10) [23].

Yucebilgin et al. [29] reported a sensitivity, specificity, positive, and negative predictive values of 85, 75, 75, and 84%, respectively, for hydrosonography in the detection of structural endometrial cavity lesions where 45 (85%) of 53 women, who were supposed to have normal findings on hydrosonography, were confirmed by hysteroscopy. They, however, suggested that hydrosonography may be a useful tool in the evaluation of intrauterine cavity structural pathologies in infertile patients with the exception of intrauterine adhesions [29].

Alborzi et al. [30] compared the diagnostic accuracy of hysterosalpingography and sonohysterosalpingography in detecting tubal and uterine abnormalities with surgical findings as the gold standard. They reported a sensitivity, specificity, positive predictive value, and negative predictive value of 78.2, 93.1, 82.7, and 91%, respectively, for the detection of total tubal and uterine pathologies compared to 76.3, 81.8, 90.9, and 59.2%, respectively, for HSG. They concluded that sonohysterosalpingography is a safe, easy, and promising procedure and more accurate than hysterosalpingography for detecting intrauterine adhesions and various forms of uterine anomalies [30].

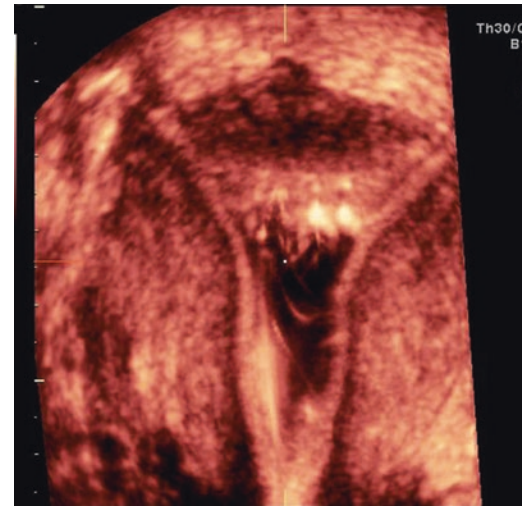

Fig. 11.1 Saline sonogram showing intrauterine adhesions

There have been reports of MRI appearances in four cases of Asherman's syndrome in which the diagnosis was confirmed by hysteroscopy. However, the full range of MRI appearances in Asherman's syndrome has not been established, and there has been only one case reported in the literature [31]. Figure 11.1 shows intrauterine adhesions using a multiplanar view after sonohysterography.

Risk Factors for IUA

Mo et al. investigated the risk factors for intrauterine adhesions in patients with artificial abortion and clinical efficacy of hysteroscopic dissection [32]. 1500 patients undergoing artificial abortion between January 2014 and June 2015 were enrolled into this study. The incidence rate for intrauterine adhesions following induced abortion is 17.0%. Univariate analysis showed that preoperative inflammation, multiple pregnancies, and suction evacuation time are the

influence risk factors of intrauterine adhesions. Multiple logistic regression demonstrates that multiple pregnancies, high intrauterine negative pressure, and long suction evacuation time are independent risk factors for the development of intrauterine adhesions following induced abortion. Additionally, intrauterine adhesions were observed in 105 mild, 80 moderate, and 70 severe cases. The cure rates for these three categories of intrauterine adhesions by hysteroscopic surgery were 100.0%, 93.8%, and 85.7%, respectively. The authors concluded that multiple pregnancies, high negative pressure suction evacuation, and long suction evacuation time are independent risk factors for the development of intrauterine adhesions following induced abortions [32].

Of 167 women treated for RPOC, 84 (50.3%) had undergone a follow-up hysteroscopic evaluation after the operative hysteroscopy and were included in the study [33]. Intrauterine adhesions were found in 16 cases (19.0%), of which only 3 (3.6%) were severe adhesions. Multivariate analysis showed that the presence of IUA was associated with RPOC after cesarean section (5 of 10 [50.5%] developed IUA, vs. 7 of 49 [14.3%] after vaginal delivery). Intrauterine adhesions were also found in 4 of 23 women (17.4%) undergoing hysteroscopy for RPOC after abortion. Patient age, gravidity, parity, and the interval between the index pregnancy and treatment for RPOC were not associated with postoperative IUA. Hysteroscopic treatment for RPOC had a 3.6% incidence of severe intrauterine adhesions formation in this descriptive series [33]. Women with RPOC occurring after delivery by cesarean section are particularly at risk for development of IUA [33].

Laparotomic myomectomy is often the only realistic solution for symptomatic women with multiple or large myomas who wish to retain their fertility. The aim of a recent study was to document the rate of uterine synechiae and their associated risk factors after laparotomic myomectomy [34]. This prospective observational study took place in a teaching hospital from May 2009 to June 2014. It included all women aged 18–45 years who had laparotomic myomectomies (without diagnostic hysteroscopy at the time of surgery) for myomas and a postoperative diagnostic office hysteroscopy 6–8 weeks later. The study included 98 women with a laparotomic myomectomy and a postoperative hysteroscopic follow-up. Women with a laparotomic myomectomy for a subserosal myoma were excluded. The intrauterine adhesion rate after laparotomic myomectomy was 25.51% (25/98); 44% (11/25) of them were complex intrauterine adhesions. Opening the uterine cavity was a major risk factor for these complex adhesions, with an OR of 6.42 (95% CI 1.27–32.52). Office hysteroscopy could be carried out after surgery in such cases [34].

Management of IUA

Diagnosis and treatment of intrauterine adhesions are integral to the optimization of fertility outcomes [15]. Surgical management of IUA presents a challenge to the hysteroscopic surgeon. Though the appropriate management is controversial [3], and more often than not, guided by the clinician's choice, skill, and operative setting, hysteroscopic adhesiolysis with antibiotic prophylaxis followed by the use of postoperative adjuvants such as systemic estrogens and intrauterine devices or systems designed to impede the development of adhesions is the treatment of choice with favorable results in terms of pregnancy and live birth rates [3, 15, 35, 36]. Clinicians should maintain a level of suspicion of intrauterine adhesions and should investigate by hysteroscopy if necessary [35]. Non-hysteroscopic techniques are also beginning to be developed, but whether they will replace the current "gold" standard of hysteroscopy remains to be seen [37]. The success of treatment regarding term deliveries and rate of abortions depends on the severity of the adhesions, and pregnancy, when achieved, may be complicated by premature labor, placenta previa, and placenta accreta [36].

Hysteroscopic Surgery

Technological progress in optic fibers and instrumentation has made it possible to video endoscope and determine the fibrous nature of the lesions and its precise localization and control

endocavitary surgeries such as hysteroscopic adhesiolysis for uterine synechiae [38]. Though sonohysterography and hysterosalpingography are useful as screening tests of intrauterine adhesions [15], hysteroscopy has been considered the mainstay of diagnosis, classification, and treatment of the intrauterine adhesions, with medical treatments having no role in management [1, 2, 4, 15, 35, 39]. Diagnostic and therapeutic hysteroscopy is a simple, feasible, safe, reproducible, effective, quick, well-tolerated, and low-cost surgical procedure that is highly successful in an outpatient setting, offering a see-and-treat approach in majority of the subjects with intrauterine adhesions [40, 41]. Hysteroscopy has also become accepted as the optimum route of surgery, the aim being to restore the size and shape of the uterine cavity, normal endometrial function, and fertility [15, 16]. Lysis of intrauterine adhesions, for the treatment of infertility and recurrent pregnancy loss, results in improved fecundability and decreased pregnancy loss. Though adhesiolysis for pain relief appears efficacious in certain subsets of women, unfortunately, even when lysed, adhesions have a great propensity to reform [16]. According to Bettocchi et al. [41], there is no consensus on the effectiveness of hysteroscopic surgery in improving the prognosis of subfertile women. However, office hysteroscopy is a powerful tool for the diagnosis and treatment of intrauterine benign pathologies, and in patients with at least two failed cycles of assisted reproductive technology, diagnostic hysteroscopy and, if necessary, operative hysteroscopy are mandatory to improve reproductive outcome [41]. A descriptive study (Canadian Task Force classification II-2) concluded that hysteroscopic adhesiolysis is an effective and safe option even for postmenopausal women with intrauterine lesions adhesions on hysteroscopy or ultrasound. It allows the correct diagnosis to be made, reduces the need for major and unnecessary surgery, and is therapeutic in most patients [42].

Treatment can range from simple cervical dilatation in the case of cervical stenosis, but an intact uterine cavity, to extensive adhesiolysis of dense intrauterine adhesions using scissors, electro- or laser energy, or a combination of blunt and sharp dissection [34, 37]. Various techniques for adhesiolysis and for prevention of scar reformation have been advocated. According to March [2], the use of miniature scissors for adhesiolysis and the placement of a balloon stent inside the uterus immediately after surgery appear to be the most efficacious [2]. Patients with more severe adhesions, in whom the uterine fundus is completely obscured, and those with a greatly narrowed fibrotic cavity present the greatest therapeutic challenge. Several techniques have been described for these difficult cases, but the outcome is far worse than in patients with mild, endometrial-type adhesions [4, 37]. A significantly obliterated cavity may require multiple hysteroscopic adhesiolysis to achieve a satisfactory anatomical and functional result [15, 39], while laparoscopic or ultrasound guidance may aid in the hysteroscopic lysis of dense scar tissue and difficult entry into the cervix [1].

Treatment Outcome

Treatment outcomes are difficult to assess as there is no universally agreed upon classification system [1]. Anatomic, but most of all functional prognosis, is directly correlated to the severity of adhesions, and the number of surgical procedures required to complete treatment [43].

Restoration of menstruation is highly successful (more than 90%), and pregnancy rates around 50–60% with live birth rates around 40–50% can be achieved [35]. The risk of complications for those that achieve pregnancy is significant with a significant risk for placenta accreta and subsequent blood loss, transfusion, and hysterectomy [12]. In perhaps the largest study, involving 6680 hysteroscopies with hysteroscopic adhesiolysis in 75 patients, 94.6% functional restoration and 93.3% anatomic resolution, with pregnancy rates ranging from 28.7% to 53.6%, were achieved. At 2-month follow-up, the uterine cavity was completely regular in 70 cases, while in four cases, a second surgical treatment was necessary [44].

Using a standard technique with a loop electrode and glycine 1.5% as distension medium, Dawood et al. [12] reported an improvement in the rate of amenorrhea from 32.3% before adhesiolysis to 9.2% after the procedure with an overall pregnancy rate of 51.2% and the live birth rate 32.6% among women who wished to conceive. Severe intrauterine adhesions were managed with the assistance of abdominal ultrasound to ensure that the uterine cavity was not breached, and the rates of pregnancy and term pregnancy among this selected group of women were similar regardless of the severity of adhesions [12].

Yu et al. [45] evaluated the outcome of hysteroscopic adhesiolysis with electrode needle or loop under direct vision in 85 women with Asherman's syndrome who presented with a history of infertility or recurrent pregnancy loss. After hysteroscopic adhesiolysis, the chances of conception among the 18.2% of women who remained amenorrheic were significantly lower than those who continued to have menses (50%). The conception rate in women who had reformation of intrauterine adhesions at second-look hysteroscopy (11.8%) was significantly lower than that of women who had a normal cavity (59.1%), suggesting that the outcome of hysteroscopic adhesiolysis for Asherman's syndrome is significantly affected by recurrence of intrauterine adhesions [45].

Hysteroscopic adhesiolysis with monopolar or bipolar energy can be performed safely and effectively for severe stage III and IV adhesions with a 97% restoration of menses, 43.8% PR, and 32.8% LBR. The pregnancy rate was significantly higher in patients ≤35 years compared to patients older than 35 years (66.6% vs. 23.5%, respectively; $p = 0.01$), suggesting that age is the main predictive factor of success: the pregnancies were at risk of abnormal placentation [46]. The impact of age on the outcome of hysteroscopic adhesiolysis is in agreement with a previous study by Capella-Allouc et al. [47] that reported a pregnancy rate of 42.8%, live birth rate of 32.1%, the pregnancy rate being much higher in patients ≤35 years compared to patients older than 35 years (62.5% vs.16.6%, respectively; $p = 0.01$) following hysteroscopic adhesiolysis in 31 patients with severe Asherman's syndrome. However, these pregnancies were at risk for hemorrhage with abnormal placentation [47].

Roy et al. [10] reported an overall conception rate of 40.4%, live birth rate of 86.1%, and a miscarriage rate of 11.1% in a mean conception time after surgery of 12.8 months following hysteroscopic adhesiolysis with the monopolar electrode knife in 89 infertile patients with Asherman's syndrome. The cumulative pregnancy rate showed that 97.2% of patients conceived within 24 months. The conception rate was higher (58%) in mild Asherman's syndrome compared to 30% conception rate in moderate and 33.3% conception rate in severe cases. There was a significantly higher likelihood of conception (44.3%) in those who continued to have improved menstrual pattern compared to only 10% likelihood of conception in those who continued to have amenorrhea after adhesiolysis. A second-look office hysteroscopy, performed after 2 months, showed reformation of adhesions in 12 patients that needed a repeat adhesiolysis with no conception in these patients. The authors concluded that hysteroscopic adhesiolysis for Asherman's syndrome is a safe and effective method of choice for restoring menstrual function and fertility [10].

Shokeir et al. [48] attempted to analyze the adhesion grade in multiple hysteroscopic-guided biopsies from IUA following the initial hysteroscopic adhesiolysis at a follow-up diagnostic hysteroscopy, performed early (2–4 weeks) after the initial operation or late, about 12 months (8–16 months). They observed that at follow-up hysteroscopy, 25% of both groups had no significant adhesions. Grade I adhesions (thin, filmy) occurred in 60% of the early hysteroscopy patients and in only 12% of the late group ($P < 0.05$). Grade II adhesions were present in 10% of the early group and in up to 41% in the late group ($P < 0.05$), whereas grade III adhesions were present in only 5% of the early hysteroscopy group but in 22% of the late one ($P < 0.05$). Correlation between hysteroscopic and histologic findings were good in most of cases in both groups. The follow-up to determine the subsequent reproductive outcome revealed similar conception rates in both groups. The authors suggested that the IUA that might be

formed immediately following hysteroscopic reproductive surgery is histologically different from those appearing a longer time after the original operation. Routine early follow-up hysteroscopy can influence the prognosis resulting from the original surgery [48].

Having excluded hormonal imbalances, premature ovarian failure, and congenital uterine abnormalities, Yasmin et al. [49] reported thick fibrous adhesions in 45% of patients, flimsy adhesions in 40%, and muscular adhesions in 15% at hysteroscopy, with 65% adhesions in the body of uterus, 25% at the site of internal os, and 1% adhesions in the cervical canal as well as the body of the uterus. Following diagnostic hysteroscopy and resection of adhesions in 20 patients (median age 26 years), presenting with scanty menses and secondary infertility (65%), secondary amenorrhea (20%), or primary infertility alone (15%), they reported a restoration of menses in 95% of the patients and conception in 10% of the patients. Though the patient number was small, the authors suggested that hysteroscopy is not only an effective procedure for diagnosing Asherman's syndrome but is equally effective for treating it [49].

Hysteroscopic adhesiolysis in women with Asherman's syndrome and poor reproductive performance (previous spontaneous abortions or a premature delivery) contributes significantly to a successful reproductive outcome. Whereas pregnancy outcome prior to the hysteroscopic adhesiolysis was 18.3% term deliveries, 3.3% premature deliveries, 62.4% first-trimester abortions, and 16.0% late abortions, after hysteroscopic adhesiolysis, the pregnancy outcome was 68.6% term deliveries, 9.3% premature deliveries, 17.4% first-trimester abortions, and 4.7% late abortions. The operative success rate, measured by delivering a healthy newborn, improved from 18.3% preoperatively to 64% postoperatively in women with two previous unsuccessful pregnancies [50], whereas in women with three or more unsuccessful pregnancies, the success rate improved from 18.3% to 75%. Successful outcome of adhesiolysis was observed in 61.9% of mild (stage I) and in 70.6% of moderate-to-severe cases (stages II and III) of intrauterine adhesions [50].

Blunt adhesiolysis with a flexible hysteroscope, following primary treatment of intrauterine adhesions with sharp adhesiolysis, has been suggested as an effective technique for the maintenance of cavity patency with an improvement in menstrual flow in 95% of the patients, relief of dysmenorrhea in 92%, 92% improvement in disease staging over the treatment interval, and a pregnancy rate of 46%. Initially, 50% had severe adhesions, 46% had moderate, and 4% had minimal disease according to the March criteria [51].

Colacurci et al. [52] analyzed the reproductive outcome in 53 women undergoing hysteroscopic lysis of intrauterine adhesions, according to their localization and severity. Hysteroscopic surgery restored an acceptable menstrual cycle in almost all the patients affected by intrauterine isolated adhesions in 52% of women with complex incomplete adhesions and in none of the patients with an entirely obliterated cavity. In isolated, isthmic, central, or marginal synechiae, a pregnancy rate of 73.3% was observed with a pregnancy rate to term, respectively, of 63.3% and of 86.3%, while in case of complex but not complete adhesions, the pregnancy rate was 25% with only two term pregnancies. There were no pregnancies in three cases of complex synechiae. The authors concluded that the basic parameter to define the functional and reproductive prognosis of the hysteroscopic lysis of intrauterine adhesions is not the menstrual profile or the histological characteristic of the lesions but rather their extension [52].

Hysteroscopy and hysteroscopic surgery have been the gold standard of diagnosis and treatment, respectively, for patients with Asherman's syndrome who presented with amenorrhea or hypomenorrhea, infertility, or recurrent pregnancy loss. However, according to most authors, despite the advances in hysteroscopic surgery, the treatment of moderate-to-severe Asherman's syndrome still presents a challenge [43, 53]. Furthermore, pregnancy after treatment remains high risk with complications including spontaneous abortion, preterm delivery, intrauterine growth restriction, placenta accreta or previa, or even uterine rupture that necessitate close antenatal surveillance and monitoring for women who

conceive after treatment [53]. According to Piketty et al. [43] despite the infrequent but well-known complications during surgery and the less frequent but often severe obstetrical complications, the benefit gained by the recovery of fertility (either spontaneous or not) remains superior to the risks of the surgical management [43].

Role of Ultrasonography in the Treatment

Serial intrauterine device-guided hysteroscopic adhesiolysis of intrauterine synechiae, especially for early intervention, may prevent complications during the treatment of severe intrauterine adhesions and may present a secure and effective alternative for constructive clinical outcomes with spontaneous pregnancy rates of 47.2 and 30% and live birth rates of 28 and 20% in patients who did and did not undergo early intervention of office hysteroscopy, 1 week after insertion of the IUD at hysteroscopic adhesiolysis, respectively [54]. Following echo-controlled hysteroscopic surgical cure of complex and/or recurrent uterine synechiae in 11 patients, Salat-Baroux et al. [38] concluded that intraoperative echography allowed hysteroscopic adhesiolysis of intrauterine adhesions at a controlled and equivalent distance from the uterine walls, enabling better treatment of the uterine cornua since the operator is informed when to limit progression to avoid massive fluid infusion into the abdominal cavity and perforation of the uterus. The intraoperative echographic control was validated in the operating theater radiographically. With this technique normal cavities with bilateral tube permeability were obtained in 72.72% of the patients and normal cycles in 90.9% of the patients [38]. Following hysteroscopic lysis under ultrasound control for significant intrauterine synechiae, Bellingham [55] reported normal menstruation in 61% of the patients and live births in 80% of the patients, of whom 50% had had severe adhesions. They reported that ultrasound control is ideally essential if the adhesions are extensive [55]. However, in both these studies, the number of patients was very small to effectively document the role of ultrasound in the treatment of IUA.

Coccia et al. [56] described a new therapeutic procedure called pressure lavage under ultrasound guidance (PLUG) for selected cases of IUA. This technique is based on sonohysterography to monitor the effects of intrauterine injections of saline solution on the continuous accumulation of saline in the uterine cavity for the mechanical disruption of IUA. In an open clinical investigation with no control group, they reported satisfactory lysis of adhesions and restoration of menses in 71.4% of the patients with mild IUA with a pregnancy rate of 66.63% following the use of the PLUG technique. A second-look hysteroscopy after 1 month showed the persistence of filmy adhesions in two patients with moderate IUA that were removed successfully during hysteroscopy. The authors suggested that PLUG is a safe and ideal in-office procedure that allows complete lysis in mild IUA cases avoiding the need for therapeutic and, possibly, follow-up hysteroscopy and may represent a useful initial step in moderate IUA cases reducing the need for operative hysteroscopy [56]. In a recent study, Taniguchi and Suginami [57] also suggested that sonohysterographic (SHG) lysis for recurrent adhesions following hysteroscopic lysis may be a treatment option for recurrent adhesions in infertile patients, with improved menstrual cycles and restored tubal patency [57].

Tiras et al. [58] demonstrated the value of laparoscopic intracorporeal ultrasound (LIU)-guided hysteroscopic adhesiolysis in a patient with amenorrhea and infertility with total intrauterine synechiae. Adequate intrauterine adhesiolysis was performed by a resectoscope with a wire loop, suggesting that complex intrauterine procedures can be easily performed by the guidance of endoscopic ultrasonography to avoid the possibility of inadvertent uterine perforation [58].

Schlaff and Hurst [59] evaluated the predictive value of preoperative endometrial sonography in the diagnosis and surgical treatment of women with amenorrhea due to severe Asherman's syndrome, characterized by complete obstruction of the cavity at hysterosalpingogram. They sug-

gested that an endometrial pattern, demonstrating a well-developed endometrial stripe on transvaginal sonography, is highly predictive of a positive surgical and clinical outcome in women with severe Asherman's syndrome with resumption of normal menses and normalization of the cavity after hysteroscopy in contrast to women with minimal endometrium who had no cavity identified and derived no benefit from surgery [59]. However, this study was limited to just seven patients, and hence, substantial evidence in this direction is lacking.

Radiographic Methods

In a small but significant study, Karande et al. [60] demonstrated that in-office lysis of intrauterine adhesions, under fluoroscopic control, using a specially designed catheter (gynecoradiologic control), can be carried out safely in the majority of patients, using minimally invasive techniques. They could successfully lyse adhesions in 76% (13/17) of the patients (9 mild, 3 moderate, and 1 severe), while in remaining 4 patients (2 moderate and 2 severe), lysis was only partially successful. Nine procedures were performed with the catheter's balloon tip and four with hysteroscopic scissors. Procedure complications resulting in the abandoning of the procedure included patient discomfort before attempting the use of scissors ($n = 1$), extravasation of dye into the myometrium making visualization difficult ($n = 1$), and thick, fibrotic adhesions that were resistant to scissors ($n = 2$). They opined that the potential cost savings with this technique in comparison with endoscopic procedures, which require utilization of expensive operating room time, are especially relevant in a cost-conscious managed care environment and only failures of in-office procedures would reach the operating room [60]. The fluoroscopic approach to adhesions was further evaluated a decade later by Chason et al. [61] who used hysteroplasty with fluoroscopic cannulation and balloon uterine dilation to treat intrauterine adhesions and cervical stenosis and lower uterine defects in select cases. They concluded that while the treatment of intrauterine adhesions resulted in an improved pregnancy outcome, albeit in a case study, the effect of lower uterine segment-filling defects from cesarean deliveries on pregnancy outcome in assisted reproductive technology cycles warrants further investigation [61]. In a 5-year retrospective, uncontrolled cohort study, Thomson et al. [62] conducted fluoroscopically guided hysteroscopic synechiolysis for Asherman's syndrome in 30 patients (13% AFS grade I, 43% AFS grade II, and 43% AFS grade III), 60% of whom were amenorrheic. They reported a 96% restoration of regular menses with a 53% pregnancy rate among patients who attempted to conceive and concluded that hysteroscopic synechiolysis, performed by injecting radiographic contrast medium and visualized under image-intensifier control, followed by cyclic high-dose estrogen therapy to stimulate endometrial proliferation, appears to be an effective treatment for Asherman's syndrome. Repeat procedures were performed monthly until the endometrial cavity was reestablished [62].

Prevention of IUA

One of the most important features of treatment for intrauterine synechiae is the prevention of recurrence [4]. Follow-up studies to assure resolution of the scarring are mandatory before the patient attempts to conceive as is careful monitoring of pregnancies for cervical incompetence, placenta accreta, and intrauterine growth retardation [2]. The best available evidence demonstrates that the newly developed adhesion barriers, such as hyaluronic acid, show promise for preventing new adhesions [4, 15]. Postoperative mechanical distention of the endometrial cavity with the use of intrauterine contraceptive devices and postoperative hormonal treatment with estrogen +/− progestogen to facilitate endometrial regrowth are important in the prevention of recurrence [15, 35].

With regard to primary adhesion formation, a recent study by Rein et al. [63] demonstrated that selective hysteroscopic resection (HR) of residual trophoblastic tissue after first- or second-

trimester miscarriage or term delivery significantly reduces the incidence of intrauterine adhesions and increases pregnancy rates compared to ultrasound-guided evacuation with a curette (D&E). They reported mild adhesion in 4.2% of the patients after selective HR compared to an incidence of 30.8% after D&E, of which 17.9% were mild, 7.7% single dense adhesions, and 2.6% with extensive endometrial fibrosis. Conception rates were significantly higher in the HR patients compared to curetted patients (68.8% vs. 59.9%, respectively; $p < 0.05$) and 78.1% vs. 66.6%, respectively; $p < 0.05$ in patients younger than 35 years of age with a significantly ($p < 0.05$) shorter time to conception (11.5 months vs. 14.5 months) [63]. Operative hysteroscopy for selective curettage of residual trophoblastic tissue instead of nonselective conventional curettage may prevent intrauterine adhesions [39].

Mechanical Barriers

The efficiency of barrier agents' postoperative hysteroscopic adhesiolysis to prevent the recurrence of adhesions has been addressed in a few clinical trials. Barrier agents have been grouped under mechanical agents (intrauterine device-IUCD, Foley catheter), fluid agents (Seprafilm, Hyalobarrier, auto-cross-linked hyaluronic acid [ACP] gel), postoperative systemic treatment (cyclic estrogen-progesterone therapy), and the latest tissue barriers (fresh or dries amnion grafts).

Several comparative studies, evaluating the efficacy of various barrier agents, have been conducted. Orhue et al. [64] compared two adjunctive treatments following intrauterine adhesiolysis—the intrauterine contraceptive device (IUCD) and the Foley catheter. In a 4-year initial period, patients with intrauterine adhesions were treated with the insertion of an IUCD after adhesiolysis. In the next 4 years, a pediatric Foley catheter balloon was used after adhesiolysis instead of the IUCD. They reported a significantly higher restoration of normal menstruation (81.4% vs. 62.7%, $p < 0.05$), less frequent persistent posttreatment amenorrhea and hypomenorrhea (18.6% vs. 37.3%; $P < 0.03$), a higher conception rate (33.9% vs. 22.5%), and a significantly lesser need for repeated treatment in the Foley catheter group compared to the IUCD group, respectively. They concluded that the Foley catheter is a safer and more effective adjunctive method of treatment of IUA compared with the IUCD [64].

Fluid Barriers

The application of auto-cross-linked hyaluronic acid (ACP) gel has been reported to significantly reduce the incidence and severity of de novo formation of intrauterine adhesions after hysteroscopic surgery, with a significant decrease in adhesion severity on staging of adhesions [65].

Tissue Barriers

The role of amnion grafts as barrier agents to prevent recurrence of adhesions has currently gained a lot of attention. In a pilot study involving 25 patients with moderate or severe intrauterine adhesions, Amer et al. [66] reported that hysteroscopic adhesiolysis followed by intrauterine application of a fresh amnion graft over an inflated balloon of a Foley catheter for 2 weeks seems to be a promising procedure for decreasing recurrence of adhesions and encouraging endometrial regeneration. They reported failure to achieve normal menstrual flow in 16.7% of the patients with moderate versus 23.1% of the patients with severe adhesions and observed adhesion reformation at follow-up hysteroscopy in 48% of the patients, all with severe adhesions. However, randomized comparative studies are needed to validate its benefits, including reproductive outcome [66].

In a more recent pilot prospective randomized comparative study (Canadian Task Force classification I), Ameret et al. [67] estimated the efficacy of inserting fresh and dried amnion graft after hysteroscopic lysis of severe intrauterine adhesions in decreasing its recurrence and encouraging endometrial regeneration in 45 patients.

Hysteroscopic lysis of intrauterine adhesions was followed by insertion of an intrauterine balloon only (group 1) or either fresh amnion graft (group 2) or dried amnion graft (group 3) for 2 weeks. Diagnostic hysteroscopy, performed at 2 to 4 months postoperatively, revealed significant improvement in adhesion grade with the amnion graft versus intrauterine balloon alone ($p = 0.003$) and significant improvement with fresh compared to dried amnion graft ($p = 0.01$). Restoration of normal menstruation (46.7% in group 3, 35.7% in group 2, 28.6% in group 1) and the conception rate (80% after amnion graft and 20% without amnion) was higher in patients with the graft compared to the balloon. The overall conception rate was 23.3% with a miscarriage rate of 60%. The authors concluded that hysteroscopic lysis of severe intrauterine adhesions with grafting of either fresh or dried amnion is a promising adjunctive procedure for decreasing recurrence of adhesions and encouraging endometrial regeneration [67].

Peng et al. set up a study to determine the safety and efficacy of amnion grafts in preventing the recurrence of intrauterine adhesions after hysteroscopic adhesiolysis in women with severe intrauterine adhesions [68]. A total of 120 patients underwent intrauterine adhesiolysis for severe intrauterine adhesions: 40 patients in the treatment group and 80 patients in the control group matched for age and adhesion scores. The mean duration of follow-up was 14.6 months. A Foley balloon with/without a fresh amnion graft was introduced into the uterine cavity after hysteroscopic adhesiolysis. In both groups, the balloon was kept in place for 7 days, cyclic hormone treatment was given for 3 months, and second-look and third-look hysteroscopies were performed 1 and 3 months after the operation. Outcome measures included the incidence of the recurrence of intrauterine adhesions, the score of intrauterine adhesions (if present), and the impact of the surgery on the amount of menstrual flow. In the study group, the menstrual score at the end of 3 months was significantly higher, and the intrauterine adhesion score at third-look hysteroscopy was significantly lower compared with those in the control group. The incidences of the recurrence of intrauterine adhesions at third-look hysteroscopy in the treatment and control groups were 30% and 48.7%, respectively ($p = 0.05$). The adhesion scores at third-look hysteroscopy in the treatment and control groups were 1.3 and 2.1, respectively ($p < 0.05$). The use of an amnion graft after intrauterine adhesiolysis appears to be beneficial in improving menstruation and reducing the recurrence of adhesion reformation [68].

Prevention Strategies

Prevention strategies, including bipolar resection, barrier gel, or postoperative estradiol, might be useful, but stronger evidence is needed, and there is a need for other randomized controlled trials to fully justify the use of adhesion barriers for clinical use [5, 9]. In view of the current knowledge, Gambadauro et al. [9] recommend a prevention strategy based on a combination of surgical trauma minimization and identification of high-risk cases, with early hysteroscopic diagnosis and lysis possibly representing the best means of secondary prevention and treatment of postoperative intrauterine adhesions [9]. Considering the decreased pregnancy outcome in patient with recurrence of adhesions, further research in Asherman's syndrome should be directed toward reduction of adhesion reformation with a view to improving outcome [45].

Hooker et al. set up a study to examine whether intrauterine application of auto-cross-linked hyaluronic acid (ACP) gel, after dilatation and curettage (D&C), reduces the incidence of intrauterine adhesions (IUAs) [69]. A total of 152 women with a miscarriage of <14 weeks with at least one previous D&C for miscarriage or termination of pregnancy were included. Women were randomly assigned to either D&C plus ACP gel (intervention group) or D&C alone (control group). A follow-up diagnostic hysteroscopy was scheduled 8–12 weeks after the D&C procedure. The primary outcome was the number of women with IUAs, and the secondary outcome was the severity of IUAs. Outcomes were available for 149 women: 77 in the intervention group and 72 in the control group. The IUAs were observed

in 10 (13.0%) and 22 women (30.6%), respectively (relative risk, 0.43; 95% confidence interval, 0.22–0.83). Mean adhesion score and the amount of moderate-to-severe IUAs were significantly lower in the intervention group according to the American Fertility Society (AFS) and European Society of Gynecological Endoscopy classifications systems of adhesions. The authors concluded that intrauterine application of ACP gel after D&C for miscarriage in women with at least one previous D&C seems to reduce the incidence and severity of IUAs but does not eliminate the process of adhesion formation completely [69].

Risk of Recurrence of IUA After Hysteroscopic Adhesiolysis

Yang et al. investigated the recurrence potential of intrauterine adhesions after hysteroscopic adhesiolysis [70]. This study included 115 women who had intrauterine adhesions completely separated during hysteroscopic surgery. The treated adhesions were classified into four groups according to their location and extent: group 1, central type (i.e., intervening space between the adhesions and both lateral uterine sidewalls) at the middle area of uterine cavity; group 2, central type at uterine cornua; group 3, cervico-isthmic; and group 4, extensive if the adhesions were dense with occlusion of part of the uterine cavity other than cervico-isthmic region. Postoperative outpatient hysteroscopic adhesiolysis was scheduled 10–14 days after the initial hysteroscopic surgery, and procedures were repeated every 10–14 days until no reformed adhesions were detected. Multivariate logistic regression models were built to examine initial adhesion characteristics and other factors associated with adhesion reformation and need for subsequent outpatient adhesiolysis. Categorical data were compared using Fisher's exact test. The location and extent of adhesions according to the allocated group was the only parameter independently related to the number of postoperative outpatient adhesiolysis procedures ($P = 0.0004$). Women with group 1 adhesions underwent a lower number of postoperative interventions compared with those with group 2, 3, and 4 adhesions ($P = 0.0355$, $P = 0.0004$, and $P = 0.0087$, respectively). There is an increased likelihood of intrauterine adhesion recurrence when successfully divided adhesions were originally located at the uterine cornua, the cervico-isthmic region or involved a large portion of the uterine cavity [70].

The aim of Xu et al.'s study was to assess the effect of early second-look hysteroscopy after hysteroscopic adhesiolysis for intrauterine adhesions (IUAs) on the pregnancy rate (PR) and live birth rate (LBR) (71). Of 151 women treated for IUAs, the general PR was 71.5%, and LBR was 53.0%. The PR and LBR were higher in the earlier second-look group (compared with second hysteroscopy later than 2 months group) and the group which received less than three times adhesiolysis ($p < 0.05$). The PR was higher in the amenorrhea group (compared with normal menses group) and recurrent miscarriage group (compared with infertility group) ($p < 0.05$). Logistic regression showed that the second-look time interval, times of operation to relieve adhesion, and pregnancy history were associated with the PR, while age and the second-look time interval were associated with the LBR. Early second-look hysteroscopic examinations within 2 months may increase the cumulative PR and LBR [71].

Recent Advances

Recently, the endometrium has been identified as a repository for anti-Mullerian hormone (AMH), with endometrial masses associated with AMH serum levels. Promberger and Ott aimed to compare AMH levels, as well as other parameters for ovarian reserve, in women with endometrial trauma due to Asherman's syndrome (AS) and matched controls [72]. In a retrospective study, nine women with hysteroscopically confirmed AS were compared to nine matched controls. Follicle-stimulating hormone, luteinizing hormone, and estradiol levels did not differ between women with and without AS, whereas significantly lower AMH levels were found in patients (median 0.50 pg/mL; IQR 0.25–0.75) than in controls (median 1.14 pg/mL; IQR 0.63–1.77;

p = 0.026). The results suggest that decreased AMH levels in patients with AS do not necessarily indicate decreased ovarian reserve. The study is limited by the small sample size, and, thus, future research on the role of AMH in endometrial tissue and function are necessary to clarify the importance of these findings [72].

In an effort to treat injured endometrium nonresponsive to conventional treatment for Asherman's syndrome (IUCD) with cyclical hormonal therapy for 6 months, Nagori et al. [73] demonstrated that placement of endometrial angiogenic stem cells in the endometrial cavity under ultrasound guidance after curettage followed by cyclical hormonal therapy can regenerate injured endometrium. These cells could be isolated from adult autologous stem cells isolated from a patient's own bone marrow using immunomagnetic isolation [73]. Gargett and Healy [74] also reported regeneration of thin endometrium refractory to estrogen stimulation following intrauterine administration of bone marrow stem/progenitor cells sufficiently to support a pregnancy in a case study. However, whether its local endometrial damage is induced by concurrent curettage that stimulated endogenous endometrial stem/progenitor cells into action, or both, is open to question [74].

Recently, stem cell transplantation has been proposed to promote the recovery process. Gan et al. investigated whether human amniotic mesenchymal stromal cells (hAMSCs), a valuable resource for transplantation therapy, could improve endometrial regeneration in rodent IUA models [75]. hAMSC transplantation promotes endometrial regeneration after injury in IUA rat models, possibly due to immunomodulatory properties. These cells provide a more easily accessible source of stem cells for future research into the impact of cell transplantation on damaged endometria [75].

There are few effective treatments due to the complex function of endometrium and shortage of native materials. 17β-estradiol (E2) is commonly used as an ancillary treatment in IUA patients, but it is limited by its poor solubility in aqueous solutions and low concentrations at the injured sites. In a recent publication, a mini-endometrial curette was used to injure the rat's endometrium to form an IUA model [76]. 17β-estradiol was encapsulated into the micelles of heparin-poloxamer, and a thermosensitive hydrogel (E2-HP hydrogel) was formed. This sustained releasing system was applied to restore the structure and function of the injured uterus. E2-HP hydrogel was constructed, and relevant characteristics including gelation temperature and micromorphology were evaluated. Sustained release of 17β-estradiol from HP hydrogel was performed both in vitro and in vivo. Ultrasonography measurement and pathologic characteristics on the IUA rats were performed to evaluate the therapeutic effect of E2-HP hydrogel. Endoplasmic reticulum (ER) stress-related apoptosis was analyzed to explore the possible mechanisms in IUA recovery. E2-HP hydrogel showed a prolonged release of E2 at the targeting region and more effective endometrium regeneration in IUA rats. Significant improvements in both gland numbers and fibrosis area were observed in the E2-HP hydrogel group [76]. The paper also demonstrated that E2-HP hydrogel in the recovery of IUA was closely related to the suppression of ER stress signals via the activation of downstream signals, PI3K/Akt and ERK1/2. HP hydrogel might be an effective approach to deliver E2 into the injured endometrium. Therapeutic strategies targeting ER stress using E2-HP hydrogel might be a promising solution for the treatment of women with intrauterine adhesions [76].

Conclusion

Intrauterine adhesions are a significant gynecological complication that requires prompt and accurate diagnosis and treatment. Despite its invasiveness, cost issues, and the technical skill required, hysteroscopy is recognized as the gold standard for the diagnosis, classification, and treatment of adhesions with an encouraging restoration of fertility in terms of menstruation, pregnancy rates, and live birth rates in patients with mild, moderate, and severe IUA, including postmenopausal women. Moreover, it offers a

see-and-treat approach in majority of the patients where therapy is required, thus obviating the need for a second intervention. Though ultrasonography is gradually gaining acceptance in the diagnosis of IUA, particularly in economically compromised settings, with the purpose of avoiding costly invasive techniques, it has limited accuracy and sensitivity in the diagnosis of IUA compared to hysteroscopy. The addition of 3D ultrasound is reported to have improved accuracy in the diagnosis, but consistent large-scale studies are lacking. However, with regard to treatment, ultrasound may have a significant role in controlling hysteroscopic surgery, especially in patients with complex severe adhesions, to avoid inadvertent uterine perforation. More large-scale randomized trials will be required before ultrasonography can be established as a more functionally effective alternative to hysteroscopy in the diagnosis and treatment of IUA.

References

1. Berman JM. Intrauterine adhesions. Semin Reprod Med. 2008;26(4):349–55.
2. March CM. Asherman's syndrome. Semin Reprod Med. 2011;29(2):83–94.
3. Fedele L, Bianchi S, Frontino G. Septums and synechiae: approaches to surgical correction. Clin Obstet Gynecol. 2006;49(4):767–88.
4. Deans R, Abbott J. Review of intrauterine adhesions. J Minim Invasive Gynecol. 2010;17(5):555–69.
5. Revaux A, Ducarme G, Luton D. Prevention of intrauterine adhesions after hysteroscopic surgery. [Article in French]. Gynecol Obstet Fertil. 2008;36(3):311–7.
6. Westendorp IC, Ankum WM, Mol BW, Vonk J. Prevalence of Asherman's syndrome after secondary removal of placental remnants or a repeat curettage for incomplete abortion. Hum Reprod. 1998;13(12):3347–50.
7. Salzani A, Yela DA, Gabiatti JR, Bedone AJ, Monteiro IM. Prevalence of uterine synechia after abortion evacuation curettage. Sao Paulo Med J. 2007;125(5):261–4.
8. Khanna A, Agrawal A. Markers of genital tuberculosis in infertility. Singapore Med J. 2011;52(12):864–7.
9. Gambadauro P, Gudmundsson J, Torrejón R. Intrauterine adhesions following conservative treatment of uterine fibroids. Obstet Gynecol Int. 2012;2012:853269.
10. Roy KK, Baruah J, Sharma JB, Kumar S, Kachawa G, Singh N. Reproductive outcome following hysteroscopic adhesiolysis in patients with infertility due to Asherman's syndrome. Arch Gynecol Obstet. 2010;281(2):355–61.
11. Tam WH, Lau WC, Cheung LP, Yuen PM, Chung TK. Intrauterine adhesions after conservative and surgical management of spontaneous abortion. J Am Assoc Gynecol Laparosc. 2002;9(2):182–5.
12. Dawood A, Al-Talib A, Tulandi T. Predisposing factors and treatment outcome of different stages of intrauterine adhesions. J Obstet Gynaecol Can. 2010;32(8):767–70.
13. Sharma JB, Roy KK, Pushparaj M, Gupta N, Jain SK, Malhotra N, Mittal S. Genital tuberculosis: an important cause of Asherman's syndrome in India. Arch Gynecol Obstet. 2008;277(1):37–41.
14. Poujade O, Grossetti A, Mougel L, Ceccaldi PF, Ducarme G, Luton D. Risk of synechiae following uterine compression sutures in the management of major postpartum haemorrhage. BJOG. 2011;118(4):433–9.
15. Kodaman PH, Arici A. Intra-uterine adhesions and fertility outcome: how to optimize success? Curr Opin Obstet Gynecol. 2007;19(3):207–14.
16. Diamond MP, Freeman ML. Clinical implications of postsurgical adhesions. Hum Reprod Update. 2001;7(6):567–76.
17. Bonilla-Musoles F, De Velasco LA, Osborn NG, MacHado LE, Flores DP, MacHado FR, Bonilla F Jr. Two-dimensional and three-dimensional ultrasound differential diagnosis of endometrial hyperplasia and endometrial adenocarcinoma. J Gynecol Surg. 2003;19(3):105–20.
18. El-Mazny A, Abou-Salem N, El-Sherbiny W, Saber W. Outpatient hysteroscopy: a routine investigation before assisted reproductive techniques? Fertil Steril. 2011;95(1):272–6.
19. Fedele L, Bianchi S, Dorta M, Vignali M. Intrauterine adhesions: detection with transvaginal US. Radiology. 1996;199(3):757–9.
20. Narayan R, Goswamy RK. Transvaginal sonography of the uterine cavity with hysteroscopic correlation in the investigation of infertility. Ultrasound Obstet Gynecol. 1993;3(2):129–33.
21. Knopman J, Copperman AB. Value of 3D ultrasound in the management of suspected Asherman's syndrome. J Reprod Med. 2007;52(11):1016–22.
22. Jorizzo JH, Riccio GJ, Chen MYM, Carr JJ. Sonohysterography: the next step in the evaluation of the abnormal endometrium. Radiographics. 1999;19:S117–30.
23. de Kroon CD, Jansen FW, Trimbos JB. Efficiency of saline contrast hysterosonography for evaluating the uterine cavity. [Article in Dutch]. Ned Tijdschr Geneeskd. 2003;147(32):1539–44.
24. Badu-Peprah A, Odoi AT, Dassah ET, Amo-Wiafe Y. Sonohysterography: time to step up its use in gynaecologic imaging in West Africa. Afr J Reprod Health. 2011;15(3):133–9.

25. Onah HE, Ezike HA, Mgbor SO. Saline sonohysterosalpingographic findings in infertile Nigerian women. J Obstet Gynaecol. 2006;26(8):788–90.
26. Kowalczyk D, Guzikowski W, Więcek J, Sioma-Markowska U. Clinical value of real time 3D sonohysterography and 2D sonohysterography in comparison to hysteroscopy with subsequent histopathological examination in perimenopausal women with abnormal uterine bleeding. Neuro Endocrinol Lett. 2012;33(2):212–6.
27. Soares SR, Barbosa dos Reis MM, Camargos AF. Diagnostic accuracy of sonohysterography, transvaginal sonography, and hysterosalpingography in patients with uterine cavity diseases. Fertil Steril. 2000;73(2):406–11.
28. Makris N, Skartados N, Kalmantis K, Mantzaris G, Papadimitriou A, Antsaklis A. Evaluation of abnormal uterine bleeding by transvaginal 3-D hysterosonography and diagnostic hysteroscopy. Eur J Gynaecol Oncol. 2007;28(1):39–42.
29. Yucebilgin MS, Aktan E, Bozkurt K, Kazandi M, Akercan F, Mgoyi L, Terek MC. Comparison of hydrosonography and diagnostic hysteroscopy in the evaluation of infertile patients. Clin Exp Obstet Gynecol. 2004;31(1):56–8.
30. Alborzi S, Dehbashi S, Khodaee R. Sonohysterosalpingographic screening for infertile patients. Int J Gynaecol Obstet. 2003;82(1):57–62.
31. Bacelar AC, Wilcock D, Powell M, Worthington BS. The value of MRI in the assessment of traumatic intra-uterine adhesions (Asherman's syndrome). Clin Radiol. 1995;50(2):80–3.
32. Mo X, Qin G, Zhou Z, Jiang X. Assessment of risk factors of intrauterine adhesions in patients with induced abortion and the curative effect of hysteroscopic surgery. J Invest Surg. 2017:1–5. https://doi.org/10.1080/08941939.2017.1376130. [Epub ahead of print].
33. Barel O, Krakov A, Pansky M, Vaknin Z, Halperin R, Smorgick N. Intrauterine adhesions after hysteroscopic treatment for retained products of conception: what are the risk factors? Fertil Steril. 2015;103(3):775–9. https://doi.org/10.1016/j.fertnstert.2014.11.016. Epub 2014 Dec 17.
34. Capmas P, Pourcelot AG, Fernandez H. Are synechiae a complication of laparotomic myomectomy? Reprod Biomed Online. 2018;36(4):450–4. https://doi.org/10.1016/j.rbmo.2018.01.010. Epub 2018 Feb 2.
35. Thomson AJ, Abbott JA, Deans R, Kingston A, Vancaillie TG. The management of intrauterine synechiae. Curr Opin Obstet Gynecol. 2009;21(4):335–41.
36. Schenker JG. Etiology of and therapeutic approach to synechia uteri. Eur J Obstet Gynecol Reprod Biol. 1996;65(1):109–13.
37. Magos A. Hysteroscopic treatment of Asherman's syndrome. Reprod Biomed Online. 2002;4(Suppl 3):46–51.
38. Salat-Baroux J, Pambou O, Guyot B. Hysteroscopic cure under ultrasonic control of complex and/or recurrent uterine synechiae. [Article in French]. Presse Med. 1995;24(17):811–4.
39. Heinonen PK. Intrauterine adhesions – Asherman's syndrome. [Article in Finnish]. Duodecim. 2010;126(21):2486–91.
40. Gulumser C, Narvekar N, Pathak M, Palmer E, Parker S, Saridogan E. See-and-treat outpatient hysteroscopy: an analysis of 1109 examinations. Reprod Biomed Online. 2010;20(3):423–9.
41. Bettocchi S, Achilarre MT, Ceci O, Luigi S. Fertility-enhancing hysteroscopic surgery. Semin Reprod Med. 2011;29(2):75–82.
42. Shushan A, Protopapas A, Hart R, Magos AL. Diagnostic and therapeutic advantages of hysteroscopic surgery in management of intrauterine lesions in postmenopausal women. J Am Assoc Gynecol Laparosc. 2001;8(1):87–91.
43. Piketty M, Lesavre M, Prat-Ellenberg L, Benifla JL. Surgical management of intrauterine adhesions: is benefice bigger than risk? [Article in French]. Gynecol Obstet Fertil. 2010;38(9):547–9.
44. Pace S, Stentella P, Catania R, Palazzetti PL, Frega A. Endoscopic treatment of intrauterine adhesions. Clin Exp Obstet Gynecol. 2003;30(1):26–8.
45. Yu D, Li TC, Xia E, Huang X, Liu Y, Peng X. Factors affecting reproductive outcome of hysteroscopic adhesiolysis for Asherman's syndrome. Fertil Steril. 2008;89(3):715–22.
46. Fernandez H, Al-Najjar F, Chauveaud-Lambling A, Frydman R, Gervaise A. Fertility after treatment of Asherman's syndrome stage 3 and 4. J Minim Invasive Gynecol. 2006;13(5):398–402.
47. Capella-Allouc S, Morsad F, Rongières-Bertrand C, Taylor S, Fernandez H. Hysteroscopic treatment of severe Asherman's syndrome and subsequent fertility. Hum Reprod. 1999;14(5):1230–3.
48. Shokeir TA, Fawzy M, Tatongy M. The nature of intrauterine adhesions following reproductive hysteroscopic surgery as determined by early and late follow-up hysteroscopy: clinical implications. Arch Gynecol Obstet. 2008;277(5):423–7.
49. Yasmin H, Nasir A, Noorani KJ. Hysteroscopic management of Ashermans syndrome. J Pak Med Assoc. 2007;57(11):553–5.
50. Katz Z, Ben-Arie A, Lurie S, Manor M, Insler V. Reproductive outcome following hysteroscopic adhesiolysis in Asherman's syndrome. Int J Fertil Menopausal Stud. 1996;41(5):462–5.
51. Robinson JK, Colimon LM, Isaacson KB. Postoperative adhesiolysis therapy for intrauterine adhesions (Asherman's syndrome). Fertil Steril. 2008;90(2):409–14.
52. Colacurci N, Fortunato N, Nasto R, Mele D, Errico G, De Franciscis P, Zarcone R. Reproductive outcome of hysteroscopic lysis of intrauterine adhesions. [Article in Italian]. Minerva Ginecol. 1997;49(7–8):325–7.
53. Yu D, Wong YM, Cheong Y, Xia E, Li TC. Asherman syndrome – one century later. Fertil Steril. 2008;89(4):759–79.

54. Pabuccu R, Onalan G, Kaya C, Selam B, Ceyhan T, Ornek T, Kuzudisli E. Efficiency and pregnancy outcome of serial intrauterine device-guided hysteroscopic adhesiolysis of intrauterine synechiae. Fertil Steril. 2008;90(5):1973–7.
55. Bellingham FR. Intrauterine adhesions: hysteroscopic lysis and adjunctive methods. Aust N Z J Obstet Gynaecol. 1996;36(2):171–4.
56. Coccia ME, Becattini C, Bracco GL, Pampaloni F, Bargelli G, Scarselli G. Pressure lavage under ultrasound guidance: a new approach for outpatient treatment of intrauterine adhesions. Fertil Steril. 2001;75(3):601–6.
57. Taniguchi F, Suginami H. Pregnancy and delivery following sonohysterographic lysis to treat recurrence after hysteroscopic lysis of severe intrauterine adhesions: a case report. Clin Exp Obstet Gynecol. 2008;35(3):215–7.
58. Tiras MB, Oktem M, Noyan V. Laparoscopic intracorporeal ultrasound guidance during hysteroscopic adhesiolysis. Eur J Obstet Gynecol Reprod Biol. 2003;108(1):80–4.
59. Schlaff WD, Hurst BS. Preoperative sonographic measurement of endometrial pattern predicts outcome of surgical repair in patients with severe Asherman's syndrome. Fertil Steril. 1995;63(2):410–3.
60. Karande V, Levrant S, Hoxsey R, Rinehart J, Gleicher N. Lysis of intrauterine adhesions using gynecoradiologic techniques. Fertil Steril. 1997;68(4):658–62.
61. Chason RJ, Levens ED, Yauger BJ, Payson MD, Cho K, Larsen FW. Balloon fluoroscopy as treatment for intrauterine adhesions: a novel approach. Fertil Steril. 2008;90(5):2005.e15–7.e15.
62. Thomson AJ, Abbott JA, Kingston A, Lenart M, Vancaillie TG. Fluoroscopically guided synechiolysis for patients with Asherman's syndrome: menstrual and fertility outcomes. Fertil Steril. 2007;87(2):405–10.
63. Rein DT, Schmidt T, Hess AP, Volkmer A, Schöndorf T, Breidenbach M. Hysteroscopic management of residual trophoblastic tissue is superior to ultrasound-guided curettage. J Minim Invasive Gynecol. 2011;18(6):774–8.
64. Orhue AA, Aziken ME, Igbefoh JO. A comparison of two adjunctive treatments for intrauterine adhesions following lysis. Int J Gynaecol Obstet. 2003;82(1):49–56.
65. Guida M, Acunzo G, Di Spiezio Sardo A, Bifulco G, Piccoli R, Pellicano M, Cerrota G, Cirillo D, Nappi C. Effectiveness of auto-crosslinked hyaluronic acid gel in the prevention of intrauterine adhesions after hysteroscopic surgery: a prospective, randomized, controlled study. Hum Reprod. 2004;19(6):1461–4.
66. Amer MI, Abd-El-Maeboud KH. Amnion graft following hysteroscopic lysis of intrauterine adhesions. J Obstet Gynaecol Res. 2006;32(6):559–66.
67. Amer MI, Abd-El-Maeboud KH, Abdelfatah I, Salama FA, Abdallah AS. Human amnion as a temporary biologic barrier after hysteroscopic lysis of severe intrauterine adhesions: pilot study. J Minim Invasive Gynecol. 2010;17(5):605–11.
68. Peng X, Li T, Zhao Y, Guo Y, Xia E. Safety and efficacy of amnion graft in preventing reformation of intrauterine adhesions. J Minim Invasive Gynecol. 2017;24(7):1204–10. https://doi.org/10.1016/j.jmig.2017.08.005. Epub 2017 Aug 12.
69. Hooker AB, de Leeuw R, van de Ven PM, Bakkum EA, Thurkow AL, Vogel NEA, et al. Prevalence of intrauterine adhesions after the application of hyaluronic acid gel after dilatation and curettage in women with at least one previous curettage: short-term outcomes of a multicenter, prospective randomized controlled trial. Fertil Steril. 2017;107(5):1223–1231.e3. https://doi.org/10.1016/j.fertnstert.2017.02.113. Epub 2017 Apr 6.
70. Yang JH, Chen CD, Chen SU, Yang YS, Chen MJ. The influence of the location and extent of intrauterine adhesions on recurrence after hysteroscopic adhesiolysis. BJOG. 2016;123(4):618–23. https://doi.org/10.1111/1471-0528.13353. Epub 2015 Mar 6.
71. Xu W, Zhang Y, Yang Y, Zhang S, Lin X. Effect of early second-look hysteroscopy on reproductive outcomes after hysteroscopic adhesiolysis in patients with intrauterine adhesion, a retrospective study in China. Int J Surg. 2018;50:49–54. https://doi.org/10.1016/j.ijsu.2017.11.040. Epub 2017 Dec 1.
72. Promberger R, Ott J. Anti-Mullerian hormone as a parameter for endometrial trauma in Asherman syndrome: a retrospective data analysis. Reprod Biol. 2017;17(2):151–3. https://doi.org/10.1016/j.repbio.2017.03.005. Epub 2017 Apr 8.
73. Nagori CB, Panchal SY, Patel H. Endometrial regeneration using autologous adult stem cells followed by conception by in vitro fertilization in a patient of severe Asherman's syndrome. J Hum Reprod Sci. 2011;4(1):43–8.
74. Gargett CE, Healy DL. Generating receptive endometrium in Asherman's syndrome. J Hum Reprod Sci. 2011;4(1):49–51.
75. Gan L, Duan H, Xu Q, Tang YQ, Li JJ, Sun FQ, Wang S. Human amniotic mesenchymal stromal cell transplantation improves endometrial regeneration in rodent models of intrauterine adhesions. Cytotherapy. 2017;19(5):603–16. https://doi.org/10.1016/j.jcyt.2017.02.003. Epub 2017 Mar 9.
76. Zhang SS, Xia WT, Xu J, Xu HL, Lu CT, Zhao YZ, Wu XQ. Three-dimensional structure micelles of heparin-poloxamer improve the therapeutic effect of 17β-estradiol on endometrial regeneration for intrauterine adhesions in a rat model. Int J Nanomedicine. 2017;12:5643–57. https://doi.org/10.2147/IJN.S137237. eCollection 2017.

12 Sonohysterography (SHG) in Reproductive Medicine

Ilan Tur-Kaspa, Alberto Revelli,
Laurel A. Stadtmauer, and David P. Cohen

Introduction

In this chapter, we will review the indication and contraindication for SHG, existing practice guidelines, and describe the optimal technique for it. The main focus will be on diagnosis of intrauterine abnormalities through SHG rather than their treatment thereafter. This will include a discussion on how to make the procedure pain-free for women by using flexible catheters, gentle movements, inflating the balloon inside the cervix rather than the uterus, and injecting the saline slowly. Practice guidelines conclude that SHG is a safe, cost-effective, accurate, and easy to perform procedure, for patients as well as for physicians, to evaluate intrauterine pathology and can be used as the primary diagnostic tool for such cases.

Practice Guidelines for SHG

The American College of Obstetrics and Gynecology (ACOG) published a technology assessment on SHG, in collaboration with the American Institute of Ultrasound in Medicine (AIUM), the Society for Reproductive Endocrinology and Infertility (SREI), an affiliate of the American Society for Reproductive Medicine (ASRM), and the American College of Radiology [1]. The reader is highly encouraged to review the published guidelines [2–5]. They describe the technique, the indications and contraindications, and the qualifications and responsibilities of the physician performing the SHG. The authors of this chapter have found it easy to adhere and to comply with the above guidelines in their practices and have incorporated them into this review.

Indication and Contraindication

The ACOG and AIUM guidelines [1, 2] describe the indications and contraindications for SHG. The most common indication for SHG is pre- and postmenopausal abnormal uterine bleeding (AUB) [6–11]. Screening of the uterine cavity prior to ART and for the evaluation of infertility and habitual abortions is the second most common indication. SHG may be performed for the evaluation of congenital or

I. Tur-Kaspa (✉) · D. P. Cohen
Institute for Human Reproduction, Chicago, IL, USA
e-mail: DrTK@infertilityIHR.com

A. Revelli
Sant'Anna Hospital, University of Turin, Department of Obstetrics and Gynecology, Turin, Italy

L. A. Stadtmauer
The Jones Institute for Reproductive Medicine, Eastern Virginia Medical School, Norfolk, VA, USA

L. A. Stadtmauer, I. Tur-Kaspa (eds.), *Ultrasound Imaging in Reproductive Medicine*,
https://doi.org/10.1007/978-3-030-16699-1_12

acquired (fibroids, polyps, and synechiae) uterine anomalies and preoperative and postoperative evaluations of the uterine cavities. SHG may also be performed for further diagnosis of any suboptimal imaging of the endometrium and when focal or diffuse endometrial thickening or abnormalities are seen on a regular TVUS.

The two main contraindications for SHG are pregnancy and pelvic infection or unexplained pelvic tenderness. Abnormal uterine bleeding (AUB) is not a contraindication, though it may make the interpretation of the findings more challenging [7]. Tur-Kaspa et al. [6] have prospectively analyzed SHG with 409 consecutive patients with AUB and have found 37.2% of intracavitary abnormalities, mainly polyps and submucosal fibroids. Goldstein [9] has suggested "ultrasound first" as an approach to women with postmenopausal bleeding. SHG may be used for triage by identifying patients with no disease vs. those with focal or global abnormalities. Furthermore, patient acceptability and diagnostic capability of SHG are high, and it reduces demand for hysteroscopy [8]. SHG-guided endometrial biopsy provided an accurate pathological diagnosis in 89% of patients compared to 52% with blind endometrial sampling [8, 12].

SHG Procedure [1, 2, 6, 13]

Menstrual dating should be documented, and pregnancy should be ruled out before performing SHG. The best timing for performing SHG is after the menstrual flow and prior to ovulation, in cycle days 5–10. This is when the endometrial lining is most symmetrical and precludes the chance for an early pregnancy. During the luteal phase, the lining is thickened and more echogenic and may be associated with a higher false-positive rate of polyps. Using birth control pills may assist in scheduling this test at any day of the menstrual cycle.

Patients should be informed of alternative procedures and the possible risks and complications of SHG (mainly discomfort, low risk of infection, and bleeding) and then sign a consent form. Pretreatment antibiotic is not recommended routinely unless the patient has a history of gynecologic infections or tubal factor infertility [14]. Several RCTs, using different analgesics, have failed to demonstrate benefits of using any drug to significantly reduce pain during or after SHG [15–18]. Unless indicated, no analgesics or sedatives are routinely needed before, during, or after SHG, since it may be considered as a pain-free procedure [6, 19].

Prior to SHG, TVUS is performed with routine evaluation and measurement of the uterus, endometrium, and ovaries. The presence of fluid in the cul-de-sac should be noted, and any pelvic abnormal findings such as hydrosalpinx should be documented. If a patient had a baseline TVUS on day 3 of her period and returns for SHG a few days later, then a quick scan for the evaluation of the uterine cavity and of fluid in the cul-de-sac may be performed after the insertion of the catheter before the injection of the saline.

A speculum is placed in the vagina to visualize the cervix. After cleansing the external os with betadine or equivalent solution, the SHG catheter is inserted into the cervical canal. The SHG catheter should be pre-filled with saline in order to avoid infusing air bubbles into the uterine cavity. There are many catheter options, including HSG/SHG curved catheters, intrauterine insemination catheters, and balloon SHG/HSG catheters. Any rigid catheter, which requires grasping the cervix with a tenaculum, may induce significant pain for the patient. If a balloon catheter is used, it is preferred to inflate the balloon intracervically rather than intrauterine, and the appropriate position of the catheter may be confirmed by pulling it slightly. An RCT recently showed a significant less fluid used for SHG and significantly less pain felt by patients when the balloon was inflated inside the cervix rather than in the lower uterine segment [20]. Furthermore, by inflating the balloon intracervically, one may avoid balloon hyperinflation inside the uterine cavity, which may displace and obscure a pathological finding, such as endometrial polyp. Next, the speculum is removed, and the TVUS probe is inserted into the vagina. Physiological saline solution is then slowly injected to distend the

endometrial lumen under direct real-time visualization. Injecting the fluid slowly is mandatory to avoid abrupt uterine distension and pain. Documentation should include images of the endometrial cavity, including the lower segment and the upper cervical canal in at least two planes, longitudinal and transverse (Fig. 12.1). The reader is encouraged to read the official guidelines set by ACOG and AIUM [1, 2].

SHG for Congenital Uterine Anomalies

SHG is a cost-effective method available in an outpatient setting which is highly accurate in identifying uterine anomalies, especially septate and bicornuate uterus [21–23]. Müllerian anomalies are congenital defects in the development of the uterus and the upper vagina. The ability of 2D

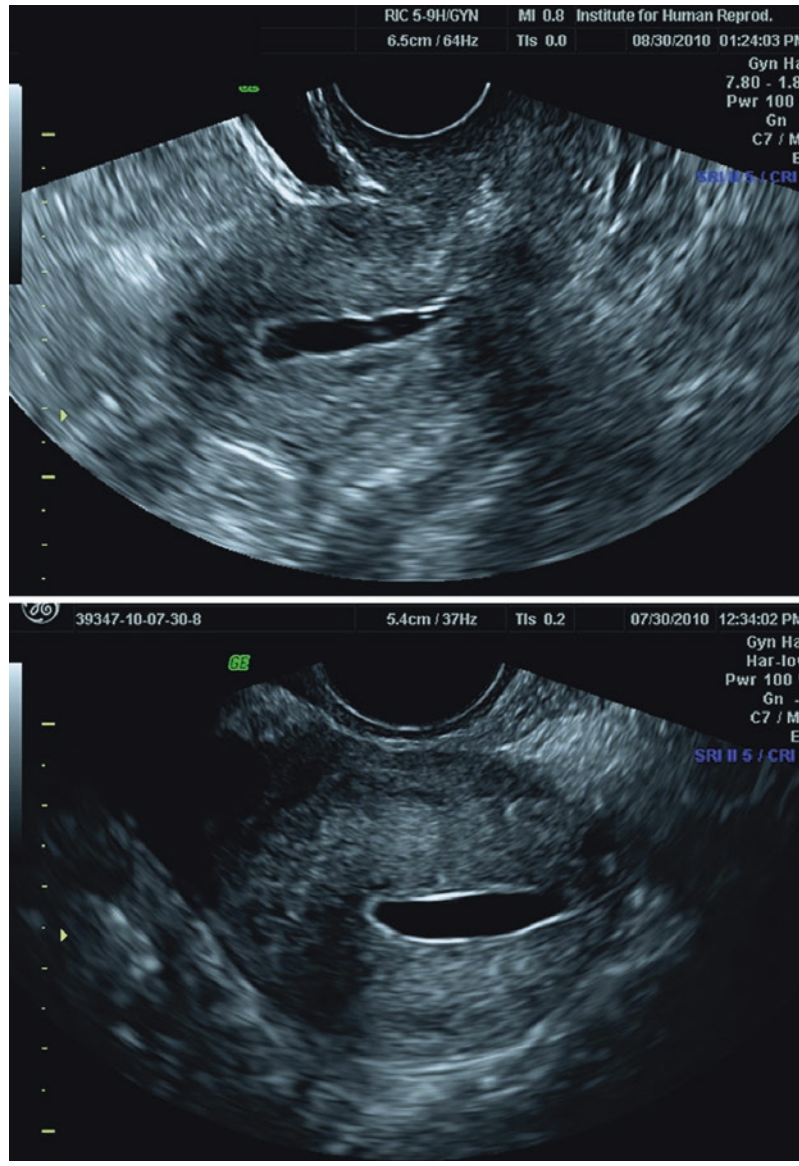

Fig. 12.1 2D longitudinal (upper image) and transverse (lower image) images of the uterus showing adequate distention of the endometrial canal with saline during SHG

US to distinguish between different types of uterine anomalies is limited and operator-dependent. The finding of a uterine anomaly may affect the management of the infertile and/or pregnant woman and the pregnancy outcome. In a recent meta-analysis [24], including 94 observational studies comprising 89,861 women, the prevalence of uterine anomalies diagnosed by optimal tests was 5.5% (95% CI, 3.5–8.5) in unselected population, 8.0% (95%CI, 5.3–12) in infertile women, 13.3.% (95% CI, 8.9–20.0) in women with a history of miscarriage, and 24.5% (95% CI, 18.3–32.8) in women with miscarriage and infertility.

Congenital uterine anomalies are associated with poor reproductive outcome [25]. All uterine anomalies are associated with an increase incidence of fetal malpresentions at delivery. Unification defects do not reduce fertility, but some defects, in particular bicornuate uteri, are associated with aberrant outcomes throughout the course of pregnancy. Canalization defects appear to reduce the chance of clinical pregnancy and to increase risk of preterm delivery. These are more profound in cases of septate uteri. Arcuate uteri, while previously considered to have no reproductive sequelae, are specifically associated with poor outcomes in late pregnancy, i.e., second-trimester miscarriage and malpresentation [25].

Uterine anomalies are defined by the criteria outlined by the American Society of Reproductive Medicine [26]. The visualization of the uterine fundus at the coronal plane is necessary for classifying uterine shape. SHG has been shown to have superior diagnostic ability compared to HSG and 2D US for the evaluation of uterine malformation. Tur-Kaspa et al. [6] studied prospectively the prevalence of uterine anomalies diagnosed by SHG in 600 consecutive infertile patients compared to 409 patients with AUB. While the prevalence of septate uterus was 3% in each group, arcuate uterus was significantly more common among the infertile patients (15% vs. 6%, respectively). All other anomalies had <1% frequency in either group. We [6], as well as others [1, 27–31], concluded that SHG is an excellent method for the evaluation of congenital uterine anomalies. 3D SHG may be needed in some cases to assist in the final diagnosis.

SHG for Acquired Uterine Abnormalities

SHG can serve as a first-line test for the evaluation of acquired intrauterine abnormalities such as adhesions (Fig. 12.2), polyps (Fig. 12.3), and fibroids [3, 10, 11, 32]. Tur-Kaspa et al. [6] have

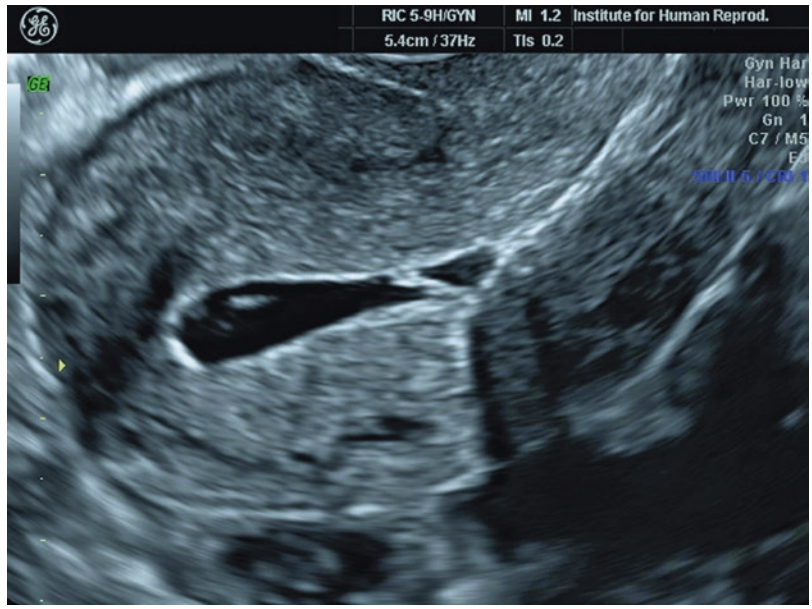

Fig. 12.2 2D longitudinal image of SHG demonstrating intrauterine adhesion at the lower uterine segment, connecting the anterior and the posterior walls of the uterus

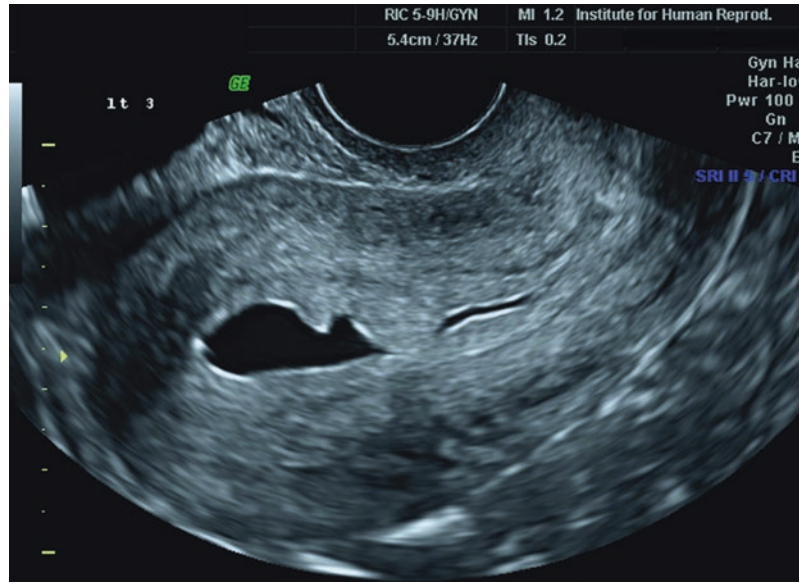

Fig. 12.3 2D longitudinal image of SHG demonstrating two polyps protruding into the uterine cavity

documented that intracavitary abnormalities are significantly more frequent among patients with AUB than with infertility. Polyps were the most common finding both among patients with AUB and infertile women (30% and 13%, respectively) [6, 33]. In addition to the negative effect a polyp may have on fertility, systematic review and meta-analysis demonstrated that the prevalence of premalignant or malignant polyps was 1.7% (68 of 3997) in reproductive-aged women (relative risk 3.86; 95% CI 2.92–5.11) compared to 5.4% (214 of 3946) in postmenopausal women [33]. Both symptomatic vaginal bleeding and postmenopausal status in women with endometrial polyps are associated with an increased risk of endometrial malignancy [33].

Submucosal fibroids were found in 9% of the AUB group and 3% among infertile women [6]. Submucosal fibroids have been shown by meta-analysis to significantly lower pregnancy rates in ART and should be removed by operative hysteroscopy [34, 35]. Besides infertility, the submucosal fibroids may cause bleeding and miscarriages. The European Society of Hysteroscopy has developed a classification system for fibroids which can also assist in the surgical approach. A Type 0 submucosal fibroid has no myometrial invasion, while a T1 has <50% extension and T2 has more than 50% extension into the myometrium. The T0 and T1 are appropriate for the hysteroscopic approach, while the T2 may require more than one procedure or be removed laparoscopically.

2D Versus 3D SHG

When the option of having a 3D SHG scan is available, it may shorten the procedure and the volume of the saline used [36]. 3D SHG vs. 2D SHG is more accurate for diagnosing congenital uterine anomalies [21]. For acquired uterine anomalies, in experienced hands, 3D will not improve the accuracy but may assist in better imaging (Figs. 12.4 and 12.5) [9, 37–41]. For the evaluation of postmenopausal bleeding, 2D and 3D SHG have similar diagnostic accuracy as hysteroscopy with higher patient acceptability of SHG [42, 43].

A 3D US in comparison to a 2D US allows for the visualization of the entire uterine cavity in the coronal view; it can detect the exact placement of uterine fibroids, polyps, and synechiae in the cavity, as well as the mean diameter of different tissues [9, 39–41, 44]. A 3D US examination comprises approximately four steps: (1) data acquisition, (2) volume calculation, (3) image animation, and (4) data storage and transfer. The scans can be obtained

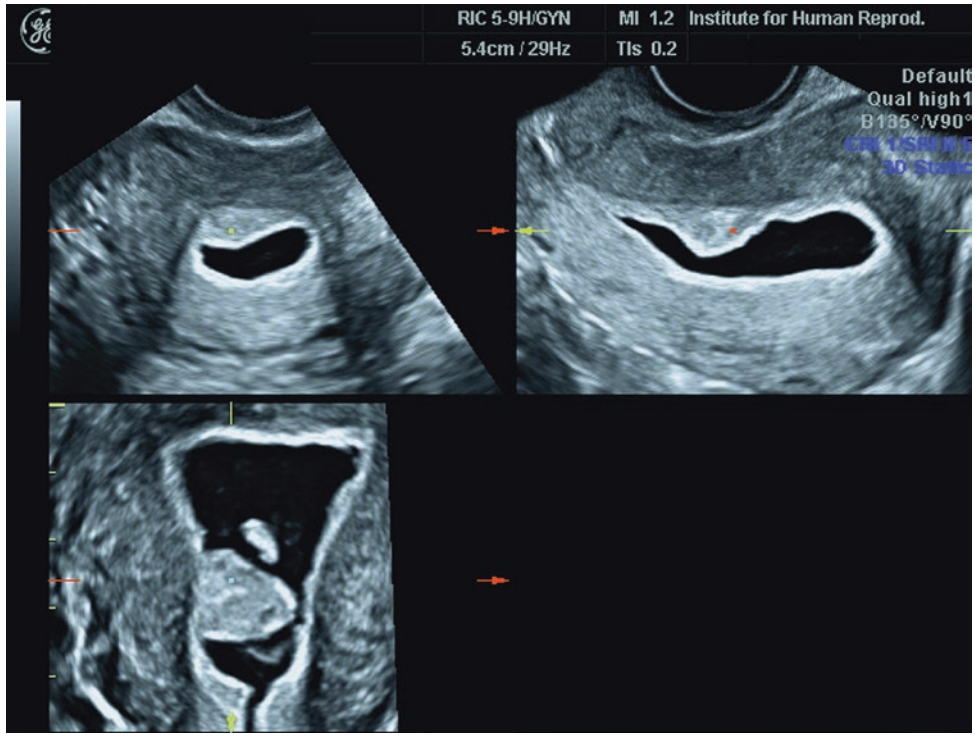

Fig. 12.4 3D SHG images of a uterine polyp. They are able to show the size and location of the stalk of the polyp more accurately in preparation for operative hysteroscopy and for consulting the patient

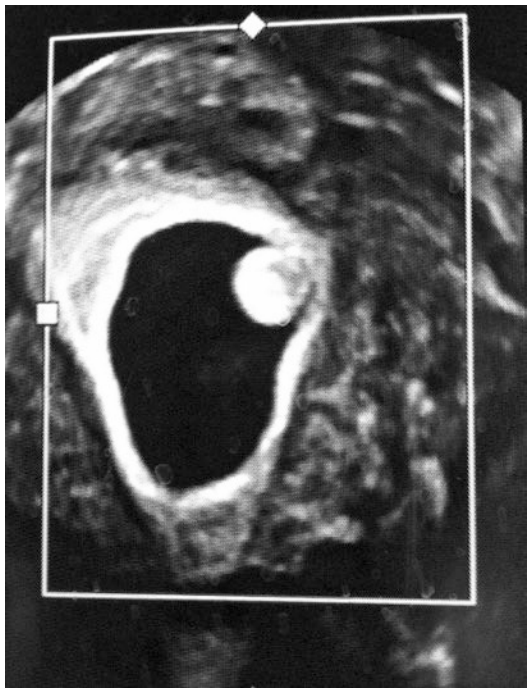

Fig. 12.5 3D SHG image of a corneal uterine polyp providing excellent information for the practitioner and patient on the size and location of the polyp

either freehand, by manual movement through the region of interest (ROI), or automatically, by sweeping through the ROI. 3D US needs post-processing of the received data. Data can be stored and visualized in various displays such as multiplanar with navigation through the planes or surface-rendering mode. For more details on 3D US technique, the reader is referred to Chap. 2.

A saline infusion enhances the contrast in a 3D US and can facilitate the accurate diagnosis of congenital uterine anomalies, especially the arcuate uterus (Fig. 12.6) compared with the septate uterus (Fig. 12.7) and the bicornuate uterus. The serosal edge and the fundal indentation can be clearly seen. Through TUI tomographic imaging, a series of images can visualize the leiomyomata protruding into the uterine cavity vs. deviating the endometrial cavity.

3D adds value to 2D SHG by improving with visualization of the uterine fundus [41, 45]. Others suggest that when the SHG is performed by an experienced examiner, 3D does not add additional value to the 2D SHG [46]. It is the

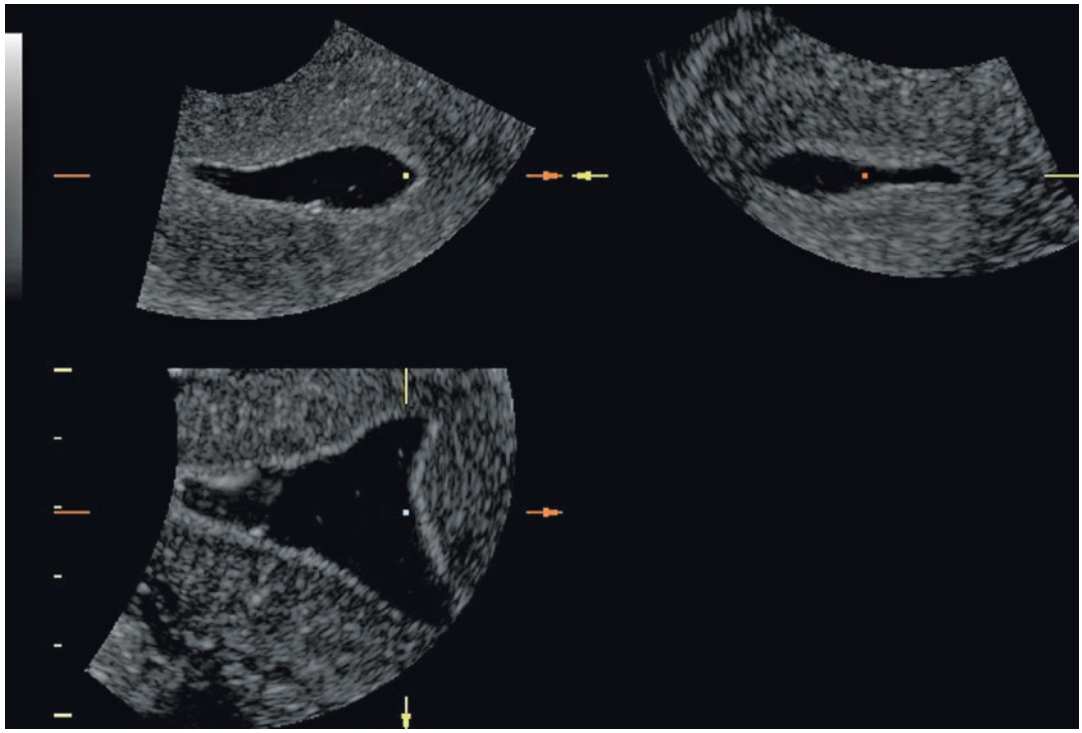

Fig. 12.6 3D SHG demonstrating an arcuate uterus. The visualization of the fundal area at the coronal plane and the ability to measure the depth of the anomaly can easily define arcuate uterus and rule out a septum

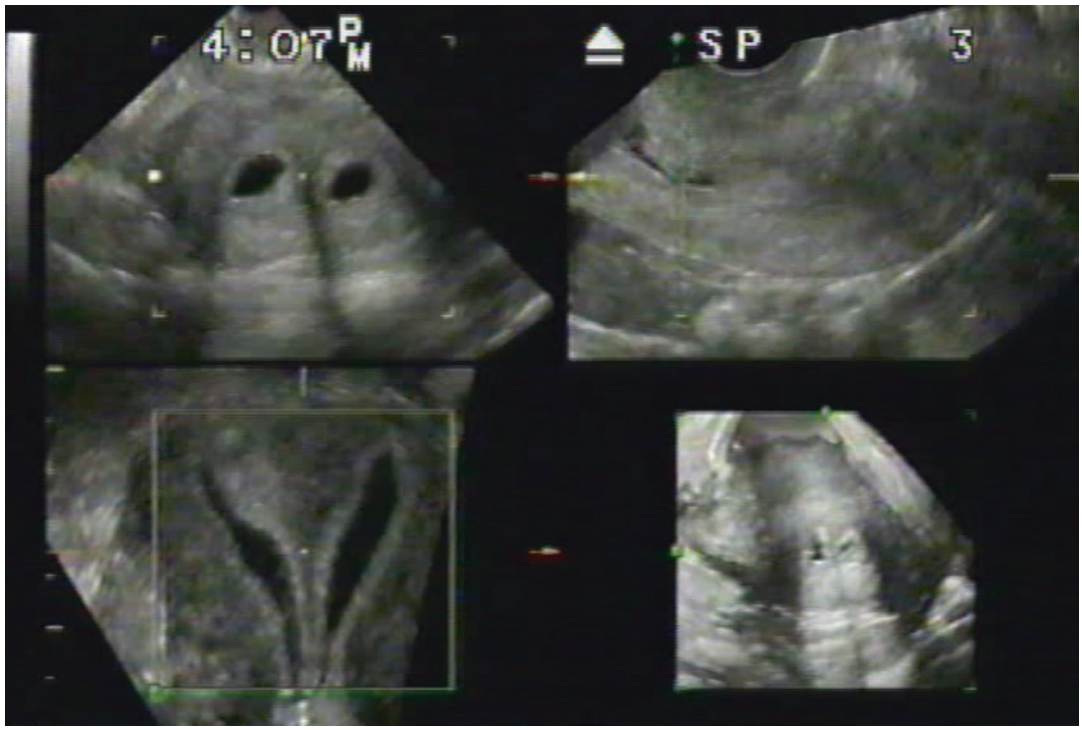

Fig. 12.7 3D SHG demonstrating a completely septated uterus. The 3D reconstruction at the coronal plane leaves no space for imagination, providing definite diagnosis and assisting in planning the surgical treatment needed as well as consulting with the patient

opinion of the authors that adding a 3D US to a 2D SHG will allow the exam to be completed faster with the same or better accuracy [39]. Still, in most cases, 2D SHG is adequate for diagnosing abnormal intracavitary finding.

Gel Instillation SHG

Gel SHG uses hydroxyethyl cellulose gel instead of saline as its medium. This is done in order to try to simplify the technique of artificial uterine cavity distension for SHG [47]. The gel provides a more stable filling of the uterine cavity, allowing a high-quality ultrasonographic visualization of intrauterine pathology by 2D and 3D US [48–53]. Still, most centers will use saline for SHG.

NO Pain with SHG

Tur-Kaspa [19] has recently summarized data supporting that SHG, as well as HSG and hysterocontrastsonography (HyCoSy), should be considered pain-free procedures. Hysterosalpingography (HSG) has a long-standing reputation of being a painful procedure. The use of modern thin catheters and nonionic media that significantly reduces pain during and after HSG [54–58] was unable to affect significantly HSG's "reputation." SHG and HyCoSy, the modern ultrasound-based procedures that are currently used instead of HSG for the evaluation of the uterine cavity and/or the fallopian tubes, "inherited" this high level of fear of pain. It is possible that this stigma discourages patients and leads them to believe that the procedure should be painful when it does not have to be. Several recent randomized controlled trials (RCT) have failed to demonstrate a significant benefit of various pharmacological strategies available to reduce pain during these procedures, suggesting that the pain is more psychological than physical [15–18]. It is the author's opinion, based on evidence data and the experience of performing thousands of these tests, that they can be pain-free for women.

One of the primary ways to make SHG a pain-free procedure is using gentle movements with a thin flexible catheter. Using a rigid catheter, which requires grasping the cervix with a tenaculum, will promote pain. If a balloon catheter is used, it is preferred to inflate the balloon intracervically rather than intrauterine, and the appropriate position of the catheter may be confirmed by pulling it slightly. An RCT recently showed significantly less fluid used for SHG and significantly less pain felt by patients when the balloon was inflated inside the cervix rather than in the lower uterine segment [20]. Warming the saline solutions to body temperature before instillation is another way of reducing patients' discomfort. It is crucial to introduce the saline solution *slowly* into the cavity to prevent abrupt overdistention of the uterus, which would induce immediate pain. While women naturally may feel embarrassed, stressed, and discomfort, as with any medical and gynecological examination, there should be no more fear of pain from procedures such as SHG, HyCoSy, and HSG [19].

SHG Versus Hysteroscopy

Sonohysterography (SHG) was first described in 1986 by Randolph et al. [59]. Randolph et al. instilled saline into the uterus to provide contrast during transabdominal US and compared the SHG findings in 61 women to hysterosalpingography (HSG) and laparoscopy/hysteroscopy. They concluded that real-time US with fluid installation provides an accurate alternative to HSG in screening for uterine abnormalities and tubal patency. Syrop and Sahakian were the first to describe transvaginal SHG in 1992, followed by Parsons and Lense in 1993 [60, 61].

For a long time, hysteroscopy with direct visualization of the intrauterine cavity was considered the gold standard for diagnosing uterine abnormalities [27–31, 34, 35, 62–64]. The percentage of intracavitary abnormalities in women screened by SHG or hysteroscopy for infertility range from 11% to 45% and with polyps range between 6% and 25% [6, 62]. In the last 15 years, accumulating evidence-based data, including

randomized control trials, systematic reviews, and meta-analyses, has demonstrated that SHG has comparable sensitivity, specificity, and accuracy in diagnosing intrauterine abnormalities as hysteroscopy [7, 27–31, 63–72]. Therefore, SHG and other ultrasonography techniques may be used as effectively as hysteroscopy for diagnosing intracavitary abnormalities [28, 30, 31]. Pre-IVF SHG was shown to be effective at limiting cycle cancellations caused by endometrial polyps [73], and it was shown to be highly valuable as a first line office-based diagnostic tool for patients with recurrent IVF implantation failure [74]. These data may explain why most of the high-performing IVF programs in the US use SHG for the evaluation of uterine cavity before ART [75].

In addition, cost analysis comparing SHG vs. hysteroscopy screening prior to IVF showed that using SHG is more cost-effective. While hysteroscopic screening is cost-effective [76], Kim and Rone [77] have shown that SHG is more cost-effective than hysteroscopy. They calculated the average cost per patient of SHG screening (n = 229) and hysteroscopy in the subset of patients who have significant and/or correctable abnormalities (n = 35; 15.3%). The cost per patient using SHG screening with additional hysteroscopy as needed was $645. If hysteroscopy was used to screen the same group of patients instead of SHG, the cost per patient would have been $1281.

Conclusion

SHG can serve as a first-line test for screening and evaluation of the uterine cavity for the diagnosis of infertility and before ART. SHG is a simple, cost-effective, safe, and easy to perform procedure for the evaluation of congenital and acquired uterine abnormalities. While using thin flexible catheters, placing them inside the cervix, and injecting the saline slowly, this procedure can be pain-free. Published guidelines on SHG by ASRM, AIUM, and ACOG are easy to implement in routine gynecological and reproductive medicine practice.

References

1. American College of Obstetricians and Gynecologists. ACOG technology assessment no. 8: Sonohysterography. Obstet Gynecol. 2012 Jun;119(6):1325 (update of ACOG technology assessment in obstetrics and gynecology no. 5: sonohysterography). Obstet Gynecol. 2008;112(6):1467–9.
2. American Institute of Ultrasound in Medicine; Society for Reproductive Endocrinology and Infertility; American Society of Reproductive Medicine. AIUM practice guideline for ultrasonography in reproductive medicine. J Ultrasound Med. 2009;28(1):128–37.
3. Practice Committee of the American Society for Reproductive Medicine. Diagnostic evaluation of the infertile female: a committee opinion. Fertil Steril. 2015;103(6):44–50.
4. American College of Nurse-Midwives (ACNM); American College of Obstetricians and Gynecologists (ACOG); American College of Osteopathic Obstetricians and Gynecologists (ACOOG); American Society for Reproductive Medicine–Society for Reproductive Endocrinology and Infertility (ASRM-SREI);Association of Women's Health, Obstetric and Neonatal Nurses (AWHONN). AIUM practice guideline for the performance of a focused reproductive endocrinology and infertility scan. J Ultrasound Med. 2012;31(11):1865–74.
5. American Institute of Ultrasound in Medicine (AIUM); American College of Radiology (ACR); American College of Obstetricians and Gynecologists (ACOG); Society for Pediatric Radiology (SPR); Society of Radiologists in Ultrasound (SRU). AIUM practice guideline for the performance of ultrasound of the female pelvis. J Ultrasound Med. 2014;33(6):1122–30.
6. Tur-Kaspa I, Gal M, Hartman M, Hartman J, Hartman A. A prospective evaluation of uterine abnormalities by saline infusion sonohysterography (SIS) in 1009 women with infertility or abnormal uterine bleeding. Fertil Steril. 2006;86:1731–5.
7. van Hanegem N, Breijer MC, Khan KS, Clark TJ, Burger MP, Mol BW, et al. Diagnostic evaluation of the endometrium in postmenopausal bleeding: an evidence-based approach. Maturitas. 2011;68(2):155–64.
8. Choudry A, Shukr I, Khan S, Hafeez H, Jamal S, Anwer A. Acceptability and accuracy of saline infusion sonohysterography in women with postmenopausal bleeding. J Coll Physicians Surg Pak. 2010;20(9):571–5.
9. Goldstein SR. Modern evaluation of the endometrium. Obstet Gynecol. 2010;116(1):168–76.
10. Bittencourt CA, Dos Santos Simões R, Bernardo WM, Fuchs LFP, Soares Júnior JM, Pastore AR, Baracat EC. Accuracy of saline contrast sonohysterography in detection of endometrial polyps and submucosal leiomyomas in women of reproductive age with abnormal uterine bleeding: systematic review and meta-analysis. Ultrasound Obstet Gynecol. 2017;50(1):32–9.

11. Bittencourt CA, Dos Santos Simões R, Bernardo WM, Fuchs LFP, Soares Júnior JM, Pastore AR, et al. Accuracy of saline contrast sonohysterography in detection of endometrial polyps and submucosal leiomyomas in women of reproductive age with abnormal uterine bleeding: systematic review and meta-analysis. Ultrasound Obstet Gynecol. 2017;50(1):32–9.
12. Moschos E, Ashfaq R, McIntire DD, Liriano B, Twickler DM. Saline-infusion sonography endometrial sampling compared with endometrial biopsy in diagnosing endometrial pathology. Obstet Gynecol. 2009;113(4):881–7.
13. Allison SJ, Horrow MM, Kim HY, Lev-Toaff AS. Saline-infused sonohysterography: tips for achieving greater success. Radiographics. 2011;31(7):1991–2004.
14. ACOG Committee on Practice Bulletins--Gynecology. ACOG practice bulletin. Antibiotic prophylaxis for gynecologic procedures. No. 104, May 2009. Obstet Gynecol. 2009;113:1180–9.
15. Ahmad G, Duffy J, Watson AJ. Pain relief in hysterosalpingography. Cochrane Database Syst Rev. 2007;(2):CD006106.
16. Ahmad G, Attarbashi S, O'Flynn H, Watson AJ. Pain relief in office gynaecology: a systematic review and meta-analysis. Eur J Obstet Gynecol Reprod Biol. 2011;155:3–13.
17. Moro F, Selvaggi L, Sagnella F, Morciano A, Martinez D, Gangale MF, et al. Could antispasmodic drug reduce pain during Sonosalpingohysterography (SSHG) in infertile patients? A randomized double-blinded clinical trial. Ultrasound Obstet Gynecol. 2012;39(3):260–5.
18. Yung SS, Lai SF, Lam MT, Lee VC, Li RH, Ho PC, et al. Randomized, controlled, double-blind trial of topical lidocaine gel and intrauterine lidocaine infusion for pain relief during saline contrast sonohysterography. Ultrasound Obstet Gynecol. 2016;47(1):17–21.
19. Tur-Kaspa I. Fear no pain: uterine cavity and tubal patency assessment tests should be pain free. Ultrasound Obstet Gynecol. 2012;39(3):247–51.
20. Spieldoch RL, Winter TC, Schouweiler C, Ansay S, Evans MD, Lindheim SR. Optimal catheter placement during sonohysterography: a randomized controlled trial comparing cervical to uterine placement. Obstet Gynecol. 2008;111(1):15–21.
21. Dreisler E, Stampe Sørensen S. Müllerian duct anomalies diagnosed by saline contrast sonohysterography: prevalence in a general population. Fertil Steril. 2014;102(2):525–9.
22. Ludwin A, Ludwin I, Pityński K, Banas T, Jach R. Role of morphologic characteristics of the uterine septum in the prediction and prevention of abnormal healing outcomes after hysteroscopic metroplasty. Hum Reprod. 2014;29(7):1420–31. [Epub ahead of print].
23. Ludwin A, Ludwin I, Banas T, Knafel A, Miedzyblocki M, Basta A. Diagnostic accuracy of sonohysterography, hysterosalpingography and diagnostic hysteroscopy in diagnosis of arcuate, septate and bicornuate uterus. J Obstet Gynaecol Res. 2011;37(3):178–86.
24. Chan YY, Jayaprakasan K, Zamora J, Thornton JG, Raine-Fenning N, Coomarasamy A. The prevalence of congenital uterine anomalies in unselected and high-risk populations: a systematic review. Hum Reprod Update. 2011;17(6):761–71.
25. Chan YY, Jayaprakasan K, Tan A, Thornton JG, Coomarasamy A, Raine-Fenning NJ. Reproductive outcomes in women with congenital uterine anomalies: a systematic review. Ultrasound Obstet Gynecol. 2011;38(4):371–82.
26. The American Fertility Society. The American Fertility Society classification of adnexal adhesions, distal tubal occlusion, tubal occlusion secondary to tubal ligation, tubal pregnancies, Mullerian anomalies and intrauterine adhesions. Fertil Steril. 1988;49:944–55.
27. van Dongen H, de Kroon CD, Jacobi CE, Trimbos JB, Jansen FW. Diagnostic hysteroscopy in abnormal uterine bleeding: a systematic review and meta-analysis. BJOG. 2007;114(6):664–75.
28. Saunders RD, Shwayder JM, Nakajima ST. Current methods of tubal patency assessment. Fertil Steril. 2011;95:2171–9.
29. Taylor E, Gomel V. The uterus and fertility. Fertil Steril. 2008;89:1–16.
30. Van Voorhis BJ. Ultrasound assessment of the uterus and fallopian tube in infertile women. Semin Reprod Med. 2008;26:232–40.
31. Devroey P, Fauser BCJM, Diedrich K, and on behalf of the Evian Annual Reproduction (EVAR) Workshop Group 2008. Approaches to improve the diagnosis and management of infertility. Hum Reprod Update. 2009;15:391–408.
32. Ludwin A, Martins WP, Ludwin I. Uterine niche by three-dimensional sonohysterography and volumetric quantification: techniques and scoring classification system. Ultrasound Obstet Gynecol. 2019;53(1):139–43.
33. Lee SC, Kaunitz AM, Sanchez-Ramos L, Rhatigan RM. The oncogenic potential of endometrial polyps: a systematic review and meta-analysis. Obstet Gynecol. 2010;116(5):1197–205.
34. Bozdag G, Aksan G, Esinler I, Yarali H. What is the role of office hysteroscopy in women with failed IVF cycles? Reprod Biomed Online. 2008;17:410–5.
35. Bosteels J, Kasius J, Weyers S, Broekmans FJ, Mol BW, D'Hooghe TM. Hysteroscopy for treating subfertility associated with suspected major uterine cavity abnormalities. Cochrane Database Syst Rev. 2013;(1):CD009461. https://doi.org/10.1002/14651858.CD009461.pub2.
36. Tur-Kaspa I, Segal S, Zohav E. The ART of imaging: three-dimensional (3D) ultrasound and ART. In: Revelli A, Tur-Kaspa I, Holte JG, Massobrio M, editors. Biotechnology of human reproduction. New York: The Parthenon Publishing Group; 2003. p. 363–73.

37. Mora-Guanche P, Sparacino L, García-Guzman R, Bennett RA, Hernández J, Palumbo A. Three-dimensional sonohysterography (SHG) has improved diagnostic accuracy for intrauterine pathology compared to two-dimensional SHG: a prospective pilot study in infertility patients. Fertil Steril. 2009;92(Suppl):S119.
38. Ludwin A, Pityński K, Ludwin I, Banas T, Knafel A. Two- and three-dimensional ultrasonography and sonohysterography versus hysteroscopy with laparoscopy in the differential diagnosis of septate, bicornuate, and arcuate uteri. J Minim Invasive Gynecol. 2013;20(1):90–9.
39. Nieuwenhuis LL, Hermans FJ, Bij de Vaate AJM, Leeflang MM, Brölmann HA, Hehenkamp WJ, et al. Three-dimensional saline infusion sonography compared to two-dimensional saline infusion sonography for the diagnosis of focal intracavitary lesions. Cochrane Database Syst Rev. 2017;(5):CD011126.
40. Inoue T, Kitajima M, Taniguchi K, Masuzaki H. Three-dimensional saline-infusion sonohysterography is useful for the identification of endometrial polyp. J Obstet Gynaecol Res. 2016;42(7):855–9.
41. Arya S, Kupesic Plavsic S. Preimplantation 3D ultrasound: current uses and challenges. J Perinat Med. 2017;45(6):745–58.
42. Katsetos C, Radhakrishnan S, Koumousidis A, Kontoyannis M, Sanoulis V, Spaliaras D, et al. Comparison of transvaginal 3D sonohysterography with outpatient hysteroscopy in the evaluation of abnormal uterine bleeding. Clin Exp Obstet Gynecol. 2013;40(1):74–7.
43. Adel M, Kandil M, Abo-Elnasr M, Sanad Z, Farag H. Three-dimensional sonohysterography may replace hysteroscopy for women with perimenopausal bleeding. Climacteric. 2014;17(1):55–9.
44. El-Sherbiny W, El-Mazny A, Abou-Salem N, Mostafa WS. The diagnostic accuracy of two- vs three-dimensional sonohysterography for evaluation of the uterine cavity in the reproductive age. J Minim Invasive Gynecol. 2015;22(1):127–31.
45. Hartman MR, Hartman JD, Oprea C, Hartman BD, Hartman A. 3D ultrasound vs 3D sonohysterography in the diagnosis of uterine anomalies: a prospective blinded study of 600 consecutive infertility patients. Fertil Steril. 2008;90(Suppl):S20.
46. Opolskiene G, Sladkevicius P, Valentin L. Two- and three-dimensional saline contrast sonohysterography: interobserver agreement, agreement with hysteroscopy and diagnosis of endometrial malignancy. Ultrasound Obstet Gynecol. 2009;33(5):574–82.
47. Exalto N, Stappers C, van Raamsdonk LA, Emanuel MH. Gel instillation sonohysterography: first experience with a new technique. Fertil Steril. 2007;87(1):152–5.
48. Marasinghe JP, Senanayake HM. Gel instillation sonohysterography: first experience with a new technique. Fertil Steril. 2007;88(2):536–7.
49. Van den Bosch T, Betsas G, Van Schoubroeck D, Daemen A, Vandenbroucke V, Cornelis A, De Moor B, et al. Gel infusion sonography in the evaluation of the uterine cavity. Ultrasound Obstet Gynecol. 2009;34(6):711–4.
50. Bij de Vaate AJ, Brölmann HA, van der Slikke JW, Emanuel MH, Huirne JA. Gel instillation sonohysterography (GIS) and saline contrast sonohysterography (SCSH): comparison of two diagnostic techniques. Ultrasound Obstet Gynecol. 2010;35(4):486–9.
51. Bij de Vaate AJ, Brölmann HA, van der Voet LF, van der Slikke JW, Veersema S, Huirne JA. Ultrasound evaluation of the Cesarean scar: relation between a niche and postmenstrual spotting. Ultrasound Obstet Gynecol. 2011;37(1):93–9.
52. Van Den Bosch T, Van Schoubroeck D, Luts J, Bignardi T, Condous G, Epstein E, et al. Effect of gel-instillation sonography on Doppler ultrasound findings in endometrial polyps. Ultrasound Obstet Gynecol. 2011;38(3):355–9.
53. Van den Bosch T, Van Schoubroeck D, Daemen A, Domali E, Vandenbroucke V, De Moor B, et al. Lidocaine does not reduce pain perception during gel instillation sonography or subsequent office hysteroscopy: results of a randomized trial. Gynecol Obstet Investig. 2011;71(4):236–9.
54. Golan A, Tur-Kaspa I. The management of the infertile patient with proximal tubal occlusion. Hum Reprod. 1996;11:1833–4.
55. Tur-Kaspa I, Seidman DS, Soriano D, Greenberg I, Dor J, Bider D. Hysterosalpingography with a balloon catheter versus a metal cannula: a prospective, randomized, blinded comparative study. Hum Reprod. 1998;13(1):75–7.
56. Tur-Kaspa I, Moscovici O, Meltzer S, Peled R, Rabinson J, Segal S. Transcervical tubal catheterization (TTC) is the treatment of choice for infertile women with proximal tubal obstruction – an experience with 1010 fallopian tubes. Fertil Steril. 2002;78(Suppl 1):S90.
57. Ricci G, Guastalla P, Ammar L, Cervi G, Guarnieri S, Sartore A. Balloon catheter vs. cervical vacuum cup for hysterosalpingography: a prospective, randomized, single-blinded study. Fertil Steril. 2007;87(6):1458–67.
58. Anserini P, Delfino F, Ferraiolo A, Remorgida V, Menoni S, De Caro G. Strategies to minimize discomfort during diagnostic hysterosalpingography with disposable balloon catheters: a randomized placebo-controlled study with oral nonsteroidal premedication. Fertil Steril. 2008;90(3):844–8.
59. Randolph JR, Ying YK, Maier DB, Schmidt CL, Riddick DH. Comparison of real-time ultrasonography, hysterosalpingography, and laparoscopy/hysteroscopy in the evaluation of uterine abnormalities and tubal patency. Fertil Steril. 1986;46:828–32.
60. Syrop C, Sahakian V. Transvaginal sonographic detection of endometrial polyps with fluid contrast augmentation. Obstet Gynecol. 1992;79:1041–3.
61. Parsons A, Lense J. Sonohysterography for endometrial abnormalities: preliminary results. J Clin Ultrasound. 1993;21:87–9.

62. Fatemi HM, Kasius JC, Timmermans A, van Disseldorp J, Fauser BC, Devroey P, et al. Prevalence of unsuspected uterine cavity abnormalities diagnosed by office hysteroscopy prior to in vitro fertilization. Hum Reprod. 2010;25(8):1959–65.
63. Grimbizis GF, Tsolakidis D, Mikos T, Anagnostou E, Asimakopoulos E, Stamatopoulos P, et al. A prospective comparison of transvaginal ultrasound, saline infusion sonohysterography, and diagnostic hysteroscopy in the evaluation of endometrial pathology. Fertil Steril. 2010;94:2720–5.
64. Brown SE, Coddington CC, Schnorr J, Toner JP, Gibbons W, Oehninger S. Evaluation of outpatient hysteroscopy, saline infusion hysterosonography, and hysterosalpingography in infertile women: a prospective, randomized study. Fertil Steril. 2000;74(5):1029–34.
65. Ayida G, Chamberlain P, Barlow D, Kennedy S. Uterine cavity assessment prior to in vitro fertilization: comparison of transvaginal scanning, saline contrast hysterosonography and hysteroscopy. Ultrasound Obstet Gynecol. 1997;10(1):59–62.
66. Loverro G, Nappi L, Vicino M, Carriero C, Vimercati A, Selvaggi L. Uterine cavity assessment in infertile women: comparison of transvaginal sonography and hysteroscopy. Eur J Obstet Gynecol Reprod Biol. 2001;100(1):67–71.
67. de Kroon CD, de Bock GH, Dieben SW, Jansen FW. Saline contrast hysterosonography in abnormal uterine bleeding: a systematic review and meta-analysis. BJOG. 2003;110:938–47.
68. Ragni G, Diaferia D, Vegetti W, Colombo M, Arnoldi M, Crosignani PG. Effectiveness of sonohysterography in infertile patient work-up: a comparison with transvaginal ultrasonography and hysteroscopy. Gynecol Obstet Investig. 2005;59:184–8.
69. Bingol B, Gunenc Z, Gedikbasi A, Guner H, Tasdemir S, Tiras B. Comparison of diagnostic accuracy of saline infusion sonohysterography, transvaginal sonography and hysteroscopy. J Obstet Gynaecol. 2011;31(1):54–8.
70. Yang T, Pandya A, Marcal L, Bude RO, Platt JF, Bedi DG, et al. Sonohysterography: principles, technique and role in diagnosis of endometrial pathology. World J Radiol. 2013;5(3):81–7.
71. Seshadri S, El-Toukhy T, Douiri A, Jayaprakasan K, Khalaf Y. Diagnostic accuracy of saline infusion sonography in the evaluation of uterine cavity abnormalities prior to assisted reproductive techniques: a systematic review and meta-analyses. Hum Reprod Update. 2015;21(2):262–74.
72. Armstrong SC, Showell M, Stewart EA, Rebar RW, Vanderpoel S, Farquhar CM. Baseline anatomical assessment of the uterus and ovaries in infertile women: a systematic review of the evidence on which assessment methods are the safest and most effective in terms of improving fertility outcomes. Hum Reprod Update. 2017;23(5):533–47.
73. Yauger BJ, Feinberg EC, Levens ED, Gustofson RL, Larsen FW, DeCherney AH. Pre-cycle saline infusion sonography minimizes assisted reproductive technologies cycle cancellation due to endometrial polyps. Fertil Steril. 2008;90:1324–6.
74. Shokeir T, Abdelshaheed M. Sonohysterography as a first-line evaluation for uterine abnormalities in women with recurrent failed in vitro fertilization-embryo transfer. Fertil Steril. 2009;91:1321–2.
75. Van Voorhis BJ, Thomas M, Surrey ES, Sparks A. What do consistently high-performing in vitro fertilization programs in the U.S. do? Fertil Steril. 2010;94(4):1346–9.
76. Kasius JC, Eijkemans RJ, Mol BW, Fauser BC, Fatemi HM, Broekmans FJ. Cost-effectiveness of hysteroscopy screening for infertile women. Reprod Biomed Online. 2013;26(6):619–26.
77. Kim AH, Rone HM. Cost of sonohysterographic (SHG) versus hysteroscopic (HS) screening prior to in vitro fertilization (IVF). Fertil Steril. 2006;86(3):S52–3.

Part V

Ultrasound and Male Infertility

Ultrasound in Male Infertility

13

Isaac Samuel Lam, Landon W. Trost,
David D. Casalino, and Robert E. Brannigan

Introduction

Infertility remains a significant issue both for the individual couple and from a public health standpoint. Although the exact prevalence is unknown, with varied results reported by region, definition, and methodology utilized, infertility is reported to affect 14–20% of couples with a male-factor contributory in 56–75% of cases [1–9]. Infertility is commonly defined as the inability of a couple to achieve pregnancy following at least 12 months of unprotected intercourse. Couples presenting with infertility are frequently evaluated concomitantly to assess for the presence of correctable male and female factors with several guidelines/algorithms available to assist treating clinicians [10–14].

In addition to medical history, physical examination, semen analysis, and laboratory assessments, ultrasonography has a role in both the evaluation and treatment of male-factor infertility. Although significant variability exists in the actual utilization, ultrasound may be employed in the initial assessment, as a confirmatory/adjunctive test to physical examination; as a predictor of underlying fertility and operative outcomes, in the treatment of certain causes of infertility; and in the acquisition of sperm for assisted reproductive techniques (ARTs). Ultrasound is frequently selected as a first-line modality among imaging options due to its noninvasive nature and ready availability.

Overview of Genitourinary Ultrasonography

The use of ultrasound for evaluation of male-factor infertility predominantly consists of scrotal and transrectal ultrasonography with occasional use of retroperitoneal imaging in select cases. Prior to imaging, patients are positioned so as to maximize image quality and patient comfort. For scrotal ultrasonography, patients are placed in a semi-recumbent versus supine position with the penis retracted cephalad. A warm probe is applied to minimize contraction of the dartos muscle. For transrectal ultrasonography, the patient is most commonly positioned

I. S. Lam
Northwestern University Feinberg School of Medicine, Department of Urology, Chicago, IL, USA

L. W. Trost
Mayo Clinic, Department of Urology, Rochester, MN, USA

D. D. Casalino
Northwestern University School of Medicine, Department of Radiology, Chicago, IL, USA

R. E. Brannigan (✉)
Northwestern Memorial Hospital, Department of Urology, Chicago, IL, USA
e-mail: r-brannigan@northwestern.edu

L. A. Stadtmauer, I. Tur-Kaspa (eds.), *Ultrasound Imaging in Reproductive Medicine*,
https://doi.org/10.1007/978-3-030-16699-1_13

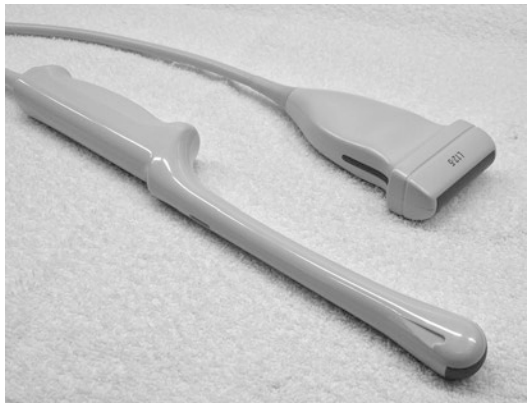

Fig. 13.1 Ultrasound probes: photo shows a high-frequency, linear array transducer above and a curved array endocavitary transducer below

in the lateral decubitus position with the knees drawn to the chest. Alternatively, the patient may be placed in dorsolithotomy or prone jackknife depending on the clinical context of the procedure. Evaluation of the retroperitoneum is performed in a sloppy lateral to full flank position, with the highest-frequency transducer utilized to permit sufficient depth of penetration.

Similar to other applications of ultrasonography, imaging is achieved through transmission of ultrasonic waves from the transducer, which are subsequently reflected and represented graphically on a monitor. Structures with increased density or points of transition between structures of varying densities reflect a greater portion of sound waves and are visualized as brighter when compared to those of lower density. Structures which do not permit passage of ultrasound waves such as calcifications result in complete reflectivity which is perceived as a bright image with an absence of signal distal to the calcification. This "shadowing" is clearly demonstrated with larger calcifications and may be imperceptible in smaller applications such as with testicular microlithiasis.

The selection of the probe utilized depends on the desired application including organ visualized and depth of penetration required (Fig. 13.1). In general, increasing frequencies are associated with improved tissue resolution and decreasing depths of penetration. Given the relatively short skin-to-organ distance with scrotal and transrectal ultrasonography, the majority of probes utilized range from 7.5 to 14 MHz.

In addition to increasing ultrasound frequency, various forms of Doppler may be utilized to enhance the diagnostic value of the imaging obtained. Power (i.e., color flow) Doppler refers to a form of pulse wave Doppler in which returning echoes are assigned a color (red if moving toward the probe, blue if moving away) so as to differentiate images with velocity (vascular structures) from nonmotile tissue. Duplex Doppler includes the combination of both spectral (flow velocity represented graphically on an *X*/*Y* axis) and flow color imaging; it is particularly useful to assess the intensity of vascular flow and to assign resistive indices (Fig. 13.2). Additional techniques including elastosonography are being evaluated for their clinical utility in routine practice.

To further discuss the role of ultrasound in the diagnosis and management of male-factor infertility, the current chapter is outlined to review normal and abnormal findings on scrotal and transrectal ultrasonography associated with infertility. When available, standard measurements and anatomic variants are reported. See Table 13.1 for a summary of ultrasound findings associated with male infertility. Brief mention is given to the management of various infertility causes when they relate to pre- and posttreatment ultrasound findings and to the use of ultrasonography with assisted reproductive techniques.

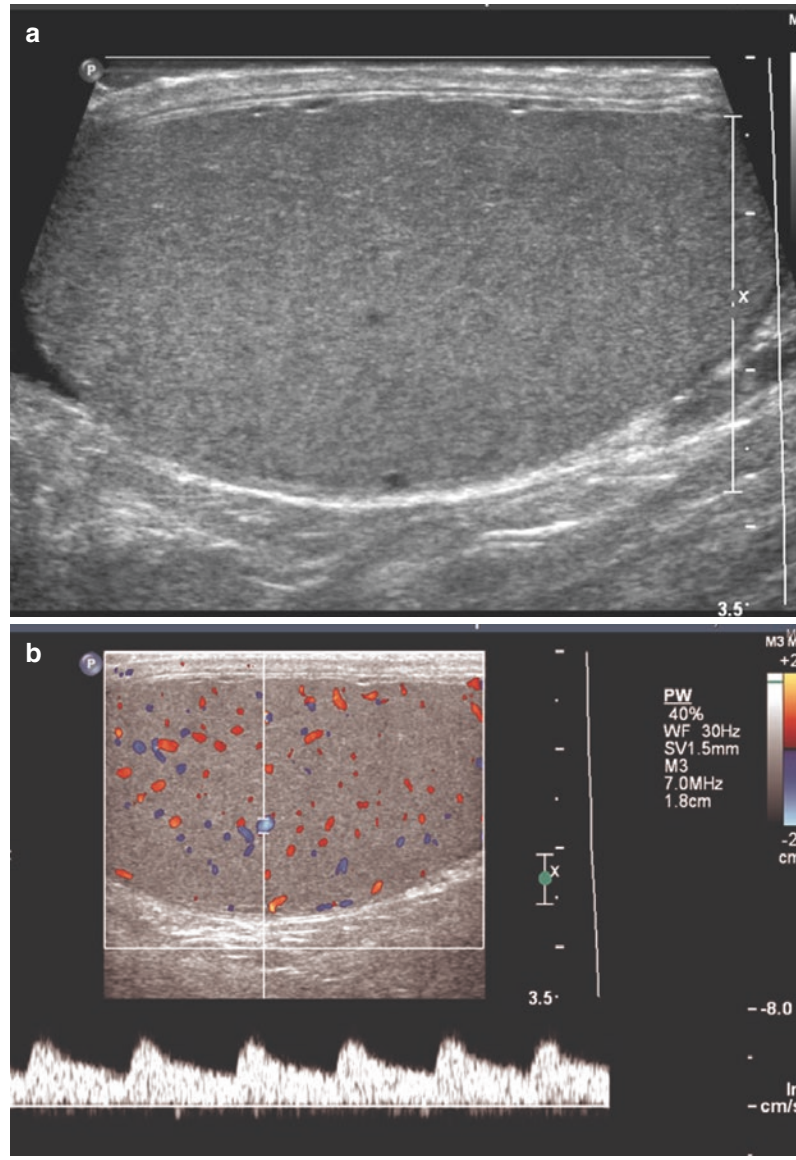

Fig. 13.2 Normal testis: longitudinal sonogram (**a**) shows the testis to have a homogeneous echogenicity and echotexture. Longitudinal color Doppler sonogram (**b**) with duplex shows a normal blood flow pattern and normal intratesticular artery velocity tracing

Table 13.1 Ultrasound findings associated with male infertility

Structure	US findings	Associations with infertility
Scrotal ultrasound		
Epididymis	Normal caput diameter 7–8 mm	
Cysts	Hypo-/anechoic, well circumscribed, commonly located at head	Simple cysts (no sperm) and spermatoceles (sperm present) not associated with infertility
Infections	Enlarged, thickened, decreased echogenicity	MAGI[a] associated with decreased motility, increased sperm DNA fragmentation, abnormal sperm morphology
Masses	Presence of vascularity, varied echotexture	Most commonly adenomatoid tumors; others include cystadenomas, mesotheliomas, sarcomas
Obstruction	Epididymal enlargement, prominence of rete testis, hypoechoic appearance	Normal-volume ejaculate with oligo-/azoospermia
Testicles		
Cysts	Hypo-/anechoic, well circumscribed, thin wall	Increased incidence, no known impact on fertility
Hydroceles	Fluid located between tunica albuginea and vaginalis	Increased incidence, no known impact on fertility
Infections	Early – decreased echogenicity, increased heterogeneity, enlargement	Associated with subsequent infertility, particularly with postpubertal mumps
	Late – atrophy, increased echogenicity	
Masses	Presence of vascularity, varied echotexture	Increased incidence of benign and malignant masses
Microlithiasis	Increased small focal echogenicity, absence of shadowing	Increased incidence, associated with carcinoma in situ, no known impact on fertility
Torsion	Early – hyperemia, increased size	Unilateral testicular loss associated with decreased sperm density, increased FSH/LH
	Late – absence of flow, "whirlpool" sign	
Trauma	May visualize seminiferous tubules, hematomas	May lead to secondary infertility, antisperm antibodies
Testicular cord		
Masses	Presence of vascularity, varied echotexture	Adenomatoid tumor most common, no known impact on fertility
Varicocele	Internal spermatic vein ≥3 mm	Decreased sperm count, motility, abnormal morphology, decreased sperm function, varicocele grade inversely associated with sperm density
Vas deferens	CBAVD[b] with dilated efferent ducts, prominent epididymal heads, and rete testes	CBAVD found in patients with cystic fibrosis, absence/anomalies of SVs[c], renal agenesis/anomalies
Transrectal ultrasound		
Prostate		
Cysts	May be located peripherally, midline, paramedian, hypo-/anechoic, thin wall	May result in obstruction, rare malignant processes
Seminal vesicles		
EDO[d]	Dilated ejaculatory duct and SVs, may have calcifications	Low-volume ejaculate, oligo-/azoospermia, decreased fructose and semen pH, requires confirmatory aspiration demonstrating sperm

[a]*MAGI* male accessory gland infections, [b]*CBAVD* congenital bilateral absence of the vas deferens, [c]*SV* seminal vesicles, [d]*EDO* ejaculatory duct obstruction

Scrotal Ultrasonography

Ultrasound is an optimal imaging modality for the primary evaluation of scrotal pathology. In addition to providing real-time assessments, including patient assistance in localization of findings (e.g., pain), advancements in technology permit increasing resolution of underlying structures, assessments of vascular flow, and tissue characteristics (elastosonography). As the scrotum typically does not consist of gas-containing or large calcified structures, a complete visualization of anatomy is available in multiple planes of imaging.

The role for scrotal ultrasonography in the evaluation of the infertile male has been previously established. Scrotal abnormalities have been reported to occur in 38–65% of infertile men, approximately 60–70% of which were not found clinically on physical examination alone [15, 16]. In reporting scrotal ultrasound findings in 545 infertile males with a mean age of 36 years, Sakamoto and colleagues identified left varicoceles in 313 (57.4%), testicular microlithiasis in 30 (5.5%), epididymal cysts in 21 (3.9%), right varicoceles in 4 (0.8%), testicular cysts in 3 (0.6%), and a testicular tumor, intrascrotal hemangioma, and hydrocele of the spermatic cord in 1 (0.2%) patient, respectively [15]. When compared to normospermic men, males with infertility have been confirmed to have significantly increased rates of scrotal findings including varicocele (35.5% vs. 16%), hydrocele (16.7% vs. 8.7%), testicular microlithiasis (9.8% vs. 2%), epididymal enlargement (9% vs. 2.6%), and epididymal cysts (7.7% vs. 2%) [17].

Color flow Doppler adds further value to scrotal ultrasonography as it provides real-time assessments with increased sensitivity to testicular blood flow. This is particularly useful in cases of testicular ischemia, trauma, differentiation of testicular/paratesticular lesions, and infectious processes. Elastosonography, which further assesses tissue firmness, has also been reported to improve characterization of testicular lesions <1 cm [18].

Mapping testicular perfusion may provide useful information for potential future procedures as well such as for testicular sperm extraction (TESE) in men with azoospermia. Limited data suggests that patients with azoospermia tend to have enhanced quality and quantity of sperm in TESE areas with increased testicular perfusion [19]. Information provided by scrotal ultrasound may allow urologists to better localize areas of high perfusion during the biopsy among men with nonobstructive azoospermia.

Testicular volume is another indicator of fertility that can be accurately characterized through ultrasound. Ultrasound is superior to the traditional orchidometer in evaluating testicular volume as the latter tends to overestimate volume, especially when measuring smaller testes that are more prevalent in infertile patients [20]. A study of almost 500 patients demonstrated a correlation between testicular volume and sperm parameters including total motile sperm, total sperm count, and sperm density [21]. A later study by Sakamoto et al. confirmed the association between decreased testicular volume and reduced total sperm counts [22]. Despite this data, it should be noted that in some cases, large testicles may be indicative of obstructive azoospermia. In addition to directly correlating to worsened sperm parameters, lower testicular volume may also suggest a potential varicocele. Both Sakamoto et al. and Diamond et al. performed studies indicating an association between smaller testicles on ultrasound with presence of a varicocele [23, 24].

A testicular resistive index (RI) also provides useful information on male infertility as well. RI is derived from scrotal ultrasound and is calculated with the peak systolic (PSV) and end diastolic velocities (EDV) from testicular vessel groups, utilizing the equation RI = PSV − EDV/PSV × 100. Generally, providers use a cutoff of greater than 0.6 to suggest possible nonobstructive infertility [25]. A higher RI has been associated with varicoceles, lower sperm count, and other scrotal pathologies [26, 27]. Obtaining a RI may therefore provide additional information in the characterization of male infertility.

Although a definitive role for ultrasound in the routine evaluation of the infertile male remains debatable, given the high rate of intrascrotal findings in infertile men, particularly the increased risk of significant pathology such as testicular tumors, scrotal ultrasound is becoming increasingly utilized in the assessment of males presenting with infertility. Additionally, it may provide helpful supplementary information as noted above.

Paratesticular Structures

Epididymis

Ultrasound evaluation of the epididymis is performed to assess for the presence of infectious findings, masses or lesions, or evidence of epididymal obstruction. Measurements of the epididymis

are obtained at the caput. A normal epididymis measures 7–8 mm in diameter, with increasing diameter associated with infectious processes [28]. Epididymitis as a clinical diagnosis may be confirmed with ultrasound findings, which include an enlarged or thickened epididymis with decreased echogenicity.

Infectious processes associated with infertility are more broadly categorized as male accessory gland infections (MAGI), which include infections of the epididymis, seminal vesicles, prostate, or bladder. Organisms commonly identified are *Chlamydia*, *Mycoplasma*, and *E. coli*. However, organisms such as tuberculosis have also been directly associated with infertility [29]. Although relatively limited data exist and vary by region, the prevalence of MAGI and infertility have been reported to occur in up to 12% of cases [30]. Several studies have identified abnormal semen parameters in patients with MAGI including decreased motility, increased abnormal forms, and a higher rate of DNA fragmentation [31, 32]. Despite these findings, the etiologic role of MAGI with male-factor infertility remains unclear, as reports have failed to demonstrate consistent findings [33, 34].

Epididymal masses may be further defined as solid versus cystic. Solid masses are most commonly benign adenomatoid tumors with additional lesions encountered including cystadenoma, mesothelioma, or sarcomas (Fig. 13.3). Cysts of the epididymis are benign lesions commonly located at the head of the epididymis and may represent simple cysts (no sperm in fluid) or spermatoceles (sperm in fluid) (Fig. 13.4). Although epididymal cysts are found more commonly among men with infertility, they have not been shown to result in epididymal obstruction or infertility [17]. In performing surgical resection of spermatoceles and hydroceles, epididymal injury has been reported to occur in 17 and 6% of cases, respectively [35]. A more recent report by Kauffman and colleagues describing a microsurgical technique of spermatocelectomy demonstrated no changes in sperm count among patients with pre- and postoperative semen analyses, suggesting the absence of iatrogenic epididymal obstruction [36].

In addition to identifying paratesticular masses and infectious processes, improvements in ultrasound resolution have led to its utility in

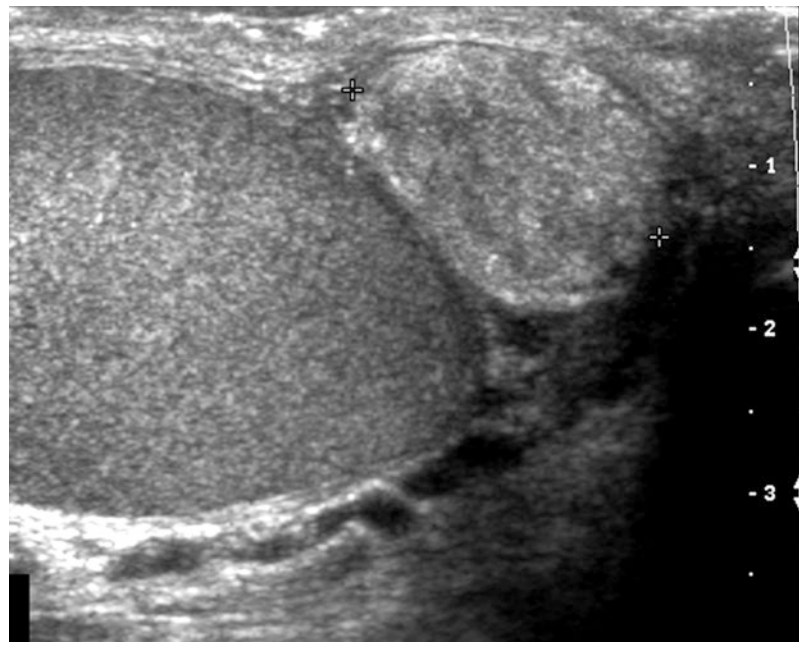

Fig. 13.3 Solid epididymal mass: longitudinal sonogram shows a normal right testis and a solid, heterogeneous mass (between calipers) of the epididymal tail that proved to be an adenomatoid tumor

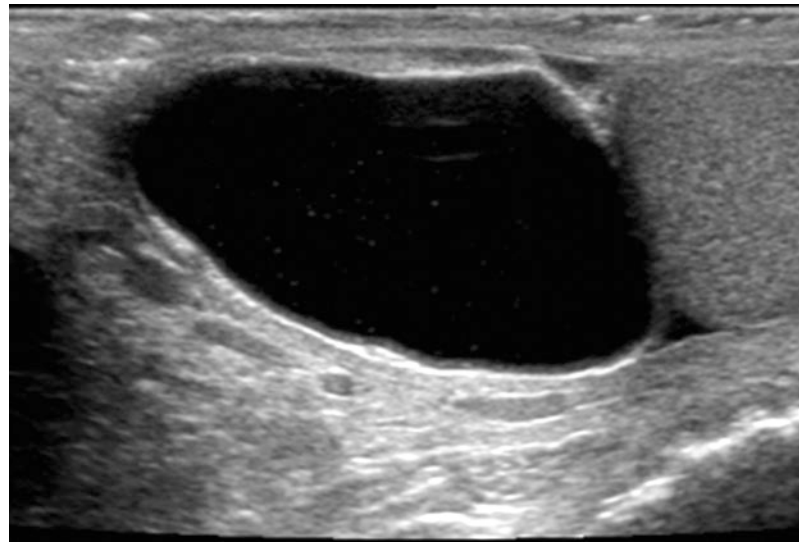

Fig. 13.4 Cystic epididymal mass: longitudinal sonogram shows a large cystic mass of the epididymal head, along the superior aspect of the testis. Spermatocele is likely a diagnosis, particularly given the few low-level echoes within the mass

diagnosing epididymal obstruction. Clinical and laboratory findings of epididymal obstruction include normal-volume ejaculate with oligo- or azoospermia. Imaging findings may demonstrate epididymal enlargement with prominence of the rete testis and a hypoechoic appearance. Epididymal findings have further been described to help delineate between congenital and acquired causes of obstructive azoospermia. In a report of 211 infertile males undergoing scrotal ultrasonography for obstructive azoospermia, men with a congenital etiology were found to have higher rates of ectasia in the epididymal head with tapering and absence of the epididymal body and tail [37]. In contrast, acquired azoospermia exhibited increased rates of epididymal body and tail duct ectasia and an epididymal inflammatory mass. Other studies have also demonstrated similar findings. Moon et al. established a correlation between epididymal abnormalities and caput diameter with obstructive azoospermia, and another study achieved over 91% in specificity using caput epididymis diameter to evaluate obstruction as the cause of azoospermia [38, 39]. Using ultrasound during the initial workup can be useful in differentiating the etiology of infertility and helpful in guiding the provider and patient in decision-making for next management steps.

Varicocele

Varicoceles are reported to occur in approximately 15–25 and 35–60% of fertile and infertile males, respectively, and remain the most common, reversible cause of male-factor infertility [15, 17, 40]. Clinical varicoceles are more common on the left and are graded on a scale of I–III with grade I varicoceles palpable in the standing position with Valsalva maneuver, grade II palpable in the standing position without Valsalva maneuver, and grade III in the standing position grossly visible. Intratesticular varicoceles identified on ultrasonography are relatively uncommon and are likely of minimal significance for male-factor infertility [41].

Ultrasonography is able to detect varicoceles with a 97% sensitivity and 94% specificity [42] (Fig. 13.5). When using the commonly accepted definition of internal spermatic veins measuring ≥3 mm in diameter, ultrasound has been demonstrated to have 53% sensitivity and 91% specificity in identifying varicoceles when compared to physical examination [43].

The presence of a varicocele is associated with infertility and impaired semen characteristics including decreased sperm count, motility, and abnormal morphology [44]. In addition, the grade of the varicocele has been shown to be

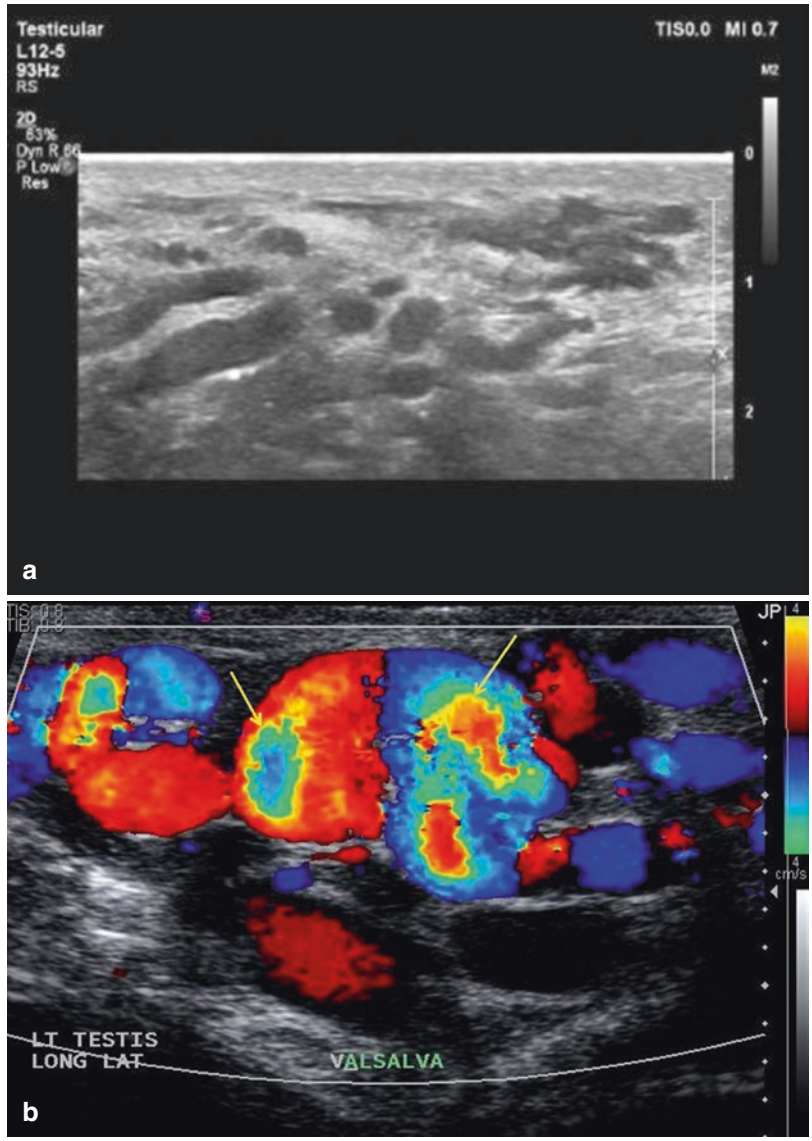

Fig. 13.5 Varicocele: longitudinal sonogram (**a**) shows multiple serpiginous, dilated scrotal veins. Longitudinal color Doppler sonogram (**b**) during Valsalva maneuver shows prominent color flow within the vessels

inversely associated with sperm density. Among infertile patients with a palpable varicocele, only 33.3% were found to have normozoospermia, highlighting the significant impact on semen characteristics [45]. Similarly, the presence of a varicocele is associated with impaired sperm function, with up to 45% of infertile males with varicoceles demonstrating an abnormal acrosome reaction [46].

Although there is controversy regarding the optimal treatment of males with clinical and subclinical (detected on imaging alone) varicoceles, correction of a palpable varicocele has been consistently shown to improve semen parameters and may prevent progressive decline [10, 47–51].

A further role for scrotal ultrasonography in the evaluation of patients with clinical varicoceles is the ability to assess and compare testicular

volumes. Men presenting with a left clinically palpable varicocele have been shown to have increased rates of ipsilateral testicular atrophy, while subclinical varicoceles have not been associated with discrepant testicular volumes [24]. These findings are significant as adolescents with testicular volume differentials >10% have been shown to have significantly lower sperm concentrations when compared to those with <10% differential. This finding was even more pronounced among those with a >20% differential volume.

Beyond its initial diagnostic role with varicoceles, ultrasonography has further prognostic value in determining paternity success following varicocelectomy. Patients with testicular atrophy were shown to have decreased paternity (11%) compared to those with normal testicular volumes (30%). Similarly, those with clinically apparent varicoceles, bilateral varicoceles, shunt-type varicoceles (both retrograde and antegrade reflux demonstrated on ultrasound), or a permanent degree of varicocele were associated with decreased paternity [52].

An additional study evaluating the impact of preoperative parameters on surgical outcomes demonstrated significant improvements following microsurgical varicocelectomy in sperm concentration, motility, and morphology in patients with testicular vein measurements (taken at the inferior pole of the testis) >2.5 mm compared to veins measuring <2.5 mm [53]. Reflux identified at the inferior pole was similarly associated with improved sperm characteristics compared to those with reflux only identified in the supratesticular venous channels.

Following surgical repair, ultrasound has been reported as a reliable tool in follow-up assessments to document decreased venous diameter at rest and with Valsalva maneuver, although this is of questionable clinical relevance [54].

Vas Deferens

Congenital bilateral absence of the vas deferens (CBAVD) is identified in 1–2% of infertile males and in approximately 10% of males with azoospermia [55, 56]. It is found in essentially all patients with cystic fibrosis and is associated with genitourinary abnormalities including absence of the vasal ampulla and seminal vesicles (SV) [57, 58]. Unilateral absence of the vas deferens is associated with both absence (90% of ipsilateral and 20% of contralateral) of the SVs and SV anomalies including hypoplasia, cysts, and calcifications [58, 59].

Patients found to have an absence of the vas deferens either unilaterally or bilaterally on physical examination can be considered for a confirmatory scrotal ultrasound. Ultrasound findings include absence of the body or tail of the epididymides as well as dilated efferent ducts with associated prominent epididymal heads and rete testis [57, 60, 61]. In the absence of cystic fibrosis, patients with unilateral or bilateral absence of the vas deferens should undergo imaging of the retroperitoneum, as up to 21 or 85% of patients, respectively, have been reported to have upper tract abnormalities (renal agenesis, renal ectopia, horseshoe kidney) [62, 63].

Testicular Ultrasound

Testicular ultrasonography provides significant information regarding potential etiologies for infertility, identification of prognostic findings, and as a screening modality for associated lesions. Testicular volume assessment may be obtained through various methodologies, with Lambert's formula (volume [mL] = length × width × AP depth [cm] × 0.71) most commonly utilized [20, 64].

Testicular volume is directly associated with semen parameters including total sperm counts, sperm density, and motility. As seminiferous tubules comprise 70–80% of testicular volume and are responsible for spermatogenesis, a reduced testicular volume has been correlated with global gonadal dysfunction, as indicated by elevated FSH and LH levels [22, 65–68]. Sakamoto and colleagues noted significant oligospermia in patients with testicular volumes <10 mL (normal 15–20 mL), including length <3.5 cm, depth <1.75 cm, and width <2.5 cm with direct correlations noted with sperm density,

total sperm count, motility, and FSH and LH levels [65]. Diminished testicular volume may be secondary to several etiologies including varicoceles, current or previous cryptorchidism, postpubertal mumps, Klinefelter's syndrome, or hormonal abnormalities, among others.

In addition to estimating testicular volume, Doppler ultrasound may be utilized to identify and assess testicular microcirculation. As spermatogenesis is dependent upon microcirculatory perfusion, diminished testicular blood flow as visualized on ultrasound directly correlates with elevated FSH levels and decreased sperm quality [19, 69, 70]. Resistive indices may be obtained to further quantify testicular tissue perfusion and are commonly obtained at the level of the testicular artery and via intratesticular branches near the rete testis. Intratesticular branch resistive indices less than 0.6 have been suggested as a threshold level of normal tissue perfusion, with elevated levels indicative of impaired microcirculation [26, 71].

Testicular ultrasound may assist in differentiating between obstructive and nonobstructive etiologies for infertility. Moon and colleagues demonstrated a reduced median testicular volume in patients with nonobstructive (8.3 mL, range 1.2–16.4) versus obstructive (11.6 mL, range 7.7–25.8) azoospermia [39]. Similarly, patients with azoospermia secondary to obstruction were shown to have dilation of the mediastinum testis, epididymis, and intrascrotal portion of the vas deferens. The sensitivity, specificity, and accuracy for differentiating obstructive versus nonobstructive azoospermia were noted to be 82.1, 100, and 87.5%, respectively. Further findings which suggest a nonobstructive etiology include reduced or absent testicular vessels, with isolated regions of visualized blood flow potentially indicative of residual spermatogenic production [72].

Cryptorchidism

Cryptorchidism is estimated to occur in approximately 2–5% of boys born at term and is associated with impaired future fertility [73]. Although there is ongoing debate as to the optimal time for orchiopexy, there is increasing consensus that earlier repair (at 6–12 months of age) results in improved long-term fertility potential [74].

In evaluating future paternity in males previously undergoing orchiopexy for undescended testes, Lee and colleagues observed successful paternity within 12 months in 90 and 65% of patients with prior unilateral or bilateral cryptorchidism, respectively [75]. This was compared against control subjects who demonstrated a 93% rate of successful paternity. The author concluded that patients with unilateral cryptorchidism have equal rates of paternity to controls, while patients with repaired bilateral cryptorchidism continue to have lifelong impairments in paternity. Further findings indicated that although patients with unilateral cryptorchidism demonstrated equal rates of paternity, they exhibited elevated levels of FSH, decreased inhibin B, and preserved levels of LH/testosterone compared to controls, suggesting subclinical impairments in spermatogenesis.

To further evaluate the effect of timing of orchiopexy on paternity outcomes among azoospermic patients undergoing IVF, Wiser and colleagues found no difference in rates of sperm retrieval, fertilization, implantation, pregnancy, or live birth rates among men with a history of unilateral (2 patients) or bilateral (40 patients) orchiopexy at ≤10 years of age versus >10 years [76]. Despite the late repairs performed, 60% of patients were found to have sperm at the time of testicular sperm extraction (TESE).

The role for ultrasonography is likely limited in the initial evaluation of patients presenting with cryptorchidism (Fig. 13.6). Tasian and colleagues performed a meta-analysis to review the diagnostic performance of ultrasonography among patients with non-palpable cryptorchidism with results demonstrating a sensitivity of 45% and specificity of 78% in localizing non-palpable testes [77]. These findings increased or decreased in the probability of actually finding an intra-abdominal testicle based on imaging from 55 to 64% and 49%, respectively. Given these low rates of precision, the authors indicated that abdominal-scrotal ultrasonography did not reliably assist in the management decision tree for patients with non-palpable testes and was therefore of limited

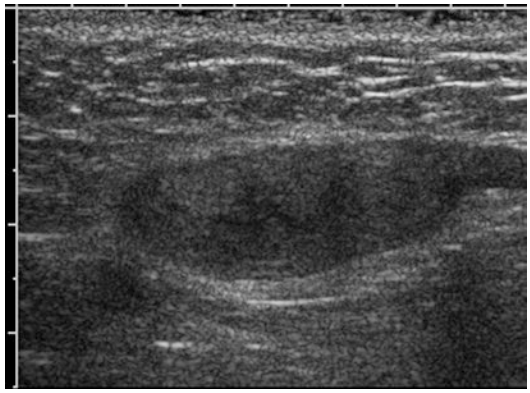

Fig. 13.6 Undescended testis: longitudinal sonogram shows a small, hypoechoic testis in the inguinal canal

utility. Other imaging modalities also demonstrate notable limitations. Given the radiation exposure and high cost that comes with CT imaging, it is not recommended for the workup of cryptorchidism. In the past, MRI had been utilized for this purpose more frequently given a somewhat greater sensitivity and specificity, but its use is currently advised against due to cost, availability, and need for anesthesia [78].

To date, there are no imaging modalities that can effectively determine the absence of a testis. In contrast, surgical exploration has high sensitivity and specificity in confirming testicular absence. Thus, diagnostic laparoscopy is the current gold standard for the diagnosis of cryptorchidism [78]. If absence of the testicle is confirmed during the procedure, then the procedure is complete. However, if a testis is found, an orchidopexy should be attempted simultaneously. A key "takeway" from the guidelines is that imaging studies rarely help in decision-making and can sometimes provide misleading information about the presence or absence of the testicle.

Although there is likely limited utility for ultrasound during the initial evaluation of undescended testes, patients with a history of cryptorchidism have a known two- to eightfold increased risk of testicular cancer, with 5–10% of men with testicular cancer having a prior history of cryptorchidism [73, 79]. This finding has led some authors to advocate for the routine use of scrotal ultrasonography as a screening tool for testicular malignancy among patients presenting with infertility, particularly those with a history of cryptorchidism [80–82].

Cysts, Hydrocele, Infectious Processes

Testicular ultrasonography is an excellent modality for identifying benign testicular structures including cysts, hydroceles, and infectious processes. Intratesticular cysts are identified as hypoechoic/anechoic regions, can represent cystic dilation of the rete testes, and may be a result of postinfectious or posttraumatic epididymal obstruction [83, 84]. Testicular cysts have been reported to occur in 1.2% of infertile men and are of unclear significance [85].

Scrotal hydroceles represent accumulation of fluid within the tunica vaginalis and are commonly the result of prior trauma, inflammatory, or infectious processes. Although there is a known increased prevalence of hydroceles in infertile males (17% vs. 9%), it is unclear if treatment of the hydrocele results in improved semen parameters or fertility [17]. Epididymal injury has been reported to occur in up to 6% of patients undergoing hydrocelectomy, and this injury may result in impaired fertility, including azoospermia [35, 86]. A long-term follow-up study of children undergoing inguinal hernia repairs demonstrated a 5% infertility rate, with 15% of patients previously undergoing hydrocelectomy at the time of herniorrhaphy [87]. To our knowledge, no study has examined the impact of hydrocelectomy on semen parameters in infertile males.

Infectious processes of the testicles visualized on ultrasonography may frequently demonstrate decreased echogenicity, increased heterogeneity, hypervascularity, and testicular enlargement (Fig. 13.7). Similar to MAGI, orchitis may be secondary to infectious (*E. coli*, *Chlamydia*, *Mycobacterium*, and mumps, among others) or noninfectious etiologies. Although there remains limited epidemiological data on the impact of orchitis on overall infertility, previous reports have demonstrated oligospermia and azoospermia occurring at follow-up among 15–33% and 8–27% of males with unilateral epididymo-orchitis,

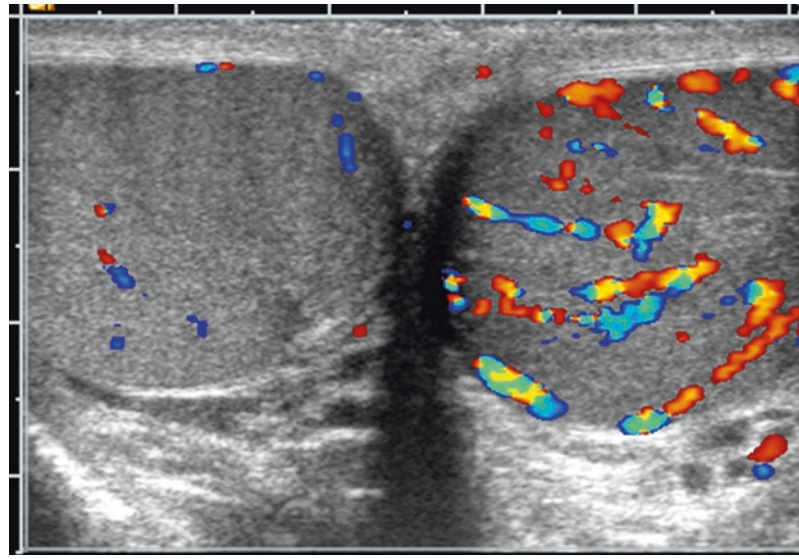

Fig. 13.7 Orchitis: transverse color Doppler sonogram shows both testes with abnormally increased blood flow in the symptomatic left testis

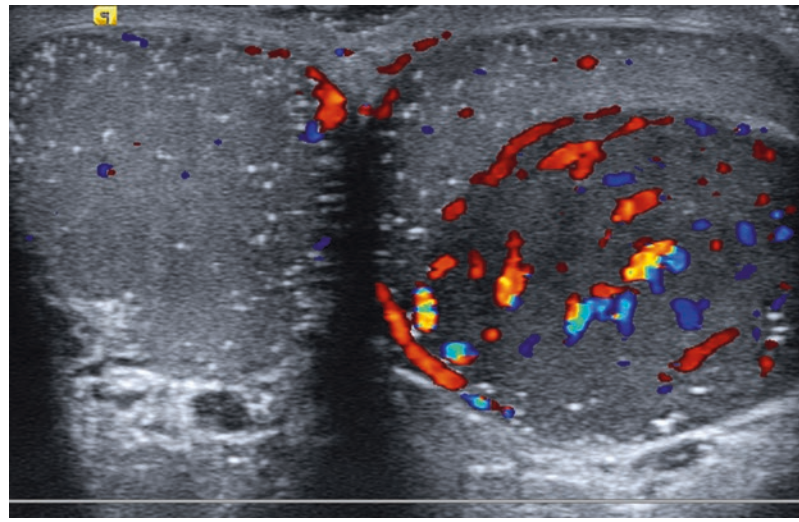

Fig. 13.8 Testicular tumor: transverse color Doppler sonogram shows a large, well-circumscribed hypoechoic mass with prominent blood flow in the left testis and both testes with numerous tiny hyperechoic foci, characteristic of microlithiasis. The mass proved to be a seminoma

respectively [88, 89]. Subsequent pathologic analysis of patients with prior epididymo-orchitis has demonstrated scarring of the seminiferous tubules involving both the ipsilateral and contralateral testicles with chronic inflammatory changes noted [88].

Mumps orchitis is the most common complication of pubertal and postpubertal mumps and is reported to occur in 5–37% of patients with mumps, with 16–65% occurring bilaterally [90]. Among patients with a history of mumps orchitis, approximately 50% will demonstrate some degree of testicular atrophy with one study demonstrating complete atrophy of seminiferous tubules in 38% of biopsies obtained [34, 91, 92]. These findings may be persistent, even in the setting of appropriate acute phase treatment [91].

Testicular Masses

Males presenting with infertility are at increased risk for both immediate and subsequent development of testicular malignancy (Fig. 13.8). The reported incidence of testicular malignancy in infertile males ranges from 0.2% to 1% and is esti-

mated to be 20–100-fold more common than in the general population [28, 93–96]. Men with abnormal semen parameters are also at an increased risk of testicular malignancy with an incidence ratio of 1.6 [97]. Additionally, infertile men continue to be at risk for malignancy following sterility with one report of subsequent development of testicular cancer occurring 14 years after initial evaluation [80]. These findings have led some authors to advocate for the routine use of ultrasound during the initial infertility evaluation [81].

The increasing utilization and improved resolution of scrotal ultrasonography have additionally resulted in an increased rate of detection of testicular lesions with series reporting incidental testicular masses in 1–6% of infertile patients [81, 98, 99]. When the criteria for an incidental testicular lesion are broadened to include hypoechoic/hyperechoic regions, 34% (49/145) of azoospermic patients are found to have focal abnormalities, with only one of the 49 cases subsequently found to represent malignancy [94].

This increased rate of detection has also led to an altered ratio of benign versus malignant lesions [100]. Carmignani and colleagues reported on a series of patients undergoing scrotal ultrasonography for infertility evaluations as well as multiple causes (varicoceles, testicular pain) with benign pathology found at surgical excision in 75–80% of incidentally discovered testicular lesions [99]. Other groups have reported higher ratios of malignancies occurring in 50% (2/4)–71% (7/9) of incidental lesions, albeit these series were comprised of relatively small numbers [81, 93]. When benign findings are reported on frozen section with later determination of malignancy on final pathology, subsequent orchiectomy specimens were found to have no residual malignancy detected [93].

Given the higher rate of incidental, benign lesions, close observation with repeat physical examinations and ultrasonography has been proposed for non-palpable testicular lesions, particularly those <1 cm [101]. Despite the increasing rate of detection of benign testicular lesions, the decision as to perform radical excision, testicular sparing surgery, or active surveillance remains an area of active debate.

Of interest, testicular ultrasound findings following sperm retrievals including PESA, TESA, and TESE demonstrate focal abnormalities which persist in 77 and 54% of patients at 5 days and 6 months, respectively [102]. These findings are not to be misinterpreted as concerning for malignancy in this otherwise at-risk population.

Microlithiasis

Microlithiasis is identified on testicular ultrasonography as hyperechoic regions measuring 3 mm or smaller without definitive shadowing present (Fig. 13.9). Among asymptomatic patients undergoing screening scrotal sonography, testicular microlithiasis is reported in 2.4–6% of individuals with a higher frequency of testicular microlithiasis present in infertile males (10% vs. 2% in controls) [103–105]. Despite the known association between testicular microlithiasis and infertility, Yee and colleagues reported no differences noted in semen analyses between infertile males with microlithiasis versus those without microlithiasis [104].

Microlithiasis has additionally been associated with a relative risk of testicular malignancy of 21.6, with testicular tumors occurring in approximately 6% of patients with microlithiasis [106, 107]. Patients with microlithiasis and unilateral testicular germ cell tumors have an increased incidence of carcinoma in situ in the

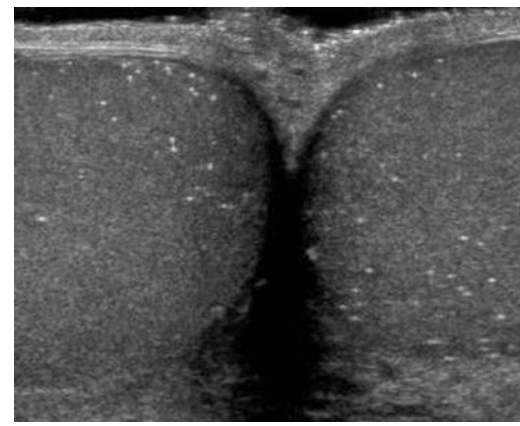

Fig. 13.9 Microlithiasis: transverse sonogram shows multiple diffuse hyperechoic foci with no acoustic shadowing in both testes

contralateral testicle, with some authors recommending routine biopsy of the contralateral testicle [108]. However, subsequent surveillance of patients with isolated testicular microlithiasis followed over a period of 7 years has not been shown to develop malignancy [109].

Given the increased incidence of testicular microlithiasis with malignancy and indeterminate clinical relevance of carcinoma in situ, routine surveillance is commonly recommended with repeat self-testicular exams with or without serial scrotal ultrasonography [106, 107]. Although there has been more research on testicular microlithiasis and testicular cancer in recent years, most of the studies have reported ambiguous results. The most robust data to date comes from a meta-analysis done by Wang et al. [110]. The meta-analysis involved 35,578 patients and suggested that individuals with testicular microlithiasis may be 12 times more likely to have testicular cancer. Based on available data of the incidence of testicular cancer, the European Association of Urology recommends that individuals with testicular microlithiasis receive routine follow-up until the age of 55 [111]. Whether the patient receives further workup depends on whether the patient has additional risk factors for testicular cancer. If the patient has isolated testicular microlithiasis, no further ultrasound or biopsy is needed [112]. However, patients with additional risk factors should receive annual ultrasounds along with month self-examinations [113]. The recommendation on when it is appropriate to perform a biopsy remains controversial.

Testicular Torsion/Trauma

Scrotal ultrasonography is an excellent imaging modality for the rapid assessment and triage of testicular injuries. In the case of testicular trauma, ultrasonography provides visualization of the tunica albuginea and assessment of rupture of seminiferous tubules, scrotal and testicular hematomas, and incidental testicular lesions [114]. In patients with an acute scrotum, Doppler ultrasonography is able to differentiate between infectious processes and testicular torsion [115]. Epididymitis and/or orchitis may present with various imaging findings

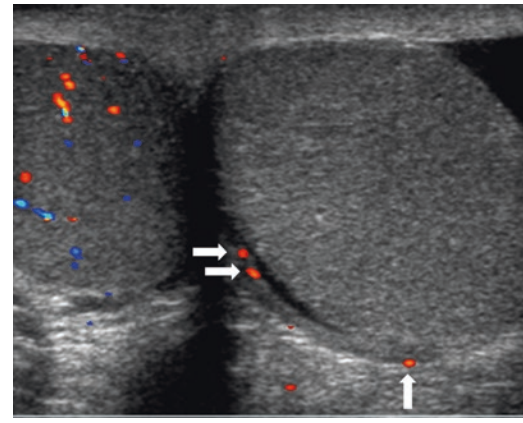

Fig. 13.10 Torsion: transverse color Doppler sonogram shows absence of blood flow in the symptomatic left testis, which is slightly enlarged and surrounded by a small hydrocele. Note normal color flow in the left extratesticular soft tissues (*arrows*)

including diffuse hypoechogenicity, enlarged epididymis/testicle, increased heterogeneity, increased Doppler flow, or straightened spermatic cord. In contrast, early or partial testicular torsion may present with venous congestion and preserved arterial inflow. Complete torsion is characterized by the absence of testicular blood flow, frequently with a proximal "whirlpool" sign (Fig. 13.10). Given the occasional difficulty in identifying early ischemic injuries, alternative imaging techniques including pulse inversion ultrasound may eventually offer a superior assessment in cases of acute ischemia [116].

Multiple studies have examined hormonal and semen profiles following unilateral testicular loss. In patients undergoing orchiectomy secondary to testicular trauma, impaired hormonal and semen characteristics were identified including decreased sperm density and elevated FSH/LH compared to fertile controls [117]. Studies comparing outcomes following orchiectomy versus orchiopexy for acute testicular torsion have reported varied results. Arap and colleagues reported decreased sperm counts and morphology with preserved hormonal levels in patients undergoing either orchiectomy or orchiopexy, while a second study noted decreased inhibin B levels in both groups, indicating possible persistent subclinical gonadal dysfunction [118, 119]. Other studies demonstrate decreased inhibin B

levels, elevated FSH, and impaired sperm density in patients undergoing orchiectomy compared to orchiopexy [120, 121].

Transrectal Ultrasonography

Transrectal ultrasonography (TRUS) is frequently utilized during the evaluation of male infertility in cases of low-volume ejaculate, azoospermia on semen analysis, or palpable asymmetry on digital rectal exam in order to rule out ejaculatory duct obstruction or to evaluate for the presence/absence of seminal vesicles. TRUS identifies pathologic findings (hypoplastic/atrophic SVs, vasal agenesis, etc.) in 75% of azoospermic males, compared to no pathology in 65% of non-azoospermic males [122].

TRUS is frequently performed with a 6.5–7.5 MHz probe with the bladder partially filled. Patients are placed in the lateral decubitus and knee-to-chest position and may alternatively be placed in the prone jackknife or dorsolithotomy positions depending on the surgical scenario.

Prostate

Transrectal ultrasonography is an excellent modality to assess obstructive etiologies of infertility, including prostatic cysts and ejaculatory duct obstruction (EDO), and may be used as an adjunctive measure in cases of suspected prostatic infections or abscesses. Infertile males with EDO or prostatic cysts may present with varied accompanying symptoms including perineal pain, low-volume ejaculate, hematospermia, painful ejaculation, or epididymal tenderness [32, 34].

Cysts

Prostatic cysts are frequently identified in cases of obstructive azoospermia/severe low-volume oligospermia and may be further classified based on location, including peripheral/parenchymal, midline, or paramedian. Midline cysts are typically of a Mullerian embryologic origin and usually do not contain sperm, while paramedian cysts are typically of Wolffian duct origin and may contain sperm upon aspiration [123, 124]. Midline cysts may further be differentiated into utricular cysts which are typically 15 mm in diameter or true Mullerian cysts which may be larger and extend posteriorly beyond the prostatic base (Fig. 13.11). Peripheral cysts may be acquired following infectious processes or rarely may represent benign or malignant processes including multilocular cystadenoma/cystadenocarcinoma [125, 126].

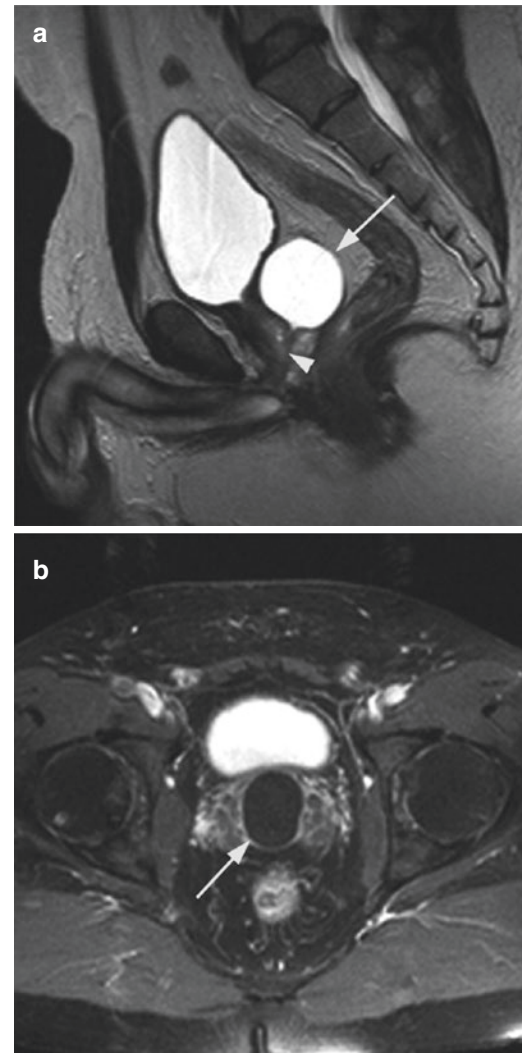

Fig. 13.11 The following image shows a Mullerian duct cyst as indicated by the arrow and prostate as indicated by the arrowhead on (**a**) sagittal T2-weighted and (**b**) axial T1-weighted post-contrast MRI

Ejaculatory Duct Obstruction

The ejaculatory duct is minimally visualized on ultrasonography in the absence of obstruction and enters the urethra at the level of the verumontanum with standard lengths of approximately 4–8 mm and a lumen of 2 mm. In contrast, ejaculatory duct obstruction (EDO) is often well demonstrated in the sagittal view and is commonly associated with dilation of the ejaculatory duct, seminal vesicles, and occasional ejaculatory ductal calcifications.

Ejaculatory duct obstruction may occur secondary to congenital processes including compression by prostatic cysts or ejaculatory duct atresia/stenosis or may be acquired from infections (UTI, sexually transmitted diseases, tuberculosis), inflammatory conditions, traumatic strictures, stone formation, or following prior surgical procedures (transurethral resection of the prostate, exstrophy repair, colorectal surgery) [127–130] (Fig. 13.12). Partial EDO may result from any of the above etiologies and has a variable presentation including low volume with varied sperm densities/total sperm on semen analysis and dilation of one or both of the SVs [131, 132].

Although TRUS findings may suggest EDO, confirmatory tests are commonly required given the relatively low specificity of TRUS alone. In males with azoospermia/severe oligospermia suspected of having EDO, TRUS with concurrent SV aspiration demonstrating the presence of sperm (common definition requiring three or more per high-power field) confirmed obstruction in 49.1% of cases [122, 133–135]. Similarly, Purohit and colleagues compared adjunctive testing including chromotubation, SV aspiration, and seminal vesiculography with confirmation of EDO in 52, 48, and 36% of cases, respectively [136]. An additional measure which is less commonly utilized includes ejaculatory ductal manometry which identifies higher opening pressures in men with EDO compared to fertile controls [137].

The treatment of EDO is frequently performed in combination with TRUS to confirm treatment success and assist in localization or extent of obstruction where indicated. Isolated cysts resulting in compression of the ejaculatory duct may be treated with aspiration alone when not in communication with the ejaculatory system or with transurethral resection of the ejaculatory duct (TURED) when communication exists [129, 138]. Results of TURED for complete EDO demonstrate improved semen quality in 50–92% of patients with complete EDO with subsequent spontaneous (without need for ART) paternity rates of 13–29% [139–143]. An alternative therapy for the treatment of EDO includes ejaculatory ductal dilation utilizing seminal vesicoscopy, with one study demonstrating equal efficacy and fewer complications compared to TURED [144].

Calcifications of the prostate are commonly visualized on transrectal ultrasonography and are of unlikely significance in regard to infertility. Increasing calcifications are associated with age and are present in 23% of asymptomatic males aged 20–29 versus 83% in males 60–69 years old [145].

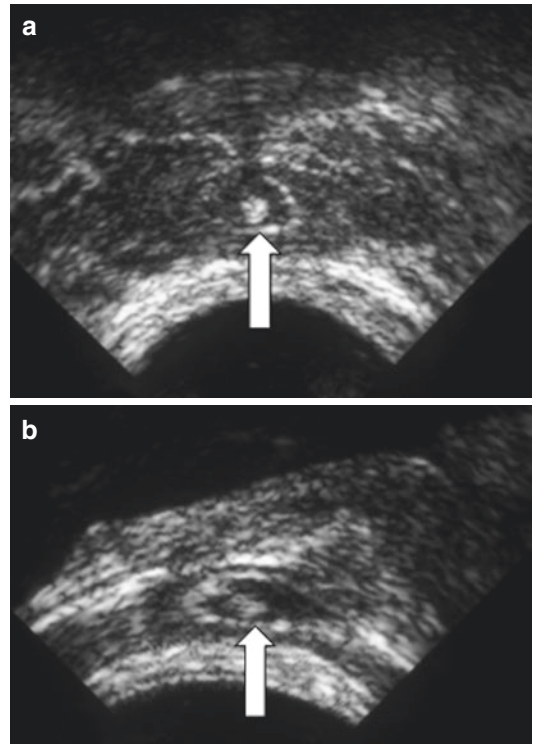

Fig. 13.12 Stone in dilated ejaculatory duct: transverse (**a**) and longitudinal (**b**) transrectal sonograms show a very small hyperechogenic stone (*arrows*) in the dilated right ejaculatory duct

Seminal Vesicles

The SVs are clearly visualized on TRUS cephalad to the prostate and posterior to the bladder and may result in decreases to semen volume, pH, and fructose concentration when abnormalities are present. Although there is variability in reported standard SV lengths, normal, hypoplastic, and atrophic are commonly classified as occurring at >24, 17–24, and <17 mm, respectively, without significant change following ejaculation [145–147].

Dilation of the SVs resulting from mechanical obstruction, particularly when >15 mm, is most commonly associated with EDO as described previously. Dilation may also be seen in patients with adult polycystic disease and infertility, ipsilateral upper urinary tract agenesis (Zinner syndrome), or diabetes mellitus and is thought to be secondary in these cases to SV hypotonicity rather than anatomic obstruction [148–150].

Absence of the SVs is associated with cystic fibrosis and unilateral/bilateral absence of the vas deferens as well as renal anomalies including renal agenesis, ectopia, and horseshoe, among others [58, 59, 62, 63]. Infections of the seminal vesicles may also be visualized on ultrasound and have been reported to impact fertility with improved semen parameters following antibiotic therapy [151].

Assisted Reproductive Techniques

In addition to the initial evaluation of the infertile male, ultrasound has been increasingly utilized in the performance of sperm retrieval for use in ARTs. Several studies have examined the use of power Doppler at the time of TESE to identify regions with increased sperm density to improve the likelihood of sperm retrieval.

Herwig and colleagues reported on the use of a laser Doppler scanner to determine perfusion rates and noted higher sperm quality and quantity based on underlying tissue perfusion. In patients with at least 70 tissue perfusion units (TPU), 72.3% of biopsies identified progressive sperm compared to 13.3% among those with ten or fewer TPUs [152]. A similar study performed in patients with nonobstructive azoospermia demonstrated successful sperm extractions in 38 and 14% of patients with subjective good versus poor vascularity, respectively [153]. A more recent Cochrane review evaluating the efficacy of various techniques for sperm aspiration demonstrated no statistically significant improvement in ultrasound-guided testicular sperm aspiration versus aspirations performed without ultrasound [154]. It is not clear, however, how these techniques compare to the results reported by Herwig and colleagues, and therefore the role for ultrasound at the time of sperm extraction remains unknown.

Further techniques to enhance extraction of sperm at the time of TESE are being developed, with Ramkumar and colleagues recently reporting their initial experience with microdissection probe-TESE (MP-TESE) [155]. The procedure utilizes a microfabricated silicon microprobe with an ultrasonic horn actuator and strain gauges to detect tissue interface boundaries between seminiferous tubules. This reportedly improves size discrimination of seminiferous tubules with the average diameter of sperm-containing tubules noted to be 41.2 ± 1.6 μm per report. Although this technology reports intriguing findings, it has yet to be validated by other groups and remains experimental at the present time.

Conclusion

Ultrasonography, including adjunctive techniques of power and duplex Doppler, is increasingly utilized in the evaluation and management of male-factor infertility. Scrotal and transrectal ultrasonographies provide both anatomic and functional information to assist in identifying underlying etiologies for infertility including infectious processes and varicoceles as well as differentiating between obstructive (EDO, epididymal obstruction, absence of the vas deferens) and nonobstructive causes. Ultrasonography may additionally detect associated findings including testicular/paratesticular lesions, upper tract renal anomalies, testicular microlithiasis, hydroceles,

and cysts. Although ultrasound currently has a limited role with ARTs, an emerging body of investigative literature suggests that its use at the time of TESE may enhance the yield of sperm obtained, thereby improving overall outcomes. As ultrasound technology continues to evolve, it will likely play an increasingly prominent role in the evaluation and treatment of male-factor infertility.

References

1. Thonneau P, Marchand S, Tallec A, Ferial ML, Ducot B, Lansac J, et al. Incidence and main causes of infertility in a resident population (1,850,000) of three French regions (1988–1989). Hum Reprod. 1991;6(6):811–6.
2. Milardi D, Grande G, Sacchini D, Astorri AL, Pompa G, Giampietro A, et al. Male fertility and reduction in semen parameters: a single tertiary-care center experience. Int J Endocrinol. 2012;2012:649149.
3. Hull MG, Glazener CM, Kelly NJ, Conway DI, Foster PA, Hinton RA, et al. Population study of causes, treatment, and outcome of infertility. Br Med J (Clin Res Ed). 1985;291(6510):1693–7.
4. Wilkes S, Chinn DJ, Murdoch A, Rubin G. Epidemiology and management of infertility: a population-based study in UK primary care. Fam Pract. 2009;26(4):269–74.
5. Sundby J. Methodological considerations in the study of frequency, risk factors and outcome of reduced fertility. Scand J Soc Med. 1989;17(2):135–40.
6. Chiamchanya C, Su-angkawatin W. Study of the causes and the results of treatment in infertile couples at Thammasat Hospital between 1999–2004. J Med Assoc Thail. 2008;91(6):805–12.
7. Bablok L, Dziadecki W, Szymusik I, Wolczynski S, Kurzawa R, Pawelczyk L, et al. Patterns of infertility in Poland - multicenter study. Neuro Endocrinol Lett. 2011;32(6):799–804.
8. Jaffe SB, Jewelewicz R. The basic infertility investigation. Fertil Steril. 1991;56(4):599–613.
9. Brugh VM 3rd, Matschke HM, Lipshultz LI. Male factor infertility. Endocrinol Metab Clin N Am. 2003;32(3):689–707.
10. Dohle GR, Colpi GM, Hargreave TB, Papp GK, Jungwirth A, Weidner W, et al. EAU guidelines on male infertility. Eur Urol. 2005;48(5):703–11.
11. Practice Committee of American Society for Reproductive Medicine. Report on varicocele and infertility. Fertil Steril. 2008;90(5 Suppl):S247–9.
12. Practice Committee of the American Society for Reproductive Medicine. Report on management of obstructive azoospermia. Fertil Steril. 2006;86(5 Suppl 1):S259–63.
13. Male Infertility Best Practice Policy Committee of the American Urological Association, Practice Committee of the American Society for Reproductive Medicine. Report on evaluation of the azoospermic male. Fertil Steril. 2006;86(5 Suppl 1):S210–5.
14. Male Infertility Best Practice Policy Committee of the American Urological Association, Practice Committee of the American Society for Reproductive Medicine. Report on optimal evaluation of the infertile male. Fertil Steril. 2006;86(5 Suppl 1):S202–9.
15. Sakamoto H, Saito K, Shichizyo T, Ishikawa K, Igarashi A, Yoshida H. Color Doppler ultrasonography as a routine clinical examination in male infertility. Int J Urol. 2006;13(8):1073–8.
16. Pierik FH, Dohle GR, van Muiswinkel JM, Vreeburg JT, Weber RF. Is routine scrotal ultrasound advantageous in infertile men? J Urol. 1999;162(5):1618–20.
17. Qublan HS, Al-Okoor K, Al-Ghoweri AS, Abu-Qamar A. Sonographic spectrum of scrotal abnormalities in infertile men. J Clin Ultrasound. 2007;35(8):437–41.
18. Grasso M, Blanco S, Raber M, Nespoli L. Elastosonography of the testis: preliminary experience. Arch Ital Urol Androl. 2010;82(3):160–3.
19. Herwig R, Tosun K, Schuster A, Rehder P, Glodny B, Wildt L, et al. Tissue perfusion-controlled guided biopsies are essential for the outcome of testicular sperm extraction. Fertil Steril. 2007;87(5):1071–6.
20. Sakamoto H, Saito K, Ogawa Y, Yoshida H. Testicular volume measurements using Prader orchidometer versus ultrasonography in patients with infertility. Urology. 2007;69(1):158–62.
21. Sakamoto H, Ogawa Y. Does a clinical varicocele influence the relationship between testicular volume by ultrasound and testicular function in patients with infertility? Fertil Steril. 2009;92(5):1632–7.
22. Sakamoto H, Ogawa Y, Yoshida H. Relationship between testicular volume and testicular function: comparison of the Prader orchidometric and ultrasonographic measurements in patients with infertility. Asian J Androl. 2008;10(2):319–24.
23. Diamond DA, Zurakowski D, Bauer SB, Borer JG, Peters CA, Cilento BG Jr, et al. Relationship of varicocele grade and testicular hypotrophy to semen parameters in adolescents. J Urol. 2007;178(4 Pt 2):1584–8.
24. Sakamoto H, Ogawa Y, Yoshida H. Relationship between testicular volume and varicocele in patients with infertility. Urology. 2008;71(1):104–9.
25. Hillelsohn JH, Chuang KW, Goldenberg E, Gilbert BR. Spectral Doppler sonography: a noninvasive method for predicting dyspermia. J Ultrasound Med. 2013;32(8):1427–32.
26. Unsal A, Turgut AT, Taskin F, Kosar U, Karaman CZ. Resistance and pulsatility index increase in capsular branches of testicular artery: indicator of impaired testicular microcirculation in varicocele? J Clin Ultrasound. 2007;35(4):191–5.
27. Middleton WD, Picus DD, Marx MV, Melson GL. Color Doppler sonography of hemodialysis vas-

cular access: comparison with angiography. AJR Am J Roentgenol. 1989;152(3):633–9.
28. Nashan D, Behre HM, Grunert JH, Nieschlag E. Diagnostic value of scrotal sonography in infertile men: report on 658 cases. Andrologia. 1990;22(5):387–95.
29. Wise GJ, Marella VK. Genitourinary manifestations of tuberculosis. Urol Clin North Am. 2003;30(1):111–21.
30. Everaert K, Mahmoud A, Depuydt C, Maeyaert M, Comhaire F. Chronic prostatitis and male accessory gland infection--is there an impact on male infertility (diagnosis and therapy)? Andrologia. 2003;35(5):325–30.
31. La Vignera S, Condorelli R, D'Agata R, Vicari E, Calogero AE. Semen alterations and flowcitometry evaluation in patients with male accessory gland infections. J Endocrinol Investig. 2012;35(2):219–23.
32. Lotti F, Corona G, Mancini M, Filimberti E, Degli Innocenti S, Colpi GM, et al. Ultrasonographic and clinical correlates of seminal plasma interleukin-8 levels in patients attending an andrology clinic for infertility. Int J Androl. 2011;34(6 Pt 1):600–13.
33. Huwe P, Diemer T, Ludwig M, Liu J, Schiefer HG, Weidner W. Influence of different uropathogenic microorganisms on human sperm motility parameters in an in vitro experiment. Andrologia. 1998;30(Suppl 1):55–9.
34. Weidner W, Krause W, Ludwig M. Relevance of male accessory gland infection for subsequent fertility with special focus on prostatitis. Hum Reprod Update. 1999;5(5):421–32.
35. Zahalsky MP, Berman AJ, Nagler HM. Evaluating the risk of epididymal injury during hydrocelectomy and spermatocelectomy. J Urol. 2004;171(6 Pt 1):2291–2.
36. Kauffman EC, Kim HH, Tanrikut C, Goldstein M. Microsurgical spermatocelectomy: technique and outcomes of a novel surgical approach. J Urol. 2011;185(1):238–42.
37. Wang ZQ, Li FH, Du J, Zheng JF. Ultrasonographic features of epididymides in obstructive azoospermia. Zhonghua Nan Ke Xue. 2010;16(11):984–9.
38. Pezzella A, Barbonetti A, Micillo A, D'Andrea S, Necozione S, Gandini L, et al. Ultrasonographic determination of caput epididymis diameter is strongly predictive of obstruction in the genital tract in azoospermic men with normal serum FSH. Andrology. 2013;1(1):133–8.
39. Moon MH, Kim SH, Cho JY, Seo JT, Chun YK. Scrotal US for evaluation of infertile men with azoospermia. Radiology. 2006;239(1):168–73.
40. Cocuzza M, Athayde KS, Alvarenga C, Srougi M, Hallak J. Grade 3 varicocele in fertile men: a different entity. J Urol. 2012;187(4):1363–8.
41. Vasilios S, Charalampos L, Elias P, Agelos K, Koutoulidis V, Lampros V. Ultrasound findings of an intratesticular varicocele. Report of a new case and review of the literature. Int Urol Nephrol. 2006;38(1):115–8.
42. Trum JW, Gubler FM, Laan R, van der Veen F. The value of palpation, varicoscreen contact thermography and colour Doppler ultrasound in the diagnosis of varicocele. Hum Reprod. 1996;11(6):1232–5.
43. Chiou RK, Anderson JC, Wobig RK, Rosinsky DE, Matamoros A Jr, Chen WS, et al. Color Doppler ultrasound criteria to diagnose varicoceles: correlation of a new scoring system with physical examination. Urology. 1997;50(6):953–6.
44. MacLeod J. Seminal cytology in the presence of varicocele. Fertil Steril. 1965;16(6):735–57.
45. Al-Ali BM, Marszalek M, Shamloul R, Pummer K, Trummer H. Clinical parameters and semen analysis in 716 Austrian patients with varicocele. Urology. 2010;75(5):1069–73.
46. Glazier DB, Marmar JL, Diamond SM, Gibbs M, Corson SL. A modified acrosome induction test. Arch Androl. 2000;44(1):59–64.
47. Romeo C, Santoro G. Varicocele and infertility: why a prevention? J Endocrinol Investig. 2009;32(6):559–61.
48. Zorba UO, Sanli OM, Tezer M, Erdemir F, Shavakhabov S, Kadioglu A. Effect of infertility duration on postvaricocelectomy sperm counts and pregnancy rates. Urology. 2009;73(4):767–71.
49. Agarwal A, Deepinder F, Cocuzza M, Agarwal R, Short RA, Sabanegh E, et al. Efficacy of varicocelectomy in improving semen parameters: new meta-analytical approach. Urology. 2007;70(3):532–8.
50. Marmar JL, Agarwal A, Prabakaran S, Agarwal R, Short RA, Benoff S, et al. Reassessing the value of varicocelectomy as a treatment for male subfertility with a new meta-analysis. Fertil Steril. 2007;88(3):639–48.
51. Zheng YQ, Gao X, Li ZJ, Yu YL, Zhang ZG, Li W. Efficacy of bilateral and left varicocelectomy in infertile men with left clinical and right subclinical varicoceles: a comparative study. Urology. 2009;73(6):1236–40.
52. Donkol RH, Salem T. Paternity after varicocelectomy: preoperative sonographic parameters of success. J Ultrasound Med. 2007;26(5):593–9.
53. Hussein AF. The role of color Doppler ultrasound in prediction of the outcome of microsurgical subinguinal varicocelectomy. J Urol. 2006;176(5):2141–5.
54. El-Haggar S, Nassef S, Gadalla A, Latif A, Mostafa T. Ultrasonographic parameters of the spermatic veins at the inguinal and scrotal levels in varicocele diagnosis and post-operative repair. Andrologia. 2012;44(3):210–3.
55. Bromage SJ, Falconer DA, Lieberman BA, Sangar V, Payne SR. Sperm retrieval rates in subgroups of primary azoospermic males. Eur Urol. 2007;51(2):534–9; discussion 9–40.
56. Jequier AM, Ansell ID, Bullimore NJ. Congenital absence of the vasa deferentia presenting with infertility. J Androl. 1985;6(1):15–9.

57. Cornud F, Amar E, Hamida K, Thiounn N, Helenon O, Moreau JF. Imaging in male hypofertility and impotence. BJU Int. 2000;86(Suppl 1):153–63.
58. Raviv G, Mor Y, Levron J, Shefi S, Zilberman D, Ramon J, et al. Role of transrectal ultrasonography in the evaluation of azoospermic men with low-volume ejaculate. J Ultrasound Med. 2006;25(7):825–9.
59. Hall S, Oates RD. Unilateral absence of the scrotal vas deferens associated with contralateral mesonephric duct anomalies resulting in infertility: laboratory, physical and radiographic findings, and therapeutic alternatives. J Urol. 1993;150(4):1161–4.
60. Cornud F, Belin X, Delafontaine D, Amar T, Helenon O, Moreau JF. Imaging of obstructive azoospermia. Eur Radiol. 1997;7(7):1079–85.
61. Sakamoto H, Yajima T, Suzuki K, Ogawa Y. Cystic fibrosis transmembrane conductance regulator (CFTR) gene mutation associated with a congenital bilateral absence of vas deferens. Int J Urol. 2008;15(3):270–1.
62. Augarten A, Yahav Y, Kerem BS, Halle D, Laufer J, Szeinberg A, et al. Congenital bilateral absence of vas deferens in the absence of cystic fibrosis. Lancet. 1994;344(8935):1473–4.
63. Donohue RE, Fauver HE. Unilateral absence of the vas deferens. A useful clinical sign. JAMA. 1989;261(8):1180–2.
64. Sakamoto H, Saito K, Oohta M, Inoue K, Ogawa Y, Yoshida H. Testicular volume measurement: comparison of ultrasonography, orchidometry, and water displacement. Urology. 2007;69(1):152–7.
65. Sakamoto H, Yajima T, Nagata M, Okumura T, Suzuki K, Ogawa Y. Relationship between testicular size by ultrasonography and testicular function: measurement of testicular length, width, and depth in patients with infertility. Int J Urol. 2008;15(6):529–33.
66. Arai T, Kitahara S, Horiuchi S, Sumi S, Yoshida K. Relationship of testicular volume to semen profiles and serum hormone concentrations in infertile Japanese males. Int J Fertil Womens Med. 1998;43(1):40–7.
67. Bujan L, Mieusset R, Mansat A, Moatti JP, Mondinat C, Pontonnier F. Testicular size in infertile men: relationship to semen characteristics and hormonal blood levels. Br J Urol. 1989;64(6):632–7.
68. Lenz S, Thomsen JK, Giwercman A, Hertel NT, Hertz J, Skakkebaek NE. Ultrasonic texture and volume of testicles in infertile men. Hum Reprod. 1994;9(5):878–81.
69. Tarhan S, Gumus B, Gunduz I, Ayyildiz V, Goktan C. Effect of varicocele on testicular artery blood flow in men--color Doppler investigation. Scand J Urol Nephrol. 2003;37(1):38–42.
70. Battaglia C, Pasini A, Mancini F, Burnelli R, Cicognani A, de Aloysio D. Role of intratesticular ultrasonographic and Doppler flow analyses in evaluating gonadal status in male survivors of childhood malignancy. Fertil Steril. 2005;83(6):1867–70.
71. Schurich M, Aigner F, Frauscher F, Pallwein L. The role of ultrasound in assessment of male fertility. Eur J Obstet Gynecol Reprod Biol. 2009;144(Suppl 1):S192–8.
72. Foresta C, Garolla A, Bettella A, Ferlin A, Rossato M, Candiani F. Doppler ultrasound of the testis in azoospermic subjects as a parameter of testicular function. Hum Reprod. 1998;13(11):3090–3.
73. Toppari J, Kaleva M. Maldescendus testis. Horm Res. 1999;51(6):261–9.
74. Ritzen EM, Bergh A, Bjerknes R, Christiansen P, Cortes D, Haugen SE, et al. Nordic consensus on treatment of undescended testes. Acta Paediatr. 2007;96(5):638–43.
75. Lee PA. Fertility after cryptorchidism: epidemiology and other outcome studies. Urology. 2005;66(2):427–31.
76. Wiser A, Raviv G, Weissenberg R, Elizur SE, Levron J, Machtinger R, et al. Does age at orchidopexy impact on the results of testicular sperm extraction? Reprod Biomed Online. 2009;19(6):778–83.
77. Tasian GE, Copp HL. Diagnostic performance of ultrasound in nonpalpable cryptorchidism: a systematic review and meta-analysis. Pediatrics. 2011;127(1):119–28.
78. Kolon TF, Herndon CD, Baker LA, Baskin LS, Baxter CG, Cheng EY, et al. Evaluation and treatment of cryptorchidism: AUA guideline. J Urol. 2014;192(2):337–45.
79. Dieckmann KP, Pichlmeier U. Clinical epidemiology of testicular germ cell tumors. World J Urol. 2004;22(1):2–14.
80. Kanto S, Takahashi K, Maehara I, Fukuzaki A, Kyono K, Arai Y. Incidental testicular cancers that subsequently developed in oligozoospermic and azoospermic patients: report of three cases. Fertil Steril. 2007;88(5):1374–6.
81. Phillips N, Jequier AM. Early testicular cancer: a problem in an infertility clinic. Reprod Biomed Online. 2007;15(5):520–5.
82. Onur MR, Firdolas F, Onur R, Kocakoc E, Akpolat N, Orhan I. Scrotal ultrasonography: should it be used in routine evaluation of infertile men? Andrologia. 2008;40(1):58–61.
83. Colangelo SM, Fried K, Hyacinthe LM, Fracchia JA. Tubular ectasia of the rete testis: an ultrasound diagnosis. Urology. 1995;45(3):532–4.
84. Older RA, Watson LR. Tubular ectasia of the rete testis: a benign condition with a sonographic appearance that may be misinterpreted as malignant. J Urol. 1994;152(2 Pt 1):477–8.
85. Jequier AM, Phillips N. Cystic dilatation of the rete testis: a hidden diagnosis among infertile men. Reprod Biomed Online. 2009;18(2):190–4.
86. Ross LS, Flom LS. Azoospermia: a complication of hydrocele repair in a fertile population. J Urol. 1991;146(3):852–3.
87. Zendejas B, Zarroug AE, Erben YM, Holley CT, Farley DR. Impact of childhood inguinal hernia

repair in adulthood: 50 years of follow-up. J Am Coll Surg. 2010;211(6):762–8.
88. Osegbe DN. Testicular function after unilateral bacterial epididymo-orchitis. Eur Urol. 1991;19(3):204–8.
89. Weidner W, Garbe C, Weissbach L, Harbrecht J, Kleinschmidt K, Schiefer HG, et al. Initial therapy of acute unilateral epididymitis using ofloxacin. II. Andrological findings. Urologe A. 1990;29(5):277–80.
90. Beard CM, Benson RC Jr, Kelalis PP, Elveback LR, Kurland LT. The incidence and outcome of mumps orchitis in Rochester, Minnesota, 1935 to 1974. Mayo Clin Proc. 1977;52(1):3–7.
91. Yeniyol CO, Sorguc S, Minareci S, Ayder AR. Role of interferon-alpha-2B in prevention of testicular atrophy with unilateral mumps orchitis. Urology. 2000;55(6):931–3.
92. Mikuz G, Damjanov I. Inflammation of the testis, epididymis, peritesticular membranes, and scrotum. Pathol Annu. 1982;17(Pt 1):101–28.
93. Powell TM, Tarter TH. Management of nonpalpable incidental testicular masses. J Urol. 2006;176(1):96–8; discussion 9.
94. Eifler JB Jr, King P, Schlegel PN. Incidental testicular lesions found during infertility evaluation are usually benign and may be managed conservatively. J Urol. 2008;180(1):261–4; discussion 5.
95. Carmignani L, Gadda F, Mancini M, Gazzano G, Nerva F, Rocco F, et al. Detection of testicular ultrasonographic lesions in severe male infertility. J Urol. 2004;172(3):1045–7.
96. Raman JD, Nobert CF, Goldstein M. Increased incidence of testicular cancer in men presenting with infertility and abnormal semen analysis. J Urol. 2005;174(5):1819–22; discussion 22.
97. Jacobsen R, Bostofte E, Engholm G, Hansen J, Olsen JH, Skakkebaek NE, et al. Risk of testicular cancer in men with abnormal semen characteristics: cohort study. BMJ. 2000;321(7264):789–92.
98. Hopps CV, Goldstein M. Ultrasound guided needle localization and microsurgical exploration for incidental nonpalpable testicular tumors. J Urol. 2002;168(3):1084–7.
99. Carmignani L, Gadda F, Gazzano G, Nerva F, Mancini M, Ferruti M, et al. High incidence of benign testicular neoplasms diagnosed by ultrasound. J Urol. 2003;170(5):1783–6.
100. Leonhartsberger N, Ramoner R, Aigner F, Stoehr B, Pichler R, Zangerl F, et al. Increased incidence of Leydig cell tumours of the testis in the era of improved imaging techniques. BJU Int. 2011;108(10):1603–7.
101. Toren PJ, Roberts M, Lecker I, Grober ED, Jarvi K, Lo KC. Small incidentally discovered testicular masses in infertile men--is active surveillance the new standard of care? J Urol. 2010;183(4):1373–7.
102. Ron-El R, Strauss S, Friedler S, Strassburger D, Komarovsky D, Raziel A. Serial sonography and colour flow Doppler imaging following testicular and epididymal sperm extraction. Hum Reprod. 1998;13(12):3390–3.
103. Aizenstein RI, DiDomenico D, Wilbur AC, O'Neil HK. Testicular microlithiasis: association with male infertility. J Clin Ultrasound. 1998;26(4):195–8.
104. Yee WS, Kim YS, Kim SJ, Choi JB, Kim SI, Ahn HS. Testicular microlithiasis: prevalence and clinical significance in a population referred for scrotal ultrasonography. Korean J Urol. 2011;52(3):172–7.
105. Serter S, Gumus B, Unlu M, Tuncyurek O, Tarhan S, Ayyildiz V, et al. Prevalence of testicular microlithiasis in an asymptomatic population. Scand J Urol Nephrol. 2006;40(3):212–4.
106. Cast JE, Nelson WM, Early AS, Biyani S, Cooksey G, Warnock NG, et al. Testicular microlithiasis: prevalence and tumor risk in a population referred for scrotal sonography. AJR Am J Roentgenol. 2000;175(6):1703–6.
107. Lam DL, Gerscovich EO, Kuo MC, McGahan JP. Testicular microlithiasis: our experience of 10 years. J Ultrasound Med. 2007;26(7):867–73.
108. Meissner A, Mamoulakis C, de la Rosette JJ, Pes MP. Clinical update on testicular microlithiasis. Curr Opin Urol. 2009;19(6):615–8.
109. Sakamoto H, Shichizyou T, Saito K, Okumura T, Ogawa Y, Yoshida H, et al. Testicular microlithiasis identified ultrasonographically in Japanese adult patients: prevalence and associated conditions. Urology. 2006;68(3):636–41.
110. Wang H, Yin X, Wu D. Novel human pathological mutations. SLC34A2. Disease: pulmonary alveolar microlithiasis. Hum Genet. 2010;127(4):471.
111. Tan IB, Ang KK, Ching BC, Mohan C, Toh CK, Tan MH. Testicular microlithiasis predicts concurrent testicular germ cell tumors and intratubular germ cell neoplasia of unclassified type in adults: a meta-analysis and systematic review. Cancer. 2010;116(19):4520–32.
112. Montgomery JS, Bloom DA. The diagnosis and management of scrotal masses. Med Clin North Am. 2011;95(1):235–44.
113. Richenberg J, Belfield J, Ramchandani P, Rocher L, Freeman S, Tsili AC, et al. Testicular microlithiasis imaging and follow-up: guidelines of the ESUR scrotal imaging subcommittee. Eur Radiol. 2015;25(2):323–30.
114. Bhatt S, Dogra VS. Role of US in testicular and scrotal trauma. Radiographics. 2008;28(6):1617–29.
115. Vijayaraghavan SB. Sonographic differential diagnosis of acute scrotum: real-time whirlpool sign, a key sign of torsion. J Ultrasound Med. 2006;25(5):563–74.
116. Paltiel HJ, Kalish LA, Susaeta RA, Frauscher F, O'Kane PL, Freitas-Filho LG. Pulse-inversion US imaging of testicular ischemia: quantitative and qualitative analyses in a rabbit model. Radiology. 2006;239(3):718–29.
117. Lin WW, Kim ED, Quesada ET, Lipshultz LI, Coburn M. Unilateral testicular injury from external

trauma: evaluation of semen quality and endocrine parameters. J Urol. 1998;159(3):841–3.
118. Romeo C, Impellizzeri P, Arrigo T, Antonuccio P, Valenzise M, Mirabelli S, et al. Late hormonal function after testicular torsion. J Pediatr Surg. 2010;45(2):411–3.
119. Arap MA, Vicentini FC, Cocuzza M, Hallak J, Athayde K, Lucon AM, et al. Late hormonal levels, semen parameters, and presence of antisperm antibodies in patients treated for testicular torsion. J Androl. 2007;28(4):528–32.
120. Taskinen S, Taskinen M, Rintala R. Testicular torsion: orchiectomy or orchiopexy? J Pediatr Urol. 2008;4(3):210–3.
121. Anderson MJ, Dunn JK, Lipshultz LI, Coburn M. Semen quality and endocrine parameters after acute testicular torsion. J Urol. 1992;147(6):1545–50.
122. Engin G, Kadioglu A, Orhan I, Akdol S, Rozanes I. Transrectal US and endorectal MR imaging in partial and complete obstruction of the seminal duct system. A comparative study. Acta Radiol. 2000;41(3):288–95.
123. Jarow JP. Transrectal ultrasonography of infertile men. Fertil Steril. 1993;60(6):1035–9.
124. Parsons RB, Fisher AM, Bar-Chama N, Mitty HA. MR imaging in male infertility. Radiographics. 1997;17(3):627–37.
125. Park JP, Cho NH, Oh YT, Choi YD. Giant multilocular prostatic cystadenoma presenting with obstructive aspermia. Yonsei Med J. 2007;48(3):554–6.
126. Tuziak T, Spiess PE, Abrahams NA, Wrona A, Tu SM, Czerniak B. Multilocular cystadenoma and cystadenocarcinoma of the prostate. Urol Oncol. 2007;25(1):19–25.
127. Pryor JP, Hendry WF. Ejaculatory duct obstruction in subfertile males: analysis of 87 patients. Fertil Steril. 1991;56(4):725–30.
128. Philip J, Manikandan R, Lamb GH, Desmond AD. Ejaculatory-duct calculus causing secondary obstruction and infertility. Fertil Steril. 2007;88(3):706 e9–11.
129. Donkol RH. Imaging in male-factor obstructive infertility. World J Radiol. 2010;2(5):172–9.
130. Goluboff ET, Stifelman MD, Fisch H. Ejaculatory duct obstruction in the infertile male. Urology. 1995;45(6):925–31.
131. Ruiz Rubio JL, Fernandez Gonzalez I, Quijano Barroso P, Herrero Payo JA, Berenguer Sanchez A. The value of transrectal ultrasonography in the diagnosis and treatment of partial obstruction of the seminal duct system. J Urol. 1995;153(2):435–6.
132. Nagler HM, Rotman M, Zoltan E, Fisch H. The natural history of partial ejaculatory duct obstruction. J Urol. 2002;167(1):253–4.
133. Jarow JP. Seminal vesicle aspiration of fertile men. J Urol. 1996;156(3):1005–7.
134. Orhan I, Onur R, Cayan S, Koksal IT, Kadioglu A. Seminal vesicle sperm aspiration in the diagnosis of ejaculatory duct obstruction. BJU Int. 1999;84(9):1050–3.
135. Engin G, Celtik M, Sanli O, Aytac O, Muradov Z, Kadioglu A. Comparison of transrectal ultrasonography and transrectal ultrasonography-guided seminal vesicle aspiration in the diagnosis of the ejaculatory duct obstruction. Fertil Steril. 2009;92(3):964–70.
136. Purohit RS, Wu DS, Shinohara K, Turek PJ. A prospective comparison of 3 diagnostic methods to evaluate ejaculatory duct obstruction. J Urol. 2004;171(1):232–5; discussion 5–6.
137. Eisenberg ML, Walsh TJ, Garcia MM, Shinohara K, Turek PJ. Ejaculatory duct manometry in normal men and in patients with ejaculatory duct obstruction. J Urol. 2008;180(1):255–60; discussion 60.
138. Stricker HJ, Kunin JR, Faerber GJ. Congenital prostatic cyst causing ejaculatory duct obstruction: management by transrectal cyst aspiration. J Urol. 1993;149(5):1141–3.
139. Yurdakul T, Gokce G, Kilic O, Piskin MM. Transurethral resection of ejaculatory ducts in the treatment of complete ejaculatory duct obstruction. Int Urol Nephrol. 2008;40(2):369–72.
140. Kadioglu A, Cayan S, Tefekli A, Orhan I, Engin G, Turek PJ. Does response to treatment of ejaculatory duct obstruction in infertile men vary with pathology? Fertil Steril. 2001;76(1):138–42.
141. Meacham RB, Hellerstein DK, Lipshultz LI. Evaluation and treatment of ejaculatory duct obstruction in the infertile male. Fertil Steril. 1993;59(2):393–7.
142. Schroeder-Printzen I, Ludwig M, Kohn F, Weidner W. Surgical therapy in infertile men with ejaculatory duct obstruction: technique and outcome of a standardized surgical approach. Hum Reprod. 2000;15(6):1364–8.
143. Heshmat S, Lo KC. Evaluation and treatment of ejaculatory duct obstruction in infertile men. Can J Urol. 2006;13(Suppl 1):18–21.
144. Xu B, Niu X, Wang Z, Li P, Qin C, Li J, et al. Novel methods for the diagnosis and treatment of ejaculatory duct obstruction. BJU Int. 2011;108(2):263–6.
145. Zackrisson B, Hugosson J, Aus G. Transrectal ultrasound anatomy of the prostate and seminal vesicles in healthy men. Scand J Urol Nephrol. 2000;34(3):175–80.
146. Tanahashi Y, Watanabe H, Igari D, Harada K, Saitoh M. Volume estimation of the seminal vesicles by means of transrectal ultrasonotomography: a preliminary report. Br J Urol. 1975;47(6):695–702.
147. Hernandez AD, Urry RL, Smith JA Jr. Ultrasonographic characteristics of the seminal vesicles after ejaculation. J Urol. 1990;144(6):1380–2.
148. La Vignera S, Vicari E, Condorelli R, D'Agata R, Calogero AE. Ultrasound characterization of the seminal vesicles in infertile patients with type 2 diabetes mellitus. Eur J Radiol. 2011;80(2):e64–7.
149. Pace G, Galatioto GP, Guala L, Ranieri G, Vicentini C. Ejaculatory duct obstruction caused by a right giant seminal vesicle with an ipsilateral upper urinary tract agenesia: an embryologic malformation. Fertil Steril. 2008;89(2):390–4.

150. Manno M, Marchesan E, Tomei F, Cicutto D, Maruzzi D, Maieron A, et al. Polycystic kidney disease and infertility: case report and literature review. Arch Ital Urol Androl. 2005;77(1):25–8.
151. Andrade-Rocha FT. Unusual presentation of seminal vesiculitis in an infertile man. Can J Urol. 2007;14(6):3750–2.
152. Herwig R, Tosun K, Pinggera GM, Soelder E, Moeller KT, Pallwein L, et al. Tissue perfusion essential for spermatogenesis and outcome of testicular sperm extraction (TESE) for assisted reproduction. J Assist Reprod Genet. 2004;21(5):175–80.
153. Tunc L, Alkibay T, Kupeli B, Tokgoz H, Bozkirli I, Yucel C. Power Doppler ultrasound mapping in non-obstructive azoospermic patients prior to testicular sperm extraction. Arch Androl. 2005;51(4):277–83.
154. Van Peperstraten A, Proctor ML, Johnson NP, Philipson G. Techniques for surgical retrieval of sperm prior to intra-cytoplasmic sperm injection (ICSI) for azoospermia. Cochrane Database Syst Rev. 2008;(2):CD002807.
155. Ramkumar A, Lal A, Paduch DA, Schlegel PN. Ultrasonically actuated silicon-microprobe-based testicular tubule metrology. Conf Proc IEEE Eng Med Biol Soc. 2010;2010:6469–72.

Part VI

Ultrasound and ART Techniques

14 Evaluation of Tubal Patency (HyCoSy, Doppler)

Kamal Ojha, Tuhina Goel,
and Dimuthu Vinayagam

Baseline Scan and Hydrosalpinges

Assessment of fallopian tubes begins with the baseline scan for fertility assessment. Interstitial part of the tube being the fixed part and within the uterus can easily be identified with three-dimensional (3D) ultrasound examination of the uterus (Fig. 14.1). Tracing this further the outline can sometimes be clearly seen, but this is not always possible. Ideally, the instillation of dye as described below is the best way to identify the fallopian tubes. However, if the distal part of the tube is blocked, then often fluid accumulates in the fallopian tube over a period of time, and this is described as hydrosalpinges. This is generally located between the uterus and the ovaries. Typically, it is elongated in shape with partial septae best identified with a transverse ultrasound examination. Unilateral or bilateral hydrosalpinges is associated with low success in women undergoing IVF examination. The walls of the hydrosalpinges are thin with clear fluid and partial septum. Identifying the ovary separately is essential to exclude ovarian cyst. The hydrosalpinges can at times completely surround the ovary. A paraovarian cyst is generally observed on either side of the ovary well clear from the uterus and appears more like an ovarian cyst with no septae.

K. Ojha (✉)
St. George's University Hospital, NHS Foundation Trust, Department of Obstetrics and Gynaecology, London, UK
e-mail: Kamal.Ojha@stgeorges.nhs.uk

T. Goel
All India Institute of Medical Sciences, New Delhi, India

Department of Obstetrics and Gynaecology, Saharanpur, Uttar Pradesh, India

D. Vinayagam
St. George's University Hospital, University of London, Cardiovascular Sciences Research Centre, London, UK

L. A. Stadtmauer, I. Tur-Kaspa (eds.), *Ultrasound Imaging in Reproductive Medicine*,
https://doi.org/10.1007/978-3-030-16699-1_14

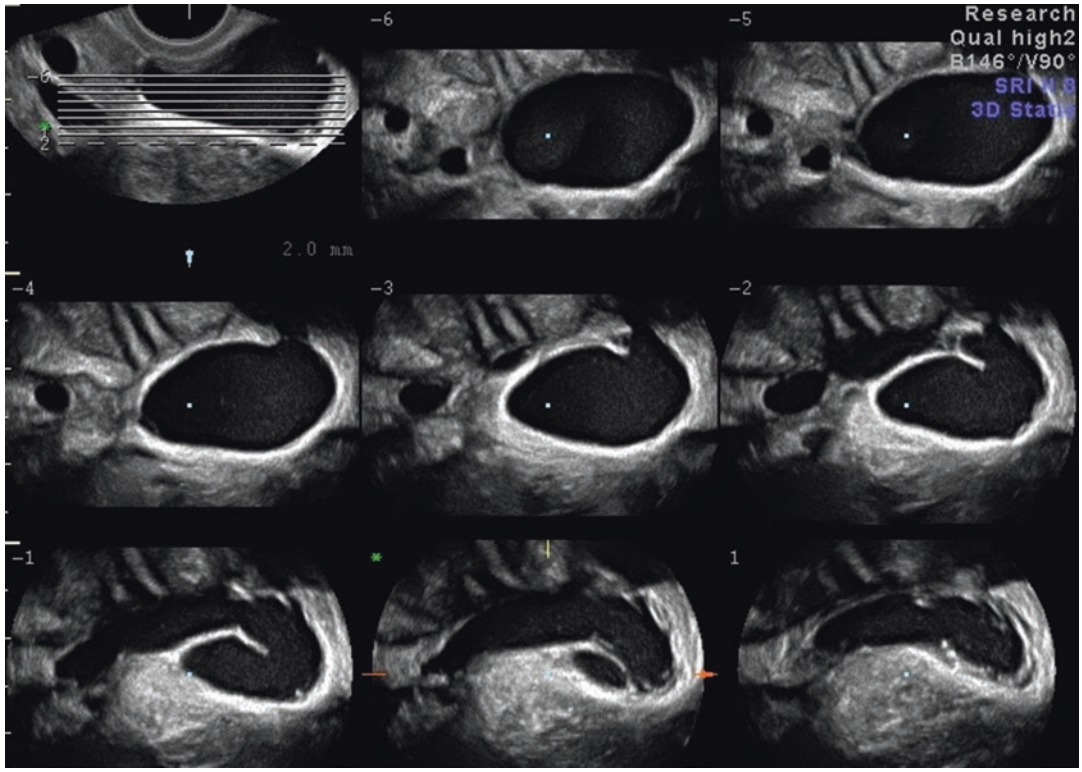

Fig. 14.1 3D TUI (tomographic ultrasound imaging) of hydrosalpinges with views at different depths within the hydrosalpinges

Laparoscopy and Dye Test (Chromopertubation)

Laparoscopy (+/− hysteroscopy) and dye testing is the gold standard method for evaluation of tubal patency. This is especially true of high-risk women who have a history of endometriosis, previous pelvic infection or abdominal surgery. Laparoscopy allows direct visualisation and concurrent treatment for various pelvic and tubal pathologies such as endometriomas, leiomyomas, pelvic endometriosis and peritubal adhesions. Methylene blue dye is introduced via the cervix, and if tubal patency is present, bilateral spill of dye can be directly visualised from each fimbrial end. This is captured either on still photographs or on video. Although laparoscopy is now a routine operation, it is still associated with risks. These include bleeding, infection, vascular damage as well as visceral injuries to other organs (bowel and bladder). Should complications at laparoscopy occur, then a laparotomy may be required. The use of general anaesthesia poses risks, and the possibility of subsequent venous thromboembolism must not be overlooked. Facilities to perform laparoscopy may not be readily available in all fertility clinic settings.

Laparoscopy is an expensive and invasive procedure when used in this context, and appropriately trained clinical and auxiliary staff are required to perform this.

Although this procedure is the gold standard method for evaluating tubal patency, it shouldn't be the first-line screening method employed on a large scale. Patients should be appropriately selected for this procedure. One possible way of risk assessing women would be to perform the inexpensive chlamydia antibody titre (CAT) blood test, and if positive, these women should be offered laparoscopy as the possibility of encountering pelvic pathology is higher in this group of patients [1]. This is already occurring in some parts of Europe where CAT testing is used as a first-line test in subfertility workup, and those

above a fixed cut-off level have postinfectious pelvic disease excluded by means of laparoscopy and chromopertubation, rather than having HSG [2, 3]. In patients who are CAT positive, HSG should be omitted in order to avoid the potential of infectious complications [4]. Patients with a high-risk history (e.g., known endometriosis and previous pelvic surgery) should have their pelvis assessed by means of a laparoscopy and dye test [5].

Hysterosalpingography (HSG)

HSG is an outpatient X-ray examination of the uterine cavity and fallopian tubes using contrast media [6]. This procedure is performed in the follicular phase of the menstrual cycle so as to not disrupt an early pregnancy. A cannula (often metal) is inserted transcervically, and a radio-opaque dye (e.g., Urografin) is passed through the cannula. X-ray images are then obtained, and patency is confirmed by visualising the bilateral peritoneal spillage of the dye. Following the procedure, patients should be advised about pelvic pain, which will be similar to dysmenorrhoea. Prophylactic antibiotics are also usually prescribed.

HSG most commonly involves the usage of a radio-opaque dye Urografin (30% for infusion contains 0.04 g sodium amidotrizoate and 0.26 g meglumine amidotrizoate), which is water-soluble.

In comparison to laparoscopy, HSG is more cost-effective, can be performed in a low-resource setting and does not require as much operator expertise. In addition, HSG can delineate uterine cavity abnormalities as well as tubal blockage. The passage of dye through the tubes can sometimes inadvertently cure the blockage, and therefore HSG can, on occasions, be therapeutic. A meta-analyses of over 4000 subjects concluded that HSG has a sensitivity of 53% and a specificity of 87% for any tubal pathology and 46 and 95% for bilateral tubal pathology [3, 7]. Both oil-soluble and water-soluble contrast media have been employed in HSG. Oil-soluble media are associated with risk of oil emboli as well as inducing inflammatory reactions within the diseased fallopian tubes. The more commonly used water-soluble agents have been shown to result in increased bleeding post HSG; however, they do produce superior radiographic images.

There has been a lot of debate regarding the use of oil-based versus water-soluble dye in HSG. A randomised controlled trial did not show any statistically significant difference in the live birth rates following oil- or water-soluble contrast media [8]. Recent evidence has highlighted the role of lipiodol (ethiodized oil), an oil-soluble contrast in fertility enhancement when compared to water-soluble contrast. A recent multicentre randomised trial including 1119 infertile women from 27 hospitals in the Netherlands was carried out comparing oil-based and water-based contrast medium in HSG. It concluded that ongoing pregnancy rates and live birth rates were significantly higher in patients where oil-based contrast medium was used [9].

Disadvantages of HSG include the radiation exposure to the pelvis. The mean dose-area product (DAP) for HSG is 2.05 Gy cm^2 versus 0.09 Gy cm^2 for a chest X-ray [10]. The use of iodine-based contrast media can result in hypersensitivity reactions and should be avoided in patients known to be sensitive to iodine-containing compounds. HSG requires the services of the radiology department for interpretation of the images produced. The procedure is associated with patient discomfort during and after the procedure. The use of thinner, non-metal cervical catheters may reduce the discomfort experienced by the patient. A study comparing HSG using a rigid, metal cannula with a balloon catheter demonstrated less patient-reported pain, less fluoroscopic time, smaller amounts of contrast medium and easier operation using the balloon catheters [11].

Some operators advise patients to take simple analgesia prior to attending for the procedure, although there is a paucity of evidence that this actually provides any significant relief.

Hysterosalpingo-Contrast-Sonography (HyCoSy)

Hysterosalpingo-contrast-sonography is an outpatient transvaginal ultrasound procedure that visualises the uterine cavity and observes spill from the fimbrial ends of the fallopian tubes.

The technique of HyCoSy was founded upon two independent observations. The initial

observation, published over 30 years ago, was that saline could be injected into the uterine cavity to delineate endometrial structures using a transvaginal ultrasound probe [12]. The same investigators noted that saline would then be present in the pouch of Douglas, indicating spill of saline had occurred through patent fallopian tubes.

Normal fallopian tubes are rarely visualised on ultrasound; however, diseased tubes (e.g., hydrosalpinx) are more readily apparent due to the presence of fluid. The notion that a fluid-filled intrauterine cavity/fallopian tubes could enhance visual diagnosis leads to the idea that injecting fluid into the uterus could be used to detect both intrauterine anomalies and tubal patency at ultrasound. Although saline was the first fluid agent to be used, its use was reported with varying degrees of success. There were limitations in observing the flow through the entire tube as well as unpredictable and not easily reproducible results. Air has also been described as a contrast agent that can be used at HyCoSy. Although it has obvious cost benefits, visualisation of the tubal course may be more challenging. This, in part, may be due to the similar echogenicities of air and the surrounding structures (e.g., bowel gas) (Fig. 14.2).

In the mid-1980s, an ultrasound contrast agent named Echovist® was being trialled for use in echocardiography. Due to its echogenic properties, Echovist® revolutionised the visualisation of the fallopian tubes using HyCoSy. Echovist® consists of galactose particles suspended in an aqueous galactose solution. Echovist® is no longer available, and SonoVue®, a second-generation agent, is now commonly used. The SonoVue® kit consists of a lyophilised powder which is mixed vigorously with normal saline to form the injectable contrast media. SonoVue consists of microbubbles of sulphur hexafluoride [13]. The interface between the sulphur hexafluoride bubble and aqueous medium acts as a reflector of the ultrasound beam, thus enhancing blood echogenicity and increasing contrast between the blood and the surrounding tissues. The most recent introduction of ExEm foam dye which contains hydroxycellulose has been specifcally been manufactured for tubal patency. The visualisation with this has hugely improved its widespready use and due to the foam used is also known as **Hyfosy** (Fig. 14.3).

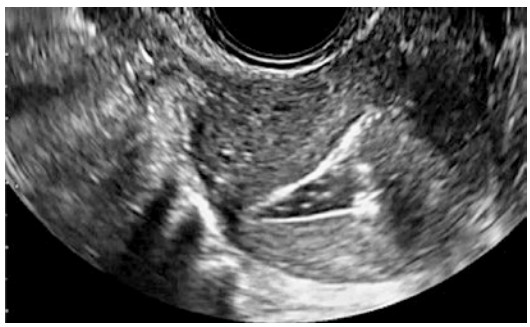

Fig. 14.2 HyCoSy with water and air: this image demonstrates air echogenic areas with a background of echo-free areas. The air bubbles are seen to move through the tube to demonstrate patency

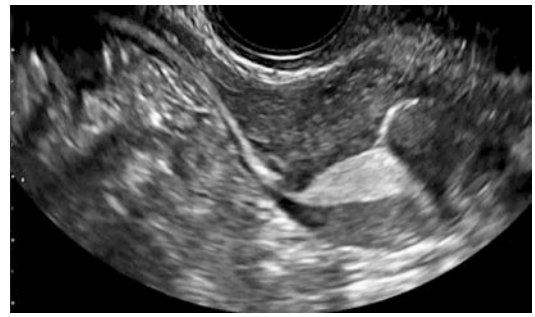

Fig. 14.3 HyCoSy with ExEm® dye showing dye in the uterine cavity and the right tube

The contrast agent produces a hyperechoic appearance on transvaginal ultrasonography. The contrast media are detected first in the uterine cavity, proximal and then distal fallopian tubes (if they are patent). Tubal patency is demonstrated by visualising intratubal flow for 5–10 seconds using B-mode scanning and until peritoneal spill is detected around the ovaries [14].

Below we outline a suggested technique for performing the procedure. There are variations to this technique, as well as inclusion and exclusion of steps that may not be routinely performed by other operators.

As HyCoSy is often performed as an outpatient procedure, it is imperative that clinicians performing this procedure remember the basics of good bedside manner, effective communica-

tion and making the patient feel at ease. Most patients will be apprehensive about the possible findings but also the anticipated discomfort. Operators performing HyCoSy should be proficient in transvaginal ultrasonography and placement of transcervical catheters and possess the relevant clinical experience and skills to perform this investigation.

It is a good practice to issue patients with an information leaflet (some time before the procedure) outlining the procedure so that they have some idea of what to expect when they attend. Leaflets can also inform patients of what to do pre-procedure and expect post-procedure and whom to contact in the event of any complications.

Some operators will perform a urinary beta-HCG test to exclude pregnancy prior to commencing the procedure, although as HyCoSy is performed in the follicular phase of the cycle, this isn't done routinely.

The Technique

1. After gaining verbal consent and a brief description of the procedure, the patient is placed into the dorsal lithotomy position.
2. A warmed, sterile and well-lubricated Cusco's (bivalve) speculum (of the appropriate size for the patient) is then carefully and slowly inserted into the vagina in order to visualise the cervix. Occasionally, the cervix may not be easily identified, and gently changing the angle of direction of the speculum may help with this.
3. Once the cervix is identified, it is cleaned with an aseptic solution.
4. The authors recommend the use of a flexible balloon catheter and not the previously used metal cannulae. Foley catheters have also been employed at this stage. The insertion of the catheter does not routinely require the use of a tenaculum; however, if tenaculum use is required, then the authors suggest a paracervical block with 1% lignocaine prior to grasping the cervix or only blocking the anterior lip when the tenaculum is applied.

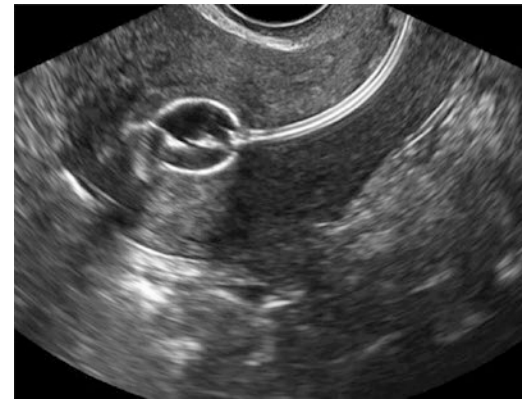

Fig. 14.4 HyCoSy catheter in cavity – ideally the catheter should be in the cervical canal. Occasionally, it is placed in the cavity to prevent displacement during the procedure

5. If a balloon catheter is used, then the authors recommend intracervical, as opposed to intrauterine, balloon dilatation. It has been demonstrated that this causes less pain, and less contrast media are required in this way too [15]. The balloon can be inflated with air or sterile water. This also allows visualisation of the lower end of the uterine cavity. If the catheter is found to be placed in the uterine cavity under ultrasound guidance, this can be withdrawn into the cervical canal. Figure 14.4 shows the balloon in the uterine cavity – this is occasionally done if the catheter does not appear to be well fixated in the cervical canal (and therefore prevents it from falling out).
6. Once the catheter is in situ and secure, the speculum (and tenaculum if applied) can be gently removed, ensuring the catheter is not dislodged. The patient is then forewarned that the transvaginal ultrasound probe will be inserted.
7. At this stage, the authors perform a conventional B-mode transvaginal scan to assess the uterus, ovaries and pouch of Douglas. The correct placement of the catheter balloon can also be checked at this point. Alternatively, a conventional scan can be performed after step 1 (before the catheter is introduced).
8. After warning the patient, the contrast medium can be injected slowly and steadily.

It is important to remember that the uterus is pressure sensitive, and as such, excessive rates and/or volumes of injecting will result in unnecessary patient discomfort. Beware that blocked fallopian tubes may increase the pain experienced by the patient. The authors suggest using no more than 10 ml of contrast media. If the balloon has been inflated correctly, there should be no leakage, and evaluation of the uterus and both tubes should be possible using less than 10 ml. In the author's experience, 2–5 ml is sufficient for demonstrating tubal patency.

9. Tubal patency is assessed by demonstrating flow along the entire length of the tube or by streaming at the cornual end for at least 10 seconds with spill into the pouch of Douglas [16].
10. A detailed examination of the uterus is performed by scanning slowly and systematically from the cervix to fundus. Any relevant lesions (e.g., submucous leiomyoma) can be closely analysed and relevant images produced.
11. Each tube is followed, in turn, until spill is visualised adjacent to the ovary.
12. Strict criteria must be adhered to in order to ensure that the fallopian tube is followed in its entirety, before it is considered to be patent. Any delay in tubal fill and/or spill must be appropriately documented. Any apparent distortion of the tubal diameter or tubal course must also be documented and preferably supplemented with the use of images/videography.
13. This could be followed by assessment of the uterine cavity with normal saline to exclude endometrial polyp or submucous fibroids.

HyCoSy (and HSG) has the significant advantage over laparoscopy of being outpatient-based (office) investigations without a need for general anaesthesia. There is no risk of visceral or vascular injuries. Patients do not need to be fasted for either procedure, and both the patient and her partner can be present whilst the investigation is being performed.

Unlike HSG, HyCoSy does not involve the use of ionising radiation and iodine-based contrast media or the use of radiology services – it can be performed by a gynaecologist/specialist in reproductive medicine, obviating the need for a radiologist. As an ultrasound-based investigation, other pelvic structures can be assessed simultaneously. HSG may preclude the need for laparoscopy in some cases, thereby improving patient satisfaction and preventing the need for invasive investigations.

HyCoSy has been shown to be at least as effective as hysterosalpingography at detecting tubal blockage. When compared with the gold standard of laparoscopy and dye testing, reported rates for sensitivity and specificity are 80 and 84%, respectively [17]. The use of HyCoSy is superior to hysterosalpingography in detecting intrauterine anomalies such as leiomyoma, polyps, septae and hydrosalpinx [18].

Two-dimensional transvaginal HyCoSy as described above, although in many ways superior to HSG, does have its limitations. Due to the tortuous course of the fallopian tubes, the entire tube will not be visualised in one scanning plane. Visualisation of the tubal course can be further limited by tubal spasms. As a result, the false-positive rate for tubal occlusion is 5–10% [19]. Due to the echogenicity of bowel, distal spill from the tubes may be difficult to distinguish from the surrounding bowel and therefore relies on a certain level of operator expertise. Interpretation can therefore be slightly more challenging as compared to hysterosalpingography. As the procedure does rely on the technical ability of the clinician performing the procedure, there can be considerable inter- and intra-observer variability.

Compared with 2D HyCoSy, 3D HyCoSy requires less time, avoids probe movements and is less dependent on operator skill. However, 3D HyCoSy is a static imaging method, cannot dis-

play the real-time process of contrast agent flow in fallopian tubes and at times makes it difficult to identify morphology of tubes in patients with myometrium venous reflux. These problems can be overcome by 4D HyCoSy, a real-time 3D HyCoSy [20].

Three-Dimensional Coded Contrast Imaging (3D CCI) During HyCoSy

Coded contrast imaging (CCI) comprises of dedicated computer software, designed to enhance the view of the fallopian tubes whilst filtering out signals from other tissues. The image which is produced is based on ultrasound signals produced by the contrast media and not by surrounding tissues.

Coded contrast imaging enhances the use of contrast media by means of low acoustic pressure, thereby enhancing visualisation of the fallopian tube by enabling the clinician to differentiate between the harmonic response of the contrast medium and signals from other surrounding organs such as bowel [19]. The software is able to filter out ultrasound signals produced by the organs and thereby display an image which is solely based on harmonic signals produced by the contrast media.

This technology has been applied in other fields including studying the microvasculature of the liver, breast lesions as well has myocardial perfusion function.

In order to further enhance the technology, second-generation contrast media are used. The first-generation contrast media (Echovist®) contain microbubbles that have rigid membranes and are therefore unable to respond with harmonic signals at low acoustic pressures. However, second-generation agents, such as SonoVue®, provide a substantial harmonic response at low acoustic pressure. The use of a second-generation contrast medium with CCI technology enables the operator to view the hyperechoic fluid firstly in the uterus and then the proximal tube and lastly spill into the abdominal cavity. Due to the detectable differences between the harmonic response between the contrast media and that of the surrounding tissue, there is a clear distinction between the contrast media and the surrounding structures.

The use of 3D imaging (without CCI) using saline-air contrast has been reported; however, the resulting image may not necessarily be clear enough to make a conclusion regarding tubal patency. However, when 3D imaging is combined with CCI, the tubal course and structure can be studied in much greater detail.

Software packages that provide the volume acquisition images are available, and when this is combined with 3D CCI, then a 3D image with the uterus and tubes, showing the tubal course in its entirety and tubal spill (if patent), is seen as a hyperechoic image in a completely anechoic pelvis (i.e., no other structures are seen).

Volume acquisition performed during HyCoSy is a static procedure and as such requires less challenging probe movements and therefore less operator experience and expertise as compared to conventional 2D TVS HyCoSy [19]. As 3D CCI visualises both fallopian tubes, less contrast media are required – this is beneficial both to the patient and also from a cost perspective. Another advantage of 3D CCI at HyCoSy is that the images can be stored (similar to Doppler imaging and HSG) and viewed by clinical colleagues, unlike conventional 2D HyCoSy which is a dynamic procedure that only the operator can interpret. However, 3D imaging requires greater funding and therefore is not accessible in resource-poor settings. A recent study [21] comparing 3D HyCoSy in 150 tubes to laparoscopy and dye testing demonstrated a sensitivity and specificity of 93.5 and 86.3%, respectively. The authors reported a positive predictive value of 87% and negative predictive value of 92.6%. These values compare favourably with previ-

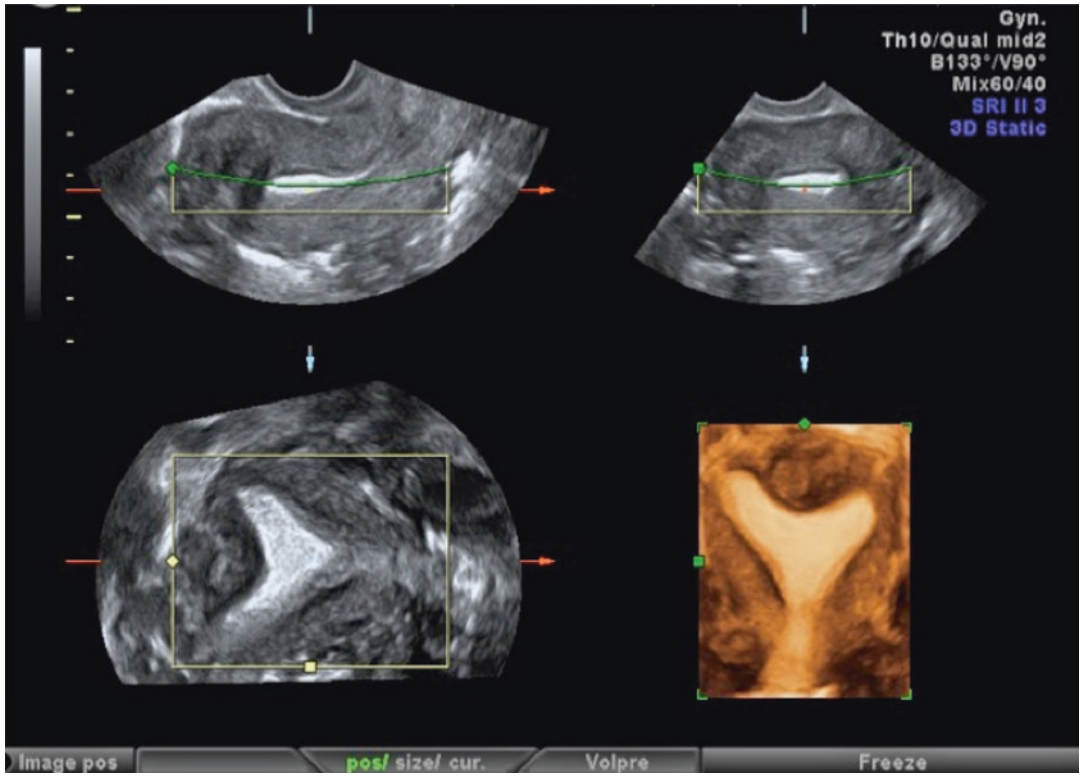

Fig. 14.5 3D HyCoSy with Echovist® dye showing the cavity

ously reported sensitivities and specificities of 2D HyCoSy.

Although more work is required to assess the diagnostic accuracy and feasibility of 3D CCI HyCoSy, it appears that this novel method of evaluating tubal patency will become widespread in the future and an integral part of the subfertility workup (Fig. 14.5).

Blood Flow and Doppler Imaging

Blood flow and Doppler are additional modalities that can be employed in conjunction with HyCoSy.

Blood flow is a relatively new technique which has been employed in other medical specialities such as vascular studies. Blood flow is an ultrasound technique developed to analyse blood flow. It does not employ the Doppler principle; rather, the reflected amplitudes of scattering particles (e.g., erythrocytes) are imaged by subtraction modes of two or four image vectors along one line. Therefore, moving particles are imaged, and stationary structures (such as vessel walls) can be subtracted. Blood flow data can

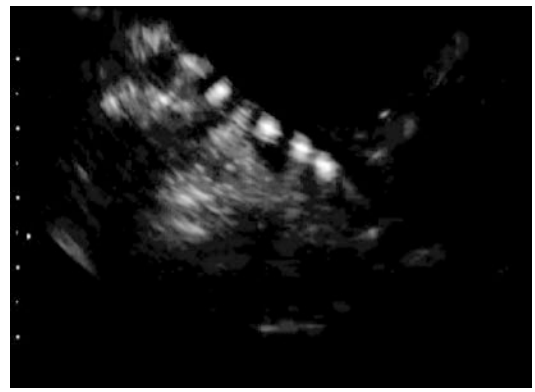

Fig. 14.6 HyCoSy with B-flow technique: this is a form of inversion mode where movement of fluid is captured in greyscale and the rest of the image appears dark. The *grey images* below the tube represent the bowel peristalsis

then be combined with B-mode information to enable a better amplitude visualisation of flow. With this technique, water can be used, and tubal patency is demonstrated with blood flow technique.

Although the application of blood flow is not yet an established method of assessment for tubal patency, increased experience and knowledge of it is likely to lead to more widespread use of this modality in the assessment of tubal function (Fig. 14.6).

Colour-coded Doppler imaging can be used as an adjunct to greyscale imaging in order to visualise the flow of media through the tubes. Doppler imaging has been shown to be valuable in cases where HyCoSy has been inconclusive [22]. When 3D power Doppler imaging (3D-PDI) is employed in conjunction with HyCoSy, it allows visualisation of contrast media throughout the entire tubal length. The use of 3D-PDI has clear advantages over the use of HyCoSy alone. It has been shown that visualisation of distal tubal spill occurs twice as often when 3D-PDI is employed [23]. As the procedure does rely on the technical ability of the clinician performing the procedure and, in the case of 3D-PDI, time for analysis, this has not been routinely implemented in clinical practice.

Conclusion

Being one of the commonest causes of subfertility, tubal patency is an essential component of the subfertility workup. In this chapter, we have provided an overview of the gold standard technique of chromopertubation and classical methods such as the hysterosalpingogram and then covered the use of ultrasound in slightly more detail. We hope we have provided the reader with a good understanding of these newer techniques involving ultrasound as well as a foundation for a technique that we employ. The methods we have outlined above are by no means exclusive, and the readers are encouraged to develop their own techniques when carrying out the procedures discussed. As the boundaries of investigative medicine continue to be expanded, there will be further development of the above employed methods as well as newer modalities. What is certain is that ultrasound does and will continue to play a pivotal role in the armamentarium we have at our disposal in the investigation of our patients.

References

1. Lim CP, Hasafa Z, Bhattacharya S, Maheswari A. Should a hysterosalpingogram be a first-line investigation to diagnose female tubal subfertility in the modern subfertility workup? Hum Reprod. 2011;26(5):967–71.
2. Coppus SFPJ, Opmeer BC, Logan S, Van der Veen F, Bhattacharya S, Mol BWJ. The predictive value of medical history taking and Chlamydia IgG ELISA antibody testing (CAT) in the selection of subfertile women for diagnostic laparoscopy: a clinical prediction model approach. Hum Reprod. 2007;22:1353–8.
3. Swart P, et al. The accuracy of hysterosalpingography in the diagnosis of tubal pathology: a meta-analysis. Fertil Steril. 1995;64(3):486–91.
4. den Hartog JE, Lardenoije CM, Severens JL, Land JA, Evers JL, Kessels AG. Screening strategies for tubal factor subfertility. Hum Reprod. 2008;23:1840–8.
5. National Collaboratry Centre for Women's and Children's Health. Fertility: assessment and treatment for people with fertility problems. Commissioned by the National Institute for Clinical Excellence (NICE). London: RCOG Press; 2004. ISBN 1-900364-97-2.
6. Steinkeler JA, Woodfield CA, Lazarus E, Hillstrom MM. Female infertility: a systematic approach to radiologic imaging and diagnosis. Radiographics. 2009;29:1353–70.
7. Broeze KA, Opmeer BC, Van Geloven N, Coppus SFPJ, Collins JA, den Hartog JE, et al. Are patient characteristics associated with the accuracy of hysterosalpingography in diagnosing tubal pathology? An individual patient data meta-analysis. Hum Reprod. 2011;17:293–300.
8. Spring DB, et al. Potential therapeutic effects of contrast materials in hysterosalpingography: a prospective randomised controlled trial. Radiology. 2000;214:53–7.
9. Dreyer K, van Rijswijk J, Mijatovic V, Goddijn M, Verhoeve HR, van Rooij IAJ, et al. Oil-based or water-based contrast for Hysterosalpingography in infertile women. NEJM. 2017;2017(25):2043–52.
10. Hart D, Hillier MC, Wall BF. HPA-RPD-029-doses to patients from radiographic and fluoroscopic X-ray imaging procedures in the UK – 2005. Review. 2009;2010:95.
11. Tur-Kaspa I, Seidman DS, Soriano D, Greenberg I, Dor J, Bider D. Hysterosalpingography with a balloon catheter versus a metal cannula: a prospective, randomized, blinded comparative study. Hum Reprod. 1998;13:75–7.
12. Nanini R, Chelo E, Branconi F, Tantini C, Scarselli GF. Dynamic echohysteroscopy: a new diagnostic

technique in the study of female infertility. Acta Eur Fertil. 1981;12:165–71.
13. Lanzani C, Savasi V, Leone FP, Ratti M, Ferrazzi E. Two-dimensional HyCoSy with contrast tuned imaging technology and a second-generation contrast media for the assessment of tubal patency in an infertility program. Fertil Steril. 2009;92:1158–61.
14. Campbell S, Bourne T, Tan S, Collins W. Hysterosalpingo-contrast-sonography (HyCoSy) and its future role within the investigation of infertility in Europe. Ultrasound Obstet Gynecol. 1994;4:245–53.
15. Spieldoch RL, Winter TC, Schouweiler C, Ansay S, Evans MD, Lindheim SR. Optimal catheter placement during sonohysterography: a randomized controlled trial comparing cervical to uterine placement. Obstet Gynecol. 2008;111:15–21.
16. Ayida G, Chamberlain P, Barlow D, Koninckx P, Golding S, Kennedy S. Is routine diagnostic laparoscopy for infertility still justified? A pilot-study assessing the use of hysterosalpingo-contrast sonography and magnetic resonance imaging. Hum Reprod. 1997;12(7):1436–9.
17. Tanawattanacharoen S, Suwajanakorn S, Uerpairojkit B, Boonkasemsanti W, Virutamesan P. Transvaginal hysterosalpingo-contrast sonography (HyCoSy) compared with chromolaparoscopy. J Obstet Gynaecol Res. 2000;26:71–5.
18. Watrelot A, Hamilton J, Grudzinskas JG. Advances in the assessment of the uterus and fallopian tube function. Best Pract Res Clin Obstet Gynaecol. 2003;17(2):187–209.
19. Exacoustos C, Di Giovanni A, Szabolcs B, Binder-Reisinger H, Gabardi C, Arduini D. Automated sonographic tubal patency evaluation with three-dimensional coded contrast imaging (CCI) during hysterosalpingo-contrast sonography (HyCoSy). Ultrasound Obstet Gynecol. 2009;34:609–12.
20. Wang Y, Qian L. Three- or four-dimensional hysterosalpingo contrast sonography for diagnosing tubal patency in infertile females: a systematic review with meta-analysis. Br J Radiol. 2016;89:20151013.
21. Zhou L, Zhang X, Chen X, Liao L, Pan R, Zhou N, Di N. Value of three-dimensional hysterosalpingo-contrast sonography with SonoVue in the assessment of tubal patency. Ultrasound Obstet Gynecol. 2012;40(1):93–8.
22. Kalogirou D, Antoniou G, Botsis G, Kassanos D, Vitoratos N, Zioris C. Is colour Doppler necessary in the evaluation of tubal patency by hysterocontrast-sonography. Clin Exp Obstet Gynecol. 1997;24(2):101–3.
23. Sladkevicius P, Ojha K, Campbell S, Nargund G. Three-dimensional power Doppler imaging in the assessment of fallopian tube patency. Ultrasound Obstet Gynecol. 2000;16(7):644–7.

Ultrasound in Follicle Monitoring for Ovulation Induction/IUI

15

Josef Blankstein, Peter Aziz, Shumal Malepati, and Jawaria Amir

Ovulation induction refers to the treatment in which ovulation is achieved by medication such as Clomid and gonadotropins to enhance fertility. Transvaginal ultrasonography has become the norm in infertility centers to provide noninvasive access to the dynamic processes such as ovarian follicular development, ovulation, and endometrial response to hormonal stimulation [1–3].

Recent advances in reproductive endocrinology have led to greater understanding of the basic regulatory mechanisms governing the reproductive process. It is fitting to introduce our topic by outlining the major morphological changes of the menstrual cycle that can be visualized by ultrasound.

J. Blankstein (✉)
Rosalind Franklin University of Medicine and Science, Chicago, IL, USA

Mount Sinai Hospital, Department of Obstetrics and Gynecology, Chicago, IL, USA
e-mail: josef.blankstein@sinai.org

P. Aziz
Mount Sinai Hospital, Department of Obstetrics and Gynecology, Chicago, IL, USA

S. Malepati
Trios Medical Group – Obstetrics & Gynecology, Kennewick, WA, USA

J. Amir
Rosalind Franklin University of Medicine and Science, The Chicago Medical School, Chicago, IL, USA

Follicular Selection: Morphological and Ultrasound Observations

In the beginning of each ovarian or menstrual cycle, many follicles may start developing; however only one is selected to continue development, while the remainders undergo atresia. While oocyte recruitment and development is predominately dependent upon genetic endowment, follicular growth, in contrast, is a gonadotropin- and sex steroid-regulated phenomenon.

The early follicular phase of the ovarian cycle is characterized by relatively elevated levels of FSH and low levels of LH, estrogens, and progesterone. During this early cycle phase, the growth of a number of follicles, referred to as a cohort of follicles, is initiated. It has been demonstrated that this oocyte selection process involves two main processes. First, a number of follicles are recruited, and second, a number of growing follicles are selected out of the recruited group to continue toward maturation. Studies supporting the "dominant follicle theory" support that new follicular growth is arrested in the presence of a single dominant follicle. The provision of more gonadotropins in stimulated or induced cycles by clomiphene citrate or human menopausal gonadotropins or both will violate the normal monovular quota. Moreover, the responsiveness of other follicles to human menopausal gonadotropins (hMG) therapy was found to be suppressed in the

L. A. Stadtmauer, I. Tur-Kaspa (eds.), *Ultrasound Imaging in Reproductive Medicine*,
https://doi.org/10.1007/978-3-030-16699-1_15

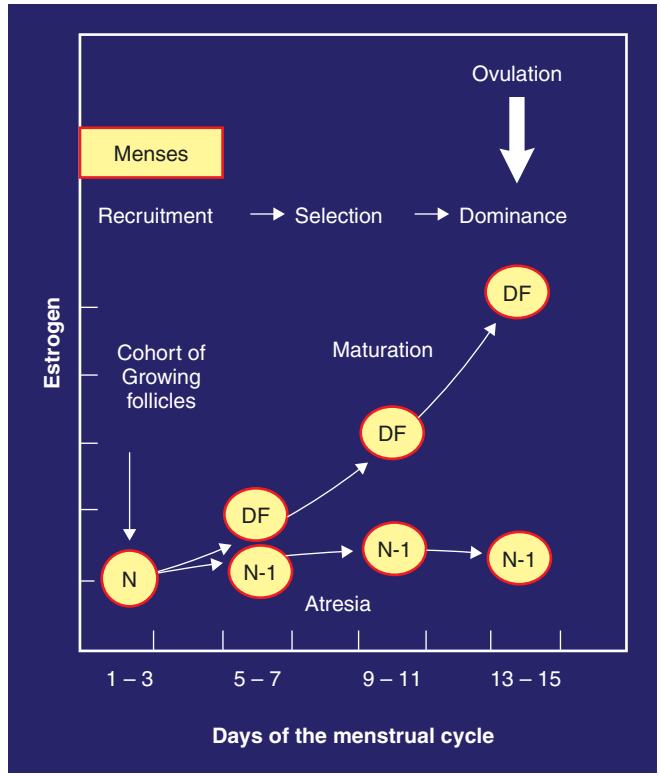

Fig. 15.1 Cyclic ovarian changes. Time course for recruitment, selection, and ovulation of the dominant ovarian follicle, with onset at atresia among other follicles of the cohort. (Reprinted from Hodgen [53]. With permission from Springer)

presence of the overt dominant follicle, while the same dose of hMG early in the follicular cycle increased the number of follicles recruited and/or selected for maturation (Fig. 15.1).

In the normal ovulatory cycle, the dominant follicle steadily increases in size, while the accompanying smaller follicles are not observed to show a similar increase. Thus, while one or more follicles will grow to full maturity and ovulate, others are destined to atresia and degeneration. This follicular atresia appears to involve genetically programed cell death within the oocyte (apoptosis).

Ovarian secretion of estradiol (E_2) and estrone, from the granulosa cells, promotes follicular maturation by increasing follicular sensitivity to gonadotropins stimulation. This is accepted to be a gonadotropin receptor-mediated process.

The temporal relationship between hormonal profile and follicular development with respect to ovulation is summarized in Fig. 15.2.

The dominant follicle is selected due to its responsiveness to elevated circulatory FSH levels. It is not uncommon to observe two, or more, follicles developing to approximately 10 mm with one achieving dominance and growing while the others regress. LH reinitiates meiosis of the oocyte, and typically, ovulation occurs within 36 hours of its "surge."

Small follicles can be visualized easily as echo-free, smooth-walled structures and usually lie toward the periphery of the more echogenic ovarian tissue. As the follicle matures, more fluid is released and accumulates into its center. The granulosa cell mass, lining the inner of the follicle, increases. Microscopically the oocyte itself, which is less than one tenth of one mm, is surrounded by a cluster of granulosa cells. This complex surrounding the oocyte is termed the cumulus oophorus. It measures approximately 1 mm and can occasionally be depicted by transvaginal scan (TVS) adjacent to the wall of a mature follicle. Immediately prior to ovulation, the cumulus separates from the wall and floats freely within the follicle's center. Today, even with the enhanced resolution afforded by TVS, the attached or floating cumulus is only rarely seen. However new technological develop-

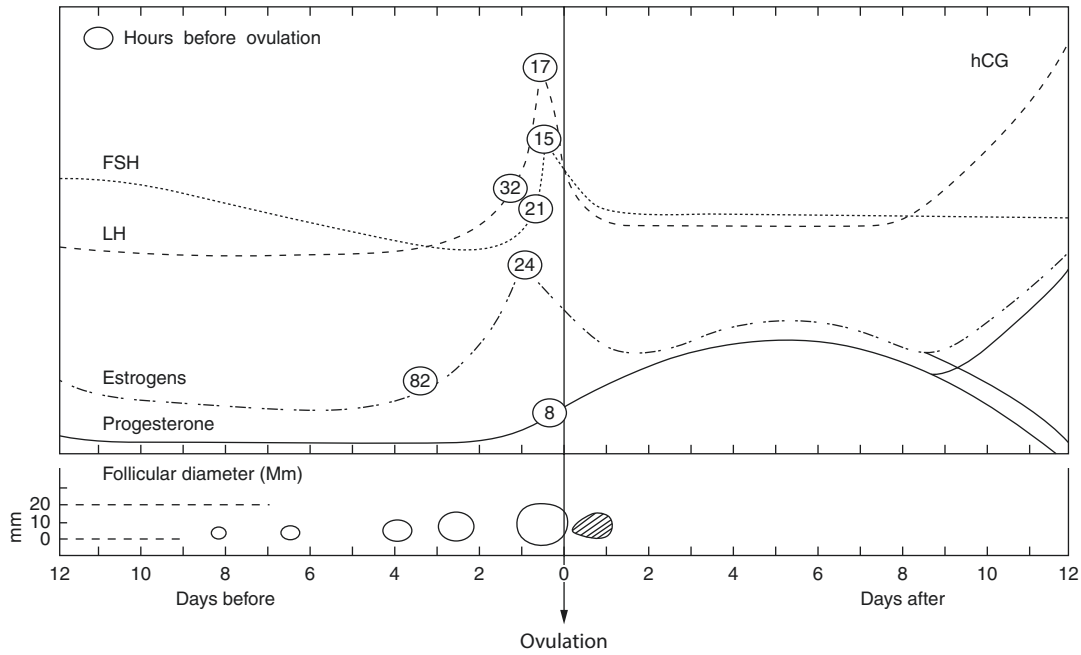

Fig. 15.2 Temporal relationships between hormonal profile and follicular development with respect to ovulation. Significant hormone levels and their preovulatory peaks are given in hours prior to ovulation (circled numbers). (From Blankstein et al. [54])

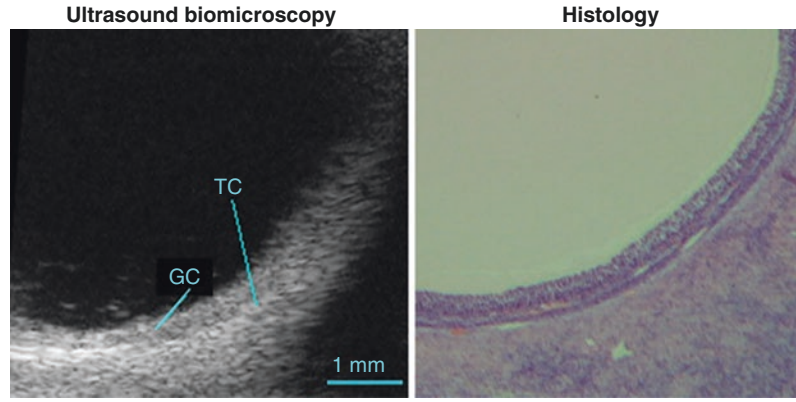

Fig. 15.3 Antrum, granulosa (GC), and the theca cells (TC) in a preovulatory follicle. (Reprinted from Palleres et al. [55]. With permission from Elsevier. https://www.fertstert.org/article/S0015-0282(08)01146-1/fulltext)

ments, mainly high-resolution probes (40 MHz), have enabled clinical researchers to clearly visualize the antrum, granulosa (GC), and the theca cells (TC) in a preovulatory follicle (Fig. 15.3).

Monitoring ovarian response to ovulation induction can be achieved by ultrasonography alone. The dimensions of the growing follicles are plotted from around day 8 of stimulation together with a measurement of endometrial thickness. The mean follicular growth rate is 1.4 mm/day in spontaneous menstrual cycle and 1.7 mm during ovarian stimulation cycles [4].

Mature follicles, those containing a mature oocyte, typically measure from 17 to 25 mm in average inner dimension. The optimal follicular size before triggering ovulation in intrauterine insemination cycles with clomiphene citrate or

letrozole was found to be in the 23–28 mm range. The optimal size of the leading follicle was not statistically significantly different between cycles using letrozole or clomiphene citrate and was closely related to the endometrial thickness [5]. Intrafollicular echoes may be observed with mature follicles, probably arising from clusters of granulosa cells that shear off the wall near the time of ovulation. After ovulation, the follicular wall becomes irregular as the follicle becomes "deflated." The fresh corpus luteum usually appears as a hypoechoic structure with an irregular internal wall and may contain some internal free-floating or fixed echoes that correspond to hemorrhage. As the corpus luteum develops 4–8 days after ovulation, it appears as an echogenic structure of approximately 15 mm in size. Its wall is thickened due to the process of luteinization. TVS shows the neovascularity within the wall that is associated with formation of the corpus luteum. In addition to delineation of changes in follicle size and structure, TVS can depict the presence of intraperitoneal fluid. It is normal to have approximately 1–3 mL of intraperitoneal fluid in the cul-de-sac throughout the cycle. When ovulation occurs, there typically is between 4 and 5 mL of fluid within the cul-de-sac. The intraperitoneal fluid resulting from ovulation may be located outside of the posterior cul-de-sac, surrounding bowel loops in the lower abdomen, and upper pelvis or in the anterior cul-de-sac superior to the uterine fundus (Fig. 15.4).

The Role of Doppler in Reproduction

The formation of new blood vessels is taking place in the ovary during folliculogenesis and corpus luteum formation, as well in the endometrium, mainly during the follicular phase. It was already recognized as early as in 1926 that neovascularization may be of prime importance in the growth and selection of ovulatory follicles, in addition to the subsequent development and function of the corpus luteum. Studies of ovarian vascular morphology showed that the capillary network of preovulatory follicles was more extensive than that of other follicles, consequently proposing that initiation and maintenance of follicular growth depends on the development of the follicular microvasculature.

A study done by Shrestha et al. [6] to determine whether ovarian perifollicular blood flow (PFBF) in the early follicular phase (EFP) is associated with treatment outcome of IVF showed high-grade ovarian PFBF in the EFP during IVF to be associated with a higher clinical pregnancy rate. Furthermore, a study done by Vural et al. [39] concluded that well-vascularized follicles are associated with good-quality oocytes

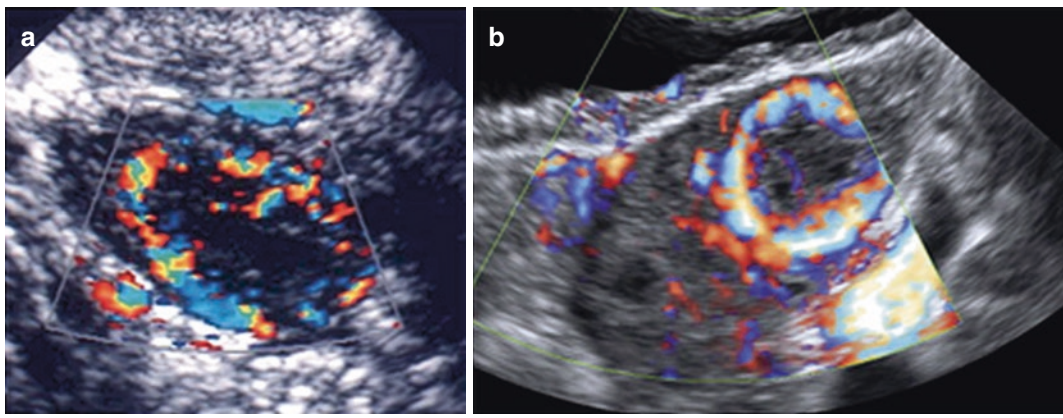

Fig. 15.4 Corpus luteum ultrasound study. (**a**) Note the irregular cystic mass with crenulated borders and low-level echoes. (**b**) Doppler findings of a hypervascular corpus luteum with low resistance index

and embryos, a well-vascularized endometrium, and increased pregnancy rates. However, a systematic review by Huyghe et al. [40] indicates that while PFBF could be a good prognostic marker for pregnancy rate after IVF/ICSI, this was not observed in studies utilizing only IUI.

Coulam et al. [7] correlated peak systolic velocity (PSV) of individual follicles with oocyte recovery, fertilization rate, and embryo quality in women undergoing in vitro fertilization (IVF) and embryo transfer. They assessed the role of quantitative and qualitative indices of follicular vascularity in predicting pregnancy after IVF and embryo transfer. Women who had PSV ≥ 10 cm/s in at least one follicle on the day of hCG administration more often became pregnant than those with PSV <10 cm/s ($P = 0.05$). Nargund et al. [8] demonstrated that there was a 70% chance of producing a grade I or II embryo if the follicular blood velocity was >10 cm/s, compared with 14% if the PSV was <10 cm/s. This study concluded that there is a physiological relationship between follicular blood velocity, oocyte recovery, and the production of a high-grade preimplantation embryo, which may form the basis of a useful clinical test. Jayaprakasan et al. [9] on the other hand concluded that ovarian vascularity as measured by 3D ultrasound is not decreased in women who demonstrate poor ovarian response to controlled ovarian stimulation as part of assisted reproduction treatment.

Perifollicular vascular perfusion appears to be an important factor in determining the outcome of stimulated cycles and may have clinical implications in assisted reproduction therapy. As there were low pregnancy rates and oocyte retrieval in the group of women with uniformly low-grade vascularity, the identification of these cycles would be valuable in terms of counseling with regard to the potential outcome in that cycle. Ideally, the identification of these women (who may also be "low recruiters") earlier in the cycle would be helpful. This could allow the cancellation of treatment after careful counseling, on the basis of perifollicular vascular perfusion, and could be cost-effective, both financially and emotionally. However, further longitudinal data would be needed before this form of prospective management of treatment cycles could be applied clinically. The risk of multiple pregnancies and their implications on the health service is also well recognized. Since there were higher multiple pregnancy rates in stimulated intrauterine insemination (IUI) cycles with uniformly high-grade follicular vascularity, perhaps these cycles in particular should be considered for follicle reduction or even cancellation. This may potentially reduce the number of developmentally competent oocytes that have a higher capability of producing more viable embryos for implantation [10].

In a prospective study by Ivanovsky et al. [11], vascular impedance was calculated using the uterine artery and arcuate artery pulsatility resistance and velocity on the day of hCG administration. It was found that optimal uterine receptivity can be accomplished by reduced vascular resistance and increased blood flow. Obviously more studies are needed to confirm their results.

The relationship between endometrial and subendometrial blood flow and pregnancy after intrauterine insemination was examined in a prospective study. The main outcomes measured were vascularization index (VI), flow index (FI), and vascularization flow index (VFI) of the endometrium as well as those of subendometrial region. These measurements were analyzed in relation to IUI outcome in pregnant vs. nonpregnant. It was found that the pregnant group had higher endometrium VI, FI, and VFI scores than the nonpregnant group. The subendometrial region VI, FI, and VFI scores did not differ between the groups [12] (Fig. 15.5).

Ovulation Induction and Intrauterine Insemination (IUI)

In conjunction with ovulation induction, IUI is a way to potentially overcome various fertility problems such as oligospermia, i.e., low sperm count, low sperm motility, cervical factor infertility (cervical mucus inactivates sperm motility), sexual dysfunction, and unexplained infertility.

By placing sperm directly into the uterine cavity, the greatest barrier, the mucus in the cervix, is

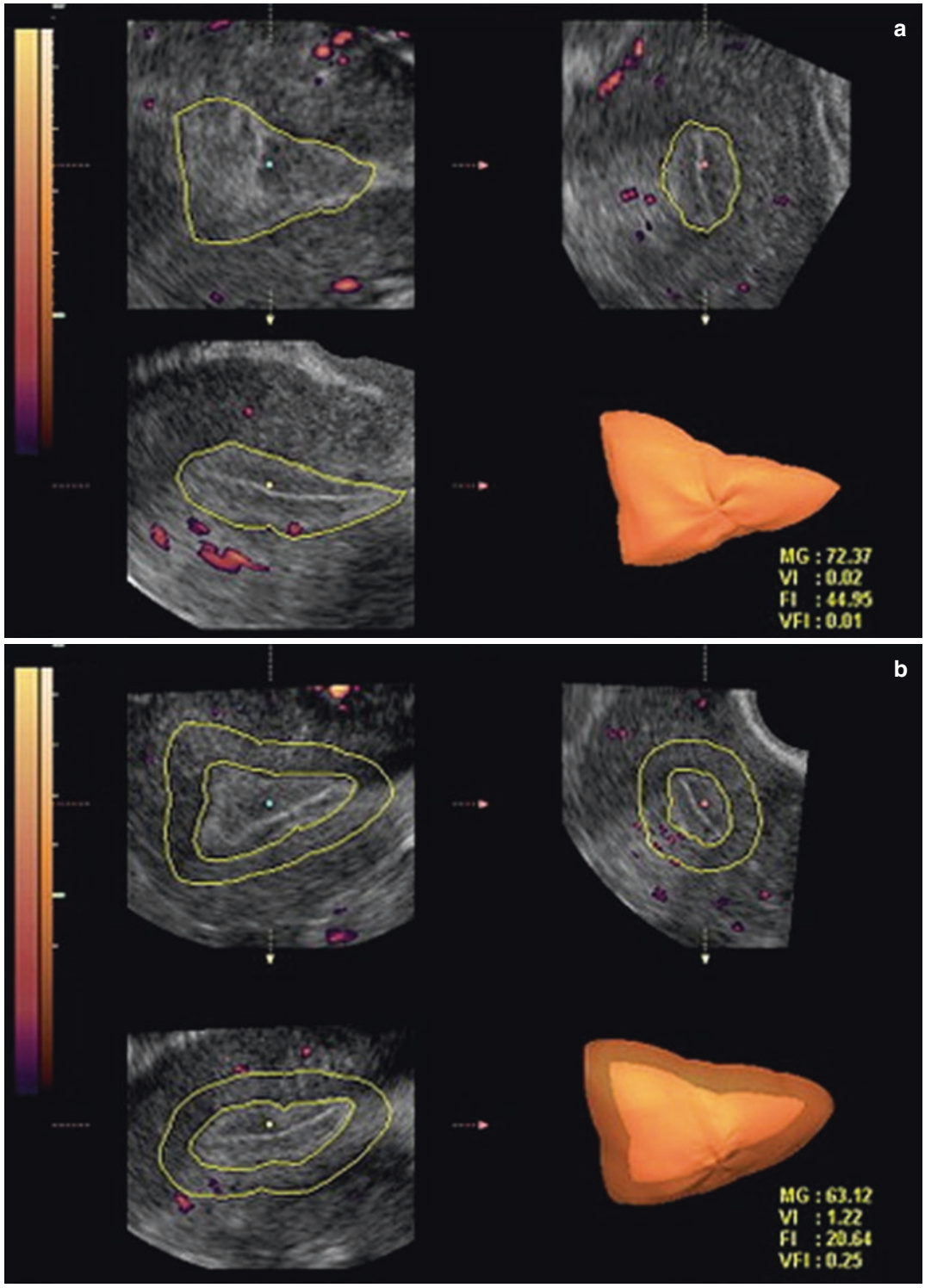

Fig. 15.5 Three-dimensional power Doppler images generated using VOCAL software. (**a**) Endometrial. (**b**) Subendometrial blood flow parameters on the day of IUI. (Reprinted from Kim et al. [12]. With permission from Elsevier. https://www.fertstert.org/article/S0015-0282(09)00754-7/fulltext)

bypassed; therefore, more sperm reaches the egg, creating a better chance of fertilization for the egg. IUI is usually combined with ovulation induction. Optimal timing of insemination is achieved either by the detection of a luteinizing hormone (LH) surge through urinary LH (uLH) testing or by ultrasound monitoring of follicular growth followed by the administration of human chorionic gonadotropin (hCG). In most centers, when the leading follicle reached >18 mm in diameter, 10,000 IU hCG was given to trigger ovulation, and IUI is timed 36+ or −2 hours later. While IUI is a natural starting point for many treatment schemes, unfortunately this therapy may be complicated by premature luteinization and hyperstimulation.

Premature Luteinization

Premature LH surge will luteinize the follicle, which is too small and not ready to ovulate. Cantineau et al. [23] studied the prevalence of premature LH surges in an IUI program. It has been concluded that 24% of IUI cycles suffer from premature LH surge, and this can result in IUI procedure cancellation. Obviously, this represents economic and psychological stress for the patients.

Manzi et al. [13] showed that patients who underwent controlled ovarian stimulation (COS)/IUI treatment and had premature LH surge demonstrated much better pregnancy rates in the subsequent cycle when a GnRH analogue was added, thus avoiding premature LH surge.

GnRH antagonists have been proposed to prevent premature LH surge [14]. These drugs do not produce flare-up effect. Moreover, the potential advantage of a GnRH antagonist is that pituitary gonadotropin secretion is suppressed immediately after the start of the therapy. Therefore, co-treatment with GnRH antagonists can be restricted to the time in the cycle where there is a risk of premature LH rise. It has been shown that a minimal dose of leuprolide depot is sufficient to prevent premature LH surge in the in vitro fertilization (IVF) programs [41]. However, Wadhwa et al. [42] showed that the delayed administration of GnRH antagonists in mild ovarian hyperstimulation (MOH) with IUI cycles when follicle size is ≥16 mm is beneficial in terms of preventing the occurrence of premature LH surge but with no improvement in pregnancy rates.

Multiple Pregnancies

Another concern with controlled ovarian stimulation COS/IUI cycles is the risk of multiple pregnancies. The problem with multiple gestations is that they are associated with major maternal and fetal risks (see Table 15.3).

This past decade has shown increasing medical, societal, and regulatory attention to controlling multiple gestations in all areas of assisted reproduction. Improved outcome-based medical procedures, such as lower gonadotropin dosages, single embryo IVF transfer, and increased utilization of cryopreservation of embryos, have all contributed to the reduction in multiple gestations from ART procedures. Regulatory pressure to lower multiple gestations has come in the form of multiple agencies publishing embryo transfer number guidelines, and a national ART tracking database through SART (Society of Reproductive Medicine). In the USA such regulations remain voluntary, while in many other countries, such guidelines are legislated and strictly enforced.

Low-dose stimulation, careful follicular monitoring, may help to reduce the risk of multiple pregnancies. The risk of multiple pregnancies after IUI is dependent on the type of stimulation (clomiphene citrate vs. gonadotropins) and on the size and number of follicles. Dickey et al. [15] reported a positive correlation of multiple pregnancies with the number of follicles 12 and 15 mm or larger. Offering oocyte aspiration of excess follicles in an effort to reduce multiple gestations has been proposed by many researchers, and this method has shown to reduce the risk of multiple pregnancies.

Stoop et al. [16] concluded that aspiration of excess oocytes in stimulated IUI cycles reduced cancellation rates and further reduced multiple

pregnancy rates. Additional studies are needed to better define the criteria and methods for oocyte aspiration of preovulatory follicles prior to hCG administration.

Polycystic Ovarian Syndrome (PCOS)

A significant disorder of concern to the reproductive endocrinologist is the polycystic ovary syndrome (PCOS). This is a common cause of anovulation with multiple etiologies. This disorder affects 5–10% of women. PCOS patients respond well to ovulation induction (see below); however, one has to remember that those patients are prone to develop hyperstimulation and multiple gestations.

For years, PCOS has been one of the most controversial entities in gynecologic endocrinology. Despite a vast amount of clinical and laboratory data that have been accumulated since the initial report of Stein and Leventhal in 1935, our knowledge of the endocrine metabolism underlying the disease is still fragmentary. The PCOS is a disorder of multiple etiologies involving a self-perpetuating imbalance between various interdependent endocrine and peripheral structures. In dealing with patients who exhibit symptoms of the PCOS, we cannot escape the suspicion that we are facing a whole series of interrelated disorders leading to manifestations often classified under this single title (Fig. 15.6).

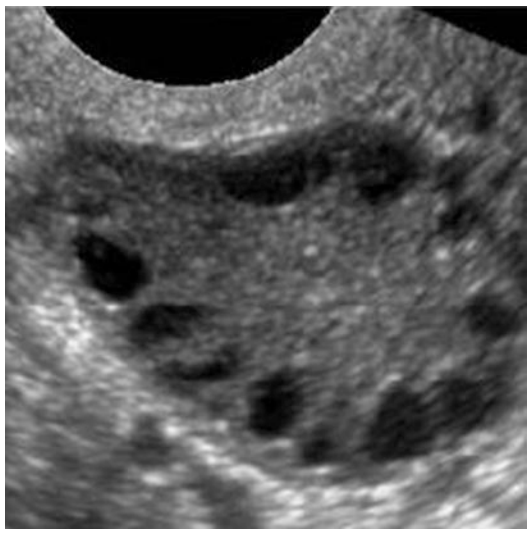

Fig. 15.6 PCOS ultrasound study (note the peripheral small cysts, "string of pearls")

The Classical Picture of PCOS

The PCO syndrome is characterized by a variety of symptoms, all of which are not necessarily present in every patient. These include (1) a broad spectrum of menstrual abnormalities, (2) signs of hyperandrogenism, (3) infertility, and (4) bilateral polycystic ovaries. Menstrual disorders observed include secondary amenorrhea (rarely primary amenorrhea may occur) and oligomenorrhea.

Grossly, the polycystic ovary appears enlarged, sometimes twice the normal size, and is characterized by a shiny, oyster-gray color, and small, embedded, bluish cysts (2–6 mm in diameter). Microscopically, the ovarian capsule is thick (approximately 144–595 u wide as opposed to 100 u in normal ovaries) and fibrous and contains numerous primordial follicles. In the substance of the ovary, there are follicles in all stages of development and atresia, and multiple cystic follicles are lined with one to three layers of granulosa cells. Luteinized follicles are present and occasionally corpora lutei have been reported. The walls of the atretic follicles often display hyperplasia of the theca interna cells.

Ultrasound Diagnosis [17]

The criteria for ultrasound diagnosis of PCO have recently been revised in the light of improved ultrasound technology and better understanding of the condition [17]. Polycystic ovarian morphology is defined as at least one ovary with an ovarian volume of greater than 10 cm^3 (or 10 mL) or an increased number of antral follicles (i.e., those that can be visualized as cysts in the ovarian cortex measuring 2–9 mm in diameter). The exact number of antral follicles, that is, the antral follicle count, to establish

the diagnosis of polycystic ovarian morphology using modern high-frequency transvaginal ultrasonography probes is now at least 12 if not higher [48].

If a large follicle is present (over 10 mm), then the volume should be calculated on a repeat scan when the ovary is quiescent to prevent overestimation of ovarian volume. Ovarian morphology is a more reliable diagnostic tool than ovarian volume for diagnosing PCOS.

Remember that imaging findings alone should not diagnose PCOS in an asymptomatic patient. In this situation further supporting evidence in terms of clinical examination and blood tests should be obtained before a firm diagnosis is made.

Induction of Ovulation

In patients whose infertility can be attributed to an ovulation abnormality, ovulation induction is indicated. Ovulation induction is also used in in vitro fertilization programs (IVF-ET) to increase the number of oocytes aspirated, which in turn increases the number of fertilized conceptus that may be transferred, thereby increasing the chance of pregnancy. Commonly used ovulation induction medications include clomiphene citrate, human menopausal gonadotropin, purified FSH, and recombinant gonadotropins. Although all of these medications result in the development of multiple follicles, they act via different mechanisms.

Transvaginal sonography has a vital role in monitoring the follicular growth rate in women receiving ovulation induction medications.

In an elegant prospective study, Baerwold [4] compared the growth rate of ovarian follicles during natural cycle and ovarian stimulation cycles using standardized techniques.

While the growth rate in natural cycles was 1.42 mm per day, the growth in stimulated cycles was significantly greater, i.e., 1.7 mm per day. Continued research on the effect of greater follicular growth rates and shorter intervals to ovulation are being conducted (Fig. 15.7).

The baseline scan of the pelvis is mandatory to rule out ovarian or uterine pathology and assess the ovarian reserve; moreover, one needs to rule out the presence of ovarian cysts [3].

The objectives of a baseline scan are as follows:

1. *To rule out ovarian or uterine pathology* requiring attention prior to beginning infertility treatment (Table 15.1)

A common adnexal finding, endometriosis [19], can be seen in over 30% of women with clinically defined infertility. Endometriosis is defined as the extrauterine presence of endometrial tissue and is likely due to retrograde menstruation and/or immunologic variations or deficiencies within the peritoneal cavity.

In mild cases small lesions are often located on the ovarian and peritubular surfaces. Cases of minimal endometriosis are not amenable to ultrasonographic diagnosis. However in more moderate cases, one can visualize an endometrioma, i.e., a cystic structure which is lined with endometrial epithelium which can involve one or both ovaries, uterosacral ligaments, etc.

Endometrioma may appear as an ovarian cyst with an echo-dense appearance of blood within a cyst; the appearance may range from anechoic to solid, depending on the amount and organization of the blood within the cystic structure; commonly one can visualize low-level echoes evenly distributed throughout the cyst (Fig. 15.8).

It is important for the physicians to familiarize him with the ultrasonographic picture of endometrioma in order to avoid aspirating the cyst because of an increased risk of infection, compared with aspiration of a simple cyst.

Since ovarian teratomas are the most common ovarian neoplasm especially in reproductive-age women [20], one may encounter them during a baseline scan; the ultrasonographic findings will depend on which elements are present: ectoderm, mesoderm, etc. Very often one can appreciate an echogenic mass with acoustic shadowing. The presence of ectodermal elements gives irregular and variable internal echogenicity (Fig. 15.9).

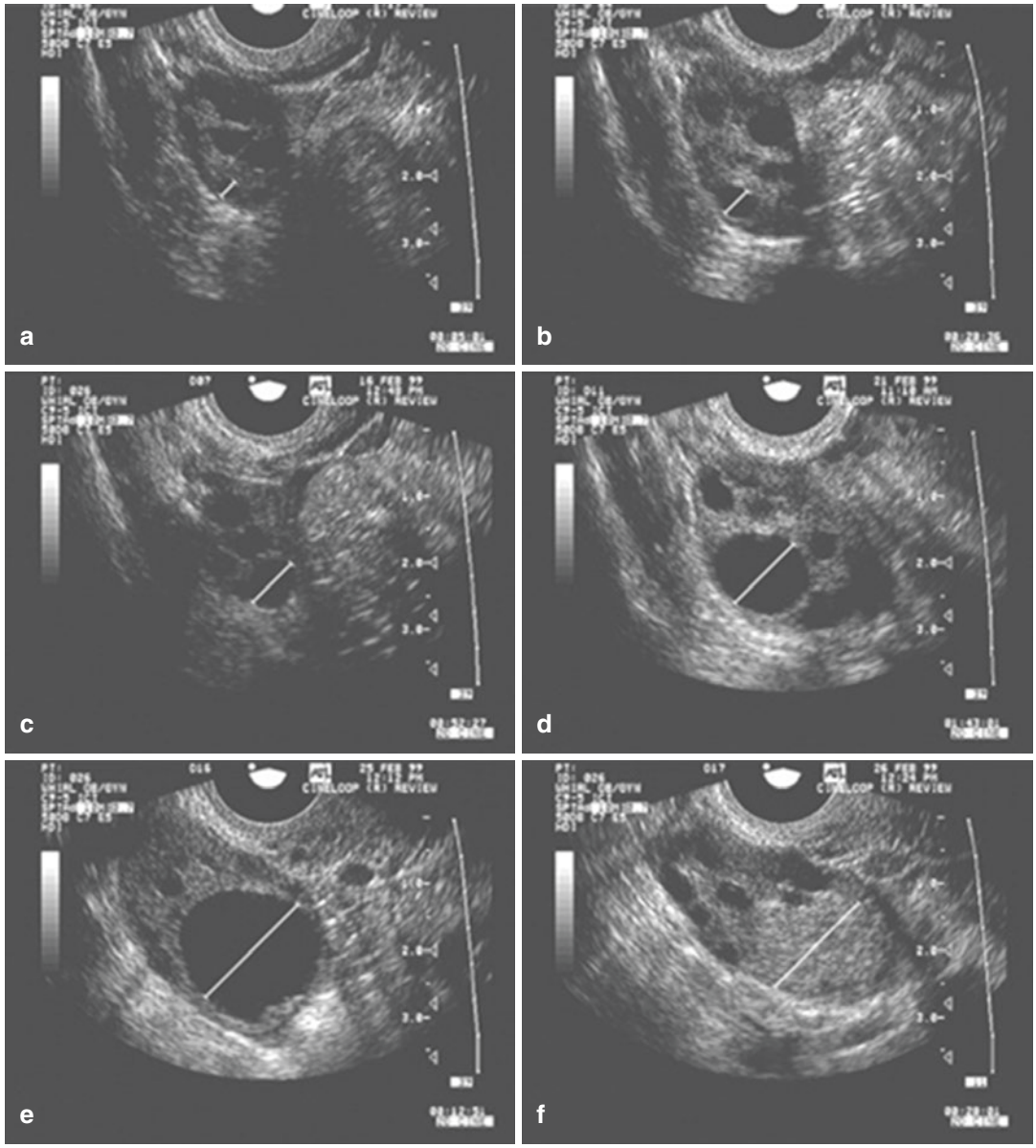

Fig. 15.7 Serial transvaginal ultrasonographic images of the right ovary of a research participant on days 1 (**a**), 4 (**b**), 7 (**c**), 11 (**d**), 16 (**e**), and 17 (**f**) of a spontaneous menstrual cycle. The same ovarian follicle is identified throughout the growth phase in (**a**)–€. The corresponding corpus luteum on the day of ovulation is shown in (**e**). (Reprinted from Baerwald et al. [4]. With permission from Elsevier. https://www.fertstert.org/article/S0015-0282(07)04116-7/fulltext)

2. *To check ovarian reserve*, which will help identify the ideal treatment protocol

Markers of ovarian reserve are associated with ovarian aging as they decline with chronologic age and hence may predict stages of reproductive aging including the menopause transition. Assessment of ovarian reserve includes measurement of serum follicle-stimulating hormone (FSH), anti-Müllerian hormone (AMH), and

inhibin B. Anti-Müllerian hormone is a glycoprotein produced by the granulosa cell of small preantral follicles, used as a marker for oocyte quality and quantity. Historically it was responsible for the Müllerian duct regression [51]. Levels gradually decline as the pool of follicles decline with age. It is undetectable at menopause. Wang et al. [45]

Table 15.1 Common adnexal masses

Cystic masses	Follicular cyst, corpus/luteum cyst, hydrosalpinx dermoid cyst, endometrioma/hemorrhagic cyst
Solid masses	Fibroma, dysgerminoma, teratoma, subserosal fibroid
Complex masses	Dermoid cyst, cyst adenoma, granulosa

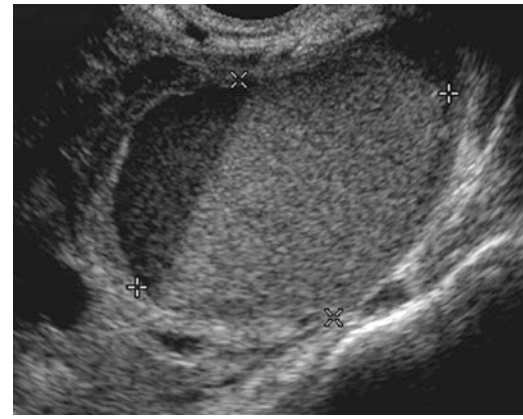

Fig. 15.8 Endometrioma ultrasound study (note the homogenous, low-level echoes "ground-glass" appearance)

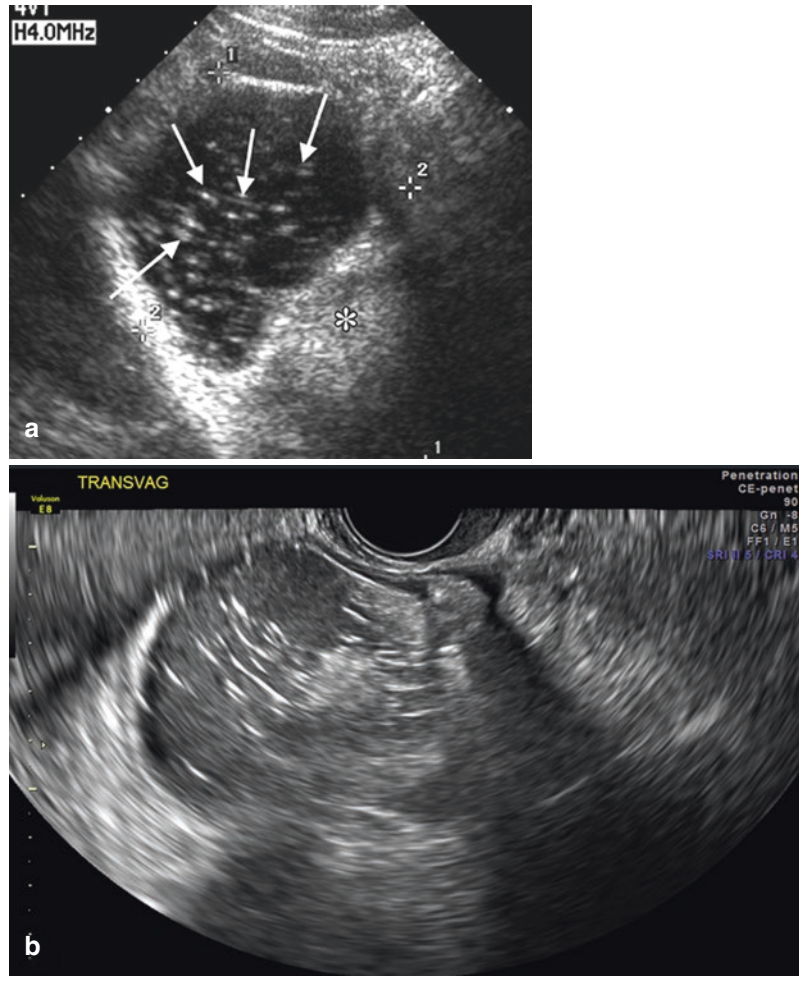

Fig. 15.9 (**a**) Teratoma ultrasound study (note the echogenic linear speckles). (**b**) Dermoid cyst

found that while both FSH and AMH are widely used to assess the ovarian reserve in women undergoing evaluation for infertility, AMH appears to be superior to FSH among all age groups. Ultrasound determination of antral follicle count (AFC), ovarian vascularity, and ovarian volume also can have a role. In infertile women, ovarian reserve markers can be used to predict low and high oocyte yield and treatment failure in women undergoing in vitro fertilization [21].

Small antral follicles (<6.0 mm) measured using 3D ultrasound and AMH show little intracycle variation and perhaps should be evaluated in prediction of ovarian reserve independent of menstrual cycle [18].

In our clinic a baseline scan involves antral follicle count and evaluation of ovarian volume. The number of antral follicles of at least 2 mm in diameter can be detected using ultrasound imaging. Generally follicles that are greater than 2 mm in diameter are highly responsive to gonadotropins; however, some follicles in this size range may be in the early states of atresia. Antral follicle count is performed on day 2–4 of a natural cycle or following pituitary downregulation. Prospective studies assessing antral follicle count demonstrate that lower counts (less than four follicles) are associated with significantly decreased pregnancy rates and increased cycle cancellation rates [22].

Low AFC did predict a higher cancellation rate. Antral follicle count did not predict implantation rate, pregnancy rate, or live birth rate per cycle start. Antral follicle count may be helpful in determining stimulation protocol, as it is the most reliable determinant of oocytes retrieved per starting FSH dose. Antral follicle count predicts ovarian response, not embryo quality or pregnancy [23]. On the contrary, AMH was found to be positively correlated to AFC in determining the number of mature oocytes and implantation rates. It has been proven by Nelson et al. [49] that AMH was a better predictor of ovarian response than AFC in ovulation induction [51].

Ovarian volume is measured using the formula volume (cm^3) = length × width × anterior posterior diameter × 0.53. In a prospective cross-sectional study, it has been shown that ovarian volume, number of follicles, and total follicular volume decreased significantly with age [24].

It has been shown that ovarian volume is inversely correlated with age. Significant decrease in ovarian volume is observed in women older than 35 years of age. The prognostic practicality of measuring early follicular ovarian volume is limited because clinically meaningful changes are only manifest at the physiologic extremes [25]. However, one has to note that ovarian volumes less than 3 cc are associated with a significant decrease in clinical pregnancy rates.

3. *To Identify Ovarian Cyst/Hydrosalpinx*

It is important to identify cysts and/or hydrosalpinx prior to stimulation since these situations could later be misinterpreted as developing follicle. Moreover, basal ovarian cyst significantly reduces ovulating events in patients treated with clomiphene citrate [26]. Thus the recommendation is to do a routine ultrasound screening in those patients with a history of prior cysts, as they are more likely to have a recurrent cyst and those not ovulating on clomiphene citrate (Fig. 15.10a).

Upon detection of an ovarian cyst, a conservative approach is generally effective. One can wait for a spontaneous menstrual bleed which indicates that endogenous ovarian hormone levels returned to base level; if the cyst is not resolving and hormone levels of E_2 are high, then cyst aspiration prior to stimulation remains a viable option.

Upon detection of suspected hydrosalpinx (Fig. 15.10b), confirmatory hysterosalpingogram and/or laparoscopy is indicated. Normal fallopian tubes are usually not visualized on ultrasound. Ultrasound findings suspicious for hydrosalpinx would be an anechoic serpiginous tubular structure adjacent in adnexa. The ampullary end is usually wider than the isthmus portion. Also often there is an abrupt transition in diameter between the wider ampullary portion of the tube and isthmus. Significant international data supports that observation that hydrosalpinx lowers the success rate for IVF and related ART procedures. It is thought that the mechanism of action involves the retrograde flow of inflammatory fluid into the uterine cavity and resultant inhibition of embryo implantation.

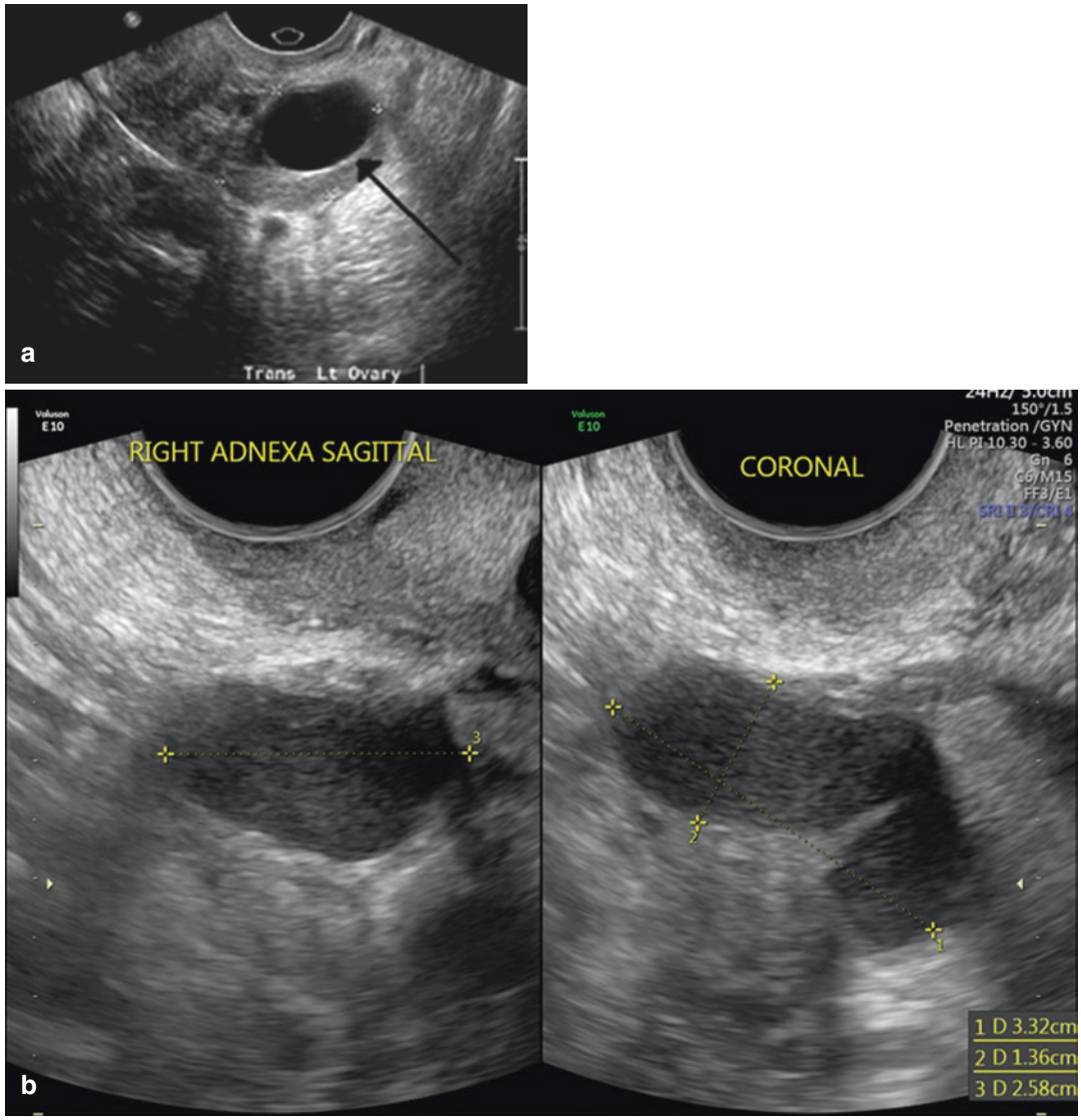

Fig. 15.10 (**a**) Ovarian cyst. (**b**) Hydrosalpinx

Selection of Patients

The ovulatory treatment options are based on WHO classification with patients separated into three main groups (Table 15.2):

- *Group I*: Hypothalamic-pituitary failure included women with primary or secondary amenorrhea, low levels of endogenous

Table 15.2 Anovulation-treatment options (based on WHO classifications)

	Option I	**Option II**
Group I Low FSH	GnRH (pulsatile) Gonadotropins Bromocriptine	Gonadotropins, bromocriptine, and clomiphene citrate
Group II Normal FSH	Clomiphene citrate	Gonadotropins Surgical approach
Group III High FSH	Ovum donation	

gonadotropins, and lack of endogenous estrogen activity. The treatment of choice for this group of patients is gonadotrophic therapy.

- *Group II*: Hypothalamic-pituitary dysfunction included patients with anovulation associated with a variety of menstrual disorders whose serum gonadotropin levels were within the normal range and who had evidence of endogenous estrogen activity.
- The treatment of choice for patients belonging to Group II is a chlorotrianisene analogue, such as clomiphene citrate.
- *Group III*: Includes patients with high FSH levels and have the only viable option for them is ovum donation.

The above classification is based on hormone levels of FSH and estrogens; however some conclusions can be drawn following a baseline ultrasound evaluation of the endometrium. In cases where the endometrium measures more than 7 mm, one can conclude that the patient had sufficient ovarian estrogen secretion and normal FSH level (i.e., Group II).

If, on the other hand, the endometrium is thin, the patient has low estrogen level, and in this case, a single FSH level will differentiate between Group I (low FSH) and Group III (high FSH).

Technical Tips on How to Scan the Ovaries and Follicular Growth

Ovaries

The ovaries are located posterior to the broad ligament and anteromedial to the internal iliac vessels which are easily located and can be used as a landmark for ovarian localization; moving laterally from the endometrial canal will produce the image of the ovary adjacent to the iliac vessels.

The pelvic organs may be scanned either transabdominally or transvaginally. In most infertility units, transvaginal ultrasound has become the routine method since it improves spatial resolution; however it has a smaller field of view. During the transvaginal approach, only a few centimeters separate the probe from the ovaries.

The best way to locate the ovaries is to scan along the lateral margin of the uterus in transverse plane from the fundus to the cervix. In cases where you cannot locate the ovaries, look for them adjacent to the iliac vessels, which are usually easily identified, or try to follow the fallopian tube laterally.

In cases when the ovary is high in the pelvis, a transabdominal scan is also necessary; in these situations begin with the abdominal transducer perpendicular at the midline just superior to the symphysis pubis. Once you locate the long axis of the uterus, move the transducer lateral until the ovary is located. Again remember that the internal iliac vessels are located immediately posterior to the ovary.

Follicles

The spatial resolution of transvaginal scans is 2–3 mm, so small follicles can be visualized easily as echo-free structures which usually lie toward the periphery of the more echogenic ovarian tissue. Since the follicles may be flattened in one plane or have their shape altered due to pressure, the internal diameter of the follicle should be measured in three planes and the mean value calculated. The intra-observer standard deviation of transabdominal follicular measurement was reported in one study to be 0.6 mm and the inter-observer standard deviation 1.2 mm, irrespective of the follicular diameter. Thus, the 95% confidence limits for any particular measurement should be $2.4mm^3$ [27], and one would expect transvaginal measurements to confer even greater accuracy [14].

Follicles can be confused with blood vessels (hypogastric vein), and they can be differentiated by rotating the transducers. If the structure is a vessel, it will appear tubular following rotation.

A baseline scan should always be done to identify cystic structures which could later be misinterpreted as follicles.

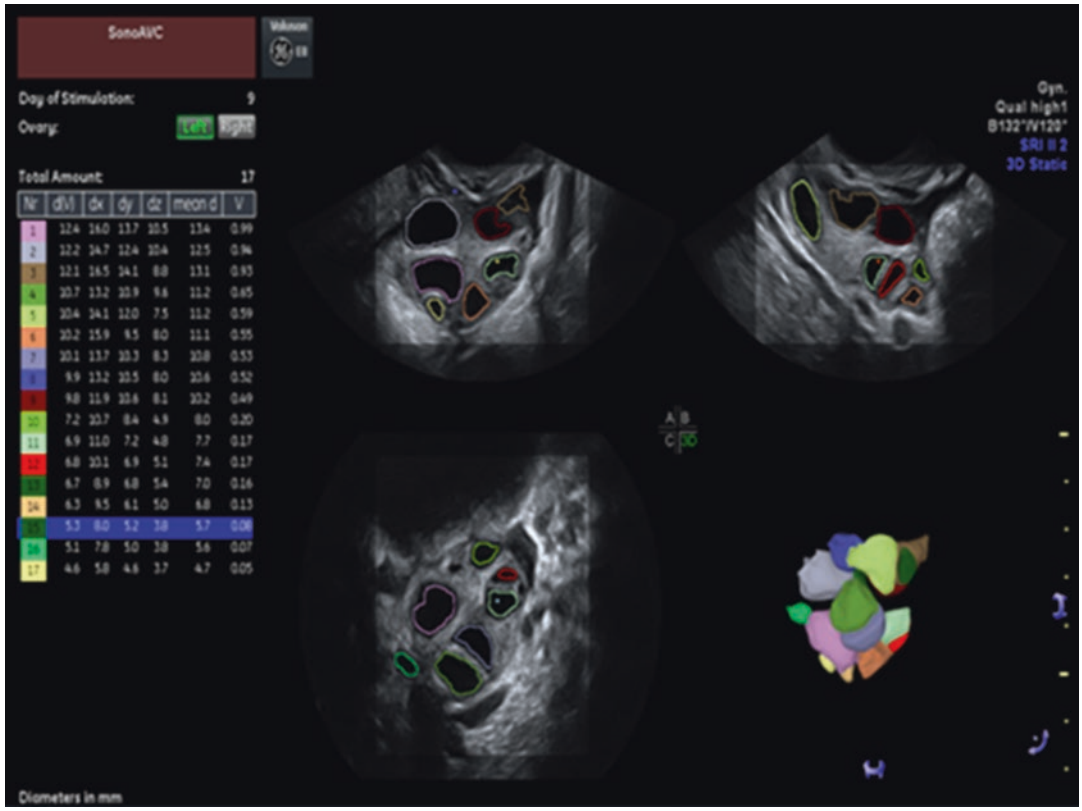

Fig. 15.11 Sono AVC ultrasound study. Automatic estimation of diameter and volume. Each volume is separately color-coded (see text)

Sono AVC (Automatic Volume Calculation)

A relatively new software program (GE) with 3D data set, which can automatically estimate the diameter and volume of each follicle, has been developed; this ultrasound program will automatically identify the ovarian follicle and the volume for each follicle (Fig. 15.11).

Raine-Fenning et al. [28] compared automatic volume measurement of each follicle to manual measurements from 2D and 3D ultrasound; sono AVC provided measurements that were more accurate than manual measurements, and obviously the time taken for measurements was significantly shorter.

Clomiphene Citrate

Clomiphene citrate (CC) is a nonsteroidal triphenylethylene compound currently used as the first choice of treatment for induction of ovulation in anovulatory or oligoovulatory women.

Mode of Action

The stereoscopic configuration of CC is sufficiently similar to that of ß-estradiol to compete with it for available estrogen receptor sites in all estrogen-dependent target cells such as the hypothalamus, pituitary, ovary, uterus, and cervical glands.

The mode of action of CC in the induction of ovulation may be tentatively described as fol-

lows. "Blinded" by CC molecules occupying the estrogen receptor sites, the hypothalamus and pituitary are unable to correctly perceive true serum estrogen levels. A false message of insufficient estrogen concentration is registered and acted upon, resulting in exaggerated FSH and LH secretion. The occupation of hypothalamic estrogen receptors by CC is a short duration, time-limited process. A fair chance exists that, by the time ovarian follicles that are stimulated by the CC-induced gonadotropin elevation reach the preovulatory stage, the hypothalamus is already free of CC influence and ready to perceive the correct steroid signal. From this moment forward, the events are regulated and controlled by the endogenous feedback mechanisms within the hypothalamic-pituitary-ovarian (HPO) axis.

Considering its mode of action, an antiestrogen such as CC should be effective in patients having a hypothalamus capable of releasing pulsatile GnRH, a pituitary gland capable of responding to GnRH, and an ovary containing normal primordial follicles. Clomiphene citrate is most effective when used in patients with hypothalamic-pituitary dysfunction. These patients lack the proper regulation within the HPO axis, but they have some endogenous GnRH secretion and estradiol production. These anovulatory women probably have irregularities in the pulsatile secretion of GnRH, even though they do have fluctuating, detectable levels of gonadotropins and estrogens. While clomiphene citrate remains first-line for ovulation induction in most cases, it has been shown that letrozole (LE) is superior to clomiphene citrate (CC) for ovulation induction in patients with polycystic ovarian syndrome (PCOS), with an improvement in live birth rate and pregnancy rates [43, 44].

Antiestrogenic Effects on the Cervix and Endometrium

The antiestrogenic effect of CC may exert an adverse effect on the uterus and the cervix (Fig. 15.12). This detrimental effect, caused by the drug's competition for estrogen receptors, is claimed to be one factor responsible for the discrepancy between the ovulation rate (85%) and the pregnancy rate (43%) of women receiving CC treatment. Jirge et al. [29] have demonstrated in a prospective crossover study that the number of follicles at the assumed time of ovulation is significantly higher in patients treated with clomiphene citrate; moreover the endometrial thickness on the same day was significantly smaller (7.6 mm vs. 8.5 mm). Most investigators report decreased secretion of mucus from the cervical glands caused by antiestrogenic agents such as CC. The antiestrogenic effect on the cervical mucus, when present, is expressed by a decreased amount of mucus, which occurs despite the relatively high levels of estrogens in the circulation. Wollman et al. [30] demonstrated that the cervical mucus can be visualized in many patients around the time of ovulation, using pelvic

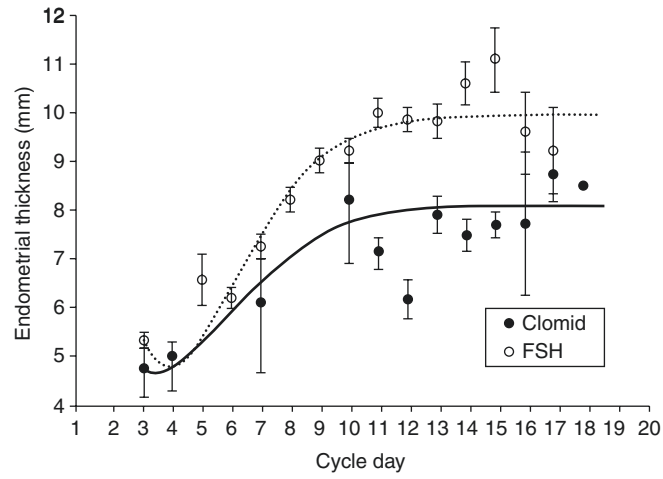

Fig. 15.12 Antiestrogenic effects of clomiphene citrate on the cervix and endometrium. (Reprinted from Bromer et al. [56]. With permission from Elsevier. https://www.fertstert.org/article/S0015-0282(07)04339-7/fulltext)

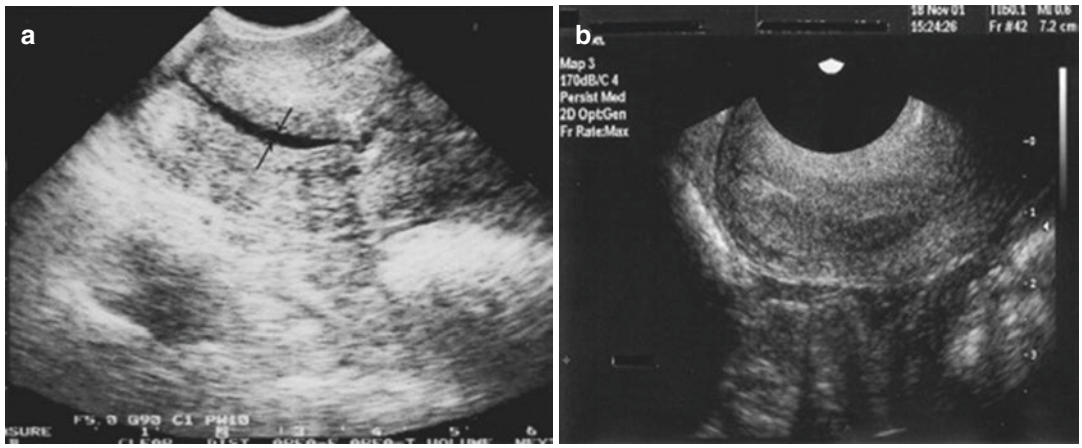

Fig. 15.13 (**a**) Cervical canal measurement near ovulation and (**b**) after ovulation. (Reprinted from Wolman et al. [30]. With permission from Elsevier. https://www.fertstert.org/article/S0015-0282(09)00104-6/fulltext)

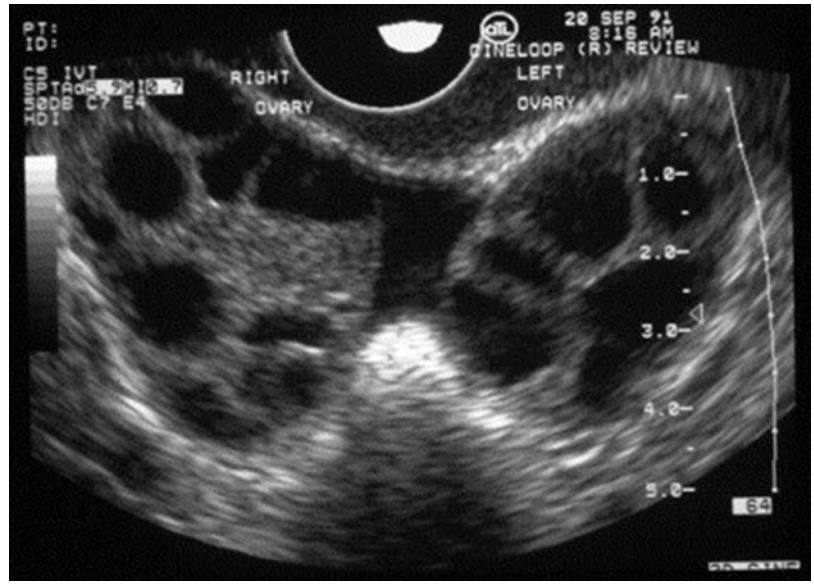

Fig. 15.14 Multiple follicles – ultrasound study

ultrasound (Fig. 15.13). In many patients given CC, the cervical mucus does not exhibit any depressed effects. To understand this phenomenon, we must remember that the antiestrogen effect on the hypothalamus will result in elevated circulating FSH and LH levels. The elevated gonadotropin levels may cause multifollicular development, which in turn enhances estrogen production. The elevated estrogen levels, five to ten times higher than in normal cycles, sometimes mask the antiestrogen effect of CC and tamoxifen citrate in the cervix and uterus (Fig. 15.14).

Treatment Schema and Monitoring of Clomiphene Citrate Therapy

Clomiphene citrate is administered orally in 50 mg tablets. Therapy should be initiated with 50 mg of CC over a period of 5 days, usually starting on the fifth day after the first appearance

of spontaneous or progestin-induced menstrual bleeding. If there is evidence of successful ovulation induction, then same dosage of CC can be used in subsequent cycles until conception occurs. However, if the initial dosage of CC failed to induce ovulation, then the dose is increased to 100 mg/day for 5 days. Dose can be increased gradually up to 150–200 mg/day. Clomiphene citrate-induced ovarian cysts often resolve spontaneously and typically do not require intervention. Up to 10% of women treated with CC fail to ovulate with the highest doses.

In addition to the baseline scan, we advocate cycle monitoring via ultrasonographic evaluation of follicular size, endometrial thickness, and cervical mucus observation. Ultrasound monitoring of patients undergoing ovulation induction cycles will ensure adequate follicular recruitment and identify those patients not responding or have delayed endometrial thickening. In cases where there is concern that cervical mucus is insufficient, often due to the antiestrogenic effect of Clomid, intrauterine insemination (bypassing the cervix) is probably the best solution. Whenever the endogenous feedback mechanism responsible for the preovulatory LH surge is not properly activated, the midcycle LH peak may consequently be inadequate, ill-timed, or entirely absent. In such instances, hCG should be administered to induce ovulation. Optimal timing for hCG ovulation trigger injections includes ultrasonographic measurement of mean follicular diameter ranging 19–20 mm. Ovulation will occur 34–36 hours following hCG injection, so the IUI is often performed 34 hours later. Recently Paltnik et al. [5] have shown that higher pregnancy rates were achieved when the leading follicle was in the 23–28 mm range.

Universal agreement is lacking as to when to introduce ultrasonographic cycle monitoring versus less complicated or costly alternatives. However, we agree with the predominant opinion that the additional ultrasound expense is justified by the prevention of protracted periods of ineffective therapy [31]; moreover it has been shown that a significant number of women (14%) developed three or more follicles, despite receiving low doses of clomiphene citrate [32].

Gonadotropins

Principles of Gonadotrophic Therapy

In order to optimally stimulate follicular maturation, both FSH and LH are required. While FSH content of the pharmacologic preparation is essential for follicular development, final maturation of the follicles and subsequent ovulation are brought about by a pituitary release and circulatory surge of LH. Thus two gonadotropins are required for induction of ovulation: one providing the required amount of FSH and another providing LH or LH-like material (hCG) of sufficient quantity to provoke ovulation and corpus luteum formation. Well-accepted ovulation induction protocols include alterations in the precise ratio of FSH to LH. Zhang [50] has proven that trigger of ovulation with GnRH agonist and hCG significantly increases the number of mature oocytes retrieved specially in poor ovarian responders.

Selection of Patients

Ideal candidates for ovulation induction with gonadotropins are patients who have low endogenous gonadotropin secretion and are amenorrheic or anovulatory (Group I-WHO). This treatment can also be given to patients with hypothalamic-pituitary dysfunction (Group II), including anovulatory patients associated with a variety of menstrual disorders. The treatment of choice for patients belonging to Group II is a clomiphene citrate alone or in conjunction with estrogen and/or hCG. Patients who fail to ovulate or conceive within a reasonable time are considered "clomiphene failures" and can be considered for hMG therapy. In fact, a study done by Peeraer et al. [46] found that low-dose hMG is superior to CC in IUI cycles with respect to clinical pregnancy rate in subfertile couples. Youssef et al. [47] have further found no evidence of a difference in pregnancy outcomes between low doses of gonadotropins and high doses of gonadotropins in ovarian stimulation regimens.

Monitoring of Therapy

Gonadotropins are given daily by injection in order to stimulate follicular development;

ovulation is actually induced by hCG. The daily dose of gonadotropins given in a particular cycle depends upon the ovarian response of the patient in that particular cycle. The response is reflected by a growth of follicles accompanied by biochemical changes mainly with respect to increased synthesis and secretion of steroidal hormones. The follicular enlargement can be visualized by ultrasonographic measurement, while estrogen secretion values can be estimated directly by blood measurement.

Nelson et al. [49] have proven that the mean number of oocytes retrieved was higher in patients treated with GnRH agonists vs. antagonists. However, in PCOS, GnRH antagonist was the preferred agent as it decreases the incidence of ovarian hyperstimulation syndrome without interfering with clinical pregnancy outcome in PCOS patients [52].

Ultrasonographic as well as biochemical monitoring of treatment cycles serves to assess the effective dose required to evoke an ovarian response, the length of time required for follicular maturation, and the appropriate time for induction of ovulation. Furthermore, such monitoring should aim to prevent ovarian hyperstimulation syndrome (OHSS) or at least lead to early detection. For these purposes, a combination of ultrasonography and estrogen determination was advocated. Given that exogenous gonadotropic stimulation usually induces the development and growth of several follicles, ultrasonographic monitoring is particularly advisable for these treatment cycles.

Sonographic visualization may thus discriminate between single and multiple follicular growths, and their measurement may aid in the interpretation of the meaning of the estrogen levels. Evidence is accumulating that follicles of diameters greater than 18–19 mm should be "ovulated." Thus, sonography can be a more precise indicator for the determination of the optimal ovulatory timing.

Follicular development should be monitored with frequent ultrasound studies. Ultrasound plays a critical role in assessing response to gonadotropins and timing of hCG administration (see Fig. 15.14).

Scanning should become more frequent when the follicle reaches 14 mm or greater. When a follicle 18 mm or greater is identified, hMG is discontinued, and hCG is administered 24 hours later to cause ovum release. Usually 10,000 units of hCG, injection, are given to trigger ovulation.

While in the past it was emphasized that ultrasound scanning should be complimentary to estradiol data, Shoham et al. [33, 34] have raised the question of whether it is possible to run a successful ovulation induction program based solely on ultrasound monitoring. In his prospective study, monitoring of ovulation induction was performed using serial ultrasound measurements and correlated with the patient's E_2 concentrations that became available at the end of each cycle. Twenty hypogonadotropic and 29 ultrasonically diagnosed polycystic ovary patients received treatment with gonadotropins. The results of this study demonstrated that transvaginal ultrasound findings including (a) follicular growth, (b) uterine measurements, and (c) endometrial thickness all strongly correlated with serum E_2 concentrations ($P < 0.0001$). Shoam et al. concluded that serial ultrasound examinations used alone (eliminating determination of serum E_2 levels) have proven to be an effective monitoring approach for ovulation induction cycles.

Wiser et al. [35] studied two groups of patients undergoing their first IVF treatment. The ultrasound-only group (study group) was monitored by US for follicle size and endometrial thickness without blood tests. In this group, only one blood test was taken before human chorionic gonadotropin (hCG) injection, to ensure a safe level of estradiol (E(2)) regarding ovarian hyperstimulation syndrome (OHSS) risk. The control group was monitored by ultrasound plus serum estradiol and progesterone concentration at each visit. No differences were found between the groups. The conclusion of the study was that ultrasound as a single monitoring tool for IVF cycles is reliable, safe, and patient-friendly and reduces treatment expenses.

Clomiphene Citrate and hMG

The rationale of clomiphene citrate followed by hMG is the utilization of the former to increase FSH in the initial phase (recruitment and selection) and maintain adequate FSH levels by administration of hMG during follicular growth phase.

It has been shown that by using the combined clomiphene citrate/hMG protocol in normogonadotropic patients, they could reduce the necessary hMG requirement by 50%. Abdelazim et al. [36] compared sequential clomiphene citrate/hMG regimen to hMG regimen for ovulation induction in clomiphene citrate-resistant women. They found that the sequential CC/hMG regimen is as effective as hMG regimen for ovulation induction, produces satisfactory pregnancy results, and reduces treatment cost.

The clomiphene citrate-hMG treatment scheme is as follows: on the fifth through the ninth day after induced or spontaneous bleeding, the normogonadotropic patient receives 100 mg of clomiphene citrate daily. From the eighth day onward, hMG is administered. The patient is carefully monitored by estrogen determination and ultrasound visualization of the growing follicle(s). This will help to determine if and when the ovulatory dose of hCG should be administered and to prevent hyperstimulation and multiple pregnancies.

The Help of Ultrasound: Assessing Complications

The major adverse effects of induction of ovulation are multiple pregnancies and OHSS.

5–8% of clomiphene-induced pregnancies and 15–25% of all pregnancies following gonadotropin-induced ovulation are multiple gestations.

While almost all of the multiple gestations conceived on clomiphene will be twins, 30% of multiple gestations following gonadotropin therapy will be triplets.

Poorly monitored ovulation induction is probably the major cause of the multiple pregnancy epidemics. Table 15.3 summarizes the clinical complication associated with twin pregnancies. It is important to diagnose multiple pregnancies early, in the first trimester, so women who conceive with high-order multiple pregnancies may consider multiple pregnancy reductions.

Table 15.3 Complications associated with twin pregnancy

Maternal complications	Fetal complications
Anemia	Premature delivery
Preeclampsia/eclampsia	Difficult delivery
Pre-/postpartum hemorrhage	Prolapse of an umbilical cord
	Hypoxia of second twin

In cases of twin pregnancy, it is recommended by the AIUM to document amnionicity and chorionicity in the early first trimester, so one can prepare for high-risk situations such as a monochorionic twin gestation.

In many countries, triggering of ovulation with hCG is only done if there are no more than two mature follicles around the assumed time of ovulation.

Adhering to strict guidelines involving ultrasound monitoring will definitely reduce the incidence of multiples.

Ovarian hyperstimulation is the most serious complication, which, in extreme situations, is potentially life-threatening. It occurs in women receiving exogenous hCG. Risk factors include young age, low BMI, PCOS, high-dose hCG, and previous history of OHSS, and the reader is referred to Chap. 19.

It is important to understand the risk factors that can be identified in high-risk patients before ovulation is being induced. The presence of polycystic ovaries puts the patient at increased risk; we have shown that a decrease in the fraction of the mature follicles and an increase in the fraction of the very small follicles around the assumed time of ovulation correlated with an augmented risk for the development of severe stimulation of the ovaries. Our data suggest [37] that ultrasonography is of good predictive value in the occurrence of clinically moderate to severe OHSS in women treated by hMG and hCG. Even with estrogen levels within accepted normal limits, it

is suggested that hMG/hCG administration should be interrupted in the presence of 11 or more preovulatory follicles, especially if most of them are immature (<9 mm).

Conclusion

Ultrasound is the most powerful tool to monitor normal and stimulated cycles; predictions of the assumed time of ovulation allow optimal timing of various procedures such as insemination, ovum aspiration, etc.

In stimulated cycles sonographic detection of too many follicles allows withholding hCG induction thus preventing hyperstimulation.

In the past ovulation function was monitored by estradiol estimation; since the development of sophisticated ultrasonographic techniques, monitoring of ovarian follicular growth by ultrasound became a routine addition to estradiol measurement in most clinics.

Accumulating data based on the Cochrane Database [38] indicate that there is no evidence from randomized trials to support cycle monitoring by ultrasound plus serum estradiol as more efficacious than cycle monitoring by ultrasound only on outcomes of live birth and pregnancy rates.

As far as OHSS, randomized trial with a sufficiently large sample is needed. Until such a trial is considered, ultrasound plus serum estradiol may need to be retained as a precautionary good practice point, in patients prone to develop hyperstimulation.

References

1. Aboulghar MM. Ultrasound monitoring for ovulation induction: pitfalls and problems. In: Ovarian stimulation. Cambridge: Cambridge University Press; 2009: online publication January 2009. ISBN: 9780511762390.
2. Pierson RA, Olatunbosun OA. Transvaginal ultrasonography and the evaluation of female infertility. In: Sciarra JJ, editor. Gynecology and obstetrics, vol. 5. Saskatoon: University of Saskatchewan; 2004. p. 1–12.
3. Blankstein J, Malepati S, Brasch J. Ultrasound to monitor ovulation induction. In: Ultrasonography in gynecology. Cambridge University Press: Publisher Springer; 2014. p231–50.
4. Baerwald A, Walker R, Pierson R. Growth rate of ovarian follicles during natural menstrual cycles, oral contraceptives cycles and ovarian stimulation cycles. Fertil Steril. 2009;91(2):440–9.
5. Palatnik A, Strawn E, Szabo A, Robb P. What is the optimal follicular size before triggering ovulation in intrauterine insemination cycles with clomiphene citrate or letrozole? Fertil Steril. 2012;97(5):1089–94. e1–3.
6. Shrestha SM, Costello MF, Sjoblom P, McNally G, Bennett M, Steigrad SJ, et al. Doppler ultrasound assessment of follicular vascularity in the early follicular phase and its relationship with outcome of in-vitro fertilization. J Assist Reprod Genet. 2006;23(4):161–9. Epub 2006 Apr 22.
7. Coulam CB, Goodman C, Rinehart JS. Colour Doppler indices of follicular blood flow as predictors of pregnancy after in vitro fertilization and embryo transfer. Hum Reprod. 1999;14(8):1979–82.
8. Nargund G, Bourne T, Doyle P, Parsons J, Cheng W, Campbell S, Collins W. Associations between ultrasound indices of follicular blood flow, oocyte recovery and preimplantation embryo quality. Hum Reprod. 1996;11(1):109–13.
9. Jayaprakasan K, Al-Hasie H, Jayaprakasan R, Campbell B, Hopkisson J, Johnson I, et al. The three-dimensional ultrasonographic ovarian vascularity of women developing poor ovarian response during assisted reproduction treatment and its predictive value. Fertil Steril. 2009;92(6):1862–9. Epub 2008 Oct 29.
10. Bhal PS, Pugh ND, Gregory L, O'Brien S, Shaw RW. Peri-follicular vascularity as a potential variable affecting outcome in stimulated intrauterine insemination treatment cycles: a study using transvaginal power Doppler. Hum Reprod. 2001;16(8):1682–9.
11. Ivanovski M, Damcevski N, Radevska B, Doicev G. Assessment of uterine and arcuate artery blood flow by transvaginal color Doppler ultrasound on the day of human chorionic gonadotropin administration as predictors of pregnancy in an in vitro fertilization program. Akush Ginekol (Sofiia). 2012;51(2):55–60.
12. Kim A, Han JE, Yoon TK, Lyu SW, Seok H, Won HJ. Relationship between endometrial and subendometrial blood flow measured by three-dimensional power Doppler ultrasound and pregnancy after intrauterine insemination. Fertil Steril. 2010;94(2):747–52.
13. Manzi DS, Dumez S, Scott LB, Nulsen JC. Selective use of leuprolide acetate in women undergoing superovulation with intrauterine insemination results in significant improvement in pregnancy outcome. Fertil Steril. 1995;63(4):866–73.
14. Kolibianakis EM, Zikopoulos K, Schiettecatte J, Smitz J, Tournaye H, Camus M, et al. Profound LH suppression after GnRH antagonist administration is associated with a significantly higher ongoing pregnancy rate in IVF. Hum Reprod. 2004;19(11):2490–6.

15. Dickey RP, Olar TT, Taylor SN, Curol DN, Rye PH, Matulich EM. Relationship of follicle number, serum estradiol, and other factors to birth rate and multiparity in human menopausal gonadotropin-induced intrauterine insemination cycles. Fertil Steril. 1991;56(1):89–92.
16. Stoop D, Van Landuyt L, Paquay R, Fatemi H, Blockeel C, De Vos M, et al. Offering excess oocyte aspiration and vitrification to patients undergoing stimulated artificial insemination cycles can reduce the multiple pregnancy risk and accumulate oocytes for later use. Hum Reprod. 2010;25(5):1213–8.
17. Rotterdam Eshre/ASRM-Sponsored PCOS Consensus Workshop Group. Revised 2003 consensus on diagnostic criteria and long-term health risks related to polycystic ovary syndrome. Fertil Steril. 2004;81(1):19–25.
18. Deb S, Campbell BK, Clewes JS, Pincott-Allen C, Raine-Fenning NJ. The intra-cycle variation in the number of antral follicles stratified by size and in the endocrine markers of ovarian reserve in women with normal ovulatory menstrual cycles. Ultrasound Obstet Gynecol. 2012;41(2):216–22.
19. Kinkel K, Frei KA, Balleyguier G, Chapron C. Diagnosis of endometriosis with imaging: a review. Eur Radiol. 2006;16:285.
20. de Silva KS, Kanumakala S, Grover SR, Chow CW, Warne GL. Ovarian lesions in children and adolescents-an 11 year review. J Pediatr Endocrinol Metab. 2004;17:951.
21. La Marca A, Argento C, Sighinolfi G, Grisendi V, Carbone M, D'Ippolito G, et al. Possibilities and limits of ovarian reserve testing in ART. Curr Pharm Biotechnol. 2012;13(3):398–408.
22. Frattearelli JL, Levi AJ, Miller BT, Segars JH. A prospective assessment of predictive value of basal antral follicles in in-vitro fertilization cycles. Fertil Steril. 2003;80:350–5.
23. Hsu A, Arny M, Knee AB, Bell C, Cook E, Novak AL, et al. Antral follicle count in clinical practice: analyzing clinical relevance. Fertil Steril. 2011;95(2):474–9.
24. Jokubkiene L, Sladkevicius P, Valentin L. Number of antral follicles, ovarian volume, and vascular indices in asymptomatic women 20 to 39 years old as assessed by 3-dimensional sonography- A prospective cross-sectional study. J Ultrasound Med. 2012;31:1635–49.
25. Hendriks DJ, Ben-Willem JM, Laszlo FJ, Egbert R, Broekmans FJM. Antral follicle count in the prediction of poor ovarian response and pregnancy after in vitro fertilization: a meta-analysis and comparison with basal follicle-stimulating hormone level. Fertil Steril. 2005;83(2):291–301.
26. Csokmay JM, Frattarelli JL. Basal ovarian cysts and clomiphene citrate ovulation induction cycles. Obstet Gynecol. 2006;107(6):1292–6.
27. Eissa MK, Hudson K, Docker MF, Sawers RS, Newton JR. Ultrasound follicular diameter measurement: and assessment of inter-observer and intra-observer variation. Fertil Steril. 1985;44:751–4.
28. Raine-Fenning NJ, Jayaprakasan K, Chamberlain S, Devlin L, Priddle H, Johnson I. Automated measurements of follicle diameter: a chance to standardize? Fertil Steril. 2009;91(4 Suppl):1469–72.
29. Jirge PR, Patil RS. Comparison of endocrine and ultrasound profiles during ovulation induction with clomiphene citrate and letrozole in ovulatory volunteer women. Fertil Steril. 2010;93(1):174–83.
30. Wolman I, Birenbaum-Gal T, Jaffa AJ. Cervical mucus status can be accurately estimated by transvaginal ultrasound during fertility evaluation. Fertil Steril. 2009;92(3):1165–7.
31. Homburg R. Clomiphene citrate- end of an era? Hum Reprod. 2005;20(8):2043–51.
32. Coughlan C, Fitzgerald J, Milne P, Wingfield M. Is it safe to prescribe clomiphene citrate without ultrasound monitoring facilities? J Obstet Gynaecol. 2010;30(4):393–6.
33. Shoham Z, DiCarlos C, Patel A, Conway GS, Jacobs HS. Is it possible to run a successful ovulation induction program based solely on ultrasound monitoring? The importance of endometrial measurements. Fertil Steril. 1992;56:836–41.
34. Shoham Z. Ultrasound is the only monitoring modality necessary for ovulation induction. OBGyn.net. 21 July 2011. http://hcp.obgyn.net/fetal-monitoring/content/article/1760982/1911450. Last accessed on 30 May 2013.
35. Wiser A, Gonen O, Ghetler Y, Shavit T, Berkowitz A, Shulman A. Monitoring stimulated cycles during in vitro fertilization treatment with ultrasound only-preliminary results. Gynecol Endocrinol. 2012;28(6):429–31.
36. Abdelazim IA, Makhlouf HH. Sequential clomiphene citrate/hMG versus hMG for ovulation induction in clomiphene citrate-resistant women. Arch Gynecol Obstet. 2013;287(3):591–7.
37. Blankstein J, Shalev J, Saadon T, Kukia EE, Rabinovici J, Pariente C, et al. Ovarian hyperstimulation syndrome: prediction by number and size of preovulatory ovarian follicles. Fertil Steril. 1987;47(4):597–602.
38. Kwan I, Bhattacharya S, et al. (Systemic review). Cochrane Menstrual Disorders and Sub-fertility Group. (*MDSG*). Cochrane Database Syst Rev. 2008;(4):40.
39. Vural F, Vural B, Doğer E, Çakıroğlu Y, Çekmen M. Perifollicular blood flow and its relationship with endometrial vascularity, follicular fluid EG-VEGF, IGF-1, and inhibin-a levels and IVF outcomes. J Assist Reprod Genet. 2016;33(10):1355–62. Epub 2016 Aug 2.
40. Huyghe S, Verest A, Thijssen A, Ombelet W. The prognostic value of perifollicular blood flow in the outcome after assisted reproduction: a systematic review. Facts Views Vis Obgyn. 2017;9(3):153–6.
41. Chen HJ, Lin YH, Huang MZ, Seow KM, Huang LW, Hsieh BC, et al. Dose-finding study of Leuplin depot for prevention of premature luteinizing hormone surge during controlled ovarian stimulation: a pilot

study in intrauterine insemination treatment. Taiwan J Obstet Gynecol. 2016;55(2):235–8.
42. Wadhwa L, Khanna R, Gupta T, Gupta S, Arora S, Nandwani S. Evaluation of role of GnRH antagonist in intrauterine insemination (IUI) cycles with mild ovarian hyperstimulation (MOH): a prospective randomised study. J Obstet Gynaecol India. 2016;66(Suppl 1):459–65. doi: Epub 2016 Feb 26.
43. Franik S, Eltrop SM, Kremer JA, Kiesel L, Farquhar C. Aromatase inhibitors (letrozole) for subfertile women with polycystic ovary syndrome. Cochrane Database Syst Rev. 2018;24(5):CD010287.
44. Hu S, Yu Q, Wang Y, Wang M, Xia W, Zhu C. Letrozole versus clomiphene citrate in polycystic ovary syndrome: a meta-analysis of randomized controlled trials. Arch Gynecol Obstet. 2018;297(5):1081–8.
45. Wang S, Zhang Y, Mensah V, Huber WJ III, Huang YT, Alvero R. Discordant anti-müllerian hormone (AMH) and follicle stimulating hormone (FSH) among women undergoing in vitro fertilization (IVF): which one is the better predictor for live birth? J Ovarian Res. 2018;11:60.
46. Peeraer K, Debrock S, De Loecker P, Tomassetti C, Laenen A, Welkenhuysen M, et al. Low-dose human menopausal gonadotrophin versus clomiphene citrate in subfertile couples treated with intrauterine insemination: a randomized controlled trial. Hum Reprod. 2015;30(5):1079–88. Epub 2015 Mar 18.
47. Youssef MA, van Wely M, Mochtar M, Fouda UM, Eldaly A, El Abidin EZ, et al. Low dosing of gonadotropins in in vitro fertilization cycles for women with poor ovarian reserve: systematic review and meta-analysis. Fertil Steril. 2018;109(2):289–301. Epub 2018 Jan 6.
48. Azziz R. Reproductive endocrinology and infertility: clinical expert series -polycystic ovary syndrome. Obstet Gynecol. 2018;132(2):321–36.
49. Nelson SM, Klein BM, Arce J-C. Comparison of anti-müllerian hormone levels and antral follicle count as predictor of ovarian response to controlled ovarian stimulation in good-prognosis patients at individual fertility clinics in two multicenter trials. Fertil Steril. 2015;103(4):930.e1. https://www.clinicalkey.es/playcontent/1-s2.0-S001502821402545X. https://doi.org/10.1016/j.fertnstert.2014.12.114.
50. Zhang S, Zhang J, Wang Y, Chen Q, Hong Q, Cai R, et al. Dual trigger of final oocyte maturation in poor ovarian responders undergoing IVF/ICSI cycles. Reprod Biomed Online. 2017;35(6):701–7. https://www.sciencedirect.com/science/article/pii/S1472648317304194. https://doi.org/10.1016/j.rbmo.2017.09.002.
51. Lehmann P, Vélez M, Saumet J, Lapensée L, Jamal W, Bissonnette F, et al. Anti-müllerian hormone (AMH): a reliable biomarker of oocyte quality in IVF. J Assist Reprod Genet. 2014;31(4):493–8. https://www.ncbi.nlm.nih.gov/pubmed/24573377. https://doi.org/10.1007/s10815-014-0193-4.
52. Kollmann M, Martins WP, Lima MLS, Craciunas L, Nastri CO, Richardson A, et al. Strategies for improving outcome of assisted reproduction in women with polycystic ovary syndrome: systematic review and meta-analysis. Ultrasound Obstet Gynecol. 2016;48(6):709–18. https://onlinelibrary.wiley.com/doi/abs/10.1002/uog.15898. https://doi.org/10.1002/uog.15898.
53. Hodgen G. Ovarian physiology and in vitro fertilization. In: Collins RC, editor. Ovulation induction. New York: Springer; 1990. p. 22–40.
54. Blankstein J, Mashiach S, Lunenfeld B. Ovulation induction and in vitro fertilization, vol. 27. Chicago: Year Book Medical Publishers; 1986.
55. Palleres P, Lealier C, Gonzales-Bulnes A. Progress toward in vitro virtual histology of ovarian follicle and corpora latea by ultrasound. Fertil Steril. 2009;91(2):624–6.
56. Bromer JG, Aldad TS, Taylor HS. Defining the proliferative phase endometrial defect. Fert Steril. 2009;91(3):698–704.

2D Ultrasound in Follicle Monitoring for ART

16

Gianluca Gennarelli, Tomer Tur-Kaspa, Alberto Revelli, Mette Toftager, and David P. Cohen

Introduction

Ultrasound (US) imaging represents an invaluable tool for the reproductive endocrinologist working with assisted reproductive technologies (ART). It allows for noninvasive monitoring of the ovarian response during controlled ovarian stimulation (COS). Ultrasound imaging of follicle maturation was first performed in 1978, when a linear correlation between follicle size and serum estradiol levels was demonstrated [1]. Later, studies performed in the early 1980s confirmed the relationship between serum estrogen concentration and both the number and size of growing follicles. An increase in uterine size and endometrial thickening during stimulation was also described [2]. Currently two-dimensional (2D) ultrasound imaging is used diagnostically and in treatment, for evaluation of all pelvic organs and for transvaginal procedures, respectively.

Most importantly, the introduction of transvaginal ultrasound in 1983 dramatically improved the safety and success of ART. Today, transvaginal ultrasound imaging is imperative when administering gonadotropins for COS, in order to optimize treatment, reduce the risk of multiple pregnancies, and avoid potentially life-threatening side effects, such as the ovarian hyperstimulation syndrome (OHSS). Indeed, the use of 2D ultrasound for assessing follicular development during gonadotropin stimulation for ART is virtually universal.

More recently, the addition of power Doppler added to 2D ultrasound has been proposed with the aim of studying ovarian and endometrial blood flow. By monitoring perifollicular blood flow, the physician can identify follicles whose oocytes may result in embryos of better developmental competence [3] (see Chaps. 3 and 4).

Why Monitor the Follicular Phase?

During in vitro fertilization (IVF) treatment, exogenous gonadotropins induce the growth of a cohort of ovarian follicles. Monitoring this phenomenon is essential in order to optimize and individualize IVF treatments, and ultrasound examination is effective at all stages of the COS.

At a baseline examination, before initiating gonadotropin administration, US monitoring can identify ovarian abnormalities, such as follicular cysts or adnexal masses that need to be addressed

G. Gennarelli · A. Revelli
Sant'Anna Hospital, University of Turin, Department of Obstetrics and Gynecology, Turin, Italy

T. Tur-Kaspa
Wesleyan University, Middletown, CT, USA

M. Toftager
Fertility Clinic, Rigshospitalet, Copenhagen University Hospital, Copenhagen, Denmark

D. P. Cohen (✉)
Institute for Human Reproduction, Chicago, IL, USA
e-mail: dcohen@infertilityihr.com

L. A. Stadtmauer, I. Tur-Kaspa (eds.), *Ultrasound Imaging in Reproductive Medicine*,
https://doi.org/10.1007/978-3-030-16699-1_16

in advance. Furthermore, a baseline count of small antral follicles (AFC) provides a hint into the probability of success, and it helps identify the optimal starting dose of gonadotropin and the most appropriate type of stimulation protocol. It has been repeatedly shown that the AFC correlates positively with the number of oocytes retrieved, the proportion of mature oocytes from the oocytes retrieved, and ultimately the probability of success of the IVF treatment [4, 5], provided a transvaginal US probe with frequency ≥7 MHz is used and the operator is adequately experienced [6].

Furthermore, in cases when GnRH agonists are used to block the endogenous gonadotropin secretion from the pituitary, US examination can verify that effective pituitary-ovarian axis suppression has been obtained before starting COS. Additionally, other useful information can be obtained before stimulation, for example, the ease with which the ovaries are accessible to transvaginal needle aspiration. Finally, during ovarian stimulation US monitoring is crucial in order to determine whether the initially suggested gonadotropin stimulation dosing protocol is optimal or needs to be adjusted.

As previously mentioned US helps predict the number of oocytes expected to be obtained, but it is also of paramount importance for minimizing the risk of OHSS. When OHSS is incipient, free fluid may be identified in the peritoneal cavity. This sign, together with the number and size of the growing follicles and the ovarian volume, is information currently used to help predict and prevent OHSS. Interestingly, to prevent OHSS in the polycystic ovarian syndrome patient resistant to standard ovulation induction, ultrasound has been suggested as a tool to guide ovarian drilling [7].

Finally, ultrasound monitoring is critical in determining the optimal time for induction of the final maturation of the growing follicles. As a matter of fact, most clinicians agree that ultrasound examination is the best modality, among those available, to monitor ovulation induction.

Normal Folliculogenesis

Before reviewing the parameters of follicular growth studied with 2D ultrasound during ART treatment, it is helpful to summarize the events which occur during normal folliculogenesis. Follicles grow through two stages, the first being gonadotropin-independent and the second gonadotropin-dependent. Primordial follicles consist of an oocyte with a thin layer of granulosa and stromal cells, and at this stage, follicles cannot be seen by ultrasound. By the time follicles develop an antral cavity, they become ultrasonographically visible, and, importantly, they have reached the gonadotropin-dependent stage. These antral follicles measure between 2 and 10 mm in mean diameter and represent the pool of follicles that may be stimulated in the ensuing follicular phase. In a natural cycle, one follicle is ultimately selected for ovulation, and that selection process occurs during the mid-follicular phase of the ovarian cycle, when the endogenous pituitary follicle stimulating hormone (FSH) level falls in response to the increasing ovarian estradiol production. Decreasing FSH levels promote a selection process in which each of the follicular microenvironments competes for the diminishing FSH needed to stimulate granulosa cells to produce aromatase and continue growth. Aromatase, in turn, is necessary to convert testosterone and androstenedione produced in the peripheral theca cells into estradiol and estrone, respectively, in the granulosa cells. Failure of this conversion from androgen to estrogen leads to an elevated androgen-to-estrogen ratio in the microenvironment of the follicle and then to follicular atresia. From this cursory review of the anatomy and physiology of oocyte maturation, it is easy to see how ovulation-inducing agents that either indirectly increase endogenous FSH (e.g., clomiphene citrate) or directly add exogenous FSH to the system diminish the competition among follicles for FSH and permit the development of multiple dominant follicles [5, 6].

Monitoring Follicular Maturation

Methods for Monitoring

It is difficult to predict the optimal number of growing ovarian follicles in an IVF cycle, since there is considerable variation in ovarian response among patients. The ovarian response depends on

age, ovarian reserve, the type of stimulation protocol, the FSH dose, FSH receptor polymorphisms, etc.

Follicular maturation in IVF cycles can be monitored clinically by:

- Serum estradiol value alone
- 2D ultrasound alone
- 3D ultrasound alone
- Serum estradiol and ultrasound combined
- Supplemental power Doppler imaging

There are numerous studies on the use of these different methods for monitoring follicular maturation. Traditional monitoring of an IVF treatment cycle includes a combination of 2D ultrasonography and serum estradiol concentrations and has long been accepted as the gold standard. However, whether estradiol monitoring adds any advantage to US monitoring remains controversial. Obviously, US examination provides more accurate measurement of follicle number and size than can be obtained by serum estradiol alone. Whereas available data are not conclusive, the most recent literature does not support the notion that measuring estradiol serum concentrations during COS is of significant advantage in terms of both results and safety [8].

The frequency of US check and the time points at which the dose of exogenous gonadotropins could be changed show wide variations, depending on the experience of the clinician and the routine applied at each IVF clinic. Some monitoring methods are very complex, whereas other methods are simpler. However, whatever the complexity of COS monitoring, the outcomes of IVF cycles does not differ significantly [9].

When viewed on ultrasound, follicles appear as echo-free structures within the more echogenic ovarian tissue. By convention, follicle size in 2D is estimated by calculating the mean of the maximum follicular internal diameter in two perpendicular planes [10]. Alternatively, the follicle size can be estimated in three dimensions, the *x*, *y*, and *z* planes, and using this technique, it is possible to calculate the volume of each follicle. Most recently, three-dimensional (3D) software programs that distinguish the echogenicity of the well-circumscribed, sharp-edged, echolucent follicular fluid from the surrounding greater echogenicity of the ovarian cortical parenchyma have automated this process and allow follicular volume calculations from data derived from 2D images. The clinician can simply sweep through the ovarian tissue, and the stored image data is analyzed, reducing the time usually needed when multiple diameters are measured for each follicle, separately. This option is particularly useful in busy practices, when a large number of follicular monitoring scans are performed every day.

Standard Ultrasound Monitoring Program

Follicular growth can be directly monitored with 2D ultrasound, since the follicular diameter increases during development in the follicular phase. Most clinicians measure the follicles at baseline (Fig. 16.1), prior to initiating gonadotropin stimulation, and then again after approximately 5 days of gonadotropin stimulation, and then every 24–48 hours depending on the rate of development (Figs. 16.2, 16.3, 16.4, and 16.5). Once the mature follicle measures 17–21 mm, the physician can trigger ovulation with human chorionic gonadotropin (hCG, a luteinizing hormone (LH) surrogate) (Fig. 16.6) or a gonadotropin-releasing hormone analog. In simple ovulation induction, confirmation of ovulation can be demonstrated by ultrasound as well, observing the sudden change of the intact follicle, made up of concentric layers of theca cells surrounding granulosa cells enclosing the follicular fluid and the oocyte that is suddenly changed after follicular rupture and ovulation. Physiologically, it is at this moment that both testosterone-secreting theca cells and estradiol-secreting granulosa cells convert intracellular steroid production to preferentially favor progesterone production. Thus, ovulation is accompanied by a dramatic loss of the concentric architecture of the preovulatory follicle and an increase in blood supply, presumably aimed at increasing dramatically the output of progesterone into the bloodstream. A very specific, nearly

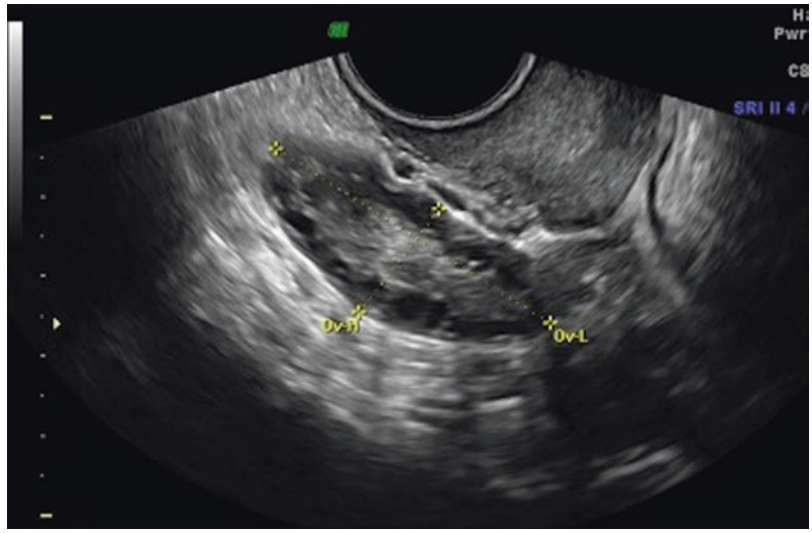

Fig. 16.1 Baseline, prior to initiating gonadotropin stimulation. Ovary with antral follicles

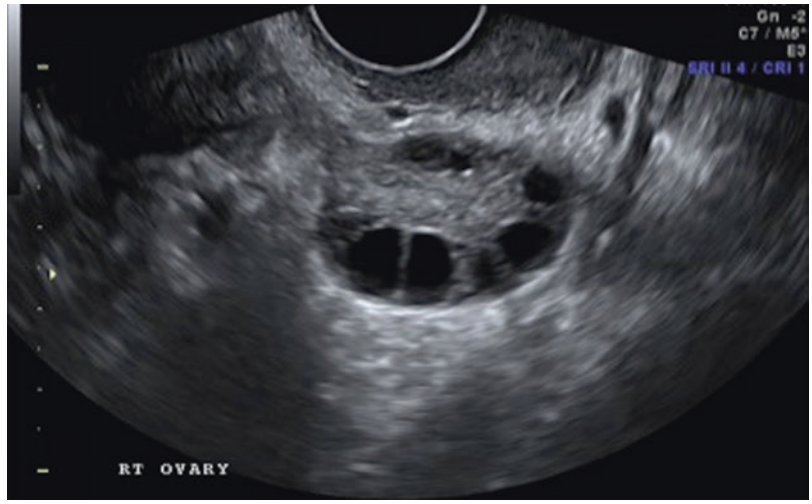

Fig. 16.2 Stimulation day 5, showing recruited follicles measuring 10–12 mm

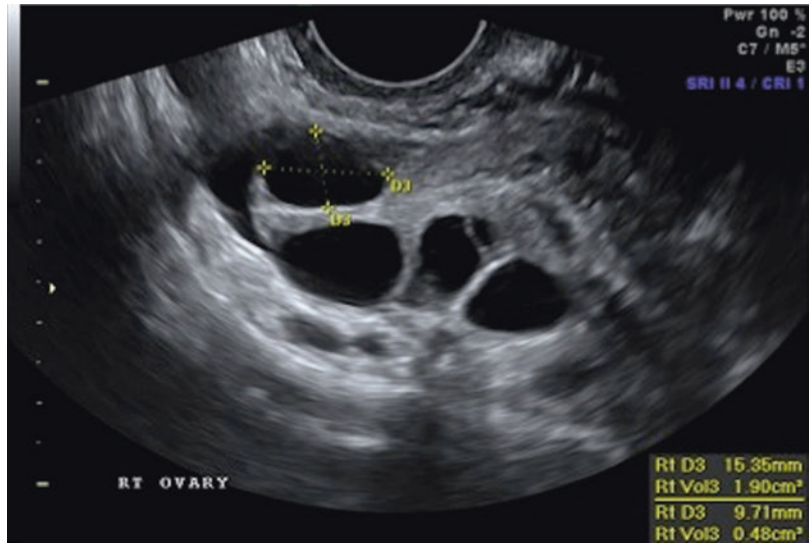

Fig. 16.3 Stimulation day 7, showing ovary with leading follicle >12 mm

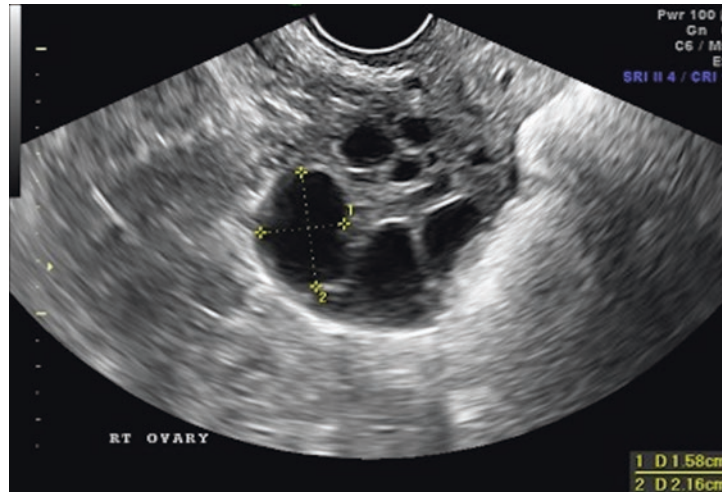

Fig. 16.4 Stimulation day 9, showing ovary with growing follicles

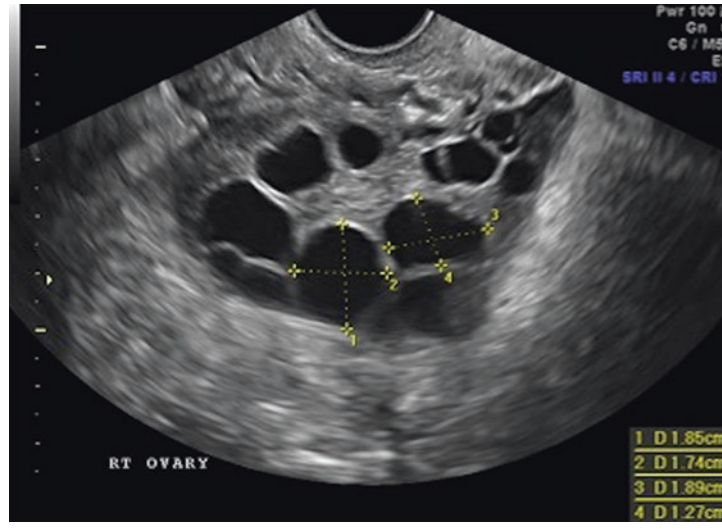

Fig. 16.5 Stimulation day 11, 2–3 follicles measuring 17–18 mm

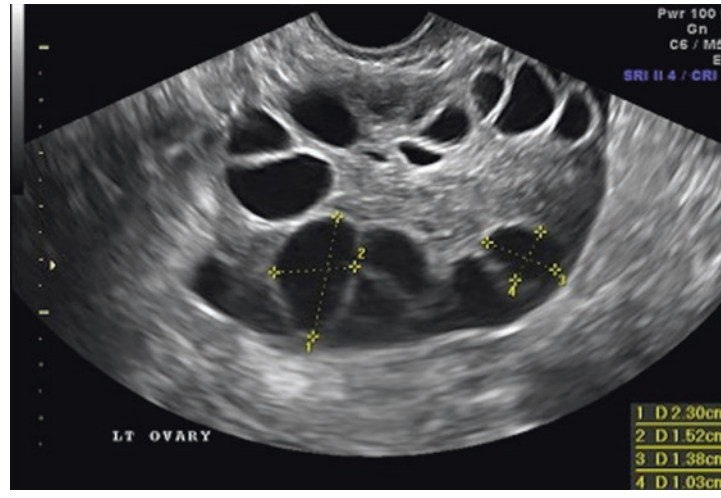

Fig. 16.6 Day of ovulation induction. Leading follicles measuring more than 18 mm

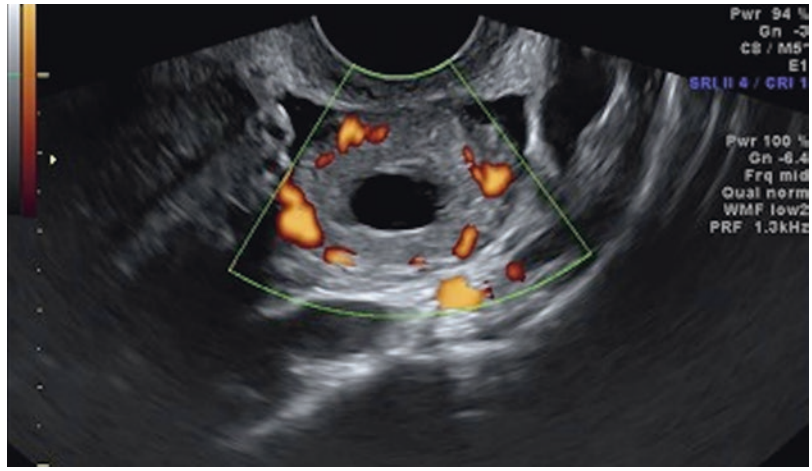

Fig. 16.7 Corpus luteum cyst – "ring of fire"

pathognomonic "ring of fire" ultrasound finding is easily discerned around each corpus luteum at this time (Fig. 16.7). Doppler technology added to the 2D image enables observation of this typical flow pattern which, in combination with the classic echogenicity of the corpus luteum, makes the diagnosis of ovulation quite simple [11].

Follicular Size and Volume

During COS for IVF, it is realistic to recruit 5–10 ovarian follicles in each ovary; however the number, the rate of growth of each follicle, and the number of stimulation days can vary greatly between patients.

After 6–7 days of gonadotropin stimulation, follicles measuring more than 10 mm are expected.

Once a dominant follicle measures more than 12 mm in mean diameter, a growth rate of 2 mm (1–3 mm) per day is expected [12]. Growth continues until follicular maturation at 17–21 mm, and at that point, the oocyte is ready to ovulate, complete meiosis in response to the LH trigger, and be released into the peritoneal cavity.

Criteria Used for Triggering Ovulation

Whereas the criteria used for triggering ovulation and inducing the final oocyte maturation vary between protocols, all aim to produce mature oocytes to be fertilized; mature oocytes are defined as those that have completed meiosis I, extruded the first polar body, and rearrested in metaphase of meiosis II. Most commonly hCG is administered to mimic the endogenous LH surge, which in turn triggers meiotic reinitiation from the oocyte's prophase I resting state. As noted previously, stimulation protocols vary and are often modified during the stimulation. However, in most cases ovulation is triggered when ≥3 follicles ≥17 mm in diameter are identified on ultrasound. Alternatively, the trigger is administered either when ≥3 follicles, each with a maximum diameter of 18 mm, are identified or when ≥1 follicle of ≥18 mm and 3 follicles of ≥15 mm are observed. Other criteria have taken into consideration serum estradiol levels as well; in these criteria, hCG is usually administered when the leading follicle reaches 18–20 mm and the coincident serum estradiol level suggests "satisfactory" follicular development. More in detail, it is suggested that induction of the final oocyte maturation be performed in the presence of at least one follicle ≥20 mm and a serum estradiol level ≥1200 pg/mL [13]. So far, there are no conclusive data in favor of any specific criteria.

How to Predict Retrieval of Mature Oocytes?

Follicular size and the volume of follicular fluid have traditionally been recognized as possible

predictors of oocyte quality, i.e., oocytes that will be fertilized and result in embryos that implant and progress into a viable pregnancy [14]. However, attempts to find a universally accepted threshold of a worth-to-be-punctured follicle size have been disappointing, due to conflicting results. What is commonly accepted is that a large follicle is more likely to lead to the retrieval of a mature oocyte than a smaller follicle. The correlation between the follicle size and the likelihood of retrieving a mature oocyte may reflect the notion that larger follicles have completed the maturation process and released the oocyte-cumulus cell mass as a free-floating structure in the antral fluid just before follicle rupture. According to early data from Teissier et al. [15], 14 mm in diameter should be considered the threshold follicle size to get an acceptable chance of finding meiotically competent oocytes at retrieval, both in normal and polycystic ovaries. However, follicles measuring as small as 11–15 mm have been reported to have as much as a 50% chance of yielding a mature oocyte [16].

Conversely, follicles with a mean diameter above 22 mm result in lower recovery of mature, fertilizable oocytes as they often contain postmature eggs, probably the result of intrafollicular atresia and degenerative phenomena [17].

More recent studies have observed a correlation between oocyte competence and ultrasound-measured follicular size prior to trigger and oocyte retrieval. A higher proportion of immature oocytes (germinal vesicle-GV-stage) are indeed found in smaller follicles, particularly those below 12 mm in mean diameter. It is important to remember, however, that this is not a universal finding since even small follicles can generate mature MII oocytes [18]. Wittmaack et al. [19] found the optimal follicle volume to be between 1 ml, which corresponds to 12 mm in mean diameter, and 6–7 ml, corresponding to 24 mm in mean diameter. Higher oocyte recovery rates, higher fertilization rates, and higher cleavage rates for follicles in this interval were reported. However, within this range, the higher the follicular volume, the higher the fertilization rate and the better the embryo quality. Furthermore, in sync with those observations, a recent study showed that delaying the oocyte maturation trigger by 1 day, once the leading follicles have reached 18 mm in diameter, would allow the retrieval of significantly more mature oocytes, provided no progesterone rise is detected [20].

Most compelling, the results of a prospective study, including 9933 follicles from 535 IVF cycles, confirmed that oocytes from follicles with a volume <1 ml (<12 mm in mean diameter) had a significantly lower fertilization rate than oocytes from larger follicles. However, the same oocytes, once fertilized, yielded embryos of comparable quality; no significant differences in the implantation rate, clinical pregnancy rate, or live birth rate were detectable from embryos derived from oocytes recovered from either small or large follicles [21].

It is also true that in general, it is not possible to identify a clear relationship between follicle size and the morphological quality of the embryos. This may be due to the fact that follicles with a volume within a certain interval contain oocytes that lead to embryos of comparable morphologic scores and/or to the fact that the male gamete contributes to embryo quality as well and should be considered along with the oocyte.

Likewise, follicular size, volume, morphology, and vascularity do not provide any predictive information on the chances of conception of a euploid fetus.

The Uterine Cavity and Monitoring of Endometrial Proliferation

During the diagnostic evaluation of the infertile couple, assessment of the uterine cavity and the patency of the fallopian tubes is essential. The standard means of assessment of these two structures is hysterosalpingography or more invasive laparoscopy and hysteroscopy. In the last decade, the use of saline infusion into the cavity to assess both the cavities in several planes using 2D and 3D (more recently) transvaginal imaging has made assessment of the uterine cavity and the tubes an office procedure that is less painful, involves no radiation, and is less expensive and more accessible.

During the proliferative phase of the menstrual cycle, several factors have been shown to correlate with a successful pregnancy. The aim of 2D monitoring of the follicular phase in ART is not solely to monitor follicular development but also to monitor endometrial development. Predicting the probability of pregnancy by assessing the degree of endometrial development on ultrasonography has been the aim of several studies. For example, a prospective study demonstrated higher pregnancy rates with endometrial thicknesses of 8 mm and greater. The same study reported more pregnancies when Doppler-identified endometrial blood flow was more penetrating into the endometrium [22].

Endometrial thickness and pattern varies throughout the menstrual cycle, especially in the follicular phase in response to estrogen secretion from ovarian follicles. The endometrium is thin immediately after menstruation (2–5 mm), thickens during the proliferative (ovarian follicular) phase, is trilaminar before ovulation, and is thick and hyperechogenic in the secretory (ovarian luteal) phase of the cycle. A small amount of endometrial fluid (0.5–1.0 mm in the middle of the uterine cavity), thought to be mucus, can be seen before ovulation: this finding is considered normal, and it rapidly disappears. In contrast, however, fluid in the endometrium at the time of embryo transfer (ET), often coexisting with a hydrosalpinx, is associated with a poorer prognosis. When this observation is made, freezing all the embryos is considered a valuable option in order to provide time to manage the pathological condition and have a lining with no fluid in it for an ET in the future.

With respect to endometrial development during the follicular phase and during COS, endometrial blood flow, endometrial echo patterns, and endometrial thickness are the US signs most often investigated.

The thickened endometrium provides the site for embryo attachment. Controversies exist, however, regarding the clinical significance of observed variations in endometrial thickness in relation to pregnancy rates during IVF. Some studies report no correlation between endometrial thickness and pregnancy rates, whereas others suggest a positive correlation. Possible reasons for this observed discordancy may be attributed to a number of confounding variables, such as different treatment protocols and/or the different etiologies of infertility. There is a general agreement, nonetheless, that a "thin" endometrium is detrimental to embryo implantation and the development of a pregnancy. Thus, patients with a thin endometrium also present the clinician with the dilemma of whether to continue the IVF cycle or to cancel the embryo transfer and cryopreserve all the embryos.

A systematic review and meta-analysis from 2014 reported no significant correlation between endometrial thickness on the day of hCG administration and the chances of pregnancy [23]. However a tendency toward lower clinical pregnancy rates was observed for cases with endometrial thickness $\leq$7 mm in comparison to cases with endometrial thickness >7 mm (23.3% vs 48.1%) [23].

More recently, a retrospective analysis performed on more than 40,000 IVF cycles, including both fresh and frozen/thawed embryo transfers, demonstrated that clinical pregnancies and live birth rates decline when endometrial thickness decreases below 8 mm and 7 mm, respectively [24].

So far, however, there are no clear cutoffs in endometrial thickness measurements that can be applied to definitively recommend cycle cancellation.

The use of endometrial blood flow to predict endometrial receptivity has also been studied. According to a recent meta-analysis, various US indices related to both endometrial and subendometrial blood flow correlate with implantation and pregnancy rates [25], whereas the absence of endometrial and sub-endometrial blood flow is associated with higher uterine artery resistance and with a thin endometrium.

There are indications that the echogenic pattern of the endometrium reflects histologic processes that are believed to be involved in embryo receptivity. This may explain the reported association between premature hyperechogenic patterns of the endometrium and poor implantation rates. Indeed higher pregnancy rates in IVF

cycles are reached when a triple-line isoechogenic pattern is observed on the day of hCG administration [26].

Although there may be a relationship between endometrial differentiation and pregnancy, the endometrial mechanisms behind implantation are probably more complex than a few ultrasound measurements can determine.

Monitoring with 2D vs 3D

Three-dimensional US follicular volume measurements provide more accurate data with respect to 2D measurements. Both manual measurement (VOCAL) and automated measurement (SonoAVC) show a 95% correlation with the real follicle volume (obtained by measuring the aspirated follicular fluid at oocyte retrieval) [27]. One advantage of the automated 3D US scanning is the reduction in interobserver and intra-observer variability [27]. However, in spite of that the results on fertility outcomes are so far conflicting [28, 29] (see Chap. 17).

Three-dimensional power Doppler angiography has been suggested for the study of perifollicular blood flow. The vascularization index (VI) and the flow index (FI) from the whole ovary seem to correlate positively with the number of embryos and their morphological scores [14].

Monitoring with Power Doppler (in Relation to 2D)

Under physiological gonadotropin stimulation, granulosa cells produce factors related to angiogenesis. These factors contribute to an increase in vascularization needed for follicle development, for ovulation, and for optimal function of the corpus luteum.

A neovascularization surrounding the dominant follicle can be detected by Doppler US, both during spontaneous ovulation and during ovulation induction. Increased perifollicular blood fluxes and decreased indices of vascular resistance are observed in the preovulatory follicle. A rapid increase in blood flow velocity occurring at the time of the LH surge in the perifollicular and stromal blood vessels has been associated with follicle maturity [30].

Early observations suggested that a perifollicular flow >10 cm/s at the time of hCG administration may enhance selection of oocytes and ultimately increase pregnancy rates [31], whereas high-grade ovarian perifollicular blood perfusion in the early follicular phase during IVF is associated with both high-grade perifollicular blood perfusion in the late follicular phase and a higher clinical pregnancy rate [32].

More recently, Jadaon et al. measured four Doppler indices in women prior to IVF treatment: peak systolic velocity (PSV), pulsatility index (PI), resistance index (RI), and systole/diastole ratio (S/D). They found a positive correlation between the number of follicles ≥14 mm on the day of hCG and PSV. The number of follicles ≥14 mm and the number of retrieved oocytes had significant negative correlations with RI and S/D ratio. Furthermore, the number of fertilized oocytes had a significant negative correlation with S/D ratio. The absence of a Doppler signal in one or both ovaries was significantly higher in the women with a poor response (31%) as compared to women with a normal response (16%) [33].

Based on these observations, it has been suggested that the Doppler blood flow analysis of the growing follicles could be used in IVF to select the best oocytes that eventually lead to embryos with better implantation potential. However, practical problems do exist. COS generates multiple follicles overlapping one another, and it may be difficult to assign a specific flow to each single follicle. Whether the use of this technology may be of real advantage in women with a low response (very few follicles) remains to be established.

Self-Monitoring

Over the years, attempts have been made in order to lessen the patients' burden of stimulation protocols, both for induction of ovulation and COS. Under this situation, self-operated endo-

vaginal telemonitoring has been suggested [34]. The technology available is 2D, and the system consists of a probe connected via a USB to a tablet (Sonaura System ™). The patient can perform an US examination and self-record a video, which is sent wireless to the clinician. Whereas this method seems to be appreciated by the patients, it requires training, and it seems to be less efficient in obese women [35, 36].

Conclusion

Bidimensional ultrasound monitoring of follicular development during controlled ovarian stimulation is an integral component of most clinical practices. Whereas it might not always be necessary, particularly when using oral agents to induce ovulation, it is now standard of care during any ovulation induction therapy in cases of intrauterine insemination or in vitro fertilization. It provides the information needed to permit the safe use of these medications and to minimize the risk of hyperstimulation syndrome and the possibility of multiple gestation. While the accuracy and ease of use of this tool are unchallenged, the positive and negative predictive values of the data obtained in relation to the chances of a successful pregnancy remain to be determined. However, whatever the clinical value, US will not replace the physician's judgment of the whole clinical presentation.

So far, 3D US monitoring and Doppler examination of the ovary and follicles are not suggested in clinical routine. Self-monitoring might be a simplification of the treatment schedule which deserves more studies.

References

1. Hackeloer BJ, Robinson HP. Ultrasound examination of the growing ovarian follicle and of the corpus luteum during the normal physiologie menstrual cycle (author's transl). Geburtshilfe Frauenheilkd. 1978;38(3):163–8.
2. Ylostalo P, Lingren PG, Nillius SJ. Ultrasonic measurement of ovarian follicles, ovarian and uterine size during induction of ovulation with human gonadotrophins. Acta Endocrinol. 1981;98(4):592–8.
3. Naredi N, Singh SK, Sharma R. Does perifollicular vascularity on the day of oocyte retrieval affect pregnancy outcome in an in vitro fertilization cycle? J Hum Reprod Sci. 2017;10(4):281–7.
4. Ben-Haroush A, Farhi J, Zahalka Y, Sapir O, Meizner I, Fisch B. Small antral follicle count (2–5 mm) and ovarian volume for prediction of pregnancy in in vitro fertilization cycles. Gynecol Endocrinol. 2011;27(10):748–52.
5. Ben-Haroush A, Farhi J, Zahalka Y, Sapir O, Meizner I, Fisch B. Correlations between antral follicle count and ultrasonographic ovarian parameters and clinical variables and outcomes in IVF cycles. Gynecol Endocrinol. 2012;28(6):432–5.
6. Coelho Neto MA, Ludwin A, Borrell A, Benacerraf B, Dewailly D, da Silva Costa F, Condous G, et al. Counting ovarian antral follicles by ultrasound: a practical guide. Ultrasound Obstet Gynecol. 2018;51(1):10–20.
7. Kandil M, Rezk M, Al-Halaby A, Emarh M, El-Nasr IS. Impact of ultrasound- guided transvaginal ovarian needle drilling versus laparoscopic ovarian drilling on ovarian reserve and pregnancy rate in polycystic ovary syndrome: a randomized clinical trial. J Minim Invasive Gynecol. 2018;25(6):1075–9. https://doi.org/10.1016/J.JMIG.2018.01.036. Epub 2018 Feb 21.
8. Kwan I, Bhattacharya S, Kang A, Woolner A. Monitoring of stimulated cycles in assisted reproduction (IVF and ICSI). Cochrane Database Syst Rev. 2014;24(8):CD005289.
9. Wikland M, Hillensjö T. Monitoring ovarian response in IVF cycles. In: Gardner DK, et al., editors. Textbook of assisted reproductive techniques. London: Informa Healthcare; 2012.
10. Penzias AS, Emmi AM, Dubey AK, Layman LC, DeCherney AH, Reindollar RH. Ultrasound prediction of follicle volume: is the mean diameter reflective? Fertil Steril. 1994;62(6):1274–6.
11. Jokubkiene L, Sladkevicius P, Rovas L, Valentin L. Assessment of changes in volume and vascularity of the ovaries during the normal menstrual cycle using three-dimensional power Doppler ultrasound. Hum Reprod. 2006;21(10):2661–8.
12. Tur-Kaspa I, Stadtmauer L. Ultrasonography in assisted reproduction. In: Gardner DK, et al., editors. Textbook of assisted reproductive techniques. London: Informa Healthcare; 2012.
13. Kolibianakis EM, Albano C, Camus M, Tournaye H, Van Steirteghem AC, Devroey P. Prolongation of the follicular phase in in vitro fertilization results in a lower ongoing pregnancy rate in cycles stimulated with recombinant follicle-stimulating hormone and gonadotropin-releasing hormone antagonists. Fertil Steril. 2004;82(1):102–7.
14. Merce LT, Bau S, Barco MJ, Troyano J, Gay R, Sotos F, Villa A. Assessment of the ovarian volume, number and volume of follicles and ovarian vascularity by three-dimensional ultrasonography and power Doppler angiography on the HCG day to pre-

dict the outcome in IVF/ICSI cycles. Hum Reprod. 2006;21(5):1218–26.
15. Teissier MP, Chable H, Paulhac S, Aubard Y. Comparison of follicle steroidogenesis from normal and polycystic ovaries in women undergoing IVF: relationship between steroid concentrations, follicle size, oocyte quality and fecundability. Hum Reprod. 2000;15(12):2471–7.
16. Shmorgun D, Hughes E, Mohide P, Roberts R. Prospective cohort study of three- versus two-dimensional ultrasound for prediction of oocyte maturity. Fertil Steril. 2010;93(4):1333–7.
17. Ectors FJ, Vanderzwalmen P, Van Hoeck J, Nijs M, Verhaegen G, Delvigne A, Schoysman R, Leroy F. Relationship of human follicular diameter with oocyte fertilization and development after in-vitro fertilization or intracytoplasmic sperm injection. Hum Reprod. 1997;12(9):2002–5.
18. Inaudi P, Germond M, Senn A, De Grandi GP. Timing of hCG administration in cycles stimulated for in vitro fertilization: specific impact of heterogeneous follicle sizes and steroid concentrations in plasma and follicle fluid on decision procedures. Gynecol Endocrinol. 1995;9(3):201–8.
19. Wittmaack FM, Kreger DO, Blasco L, Tureck R, Mastroianni LJ, Lessey BA. Effect of follicular size on oocyte retrieval, fertilization, cleavage, and embryo quality in in vitro fertilization cycles: a 6-year data collection. Fertil Steril. 1994;62(6):1205–10.
20. Vandekerckhove F, Gerris J, Vansteelandt S, De A, Baerdemaeker TK, De Sutter P. Delaying the oocyte maturation trigger by one day leads to a higher metaphase II oocyte yield in IVF/ICSI: a randomised controlled trial. Reprod Biol Endocrinol. 2014;12(31):1–9.
21. Detti L, Yelian FD, Kruger ML, Diamond MP, Puscheck EE. Endometrial thickness dynamics and morphologic characteristics during pituitary downregulation with antagonists in assisted reproductive technology cycles. J Ultrasound Med. 2008;27(11):1591–6.
22. Kader MA, Abdelmeged A, Mahran A, Abu Samra MF, Bahaa H. The usefulness of endometrial thickness, morphology and vasculature by 2D Doppler ultrasound in prediction of pregnancy in IVF/ICSI cycles. Egypt J Radiol Nucl Med. 2016;47(1):341–6.
23. Kasius A, Smit JG, Torrance HL, Eijkemans MJ, Mol BW, Opmeer BC, Broekmans FJ. Endometrial thickness and pregnancy rates after IVF: a systematic review and meta-analysis. Hum Reprod Update. 2014;20(4):530.
24. Liu KE, Hartman M, Hartman A, Luo ZC, Mahutte N. The impact of a thin endometrial lining on fresh and frozen-thaw IVF outcomes: an analysis of over 40 000 embryo transfers. Hum Reprod. 2018;33(10):1883–8.
25. Wang J, Xia F, Zhou Y, Wei X, Zhuang Y, Huang Y. Association between endometrial/subendometrial vasculature and embryo transfer outcome: a meta-analysis and subgroup analysis. J Ultrasound Med. 2018;37(1):149–63.
26. Zhao J, Zhang Q, Wang Y, Li Y. Endometrial pattern, thickness and growth in predicting pregnancy outcome following 3319 IVF cycle. Reprod Biomed Online. 2014;29(3):291–8.
27. Salama S, Arbo E, Lamazou F, Levaillant JM, Frydman R, Fanchin R. Reproducibility and reliability of automated volumetric measurement of single preovulatory follicles using SonoAVC. Fertil Steril. 2010;93(6):2096–73.
28. Singh N, Usha BR, Malik N, Malhotra N, Pant S, Vanamail P. Three-dimensional sonography-based automated volume calculation (SonoAVC) versus two-dimensional manual follicular tracking in in vitro fertilization. Int J Gynaecol Obstet. 2015;131(2):166–9.
29. Wertheimer A, Nagar R, Oron G, Meizner I, Fisch B, Ben-Haroush A. Fertility treatment outcomes after follicle tracking with standard 2-dimensional sonography versus 3-dimensional sonography-based automated volume count: prospective study. J Ultrasound Med. 2018;37(4):859–66.
30. Ardaens Y, Gougeon A, Lefebvre C, Thomas P, Leroy M, Leroy JL, et al. Contribution of ovarian and uterine color Doppler in medically assisted reproduction techniques (ART). Gynecol Obstet Fertil. 2002;30(9):663–72.
31. Nargund G, Doyle PE, Bourne TH, Parsons JH, Cheng WC, Campbell S, Collins WP. Ultrasound derived indices of follicular blood flow before HCG administration and the prediction of oocyte recovery and preimplantation embryo quality. Hum Reprod. 1996;11(11):2512–7.
32. Shrestha SM, Costello MF, Sjoblom P, McNally G, Bennett M, Steigrad SJ, Hughes GJ. Power Doppler ultrasound assessment of follicular vascularity in the early follicular phase and its relationship with outcome of in vitro fertilization. J Assist Reprod Genet. 2006;23(4):161–9.
33. Jadaon JE, Ben-Ami M, Haddad S, Radin O, Bar-Ami S, Younis JS. Prospective evaluation of early follicular ovarian stromal blood flow in infertile women undergoing IVF-ET treatment. Gynecol Endocrinol. 2012;28(5):356–9.
34. Gerris J. Telemonitoring in IVF/ICSI. Curr Opin Obstet Gynecol. 2017;29(3):160–7.
35. Gerris J, Vandekerckhove F, De Sutter P. Outcome of one hundred consecutive ICSI attempts using patient operated home sonography for monitoring follicular growth. Facts Views Vis Obgyn. 2016;8(3):141–6.
36. Pereira I, von Horn K, Depenbusch M, Schultze-Mosgau A, Griesinger G. Self-operated endovaginal telemonitoring: a prospective, clinical validation study. Fertil Steril. 2016;106(2):306–310.e1.

SonoAVC (Sonographic-Based Automated Volume Count)

17

Adela Rodrıguez-Fuentes,
Jairo Hernández, Jean Paul Rouleau,
and Angela Palumbo

Introduction

Recent advances in three-dimensional (3D) ultrasound technology have resulted in the development of specific software tools for automatic volume calculation. This new technology minimizes the dependence on the operator experience, which is the classical inconvenience of ultrasound. These software are applicable in several medical fields: cardiology, nephrology, fetal ultrasound [1–4], and ovulation induction monitoring [5–11].

Focusing on reproductive medicine, the ovary is the perfect organ for the application of automatic volume calculation. The new software allows quick and precise evaluation of ovarian volume and follicles both at baseline and during ovarian stimulation.

Assessment of ovarian reserve is of paramount importance to decide clinical attitude. Besides biochemical markers of ovarian reserve such as anti-mullerian hormone (AMH), day 2 follicle stimulation hormone (FSH), and estradiol, sonographic evaluation of ovarian volume and antral follicle count (AFC) has become a crucial step in the evaluation of the infertile patient. A new tool allowing automatic AFC has recently become available and is under study in the clinical setting. In IVF (in vitro fertilization), follicular monitoring during ovarian stimulation is essential to determine the optimal timing of trigger. Ideally, "optimal timing" allows retrieval of the maximum number of mature oocytes without compromising oocyte quality and endometrial receptivity. The possibility of assessing the volume of individual follicles in a reliable and reproducible manner represents an important innovation. Clinical decisions may be guided by follicular volumes rather than mean diameter, and this may help improve final results in terms of achieving the optimal number of healthy mature oocytes.

Before introduction of 3D ultrasound, evaluation of ovarian volume and AFC as well as follow-up of follicular growth were performed by 2D ultrasound. Leading follicles' mean diameter over 16–18 mm was the classic parameter to decide administration of hCG (human chorionic gonadotropin) to induce final oocyte maturation. The idea of using follicular volume as a possible improved indicator of oocyte matu-

Electronic Supplementary Material The online version of this chapter (https://doi.org/10.1007/978-3-030-16699-1_17) contains supplementary material, which is available to authorized users.

A. Rodrıguez-Fuentes (✉)
Universidad de La Laguna, Centro de Asistencia a la Reproducción Humana de Canarias, San Cristobal de La Laguna, Spain

J. Hernández · J. P. Rouleau · A. Palumbo
Centro de Asistencia a la Reproducción Humana de Canarias, San Cristobal de La Laguna, Spain

L. A. Stadtmauer, I. Tur-Kaspa (eds.), *Ultrasound Imaging in Reproductive Medicine*,
https://doi.org/10.1007/978-3-030-16699-1_17

rity instead of leading follicles' mean diameter was introduced in 1994 by Wittmaack et al. [12]. They estimated follicular volume from the two greatest diameters considering the follicle as if it was a sphere ($v = 4/3\pi r^3$) and suggested an ideal volume of 1 to 7 cc (Fig. 17.1). These results were compared with real aspirated follicular fluid concluding that there was a good correlation ($r^2 = 0.79$) between them; however, there was an overall overestimation of the volume with this method. Wittmaack focused on a pool of follicles in the volume range of maturity (1–7 cc) instead of the leading follicle mean diameter to decide the optimal moment for triggering. Follicles under 1 cc or above 7 cc had a lower percentage of oocytes harvested. In this study, follicles between 0.1 cc and 1 cc were included in the same group.

At the beginning of this century, papers about 3D technology began to appear introducing Virtual Organ Computer-aided AnaLysis program (VOCAL). Raine-Fenning [13] published about the accuracy and reproducibility of ovarian volume measured on 2D image applying the prolate ellipsoid formula (Fig. 17.2) compared with those using the 3D rotational technique (VOCAL). Their results showed that 2D and 3D volume calculations are both reliable and valid with rotational techniques being superior to conventional ones.

Mercé and coauthors [14] studied not only ovarian volume reproducibility using 3D data but

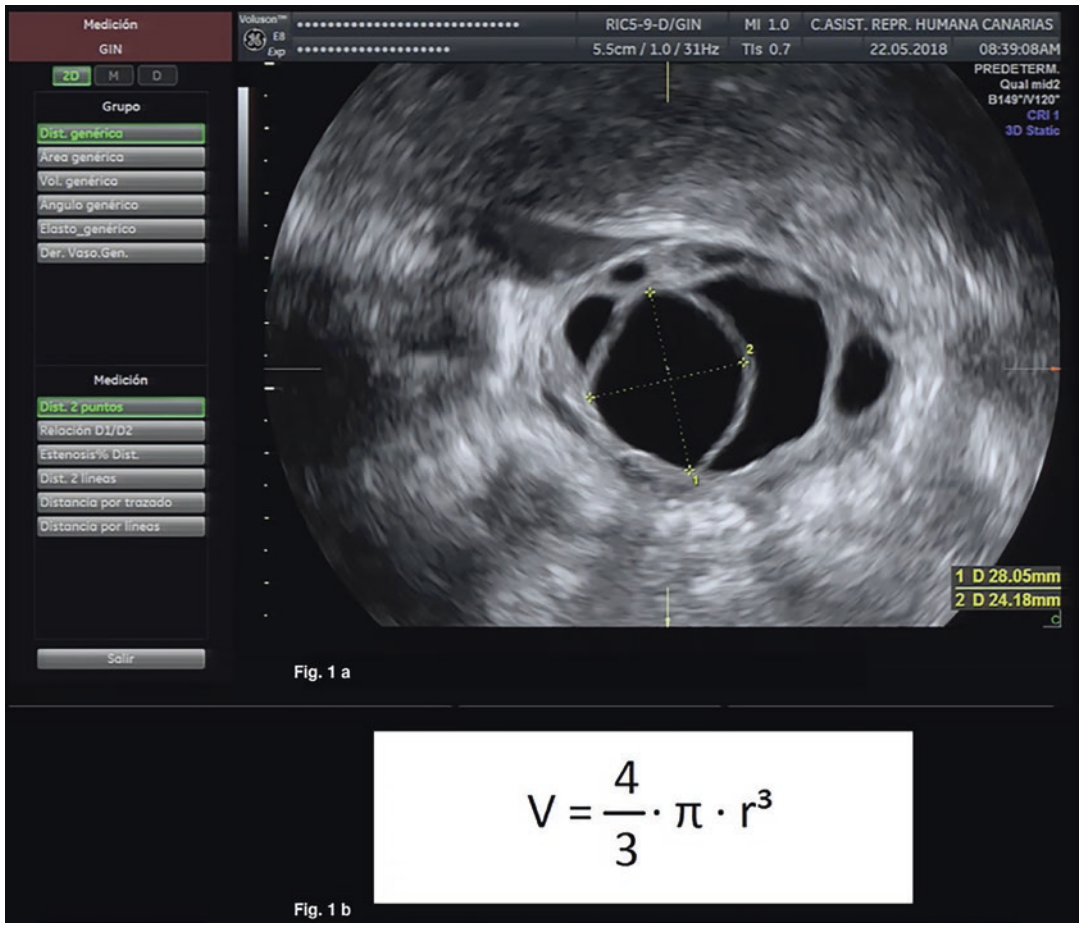

Fig. 17.1 (**a**) Measurement of the two greatest diameters of a follicle. (**b**) Sphere formula to estimate volumes from 2D images

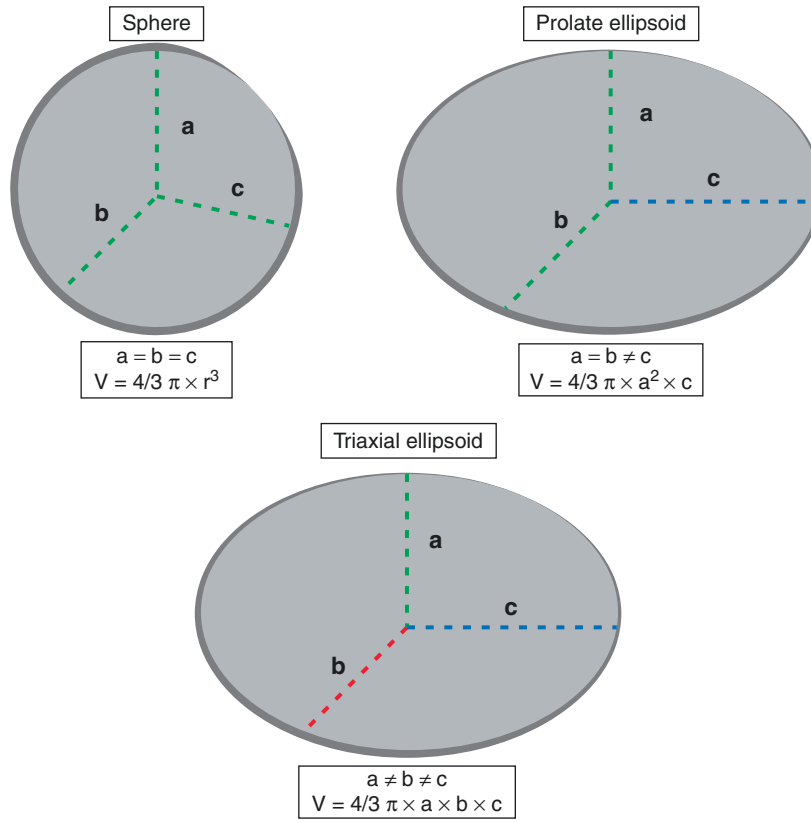

Fig. 17.2 Formula for the volume of a sphere, a prolate ellipsoid and a triaxial ellipsoid

also AFC and 3D power Doppler indices: vascularization index (VI), flow index (FI), and vascularization flow index (VFI). They confirmed the accuracy of automatic measurements of volume and also a good inter- and intraobserver correlation coefficient in power Doppler indices and AFC.

Shmorgun [15] studied the correlation between follicular volumes and oocyte maturity comparing 2D and 3D techniques. In their study volume was either estimated from follicular diameters measured by 2D US assuming that each follicle is a perfect sphere ($v = 4/3\pi r^3$) or measured with VOCAL using 3D ultrasound. The authors concluded that volumes obtained from 3D acquisitions correlated better with oocyte maturity, but with the available technology at the time, it was considered cumbersome and time-consuming (Figs. 17.3 and 17.4).

Finally, in the period between 2008 and 2010 SonoAVC*follicle* became available and was proposed in several papers as the most accurate technique to assess follicular volume taking as the gold standard aspirated follicular fluid on the day of egg retrieval [5, 6].

SonoAVC*follicle* is an automatic software developed by GE Healthcare (Austria) to study stimulated ovaries, detecting hypoechogenic objects (follicles) localized in a certain area of interest (ovary). It analyzes its volume and shape, calculating the mean diameter of each structure in the three planes of the space, with all follicles being shown in a list in decreasing order of size with a color code (Fig. 17.5).

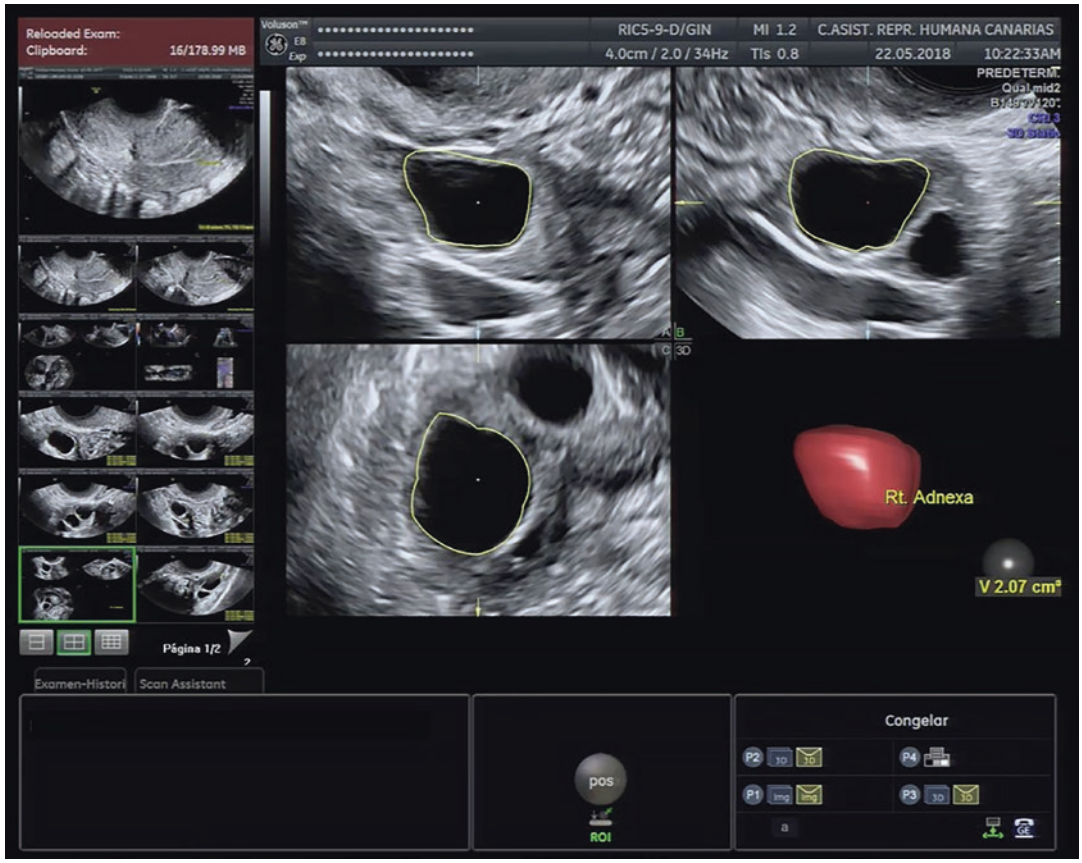

Fig. 17.3 Volume of a single follicle measured using VOCAL (Virtual Organ Computer-aided AnaLysis)

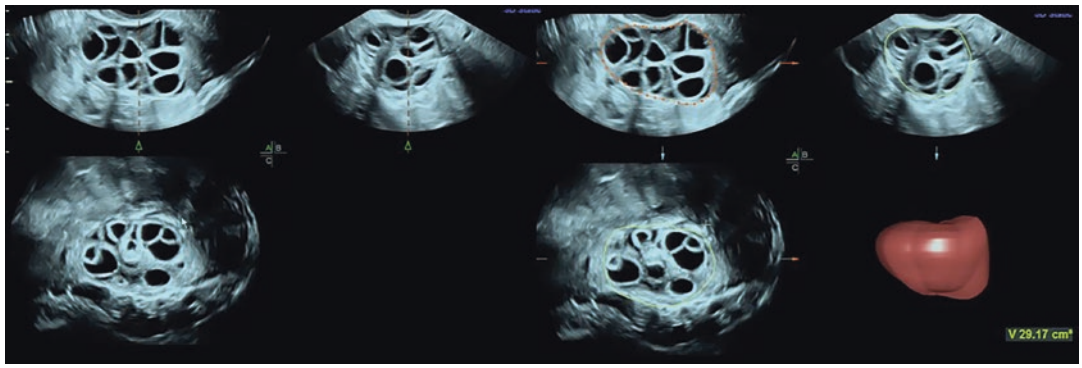

Fig. 17.4 Multiplanar view of the ovary is presented on the left. On the right, ovarian volume measured with VOCAL

How Does One Apply SonoAVC?

It is a quite simple and intuitive process. First of all, it is mandatory to adjust the parameters of a 2D image in order to obtain an optimal quality image. In that way one improves the final results of a 3D acquisition thereby reducing post-processing efforts.

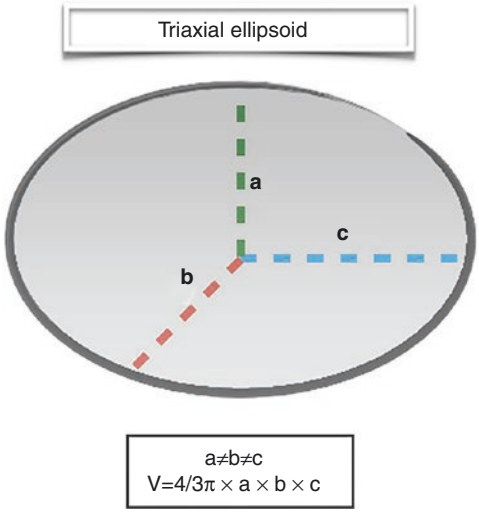

Ovario: Izq.
N. °total: 9

Núm.	d(v) mm	dx mm	dy mm	dz mm	mn. d mm	v cm³
1	16.9	21.6	17.5	13.8	17.6	2.52
2	16.8	20.6	16.5	14.8	17.3	2.49
3	15.7	24.9	18.4	11.5	18.3	2.02
4	13.2	16.7	13.8	11.0	13.8	1.20
5	11.0	13.8	12.8	7.8	11.5	0.69
6	8.3	9.8	9.3	6.5	8.5	0.30
7	7.8	13.5	9.9	4.3	9.2	0.25
8	3.3	4.7	3.8	2.0	3.5	0.02

Fig. 17.5 On the right, a SonoAVC*follicle* report is presented. Notice that mean diameter of each follicle is specified in the three planes of the space

Ideally we have different settings that have been previously adjusted for each type of exploration. To study ovarian follicles, we use our own protocol called ovaryAVC, which has a high contrast on gray scale (high dynamic range). Despite this, there are some functions that we must recognize to optimize image quality when needed:

1. Gain: It amplifies all signals by a constant factor regardless of depth.
2. TGC (Time Gain Compensation): Ability to compensate for the attenuation of ultrasound echo signals as a sound wave travels through tissue in the body. It modifies gain in different depth layers.
3. Focal zone: The region over which the optimal sharpness of the ultrasound beam is. We can increase the number of focal zones being aware of the consequent deceleration of the frame rate.
4. Depth: The region of interest must be localized in the center of the screen.
5. Quality of Image: Maximum quality increases the acquisition time. This may be a problem when the region of interest (ROI) is in movement, but this is not the case of when viewing the ovary.
6. Dynamic range: Ratio of the largest to the smallest signals. It controls the contrast on the ultrasound image making an image look either very gray or very black and white.
7. Spatial compounding (CrossXBeam): Ultrasound beam emission in different directions resulting in a better contrast resolution and organ sharpness or its margins.
8. SRI (Speckle Reduction Imaging): It softens a final image so that it may become blurred – should be used with caution.

After optimizing the 2D image, we have to select the 3D mode, adjust the 3D box, and stand still, while the automatic acquisition is made. We must make sure that the larger diameter of the ovary is inside the region of interest (ROI) before the scanning starts (Video 17.1).

Once the volume is acquired, it is shown on the screen on the multiplanar view. We must check that the entire ovary has been scanned and that there is no shadowing hindering its visualization before proceeding. Then we select the [SonoAVC*follicle*] button, adjust the area of study to the ovarian parenchyma and press right/left ovary to start automatic volume calculation (Fig. 17.6). In a few seconds, every anechoic structure will be represented. On the superior left corner of the screen, one will find the report. Each follicle has the same color code in the report as well as in the multiplanar view and render mode (Fig. 17.7, Video 17.2).

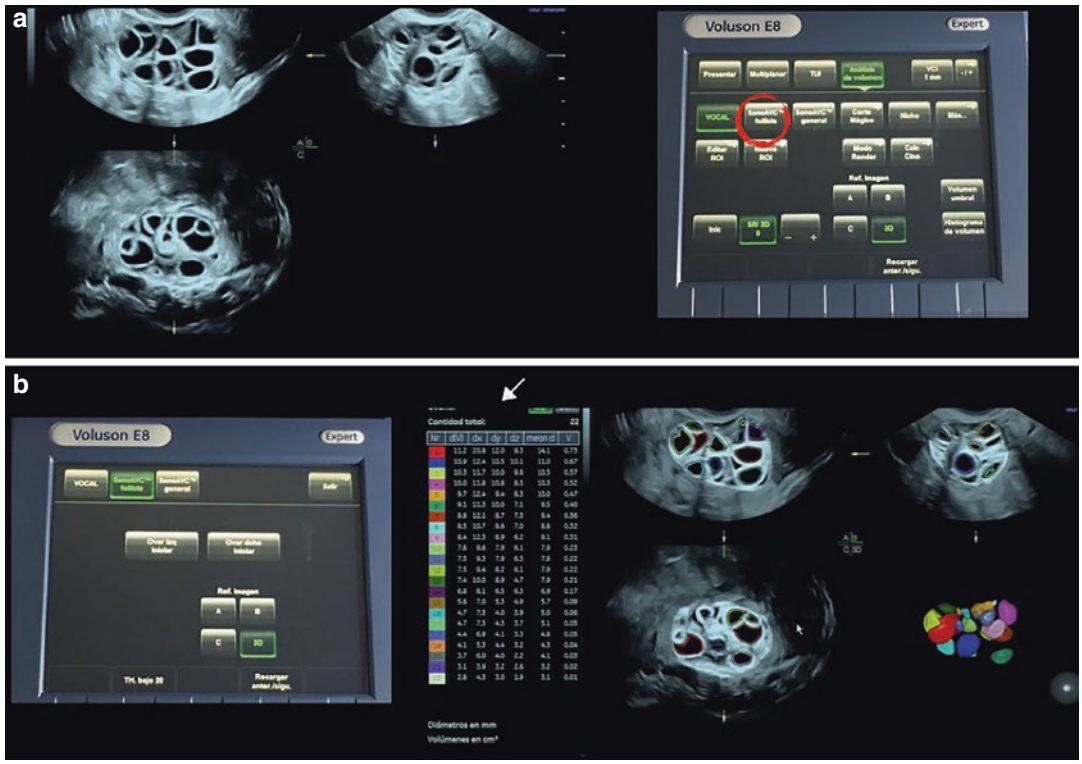

Fig. 17.6 (**a**) Left: there is a multiplanar view of the ovary. Right: screen with volume analysis options: in this case the SonoAVC*follicle* option (red circle) is selected. (**b**) On the next step, after choosing "right/left ovary," the report (white arrow) together with a 3D representation of the ovary with color-coded follicles will be shown after a few seconds

The report is in decreasing order of size with the following specific information (Fig. 17.8):

- d (*V*): Mean diameter calculated as if it was a perfect sphere
- dx: *X* axis length of the ellipsoid
- dy: *Y* axis length of the ellipsoid
- dz: *Z* axis length of the ellipsoid
- mn.d: mean diameter
- *V*: object volume
- If one is not completely satisfied with the global results, some post-processing work can be performed (Video 17.3).
- If follicles are under-/overestimated in size: adjust growth.
- If the program has recognized two different follicles as a single structure or vice versa: adjust separation.
  - In both functions the default value is "mid." Possible values go from −3 to +3.
- Use add/remove functions to include or exclude structures and cut/merge functions to manually separate or fuse follicles or part of them.
- To reverse or repeat recent actions, use "undo" or "redo" options.

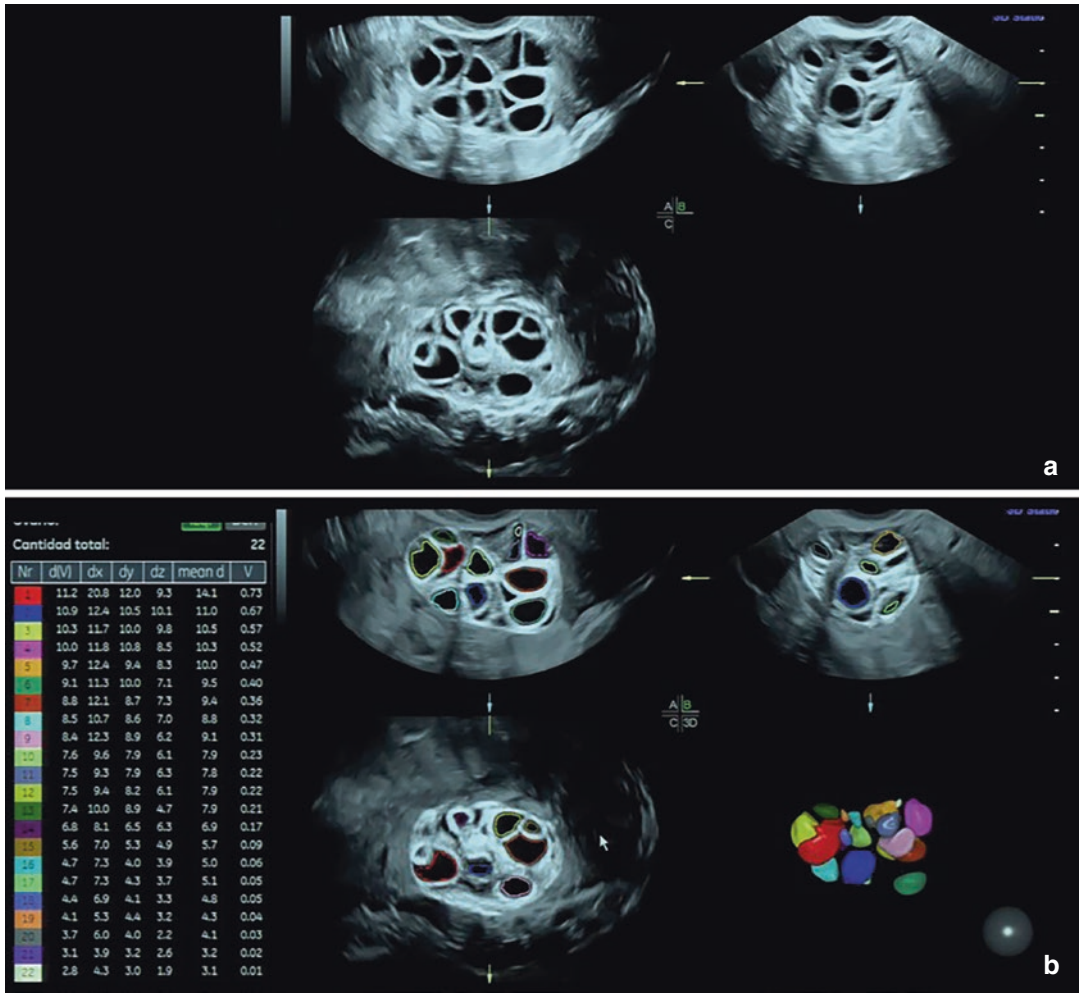

Fig. 17.7 (**a**) Multiplanar view of the ovary. (**b**) SonoAVC*follicle* calculation over the three orthogonal planes with a render presentation of the ovary on the right lower corner. On the left side of the screen, the report is shown; every follicle is color-coded

The Introduction of SonoAVC into Clinical Practice

Follicular Monitoring

As mentioned above, the reliability of SonoAVC in follicular monitoring has been widely validated during the past 10 years. Salama et al. and other authors [5, 6] concluded that follicular volume measured by SonoAVC correlated better with aspirated follicular fluid than VOCAL or 2D measurements did.

Many studies support the concept that SonoAVC calculations are comparable to man-

Left ovary

N. ° total: 28

Núm.	d(v) mm	dx mm	dy mm	dz mm	d med mm	v cm³
1	20.4	23.5	22.0	18.6	21.4	4.47
2	19.9	26.9	20.7	17.5	21.7	4.14
3	17.9	28.0	17.1	15.3	20.1	3.00
4	16.8	27.8	19.0	11.4	19.4	2.47
5	16.8	22.2	18.6	13.0	17.9	2.46
6	15.3	26.3	15.1	10.0	17.1	1.88
7	15.1	22.8	16.0	10.2	16.4	1.80
8	14.6	20.1	18.0	9.9	16.0	1.63
9	14.0	20.3	15.1	9.8	15.1	1.45
10	13.3	20.9	14.4	10.1	15.1	1.24
11	12.2	18.5	14.7	7.0	13.4	0.95
12	12.2	15.9	12.6	9.6	12.7	0.94
13	11.6	16.4	12.8	7.9	12.4	0.83
14	11.4	17.9	10.0	8.8	12.2	0.78
15	10.8	17.9	13.2	7.5	12.9	0.66
16	10.3	14.6	9.8	7.9	10.8	0.58
17	10.1	13.9	10.8	6.9	10.6	0.53
18	9.9	15.1	9.5	7.5	10.7	0.50
19	9.7	18.1	9.6	6.7	11.5	0.48
20	8.9	11.7	8.9	6.9	9.1	0.37
21	8.8	14.4	8.3	7.2	9.9	0.36
22	8.8	14.9	8.5	6.9	10.1	0.36
23	8.7	11.1	8.7	7.0	8.9	0.34
24	8.1	12.7	8.4	5.5	8.8	0.28
25	7.6	10.8	8.0	5.8	8.2	0.23
26	6.3	8.6	7.0	4.3	6.7	0.13
27	6.2	9.9	7.3	3.6	6.9	0.13
28	4.8	7.1	7.1	3.5	5.3	0.06

Right ovary

N. ° total: 28

Núm.	d(v) mm	dx mm	dy mm	dz mm	d med mm	v cm³
1	16.2	23.3	15.3	13.3	17.3	2.23
2	16.0	21.8	18.5	12.0	17.5	2.14
3	15.1	23.6	17.9	9.1	16.9	1.79
4	14.7	22.0	15.7	10.3	16.0	1.68
5	14.7	19.7	15.8	11.0	15.5	1.68
6	14.4	25.9	19.2	8.5	17.9	1.56
7	14.2	20.0	13.5	11.9	15.1	1.51
8	13.9	19.1	13.1	12.4	14.9	1.39
9	13.7	16.0	13.5	12.6	14.0	1.34
10	13.6	15.6	13.8	11.9	13.8	1.31
11	13.5	19.5	14.1	11.0	14.9	1.29
12	13.1	24.1	13.2	7.9	15.1	1.17
13	12.6	18.3	12.6	10.1	13.7	1.04
14	12.2	19.1	11.6	10.9	13.9	0.96
15	11.9	15.1	13.0	9.4	12.5	0.89
16	11.8	19.1	17.8	7.0	14.6	0.86
17	11.7	16.4	13.1	8.2	12.6	0.84
18	11.5	18.3	12.4	7.3	12.7	0.79
19	11.2	12.1	11.7	10.1	11.3	0.73
20	10.6	15.8	10.9	8.9	11.8	0.62
21	10.0	14.1	10.6	9.1	11.3	0.53
22	7.3	10.4	7.0	5.7	7.7	0.20
23	7.0	10.9	7.0	5.7	7.9	0.18
24	7.0	9.6	6.5	6.1	7.4	0.18
25	5.6	8.2	5.4	4.8	6.2	0.09
26	4.7	11.0	5.6	2.5	6.4	0.06
27	4.0	5.8	3.5	3.1	4.1	0.03
28	2.2	5.6	2.2	1.3	3.0	<0.01

Fig. 17.8 Example of a SonoAVC*follicle* report

ual measurements of 3 diameters from 3D volumes or to VOCAL measurements [7–9]. Another benefit of the automated method is the amount of time saved in the examination room [5–7, 10].

At this point it is known that SonoAVC is a quick, accurate, and reproducible software. But does it improve fertility treatment outcomes? This answer is still controversial. One of the reasons for this controversy may be that the success of treatment, in terms of pregnancy and live birth, not only depends on the number of mature oocytes retrieved but is a multifactorial process influenced by multiple factors such as maternal age, embryo quality, cause of infertility, male factor, etc.

In 2010 we published our first article on SonoAVC [10] suggesting a possible volume cutoff point of 0.6 cc that correlated better with oocyte maturity. When we analyzed data individually by patient trying to be more accurate, we obtained a cutoff value of 0.7 cc [11]. To extrapolate the follicular volume associated with mature oocytes, we selected 63 patients with good image quality on SonoAVC. On the day of hCG administration, 937 follicles were analyzed. At egg retrieval, a total of 673 oocytes were obtained, 505 of which were mature

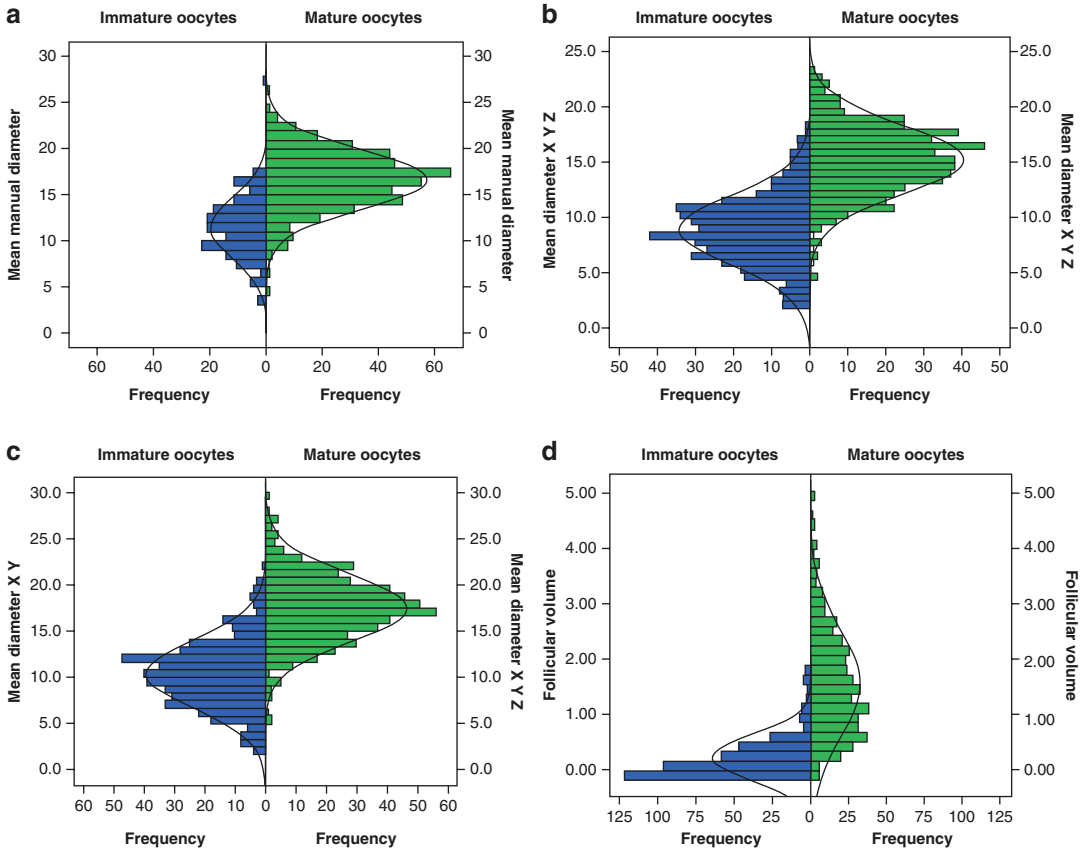

Fig. 17.9 Distribution of mature oocytes as a function of different follicular measurements: (**a**) average of manual diameters, (**b**) average of three automatic diameters, (**c**) average of two automatic diameters, and (**d**) follicular volume. In all of them, there is an overlap between the size of follicles containing immature and mature oocytes. This is the area of interest to estimate the minimum diameter or volume of follicles containing a mature oocyte

oocytes. The pairing of SonoAVC report measurements and the oocytes obtained at the pickup was done assigning the mature oocytes to larger follicles. Figure 17.9 illustrates the distribution of mature oocytes as a function of different follicular measurements: (a) average of manual diameters, (b) average of three automatic diameters, (c) average of two automatic diameters, and (d) follicular volume. In all of them, there is an overlap between the size of follicles containing immature and mature oocytes. This is the area of interest to estimate the minimum diameter or volume of follicles containing a mature oocyte. The Receiver Operating Characteristic (ROC) curve was used to determine which of these parameters is more accurate to indicate the cutoff value between immature and mature oocytes. According to ROC curve results, the parameter that generates the greater area under the curve is the most predictive one.

The representation of the ROC curve (Figure 17.10a) shows follicular volume in blue, the average of two automatic diameters in green, the average of 3 automatic diameters in yellow, and the average of manual diameters in red. According to the data, follicular volume is the variable with the greatest area under the curve, having the greatest predictive value to accurately establish the relationship between follicular size and the state of maturity of the oocyte inside the follicle. In our study a volume of 0.7 cc. was the minimum follicular volume to obtain a mature oocyte with the highest probability of true positive and with the lowest probability of a false

a

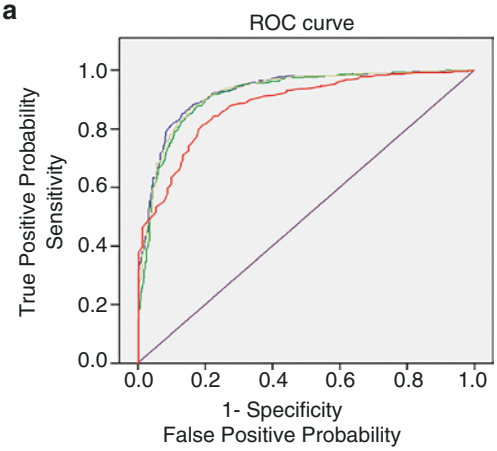

Variables resultado de contrasto	Area	Error tip. (a)	Sig. asintotica (b)	Intervalo de confianza asintotico al 95%	
				Limite superior	Limite inferior
volumen foliculos	.927	.009	.000	.910	.943
Media diametro X Y Z	.923	.009	.000	.906	.940
Media diametro X Y	.917	.009	.000	.899	.935
Media diametro manual	.880	.015	.000	.851	.908

b

Volume cc	True positive probability	False positive probability
0,615	0,887	0,181
0,625	0,885	0,171
0,635	0,883	0,164
0,645	0,875	0,162
0,655	0,875	0,157
0,665	0,873	0,155
0,675	0,865	0,153
0,685	0,863	0,146
0,695	0,863	0,144
0,705	0,855	0,141
0,715	0,851	0,132
0,725	0,840	0,127
0,735	0,832	0,125
0,745	0,830	0,120
0,755	0,826	0,118

Fig. 17.10 (**a**) ROC curve shows follicular volume in blue, the average of two diameters in green, the average of three diameters in yellow, and the average manual diameters in red. According to the data, follicular volume is the variable with the greatest area under the curve, having the greatest predictive value to accurately establish the relationship between follicular size and the state of maturity of the oocyte inside the follicle. (**b**) In our study, a volume of 0.7 cc. was the minimum follicular volume to obtain a mature oocyte with the highest probability of true positive and with the lowest probability of a false positive

positive (Figure 17.10b). Our study shows that a follicular volume of 0.7 cc has a greater than 85% probability of being associated with a mature egg. These results led us to suggest that the new parameter easily measured by SonoAVC – follicular volume – gives valuable information during ovarian stimulation that improves individualization of treatment for each patient. This is the reason why we routinely apply this information to make clinical decisions in our center.

There are patients that fulfill classical ultrasound parameters in terms of leading follicles mean diameters but also have a pool of follicles that may need one more day to achieve maturity. The SonoAVC report, together with other clinical parameters (estradiol and progesterone levels, days of stimulation, and information of previous cycles if applicable), is taken into account to decide the time of hCG administration. On the contrary, sometimes leading follicles' mean diameters are slightly under 18, but we are on the boundary of days of stimulation or progesterone levels; in these cases the data on volumes obtained by SonoAVC help to support our decisions. Below we describe some clinical cases from our center that illustrate these situations.

Case 1

- Clinical information: 39-year-old patient undergoing follicular stimulation for IVF. Preimplantation genetic testing – aneuploidy (PGT-A) needed
- AFC: 9 follicles on the right ovary and 5 follicles on the left

Figure 17.11 shows the follicular monitoring patient sheet. As you can observe, on day 11 we had two follicles over 18 mm with a progesterone level slightly above 1 ng/ml. If we look at the SonoAVC on the same day (Fig. 17.12), there

E2						874		1528	2259	2645	4039	
P										1.09	1.4	
DAY OF STIMULATION	2	3	4	5	6	7	8	9	10	11	12	13
	RIGHT ADNEXA					11 × 11 9 × 9 10 × 7 11 × 10 7 × 6 8 × 7 6 × 5 6 × 6 6 × 4		12 × 12 12 × 10 11 × 10 11 × 9 10 × 9 10 × 7 10 × 8 10 × 6 8 × 7 12 × 10 10 × 7 11 × 8 8 × 6	17 14 14 14 13 14 11 10 10 10 8 8 8 7 6 5	18 17 14 14 14 14 15 12 13	17 17 15 13 18 15 16	
	LEFT ADNEXA					13 × 8 7 × 6 10 × 9 7 × 5 4 × 6 13 × 9 3 × 3 6 × 7 6 × 6 6 × 5		15 × 13 17 × 11 10 × 7 11 × 8 10 × 9 7 × 4 8 × 6 11 × 9 10 × 6 13 × 12 10 × 8 10 × 8 10 × 8	15 15 14 10 13 10 11 10 10 7 6 3 2 6	17 16 19 14 12 13 14	21 21 20 17 16 14	

Fig. 17.11 Case 1. Manual follicular monitoring patient sheet. On day 11 there are two follicles equal or above 18 mm (red circles), and progesterone level is above 1 ng/ml. We decided to wait one more day based on the SonoAVC report (see Fig. 17.12) that indicated the possibility of obtaining four additional mature oocytes

were 16 follicles over 0.7 cc that might be mature at that time. Notice that there were four follicles between 0.6 and 0.7 that could reach maturity in one more day.

Since this patient needed PGT and blastocyst vitrification with subsequent cryotransfer, we decided to wait one more day and retrieve as many mature oocytes as possible. In this situation we could focus our attention on follicular growth without considering a possible worse implantation due to rising progesterone levels. Finally, 22 mature oocytes were retrieved, and 18 follicles were over 0.7 cc on the SonoAVC report (see Fig. 17.12).

Case 2

- Clinical information: 42-year-old patient undergoing follicular stimulation for IVF
- AFC: nine follicles on the right ovary and six follicles on the left

Figures 17.13 and 17.14 correspond to manual and automatic reports of follicular monitoring, respectively. In this case progesterone levels rose to 1.2 ng/ml on day 8 with two follicles over 18 mm. How were we supposed to proceed? Based on 2D measurements, we could have trig-

(SonoAVC)
Ovario derecho

Sono AVC day 11

N°	D(V)	Dx	Dy	Dz	Dm	Vol
1	13,9	19,0	13,0	11,5	14,5	1,41
2	13,4	19,1	16,4	9,4	15,0	1,26
3	13,2	22,0	13,9	8,7	14,9	1,22
4	13,0	27,3	11,3	8,2	15,6	1,14
5	12,9	18,2	13,9	9,4	13,8	1,12
6	12,8	21,4	17,0	8,5	15,6	1,11
7	12,7	19,0	11,5	9,9	13,5	1,08
8	12,1	17,8	10,9	9,5	12,7	0,93
9	12,0	18,3	12,0	9,1	13,1	0,90
10	11,8	15,7	11,6	9,9	12,4	0,86
11	11,6	19,0	14,2	6,3	13,2	0,82
12	11,3	14,6	12,3	8,2	11,7	0,75
13	10,6	13,5	11,6	8,6	11,2	0,66
14	10,0	13,3	9,8	8,7	10,6	0,53
15	9,1	21,7	10,1	6,2	12,7	0,39

Medicacion
Ovario izquierdo

N°	D(V)	Dx	Dy	Dz	Dm	Vol
1	16,3	23,5	15,7	13,1	17,4	2,25
2	14,1	21,0	13,2	11,4	15,2	1,46
3	13,9	20,7	14,2	9,7	14,9	1,39
4	12,5	15,7	13,7	9,9	13,1	1,03
5	10,7	14,9	10,2	8,6	11,2	0,66
6	10,7	15,5	11,7	8,3	11,8	0,64
7	10,4	14,0	11,5	7,3	10,9	0,59
8	10,3	19,0	8,2	7,6	11,6	0,58
9	10,0	14,9	10,0	7,5	10,8	0,53
10	9,1	14,8	8,9	6,5	10,1	0,39
11	9,0	17,9	7,6	6,7	10,7	0,38
12	8,7	12,5	9,6	5,9	9,3	0,34
13	8,5	14,0	8,8	5,7	9,5	0,32
14	7,9	12,5	8,1	5,4	8,7	0,26
15	7,6	11,8	6,7	6,4	8,3	0,23

(SonoAVC)
Ovario derecho

Sono AVC day 12

N°	D(V)	Dx	Dy	Dz	Dm	Vol
1	16,4	24,0	17,0	13,3	18,1	2,30
2	15,5	17,8	15,5	14,6	16,0	1,95
3	14,9	19,4	16,7	13,7	16,6	1,73
4	14,9	20,1	13,9	13,5	15,8	1,72
5	14,2	17,6	14,7	12,8	15,0	1,50
6	13,4	16,2	15,6	11,5	14,4	1,26
7	12,9	16,6	13,8	11,3	13,9	1,12
8	12,8	16,1	14,6	9,9	13,5	1,09
9	11,7	16,4	11,8	9,3	12,5	0,83
10	11,6	20,5	15,2	7,3	14,4	0,82
11	8,8	13,0	10,4	6,1	9,9	0,36
12						
13						
14						
15						

Medicacion
Ovario izquierdo

N°	D(V)	Dx	Dy	Dz	Dm	Vol
1	16,6	21,7	20,8	11,4	18,0	2,40
2	16,1	20,4	16,2	14,2	16,9	2,20
3	15,1	20,9	16,0	11,2	16,0	1,81
4	13,8	21,0	15,5	10,1	15,5	1,37
5	12,7	17,7	13,2	9,5	13,5	1,08
6	12,3	20,5	11,5	9,1	13,7	0,97
7	11,6	20,4	12,1	7,1	13,2	0,83
8	11,4	13,7	11,1	10,5	11,8	0,78
9	11,0	14,5	11,7	8,5	11,6	0,69
10	10,5	18,4	9,2	8,3	12,0	0,60
11	9,2	15,2	9,4	8,0	10,9	0,40
12	7,3	9,7	8,8	5,0	7,8	0,21
13	5,7	14,2	6,5	3,4	8,0	0,10
14	3,7	5,8	4,5	2,4	4,2	0,03
15	2,3	16,3	1,0	0,6	6,0	0,01

Fig. 17.12 Case 1. SonoAVC*follicle* report. On day 11 there were four follicles between 0.6 and 0.7 cc that could reach maturity in one more day. We decided to wait one additional day

E2							2374	2811				
P							1.2	1.4				
DAY OF STIMULATION	2	3	4	5	6	7	8	9	10	11	12	13
	RIGHT ADNEXA						15 13 11 13 19 14 11	17 17 11 13 21 15 13				
	LEFT ADNEXA						16 18 10 11 12	18 18 14 14 13 8				

Fig. 17.13 Case 2. Manual follicular monitoring patient sheet. On day 8 progesterone level started to rise (blue arrow), and two follicles were over 18 mm (red circles). There were two follicles of 15 and 16 mm. One day later we obtained one additional follicle over 18 mm (green circles). See Fig. 17.14 to analyze automated monitoring report information

(SonoAVC) Day 8 Medicacion

Ovario derecho

N°	D(V)	Dx	Dy	Dz	Dm	Vol
1	16,3	23,4	18,8	11,8	18,0	2,27
2	16,1	21,8	19,7	12,0	17,9	2,19
3	13,8	25,2	13,8	8,9	16,0	1,38
4	13,1	19,3	12,7	10,4	14,1	1,18
5	11,9	16,9	11,9	9,1	12,6	0,87
6	10,6	13,9	11,8	8,2	11,3	0,63
7	10,4	17,1	14,1	5,0	12,1	0,58
8	10,1	14,6	12,7	6,3	11,2	0,53
9	9,6	14,3	10,3	6,8	10,5	0,47
10	9,5	15,4	10,6	6,4	10,8	0,44
11	8,1	18,8	10,0	4,0	10,9	0,28
12	6,5	10,2	6,9	4,1	7,1	0,14
13	3,5	5,0	3,6	2,7	3,8	0,02
14						
15						

Ovario izquierdo

N°	D(V)	Dx	Dy	Dz	Dm	Vol
1	16,4	21,5	17,0	13,4	17,3	2,30
2	12,3	15,3	13,5	9,2	12,7	0,97
3	11,4	15,6	13,4	8,2	12,4	0,77
4	10,1	13,9	10,9	7,1	10,6	0,54
5	8,4	12,8	9,5	5,5	9,3	0,31
6	8,1	9,7	8,0	7,4	8,4	0,28
7	7,9	11,8	9,7	4,6	8,7	0,26
8	7,3	11,3	7,0	5,6	8,0	0,20
9	6,2	7,9	7,0	4,6	6,5	0,13
10	6,1	13,1	8,0	3,0	8,0	0,12
11	2,9	4,2	3,2	2,0	3,1	0,01
12						
13						
14						
15						

(SonoAVC) Day 9 Medicacion

Ovario derecho

N°	D(V)	Dx	Dy	Dz	Dm	Vol
1	18,0	29,5	17,5	13,1	20,0	3,05
2	17,5	27,1	21,4	11,1	19,9	2,81
3	14,4	22,4	15,8	10,5	16,2	1,57
4	13,0	17,4	14,3	10,5	14,1	1,14
5	12,5	17,4	15,1	8,1	13,5	1,02
6	12,1	19,5	11,5	9,5	13,5	0,94
7	10,9	14,1	10,3	9,5	11,3	0,67
8	10,8	17,2	11,0	7,3	11,8	0,66
9	10,3	15,2	13,6	5,9	11,6	0,58
10	10,2	26,7	15,6	7,1	16,5	0,55
11	8,8	15,9	7,6	6,4	10,0	0,36
12	7,0	11,2	6,7	4,8	7,6	0,18
13	2,2	10,0	2,8	0,5	4,4	0,01
14	2,1	6,4	3,1	0,7	3,4	0,01
15	2,1	5,4	3,7	0,6	3,2	

Ovario izquierdo

N°	D(V)	Dx	Dy	Dz	Dm	Vol
1	15,2	21,1	16,6	11,7	16,5	1,85
2	13,4	16,3	15,1	10,1	13,8	1,25
3	12,9	16,9	15,3	9,6	13,9	1,13
4	12,3	18,4	12,3	9,2	13,3	0,96
5	10,5	12,0	11,7	8,7	10,8	0,60
6	9,7	13,7	11,0	7,1	10,6	0,47
7	8,6	13,9	10,3	5,3	9,9	0,34
8	6,6	8,1	7,1	5,5	6,9	0,15
9	5,2	10,2	5,5	4,4	6,7	0,07
10	5,1	6,3	6,0	3,9	5,4	0,07
11						
12						
13						
14						
15						

Fig. 17.14 Case 2. SonoAVC*follicle* report: On day 8 there were eight follicles over 0.7 cc and 3 between 0.6 and 0.7 cc that could achieve maturity with one additional day of stimulation. On day 9 we triggered ovulation due to rising progesterone level

gered ovulation. The SonoAVC report (see Fig. 17.14) showed eight follicles with a probably mature egg, and with an additional day, 3 more follicles might have achieved the cutoff value for maturity (0.7 cc). With this information, we decided to wait an additional day. According to the day 9 SonoAVC report, there was still a pool of follicles with potential to mature, but if we had continued the stimulation, we would have been at risk to damage implantation due to high progesterone levels. So we triggered ovulation. Finally, seven mature follicles

were retrieved, and ten follicles were over 0.7 cc according to the SonoAVC report (see Fig. 17.14).

Case 3

- Clinical information: 40-year-old patient undergoing her second cycle of follicular stimulation for IVF
- AFC: nine follicles on the right ovary and eight follicles on the left

Figure 17.15 shows manual follicular monitoring where it can be observed that on day 12, there was only one follicle measuring 18 mm, three between 16 and 17 mm, and four of 13–14 mm, while progesterone was 1.3 ng/ml. Should one put implantation at risk with waiting an additional day? Are those follicles big enough to be mature? What happens with follicles of 13–14 mm?

In Fig. 17.16**,** we present the SonoAVC report. This shows that follicles under 0.7 cc were too small to achieve maturity in 1 day. Based on this information, we decided to administer hCG

E2										1622	2040	
P										0.8	1.3	
DAY OF STIMULATION	2	3	4	5	6	7	8	9	10	11	12	13
	RIGHT ADNEXA									12 12 11 10 13 10 9	17 13 13 11 11 11 7	
	LEFT ADNEXA									16 14 14 12 15 15	18 17 16 14 14 10 10 9	

Fig. 17.15 Case 3. Manual follicular monitoring patient sheet. After 12 days of stimulation, there was only one follicle of 18 mm (red circle), but progesterone level was slightly over 1 ng/ml. There were three follicles between 16 and 17 mm; should one put implantation at risk with waiting an additional day? See Fig. 17.16 to analyze automated monitoring report information

(SonoAVC)

Ovario derecho

N°	D(V)	Dx	Dy	Dz	Dm	Vol
1	17,7	35,0	18,0	14,2	22,4	2,90
2	14,7	27,8	12,9	10,7	17,1	1,66
3	13,9	27,0	12,8	10,1	16,6	1,40
4	12,8	17,7	13,4	10,6	13,9	1,11
5	12,2	40,2	9,9	6,5	18,9	0,96
6	11,6	25,8	10,2	8,9	15,0	0,81
7	11,3	13,6	12,4	9,1	11,7	0,76
8	7,6	10,5	8,1	5,6	8,1	0,23
9	7,0	26,4	6,5	2,9	11,9	0,18
10	7,0	38,0	7,3	1,6	15,6	0,18
11	4,8	8,4	6,4	2,5	5,8	0,06
12	4,6	11,1	7,2	2,1	6,8	0,05
13	4,2	5,0	4,7	3,5	4,4	0,04
14	3,9	7,8	5,4	2,0	5,1	0,03
15	2,6	3,5	2,9	1,8	2,7	0,01

Medicacion

Ovario izquierdo

N°	D(V)	Dx	Dy	Dz	Dm	Vol
1	16,1	21,4	17,5	12,3	17,0	2,18
2	16,0	20,7	16,7	12,8	16,7	2,14
3	15,1	20,1	15,2	12,3	15,9	1,81
4	14,8	19,2	15,5	12,3	15,7	1,71
5	14,5	21,7	15,5	11,0	16,0	1,59
6	11,9	16,3	13,0	8,6	12,7	0,88
7	11,6	17,8	12,1	8,0	12,6	0,82
8	11,0	21,6	11,1	7,8	13,5	0,70
9	7,2	9,0	7,6	5,5	7,4	0,19
10	3,9	14,4	3,6	2,1	6,7	0,03
11	3,4	5,1	3,7	2,4	3,7	0,02
12	3,2	4,8	3,6	1,9	3,4	0,02
13	2,4	3,7	2,4	1,7	2,6	0,01
14	2,4	11,9	2,0	0,8	4,9	0,01
15	2,1	4,7	2,6	1,5	3,0	0,01

Fig. 17.16 Case 3. SonoAVC*follicle* report shows that follicles under 0.7 cc are too small (<0.2 cc) to mature; therefore, there would be no benefit in prolonging treatment

obtaining ten mature oocytes, nine of which became good-quality embryos.

In conclusion, while our studies and clinical experience suggest that monitoring with SonoAVC may improve the results of ovarian stimulation in terms of mature oocytes, this is a subject of controversy. Raine-Fenning [16] performed a randomized study in 2010 comparing patients monitored manually with 2D US, and patients monitored with 3D US using SonoAVC. They used the classical criteria of three or more follicles of 18 mm or above to decide hCG administration, finding no significant differences between both groups in terms of number of mature oocytes collected, number of fertilized oocytes, and clinical pregnancy rates. These results demonstrated, as previous studies, that SonoAVC has at least the same results as 2D monitoring when looking at leading follicles' diameters, but there is no information about volumes.

In summary, SonoAVC has demonstrated its utility in follicular monitoring, being an accurate and reproducible method that saves time in the examination room. As every technique, it requires a learning curve even for trained 2D sonographers [17]. Further studies must be performed to clarify its role in improving fertility treatment outcomes.

Antral Follicle Count

Classical biochemical markers of ovarian reserve are basal FSH and estradiol and serum AMH concentrations, but there are several limitations.

While high baseline concentrations of FSH have been correlated with poor ovarian response and reduced pregnancy rates in IVF cycles [18], several studies have shown that basal FSH presents high intercycle variability and absence of a cutoff value with acceptable sensitivity and specificity [19, 20].

AMH has been proposed as a predictor of ovarian reserve and IVF success [21–23], but other studies suggest that AMH in itself is not predictive of pregnancy outcomes [24, 25].

AFC may well represent the actual functional ovarian reserve and highly correlates to the number of oocytes retrieved [26]. Antral follicle response to gonadotrophins is variable, so besides the total number of basal follicles, we have to consider their behavior during ovarian stimulation. AFC cannot predict the oocyte/embryo quality or the IVF outcome [27]. The impact of AFC in clinical outcomes was suggested in 2002 by Kupesic et al. [28]. They tried to elucidate whether AFC, ovarian volume, stromal area, and stromal blood flow were predictive of IVF out-

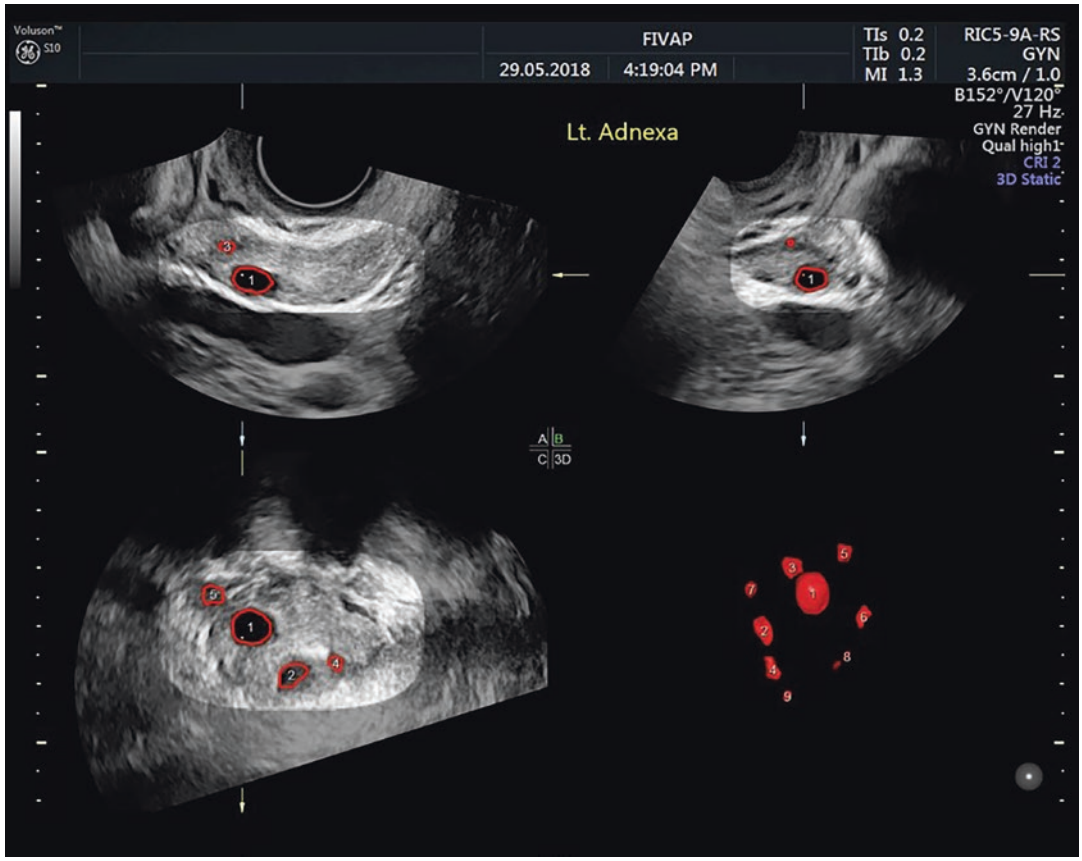

Fig. 17.17 SonoAVC*antral*

comes. All variables were measured by 3D ultrasound and power Doppler. Their results showed that AFC was the factor with the highest positive predictive value for favorable outcomes.

Despite the common use of AFC in clinical practice for years, normal ranges are still unclear although a nomogram of basal follicles in infertile women was published in 2010 [29]. Moreover, we have to keep in mind that it is not an objective parameter given that it is obtained by an operator-dependent technique.

In an attempt to standardize AFC, two consecutive papers, performed in 2009 and 2010 by Deb et al. [30, 31], studied the accuracy of AFC using SonoAVC. The first article compared SonoAVC pre- and post-processing work with 2D real-time and manual AFC in the 3D multiplanar view. The second paper recorded the total number and the mean diameter of antral follicles. The results showed that SonoAVC with post-processing work is a reliable method to measure the total amount of antral follicles giving information of its dimensions in a shorter time. The authors observed that there were a greater number of total follicles in the 2D count, as a result of including the same follicle twice. Obviously, the SonoAVC*follicle* software was designed to detect stimulated follicles and is not ideal for antral follicles. Given the importance of AFC, a dedicated software was recently developed called SonoAVC*antral* (GE Healthcare, Austria) (Fig. 17.17). This software improves the detection of small follicles; thus diminishing the post-processing work described in the literature [31]. Our experience with this software is limited. A research project is currently ongoing in our center to determine whether it is applicable to clinical practice and if it gives us a

more accurate idea of ovarian reserve prior to commencing stimulation.

There is another parameter that has been proposed to represent the potential of the ovarian follicles to be stimulated called Follicular Output Rate (FORT). FORT is the ratio between the total number of stimulated follicles (over 15 mm the day of hCG administration) and the number of antral follicles on day 2. Its importance lies in the concept that adequately responding antral follicles have more reproductive potential and are associated with an increased pregnancy rate after IVF/ICSI procedures [32]. FORT is considered a new objective parameter to estimate the ovarian response and a useful tool to study the regulation of follicle responsiveness [33, 34].

In conclusion, 3D ultrasound represents an important improvement in the study of the ovary, making all measurements more reliable and accurate. Automatic software are useful to save time, obtaining at least the same results as 2D methods with the advantage of volume data assisting to individualize clinical decisions both in routine patients and in difficult cases.

The utility of automatic volume calculation software to improve IVF treatment outcomes should not be measured only in terms of pregnancy rates or embryo quality, all variables that depend on multiple factors. The right question to be addressed in future studies may be if this softwares allows us to improve the effectiveness of stimulation and to achieve as many mature oocytes as possible without worsening implantation rates.

References

1. Bakker M, Mulder P, Birnie E, Bilardo CM. Intra-operator and inter-operator reliability of manual and semiautomated measurement of fetal nuchal translucency: a cross sectional study. Prenat Diagn. 2013;33:1264–71.
2. Chen PW, Chen M, Leung TY, Lau TK. Effect of image settings on nuchal translucency thickness measurement by a semi-automated system. Ultrasound Obstet Gynecol. 2012;39:169–74.
3. Żygadło A, Kaźnica-Wiatr M, Błaut-Jurkowska J, Knap K, Lenart-Migdalska A, Smaś-Suska M, et al. Evaluation of the clinical suitability of automated left ventricles fraction and volume measurements in 3-dimensional echocardiography compared to values obtained in magnetic resonance imaging (pilot study). Pol Merkur Lekarski. 2017;43:154–7.
4. Duin LK, Willekes C, Vossen M, Offermans J, Nijhuis JG. Reproducibility of fetal renal pelvis volume assessed by three-dimensional ultrasonography with two different measurement techniques. J Clin Ultrasound. 2013;41:230–4.
5. Raine-Fenning N, Jayaprakasan K, Clewes J, Joergner I, Bonaki SD, Chamberlain S, et al. So noAVC: a novel method of automatic volume calculation. Ultrasound in Obstet & Gynecol. 2008;31:691–6.
6. Salama S, Arbo E, Lamazou F, Levailllant JM, Frydman R, Fanchin R. Reproducibility and reliability of automated volumetric measurement of single preovulatory follicles using SonoAVC. Fertil Steril. 2010;93:2069–73.
7. Deutch T, Joergner I, Matson D, Oehninger S, Bocca S, Hoenigmann D, et al. Automated assessment of ovarian follicles using a novel three-dimensional ultrasound software. Fertil Steril. 2009;92:1562–8.
8. Lamazou F, Arbo E, Salama S, Grynberg M, Frydman R, Fanchin R. Reliability of automated volumetric measurement of multiple growing follicles in controlled ovarian hyperstimulation. Fertil Steril. 2010;94:2172–6.
9. Ata B, Seyhan A, Reinblatt SL, Shalom-Paz E, Krishnamurthy S, Tan SL. Comparison of automated and manual follicle monitoring in an unrestricted population of 100 women undergoing controlled ovarian stimulation for IVF. Hum Reprod. 2010;26:127–33.
10. Rodríguez-Fuentes A, Hernández J, García-Guzman R, Chinea E, Iaconianni L, Palumbo A. Prospective evaluation of automated follicle monitoring in 58 in vitro fertilization cycles: follicular volume as a new indicator of oocyte maturity. Fertil Steril Jan; (93): 616–620.
11. Hernández J, Rodríguez-Fuentes A, Puopolo M, Palumbo A. Follicular volume predicts oocyte maturity: a prospective cohort study using three-dimensional ultrasound and SonoAVC. Reprod Sci. 2016;23:1639–43.
12. Wittmaack FM, Kreger DO, Blasco L, Tureck RW, Mastroianni L, Lessey BA. Effect of follicular size on oocyte retrieval, fertilization, cleavage, and embryo quality in in vitro fertilization cycles: a 6-year data collection. Fertil Steril. 1994;6:1205–10.
13. Raine-Fenning NJ, Campbell BK, Clewes JS, Johnson IR. The interobserver reliability of ovarian volume measurement is improved with three-dimensional ultrasound, but dependent upon technique. Ultrasound Med Biol. 2003;29:1685–90.
14. Luis T. Mercé, Gomez B, Engels V, Bau S, Bajo JM. Intraobserver and interobserver reproducibility of ovarian volume, antral follicle count, and vascularity indices obtained with transvaginal 3-dimensional ultrasonography, power doppler angiography, and the virtual organ computer-aided analysis imaging program. J Ultrasound Med. 2005;24:1279–87.
15. Shmorgun D, Hughes E, Mohide P, Roberts R. Prospective cohort study of three-versus two dimensional ultrasound for prediction of oocyte maturity. Fertil Steril. 2010;93:1333–7.

16. Raine-Fenning N, Deb S, Jayaprakasan K, Clewes J, Hopkisson J, Campbell B. Timing of oocyte maturation and egg collection during controlled ovarian stimulation: a randomized controlled trial evaluating manual and automated measurements of follicle diameter. Fertil Steril. 2010;94:184–8.
17. Rodriguez A, Guillén JJ, López MJ, Vassena R, Coll O, Vernaev V. Learning curves in 3-dimensional sonographic follicle monitoring during controlled ovarian stimulation. J Ultrasound Med. 2014;33:649–55.
18. Jurema M, Bracero N, Garcia J. Fine tuning cycle day 3 hormonal assessment of ovarian reserve improves in vitro fertilization outcome in gonadotropin-releasing hormone antagonist cycles. Fertil Steril. 2003;80:1156–61.
19. Bancsi LF, Broekmans FJ, Mol B, Habbema JD, Velde ER. Performance of basal follicle-stimulating hormone in the prediction of poor ovarian response and failure to become pregnant after in vitro fertilization: a meta-analysis. Fertil Steril. 2003;79:1091–100.
20. Bancsi LF, Broekmans FJ, Looman CW, Habbema JD, Velde ER. Predicting poor ovarian response in IVF: use of repeat basal FSH measurement. JRM. 2004;49:187–94.
21. Barad DH, Weghofer A, Gleicher N. Comparing anti-Mullerian hormone (AMH) and follicle-stimulating hormone (FSH) as predictors of ovarian function. Fertil Steril April. 2009;91:1553–5.
22. Lekamge DN. Anti-Müllerian hormone as a predictor of IVF outcome. RBM. 2007;14:602–10.
23. Wunder DM, Guibourdenche J, Birkhauser MH, Bersinger NA. Anti-Mullerian hormone and inhibin B as predictors of pregnancy after treatment by in vitro fertilization/ intracytoplasmic sperm injection. Fertil Steril. 2008;90:2203–10.
24. Lee TH, Liu CH, Huang CC, Wu YL, Shih YT, Ho HN, et al. Serum anti-müllerian hormone and estradiol levels as predictors of ovarian hyperstimulation syndrome in assisted reproduction technology cycles. Hum Reprod. 2008;23(1):160–7.
25. Smeenk J, Sweep F, Zielhuis G, Kremer J, Thomas C, Braat D. Antimüllerian hormone predicts ovarian responsiveness, but not embryo quality or pregnancy, after in vitro fertilization or intracytoplasmic sperm injection. Fertil Steril. 2007;87(1):223–6.
26. Broer S, Mol B, Hendriks D, Broekmans F. The role of antimullerian hormone in prediction of outcome after IVF: comparison with the antral follicle count. Fertil Steril. 2009;91(3):705–14.
27. Barreto Melo M, Garrido N, Alvarez C, Bellver J, Meseguer M, Pellicer A, et al. Antral follicle count (AFC) can be used in the prediction of ovarian response but cannot predict the oocyte/embryo quality or the in vitro fertilization outcome in an egg donation program. Fertil Steril. 2009;91:148–56.
28. Kupesic S, Kurjak A. Predictors of IVF outcome by three-dimensional ultrasound. Hum Reprod. 2002;17:950–5.
29. Almog B, Shehata F, Shalom-Paz E, Tan SL, Tulandi T. Age-related nomogram for antral follicle count: McGill reference guide. Fertil Steril. 2011;95:663–6.
30. Deb S, Jayaprakasan K, Campbell BK, Clewes JS, et al. Intraobserver and interobserver reliability of automated antral follicle counts made using three-dimensional ultrasound and SonoAVC. Ultrasound Obstet Gynecol. 2009;33:477–83.
31. Deb S, Campbell BK, Clewes JS, Raine-Fenning NJ. Quantitative analysis of antral follicle number and size: a comparison of two-dimensional and automated three-dimensional ultrasound techniques. Ultrasound Obstet Gynecol. 2010;35:354–60.
32. Zhang N, Hao C, Zhuang L, Liu X, Gu HF, Liu S, et al. Prediction of IVF/ICSI outcome based on the follicular output rate. RBM. 2013;27:147–53.
33. Rehman R, Mustafa R, Baig M, Arif S, Hashmi MF. Use of follicular output rate to predict Intracytoplasmic sperm injection outcome. Int J Fertil Steril. 2016;10(2):169–74.
34. Hassan A, Kotb M, AwadAllah A, Wahba A, Shehata N. Follicular output rate can predict clinical pregnancy in women with unexplained infertility undergoing IVF/ICSI: a prospective cohort study. RBM. 2017;34:598–604.

Ultrasound-Guided Surgical Procedures

18

Audrey M. Marsidi, Donna R. Session, and Jennifer Fay Kawwass

Introduction

Ultrasonography plays an integral role not only in diagnostic testing but also in guiding hysteroscopic procedures, difficult intrauterine device insertion and removal, and ART procedures such as oocyte retrieval and embryo transfer.

The use of ultrasonography at the time of intrauterine procedures provides visualization of the intrauterine contents as well as the myometrium and may decrease procedure-associated risks, particularly uterine perforation. For hysteroscopic procedures such as uterine septum, myoma, or synechiae resection, operative ultrasonographic guidance provides an alternative to laparoscopy and, as a result, shortens overall operating time, decreases cost, and eliminates the risk of laparoscopy. In addition, performing intrauterine procedures under ultrasonographic guidance may increase the likelihood of completing the procedure in a single operation.

A. M. Marsidi
Emory University Hospital Midtown, Department of Gynecology and Obstetrics, Atlanta, GA, USA

D. R. Session
Vanderbilt University Medical Center, Department of Obstetrics and Gynecology, Franklin, TN, USA

J. F. Kawwass (✉)
Emory Reproductive Center, Atlanta, GA, USA

Emory University, Department of Reproductive Endocrinology and Infertility, Atlanta, GA, USA
e-mail: jennifer.kawwass@emory.edu

Assisted reproductive technology (ART) procedures such as oocyte retrieval and embryo transfer require ultrasonographic guidance for improved outcomes. In addition, ultrasound guidance is used for aspiration of ascites resulting from ovarian hyperstimulation syndrome, a complication of ART.

Ultrasound guidance has been described in IUD placement, cervical stenosis, tubal cannulation, and suction curettage for pregnancy loss [1, 2].

Ultrasound Guidance at Time of Uterine Surgery: Uterine Septum Resection, Myoma Excision, Synechiae Lysis, Intrauterine Foreign Bodies, and Hematometra

Before starting the procedure, the bladder is completely drained so that the amount of water inserted into the bladder can be accurately quantified and overdistention can be avoided. Next, the urethral catheter is flushed with water and the syringe filled with water and cleared of air. The bladder is then retrograde-filled with 200–400 cc of warm water. A three-contrast technique has been described by Lin et al. in which saline is injected into the abdomen in addition to the bladder [3]. Shalev and Zuckerman claimed that there is little advantage to the three-contrast method, because a clear view of the uterus and uterine cavity is obtained with the distending media used

L. A. Stadtmauer, I. Tur-Kaspa (eds.), *Ultrasound Imaging in Reproductive Medicine*,
https://doi.org/10.1007/978-3-030-16699-1_18

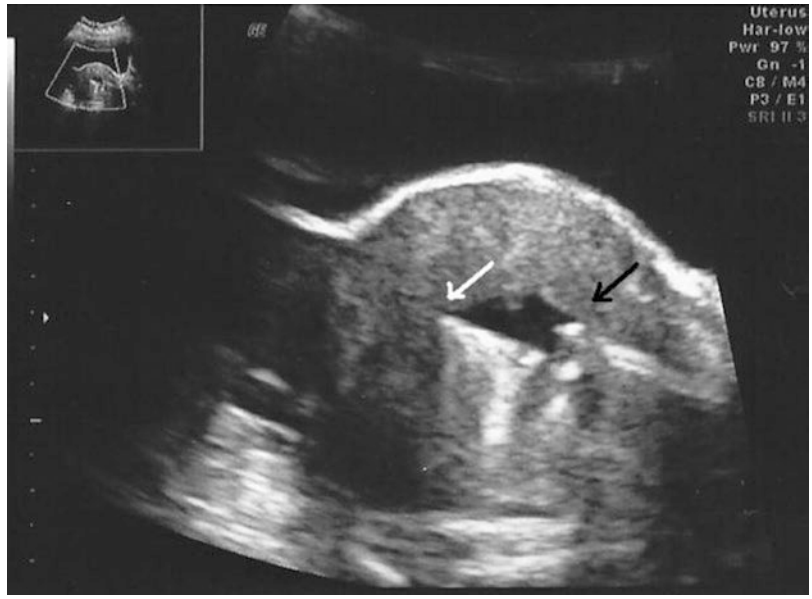

Fig. 18.1 Ultrasound guidance at time of hysteroscopy (*black arrow* pointing at hysteroscope, *white arrow* pointing at hysteroscopic scissors)

in hysteroscopy [4]. Moreover, the benefits of the three-contrast technique may not outweigh the potential risks. An abdominal ultrasound covered with a sterile sheath can be used to visualize boundaries of the uterine cavity, the instrument's location within the cavity, and the extent of resection/depth of remaining myometrium (Fig. 18.1). The ultrasonographic operator may provide a narrative of position of the instruments and depth of the uterine wall at the operative site. Alternatively, the surgeon may view the ultrasonographic and hysteroscopic images simultaneously.

Uterine Septum

The incidence of congenital uterine anomalies is estimated to be 3–4% of reproductive age women and 5–10% in women with recurrent miscarriages [5, 6]. The anomalies may be asymptomatic or result in infertility, recurrent pregnancy loss, intrauterine growth retardation, or endometriosis when obstruction is present. Uterine septum, which results from incomplete resorption of the medial septum between two normally fused hemi-uteri, is not only the most common uterine anomaly but also is the malformation most highly associated with poor pregnancy outcomes [5, 7]. Case series report a spontaneous miscarriage rate ranging from 65% to 88% in the presence of a uterine septum [8, 9]. It is hypothesized that implantation on a poorly vascularized septum may contribute to this increased risk of miscarriage. After resection, spontaneous miscarriage rates return to the baseline rate of approximately 15%; and 80% of pregnancies post-resection result in term delivery [7, 8].

The high degree of accuracy of magnetic resonance imaging (MRI) and three-dimensional (3D) ultrasound in the diagnosis of congenital anomalies has decreased the previous need for diagnostic laparoscopy at the time of surgery to aid in characterization of the type of anomaly. Three-dimensional ultrasound has been shown to have 98% specificity and 100% sensitivity of accurate septum diagnosis [10]. Although diagnostic hysteroscopy/laparoscopy has long been considered the gold standard, MRI and 3D ultrasound are accepted alternatives with lower risk and cost.

Upon diagnosis, a uterine septum is treated by noninvasive outpatient hysteroscopic surgical resection which results in significant improvement in subsequent pregnancy outcomes [5, 7, 11]. Ultrasonographic guidance without the aid of hysteroscopy has also been described; 11 patients had postprocedural evaluation of the

uterine cavity, 2 patients had a residual septum, and 1 patient had extensive synechiae [12]. Although the number of cases is limited, the results with ultrasonographically guided hysteroscopy appear better than metroplasty without the use of hysteroscopy. Hysteroscopic metroplasty can be successfully performed using microscissors, laser, or electrocautery with comparable improvements in future pregnancy outcomes [7]. The procedure is complete once both ostia are visible simultaneously and when less than 1 cm of myometrium remains [13]. Discontinuing the procedure once a fundal thickness of 8–10 mm is obtained was associated with a normal intrauterine contour on hysterosalpingography [14]. Postoperative hysterosalpingography revealed incomplete resection of the septum when thicknesses of 11–16 mm were used [14].

A prospective, open study including 81 patients undergoing ultrasound-guided operative hysteroscopy for uterine septum or submucosal myoma compared outcomes to that of a historical control group of 45 patients who underwent the same procedure under laparoscopic guidance [15]. All patients in the ultrasound group were successfully treated with a single surgery, and none required conversion to laparoscopy. In contrast, four of the control group patients required additional surgery to resect residual fibroid or septum. Ultrasound guidance allowed the surgeon to accurately determine depth of remaining septum and the outer limit of uterine fundus.

Submucosal Fibroids

Uterine fibroids, the most common benign tumors in females, have a prevalence of 8–28% in the general population and are often asymptomatic [16–18]. Symptomatic fibroids can cause pelvic pain, menorrhagia, abdominal fullness, and occasional urinary and bowel symptoms. Fibroid size and location affect the type and degree of patient symptoms and may also have reproductive consequences including pregnancy loss and infertility.

As with uterine septa, resection of submucosal fibroids benefits from ultrasound guidance at time of hysteroscopy. The extent of uterine fibroids' effect on pregnancy rates and outcomes remains controversial. However, submucosal myomas that significantly distort or encroach on the uterine cavity may lower implantation and pregnancy rates in infertile women undergoing IVF [19]. Several recent studies evaluated the effect of fibroids on in vitro fertilization cycles; the balance of data suggests that pregnancy outcomes and implantation rates are adversely affected by submucosal myomas that enter the uterine cavity but not by subserosal or intramural fibroids that are less than 5–7 cm in size [20–23]. Resection of submucosal fibroids clearly within the uterine cavity is likely warranted in patients with dysfunctional uterine bleeding, infertility, or pregnancy loss who desire to optimize future fertility. A hysteroscopic approach is reasonable if the majority of the fibroid is within the cavity or if subtotal hysteroscopic myomectomy is deemed preferable to abdominal myomectomy. Hysteroscopic resection may be performed using a hysteroscopic morcellator or resectoscope. A resectoscope allows for the use of electrocautery at time of resection but, as a result, requires electrolyte-poor distending media such as mannitol, sorbitol, or glycine. Morcellating devices resect using a rotating blade rather than electrocautery and allow for use of isotonic distending media such as normal saline or lactated ringers which have lower risk for fluid overload and subsequent electrolyte imbalance. The avoidance of electrocautery also has a theoretical benefit of avoiding thermal damage to the myometrium and decreasing chance of future uterine rupture at time of pregnancy. Both methods incur a risk of procedure abortion secondary to reaching maximum fluid deficit or bleeding. Prior to starting the hysteroscopy, injection of vasopressin into the cervical stroma can be used to help decrease myoma bleeding. If bleeding is encountered intraoperatively, conversion from morcellator to electrocautery or use of uterine balloon for tamponade and uterine compression can be used to help achieve hemostasis. Lin et al. resected six submucosal myomas under ultrasonographic

guidance [24]. All cases were completed in less than 1 hour. There were no traumatic complications. None of the patients required laparotomy or blood transfusion. Postoperative electrolyte values revealed no significant change from preoperative values. Menorrhagia and metrorrhagia improved. Postoperative hysteroscopy revealed no intrauterine adhesions, and the endometrium at the operative site appeared normal. Wortman and Dagget used ultrasonographic control to remove large submucosal myomas [25]. These authors claimed that ultrasonography may help prevent perforation and obviate laparoscopy [25].

Synechiae

Asherman's syndrome, scarring of the endometrial cavity that may have resulted from preexisting infection or uterine instrumentation, may be manifested as hypomenorrhea, amenorrhea, infertility, or recurrent pregnancy loss. Hysteroscopic lysis of adhesions remains the treatment of choice. In severe cases of intrauterine adhesions, it is difficult to determine, without ultrasonography, which part of the cavity is being observed during hysteroscopy. Shalev et al. performed hysteroscopic lysis of intrauterine adhesions using ultrasound (rather than laparoscopic) guidance in 106 women with varying degrees of Asherman's syndrome. Adhesiolysis was successful in all cases; there were no complications [26]. In cases of moderate-to-severe intrauterine synechiae, ultrasonographic guidance permits the accurate localization of the instruments within the uterus and of myometrial depth. This may result in a greater chance of success in a single surgical procedure with a lower perforation rate. A recent retrospective cohort study including 159 procedures affirms a lower uterine perforation rate for ultrasound-guided (1.9%) compared to laparoscopic (8.7%) or blind (5.3%) hysteroscopic uterine septum resection [17]. Cost was also significantly less for the ultrasound rather than laparoscopic-guided resections [17].

After significant adhesiolysis, the placement of an intrauterine balloon stent to provide mechanical separation and administration of estrogen to promote endometrial proliferation have been shown to decrease postoperative synechiae formation [20, 27–29]. Initial extent of adhesions has been shown to correlate with adhesion reformation [30]. Both uterine balloons and intrauterine devices have been evaluated for postoperative Asherman's management. A 1993 study revealed significantly improved outcomes (resumption of menses, increased conception, and decreased need for reoperation) in patients for whom a uterine balloon was placed for 10 days as compared to those who received a nonhormonal copper intrauterine device for 3 months [28]. More recently, investigators are comparing the effectiveness of newer synthetic barrier methods such as Seprafilm and hyaluronic acid gel compounds [31, 32]. Preliminary results are promising; however, larger randomized studies have not yet been performed. Of note, antibiotic prophylaxis is recommended for as long as a foreign intrauterine device remains in place.

The exact regimen and dose of oral estrogen remains unclear. Accepted supplementation ranges from 4 to 6 mg daily (often dosed bi-daily) for 4–10 weeks duration.

Intrauterine Foreign Bodies

The use of ultrasonographic guidance for the retrieval of an intrauterine foreign body has been described. Retained bony fragments after a therapeutic abortion were removed successfully with the use of an ultrasonographically guided resectoscope [3, 33]. Ultrasonography allowed visualization of bone embedded in the myometrium.

Hematometra

As in the case of intrauterine foreign body, ultrasonography can direct the surgeon to the pathologic site within the uterus when this is not evident by direct hysteroscopic vision, as in hematometra. Kohlenberg et al. described five cases of hematometra following endometrial ablation [34]. Ultrasonography was used to guide the hysteroscope to the cornua where these col-

lections were located. Similarly, Goudas and Session described a case of successful treatment of cervical stenosis and hematometra with ultrasonographically guided hysteroscopy [35].

Limitations of the Technique

Replacing laparoscopy with ultrasound at time of hysteroscopic resection of a uterine septum, myoma, or adhesive disease usually decreases potential risk while shortening operative time and maintaining optimal surgical results [26, 36]. However, in a limited number of patients in whom abdominal pathology is suspected, laparoscopy concurrent with hysteroscopy may reveal an intra-abdominal abnormality that can be treated laparoscopically. Additionally, severe retroversion and cul-de-sac adhesions may hinder clear transabdominal ultrasound visualization. Furthermore, diathermy heat may alter tissue or distending fluid by creating microbubbles or produce electrical interference that appears as a "snowstorm" that impedes ultrasonographic imaging [34]. Nonetheless, it is still usually possible to measure myometrial depth, although hysteroscopic localization within the area may be difficult. Additionally, the majority of hysteroscopic procedures can now be performed without cautery using new hysteroscopic morcellating devices.

Summary

For uterine septa, submucosal fibroids, and uterine synechiae, ultrasound guidance helps obtain complete resection while minimizing risk of uterine perforation [25].

Ovarian Cyst and Hydrosalpinx Aspiration

Both ovarian cysts and tubal fluid can be easily aspirated while using transvaginal ultrasound guidance. A needle guide fits on the superior aspect of a standard transvaginal ultrasound allowing the sonographer/surgeon to advance the needle in a predictable, visible plane. Ultrasound color Doppler can be used to confirm an avascular path from the vagina to the ovary or tube.

Ovarian Cyst Aspiration

Large, simple ovarian cysts can form spontaneously, after previous stimulation cycles or as the result of a flare response from GnRH agonist treatment and have potential to cause pain or interfere with subsequent stimulation. Usually, cysts rupture or are reabsorbed within 6 months without need for intervention; a meta-analysis including eight randomized controlled trials found no benefit to oral contraceptive use to hasten cyst resolution [37]. However, if a cyst is causing significant pain, persists for several months, and grows large enough to pose a significant bleeding or torsion risk, or if time constraints exist for a subsequent cycle, a role remains for cyst aspiration. Cysts may be either functional (hormone-secreting) or nonfunctional. Small (<15–20 mm), nonfunctional (<50 pg/mL estradiol) cysts likely have little effect on fertility treatment; however, functional cysts can deleteriously affect number and quality of retrieved oocytes, fertilization rates, implantation rates, miscarriage rates, and cycle continuation rates [38, 39].

Small, nonfunctional cysts usually do not require intervention. Larger, functional cysts may be managed conservatively either by prolonging downregulation with GnRH agonist prior to stimulation start or by surgical aspiration. In this situation, no clear benefit to surgical aspiration exists [40]. In fact, even for larger (>15 mm), estrogen-producing (>50 pg/mL estradiol) cysts, the majority of evidence suggests no improvement in number of retrieved oocytes, embryo quality, fertilization rate, and implantation and pregnancy rates between women whose cysts were aspirated and those whose cysts were not [40–43]. The deleterious impact of functional cysts on in vitro fertilization cycles persists and, unfortunately, has not been shown to be blunted by cyst aspiration.

Occasionally, however, time pressure, inability to prolong stimulation start, or patient discomfort drive the need for surgical cyst aspiration. Aspirated fluid may be collected and sent to pathology for further cytologic evaluation. A 1992 study including 1544 oocyte retrievals sent aspirated follicular fluid for cytologic evaluation and found no cases of malignancy [44].

Hydrosalpinx Aspiration

Evidence suggests that the presence of a hydrosalpinx may have a deleterious effect on implantation and pregnancy rates in IVF. This may result from a direct embryo toxic effect of the hydrosalpinx fluid on inhibition of implantation, a reduction of endometrial receptivity, or from a more direct mechanical flushing effect. Implantation rates have been improved by aspiration of hydrosalpinges during the IVF cycle following oocyte aspiration, by salpingectomy or tubal occlusion prior to the IVF cycle, and by extended antibiotic treatment during the IVF cycle [45–48]. Diagnosed hydrosalpinx is usually treated (excised or occluded) prior to initiation of IVF. However, the size of a hydrosalpinges varies during the menstrual cycle [49]. As a result, patients may not have a visible hydrosalpinx prior to stimulation but may accumulate fluid during an IVF cycle. In such situations, mixed evidence exists regarding benefit of aspiration at time of retrieval. A controlled retrospective analysis of 151 women compared implantation rates in patients with hydrosalpinx at time of retrieval and found no benefit to drainage at time of retrieval but confirmed an overall reduction in implantation rates in the presence of hydrosalpinx compared to patients without tubal disease [50]. However, a smaller retrospective study (n = 34) reported significantly improved implantation rates (14% versus 1% p = 0.015) with transvaginal aspiration of the hydrosalpinges at time of oocyte retrieval [46]. Possible concerns with this approach include the risk of pelvic infection caused by aspiration of the hydrosalpinx and rapid reaccumulation of hydrosalpinx fluid. A randomized controlled trial of 161 patients with visible hydrosalpinx at the time of oocyte retrieval reported similar implantation and pregnancy rates among patients undergoing salpingectomy versus aspiration (40% versus 27.5% p = 0.132). However, among the group receiving aspiration, 34% of patients experienced rapid reaccumulation of hydrosalpinx fluid within 2 weeks of embryo transfer. Compared to those undergoing salpingectomy, the implantation and clinical pregnancy rates were significantly lower in patients with reaccumulation of fluid (42.67% versus 19.23% p = 0.036) [51]. Nonetheless, aspiration of tubal fluid rather than cryopreservation of all embryos may be useful when hydrosalpinges become evident during an IVF cycle. It is important to note, however, that when a hydrosalpinx is present prior to initiation of an IVF cycle, tubal occlusion is generally recommended. Furthermore, a 2017 systematic review and meta-analysis by Xu et al. concluded that when compared to hysteroscopic tubal occlusion, laparoscopic salpingectomy and laparoscopic proximal tubal occlusion resulted in significantly higher clinical pregnancy rates (34.1% versus 44.0%, RR 0.71; 95% CI 0.51–0.98) [52].

Oocyte Retrieval

Although initially performed laparoscopically, oocyte retrieval is now routinely performed using ultrasound guidance due to decreased operative risk and a higher rate of oocytes retrieved. Ultrasound-guided aspiration was first described by Lenz in 1981 [53]. Aspiration techniques have included transabdominal, transvesical, and transurethral approaches using sterile-draped abdominal ultrasound and either a guided or freehand needle. The procedure may be performed using mineral oil rather than potentially oocyte-toxic ultrasound gel in a manner similar to amniocentesis [54]. Transvaginal aspiration, first described by Gleicher in 1983, has replaced other routes of aspiration, except when the ovary is not accessible vaginally such as in some cases of Mullerian anomalies [55, 56]. As with all surgical intervention, oocyte retrieval incurs a risk of infection, bleeding, and damage to nearby structures. Such

risks are <1% and are minimized by adequate visualization and proper surgical technique [57]. For transvaginal aspiration, the patient is placed in the dorsal lithotomy position. After sedation is obtained by either a local, regional, or intravenous route, the vagina is prepped with saline lavage or antiseptic to decrease bacterial counts. Prophylactic antibiotics may be given to reduce the occurrence of possible pelvic inflammatory disease particularly in patients with endometriosis [58]; however, peri-retrieval antibiotics have not been shown to affect clinical pregnancy rates [59]. As with cyst and hydrosalpinx aspiration, a transvaginal ultrasound probe is placed in a sterile sheath and fitted with a needle guide through which a single- or double-lumen 16–17 gauge needle is passed to sharply puncture ovarian follicles and aspirate (at 100–200 mmHg) follicular fluid and oocytes. The tip of the needle is etched to increase echogenicity.

Puncture site is determined by visual observation and use of color Doppler for avoidance of vaginal and pelvic blood vessels. The planned course of the needle can be clearly visualized with the biopsy line setting on the ultrasound machine, and the probe rotated in such a manner as to avoid blood vessels (Fig. 18.2). The absence of vasculature in the needle's course can be confirmed with color Doppler. Additionally, if an ovary is malpositioned, its location can be improved with abdominal pressure or by rotation of the surgical table.

The decision to use a single- or double-lumen needle depends on the physicians desire to flush aspirated follicles with culture media to attempt to increase oocyte yield. Flushing requires a double-lumen needle, while direct aspiration can be performed using a single-lumen needle. Proponents of flushing contend that it increases oocyte yield and may be clinically significant in poor responders for whom even one additional oocyte may improve pregnancy potential. Waterstone and Parsons found a 20% increase in oocyte yield in the first 3 flushes after direct aspiration in 50 patients for whom oocyte yield was quantified after direct aspiration, after 3 flushes, and after 6 flushes [59–61]. However, a Cochrane review including 4 randomized trials with number of study participants ranging from 4 to 100 found no significant difference in oocyte yield or clinical pregnancy rates for flushed compared to directly aspirated follicles [61]. Flushing required statistically significant increased operative time and analgesia use [61].

After retrieval completion, assessment of hemostasis is essential. A survey of the pelvis with Doppler ultrasound before and after the retrieval should be performed to look for fluid pockets and for active sources of bleeding. If observed, focused bimanual pressure usually suf-

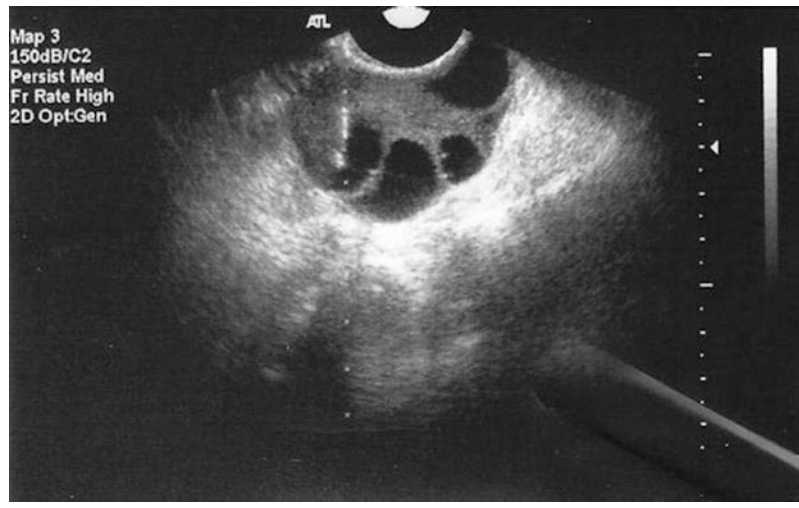

Fig. 18.2 Transvaginal oocyte retrieval (*dotted line* denotes "needle biopsy line")

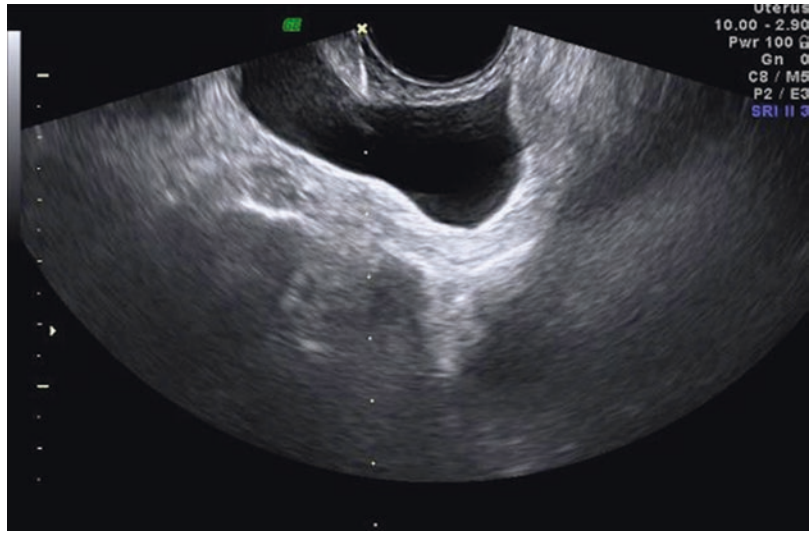

Fig. 18.3 Transvaginal aspiration of ascitic fluid in patient with ovarian hyperstimulation syndrome. Needle visualized along *dotted biopsy line*

fices to tamponade active bleeding. After abdominal hemostasis has been confirmed, a speculum should be placed in the vagina to inspect puncture sites. Bleeding vaginal sites also usually stop either with direct pressure, vaginal packing, application of an atraumatic clamp for focal direct pressure, or rarely with placement of a nonreactive vaginal suture.

Ovarian hyperstimulation is a complication of assisted reproductive technology (ART). Ascites results from increased vascular permeability. Paracentesis may decrease pain, shortness of breath, and oliguria [62]. Both transvaginal and transabdominal aspiration have been described under ultrasound guidance (Fig. 18.3) [62].

Endometrial Thickness

Endometrial characteristics such as thickness and pattern are often used as prognostic features in assisted reproductive techniques. Endometrial thickness is easily measured by transvaginal ultrasound and provides an indirect marker for serum estrogen, increasing in thickness as estrogen levels rise. A thin endometrium is thought to be associated with lower pregnancy rates, possibly resulting from excess oxygen exposure within an inadequate functional layer [63]. While studies attempting to correlate endometrial thickness and IVF outcomes have been conflicting, a systematic review and meta-analysis from 2014 concluded clinical pregnancy rates are significantly reduced among women with endometrial measurements <7 mm ($p = 0.0003$) [64]. Furthermore, A retrospective analysis among 606 women found lower success rates associated with both endometrial thickness below 8 mm and above 14 mm [65]. In 2018, a large retrospective cohort of 3350 IVF cycles reaffirmed the correlation between endometrial thickness and pregnancy outcomes. These authors found live birth rates were decreased with an endometrial thickness below 7 mm ($p < 0.001$). In addition, the same authors found a thin endometrial stripe, defined as <7.0 mm, was associated with lower neonatal birth weights [66].

Endometrial patterns are classified as pattern A—a triple line pattern with a central hyperechoic line surrounded by two hypoechoic layers, pattern B—an intermediate isoechogenic pattern with similar echogenicity as the myometrium and a poorly defined central echogenic line, and pattern C—homogenous, hyperechogenic endometrium. Significantly higher pregnancy rates were noted in patients with pattern A on the day of trigger, compared to pattern B or C ($p < 0.05$) [67].

Despite the controversy in the literature, evaluation of the endometrium for pattern and thickness has become standard monitoring during

fertility treatments. However, more studies are needed to fully correlate the sonographic findings with molecular and genetic markers of endometrial receptivity.

Embryo Transfer

Ultrasound guidance has potential to play an integral part in IVF embryo transfer. Pregnancy rates may be affected by embryo transfer techniques in IVF. Embryo transfer techniques that have been demonstrated to have an effect on pregnancy outcome include type of catheter [68], trial transfer attempt prior to the IVF cycle [69], technique of catheter loading [70], time to withdrawal of the catheter [71, 72], an atraumatic transfer [73], and location and migration of the transfer within the uterus [74, 75]. Abdominal ultrasound guidance for embryo transfer has been evaluated by several investigators.

Embryos are loaded into a catheter with the placement marked by air bubbles. Under abdominal ultrasound guidance with a full bladder, the placement of the catheter can be confirmed, and the air bubble visualized when injected into the uterus (Fig. 18.4). Of note, the bladder should be filled to aid in visualization (to the fundus of the uterus) but not "overfilled" as excess distention, particularly for retroverted uteri, may hinder transfer ability and also result in significant patient discomfort. Embryo catheters with an echodense tip may improve visualization of the catheter [76]. However, the impact of ultrasound on embryo placement was once controversial. In 1985, Strickler et al. reported ultrasound-guided embryo transfer in 16 patients. It was noted that the transfer catheter tip could be accurately positioned in the uterine cavity and ejection of the transfer media and air bubble could be documented [77] (Fig. 18.5). Woolcott and Stranger suggest that blind tactile feedback is unreliable for ascertaining proper embryo placement [77]. They describe abnormal placement near the internal tubal ostia in 9 of 121 transfers of the embryo transfer catheter documented by ultrasound [78]. The authors suggest that ultrasound guidance may decrease ectopic pregnancy rate by avoiding transfer near the tubal ostia. Similarly, Hurley et al. found tactile feedback unreliable; they identified 19 of 94 cases of ultrasound-guided embryo transfer where the physician unknowingly misplaced the catheter (6 in the cervix, 12 in the lower uterine segment, and 1 in a false passage). However, they did not find a significant difference in implantation rate with and without ultrasound, 20.2 and 17.5%, respectively [79]. A randomized controlled trial by Kan et al. also found no significant difference in implantation rate in the ultrasound-guided group (20.4%) compared to the control (16.2%) [80]. This study controlled for the pregnancy rate of the physician

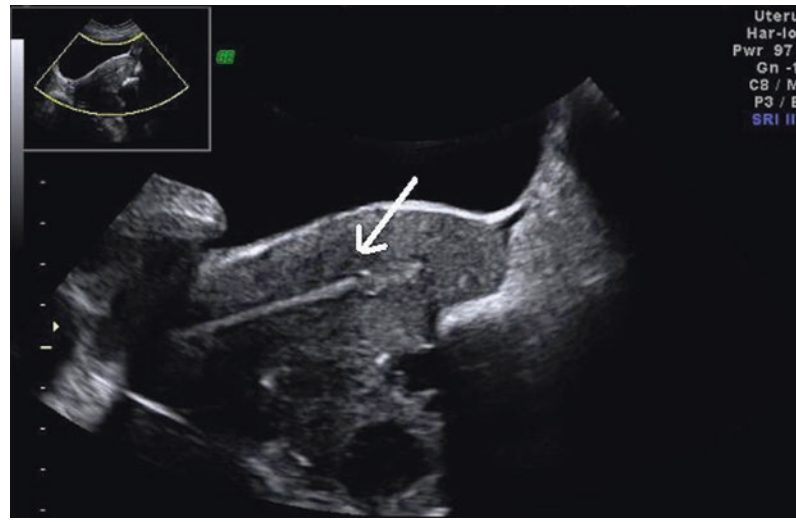

Fig. 18.4 Embryo transfer (*arrow* denotes transfer catheter and air bubble containing embryos)

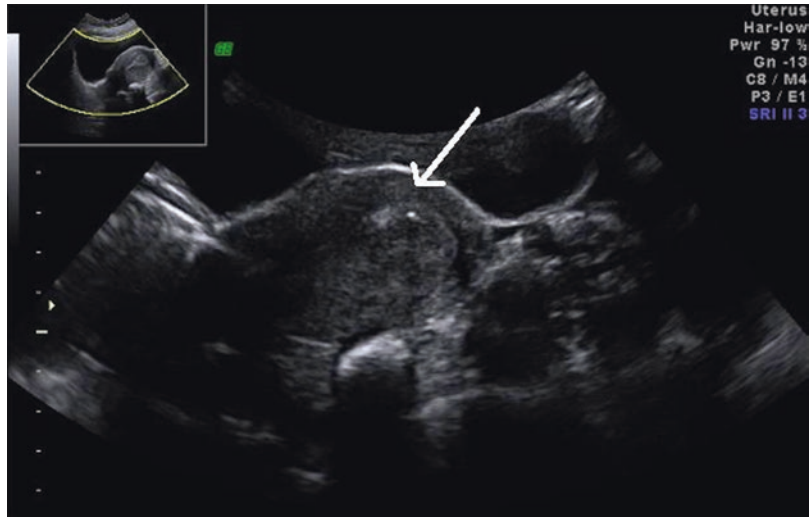

Fig. 18.5 Embryo transfer (*arrow* denotes location of embryo-containing media)

performing the procedure and day of the procedure (the control patient was selected on the same day as the study patient). Although not significant, the implantation rate of difficult transfers was 54.5% in the study group and 10.0% in the control group [80]. This group suggested that ultrasound guidance may be useful in patients with difficult transfers. In contrast, Coroleu performed a randomized trial in 362 patients and found a significant difference in implantation rate: 25.3% in the ultrasound-guided group compared to 18.1% in the control group [81]. However, they failed to control for the pregnancy rate of the physician performing the procedure. In addition, the location of embryo transfer differed between the two groups. In the ultrasound-guided group, the embryos were transferred to within 1.5 cm of the fundus, while the control group had embryos transferred as close to the fundus as possible without touching. Coroleu et al. in 2002 prospectively randomized 180 consecutive patients to embryo transfer at 10 mm from the fundus, 15 mm from the fundus, and 20 mm from the fundus [74]. All groups were equal in regard to patient age, BMI, diagnosis, duration of infertility, number of embryos transferred, and the degree of difficulty with transfers. Implantation rates were 26% if transferred 10 mm from the fundus, 31.3% at 15 mm, and 33.3% at 20 mm. The benefit of ultrasound guidance appears to occur by placing embryos in the thickest portion of endometrium at a distance of at least 15 mm from the fundus [74, 81]. Ficicioglu et al. further suggested that pregnancy rate is affected not only by the position in the uterus at the time of transfer, but also by the migration of the embryo air bubble following transfer. In a study of 220 ultrasound-guided embryo transfers, clinical pregnancy rates were found to be higher in those with air bubble migration toward the fundus, compared to static or cervical migration ($p < 0.1$). Ninety-seven percent of clinical pregnancies occurred in women with air bubble migration to <15 mm from the fundus within 60 minutes after embryo transfer. Migration of air bubble toward the cervical canal was associated with a decreased pregnancy rate [75].

Additionally, it is generally well accepted that an easy, atraumatic bloodless transfer improves implantation rates [73]. Trauma and bleeding increase the likelihood of uterine contractions and increase embryo expulsion [82]. Blood on the tip of the embryo catheter has been associated with a six- to sevenfold decrease in clinical pregnancy rate [83].

A 2003 meta-analysis including eight randomized controlled trials revealed improved implantation (OR 1.39) and clinical pregnancy rates (OR 1.44) in the ultrasound compared to "clinical touch" groups [84]. The group attributes previously reported insignificance to lack of power [83]. These significant findings favoring

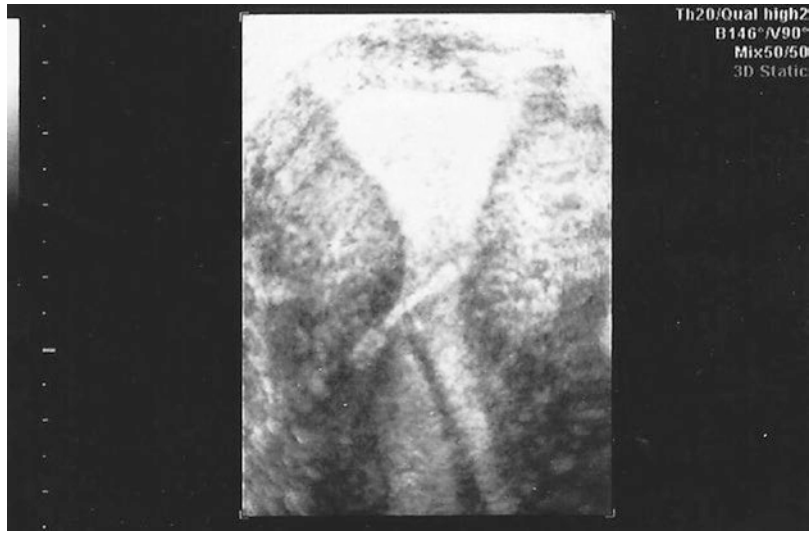

Fig. 18.6 Misplaced intrauterine device within the lower uterine segment (3D ultrasound image)

ultrasound use were affirmed by a 2010 Cochrane review and a 2018 meta-analysis including 14 randomized controlled trials [85, 86].

Although initially controversial, ultrasound guidance appears to play a beneficial role in embryo transfer. While the only disadvantages include the need for additional time, equipment, and skilled personnel, ultrasonography has the potential to aid in ideal embryo placement 15–20 mm from the fundus, to decrease uterine contractions, to increase the frequency of "easy" atraumatic transfers, and most importantly to improve implantation and pregnancy rates [87].

Intrauterine Device Placement and Removal

The intrauterine device (IUD) is one of the most effective forms of reversible contraception; the failure rate is 0.1–0.8% in the first year of use, and risk of complications such as perforation or expulsion is extremely low, 0–2% and 2–3%, respectively [88, 89]. Occasionally, a tortuous cervical canal may make insertion difficult. In such instances, using the aforementioned techniques to obtain visualization of the cervical path and uterine contour, transabdominal ultrasound can be used to help with difficult intrauterine device insertion. In addition, the use of misoprostol before the procedure may soften the cervix and make the procedure easier to perform [2]. Similarly, ultrasound can be used to confirm appropriate IUD placement and also can be used to help with device localization if IUD strings are not visible at time of desired removal (Fig. 18.6). A role for ultrasound guidance has also been reported for immediate postpartum IUD placement at which time theoretical risk of uterine perforation or IUD expulsion is greater [90]. Routine transvaginal ultrasound use has not been shown to be beneficial at time of IUD insertion [91].

Conclusion

The use of ultrasonography at the time of intrauterine procedures provides visualization of the intrauterine instruments as well as the myometrium. Therefore, ultrasonographic guidance may decrease the risk of perforation and increase the chance of a successful procedure. As an alternative to laparoscopy, ultrasonographic guidance may also shorten procedure time, decrease cost, and eliminate the risk of an additional surgical procedure. Not all procedures require ultrasound guidance; however, for selected cases, ultrasonography provides valuable assistance in carrying out the surgical procedure successfully and with lower risk.

Ultrasonography also plays an integral role in assisted reproductive treatment; effective egg retrieval relies on ultrasonography, and current literature suggests that ultrasound guidance at time of embryo transfer improves implantation and clinical pregnancy rates.

References

1. Session DR, Lerner JP, Tchen CK, Kelly AC. Ultrasound-guided fallopian tube cannulation using Albunex. Fertil Steril. 1997;67(5):972–4.
2. Christianson MS, Barker MA, Lindheim SR. Overcoming the challenging cervix: techniques to access the uterine cavity. J Low Genit Tract Dis. 2008;12(1):24–31.
3. Wu MH, Hsu CC, Lin YS. Three-dimensional ultrasound and hysteroscopy in the evaluation of intrauterine retained fetal bones. J Clin Ultrasound. 1997;25(2):93–5.
4. Shalev E, Zuckerman H. Operative hysteroscopy under real-time ultrasonography. Am J Obstet Gynecol. 1986;155(6):1360–1.
5. Grimbizis GF, Camus M, Tarlatzis BC, Bontis JN, Devroey P. Clinical implications of uterine malformations and hysteroscopic treatment results. Hum Reprod Update. 2001;7(2):161–74.
6. Acien P. Incidence of Mullerian defects in fertile and infertile women. Hum Reprod. 1997;12(7):1372–6.
7. Homer HA, Li TC, Cooke ID. The septate uterus: a review of management and reproductive outcome. Fertil Steril. 2000;73(1):1–14.
8. Propst AM, Hill JA 3rd. Anatomic factors associated with recurrent pregnancy loss. Semin Reprod Med. 2000;18(4):341–50.
9. Selvaraj P, Selvaraj K. Reproductive outcome of septate uterus following hysteroscopic septum resection. J Hum Reprod Sci. 2010;3(3):143–5.
10. Kupesic S, Kurjak A. Septate uterus: detection and prediction of obstetrical complications by different forms of ultrasonography. J Ultrasound Med. 1998;17(10):631–6.
11. Daly DC, Maier D, Soto-Albors C. Hysteroscopic metroplasty: six years' experience. Obstet Gynecol. 1989;73(2):201–5.
12. Querleu D, Brasme TL, Parmentier D. Ultrasound-guided transcervical metroplasty. Fertil Steril. 1990;54(6):995–8.
13. Fedele L, Bianchi S, Marchini M, Mezzopane R, Di Nola G, Tozzi L. Residual uterine septum of less than 1 cm after hysteroscopic metroplasty does not impair reproductive outcome. Hum Reprod. 1996;11(4):727–9.
14. Dabirashrafi H, Moghadami-Tabrizi N. Establishing the accuracy of ultrasound-guided transcervical metroplasty. Fertil Steril. 1991;56(1):152–3.
15. Coccia ME, Becattini C, Bracco GL, Bargelli G, Scarselli G. Intraoperative ultrasound guidance for operative hysteroscopy. A prospective study. J Reprod Med. 2000;45(5):413–8.
16. Cook H, Ezzati M, Segars JH, McCarthy K. The impact of uterine leiomyomas on reproductive outcomes. Minerva Ginecol. 2010;62(3):225–36.
17. Kresowik J, Syrop C, Van Voorhis B, Ryan G. Ultrasound is the optimal choice for guidance in difficult hysteroscopy. Ultrasound Obstet Gynecol. 2012;39:715–8.
18. Marsh EE, Ekpo GE, Cardozo ER, Brocks M, Dune T, Cohen LS. Racial differences in fibroid prevalence and ultrasound findings in asymptomatic young women (18–30 years old): a pilot study. Fertil Steril. 2013;99(7):1951–7.
19. Olive DL. The surgical treatment of fibroids for infertility. Semin Reprod Med. 2011;29(2):113–23.
20. Farhi J, Bar-Hava I, Homburg R, Dicker D, Ben-Rafael Z. Induced regeneration of endometrium following curettage for abortion: a comparative study. Hum Reprod. 1993;8(7):1143–4.
21. Ramzy AM, Sattar M, Amin Y, Mansour RT, Serour GI, Aboulghar MA. Uterine myomata and outcome of assisted reproduction. Hum Reprod. 1998;13(1):198–202.
22. Jun SH, Ginsburg ES, Racowsky C, Wise LA, Hornstein MD. Uterine leiomyomas and their effect on in vitro fertilization outcome: a retrospective study. J Assist Reprod Genet. 2001;18(3):139–43.
23. Surrey ES, Lietz AK, Schoolcraft WB. Impact of intramural leiomyomata in patients with a normal endometrial cavity on in vitro fertilization-embryo transfer cycle outcome. Fertil Steril. 2001;75(2):405–10.
24. Lin CC, Ou MC, Hsiao SM, Lin HH. Myomectomy through the uterine cervix using forceps under sonographic guidance. Ultrasound Obstet Gynecol. 2009;33(2):228–31.
25. Wortman M, Dagget A. Hysteroscopic myomectomy. J Am Assoc Gynecol Laparosc. 1995;3(1):39–46.
26. Shalev E, Shimoni Y, Peleg D. Ultrasound controlled operative hysteroscopy. J Am Coll Surg. 1994;179(1):70–1.
27. Myers EM, Hurst BS. Comprehensive management of severe Asherman syndrome and amenorrhea. Fertil Steril. 2012;97(1):160–4.
28. Orhue AA, Aziken ME, Igbefoh JO. A comparison of two adjunctive treatments for intrauterine adhesions following lysis. Int J Gynaecol Obstet. 2003;82(1):49–56.
29. Amer MI, Nadim EA, Karim H. The role of intrauterine balloon after operative hysteroscopy in the prevention of intrauterine adhesions; a prospective controlled study. Middle East Fertil Soc. 2005;10:135–9.
30. Pabuccu R, Atay V, Orhon E, Urman B, Ergün A. Hysteroscopic treatment of intrauterine adhesions is safe and effective in the restoration of normal menstruation and fertility. Fertil Steril. 1997;68(6):1141–3.
31. Tsapanos VS, Stathopoulou LP, Papathanassopoulou VS, Tzingounis VA. The role of Seprafilm biore-

sorbable membrane in the prevention and therapy of endometrial synechiae. J Biomed Mater Res. 2002;63(1):10–4.
32. Acunzo G, Guida M, Pellicano M, Tommaselli GA, Di Spiezio Sardo A, Bifulco G, et al. Effectiveness of auto-cross-linked hyaluronic acid gel in the prevention of intrauterine adhesions after hysteroscopic adhesiolysis: a prospective, randomized, controlled study. Hum Reprod. 2003;18(9):1918–21.
33. Letterie GS, Case KJ. Intraoperative ultrasound guidance for hysteroscopic retrieval of intrauterine foreign bodies. Surg Endosc. 1993;7(3):182–4.
34. Kohlenberg CF, Pardey J, Ellwood DA. Transabdominal ultrasound as an aid to advanced hysteroscopic surgery. Aust N Z J Obstet Gynaecol. 1994;34(4):462–4.
35. Goudas VT, Session DR. Hysteroscopic cervical cannulation under ultrasound guidance. A case report. J Reprod Med. 1998;43(8):696–8.
36. Dabirashrafi H, Mohamad K, Moghadami-Tabrizi N. Three-contrasts method hysteroscopy: the use of real-time ultrasonography for monitoring intrauterine operations. Fertil Steril. 1992;57(2):450–2.
37. Grimes DA, Jones LB, Lopez LM, Schulz KF. Oral contraceptives for functional ovarian cysts. Cochrane Database Syst Rev. 2011;9:CD006134.
38. Qublan HS, Amarin Z, Tahat YA, Smadi AZ, Kilani M. Ovarian cyst formation following GnRH agonist administration in IVF cycles: incidence and impact. Hum Reprod. 2006;21(3):640–4.
39. Jenkins JM, Davies DW, Anthony F, Wood P, Gadd SG, Watson RH, et al. The detrimental influence of functional ovarian cysts during in-vitro fertilization cycles. Hum Reprod. 1992;7(6):776–80.
40. Firouzabadi RD, Sekhavat L, Javedani M. The effect of ovarian cyst aspiration on IVF treatment with GnRH. Arch Gynecol Obstet. 2010;281(3):545–9.
41. Rizk B, Tan SL, Kingsland C, Steer C, Mason BA, Campbell S. Ovarian cyst aspiration and the outcome of in vitro fertilization. Fertil Steril. 1990;54(4):661–4.
42. Parinaud J, Cohen K, Oustry P, Perineau M, Monroziès X, Rème JM. Influence of ovarian cysts on the results of in vitro fertilization. Fertil Steril. 1992;58(6):1174–7.
43. Tarlatzis BC, Bili H, Bontis J, Lagos S, Vatev I, Mantalenakis S. Follicle cyst formation after administration of different gonadotrophin-releasing hormone analogues for assisted reproduction. Hum Reprod. 1994;9(11):1983–6.
44. Greenebaum E, Mayer JR, Stangel JJ, Hughes P. Aspiration cytology of ovarian cysts in in vitro fertilization patients. Acta Cytol. 1992;36(1):11–8.
45. Hurst BS, Tucker KE, Awoniyi CA, Schlaff WD. Hydrosalpinx treated with extended doxycycline does not compromise the success of in vitro fertilization. Fertil Steril. 2001;75(5):1017–9.
46. Van Voorhis BJ, Sparks AE, Syrop CH, Stovall DW. Ultrasound-guided aspiration of hydrosalpinges is associated with improved pregnancy and implantation rates after in-vitro fertilization cycles. Hum Reprod. 1998;13(3):736–9.
47. Vandromme J, Chasse E, Lejeune B, Van Rysselberge M, Delvigne A, Leroy F. Hydrosalpinges in in-vitro fertilization: an unfavourable prognostic feature. Hum Reprod. 1995;10(3):576–9.
48. Meyer WR, Castelbaum AJ, Somkuti S, Sagoskin AW, Doyle M, Harris JE, et al. Hydrosalpinges adversely affect markers of endometrial receptivity. Hum Reprod. 1997;12:1393–8.
49. Osuga Y, Koga K, Hirata T, Hiroi H, Taketani Y. A case of hydrosalpinx associated with the menstrual cycle. Fertil Steril. 2008;90(1):199.e9–11.
50. Sowter MC, Akande VA, Williams JA, Hull MG, et al. Is the outcome of in-vitro fertilization and embryo transfer treatment improved by spontaneous or surgical drainage of a hydrosalpinx? Hum Reprod. 1997;12(10):2147–50.
51. Fouda UM, Sayed AM, Abdelmoty HI, Elsetohy KA. Ultrasound guided aspiration of hydrosalpinx fluid versus salpingectomy in the management of patients with ultrasound visible hydrosalpinx undergoing IVF-ET: a randomized controlled trial. BMC Womens Health. 2015;15:21.
52. Xu B, Zhang Q, Zhao J, Wang Y, Xu D, Li Y. Pregnancy outcome of in vitro fertilization after Essure and laparoscopic management of hydrosalpinx: a systematic review and meta-analysis. Fertil Steril. 2017;108(1):85–95.
53. Lenz S, Lauritsen JG, Kjellow M. Collection of human oocytes for in vitro fertilisation by ultrasonically guided follicular puncture. Lancet. 1981;1(8230):1163–4.
54. Barton SE, Politch JA, Benson CB, Ginsburg ES, Gargiulo AR. Transabdominal follicular aspiration for oocyte retrieval in patients with ovaries inaccessible by transvaginal ultrasound. Fertil Steril. 2011;95(5):1773–6.
55. Gleicher N, Friberg J, Fullan N, Giglia RV, Mayden K, Kesky T, et al. EGG retrieval for in vitro fertilisation by sonographically controlled vaginal culdocentesis. Lancet. 1983;2(8348):508–9.
56. Damario MA. Transabdominal-transperitoneal ultrasound-guided oocyte retrieval in a patient with mullerian agenesis. Fertil Steril. 2002;78(1):189–91.
57. Weinerman R, Grifo J. Consequences of superovulation and ART procedures. Semin Reprod Med. 2012;30(2):77–83.
58. Moini A, Riazi K, Amid V, Ashrafi M, Tehraninejad E, Madani T, Owj M. Endometriosis may contribute to oocyte retrieval-induced pelvic inflammatory disease: report of eight cases. J Assist Reprod Genet. 2005;22(7–8):307–9.
59. Kroon B, Hart RJ, Wong BM, Ford E, Yazdani A. Antibiotics prior to embryo transfer in ART. Cochrane Database Syst Rev. 2012;(3):CD008995.
60. Waterstone JJ, Parsons JH. A prospective study to investigate the value of flushing follicles during trans-

vaginal ultrasound-directed follicle aspiration. Fertil Steril. 1992;57(1):221–3.
61. Wongtra-Ngan S, Vutyavanich T, Brown J. Follicular flushing during oocyte retrieval in assisted reproductive techniques. Cochrane Database Syst Rev. 2010;(9):CD004634.
62. The Practice Committee of the American Society for Reproductive Medicine. Ovarian hyperstimulation syndrome. Birmingham: ASRM; 2008.
63. Casper RF. Its time to pay attention to the endometrium. Fertil Steril. 2011;96(3):519–21.
64. Kasius A, Smit JG, Torrance HL, Eijkemans MJ, Mol BW, Opmeer BC, Broekmans FJ. Endometrial thickness and pregnancy rates after IVF: a systematic review and meta-analysis. Hum Reprod. 2014;20(4):530–41.
65. Lamanna G, Scioscia M, Lorusso F, Serrati G, Selvaggi LE, Depalo R. Parabolic trend in endometrial thickness at embryo transfer in in vitro fertilization/intracytoplasmic sperm injection cases with clinical pregnancy evidence. Fertil Steril. 2008;90:1272–4.
66. Ribeiro VC, Santos-Ribeiro S, De Munck N, Drakopoulos P, Polyzos NP, Schutyser V, et al. Should we continue to measure endometrial thickness in modern-day medicine? The effect on live birth rates and birth weight. Reprod Biomed Online. 2018;36:416–24.
67. Zhao J, Zhang Q, Li Y. The effect of endometrial thickness and pattern measured by ultrasonography on pregnancy outcomes during IVF-ET cycles. Reprod Biol Endocrinol. 2012;10:100.
68. Penzias AS, Harris D, Barrett CB, Alper MM, Berger MJ, Oskowitz SP. Outcome oriented research in an IVF program: transfer catheter type affects IVF outcome. Cincinnati: ASRM; 1997.
69. Mansour R, Aboulghar M, Serour G. Dummy embryo transfer: a technique that minimizes the problems of embryo transfer and improves the pregnancy rate in human in vitro fertilization. Fertil Steril. 1990;54(4):678–81.
70. Poindexter AN 3rd, Thompson DJ, Gibbons WE, Findley WE, Dodson MG, Young RL. Residual embryos in failed embryo transfer. Fertil Steril. 1986;46(2):262–7.
71. Leong M, Leung C, Tucker M, Wong C, Chan H. Ultrasound-assisted embryo transfer. J In Vitro Fert Embryo Transf. 1986;3(6):383–5.
72. Martinez F, Coroleu B, Parriego M, Carreras O, Belil I, Parera N, et al. Ultrasound-guided embryo transfer: immediate withdrawal of the catheter versus a 30 second wait. Hum Reprod. 2001;16(5):871–4.
73. Matorras R, Urquijo E, Mendoza R, Corcóstegui B, Expósito A, Rodríguez-Escudero FJ. Ultrasound-guided embryo transfer improves pregnancy rates and increases the frequency of easy transfers. Hum Reprod. 2002;17(7):1762–6.
74. Coroleu B, Barri PN, Carreras O, Martínez F, Parriego M, Hereter L, et al. The influence of the depth of embryo replacement into the uterine cavity on implantation rates after IVF: a controlled, ultrasound-guided study. Hum Reprod. 2002;17(2):341–6.
75. Ficicioglu C, Özcan P, Koçer MG, Yeşiladalı M, Alagöz O, Özkara G, et al. Effect of air bubbles localization and migration after embryo transfer on assisted reproductive technology outcome. Fertil Steril. 2018;109(2):310–4.
76. Letterie GS, Marshall L, Angle M. A new coaxial catheter system with an echodense tip for ultrasonographically guided embryo transfer. Fertil Steril. 1999;72(2):266–8.
77. Strickler RC, Christianson C, Crane JP, Curato A, Knight AB, Yang V. Ultrasound guidance for human embryo transfer. Fertil Steril. 1985;43(1):54–61.
78. Woolcott R, Stanger J. Potentially important variables identified by transvaginal ultrasound-guided embryo transfer. Hum Reprod. 1997;12(5):963–6.
79. Hurley VA, Osborn JC, Leoni MA, Leeton J. Ultrasound-guided embryo transfer: a controlled trial. Fertil Steril. 1991;55(3):559–62.
80. Kan AK, Abdalla HI, Gafar AH, Nappi L, Ogunyemi BO, Thomas A, et al. Embryo transfer: ultrasound-guided versus clinical touch. Hum Reprod. 1999;14(5):1259–61.
81. Coroleu B, Barri PN, Carreras O, Martínez F, Veiga A, Balasch J. The usefulness of ultrasound guidance in frozen-thawed embryo transfer: a prospective randomized clinical trial. Hum Reprod. 2002;17(11):2885–90.
82. Lesny P, Killick SR, Tetlow RL, Robinson J, Maguiness SD. Embryo transfer–can we learn anything new from the observation of junctional zone contractions? Hum Reprod. 1998;13(6):1540–6.
83. Goudas VT, Hammitt DG, Damario MA, Session DR, Singh AP, Dumesic DA. Blood on the embryo transfer catheter is associated with decreased rates of embryo implantation and clinical pregnancy with the use of in vitro fertilization-embryo transfer. Fertil Steril. 1998;70(5):878–82.
84. Buckett WM. A meta-analysis of ultrasound-guided versus clinical touch embryo transfer. Fertil Steril. 2003;80(4):1037–41.
85. Brown J, Buckingham K, Abou-Setta AM, Buckett W. Ultrasound versus 'clinical touch' for catheter guidance during embryo transfer in women. Cochrane Database Syst Rev. 2010;(1):CD006107.
86. Cozzolino M, Vitagliano A, Di Giovanni MV, Laganà AS, Vitale SG, Blaganje M, et al. Ultrasound-guided embryo transfer: summary of the evidence and new perspectives. A systematic review and meta-analysis. Reprod Biomed Online. 2018;36(5):524–42.
87. The Practice Committee of the American Society for Reproductive Medicine. Performing the embryo transfer: a guideline. Birmingham: ASRM; 2017.
88. Trussell J, Vaughan B. Contraceptive failure, method-related discontinuation and resumption of use: results from the 1995 National Survey of Family Growth. Fam Plan Perspect. 1999;31(2):64–72, 93.
89. Kaislasuo J, Suhonen S, Gissler M, Lähteenmäki P, Heikinheimo O. Intrauterine contraception: inci-

dence and factors associated with uterine perforation–a population-based study. Hum Reprod. 2012;27(9):2658–63.
90. Hayes JL, Cwiak C, Goedken P, Zieman M. A pilot clinical trial of ultrasound-guided postplacental insertion of a levonorgestrel intrauterine device. Contraception. 2007;76(4):292–6.
91. de Kroon CD, van Houwelingen JC, Trimbos JB, Jansen FW. The value of transvaginal ultrasound to monitor the position of an intrauterine device after insertion. A technology assessment study. Hum Reprod. 2003;18(11):2323–7.

19 Ultrasound and Ovarian Hyperstimulation Syndrome

Laura P. Smith

Ultrasound in the Prediction of Ovarian Hyperstimulation Syndrome

Because ovarian hyperstimulation syndrome (OHSS) is one of the most severe iatrogenic complications of in vitro fertilization (IVF), there have been many attempts to predict which patients are most at risk. Unfortunately, there are no perfect tests to anticipate the development of OHSS. Ultrasound determination of antral follicle count, size and follicular number at the time of egg retrieval, sonographic evidence of polycystic ovary syndrome, assessment of ovarian volume, and Doppler flow studies of ovarian vasculature have all been evaluated as markers to identify a higher likelihood of developing OHSS.

Among the sonographic tools used in the prediction of OHSS, quantitation of the antral follicle count (AFC) is one of the most accurate tests. Antral follicles are the 2–10-mm follicles that can be identified by ultrasound in the early follicular phase. Antral follicles appear as round, hypoechoic structures scattered throughout the ovary when viewed by 2D transvaginal ultrasound (Fig. 19.1). The size of the antral follicle pool is considered to reflect the total number of remaining follicles [1]. Generally, a low antral follicle count suggests a poor response to ovarian stimulation, and a high antral follicle count suggests better ovarian response to gonadotropin stimulation and higher oocyte yield.

Several investigators have evaluated AFC to predict the development of OHSS. Kwee et al. evaluated 110 patients with unexplained infertility, male factor, or cervical factor infertility, counted antral follicles in all patients, and correlated the number of antral follicles with level of ovarian response to IVF [2]. They categorized ovarian response as poor, normal, and high and then calculated the AFC cutoff which most accurately identified each group. The AFC value of >14 identified hyper-responders with a sensitivity of 82% and a specificity of 89%. Ocal et al. also evaluated the predictive role of AFC in OHSS in 41 women identified to have moderate to severe OHSS and 41 age-matched controls who did not develop OHSS [3]. They found that AFC had a moderate accuracy to predict the development of OHSS. Using an AFC cutoff of 8, much lower than the AFC cutoff used by Kwee et al., they calculated 78% sensitivity and 65% specificity. In a meta-analysis done by Broer et al. investigating AFC as a predictor of ovarian hyperstimulation, five studies were identified which met criteria for inclusion [4]. Two reported on AFC alone, three reported on both anti-Mullerian hormone (AMH) and AFC, and all five were prospective cohort studies. Among the included studies, the definition of excessive

L. P. Smith (✉)
Reproductive Medicine and Surgery Center of Virginia, PLC, Charlottesville, VA, USA
e-mail: laura.smith@rmscva.com

L. A. Stadtmauer, I. Tur-Kaspa (eds.), *Ultrasound Imaging in Reproductive Medicine*,
https://doi.org/10.1007/978-3-030-16699-1_19

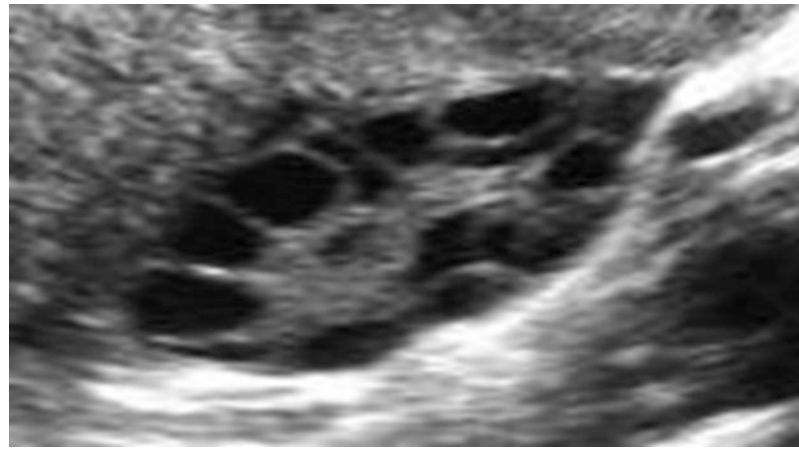

Fig. 19.1 Antral follicle count

ovarian response to IVF varied between ≥15 and ≥20 oocytes. Importantly, the number of oocytes retrieved was used as a surrogate for risk of OHSS; no study specifically identified the patients who met diagnostic criteria for OHSS. When these five studies of AFC were evaluated together, the sensitivity of AFC to predict ovarian hyper-response was seen to vary between 20% and 94% depending on the AFC cutoff used, and the specificity varied between 33% and 98%. From these values, the authors calculated a sum estimate of the sensitivity to be 82% and a sum estimate of the specificity to be 80%. Considering this evidence, there is a clear association between increased AFC and increased risk of OHSS. Given the sensitivity and specificity estimates of AFC in the studies to date, if the AFC is found to be greater than 14–16, caution should be executed in the initial gonadotropin dosing and choice of stimulation protocol since there is clearly increased risk of ovarian hyper-response in such patients.

When proposing the use of AFC to predict OHSS, it is important to be aware of the variability both in definition of antral follicle and operator technique in follicle counting [5]. Interestingly, some authors adhere to the definition of antral follicle as those follicles which are measured to be 2–10 mm in the early follicular phase, as above; but other authors limit that definition to only those follicles that measure 2–5 mm. The precise menstrual timing of the measurement of AFC also may or may not be important. Historical dogma has asserted that AFC should be performed either between cycle day 2 and 4 or while on oral contraceptive pills for greatest accuracy and reproducibility. A few recent studies have contradicted this strict time limitation on AFC, however, asserting that antral follicle count is predictive of poor ovarian response when measured at any time in the menstrual cycle [6, 7].

The number of growing follicles in response to gonadotropin stimulation during assisted reproductive technologies (ART) is another sonographic test which has been proposed to predict the development of OHSS. Clearly, there is a connection between the ovarian response to stimulation and AFC, as patients with higher baseline AFC would be expected to have a more robust ovarian response to treatment. Papanikolaou et al. sought to correlate the number of follicles ≥11 mm growing in response to gonadotropin treatment during IVF with the likelihood of developing moderate or severe ovarian hyperstimulation syndrome [8]. They evaluated 1801 patients undergoing IVF treatment over a 2-year period. Factors such as peak estradiol level and number of follicles ≥11 mm were correlated with the development of OHSS. In this cohort, 53 patients were hospitalized because of OHSS. They found that a threshold of ≥13 follicles measuring ≥11 mm was predictive of the development of OHSS with a sensitivity of 85.5% and a specificity of 69%. Interestingly, the

number of follicles ≥11 mm was a much better predictor of OHSS than the peak serum estradiol level, which had only a 53% sensitivity and 77% specificity. Tarlatzi et al. also investigated this question in a more recent study [9]. They performed an analysis of all IVF cycles during a 5-year interval (2009–2014), counted the number of follicles ≥10 mm on the day of oocyte final "trigger" shot, and performed logistic and multivariable regression analyses to determine association between follicle number and risk of severe OHSS. A secondary outcome was the occurrence of moderate OHSS. Of the 2982 patients who underwent 5493 IVF cycles evaluated in this study, severe OHSS was diagnosed in 20 cycles, and moderate OHSS was diagnosed in 74 cycles. The authors determined that if there were ≥ 15 follicles ≥10 mm on the day of trigger shot, the development of severe OHSS could be predicted with a sensitivity of 89.5% and specificity of 64.2% (OR 28.7, 95% CI 8.5–97.1) [9]. Therefore, using the Papanikolaou et al. and Tarlatzi et al. data, if it becomes apparent during an IVF cycle that there are 13–15 or more follicles measuring ≥10 mm, the patient and physician should both be cognizant of the increased risk of developing OHSS regardless of the serum estradiol level.

Because patients who have higher baseline AFC and higher functional ovarian response to stimulation have been found to have a greater likelihood of developing OHSS, it is important to identify such patients early in clinical care. It is well known that patients with polycystic ovary syndrome (PCOS) have by definition a high antral follicle count and magnified response to IVF. Ultrasound assessment of ovarian morphology serves as one of the key tests for the diagnosis of PCOS by the Rotterdam criteria [10]. The sonographic findings which meet Rotterdam diagnostic criteria are either 12 or more follicles in each ovary measuring 2–9 mm in diameter and/or increased ovarian volume > 10 mL [11] (Fig. 19.2). In combination with either anovulation/oligo-ovulation or clinical/biochemical hyperandrogenism, and having excluded other endocrine conditions as Cushing's syndrome and congenital adrenal hyperplasia, a patient could be diagnosed as having PCOS. Interestingly, even women who do not technically meet criteria for PCOS but have isolated polycystic-appearing ovaries on ultrasound have been found to have a higher risk of developing OHSS [10]. Therefore, clinical management including gonadotropin dosing and choice of stimulation protocol should incorporate knowledge of PCOS or

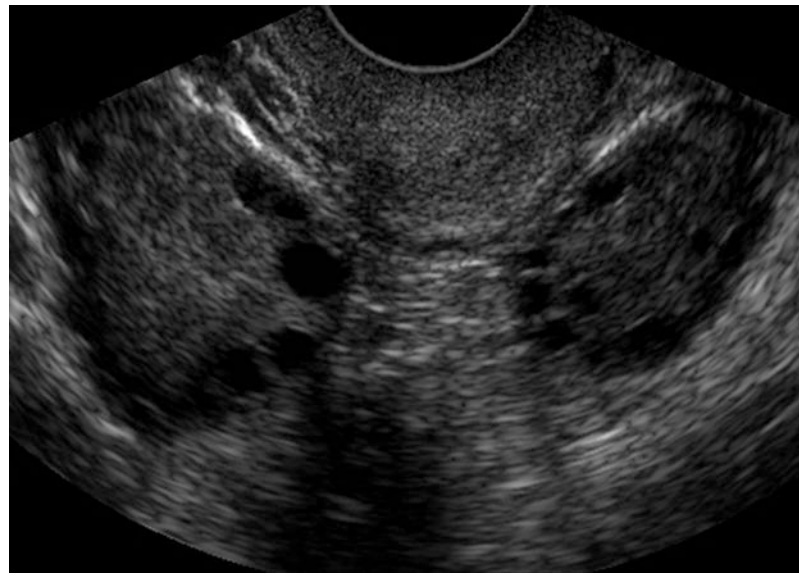

Fig. 19.2 AFC of PCOS ovary in 2D ultrasound

polycystic-appearing ovaries on ultrasound in an attempt to minimize the development of OHSS in these patients.

Using patients with PCOS as a model for other patients at risk for OHSS, researchers have investigated ultrasound calculation of baseline ovarian volume alone as a predictive marker. Danninger et al. studied 101 patients undergoing IVF, all of whom had 3D volumetric assessment of ovarian volume starting on stimulation day 1 [12]. The authors then re-measured ovarian volume on the day of human chorionic gonadotropin (hCG) and correlated those findings with the development of OHSS. They found a significant correlation between the baseline ovarian volume and OHSS ($p = 0.03$) with a greater baseline ovarian volume in women who subsequently developed OHSS compared to those who did not. The authors estimated an ovarian volume cutoff of 10 mL as predictive of OHSS. Importantly, this sonographic finding was not as robust as some of the other markers already discussed. Even in the 34 patients identified to have an ovarian volume >10 mL, only 23.5% ultimately developed OHSS. Although it is logical in the context of PCOS and the PCOS-associated risk of OHSS, the measurement of ovarian volume is not considered to be a standard marker at this time to predict OHSS.

The final ultrasound characteristics which have been used to attempt to predict the development of OHSS are Doppler flow studies of ovarian vasculature. The concept behind the assessment of ovarian vascular resistance and flow is that because OHSS involves third spacing of fluid secondary to increased vascular permeability, one might expect changes in ovarian vascular flow which may occur prior to clinical signs or symptoms of OHSS and therefore could be used to predict the development of OHSS [13]. Coupled with increased vascular permeability, there is also abnormal intraovarian angiogenesis in OHSS leading to low vascular impedance. Multiple authors have investigated sonographic characterization of ovarian vascular flow, resistance, peak systolic velocity, and pulse-wave power Doppler to try to correlate vascular chances with the likelihood of developing OHSS. In 1997, Moohan et al. evaluated 30 patients with who were diagnosed with mild or severe OHSS within 2–15 days of oocyte retrieval [13]. All patients underwent transabdominal ultrasound at the time of diagnosis of OHSS with color Doppler done on low-flow setting to characterize the flow velocity waveforms within the ovarian vessels. Vascular pulsatility index, resistance index, S-D ratio, and maximal peak systolic velocity were calculated. The authors found that in patients with severe OHSS, there was markedly reduced vascular impedance with a statistically significantly higher resistance index in patients with mild OHSS compared to severe (0.49 vs. 0.41, $p < 0.005$). Surprisingly, there was no difference in maximal peak systolic velocity, but pulsatility index and S-D ratio also differed significantly between patients with mild and severe OHSS. Of importance, this study evaluated only patients diagnosed with OHSS. There was no comparison with patients who did not develop OHSS, so it is impossible to know if these differences in vascular flow could have been used to predict the development of OHSS. Other authors including Agrawal et al. did compare patients with OHSS to controls and found a difference in ovarian stromal peak systolic velocity and time-averaged maximal velocity between patients with and without OHSS [14]. In the study by Agrawal et al. published in 1998, ovarian Doppler flow velocity was statistically significantly higher in patients with OHSS than controls, but pulsatility index and resistance index did not differ between the groups. The authors concluded that the changes in flow velocity correlated with changes in vascular endothelial growth factor (VEGF) serum and follicular fluid concentrations. More recently, Jayaprakasan et al. used three-dimensional (3D) power Doppler angiography to attempt to predict OHSS [15]. In 118 patients, of whom 18 developed moderate or severe OHSS, ovarian vascular flow indices were quantified by 3D ultrasound. Unexpectedly, there was no difference in vascularization index, flow index, or vascularization flow index between either patients with OHSS vs. controls or the subgroups of patients with moderate vs. severe OHSS. Therefore, although the pathophysiology

of OHSS involves known changes in vascular permeability which logically suggest a connection between Doppler measurements of ovarian vascular flow and the development of OHSS, unfortunately no studies to date have convincingly shown that ultrasound measurement of ovarian vascular parameters can be used to predict the risk of OHSS and this test is not considered clinically useful at this time.

In summary, ultrasound has been investigated as a tool to predict the development of OHSS through assessment of AFC, quantitation of follicular development during IVF, identification of polycystic-appearing ovaries or PCOS, determination of ovarian volume, and Doppler flow studies of ovarian vasculature. Of these potential sonographic markers, AFC and the number of growing follicles during an IVF cycle are the most significant predictors of the development of OHSS and should be used to guide management. There is also evidence linking the diagnosis of PCOS with the risk of OHSS, so IVF protocol and gonadotropin dosing should be carefully considered in these patients. To date, the other ultrasound tools including ovarian volume and vascular flow analysis do not have clinical utility in the prediction of OHSS.

As these sonographic variables are being considered, it is clear that they must be combined with demographic data (patient age, BMI, etc.), serum markers such as anti-Mullerian hormone (AMH), peak serum estradiol during IVF stimulation, and number of oocytes retrieved to arrive at a meaningful prediction of the risk of OHSS. There are specific patient characteristics such as younger age, lower BMI, and black race, which have been found to be associated with an increased risk of OHSS [16]. Likewise, ovarian reserve markers such as AMH are useful in the prediction of OHSS [17]. Lee et al. showed that an AMH > 3.36 ng/mL can predict OHSS with a sensitivity of 90.5% and specificity of 81.3% [18]. These baseline patient characteristics need to be considered in the context of an IVF cycle as the serum estradiol level is being checked, follicular growth monitored, gonadotropin dosing continues, and final egg yield determined. Peak serum estradiol during an IVF cycle has long been attempted to be used in isolation to predict OHSS risk. Unfortunately, there is no single estradiol level during IVF which can unfailingly predict the development of OHSS. What is clear is that there seems to be a range of estradiol levels above which the risk is increased in specific patients. In a large retrospective cohort study performed in 2017, Tarlatzi et al. found that a serum concentration of estradiol ≥2021 pg/mL increased the odds of severe OHSS by 13.2 times and identified 85% of the cycles complicated by severe OHSS [9]. Egg yield with IVF is logically related to developing follicle number and estradiol level but has been independently evaluated for its predictive capacity in the development of OHSS. Studies have shown that retrieval of >15–20 eggs substantially increases the risk of OHSS [19, 20]. In summary, the ultrasound tools described above can be used to attempt to predict OHSS; but they are not intended to be used in isolation. Rather, they are most meaningful if they are employed in combination with assessment of clinical variables such as patient demographics, ovarian reserve markers, and the specific details of IVF cycle progression to best predict the development of OHSS.

Ultrasound in the Diagnosis of Ovarian Hyperstimulation Syndrome

Once OHSS is suspected on clinical grounds, the diagnosis is aided by ultrasound findings. OHSS is categorized into mild, moderate, and severe disease. The differentiation involves sonographic features including the degree of ovarian enlargement, presence and volume of abdominal ascites, and presence or absence of pleural effusions and Doppler studies showing venous thromboembolism [21].

The clinical findings of OHSS encompass a spectrum ranging from mild disease, unpleasant for the patient but not considered to be dangerous, to severe OHSS with significant consequences and risk of death. Mild OHSS is common and involves symptoms such as lower

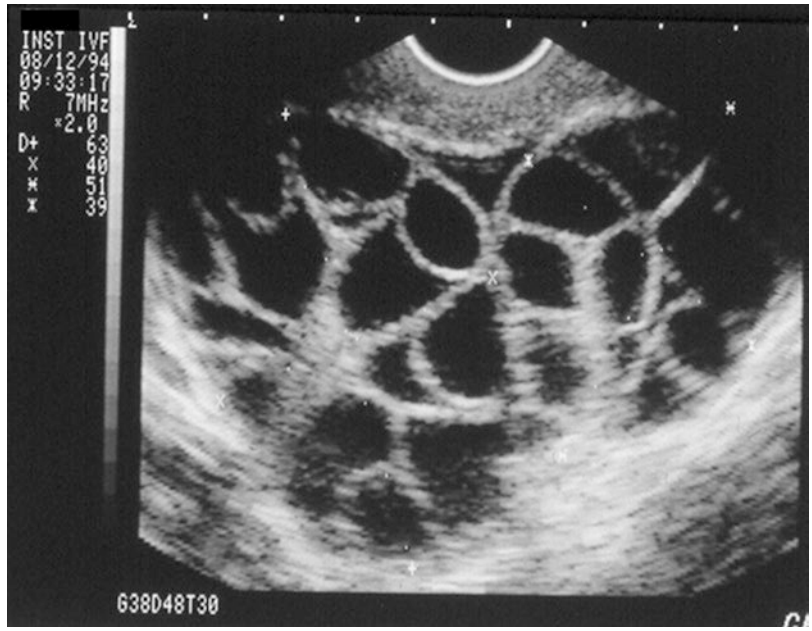

Fig. 19.3 Hyperstimulated ovary after gonadotropin therapy

abdominal or pelvic discomfort, gastrointestinal complaints including nausea, emesis, and diarrhea, and some degree of abdominal distention [22]. The process of superovulation frequently leads to these mild manifestations of OHSS, and up to a third of IVF cycles may involve these complaints. The only sonographic characteristic of mild OHSS may be enlarged ovaries (5–12 cm) [23] (Fig. 19.3).

Moderate OHSS consists of intensified pain, nausea or emesis, enlarged ovaries seen on ultrasound, and sonographic identification of abdominal or pelvic ascites with normal serum laboratory parameters (Fig. 19.4). Some authors have described OHSS as an abdominal compartment syndrome because the rapid accumulation of ascites can lead to increased intra-abdominal pressure [24]. Increased intra-abdominal pressure can become acute and lead to organ dysfunction. In severe forms, abdominal compartment syndrome affects respiratory function, as in the case of severe OHSS.

Given that abdominal ascites is a key characteristic of the diagnosis of moderate OHSS, it is critical that the ultrasound findings be interpreted correctly in the context of the clinical presentation. Gunabushanam et al. reported the case of a 22-year-old woman who had received fertility treatments and presented to the emergency department complaining of a 12-h history of severe lower abdominal pain [25]. Transabdominal ultrasound showed enlarged ovaries bilaterally (7 × 5 × 5 cm) with significant anechoic peritoneal free fluid felt consistent with ascites. She was diagnosed with OHSS. She then began to clinically decompensate with the development of pallor and peritoneal signs and underwent diagnostic paracentesis notable for nonclotting blood. Ultimately, she was taken to the operating room for emergent laparotomy, and a bleeding ovarian cyst was identified and treated. This case demonstrates the dangers of assuming the diagnosis of OHSS in all patients undergoing fertility treatments, as other pelvic pathology can clearly lead to the accumulation of pelvic fluid. Cyst rupture can certainly lead to significant intraperitoneal bleeding with risk of death, and accurate communication between the sonographer, radiologist, emergency department physician, and reproductive endocrinologist is critical to appropriate and timely diagnosis.

Severe OHSS is one of the most serious complications of ovarian hyperstimulation. The incidence of severe OHSS is estimated between

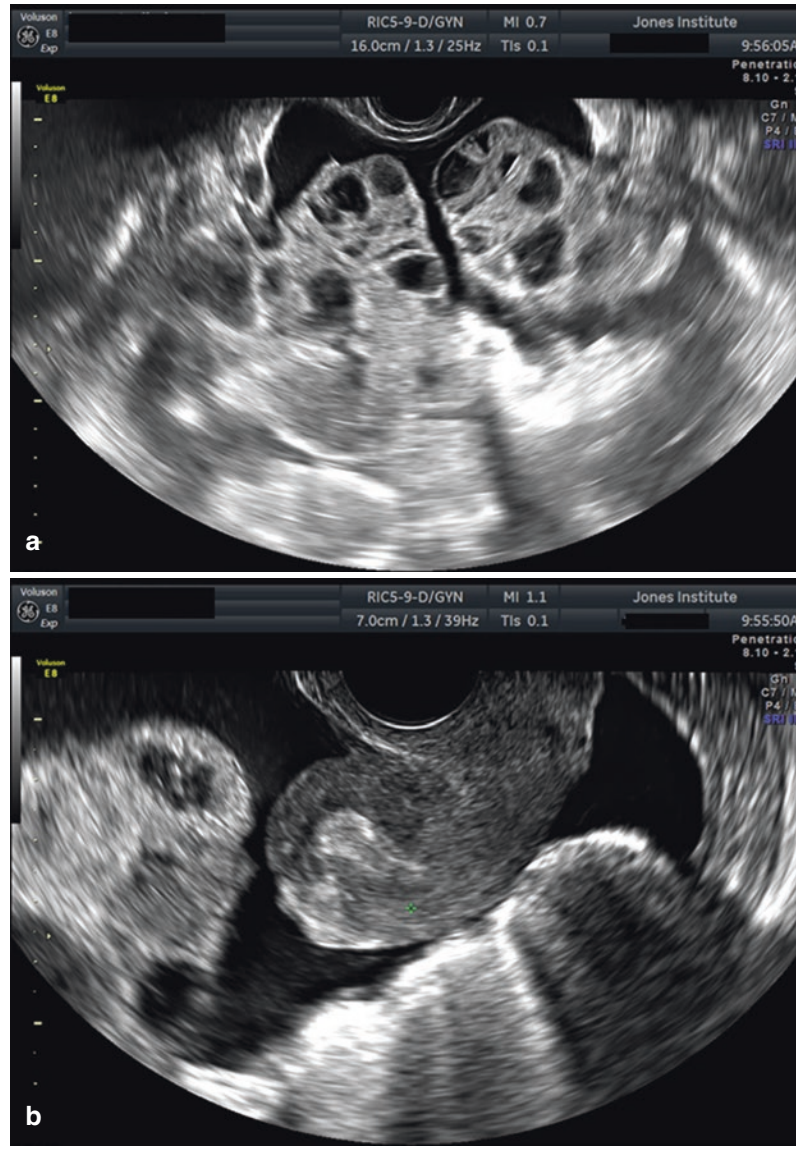

Fig. 19.4 (**a**) Ultrasound of moderate OHSS with ascites. (**b**) Ultrasound of ascites in the cul-de-sac with severe OHSS

0.5% and 5% per IVF cycle. Severe OHSS has been reported to be fatal, so the prompt diagnosis and treatment is paramount [26]. Patients with severe OHSS describe rapid weight gain, significant abdominal distention with inability to fit into usual clothes, shortness of breath, pain which can be refractory to oral medications, oliguria, and severe and unrelenting nausea or emesis with inability to tolerate oral intake. Clinical findings include all of the features of moderate OHSS plus clinical ascites, sonographic ascites, ultrasound evidence of pleural effusions, and serum laboratory abnormalities such as hemoconcentration, coagulopathy, electrolyte imbalance, and renal and hepatic dysfunction or failure [27].

Current research indicates that the fluid shifts which occur in OHSS are directly caused by increased VEGF. VEGF leads to increased vascular permeability, reduced colloid osmotic gradient, and spillage of fluid out of the vascular compartment and into the extravascular spaces

[28]. These fluid shifts can be identified sonographically, and it is recommended that in the evaluation of the patient suspected to have moderate or severe OHSS, ultrasound should be used to check for abdominal ascites or pleural effusions. Generally, the volume of accumulated fluid is not subtle and can easily be identified either through abdominal or vaginal ultrasound or ultrasound of the lung bases. The third spacing of fluid into the peritoneal and pleural cavities leads to respiratory compromise, hypotension, increased intra-abdominal pressure, and renal compromise related to decreased perfusion [29].

The hemoconcentration and resultant hypercoagulability of severe OHSS can lead to venous and arterial thromboembolism both in the typical locations such as lower extremities and lungs and in sites which seem more specific to OHSS such as the subclavian and internal jugular vessels. It is unclear why thrombosis may be localized to the neck rather than the lower extremities; some have hypothesized that increased peritoneal fluid containing inflammatory mediators drains into the thoracic duct and directly into the subclavian veins, possibly locally increasing coagulation at those sites [30]. Rova et al. evaluated the risk of venous thromboembolism in all IVF cycles and particularly in the subset complicated by OHSS [30]. They found that the incidence of venous thromboembolism from the time of the IVF cycle into the first trimester of pregnancy was 0.17% (32 out of 19,194 patients), which was a tenfold increase over the background risk in spontaneous conceptions. Furthermore, in patients diagnosed with OHSS, the risk of venous thromboembolism was 1.4% (19/1272), a 100-fold increase. Given this markedly increased risk, Doppler studies to evaluate for thromboembolism are a critical part of the evaluation of the patient with suspected moderate or severe OHSS. Even if thrombosis is not identified, it is generally recommended to initiate prophylactic anticoagulation in hemoconcentrated patients with heparin or low molecular weight heparin when the hematocrit is found to be 45–50% in order to mediate this risk [31].

Ultrasound in the Management and Treatment of Ovarian Hyperstimulation Syndrome

Timely and accurate diagnosis of OHSS facilitates proactive management and treatment. The management strategy varies in the literature, from some authors recommending immediate hospitalization upon the diagnosis of moderate or severe OHSS to others advocating active outpatient treatment. Regardless of the location, ultrasound is critical in the management and treatment of OHSS. Sonographic monitoring can determine decrease in volume of abdominal ascites which would indicate improving disease. Ultrasound-guided transabdominal and transvaginal paracentesis have been shown to markedly improve patient symptoms of OHSS and avoid the need for hospitalization. Ultrasound-guided placement of pigtail catheters has been used in the past for continuous drainage of ascites. Thoracentesis to drain pleural effusions is also aided by ultrasound guidance [22]. By fully and accurately using ultrasound, clinicians can optimize the care of patients with this serious complication.

OHSS can be diagnosed early or late in the IVF process, either during initial ovarian stimulation with gonadotropins, around the time of the oocyte retrieval, or, more commonly, 1–2 weeks following embryo transfer when the serum beta human chorionic gonadotropin (*B*-hCG) begins to rise. "Early" OHSS generally presents 3–7 days after the hCG trigger shot, while "late" OHSS occurs 12–17 days after the hCG trigger [32]. When OHSS is identified early during IVF treatment, generally ultrasound is used to monitor the progression of ascites and in conjunction with clinical assessment of the patient's stability, a determination made about the safety of proceeding with embryo transfer. If the risks of embryo transfer are felt to exceed the benefits, then one of a number of strategies can be employed including cycle cancellation with withholding of the hCG trigger, decreased hCG trigger dosing, agonist trigger, and cryopreservation of all embryos [21]. The data on the effectiveness of any of these strategies is mixed. The most

effective preventative technique is unquestionably outright cycle cancellation.

If the IVF cycle proceeds and embryo transfer is performed, then OHSS may develop within a few days to a few weeks of the embryo transfer. It is clear that in the case of pregnancy, OHSS is perpetuated by placental *B*-hCG and can become both more severe and of longer duration than if pregnancy does not occur. When there is concern for OHSS, the first step is clear communication about symptoms between the patient and the IVF staff. Early urgent clinic visits for evaluation of the stage of OHSS are extremely important for active management. If in the course of evaluation abdominal ascites is identified, transabdominal or transvaginal paracentesis with ultrasound guidance can lead to dramatic improvement in patient symptoms.

Paracentesis is not a new treatment for OHSS. It was first described by Rabau et al. in 1967, and since that time, many authors have proposed active use of both transabdominal and transvaginal ultrasound-guided paracenteses in patients with OHSS [33]. The idea for paracentesis in OHSS actually originated in the care of other patients with ascites: cirrhotic patients who underwent large-volume paracentesis when they became refractory to diuretics [34, 35]. In these cirrhotics, when at least 750 mL of ascitic fluid was removed, intra-abdominal pressure decreased, venous return improved, and renal perfusion improved. Distinct from the situation with cirrhosis, in patients with OHSS, there also appears to be a compounded therapeutic effect of the direct removal of inflammatory and vasoactive substances from the peritoneal cavity [36].

Several authors have studied the clinical consequences of paracentesis in patient with OHSS. Universally, there has been identified to be improvement in hemodynamic parameters such as uterine and renal artery perfusion [37]. These changes then lead to cardiovascular stabilization, improvement in oliguria, improved respiratory function, and dramatic relief from abdominal distention and pain. Paracentesis can be performed via a transabdominal or transvaginal approach, depending on the available equipment and the familiarity of the operator. The original reports of paracentesis described a transabdominal approach using ultrasound guidance, but more recent reports have focused on transvaginal paracentesis. Enthusiastic proponents of transvaginal paracentesis tout the ease and similarity to the technique of transvaginal oocyte retrieval, ability to perform the procedure on an outpatient basis, and improved patient pain and tolerance to the procedure [31, 38, 39]. In general, the procedure for transvaginal ultrasound-guided paracentesis starts with minimal intravenous (IV) sedation. It can be done with the injection of local anesthesia in the vaginal fornices using a spinal needle, but generally patient comfort is improved with light sedation. The vagina is cleansed with povidone-iodine (Betadine), and then a no. 17 egg retrieval needle is affixed to conventional operating room suction tubing and attached to wall suction. The suction can be set at any pressure; generally 200 mm Hg speeds the procedure. A vaginal ultrasound probe with a standard needle guide is then inserted and the posterior cul-de-sac with dependent ascites visualized. It is often helpful to place the patient in reverse Trendelenburg position in order to allow gravity to assist with ascites pooling. Under direct ultrasound visualization, the egg retrieval needle is advanced into the deepest pocket of ascites, taking care to avoid vital structures including the cervix, uterus, bowel, and vessels. Wall suction is activated and ascitic fluid drained. Paracentesis is continued until the fluid is identified to be maximally removed. There is no particular limit to the amount of ascites which may be aspirated. Generally, we limit the volume to <5 liters of fluid per paracentesis given the hemodynamic changes which can occur, but larger volume paracenteses have been reported.

In the largest series evaluating outpatient management of severe OHSS using transvaginal paracentesis, we identified 183 patients with OHSS presenting between 1999 and 2007 [31]. During this time frame, 96 patients with OHSS underwent 146 outpatient transvaginal paracenteses. Of these patients, 36% (35/96) required two paracenteses, 8% (8/96) required three

paracenteses, 3% (3/96) required a fourth procedure, and 1 patient underwent five transvaginal paracenteses until OHSS symptoms resolved and ascitic fluid no longer accumulated leading to clinical symptoms. The mean volume of ascites aspirated was 2155 mL (range 500–4500 mL). There were no procedure-related complications and no instances of pregnancy loss in this group. The use of aggressive outpatient transvaginal paracentesis not only decreased the need for hospitalization but was also associated with a decreased hospital stay in cases when hospitalization was required [31].

Other uses of ultrasound in the management of OHSS have included ultrasound-guided drainage with autotransfusion of ascitic fluid as well as transabdominal and transvaginal attempts at pigtail catheter placement for continuous drainage of ascites. In 1992 Aboulghar et al. reported three patients with OHSS who underwent transvaginal aspiration of ascites which was then autotransfused [40]. They described rapid improvements in hematologic parameters and improved clinical symptoms. Another group in Japan also described reinfusion of ascitic fluid in two patients in 1994 [41]. In that report, ascites was removed, underwent ultrafiltration, and was then reinfused, leading to resolution of the severe OHSS. Subsequent reports moved away from autotransfusion and transitioned to the placement of pigtail catheters for continuous ascites drainage. In 2003, Abuzeid et al. reported transabdominal-guided placement of an abdominal pigtail catheter which was left in place until ascitic fluid ceased to drain [42]. In that report, 26 patients with severe OHSS were identified. Half (13) underwent placement of a pigtail catheter, and the other half were hospitalized without intervention. They described the placement of a 6-0 French, 2-mm pigtail catheter through the abdominal wall into the largest pocket of ascitic fluid under continuous abdominal ultrasound guidance. The catheter was then attached to a drainage bag and left in place until ascites resolved. In those patients who underwent ultrasound-guided pigtail catheter placement, the catheter was left in place for an average of 12–13 days, and mean amount of ascites drained was 11 L. There were no documented infections and no impact on the pregnancy rates between the two groups. The authors concluded that pigtail catheter placement was safe and effective and could be an alternative to multiple paracenteses in patients with severe OHSS. Another group tested the efficacy of transvaginal pigtail catheter placement for continuous ascites drainage [43]. They reported on one patient with severe OHSS, obesity, and generalized edema who had an extremely thick abdominal wall (15 cm) which limited ultrasound visualization of both ascites and internal organs. She therefore had an Oosterlinck drainage catheter placed vaginally and left in place for continuous drainage for a total of 4 days. A total of 17.45 liters of ascites were drained over this time frame, and she was ultimately discharged to home in good condition without complications. The investigators concluded that ultrasound-guided transvaginal pigtail catheter placement was an alternative to the transabdominal approach when body habitus limits abdominal visualization.

The final way in which ultrasound may be used in the management and treatment of OHSS is to assist with thoracentesis in the case of severe OHSS with pulmonary compromise and pleural effusions. Similar to the case of abdominal ascites, protein-poor fluid can accumulate in the pleural cavity and lead to problems due to restriction of diaphragm movement, restriction of lung expansion with collapse of pulmonary parenchyma, poor ventilation, and shunting [44]. It is estimated that pleural effusions occur in about 10% of patients with severe OHSS. Chest x-ray (CXR) is the typical imaging modality used to diagnose pleural effusions, with ultrasound used to guide needle placement for thoracentesis as in the case of paracentesis. Abramov et al. in 1999 evaluated 2902 patients with OHSS between 1987 and 1996, 209 of whom were diagnosed with severe OHSS [44]. They characterized the pulmonary findings in these patients and the required interventions. Not surprisingly, 92.3% (193) presented with dyspnea and 71% had bilaterally elevated diaphragms on CXR. Almost a third (29%) were diagnosed with pleural effusions on CXR, right lung > left lung, and 13% underwent thoracentesis. The

hypothesis for the laterality of pleural effusions which seem to favor the right lung is that in the face of massive ascites, diaphragmatic lymphatics channel the fluid to the right pleural space via the thoracic duct. Man et al. also investigated pleural effusions in four patients with severe OHSS [45]. They characterized the location and volume of the fluid drained. Interestingly, 3/4 patients presented with right-sided pleural effusions. All ultimately underwent thoracentesis secondary to pulmonary symptoms, and a total of 1200–2000 mL was drained. Finally, isolated pleural effusions in the absence of abdominal ascites or other signs or symptoms of OHSS have been reported [46]. Mullin et al. in 2011 reported symptomatic isolated pleural effusion as a sole manifestation of OHSS. They note that isolated pleural effusions in severe OHSS occur with an incidence of 0.65%. The two patients reported both underwent therapeutic thoracentesis with resolution of dyspnea. Therefore, in patients with OHSS and clinical evidence of pulmonary compromise, pleural effusions should be actively sought and treated. It should not be simply assumed that dyspnea is attributable to abdominal distension from ascites and compression of the lung bases since pleural effusions are found in approximately 10–30% of patients with severe OHSS and may require treatment with thoracentesis.

In conclusion, ultrasound plays important roles in the prevention, diagnosis, and treatment of OHSS. By fully and accurately using ultrasound, clinicians can be proactive in the evaluation and management of this severe iatrogenic complication of ovulation induction. By using ultrasound to determine AFC, diagnose PCOS, and monitor follicle development during gonadotropin stimulation, clinicians may anticipate the risk of OHSS and modulate the IVF treatment plan. If clinically suspected, ultrasound is key to speedy diagnosis of OHSS into mild, moderate, or severe disease. Once OHSS is found to occur, ultrasound guidance for transabdominal or transvaginal paracentesis, sonographic monitoring for improvement in ascites, and ultrasound assistance for thoracentesis will improve patient symptoms and lessen hemodynamic, pulmonary, and renal compromise and may avoid the need for hospitalization.

References

1. Papanikolaou EG, Humaidan P, Polyzos NP, Tarlatzis B. Identification of the high-risk patient for ovarian hyperstimulation syndrome. Semin Reprod Med. 2010;28(6):458–62.
2. Kwee J, Elting ME, Schats R, McDonnell J, Lambalk CB. Ovarian volume and antral follicle count for the prediction of low and hyper-responders with in vitro fertilization. Reprod Biol Endocrinol. 2007;5:9.
3. Ocal P, Sahmay S, Cetin M, Irez T, Guralp O, Cepni I. Serum anti-mullerian hormone and antral follicle count as predictive markers of OHSS in ART cycles. J Asst Reprod Genet. 2011;28:1197–203.
4. Broer SL, Dolleman M, Opmeer BC, Fauser BC, Mol BW, Broekmans FJM. AMH and AFC as predictors of excessive response in controlled ovarian hyperstimulation: a meta-analysis. Hum Reprod Update. 2011;17(1):46–54.
5. Broekmans FJM, de Ziegler D, Howles CM, Gougeon A, Trew G, Oliviennes F. The antral follicle count: practical recommendations for better standardization. Fertil Steril. 2010;94(1):044–51.
6. Rombauts LR, Onwude JL, Chew HW, Vollenhoven BJ. The predictive value of antral follicle count remains unchanged across the menstrual cycle. Fertil Steril. 2011;96(6):1,514–8.
7. Mavrelos D, Al Chami A, Talaulikar V, Burt E, Webber L, Ploubidis G, Yasmin E. Variation in antral follicle count at different times in the menstrual cycle: does it matter? Reprod Biomed Online. 2016;33:174–9.
8. Papanikolaou EG, Pozzobon C, Kolibianakis EM, Camus M, Tournaye H, Fatemi HM, Van Steirteghem AV, Devroey P. Incidence and prediction of ovarian hyperstimulation syndrome in women undergoing gonadotropin-releasing hormone antagonist in vitro fertilization cycles. Fertil Steril. 2006;85(1):112–20.
9. Tarlatzi TB, Enetis CH, Devreker F, Englert Y, Delbaere A. What is the best predictor of severe ovarian hyperstimulation syndrome in IVF? A cohort study. J Asst Reprod Genet. 2017;34(1):341–51.
10. Humaidan P, Quartarolo J, Papanikolaou EG. Preventing ovarian hyperstimulation syndrome: guidance for the clinician. Fertil Steril. 2010;94(2):389–400.
11. Rotterdam ESHRE/ASRM-Sponsored PCOS Consensus Workshop Group. Revised 2003 consensus on diagnostic criteria and long-term health risks related to polycystic ovary syndrome. Fertil Steril. 2004;81(1):19–25.
12. Danninger B, Brunner M, Obruca A, Feichtinger W. Prediction of ovarian hyperstimulation syndrome of baseline ovarian volume prior to stimulation. Hum Reprod. 1996;11(8):1,597–9.

13. Moohan JM, Curcio K, Leoni M, Healy D, Hurley V. Low intraovarian vascular resistance: a marker for severe ovarian hyperstimulation syndrome. Fertil Steril. 1997;67(4):728–32.
14. Agrawal R, Conway G, Sladkevicius P, Tan SL, Engmann L, Payne N, Bekir J, Campbell S, Jacobs H. Serum vascular endothelial growth factor and Doppler blood flow velocities in in vitro fertilization: relevance to ovarian hyperstimulation syndrome and polycystic ovaries. Fertil Steril. 1998;70(4):651–8.
15. Jayaprakasan K, Jayaprakasan R, Al-Hasie HA, Clewes JS, Campbell BK, Johnson IR, Raine-Fenning NJ. Can quantitative three-dimensional power Doppler angiography be used to predict ovarian hyperstimulation syndrome? Ultrasound Obstet Gynecol. 2009;33:583–91.
16. Practice Committee of the American Society for Reproductive Medicine. Prevention and treatment of moderate and severe ovarian hyperstimulation syndrome: a guideline. Fertil Steril. 2016;106(7):1634–47.
17. Pilsgaard F, Grynnerup AG-A, Loessl K, Bungum L, Pinborg A. The use of anti-Mullerian hormone (AMH) for controlled ovarian stimulation in assisted reproductive technology and for fertility assessment and counseling. Acta Obstetric Gynecol Scand. 2018;97:1105. https://doi.org/10.1111/aogs.13334.
18. Lee TH, Liu CH, Huang CC, Wu YL, Shih YT, Ho HN, et al. Serum anti-Mullerian hormone and estradiol levels are predictors of ovarian hyperstimulation syndrome in assisted reproduction technology cycles. Hum Reprod. 2008;23:160–7.
19. Kahnberg A, Enskog A, Brannstrom M, Lundin K, Bergh C. Prediction of ovarian hyperstimulation syndrome in women undergoing in vitro fertilization. Acta Obstet Gynecol Scand. 2009;88:1,373–81.
20. Steward RG, Lan L, Shaa AA, Yeh JH, Price TM, Goldfarb JM, et al. Oocyte number as a predictor for ovarian hyperstimulation syndrome and live birth: an analysis of 256,381 in vitro fertilization cycles. Fertil Steril. 2014;101:967–73.
21. Alper MM, Smith LP, Sills ES. Ovarian hyperstimulation syndrome: current views on pathophysiology, risk factors, prevention, and management. J Exp Clin Asst Reprod. 2009;6:3.
22. Practice Committee of the American Society for Reproductive Medicine. Ovarian hyperstimulation syndrome. Fertil Steril. 2008;90(3):S188–93.
23. Whelan JG, Vlahos NF. The ovarian hyperstimulation syndrome. Fertil Steril. 2000;73(5):883–96.
24. Grossman LC, Michalakis KG, Browne H, Payson MD, Segars JH. The pathophysiology of ovarian hyperstimulation syndrome: an unrecognized compartment syndrome. Fertil Steril. 2010;94(4):1392–8.
25. Gunabushanam G, Mandal K, Lal S. Hemoperitoneum from ruptured cyst in a hyperstimulated ovary: a sonographic mimic of ovarian hyperstimulation syndrome. J Clin Ultrasound. 2007;35(5):281–3.
26. Brinsden PR, Wada I, Tan SL, Balen A, Jacobs HS. Diagnosis, prevention, and management of ovarian hyperstimulation syndrome. Br J Obstet Gynecol. 1995;102:767–72.
27. Rizk B, Aboulghar M. Modern management of ovarian hyperstimulation syndrome. Hum Reprod. 1991;6(1):082–7.
28. Tollan A, Holst N, Forsdahl F, Fadnes HO, Oian P, Maltau JM. Transcapillary fluid dynamics during ovarian stimulation for in vitro fertilization. Am J Obstet Gynecol. 1990;162:554–8.
29. Scheppach W. Abdominal compartment syndrome. Best Pract Res Clin Gastroent. 2009;23:25–33.
30. Rova R, Passmark H, Lindqvist PG. Venous thromboembolism in relation to in vitro fertilization: an approach to determining the incidence and increase in risk in subsequent cycles. Fertil Steril. 2012;97(1):95–100.
31. Smith LP, Hacker MR, Alper MM. Patients with severe ovarian hyperstimulation syndrome can be managed safely with aggressive outpatient transvaginal paracentesis. Fertil Steril. 2009;92:1953–9.
32. Mathur RS, Akande AV, Keay SD, Hunt LP, Jenkins JM. Distinction between early and late ovarian hyperstimulation syndrome. Fertil Steril. 2000;73(5):901–7.
33. Rabau E, David A, Serr DM, Mashiach S, Lunenfeld B. Human menopausal gonadotropin for anovulation and sterility. Am J Obstet Gynecol. 1967;98:92–8.
34. Cabrera J, Falcon L, Gorriz E, Pardo MD, Granados R, Quinones A, Maynar M. Abdominal decompression plays a major role in early post paracentesis hemodynamic changes in cirrhotic patients with tense ascites. Gut. 2001;48:384–9.
35. Forouzandeh B, Konicek F, Sheagren JN. Large-volume paracentesis in the treatment of cirrhotic patients with refractory ascites: the role of postparacentesis volume expansion. J Clin Gastroenterol. 1996;22:207–10.
36. Delbaere A, Bergmann PJ, Gervy-Decoster C, Staroukine M, Englert Y. Angiotensin II immunoreactivity is elevated in ascites during severe ovarian hyperstimulation syndrome: implications for pathophysiology and clinical management. Fertil Steril. 1994;62:731–7.
37. Chen C-D, Yang J-H, Chao K-H, Chen S-U, Ho H-N, Yang Y-S. Effects of repeated abdominal paracentesis on uterine and intraovarian haemodynamics and pregnancy outcome in severe ovarian hyperstimulation syndrome. Hum Reprod. 1998;13(8):2077–81.
38. Fluker MR, Copeland JE, Yuzpe AA. An ounce of prevention: outpatient management of the ovarian hyperstimulation syndrome. Fertil Steril. 2000;73(4):821–4.
39. Aboulghar MA, Mansour RT, Serour GI, Amin Y. Ultrasonically guided vaginal aspiration of ascites in the treatment of ovarian hyperstimulation syndrome. Fertil Steril. 1990;53:933–5.
40. Aboulghar MA, Mansour RT, Serour GI, Riad R, Ramzi AM. Autotransfusion of the ascitic fluid in the treatment of severe ovarian hyperstimulation syndrome. Fertil Steril. 1992;58(5):1056–9.
41. Fukaya T, Chida S, Terada Y, Funayama Y, Yajima A. Treatment of severe ovarian hyperstimulation

syndrome by ultrafiltration and reinfusion of ascitic fluid. Fertil Steril. 2004;61(3):561–4.
42. Abuzeid MI, Nassar Z, Massaad Z, Weiss M, Ashraf M, Fakih M. Pigtail catheter for the treatment of ascites associated with ovarian hyperstimulation syndrome. Hum Reprod. 2003;18(2):370–3.
43. Raziel A, Friedler S, Schachter M, Strassgurger D, Bukovsky I, Ron-El R. Transvaginal drainage of ascites as an alternative to abdominal paracentesis in patients with severe ovarian hyperstimulation syndrome, obesity, and generalized edema. Fertil Steril. 1998;69(4):780–3.
44. Abramov Y, Elchalal U, Schenker JG. Pulmonary manifestations of severe ovarian hyperstimulation syndrome: a multicenter study. Fertil Steril. 1999;71(4):645–51.
45. Man A, Schwarz Y, Greif J. Pleural effusion as a presenting symptom of ovarian hyperstimulation syndrome. Eur Respir J. 1997;10:2425–6.
46. Mullin CM, Fino ME, Reh A, Grifo JA, Licciardi F. Symptomatic isolated pleural effusion as an atypical presentation of ovarian hyperstimulation syndrome. Case Rep Obstet Gynecol. 2011;. ; Epub 2011 Aug 7.;2011:1.

Ultrasound Guidance in Embryo Transfer

20

Alberto Revelli, Tomer Tur-Kaspa, and Edmond Confino

Introduction

High-resolution, high-frequency transvaginal US has become an integral part of infertility evaluation and follicular growth monitoring during controlled ovarian stimulation (COS), as well as the method of choice to achieve an efficient and rapid oocyte harvesting [1, 2].

Embryo transfer (ET) is a more difficult procedure to master than oocyte retrieval and more profoundly affects IVF outcome. In fact, the type of catheter [3], the operator's experience [4], the site of embryo discharge [5–8], the catheter tip contamination with mucus or blood [9], the presence of uterine contractions, and the difficulty to pass through the cervix [10–12] have all been regarded as factors potentially affecting IVF results.

For several years, ET was performed inserting the catheter into the cervix and blindly discharging the embryos approximately in the middle of the uterine cavity ("clinical touch" ET (CTET)). While today US is routinely used for it, pre-IVF evaluation of the uterine and cervical anatomy was previously performed by using hysterosalpingography (HSG), magnetic resonance imaging (MRI), and/or computerized tomography (CT) (Figs. 20.1, 20.2, and 20.3). US availability and ease of performance have made sonohysterography (HSN) (see Chap. 12) the preferred and cost-effective visualization method of the uterus prior to ET [13, 14]. The so-called mock ET was sometimes performed some days in advance in order to predict the conditions that would have been found during ET, but its predictive accuracy resulted to be quite poor [15, 16]; pre-ET US measurement of the cervical uterine depth could verify the mock transfer data but still was a poor predictor of ET success (Fig. 20.3). Routine US use before, during, and post ET has now largely eliminated the discordance between mock ET and live ET [17].

In 1985, Strickler [18] was the first to describe the use of US to guide ET. Since then, US guidance has gradually been added to achieve an atraumatic, controlled, quick, and anatomically defined ET. Indeed US guidance allows for better control of the cervical trajectory and the uterine depth, as well as to more precisely define the site of embryo replacement. Transabdominal US allows for the visualization of the catheter tip in real time, and both transabdominal and transvaginal techniques allow physicians and patients to see an echogenic spot inside the uterus immedi-

A. Revelli
Sant'Anna Hospital, University of Turin, Department of Obstetrics and Gynecology, Turin, Italy

T. Tur-Kaspa (✉)
Wesleyan University, Middletown, CT, USA

E. Confino
Feinberg School of Medicine, Northwestern University, Chicago, IL, USA

L. A. Stadtmauer, I. Tur-Kaspa (eds.), *Ultrasound Imaging in Reproductive Medicine*,
https://doi.org/10.1007/978-3-030-16699-1_20

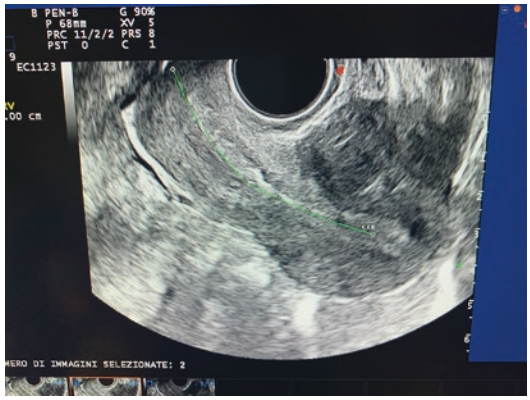

Fig. 20.1 Pre-ET vaginal measurement of cervical-fundal distance allows to calculate the site of embryo discharge

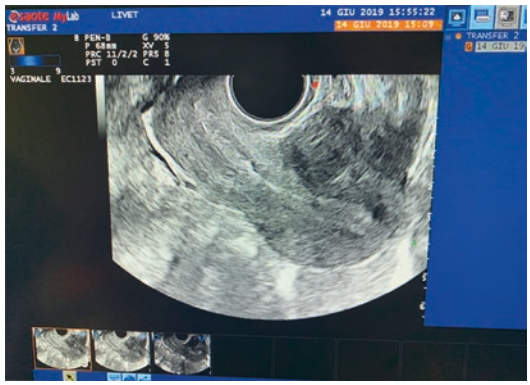

Fig. 20.2 The mock transfer catheter is placed reaching the site of embryo discharge

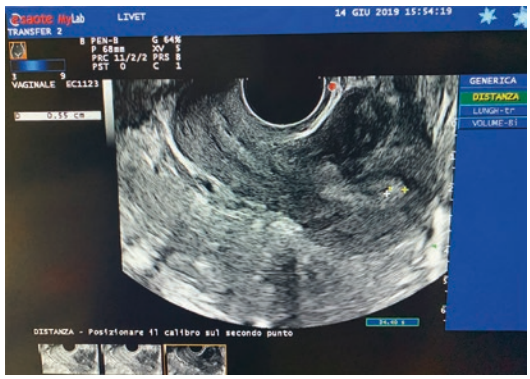

Fig. 20.3 A hyper-echogenic spot (bubble) after embryo discharge indicates the place where the embryo has been transferred

ately after embryo discharge, giving a rather precise esteem of embryo position after ET.

Several prospective, randomized controlled trials (RCTs) and meta-analyses have been performed to compare CTET to US-guided ET and concluded that US guidance significantly increases the rate of easy transfers, ultimately improving the clinical pregnancy rate and the chance of a live birth [19–25].

This chapter will review the data available today on the important role of US in ET.

Clinical Touch ET Versus Transabdominal US-Guided ET

Several RCTs and systematic reviews compared the results obtained using the "blind" clinical touch embryo transfer (CTET) technique with those of the transabdominal US-guided transfer [19–25]. The main outcomes, being implantation rate, clinical pregnancy rate, and live birth rate, of IVF after clinical touch ET were compared to those after US-guided ET. In addition, other parameters were investigated: miscarriage rate, multiple and ectopic pregnancy rate, rate of difficult or failed transfers, need for instrumental assistance during ET (e.g., stylette, tenaculum, dilatation), signs of cervical or endometrial trauma (e.g., presence of blood, mucus, or both on the catheter tip), and percentage of retained embryos. Most RCTs and meta-analysis concluded that US guidance improves the chances of clinical pregnancy and live birth compared to the clinical touch method [19–25].

The presence of blood on the catheter tip that is associated with decreased implantation, clinical pregnancy, and live birth rates, when compared to no blood, appeared to be less frequent when performing ET under US guidance, as it was much easier to avoid unwillingly touching the fundus of the uterine cavity [26]. Furthermore, allowing visualization of the cervical canal, US guidance reduced unrecognized events such as 180° curling of the inner catheter and cervical deposition of the embryos, the need

for instrumental assistance, and the failure to transfer with the assigned catheter. US guidance makes the ET procedure easier to perform, thus it significantly decreases the rate of diffuclt transfers [27]. Differently, adding US guidance had no significant effect on finding mucus on the catheter tip, on the percentage of transfer with retained embryos, and on the rate of multiple pregnancy, ectopic pregnancy, and spontaneous miscarriage [19–25].

There are at least two mechanisms by which US-guided ET may improve ART outcome: the full bladder needed for transabdominal US straightens the angle between the cervix and the uterus, and by confirming the position of the catheter tip, the embryo is discharged close to the desired site. The optimal area of embryo deposition in the uterine cavity, resulting in higher PR, has been demonstrated to be between 1.0 and 1.5 cm from the fundus of the cavity [7–9].

US guidance may also allow physicians to perform, in the infrequent occasion when catheter access into the uterus is impossible, a transmyometrial ET (Fig. 20.4) which is performed under conscious sedation using a coaxial needle outfitted with a matching ET catheter [28, 29]; this technique abolishes the need of an unplanned laparoscopic intratubal ET.

The use of transabdominal US during ET also has some disadvantages vs. CTET: (1) US equipment and a second operator (physician, nurse, or a technician) with adequate training in transabdominal US are needed, increasing the overall cost; (2) visualization of the catheter tip might be suboptimal in overweight patients or in a patient with a retroverted uterus—moving the catheter back and forth inside the uterus may be needed to better identify its position, but this may potentially damage the endometrium; (3) the time needed to perform ET is longer with US guidance than with CTET; (4) the patient must keep a full bladder for some time, and this may cause discomfort and cramping, possibly severe if a delay occurs for any reason; and (5) the patient's discomfort, in turn, may stimulate uterine contractions. Moreover, some physicians prefer CTET to minimize the need to observe the cervix and the US screen simultaneously.

Transvaginal Versus Transabdominal US Guidance for ET

The use of transvaginal US to guide ET (TVET) was proposed claiming that it could be preferable vs. transabdominal-guided ET in some patients (overweight or with uterine retroversion), more tolerable (no need of a full bladder), and more convenient (single operator needed) [30, 31]. Indeed, TVET could potentially have some advantages. It does not require a full bladder, allows an optimal detection of the utero-cervical angle even in case of uterine retroversion or overweight patients, and can visualize the catheter tip better than transabdominal US. On the other side, however, it might be difficult for the physician since it requires manual skills to be performed simultaneously by a single operator and can be uncomfortable for the patient because of the necessity to insert the US vaginal probe into the vagina while the speculum is still in place. Then the outer part of the transfer catheter will be inserted into the cervix, and the speculum will be removed while maintaining the probe in the vagina. The final step is inserting the softer part of the catheter, loaded with the embryo(s), and performing the ET under TVUS.

A couple of retrospective studies reported significantly better IVF outcome using TVET vs. CTET [32, 33], and two RCTs comparing TVET vs. transabdominal-guided ET reported comparable clinical pregnancy and implantation rates [34, 35] but were underpowered to reach convincing conclusions. While the duration of the procedure was observed to be significantly longer with TVET, it was associated with increased patient comfort due to the absence of bladder distension.

A simpler variant of TVET was recently proposed: transvaginal US is used just before ET in order to measure the uterine length and calcu-

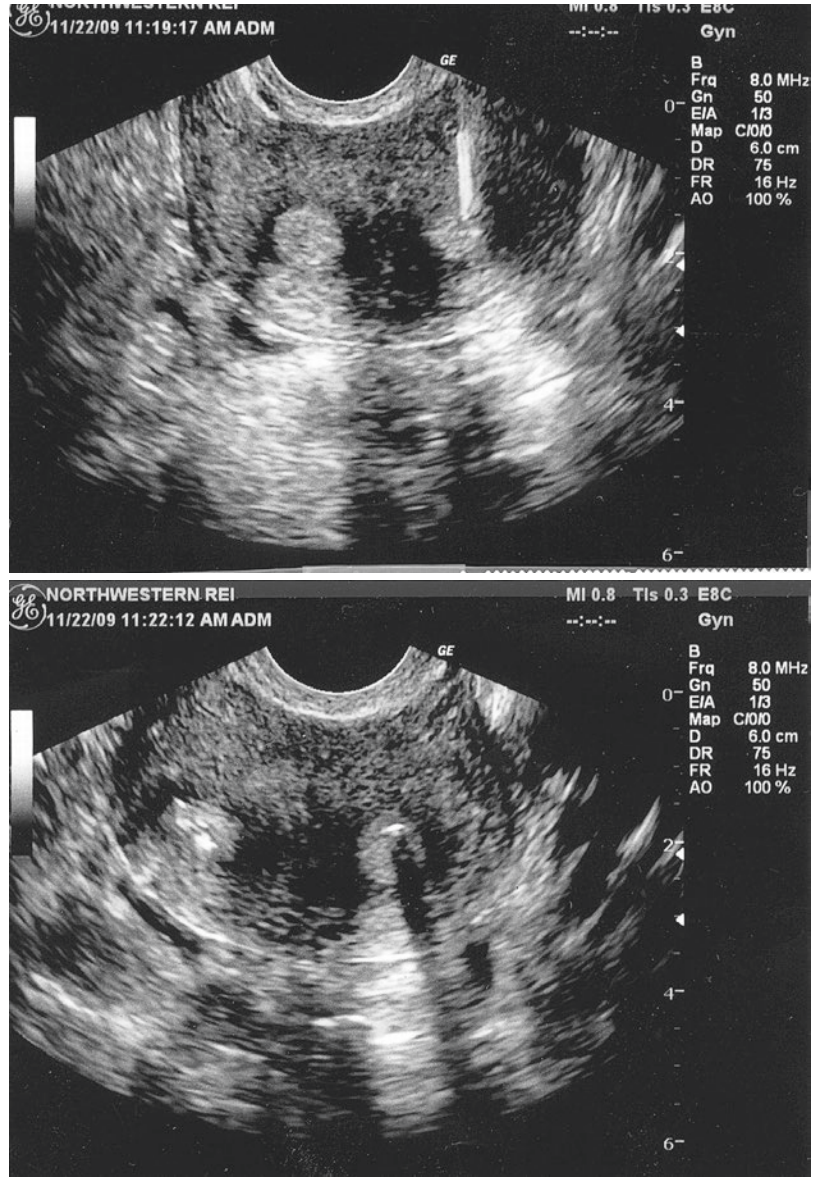

Fig. 20.4 Vaginal US-guided transmyometrial needle placement in a partially fused bicornuate uterus (upper figure right). Bubble markers are present in both right and left uterine horns depicting proper bilateral placement of one embryo in each uterine cavity (lower figure)

late the optimal site for embryo discharge; then, a clinical touch ET is performed, guiding the embryo-loading cannula to the previously calculated discharge site [36–39]. The uterine length measurement followed by CTET was already reported to obtain the same IVF outcome as transabdominal-guided ET in a retrospective study using historical controls [36]. The equivalence of the two methods was also observed in a small RCT [37], whereas another larger randomized trial (200 patients) showed slightly higher implantation and pregnancy rates in the group receiving CTET with previous uterine length measurement [38]. The largest RCT [39], that was designed as a non-inferiority trial and adequately powered to detect a clinically relevant difference in IVF outcome, demonstrated that using uterine length measurement

followed by CTET resulted in a similar implantation rate and clinical and ongoing pregnancy rates compared to transabdominal-guided ET. Moreover, the former technique was less time-demanding, more easily performed by a single operator, and standardized between physicians with different manual skills.

Training in Embryo Transfer

US guidance may be successfully applied to teach the transfer technique to young doctors without compromising IVF outcome; it prevents an involuntary touch of the uterine cavity fundus, potentially able to elicit myometrial contractility and reduce the likelihood of embryo implantation.

The post-ET marker bubbles visualized on US verify mid-cavity embryo placement (Fig. 20.5) and allow the physician, patient, and spouse to observe the position of the embryo placement. Although it is likely that embryos move inside the uterine cavity according to fluxes in uterine fluids [40, 41], visualizing marker bubbles on the screens just after ET may be reassuring about a correct embryo discharge. Shah et al. [42] recently demonstrated that the most important factor in learning a correct ET technique obtaining high ET success rates was the actual performing of live ETs rather than practicing US-guided intrauterine inseminations. Also, the clinical experience of the ultrasonographer assisting US-guided ET was observed to have no effect on the clinical outcome [43].

Coaxial catheter US-guided ET approach involves initial placement of an outer catheter in the internal uterine os (Fig. 20.6). The outer catheter protects the inner catheter from mucus exposure and eliminates the need to renegotiate a deviated or a branching cervical canal. In this instance, time is not a limiting factor because the embryos are loaded into the inner catheter, while the outer catheter is already in place. US will then allow ET time to be less than 30 s (Fig. 20.7). US guidance is extremely instructive at training facilities as it can provide feedback and reassurance to physicians in training. Coaxial live ultrasound-guided ET allows for the teaching of ET without a decline in PR.

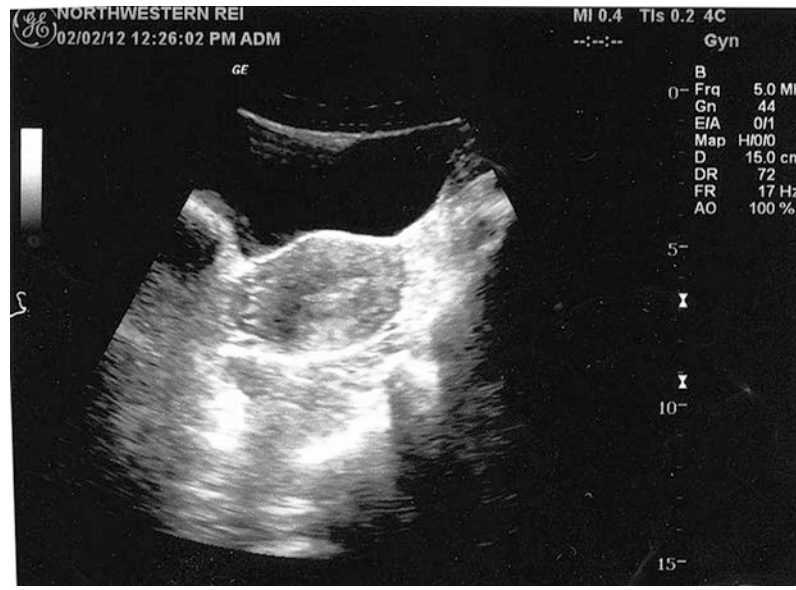

Fig. 20.5 Abdominal US with full bladder depicts two marker bubbles visualized in mid-uterine cavity and confirming a perfect placement of embryos

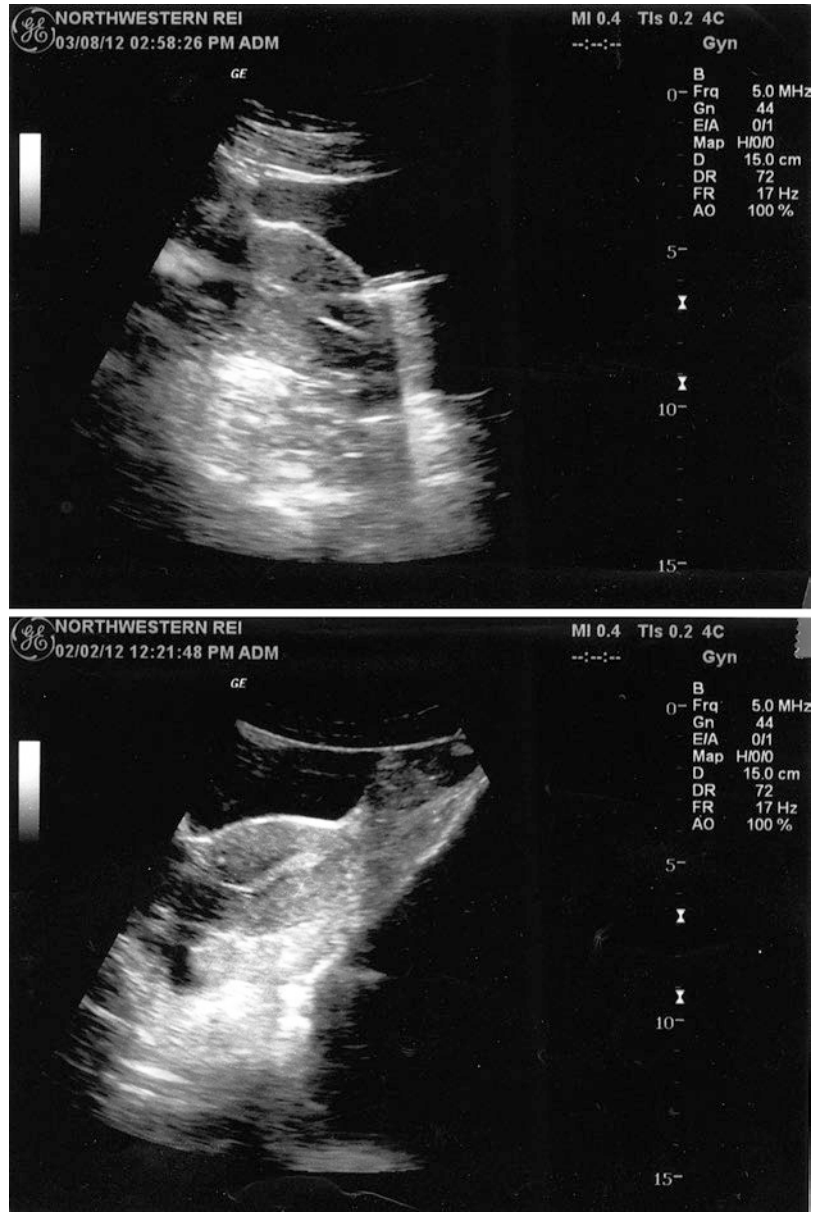

Fig. 20.6 Abdominal US depicts the external coaxial catheter wedged into the endometrium in an anteverted uterus (lower figure). Sliding a rehearsal inner catheter allows proper placement in the lower uterine segment (upper figure)

The American Society for Reproductive Medicine (ASRM) published in 2017 a practice guideline for performing ET, as well as a standard ET protocol template [3, 44]. Based on evidence-based medicine, the ASRM recommends the following steps to improve pregnancy rates: the use of abdominal US guidance for ET, the removal of cervical mucus, the use of a soft catheter for ET, and placing the embryo inside the uterine cavity at least over 1.0 cm from the fundus. In addition, immediate ambulation following ET is also recommended [3, 44]. The ASRM was actively involved in developing an ET simulator which has been shown to improve pregnancy rates and to decrease time to proficiency in training REI fellows [45].

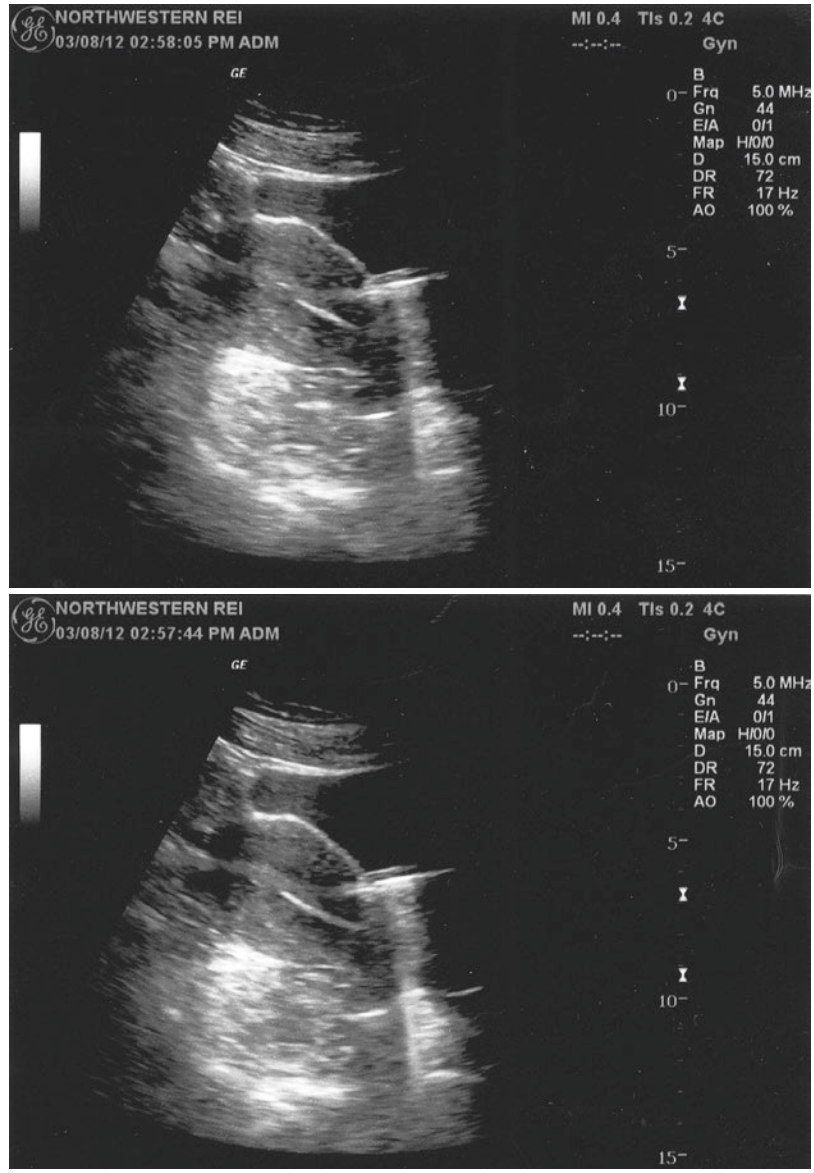

Fig. 20.7 Abdominal US demonstrates that the outer coaxial catheter is withdrawn leaving the inner soft embryo loaded catheter at 1 cm from the uterine fundus (lower figure). Under live US observation, the embryo is injected, and the marker bubble is observed in mid-cavity (upper figure)

Conclusion

Recommendations to get an optimal ET, based on expert opinions, include the performance of a meticulous cervical mucus removal, mid-uterine cavity embryo placement, a slow catheter withdrawal to avoid embryo dragging to the cervix, and a short embryo load to unload time [46–48]. In addition, evidence-based guidelines encourage US guidance in ET as it will result in easier ETs and improved IVF outcome.

US has become an indispensable tool to guide and verify proper embryo deposition in the uterus. Importantly, patients take great comfort in having the ability to visualize on the screen the final step of a difficult process.

The use of US guidance is now an integral part of an ET worldwide. With the improvement in

imaging and the possibility of utilizing 3D and 4D US [49], ultrasound guidance may assist in maximizing the potential for embryo implantation after ET and thus will further improve ART outcome [3].

References

1. Tarlatzis BC, Laufer N, Decherney AH. The use of ovarian ultrasonography in monitoring ovulation induction. J In Vitro Fert Embryo Transf. 1984;1:226–32.
2. Peluso JJ, Damien M, Nulsen JC, Luciano AA. Identification of follicles with fertilizable oocytes by sequential ultrasound measurements during follicular development. J In Vitro Fert Embryo Transf. 1990;7:304–9.
3. Practice Committee of the American Society for Reproductive Medicine. Performing the embryo transfer: a guideline. Fertil Steril. 2017;107:882–96.
4. Uyar A, Bener A, Ciray HN, Bahceci M. Physician experience in performing embryo transfers may affect outcome. Fertil Steril. 2011;95:1860–2.
5. Coroleu B, Barri PN, Varreras O, Martinez F, Parriego M, Hereter L, Parera N, Veiga A, Balasch J. The influence of the depth of embryo replacement into the uterine cavity on implantation rates after IVF: a controlled, ultrasound-guided study. Hum Reprod. 2002;17:341–6.
6. Cenksoy PO, Fıcıcıoglu C, Yesiladali M, Akcin OA, Kaspar C. The importance of the length of uterine cavity, the position of the tip of the inner catheter and the distance between the fundal endometrial surface and the air bubbles as determinants of the pregnancy rate in IVF cycles. Eur J Obstet Gynecol Reprod Biol. 2014;172:46–50.
7. Frankfurter D, Trimarchi JB, Silva CP, Keefe DL. Middle to lower uterine segment embryo transfer improves implantation and pregnancy rates compared with fundal embryo transfer. Fertil Steril. 2004;81:1273–7.
8. Pope CS, Cook EKD, Arny M, Novak A, Grow D. Influence of embryo transfer depth on in vitro fertilization and embryo transfer outcome. Fertil Steril. 2004;81:51–8.
9. Rovei V, Dalmasso P, Gennarelli G, Lantieri T, Basso G, Benedetto C, et al. IVF outcome is optimized when embryos are replaced between 5 and 15 mm from the fundal endometrial surface: a prospective analysis on 1184 IVF cycles. Reprod Biol Endocrinol. 2013;11:114–20.
10. Alvero R, Hearns-Stokes RM, Catherino WH, Leondires MP, Segars JH. The presence of blood in the transfer catheter negatively influences outcome at embryo transfer. Hum Reprod. 2003;18:1848–52.
11. Fanchin R, Righini C, Olivennes F, Taylor S, de Ziegler D, Frydman R. Uterine contractions at time of embryo transfer alter pregnancy rates after in vitro fertilization. Hum Reprod. 1998;13:1968–74.
12. Lesny P, Killick SR, Tetlow RL, Robinson J, Maginess SD. Embryo transfer - can we learn anything from the observation of junctional zone contractions? Hum Reprod. 1998;13:1540–6.
13. Gera PS, Allemand MC, Tatpati LL, Galanits TM, Morbeck D, Coddington CC. Role of saline infusion sonography in uterine evaluation before frozen embryo transfer cycle. Fertil Steril. 2008;89:562–6.
14. Sankpal RS, Confino E, Matzel A, Cohen LS. Investigation of the uterine cavity and fallopian tubes using three-dimensional saline sonohysterosalpingography. Int J Gynaecol Obstet. 2001;73:125–9.
15. Yoldemir T, Erenus M. Does the timing of mock embryo transfer trial improve implantation in intracytoplasmic sperm injection cycles? Gynecol Endocrinol. 2011;27:396–400.
16. Mansour R, Aboulghar M, Serour G. Dummy embryo transfer: a technique that minimizes the problems of embryo transfer and improves the pregnancy rate in human in vitro fertilization. Fertil Steril. 1990;54:678–81.
17. Henne MB, Milki AA. Uterine position at real embryo transfer compared with mock embryo transfer. Hum Reprod. 2004;19:570–2.
18. Strickler RC, Christianson C, Crane JP, Curato A, Knight AB, Yang V. Ultrasound guidance for human embryo transfer. Fertil Steril. 1985;43:54–61.
19. Sallam HN, Sadek SS. Ultrasound-guided embryo transfer: a meta-analysis of randomized controlled trials. Fertil Steril. 2003;80:1042–6.
20. Matorras R, Urquijo E, Mendoza R, Corcostegui B, Exposito A, Rodriguez-Escudero FJ. Ultrasound-guided embryo transfer improves pregnancy rates and increases the frequency of easy transfers. Hum Reprod. 2002;17:1762–6.
21. Abou-Setta AM, Mansour RT, Al-Inany HG, Aboulghar MM, Aboulghar MA, Serour GI. Among women undergoing embryo transfer, is the probability of pregnancy and live birth improved with ultrasound guidance over clinical touch alone? A systemic review and meta-analysis of prospective randomized trials. Fertil Steril. 2007;88:333–41.
22. Brown J1, Buckingham K, Buckett W, Abou-Setta AM. Ultrasound versus 'clinical touch' for catheter guidance during embryo transfer in women. Cochrane Database Syst Rev. 2016;(3):CD006107.
23. Flisser E, Grifo JA. Is what we clearly see really so obvious? Ultrasonography and transcervical embryo transfer--a review. Fertil Steril. 2007;87:1–5.
24. Buckett WM. A meta-analysis of ultrasound-guided versus clinical touch embryo transfer. Fertil Steril. 2003;80:1037–41.
25. Teixeira DM, Dassunção LA, Vieira CV, Barbosa MA, Coelho Neto MA, Nastri CO, Martins WP. Ultrasound guidance during embryo transfer: a systematic review

and meta-analysis of randomized controlled trials. Ultrasound Obstet Gynecol. 2015;45:139–48.
26. Tiras B, Korucuoglu U, Polat M, Saltik A, Zeyneloglu HB, Yarali H. Effect of blood and mucus on the success rates of embryo transfers. Eur J Obstet Gynecol Reprod Biol. 2012;165:239–42.
27. Allahbadia GN, Kadam K, Gandhi G, Arora S, Valliappan JB, Joshi A, et al. Embryo transfer using the SureView catheter-beacon in the womb. Fertil Steril. 2010;93:344–50.
28. Kato O, Takatsuka R, Asch RH. Transvaginal-transmyometrial embryo transfer: the Towako method; experiences of 104 cases. Fertil Steril. 1993;59:51–3.
29. Groutz A, Lessing JB, Wolf Y, Azem F, Yovel I, Amit A. Comparison of transmyometrial and transcervical embryo transfer in patients with previously failed in vitro fertilization-embryo transfer cycles and/or cervical stenosis. Fertil Steril. 1997;67:1073–6.
30. Hurley VA, Osborn JC, Leoni MA, Leeton J. Ultrasound-guided embryo transfer: a controlled trial. Fertil Steril. 1991;55:559–62.
31. Woolcott R, Stanger J. Potentially important variables identified by transvaginal ultrasound-guided embryo transfer. Hum Reprod. 1997;12:963–6.
32. Kojima K, Nomiyama M, Kumamoto T, Matsumoto Y, Iwasaka T. Transvaginal ultrasound-guided embryo transfer improves pregnancy and implantation rates after IVF. Hum Reprod. 2001;16:2578–82.
33. Anderson RE, Nugent NL, Gregg AT, Nunn SL, Behr BR. Transvaginal ultrasound-guided embryo transfer improves outcome in patients with previous failed in vitro fertilization cycles. Fertil Steril. 2002;77:769–75.
34. Porat N, Boehnlein LM, Schouweiler CM, Kang J, Lindheim SR. Interim analysis of a randomized clinical trial comparing abdominal versus transvaginal ultrasound-guided embryo transfer. J Obstet Gynaecol Res. 2010;36:384–92.
35. Bodri D, Colodrón M, García D, Obradors A, Vernaeve V, Coll O. Transvaginal versus transabdominal ultrasound guidance for embryo transfer in donor oocyte recipients: a randomized clinical trial. Fertil Steril. 2011;95:2263–8.
36. Lambers MJ, Dogan E, Kostelijk H, Lens JW, Schats R, Hompes PGA. Ultrasonographic-guided embryo transfer does not enhance pregnancy rates compared with embryo transfer based on previous uterine length measurement. Fertil Steril. 2006;86:867–72.
37. Maldonado LG, Ajzen SA, Busato WC, Iaconelli A Jr, Bibancos M, Borges E Jr. Impact of previous hysterossonometry on embryo transfer. Fertil Steril. 2005;84:S364.
38. Maldonado LG, Aoki T, Busato W, Pasqualotto FF, Iaconelli A Jr, Borges E Jr. Embryo transfer based on previous uterine length measurement: a prospective randomized study. Hum Reprod. 2010;25:i99.
39. Revelli A, Rovei V, Dalmasso P, Gennarelli G, Racca C, Evangelista F, Benedetto C. Large randomized trial comparing transabdominal ultrasound-guided embryo transfer with a technique based on uterine length measurement before embryo transfer. Ultrasound Obstet Gynecol. 2016;48:289–95.
40. Woolcott R, Stanger J. Ultrasound tracking of the movement of embryo-associated air bubbles on standing after transfer. Hum Reprod. 1998;13:2107–9.
41. Confino E, Zhang J, Risquez F. Air bubble migration is a random event post embryo transfer. J Assist Reprod Genet. 2007;24:223–6.
42. Shah DK, Missmer SA, Correia KF, Racowsky C, Ginsburg E. Efficacy of intrauterine inseminations as a training modality for performing embryo transfer in reproductive endocrinology and infertility fellowship programs. Fertil Steril. 2013;100(2):386–91.
43. Harris ID, Styer AK, Petrozza JC. Ultrasonographer experience does not impact outcomes following ultrasound-guided embryo transfer. Fertil Steril. 2009;92:918–22.
44. Practice Committee of the American Society for Reproductive Medicine. ASRM standard embryo transfer protocol template: a committee opinion. Fertil Steril. 2017;107:897–900.
45. Heitmann RJ, Hill MJ, Csokmay JM, Pilgrim J, AH DC, Deering S. Embryo transfer simulation improves pregnancy rates and decreases time to proficiency in reproductive endocrinology and infertility fellow embryo transfers. Fertil Steril. 2017;107:1166–72.
46. Ebner T, Yaman C, Moser M, Sommergruber M, Polz W, Tews G. The ineffective loading process of the embryo transfer catheter alters implantation and pregnancy rates. Fertil Steril. 2001;76:630–2.
47. Mains L, Van Voorhis BJ. Optimizing the technique of embryo transfer. Fertil Steril. 2010;94:785–90.
48. Lee MS, Cardozo ER, Karmon AE, Wright DL, Toth TL. Impact of transfer time on pregnancy outcomes in frozen-embryo transfer cycles. Fertil Steril. 2018;109:467–72.
49. Saravelos SH, Kong GW, Chung JP, Mak JS, Chung CH, Cheung LP, Li TC. A prospective randomized controlled trial of 3D versus 2D ultrasound-guided embryo transfer in women undergoing ART treatment. Hum Reprod. 2016;31:2255–60.

21 Virtual Hysterosalpingography: A Noninvasive Diagnostic Technique for the Evaluation of the Female Reproductive Tract

Patricia Carrascosa, Carlos Capuñay, Juan Mariano Baronio, and Carlos E. Sueldo

General Concepts

Virtual studies started to be implemented in 1994, with the introduction of the computed tomography (CT) virtual colonoscopy. Since then, new CT virtual evaluations of several organs, such as the airways and the urinary tract, among others, started to be developed. However, it was not until several years later that this novel technique was used in the evaluation of the female reproductive system.

After 8 years of development and improvement of both acquisition protocols, technique of realization and CT scanner capabilities, CT virtual hysterosalpingography (VHSG) was introduced in the clinical scenario by October 2006 [1–3]. Nowadays, this technique allows, in about 2 s, the full evaluation of the entire female reproductive system, giving information on the cervix, uterine cavity plus uterine walls, fallopian tubes, and other pelvic structures.

P. Carrascosa · C. Capuñay (✉)
Department of Computed Tomography and Magnetic Resonance, Diagnóstico Maipú, Buenos Aires, Argentina
e-mail: carloscapunay@diagnosticomaipu.com.ar

J. M. Baronio
Department of Fertility, CEGYR, Buenos Aires, Argentina

C. E. Sueldo
University of California San Francisco-Fresno, Department of Obstetrics and Gynecology, Fresno, CA, USA

Virtual hysterosalpingography should be performed, using multislice CT scanners with at least 64 rows, to assure an adequate CT acquisition, in order to optimize its diagnostic potential [4]. The temporal, spatial, and contrast resolutions of the study will be based on the number of rows present in the CT scanner (currently, there are scanners with up to 520 detector rows).

The temporal resolution is mandatory, to capture the complete anatomy and patency of the fallopian tubes. Temporal resolution varies according to the gantry rotation time, which ranges from 350 to 270 ms. The faster the gantry rotation time, the better its temporal resolution [5].

The entire examination is performed in a very short period of time that varies from 1.3 to 3 s. During this time, CT images are acquired and subsequently processed in a workstation, using different algorithms, such as multiplanar reconstructions, maximum-intensity projections, volume-rendering 3D images, and endoscopic views.

Patient Preparation for the Study

It is mandatory to perform the study between days 6 and 11 of the menstrual cycle. In order to avoid any potential pregnancy, sexual abstinence during 2 days before and 2 days after the day of the study is recommended. Contraindications to

L. A. Stadtmauer, I. Tur-Kaspa (eds.), *Ultrasound Imaging in Reproductive Medicine*,
https://doi.org/10.1007/978-3-030-16699-1_21

perform the study besides pregnancy are pelvic infections or bleeding.

The day of the exam, patients are asked to avoid emptying the bladder for 2 h before the study, in order to straighten the uterine axis in anteverted uterus, as it contributes to change it to a more neutral position. Additionally, patients can take analgesics 1 h before the study.

Preparation of Patients in the CT Room

Patients are placed on the CT table in gynecologic position. After cleaning the perineum and vagina with povidone-iodine solution, a speculum is placed into the vagina to visualize the external cervical os. Complete sterilization of the vagina and the uterine cervix is carried out.

In order to instill an iodine contrast dilution (3 mL of water-soluble iodine contrast and 17 mL of saline solution) into the uterine cavity, a device specially designed for this purpose is positioned in the lateral portion of the speculum (Fig. 21.1). It will keep centered in place a plastic cannula positioned at the external cervical os. This cannula will be connected to a power injector, which will inject the mixed solution at a very slow rate (0.3 ml/s), in order to reduce patient's discomfort during the procedure and to assure an optimal uterine distention. The CT image acquisition begins 12 s after starting the mixture instillation. Using a 256 or 320 slice CT scanners, the study is completed in only 1.3 s, making VHSG a real-time study with easy visualization of the contrast, as it passes into the peritoneum.

Technical parameters of these studies are slice thickness, 0.625 mm; gantry rotation time, 270–350 ms; kV, 80–120; and mAs, 100–200. X-ray tube current and potency are adjusted in relation to patient's weight and body mass index. It is always preferable to use the least mAs and kV necessary. Small patients usually receive 80 kV–100 mAs, with an exposure radiation dose of 0.3 mSv. After performing an anteroposterior scout view of the pelvis, a 10-cm length CT scan is planned, centered on the pelvic region. Once the CT images are acquired and checked by the physician performing the examination, the cannula and speculum are removed, and the perineum is cleansed with povidone-iodine solution. Patients can return immediately to routine activities.

Complications of the Procedure

The rate of complications of VHSG in our experience is extremely low; in over 15,000 VHSG studies performed since 2006, we did not find any cases of infection, bleeding, or other significant complications requiring hospitalization. In a few cases we observed intravascular passage of contrast through the uterine plexus, and only three patients experienced an allergic-like reaction requiring medical treatment, with symptoms improving in a very short time.

Patient's Acceptance

VHSG is a well-tolerated exam, as is commonly not associated with any significant discomfort. From all cases of VHSG performed in our center, the majority of the patients (85%) classified the procedure as having no discomfort or mild discomfort only [6, 7].

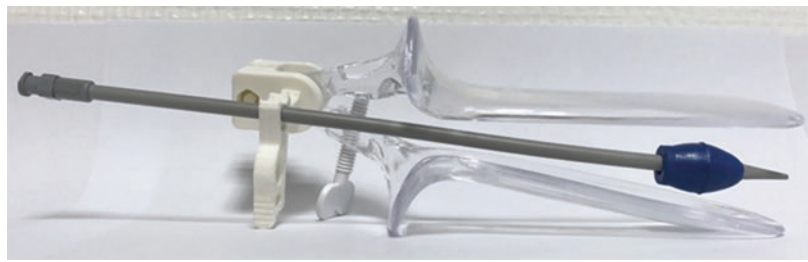

Fig. 21.1 Instruments used in VHSG exams

Contraindications

Contraindications to perform the procedure are pregnancy and active pelvic infection. Allergy to iodine is a relative contraindication, and in known cases, gadolinium can be used instead [8]. Our group conducted a study including 50 patients, comparing the diagnostic performance of VHSG using the conventional iodine-saline solution mixture versus those using a mixture of gadolinium and saline solution. Diagnostic results were similar; and the main limitation of using gadolinium is its higher cost; for that reason we prefer using iodine, as the contrast agent.

Radiation

Although in the first developmental stages of the procedure, more than 10 years ago, radiation doses of VHSG were more than 1 mSv, nowadays with the introduction of new CT scanners and the implementation of iterative reconstruction algorithms, radiation doses are significantly reduced to around 0.3 mSv. With these values, VHSG gives a lower radiation doses than a conventional X-ray hysterosalpingography, which has a variable radiation dose of 1–3 mSv, based on the fluoroscopy time and number of X-ray spots. The use of a radiation dose as low as reasonably achievable (ALARA) is mandatory, particularly when relatively young patients and the gonadal region are involved in the study.

Image Post-Processing

Once the images are acquired, two- and three-dimensional evaluations are routinely performed by the physician at a workstation, to perform the diagnosis. During the image interpretation and analysis, as mentioned earlier, different post-processing algorithms are used:

Multiplanar Reconstructions (MPR) These types of image reconstructions show the complete reproductive tract in different views and angles (coronal, sagittal, and oblique planes).

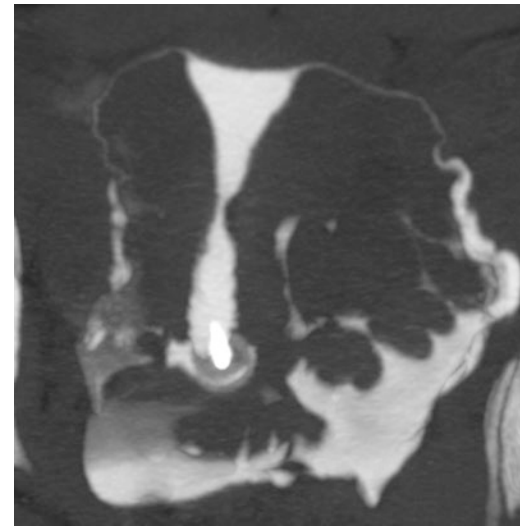

Fig. 21.2 VHSG maximum-intensity projection image of normal, patent fallopian tubes

Even curved multiplanar reconstructions can be created, unfolding the cervix and uterine cavity in a single view. MPR can assess all types of pathologies, such as polyps, synechiae, and uterine anomalies, among others, and perform all sorts of measurements (Fig. 21.2). Also extra-gynecologic pelvic structures can be evaluated.

Maximal Intensity Projection (MIP) These images provide excellent definition of the anatomy and lumen of the fallopian tubes, in a gray-scale tridimensional dimension (Fig. 21.3), facilitating the detection of hydrosalpinx, as well as tubal obstructions.

Volume-Rendering (VR) Images These images created tridimensional views of the reproductive tract, using a window that recognizes the intrauterine contrast. These reconstructions detect a large spectrum of uterine and tubal pathology, such as cervical stenosis, polyps, and tubal disease (Figs. 21.4, 21.5, and 21.6). They are also very useful in confirming suspected findings visualized on the MPR.

Virtual Endoscopy (VE) Images This analysis is the last step in the image interpretation process, and it allows performing a final diagnosis.

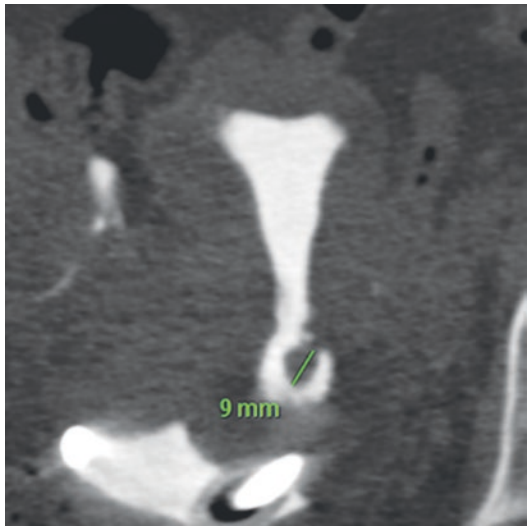

Fig. 21.3 VHSG coronal multiplanar reconstruction of a 9-mm endocervical polyp

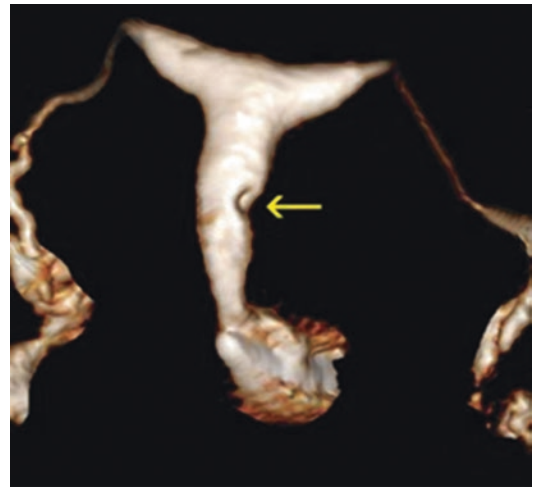

Fig. 21.5 VHSG volume-rendering image of an endometrial polyp (arrow)

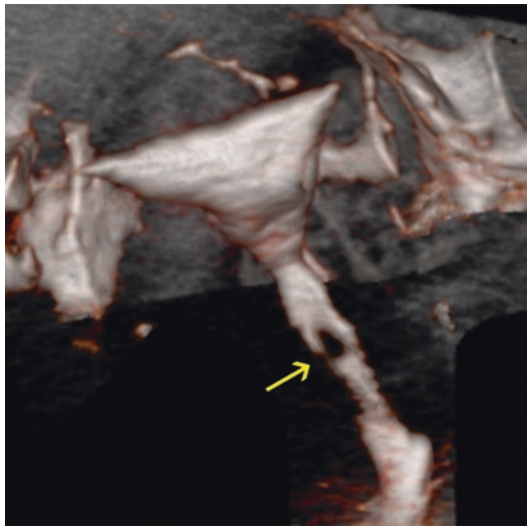

Fig. 21.4 VHSG volume-rendering image of a cervical synechiae (arrow)

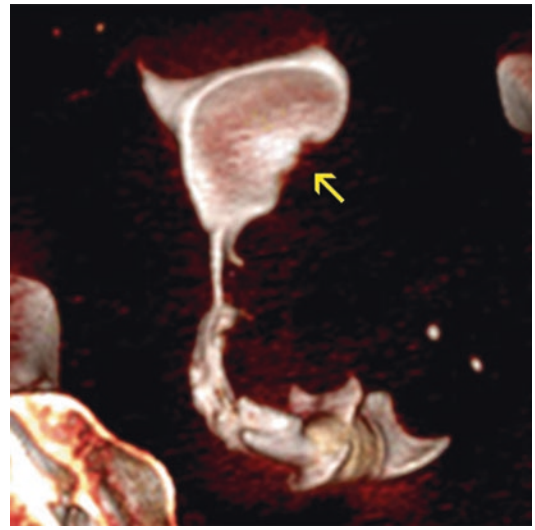

Fig. 21.6 VHSG volume-rendering image of a submucosal myoma (arrow)

Images are very similar to gold standard invasive diagnostic methods, such as hysteroscopy and falloposcopy (Fig. 21.7). Nevertheless, there are some differences between endoscopic views by VHSG and conventional hysteroscopy. VHSG endoscopic images can show all views in any angle, plus the software can display navigation from the cervix to the uterine fundus and fallopian tubes or in the opposite direction, while conventional hysteroscopy can only show navigation in a single direction.

A limitation of VHSG is that the endoscopic views do not show the real color of the mucosa and that it is only a diagnostic modality, meaning it is not therapeutic, as is the case with

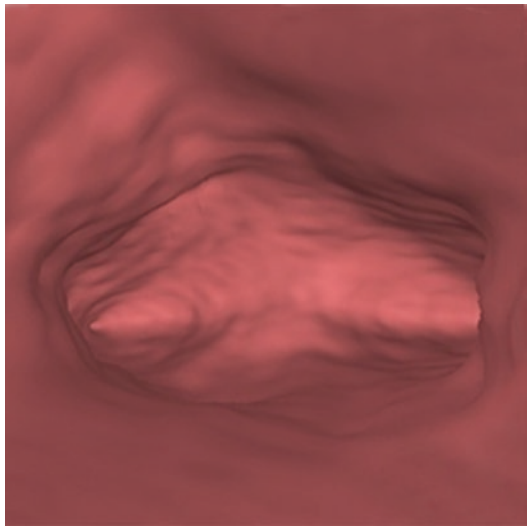

Fig. 21.7 Virtual endoscopy view of normal uterine cavity

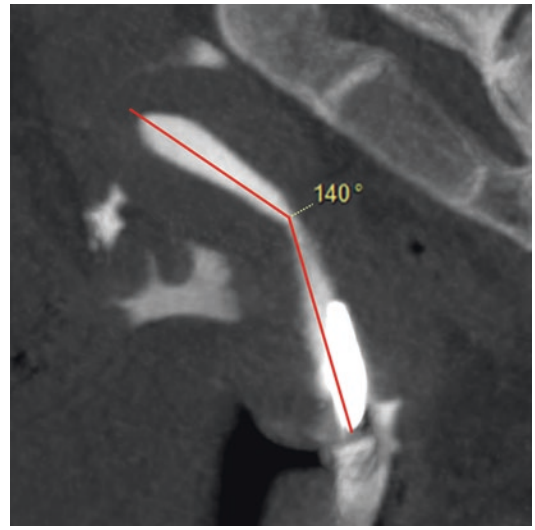

Fig. 21.8 VHSG sagittal maximum-intensity projection image showing a wide cervical-uterine angle

conventional hysteroscopy, in cases where pathology is encountered.

Clinical Experience with Virtual Hysterosalpingography in Reproductive Medicine Cervical Pathology in Infertility

The cervical anomalies may include different types of pathologies, such as cervical stenosis, synechiae, cervical wall irregularities, polyps, and diverticula. Many of these processes can reduce the lumen of the cervical canal and obstruct the intracavitary access in patients undergoing intrauterine inseminations or embryo transfers, negatively impacting outcome. Also a narrow cervical-uterine angle decreases the performance of these procedures. This angle, determined by the intersection on a line passing through the longitudinal axis of the cervical canal and other through the longitudinal axis of the uterine cavity, can be routinely measured on the VHSG studies. Regarding that its value varies according to bladder distention, it should be measured with full bladder; an angle greater than 90° facilitates the performance of the embryo transfer procedures (Fig. 21.8).

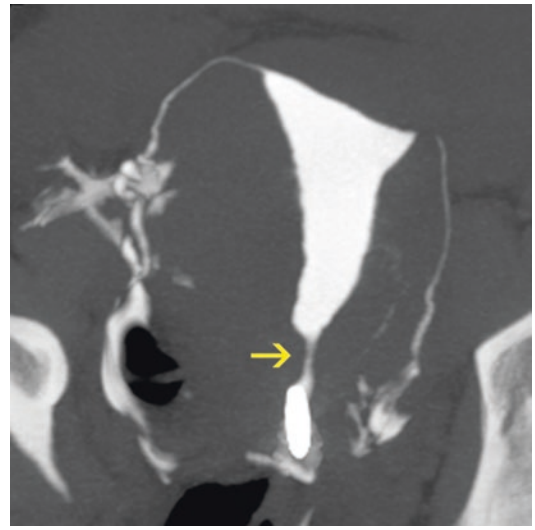

Fig. 21.9 VHSG maximum-intensity projection image of cervical stenosis (arrow)

Narrowing of the cervical canal has different etiologies such as congenital or postsurgical/instrumental trauma or post-infection. VHSG can evaluate the complete cervix without any blind spot after image reconstruction. The MPR, MIP, and VR images are extremely useful in the diagnosis of cervical stenosis (Fig. 21.9), while VE images allow the navigation through the cervical lumen clearly identifying the cervical alterations.

Cervical synechiae are characterized by the presence of fibrous tissue bands that partially or totally occupy the cervical canal. VHSG identifies elevated irregular soft tissue lesions extending from the cervical wall toward the cervical lumen. In severe cases, the lumen can be severely reduced, and the synechiae extend diffusively from one wall to the other (Fig. 21.10).

Cervical polyps are elevated lesions which vary in size and number. They may result from an abnormal response to the presence of high levels of estrogens, chronic inflammation, etc. and can be either asymptomatic or present with vaginal bleeding during intercourse or any other cervical manipulation. They are rarely malignant, but after removal they should always be sent to pathology. They are seen by VHSG partially or totally obstructing the lumen; the MPRs show a soft tissue lesion projecting into the uterine cavity, and the virtual endoscopy shows the endoluminal view of the polyp (Fig. 21.11).

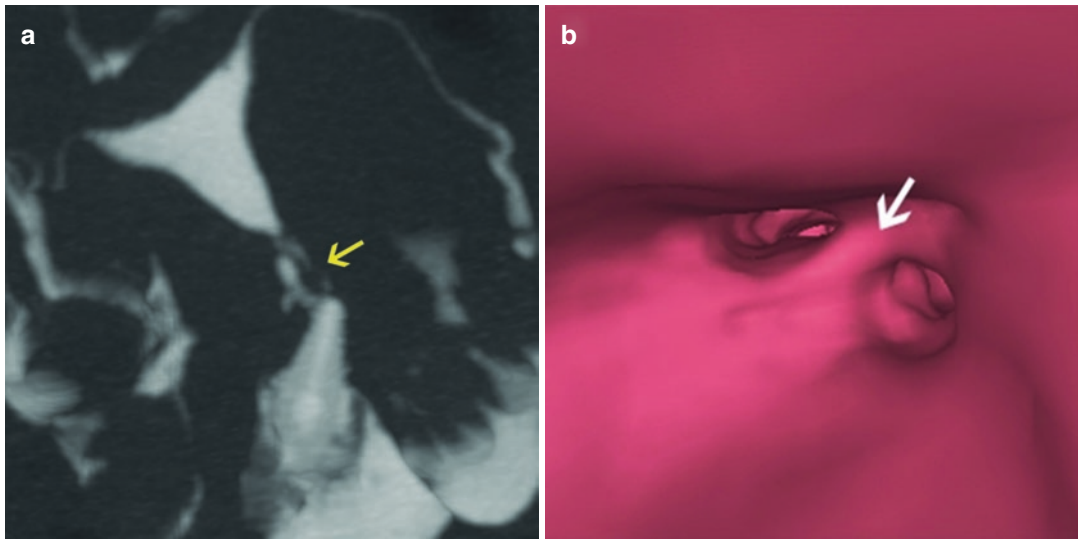

Fig. 21.10 Cervical synechiae (arrow) seen by (**a**) VHSG maximum-intensity projection image and (**b**) virtual endoscopy view

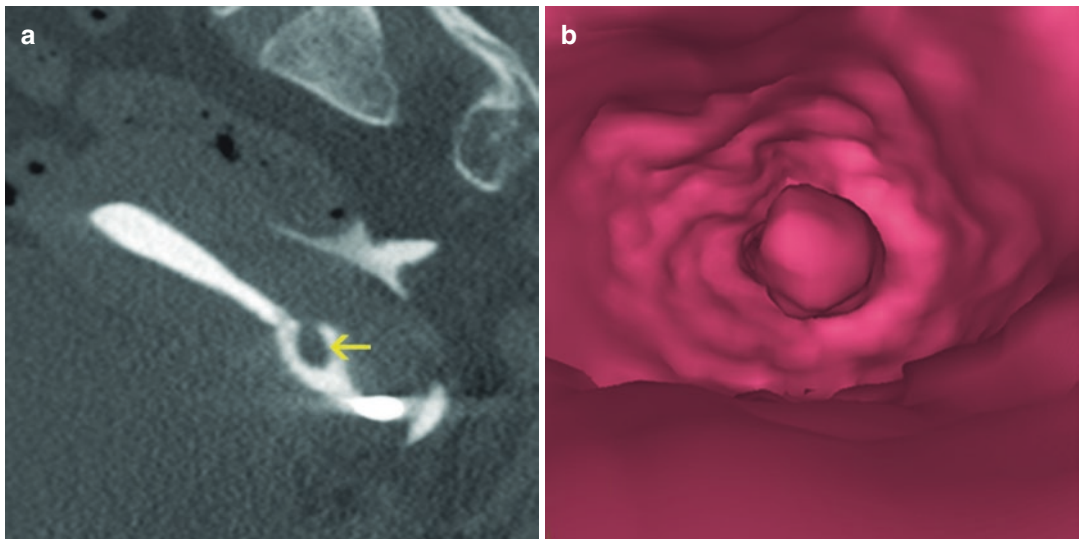

Fig. 21.11 Cervical polyp (arrow) seen by (**a**) VHSG sagittal multiplanar reconstruction and (**b**) virtual endoscopy view

The cervical diverticula are herniations of the cervical wall that can be seen by VHSG through tridimensional and endoscopic views, where one can clearly detect the neck of the diverticulum projecting into the lumen. It is unclear if diverticula play a role in human infertility.

Pathology of the Endometrial Cavity in Infertility

Different pathologies can affect the endometrial cavity and can compromise sperm transport, embryo implantation, or embryo growth, potentially increasing the rate of spontaneous miscarriages [9]. VHSG can detect all of them in a noninvasive manner with excellent diagnostic accuracy. Our group has done a comparison between VHSG and conventional hysteroscopy in 69 infertile patients, showing a sensitivity of 96%, a specificity of 86%, a positive predictive value of 90%, and a negative predictive value of 95.6% for all lesions in comparison with the gold standard technique of hysteroscopy.

Uterine congenital anomalies are well assessed by VHSG [10]. Although magnetic resonance imaging has been considered the modality of choice for their diagnosis, VHSG has shown similar results for their identification with the potential advantage of identifying associated lesions, such as polyps or synechiae, among others. Septate uterus can be clearly differentiated from bicornuate uterus by VHSG. An accurate diagnosis is important in order to properly advise patients about the best treatment to be implemented. Recently, we demonstrated the value of VHSG in the differential diagnosis of these uterine anomalies, as one can easily outline the external surface of the uterine fundus. VHSG with volume-rendering reconstruction allows the visualization of the endometrial cavity plus the adjacent flat or minimally indented myometrium consistent with a septate uterus (Fig. 21.12). On the other hand, when the indentation in the uterine fundus is deeper than 15 mm, creating the presence of two separate horns, the diagnosis of bicornuate uterus is made (Fig. 21.13); the endoscopic view of the cavity is unable to differentiate between septate and bicornuate uterus (Fig. 21.14).

Uterine synechiae can also be easily observed by VHSG, as fibrous bands that connect the

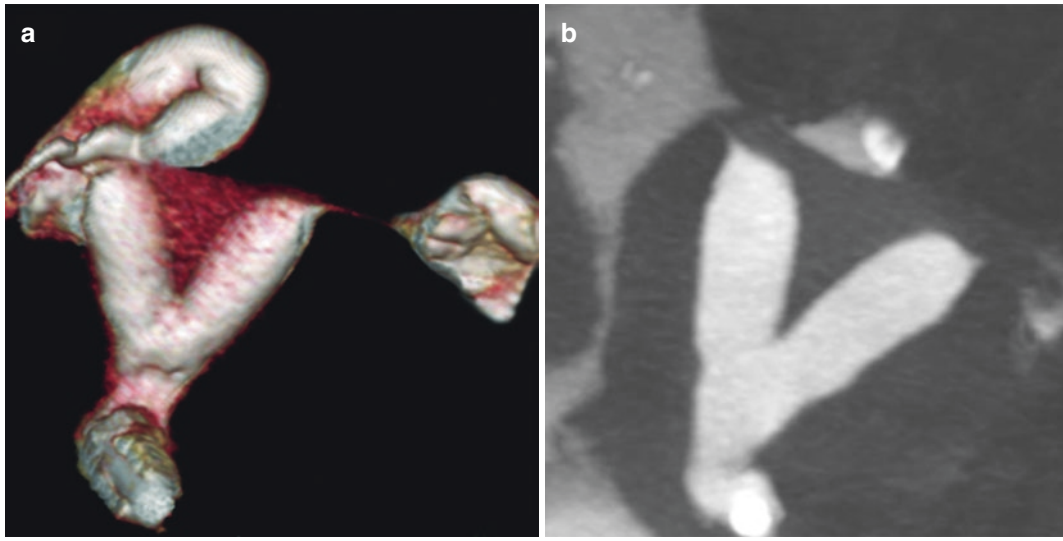

Fig. 21.12 Partial septate uterus seen by (**a**) VHSG volume-rendering image and (**b**) maximum-intensity projection image

uterine walls to one another. They represent scars usually caused by trauma, the result from an aggressive curettage post-abortion or postpartum. Their presence may be localized in a small section of the uterine cavity or extensively spread out in a diffuse manner, obliterating large sectors of the uterine cavity (Fig. 21.15). They can cause infertility or repeated pregnancy losses. VHSG is an excellent diagnostic tool as MPR shows irregularly elevated lesions with soft tissue density, while volume-rendering reconstructions show filling defects where the synechiae are located. Endometrial polyps consist of focal overgrowths of the endometrium, and they are also easily diagnosed by VHSG, as focal elevations of the endometrium projecting from the uterine wall to the endometrial cavity. Multiplanar reconstructions allows to accurately measure their sizes, while the VR images show them as filling defects in the uterine morphology. Finally VE images show the elevated lesion projected into the uterine cavity (Fig. 21.16).

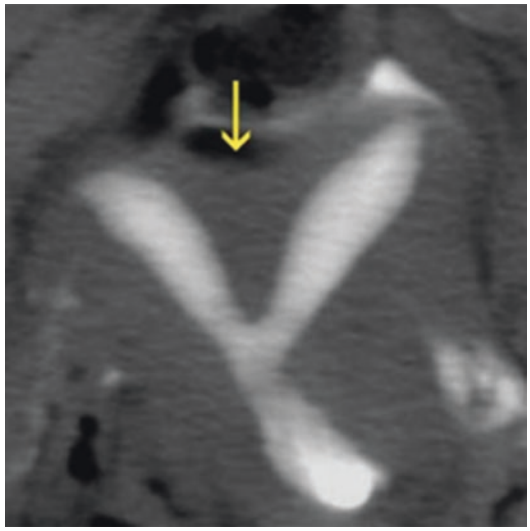

Fig. 21.13 Bicornuate uterus seen by VHSG coronal multiplanar reconstruction showing the indentation in the uterine fundus (arrow)

The association between polyps and infertility is controversial, but there is some consensus that those polyps larger than 1 cm should be removed, especially when present in patients going for in vitro fertilization or similar procedures.

Submucous myomas are generally benign tumors from the smooth muscle, single or multiple, with a variable size, number, and location. They may be a cause of infertility depending on their location and size, as they may interfere with sperm transport and/or embryo implantation; they may also be a cause of repeated miscarriages. VHSG can help in showing the exact location of the lesion, to determine the best sur-

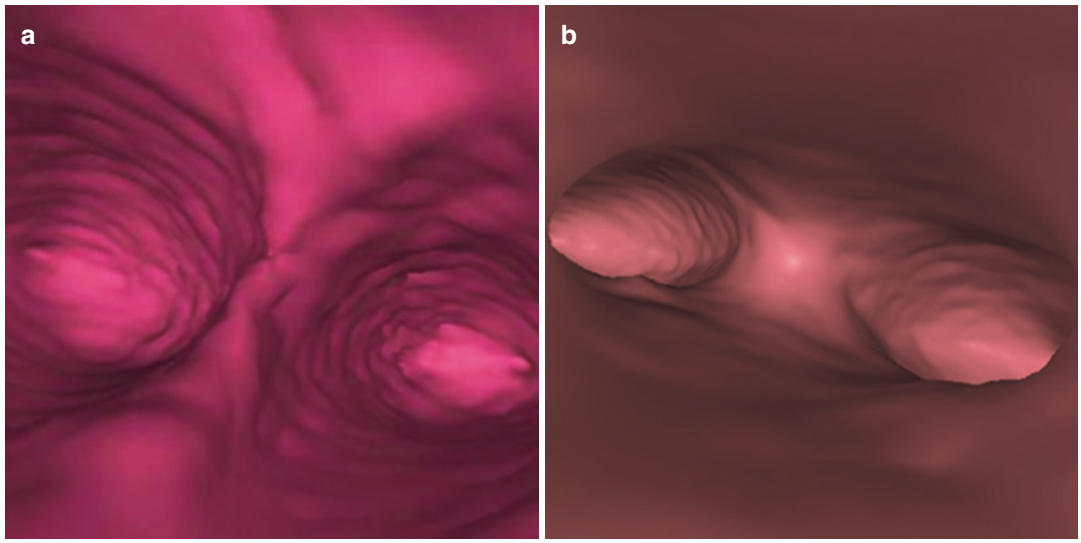

Fig. 21.14 Virtual endoscopy view of (**a**) partial septate uterus and (**b**) bicornuate uterus

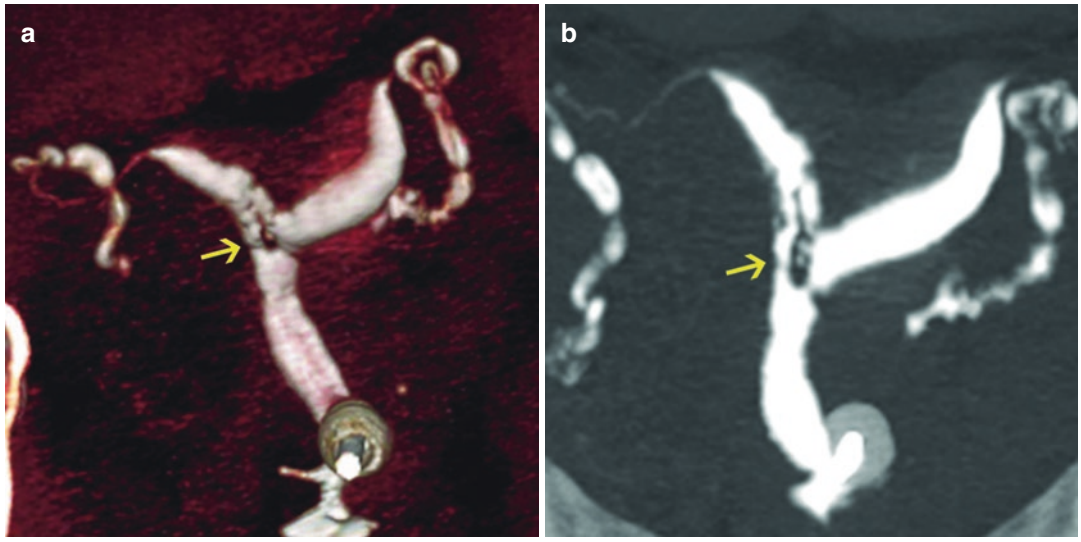

Fig. 21.15 Uterine synechiae (arrow) in a bicornuate uterus seen by (**a**) VHSG volume-rendering image and (**b**) maximum-intensity projection image

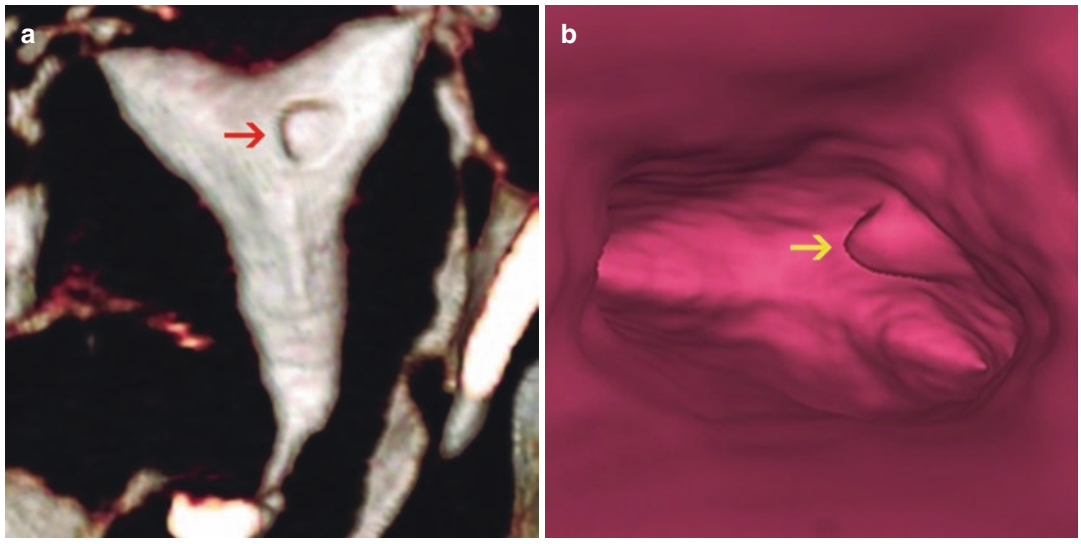

Fig. 21.16 Endometrial polyp (arrow) seen by (**a**) VHSG volume-rendering image and (**b**) virtual endoscopy view

gical approach for its removal and predict the chances of success for the procedure (Fig. 21.17).

Evaluation of the Fallopian Tubes

Conventional X-ray hysterosalpingography has traditionally been considered the gold standard for assessment of the fallopian tube morphology and patency. Currently, VHSG can also play an important role in their evaluation. As mentioned, it is mandatory to perform the VHSG studies with CT scanners of 64 or more rows, in order to capture the fallopian tubes distended with contrast along its whole length. MIP images are the best image post-processing tool to evaluate their morphology and identify any kind of pathology such as tubal obstruction, hydrosalpinx, tubal polyps, or adhesions (Fig. 21.18).

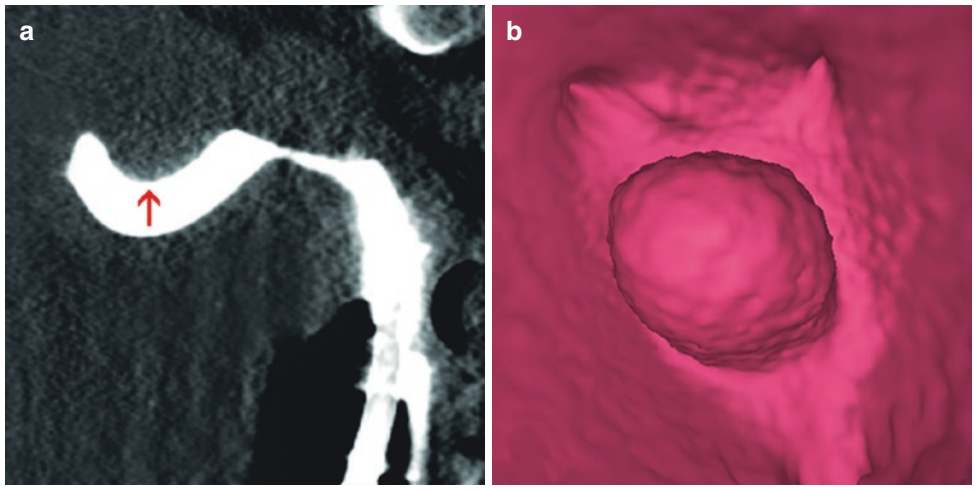

Fig. 21.17 Submucosal myoma (arrow) seen by (**a**) VHSG maximum-intensity projection image and (**b**) virtual endoscopy view

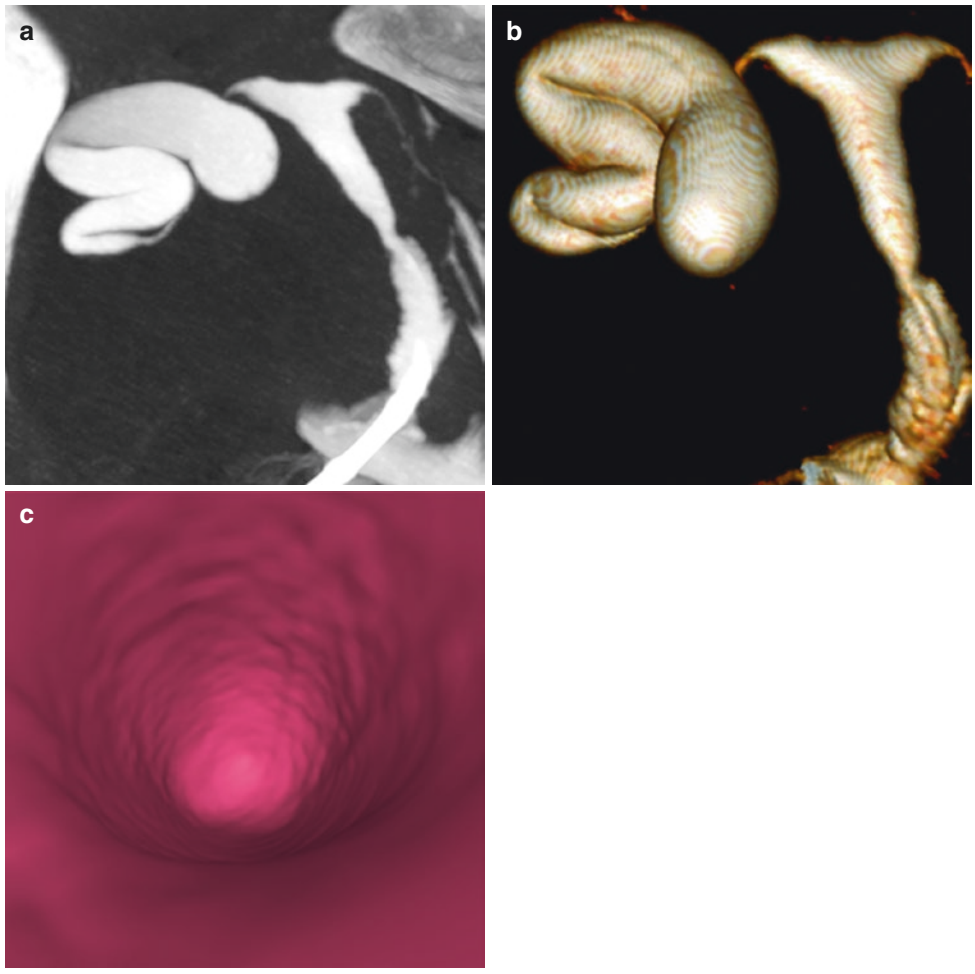

Fig. 21.18 Large right hydrosalpinx seen by (a) VHSG maximum-intensity projection image, (b) VHSG volume-rendering image, and (c) virtual endoscopy view

Conclusion

VHSG has been used clinically for several years, showing excellent diagnostic performance in comparison with other imaging modalities. The study provides high-quality images of the entire female reproductive system, and it is very well accepted by patients and referring physicians, as it offers simultaneously in a single modality the information provided by several diagnostic techniques, such as conventional X-ray hysterosalpingography, sonohysterography, and magnetic resonance imaging. Furthermore, it is a well-tolerated study that takes little time to perform and uses low radiation. The complication rate is also very low; all these qualities make VHSG the preferred imaging study for the evaluation of the female reproductive tract.

References

1. Carrascosa P, Capuñay C, Baronio M, López EM, Jorge C, Borghi M, et al. Virtual hysteroscopy by multidetector computed tomography. Abdom Imaging. 2008;33(4):381–7.
2. Carrascosa P, Baronio M, Capuñay C, López EM, Vallejos J, Borghi M, et al. Multidetector computed tomography virtual hysterosalpingography in the investigation of the uterus and fallopian tubes. Eur J Radiol. 2008;67(3):531–5.
3. Carrascosa P, Capuñay C, Vallejos J, Carpio J, Baronio M, Papier S. Two-dimensional and three-dimensional imaging of uterus and fallopian tubes in female infertility. Fertil Steril. 2016;105(6):1403–20.
4. Carrascosa P, Baronio M, Capuñay C, López EM, Sueldo C, Papier S. Clinical use of 64-row multislice computed tomography hysterosalpingography in the evaluation of female factor infertility. Fertil Steril. 2008;90(5):1953–8.
5. Carrascosa P, Capuñay C, Baronio M, Martín López E, Vallejos J, Borghi M, et al. 64-Row multidetector CT virtual hysterosalpingography. Abdom Imaging. 2009;34(1):121–33.
6. Carrascosa PM, Capuñay C, Vallejos J, Martín López EB, Baronio M, Carrascosa JM. Virtual hysterosalpingography: a new multidetector CT technique for evaluating the female reproductive system. Radiographics. 2010;30(3):643–61.
7. Celik O, Karakas HM, Hascalik S, Tagluk ME. Virtual hysterosalpingography and hysteroscopy: assessment of uterine cavity and fallopian tubes using 64-detector computed tomography data sets. Fertil Steril. 2010;93(7):2383–4.
8. Carrascosa P, Capuñay C, Vallejos J, Martin Lopez E, Baronio M, Sueldo C. Gadolinium vs iodine virtual hysterosalpingography: an alternative for allergic patients? Fertil Steril. 2008;90:S157.
9. Carrascosa P, Capuñay C, Vallejos J, Baronio M, Carrascosa J. Virtual hysterosalpingography: experience with over 1000 consecutive patients. Abdom Imaging. 2011;36(1):1–14.
10. Carrascosa P, Sueldo C, Capuñay C, Baronio M, Papier S. Virtual hysterosalpingography in the diagnosis of bicornuate versus septate uterus. Fertil Steril. 2011;96(5):1190–2.

Modern Evaluation of Endometrial Receptivity

22

Jose Miravet-Valenciano, Maria Ruiz-Alonso, and Carlos Simón

Introduction

Endometrial receptivity is an essential component in human reproduction defined as a physiological status in which the endometrium acquires an adhesive phenotype that permits embryo implantation. Adequate proliferation and differentiation during the proliferative phase must be followed by timely secretory changes during the luteal phase with stromal decidualization. However, an impaired synchronization between embryo and endometrium will lead to implantation failure. The acquisition of endometrial receptivity occurs during a specific period of time known as the window of implantation (WOI) in the midsecretory phase of the menstrual cycle [1, 2].

During the WOI, the luminal epithelial cells suffer morphological remodelling leading to polarity loss, while apical microvilli known as pinopodes appear in the luminal surface while adhesive molecules as integrins and mucins, and some specific cytokines have been found to be overexpressed during the WOI. At the same time, the glandular epithelial cells increase in size and secrete the required factors to nurture the implanting embryo. Then, the endometrial stromal cells start a differentiation process referred to as decidualization characterized by acquisition of rounded phenotype, increased storage of nutrients, accumulation of uterine natural killer cells, and the vascular reorganization surrounding the site in which implantation is to occur.

Wilcox et al. [3] determined that the human embryo implants 8–10 days after ovulation. The methods they used to determine ovulation were never officially adopted; however, the clinical community has accepted their assertion that the endometrium in all patients becomes receptive during that time. Additionally, implantation has been believed to be equally successful over these 3 days, regardless of individual variations or hormonal treatment received (this is observed to occur within natural cycles, controlled ovarian stimulation, and hormonal replacement cycles). If the embryo does not implant, the decidualized endometrium is shed leading to menstruation, and a new functional endometrial layer is regenerated in the next menstrual cycle.

However, recent studies have demonstrated that the WOI varies between patients [4] and that endometrial microbiome plays a paramount role in implantation [5], leading the diagnosis of

J. Miravet-Valenciano · M. Ruiz-Alonso
Igenomix, Valencia, Spain

C. Simón (✉)
Valencia University, Valencia, Spain

Igenomix Academy and Igenomix, Valencia, Spain

Department of Obstetrics and Gynecology, Stanford University, Stanford, CA, USA

Department of Obstetrics and Gynecology, Baylor College of Medicine, Houston, TX, USA
e-mail: simon@igenomix.com

L. A. Stadtmauer, I. Tur-Kaspa (eds.), *Ultrasound Imaging in Reproductive Medicine*,
https://doi.org/10.1007/978-3-030-16699-1_22

endometrial receptivity to a crucial role in ART to avoid implantation failure and, consequently, improve pregnancy outcomes.

The aim of this chapter is to review the current methodologies used in evaluating the endometrial function.

A Quick Look Back at Endometrial Assessment Approaches

Several studies have composed a puzzle of endometrial factor where 360° must be considered. The pieces of this puzzle belong to diverse scientific approaches to find the proper moment for embryo implantation.

The Noyes criteria [6], based on the histological features of the different compartments of the endometrium across the menstrual cycle, reflect the differentiation of the endometrium each day of the luteal phase. However, the accuracy and functional relevance of these criteria as a predictor of endometrial receptivity have been questioned in randomized studies [7, 8], leading to the discontinuation of this diagnostic method.

The use of high-resolution ultrasonography as a cheap and noninvasive method of assessment of uterine receptivity arose as a necessity to the evaluation of the endometrial development. In the 1990s, magnetic resonance imaging (MRI) demonstrated significant differences in the relative MRI signal intensities of the myometrium between conception and non-conception cycles [9], but the translation of this technique to the clinic did not succeed due to practical obstacles such as availability and cost. Ultrasonography, color Doppler, and most recently 3D ultrasonography and power Doppler angiography can help to assess several markers of implantation in a quick, noninvasive and relatively low-cost way (Fig. 22.1). Such techniques have also been used to study reproductive disorders as the effects of hydrosalpinx in the regulation of endometrial receptivity [10] and to identify intrauterine adhesions in infertile women with Asherman's syndrome undergoing hysteroscopic adhesiolysis in order to help the improvement of endometrial receptivity [11]. However, data extracted from studies analyzing the role of ultrasound for predicting endometrial receptivity are controversial.

Immunohistochemical staining has been used to complement the analysis of endometrial dating by Noyes criteria. For this purpose, several markers of endometrial receptivity have been used to assess the abundance and localization of adhesion proteins, cell cycle progression of

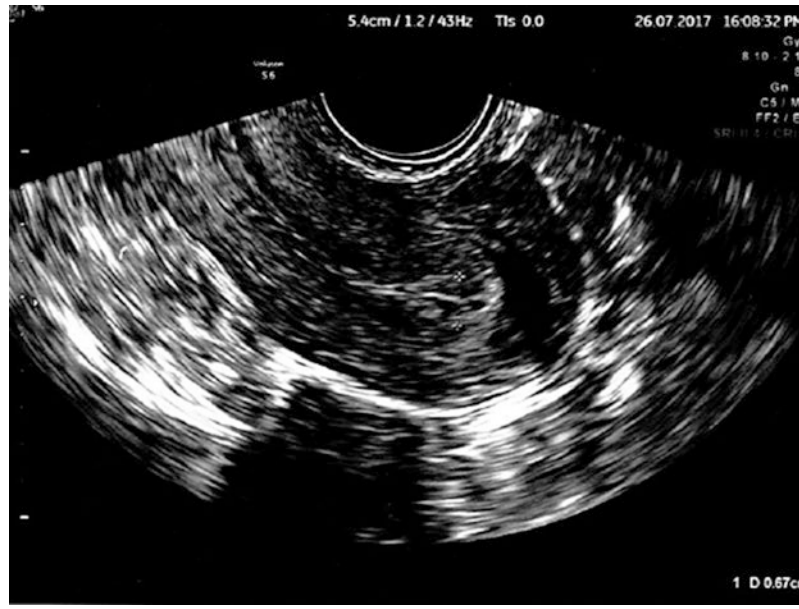

Fig. 22.1 Trilaminar endometrium assessed by ultrasound

endometrial cells, or the regulation of immune cells in endometrial specimens. Because endometrial receptivity involves an adhesive phenotype, the abnormal expression of adhesion proteins has been studied as potential markers of uterine receptivity. In this regard, alpha-1, alpha-4, and beta-3 integrins are observed in women with unexplained infertility [12] and constitute the basis of E-tegrity a clinical diagnosis test of endometrial receptivity (http://www.etegritytest.com). However, the association of beta-3 integrin with endometriosis is the main limitation of this test that may present cofounding results. Also, the expression and subcellular localization of two proteins involved in endometrial cell's mitotic cycle, cyclin E and cyclin-dependent kinase inhibitor p27, have been used to determine the endometrial receptivity in donor ovum recipients [13] and are the rationale of the endometrial function test® (EFT®) (http://klimanlabs.yale.edu/infertility/eft/).

Endometrial receptivity has been also analyzed by the immunohistochemical detection of immune cells involved in maternal adaptation to the semiallogenic developing embryo, especially uterine natural killer (uNK) cells. In this regard, it has been reported that high abundance of cytotoxic CD16(+) cells or the ratio NKp46(+):CD56(+) can be used as a marker of increased endometrial inflammation that correlates with implantation failure or pregnancy loss. However, the prognosis value of measuring total uNK cells or CD56(+) cells in endometrial specimens remains uncertain [14].

Using the single-molecule approach, many putative biochemical markers have been proposed as predictors of endometrial receptivity, but none of them have achieved the status of a diagnostic or predictive clinical tool [15]. More recently, the status of human endometrium has been more objectively classified by using transcriptomic profiling throughout the menstrual cycle [16, 17], as well as during the window of receptivity [18]. These pioneering diagnostic techniques, in conjunction with accumulated evidence that the endometrial molecular profile is unique during the WOI, prompted us to translate the molecular expression profile of the endometrium as it relates to endometrial function using transcriptomics.

Transcriptomic Assessment of Endometrial Receptivity

For more than 65 years, histologic evaluation has been the standard for clinical diagnosis based on morphological observations. The limitations of this method underscore a need to understand the genetic mechanisms underlying the observed histological changes. The possibility of classifying the endometrium using transcriptomic profiles offers an objective and powerful tool in clinical applications and is independent of the specific functional meaning of the transcriptomic signature [19].

The transcriptome reflects the genes that are being actively expressed at any given time in a specific cell population. Transcriptomics also allows gene expression characterization at the messenger RNA (mRNA) level of a population, leading to a sample-specific molecular profile. Several areas have been covered, from the transcriptomic expression throughout the menstrual cycle to the changes identified under different treatments or gynecological conditions. However, the main interest has been the identification of the specific transcriptomic signature that can diagnose the receptive function to develop a mathematical function based on the expression profiles that can accurately predict the biologic group, diagnostic category, or prognostic stage and improve the effectiveness of reproductive treatments.

Based on this research, in 2011 our group identified the transcriptomic signature of endometrial receptivity, characterized by the expression of 238 genes unique to the WOI [4]. This led to the launch of the endometrial receptivity analysis (ERA) (https://www.igenomix.com/tests/endometrial-receptivity-test-era/).

The original design of the ERA test was based on microarray data. Following the accumulation of data after 7 years from the analysis of more than 35,000 transcriptomic profiles, algorithms have been developed to provide a new

computational predictor based on next-generation sequencing (NGS) technology. The new ERA predictor defines a shorter, optimal WOI frame. To define this receptivity signature, the training of the new predictor was performed by selecting well-defined and curated endometrial profiles. Only receptive profiles from patients that were receptive and became pregnant in this cycle were used. For the non-receptive stages, training was performed using only samples in which receptivity was reached after following the specific recommendation associated with that profile. This technique has been refined and improved such that the predictor potency provides more detailed insights into the use of gene signature profiles for patient stratification.

To perform ERA, mRNA is extracted from an endometrial sample. After determining its quantity and quality, the sample is analyzed using NGS coupled with a computational predictor and an algorithm able to identify the receptivity of the endometrial sample (Fig. 22.2).

Although it has been classically considered that the WOI opened the same "standard" day of the menstrual cycle for all the women, it is possible that a displacement of the WOI occurs in some women. In these cases, the assay provides the personalized WOI of a specific patient independent of endometrial histology (Fig. 22.3). This strategy allows performing a personalized embryo transfer (pET) on the day in which the endometrium is receptive [20] (Fig. 22.4).

Interpretation of Era Results

Receptive

A receptive endometrial profile is divided into three sub-signatures: optimal receptive, early receptive, and late receptive.

- An optimal receptive profile indicates an optimally receptive endometrium. In this case, it is recommended to proceed with the embryo transfer in the same type of cycle and on the same day in which the endometrial biopsy was performed.
- An early receptive profile indicates that the endometrium is entering the receptive phase but needs 12 more hours of progesterone administration in a hormone replacement therapy (HRT) cycle to acquire an optimally receptive profile.
- A late receptive profile indicates that progesterone administration should be reduced by 12 hours in a further cycle to achieve optimal receptivity.

The early and late receptive profiles are considered transitional profiles, and it is recommended that personalized embryo transfer be performed after following the indicated treatment with progesterone (12 more or less hours) without need of further verification.

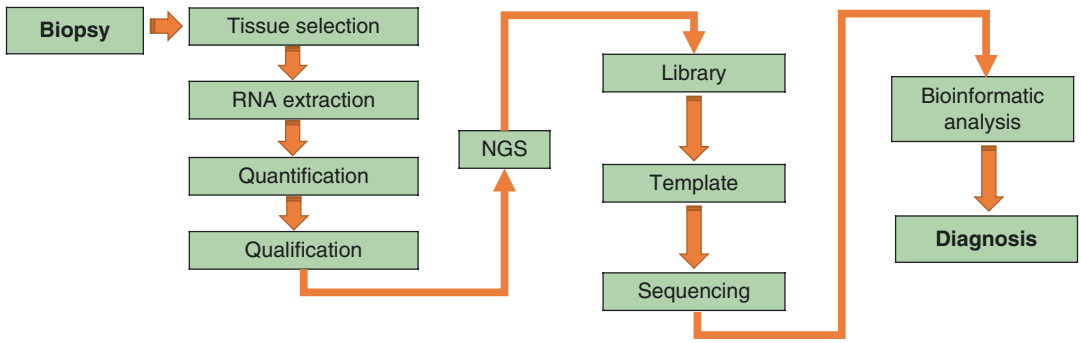

Fig. 22.2 Flow chart of the ERA laboratory and data analysis procedure

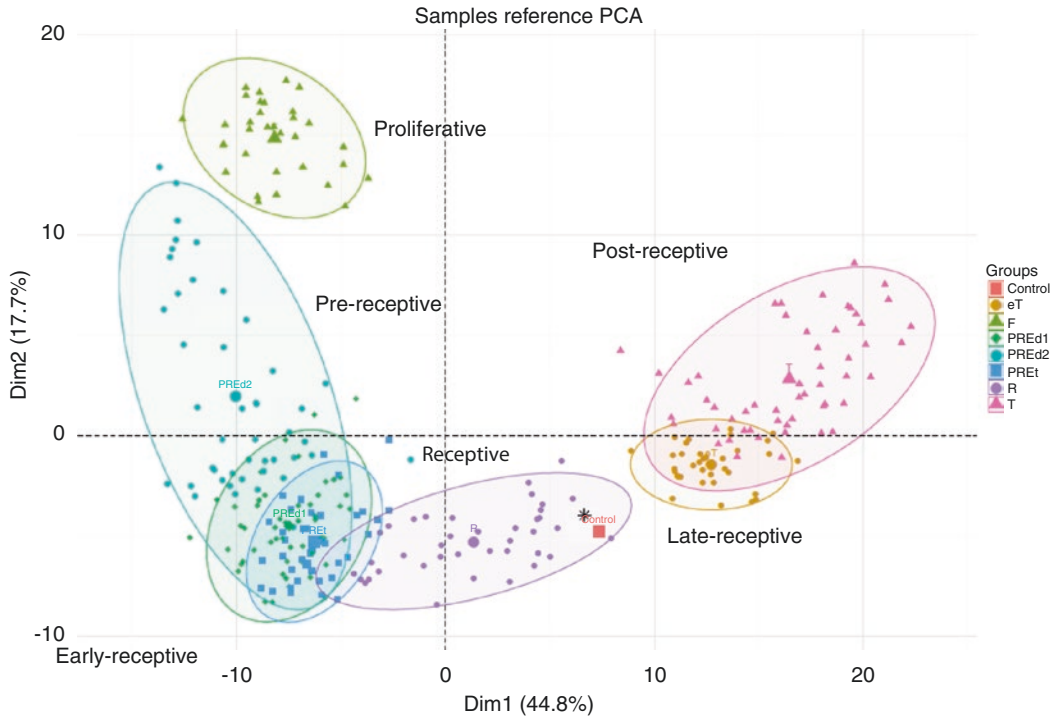

Fig. 22.3 Individual variations of the window of implantation and personal embryo transfer

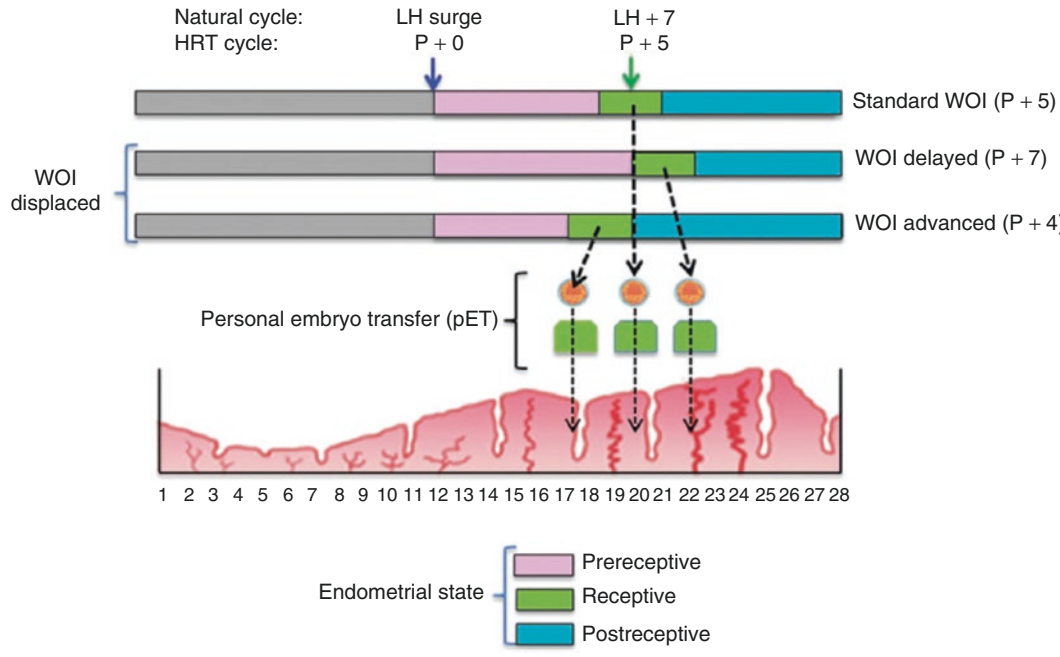

Fig. 22.4 Principal component analysis of the ERA predictor set and the classification parameters for all transcriptomic profiles

Non-receptive

Our algorithm revealed that the gene expression profile in a non-receptive endometrium is usually due to a physiological displacement of the WOI. In addition to a proliferative profile, which generally indicates that the endometrium has not been exposed to endogenous or exogenous progesterone, a non-receptive patient can also show a pre-receptive or a post-receptive transcriptomic profile.

- A pre-receptive diagnosis indicates that the transcriptional activation necessary to achieve receptivity has not yet occurred. The patient needs 1 or 2 more days of progesterone administration from the day of cycle in which the biopsy was taken to reach the receptive state.
- A post-receptive diagnosis indicates that the endometrium has already passed the ideal window for embryo implantation in the day of the cycle when the biopsy was performed, so 1 or 2 days less of progesterone administration is required to achieve receptive status.

A recent study [21] investigated whether the contribution of the endometrial factor could be identified with the ERA test and if actionable results can lead to improved outcomes. In this study 88 patients with a history of euploid blastocyst implantation failure underwent ERA testing between 2014 and 2017. Reproductive outcomes were compared for patients undergoing FET using a standard progesterone protocol versus those with non-receptive results by ERA and subsequent FET according to a personalized embryo transfer (pET) protocol. Results show that 22.5% of patients with at least one previously failed euploid FET had a displaced WOI diagnosed by ERA and qualified for pET. After pET, implantation and ongoing pregnancy rates were higher (73.7 vs 54.2% and 63.2 vs 41.7%, respectively) compared to patients without pET, supporting the optimal results obtained by ERA.

An international randomized controlled study is underway to perform endometrial assessment during fertility screening at the beginning of reproductive care (the ERA as a diagnostic guide for personalized embryo transfer. ClinicalTrials.gov Identifier: NCT01954758). An ERA RCT consortium was created to include 28 clinics worldwide. This randomized study included patients undergoing transfer at the blastocyst stage (day 5 or day 6) in their first IVF/ICSI cycle with a body mass index (BMI) between 18.5 and 30, younger than 37 years old, and a normal ovarian reserve. If any pathology affecting the endometrial cavity existed, patients were previously operated. Exclusion criteria were recurrent pregnancy loss and/or severe male factor.

The study consists of three arms comparing fresh embryo transfer under stimulation protocol, frozen embryo transfer at P + 5 in HRT cycles, and pET guided by ERA with frozen embryos in HRT cycles. At the midpoint of recruitment, results show significant differences between pregnancy rate (PR) for pET arm (85.7%) versus fresh embryo transfer (FET) (61.7%) and deferred embryo transfer (DET) (60.8%). Although not yet significant, there are also differences in implantation rate (IR) (47.8% for pET, 35.3% for FET, and 41.4% for DET) and in ongoing pregnancy rate (OPR) per embryo transfer (55.1% for pET, 43.3% for FET, and 44.6% for DET). These interim results were published in the American Society of Reproductive Medicine (ASRM) 2016 scientific congress [22] and show that 14% of patients have a displaced WOI whose correction would likely result in an effective cost-benefit strategy at the first clinical appointment.

Other studies have attempted to describe the transcriptomic profile of endometrial receptivity [23]. A lately meta-analysis found that 57 genes, including genes present in the ERA (i.e., SPP1, ANXA4, CLDN4, DPP4, GPX3, MAOA, and PAEP), were identified as potential receptivity biomarkers in multiple studies and are the most representative panel for predicting the WOI [24]. However, these findings have not been translated to the clinic.

Endometrial Microbiome: The New Kid on the Block

Humans are inhabited by trillions of microbes, residing in different body sites. The advent of highly sensitive molecular techniques, especially next-generation sequencing, has opened up new possibilities to explore the microbiota of body sites that were previously unexplored or considered sterile and how they participate in our physiology. In fact, a recent study has reported the microbiota across the female reproductive tract [25], showing that there is a continuum of slightly different microbiota expanding gradually from the vagina to the ovaries.

According to recent publications [26, 27], up to 40% of patients undergoing IVF treatments present abnormal vaginal microbiota, being bacterial vaginosis the most common vaginal disorder in reproductive age women and resulting in millions of health care visits per year. It is associated with infertility, endometritis, pelvic inflammatory disease, and increased risk of acquiring HIV, which implies a decrease in reproductive outcomes.

Aiming to find out if there is a specific endometrial microbiota and its putative role in endometrial receptivity and pregnancy outcomes, our group carried out three separate prospective studies which were published in 2016 [5]. In this study, the species-specific sequences of the variable regions of the 16S rRNA gene were analyzed by NGS to evaluate the relative abundances of each microorganism present in the microbial population.

In the first part of the study, it was compared the microbiota of paired samples of endometrial fluid and vaginal aspirates from 13 healthy and fertile subjects in pre-receptive (LH + 2) and receptive phase (LH + 7) in natural cycles. From all the samples, nine were colonized only by *Lactobacillus* spp., while the rest showed a combination of different operational taxonomic units (OTUs) in addition to *Lactobacillus*. In 24 out of 26 paired of samples, there were found slight differences between endometrial and vaginal microbiota, but in 6 of them the bacterial communities were completely different with a high proportion of potential pathogens in the endometrium or in the vagina; the same bacterial OTUs were present in only two pair of samples. The conclusion was that the uterine cavity is not sterile and endometrial and vaginal microbiomes are different in asymptomatic women.

The second part of the study consisted in investigating the hormonal regulation of the endometrial microbiota. For this purpose, the endometrial fluid from 22 healthy and fertile women in natural cycle was taken in LH + 2 and LH + 7 in the same cycle. The bacterial communities found were clustered according to the bacterial different OTUs identified and their abundances. The resulting heatmap showed two sets of samples classifying depending on the percentage of *Lactobacillus* OTUs identified. The first set of samples included those with a high abundance of *Lactobacillus* (over 90%) and very low or nonexistent other OTUs. The second set of samples was formed by lower *Lactobacillus* abundances that coexisted with bacteria represented by other OTUs. Clustering of individual samples showed two groups depending on the abundance of *Lactobacillus* OTUs. This part of the study concluded that endometrial microbiome is not regulated by hormones during the acquisition of endometrial receptivity.

Finally, the functional impact of the endometrial microbiota composition on reproductive outcome in patients undergoing IVF was studied, concluding that low abundance of *Lactobacillus* in endometrial microbiota is associated with poor reproductive outcomes in IVF patients. In fact, subjects with a non-*Lactobacillus* dominant microbiota had significantly lower implantation (60.7% vs 23.1%, $p = 0.02$), pregnancy (70.6% vs 33.3%, $p = 0.03$), ongoing pregnancy (58.8% vs 13.3%, $p = 0.02$), and live birth (58.8% vs 6.7%, $p = 0.002$) rates, as well as higher miscarriage rates (16.7% vs 60%, $p = 0.007$), although this was not statistically significant, compared to those with a *Lactobacillus* dominant microbiota.

In conclusion, the uterine cavity is not sterile. A human endometrial microbiota exists, and it is different from the vaginal microbiomes in asymptomatic women. Furthermore, the endometrial microbiome is not hormonally regulated during the acquisition of endometrial receptivity, and the existence of non-*Lactobacillus* bacteria is related to negative impacts in reproduction.

The molecular microbiology method has also been used to identify culturable and nonculturable endometrial pathogens associated with chronic endometritis such as *Enterobacteriaceae*, *Enterococcus*, *Streptococcus*, *Staphylococcus*, *Mycoplasma*, and *Ureaplasma* [28].

Chronic endometritis is a persistent inflammation of the endometrial mucosa that can be asymptomatic, but it is found in up to 40% of infertile patients and is responsible for repeated implantation failure and recurrent miscarriage.

With this aim, the classical methods used to diagnosis of chronic endometritis (hysteroscopy of the uterine cavity, endometrial biopsy with plasma cells being identified histologically, and microbial culture) were compared to the molecular method by evaluating 113 endometrial samples from patients assessed for chronic endometritis by real-time PCR. The results were lately confirmed by the microbiome assessed by next-generation sequencing. In the endometrial samples with concordant results in the three classic methods, the molecular microbiology diagnosis demonstrates 75% sensitivity, 100% specificity, 100% positive and 25% negative predictive values, and 0% false-positive and 25% false-negative rates, concluding that the molecular microbiology method is a fast and inexpensive diagnostic tool that allows for the identification of culturable and nonculturable endometrial pathogens associated with chronic endometritis.

Improving Endometrial Receptivity Assessment

Despite careful embryo selection, reproductive outcomes resulting from ART remain lower than optimal. Among the multiple factors implied in effective IVF treatment, the primary limiting factor is successful embryo implantation. Implantation failures are caused primarily by poor endometrial receptivity, defects in the embryo, diseases or disorders in the endometrium, and unbalance endometrial microbiome. It is accepted that two-thirds of these implantation failures have their origin in low endometrial receptivity or in a defective endometrium-embryo dialogue.

The functional genomics of endometrial receptivity has been extensively investigated to find transcriptomic markers of endometrial receptivity during the implantation window, with the vision of using this information in diagnosing endometrial receptivity. This advance implies the substitution of other classic biochemical and morphological markers, whose effectiveness has been frequently questioned. The ERA has become the gold standard for the diagnosis of WOI displacement in patients with RIF based on the transcriptomic profile of endometrial samples and has been used for clinical and academic research in endometrial receptivity. Currently, our group is validating a noninvasive test to provide consistent results and make it easier for clinicians to obtain samples and avoid unnecessary pain and discomfort to the patients.

Furthermore, technological advances in genetics have enabled the association of single-nucleotide polymorphisms or genetic variants with several traits and diseases. Genome-wide association studies (GWAS) would be helpful to identify genetic variants in non-receptive patients that are causative of a displacement of the WOI. If such association is found, this information could be finally used for the development of less-invasive test in blood samples for endometrial receptivity assessment, and the genes identified can be target for new research lines oriented to the clinical management of infertile patients with endometrial factor.

References

1. Hertig AT, Rock J, Adams EC. A description of 34 human ova within the first 17 days of development. Am J Anat. 1956;98(3):435–93.

2. Navot D, Scott RT, Droesch K, Veeck LL, Liu H-C, Rosenwaks ZJF, et al. The window of embryo transfer and the efficiency of human conception in vitro. Fertil Steril. 1991;55(1):114–8.
3. Wilcox AJ, Baird DD, Weinberg CR. Time of implantation of the conceptus and loss of pregnancy. N Engl J Med. 1999;340(23):1796–9.
4. Díaz-Gimeno P, Horcajadas JA, Martínez-Conejero JA, Esteban FJ, Alamá P, Pellicer A, et al. A genomic diagnostic tool for human endometrial receptivity based on the transcriptomic signature. Fertil Steril. 2011;95(1):50–60, 60.e1–15.
5. Moreno I, Codoñer FM, Vilella F, Valbuena D, Martinez-Blanch JF, Jimenez-Almazán J, et al. Evidence that the endometrial microbiota has an effect on implantation success or failure. Am J Obstet Gynecol. 2016;215(6):684–703.
6. Noyes R, Hertig A, Rock J, Survey G. Dating the endometrial biopsy. Am J Obstet Gynecol. 1950;5(4):561–4.
7. Murray MJ, Meyer WR, Zaino RJ, Lessey BA, Novotny DB, Ireland K, et al. A critical analysis of the accuracy, reproducibility, and clinical utility of histologic endometrial dating in fertile women. Fertil Steril. 2004;81(5):1333–43.
8. Coutifaris C, Myers ER, Guzick DS, Diamond MP, Carson SA, Legro RS, et al. Histological dating of timed endometrial biopsy tissue is not related to fertility status. Fertil Steril. 2004;82(5):1264–72.
9. Turnbull L, Rice C, Horsman A, Robinson J, Killick SR. Diagnostic techniques: magnetic resonance imaging and transvaginal ultrasound of the uterus prior to embryo transfer. Hum Reprod. 1994;9(12):2438–43.
10. Cheng F, Li T, Wang Q-L, Zhou H-L, Duan L, Cai X, et al. Effects of hydrosalpinx on ultrasonographic parameters for endometrial receptivity during the window of implantation measured by power color Doppler ultrasound. Int J Clin Exp Med. 2015;8(4):6103–8.
11. Malhotra N, Bahadur A, Kalaivani M, Mittal S. Changes in endometrial receptivity in women with Asherman's syndrome undergoing hysteroscopic adhesiolysis. Arch Gynecol Obstet. 2012;286(2):525–30.
12. Lessey BA, Castelbaum AJ, Sawin SW, Sun J. Integrins as markers of uterine receptivity in women with primary unexplained infertility. Fertil Steril. 1995;63(3):535–42.
13. Kliman H, Honig S, Walls D, Luna M, McSweet J, Copperman AB, et al. Optimization of endometrial preparation results in a normal endometrial function test®(EFT®) and good reproductive outcome in donor ovum recipients. J Assist Reprod Genet. 2006;23(7–8):299–303.
14. Giuliani E, Parkin KL, Lessey BA, Young SL, Fazleabas AT. Characterization of uterine NK cells in women with infertility or recurrent pregnancy loss and associated endometriosis. Am J Reprod Immunol. 2014;72(3):262–9.
15. Aghajanova L, Hamilton A, Giudice L, editors. Uterine receptivity to human embryonic implantation: histology, biomarkers, and transcriptomics. Semin Cell Dev Biol. 2008;19(2):204–11.
16. Díaz-Gimeno P, Ruíz-Alonso M, Blesa D, Simón C. Transcriptomics of the human endometrium. Int J Dev Biol. 2014;58(2–4):127–37.
17. Garrido-Gómez T, Ruiz-Alonso M, Blesa D, Diaz-Gimeno P, Vilella F, Simón CJF, et al. Profiling the gene signature of endometrial receptivity: clinical results. Fertil Steril. 2013;99(4):1078–85.
18. Kao L, Tulac S, Lobo S, Imani B, Yang J, Germeyer A, et al. Global gene profiling in human endometrium during the window of implantation. Endocrinology. 2002;143(6):2119–38.
19. Shi W, Bessarabova M, Dosymbekov D, Dezso Z, Nikolskaya T, Dudoladova M, et al. Functional analysis of multiple genomic signatures demonstrates that classification algorithms choose phenotype-related genes. Pharmacogenomics J. 2010;10(4):310–23.
20. Ruiz-Alonso M, Blesa D, Díaz-Gimeno P, Gómez E, Fernández-Sánchez M, Carranza F, et al. The endometrial receptivity array for diagnosis and personalized embryo transfer as a treatment for patients with repeated implantation failure. Fertil Steril. 2013;100(3):818–24.
21. Tan J, Kan A, Hitkari J, Taylor B, Tallon N, Warraich G, et al. The role of the endometrial receptivity array (ERA) in patients who have failed euploid embryo transfers. J Assist Reprod Genet. 2018;35(4):683–92.
22. Simon C, Vladimirov I, Cortes GC, Ortega I, Cabanillas S, Vidal C, et al. Prospective, randomized study of the endometrial receptivity analysis (ERA) test in the infertility work-up to guide personalized embryo transfer versus fresh transfer or deferred embryo transfer. Fertil Steril. 2016;106(3):e46–e7.
23. Gómez E, Ruíz-Alonso M, Miravet J, Simón C. Human endometrial transcriptomics: implications for embryonic implantation. Cold Spring Harb Perspect Med. 2015;5(7):a022996.
24. Altmäe S, Koel M, Võsa U, Adler P, Suhorutšenko M, Laisk-Podar T, et al. Meta-signature of human endometrial receptivity: a meta-analysis and validation study of transcriptomic biomarkers. Sci Rep. 2017;7(1):10077.
25. Chen C, Song X, Wei W, Zhong H, Dai J, Lan Z, et al. The microbiota continuum along the female reproductive tract and its relation to uterine-related diseases. Nat Commun. 2017;8(1):875.
26. Franasiak JM, Scott RT Jr. Introduction: microbiome in human reproduction. Fertil Steril. 2015;104(6):1341–3.
27. Miles SM, Hardy BL, Merrell DS. Investigation of the microbiota of the reproductive tract in women undergoing a total hysterectomy and bilateral salpingo-oopherectomy. Fertil Steril. 2017;107(3):813–820.e1.

28. Moreno I, Cicinelli E, Garcia-Grau I, Gonzalez-Monfort M, Bau D, Vilella F, et al. The diagnosis of chronic endometritis in infertile asymptomatic women: a comparative study of histology, microbial cultures, hysteroscopy, and molecular microbiology. Am J Obstet Gynecol. 2018;218(6):602.e1–602.e16.

List of Relevant Websites

E-tegrity: http://www.etegritytest.com/
EFT®: http://klimanlabs.yale.edu/infertility/eft/
ERA: https://www.igenomix.com/tests/endometrial-receptivity-test-era/

Part VII

Ultrasound and Pregnancy

Early Pregnancy Ultrasound

23

Laura Detti

Introduction

Early pregnancy ultrasound is performed to assess the location of a pregnancy (intrauterine or extrauterine) and its viability. It also appraises the number of embryos and their chorionicity and amnionicity and often is instrumental in predicting the development, and dictates the management, of a pregnancy in the second and third trimester. Among the main objectives of the early pregnancy ultrasound are correct dating, evaluation of early pregnancy landmarks and placental location, and distinguishing normal from abnormal pregnancy. In addition, first trimester ultrasound allows evaluation of the ovaries and the corpus luteum.

Temporally, the first structure to be appreciated by ultrasound is the gestational sac, followed by the yolk sac, the embryo, and, when present, the embryonal cardiac activity. There is general consensus that the best technique to assess the early pregnancy is by transvaginal ultrasound: the higher resolution and the closer proximity of the transvaginal transducer allow the identification of structures such as a 2-mm gestational sac, or a 1-mm yolk sac, in addition to allowing excellent anatomical details of the embryo. In this chapter we will describe the evaluation of the first trimester singleton and multiple pregnancy using the transvaginal ultrasound technique.

Pregnancy Location

It is of foremost importance to locate a pregnancy in a woman with a positive pregnancy test. An intrauterine pregnancy can be identified with a β-hCG level as low as 1500 mIU/ml, depending on the ultrasound machine capabilities. A conservative discriminatory β-hCG level of 3000 mIU/ml has been set forth by the American Institute of Ultrasound in Medicine and the Society of Radiologists in 2012 [1]. Based on these societies' panel, presumptive treatment for ectopic pregnancy with the use of methotrexate or other pharmacologic or surgical means should be undertaken only if a single β-hCG measurement is greater than 3000 mIU/ml. Under this condition, a viable intrauterine pregnancy is possible but unlikely, and treatment can be initiated, especially if a repeat β-hCG level confirms the first one. The American College of Obstetrics and Gynecology has recently endorsed this conservative approach without giving a specific discriminatory β-hCG level, as each institution should have their own based on the level of expertise, as well as laboratory thresholds, and ultrasound capabilities [2].

L. Detti (✉)
University of Tennessee Health Science Center,
Department of Obstetrics and Gynecology,
Memphis, TN, USA
e-mail: ldetti@uthsc.edu

L. A. Stadtmauer, I. Tur-Kaspa (eds.), *Ultrasound Imaging in Reproductive Medicine*,
https://doi.org/10.1007/978-3-030-16699-1_23

A true gestational sac within one side of the endometrial echo is a reliable sign of intrauterine pregnancy; however, an astute clinician must always have concern for life-threatening concurrent ectopic pregnancy (heterotopic) or pregnancy loss. In the presence of an uncertain situation, the clinician must decide what signs and symptoms are normal or abnormal in early pregnancy.

Embryonal Landmarks and Temporal Appearance

Transvaginal ultrasound (TUS) features high-resolution images, low interobserver variability, and high reliability and is conventionally used to make diagnosis of intrauterine pregnancy and to follow up with its development. Gestational sac, yolk sac, crown-rump length, heart rate, and amniotic sac are the features evaluated to assess the early pregnancy.

Gestational Sac (GS)

It is the first structure to develop from the implanted embryo, and it is present as early as 4 complete weeks' gestation. By TUS, it can be visualized as an echoic ring (trophectoderm) surrounding an anechoic center (fluid), embedded in one side of the endometrium (eccentric). Typically, it is measured by averaging the three diameters in the two orthogonal planes (Hellman's method), but more recently it is measured by only the largest diameter (Rempen's method). The algorithm in the individual ultrasound machines will calculate the gestational age based on one of the two methods. Figure 23.1 shows the correct measurement of a GS based on three diameters in the two orthogonal planes. The GS's average diameter grows linearly during the first 12 weeks of pregnancy. This trend has been confirmed by cross-sectional [3], as well as longitudinal [4], studies. Figure 23.2a shows the GS growth based on longitudinal data from 193 pregnancies that ended in live birth.

Yolk Sac (YS)

The secondary YS is the second structure to develop, together with the embryo; however, in most instances it is the first of the two to be visualized. It should always be visualized when the GS is greater than 8 mm in diameter [5]. It is

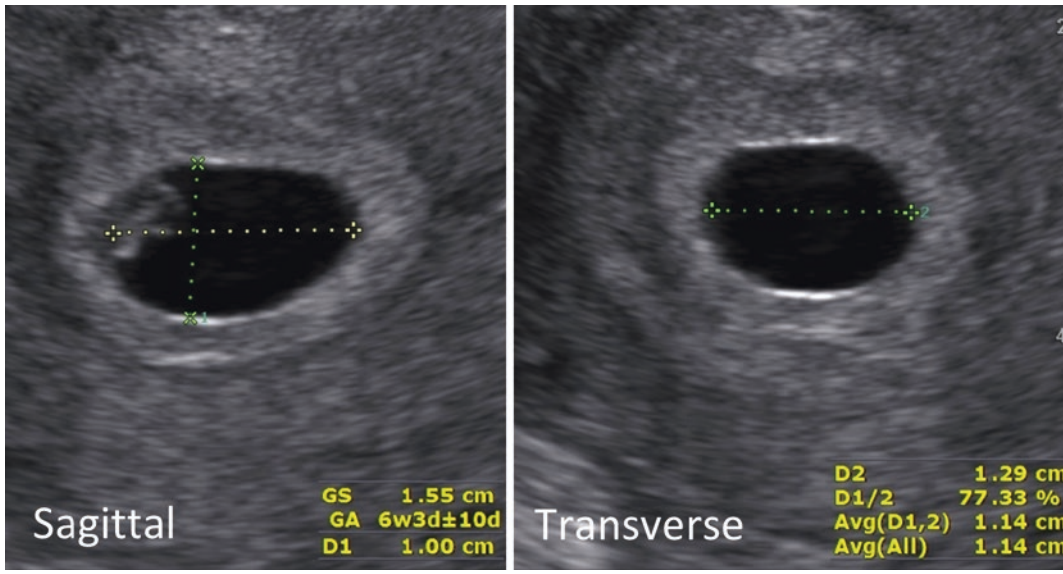

Fig. 23.1 Measurement of a gestational sac in the two orthogonal planes. Six weeks and 3 days – normal GS

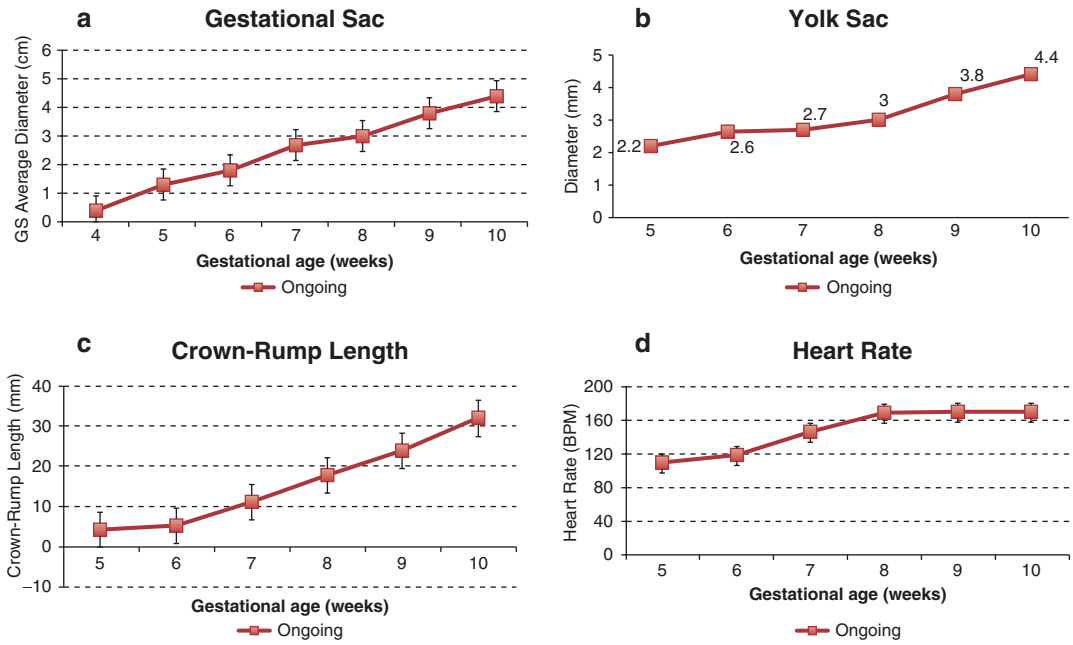

Fig. 23.2 Ultrasonographic measurement of various parameters during the first 10 weeks of pregnancy. (**a**) Gestational Sac; (**b**) Yolk Sac; (**c**) CRL, or Crown-Rump Length; (**d**) Heart Rate

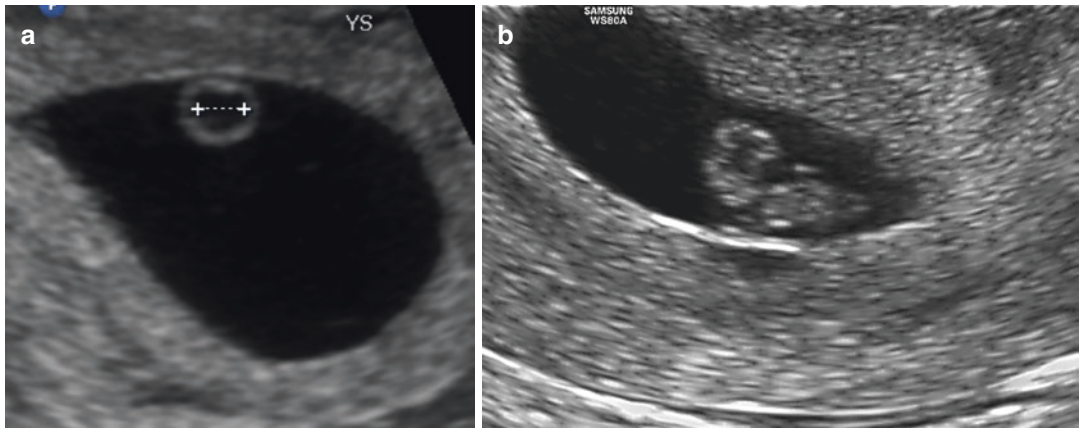

Fig. 23.3 (**a**) Correct measurement of the yolk sac. (**b**) A misshapen yolk sac

measured placing the cursor from the inner rim to the opposite inner rim, and, if misshapen, the three dimensions in the two orthogonal planes should be averaged. The YS grows linearly during the first 10 weeks of pregnancy, 0.44 mm per week (Fig. 23.2b) [6], and is then progressively distanced from the embryo by the developing amniotic sac. Figure 23.3 shows a normal YS with the correct measurement (a) and a misshapen YS (b).

Embryo and Crown-Rump Length (CRL)

The embryo develops together with the secondary yolk sac; however, because of its discoid shape and the adjacent yolk sac, it is not easily visualized until almost 6 weeks' gestation. Between 5 and 6 complete weeks' gestation, the embryo assumes a tubular shape, and, as the neural tube is sealed on both ends, it gradually

assumes a C-shaped conformation. At this time the amniotic sac becomes visible as a translucent membrane projecting from the embryo's stalk within the GS. Until 53 days (= 9.4 weeks' gestation), the caudal portion of the embryo is the tail. Only after 60 days (= 10.5 weeks' gestation) does the head become the most cephalad portion of the embryo/fetus. This means that until 11 weeks' gestation, we measure the longest fetal diameter rather than the real CRL. Nonetheless, measuring the CRL is the most reliable way to date a pregnancy when the last menstrual period is not known. In addition, when in the first trimester the estimated gestational age by CRL differs greater than ±7 days from the gestational age by LMP, the estimated date of delivery should be changed.

From 6 to 9.4 weeks, the CRL grows approximately 1 mm/day [3, 4], as seen in Fig. 23.2c. Figure 23.4 shows an ultrasound picture (a) and an electronic microscopy picture (b), of an embryo at 5 weeks' gestation. As seen, the embryo is still discoid and the secondary YS is adjacent to the embryo. Figure 23.5 shows the

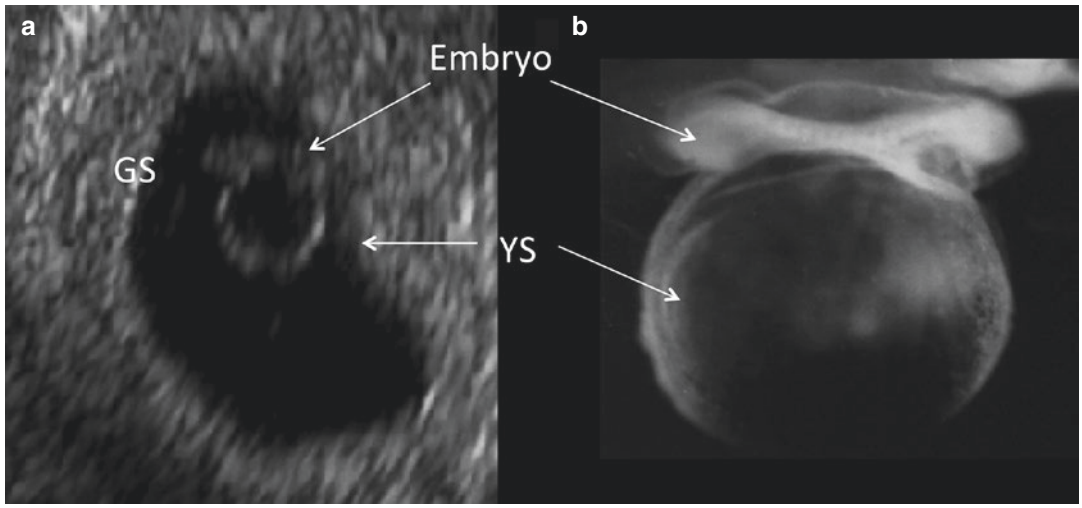

Fig. 23.4 Ultrasound (**a**) and electronic microscopy (**b**) images of a 5 weeks' gestation embryo

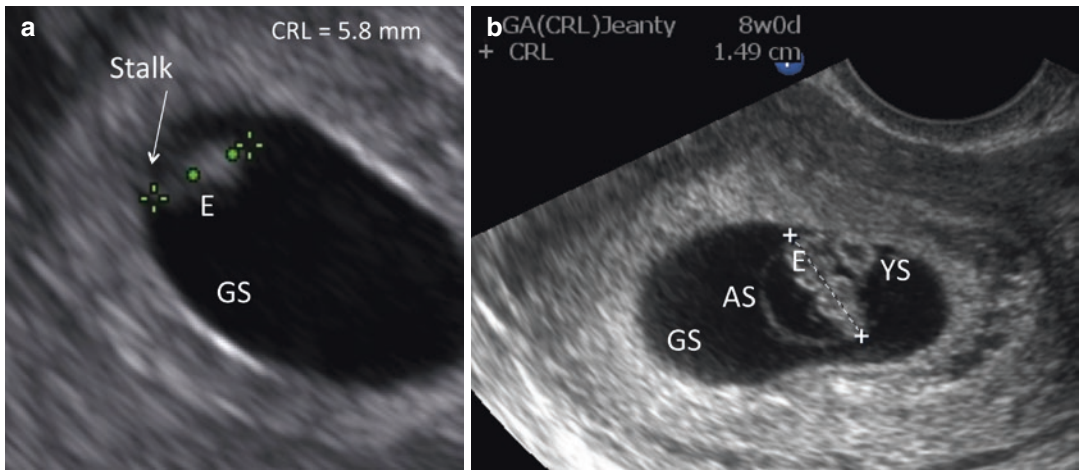

Fig. 23.5 Measurement of the CRL at 6 weeks and 3 days' (**a**) and at 8 weeks' gestation (**b**)

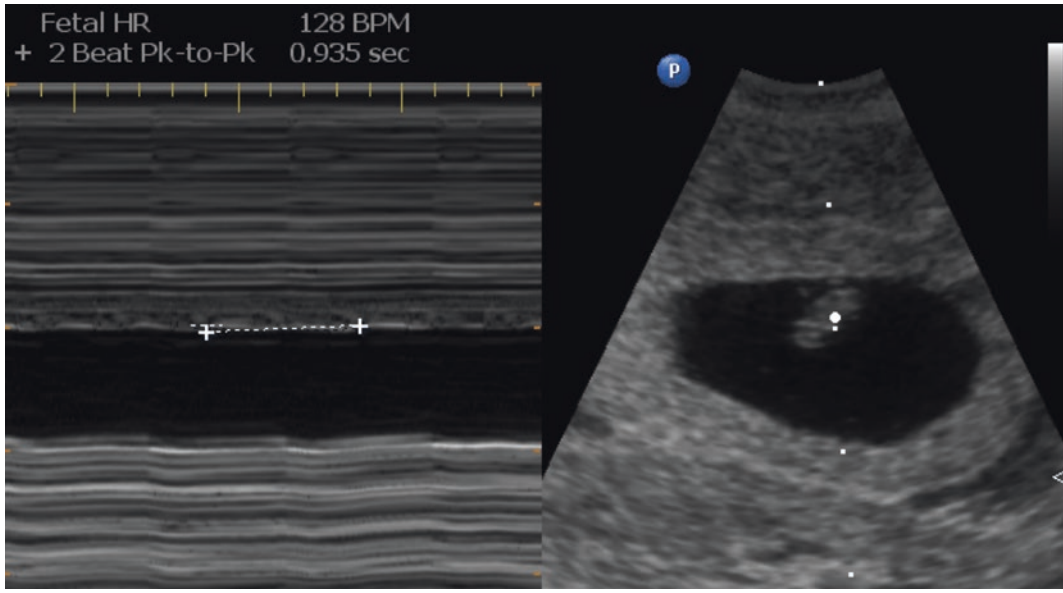

Fig. 23.6 M-mode for measurement of embryonal heart rate at 6 weeks and 4 days' gestation

correct CRL measurement and the embryonal stalk at 6 weeks' and at 8 weeks' gestation.

Embryonal Heart Rate (EHR)

The heart starts contracting to propel blood before it is fully formed during the third week of embryonal life or 5 weeks' gestation. The rate of its contractions (beats per minute = BPM) is slow in the beginning, and it progressively increases until 8 complete weeks, when it reaches approximately 180 BPM [7]. Between 5 and 6 weeks, the EHR is about 100 BPM; however, it could be slower (Fig. 23.2d). Figure 23.6 shows the M-mode technique to measure the EHR. The Doppler technique to measure the EHR should not be used until after the completion of the first trimester of pregnancy, to avoid overheating of the delicate embryonal structures and possible development of congenital defects and/or intrauterine growth restriction [in accordance with the as low as reasonably achievable (ALARA) principle] [8]. EHR increases exponentially from 5 to 8 complete weeks' gestation, and it then decreases to reach a plateau of 140–150 BPM at 15 weeks'.

Pregnancy Dating

Of the parameters previously described, the only one that has proven reliability and reproducibility to determine a pregnancy's age is the CRL. When an EHR is present, the CRL measurement can reliably diagnose the gestational age. However, if EHR is absent and the CRL measures less than 7 mm (7 weeks' gestation), it becomes critical to assess the presence of the AS. Since the AS becomes visible on ultrasound at 7 weeks' gestation, even if the CRL measures 5 or 6 complete weeks' gestation, the presence of an AS would date a pregnancy at least at 7 weeks'. Figure 23.7 shows an example of a pregnancy lost at 7 weeks and 2 days, with the CRL measuring 5.6 mm: the CRL would date the pregnancy at 6 weeks and 3 days; however, the presence of the AS dates the pregnancy to after 7 weeks'. The "double-bleb" sign, initially described as a sign of genetically abnormal pregnancy, actually represents the yolk

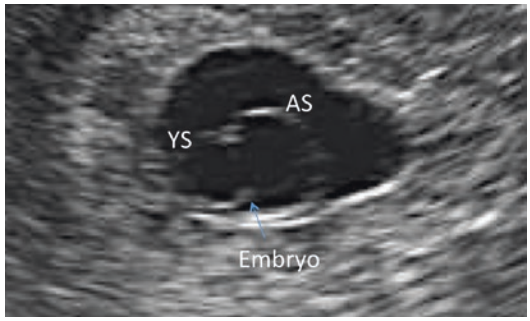

Fig. 23.7 The double-bleb sign made of the yolk sac and the amniotic sac with a faintly visualized embryo in between

sac (left "bleb") and the AS (right "bleb") with the embryo faintly visualized in between. These findings characterize a new concept of growth restriction in the first trimester, which could be important in establishing the causes of a pregnancy loss, especially in the instance of recurrent early pregnancy loss.

Diagnosis of Placental Location

During implantation, the embryo penetrates the functional layer of the endometrium with the inner cell mass facing its basal layer. Upon contact, the cytotrophoblast, the outer cell layer of the blastocyst, starts proliferating to create the trophoblastic shell. This shell is comprised of a cytotrophoblast layer with intermingled syncytial cells, which then coalesce to form the syncytiotrophoblast [9]. During the third week of embryo development, or 5 weeks gestation, the cytotrophoblast and syncytiotrophoblast form the villous chorion. At this point, embryonic blood begins to flood the villi via the umbilical arteries through the embryonal stalk, which will progressively elongate to form the umbilical cord. The embryonal blood causes development of the chorionic villi located above the basal decidua, which will then anchor the chorion frondosum with the apposed amnion.

Traditionally, placental location is identified by TUS after 8 weeks gestation, when the placenta forms by anchoring the chorion frondosum with the apposed amnion in the basal decidua [10]. The circulation in the chorion frondosum starts becoming prominent, thus appearing hyperechogenic on ultrasound and allowing its localization in relationship to the uterine wall [11]. Placental location has also been visualized using power Doppler before 10 weeks of gestation, at which point scattered vessels can be identified surrounding the gestational sac [12]. However, identification of embryonal stalk, and thus future location of the chorion frondosum and the placenta, is possible via ultrasound by 5–6 weeks gestation, and its reliability has been confirmed by a pioneer study by our group [13]. In fact, placental location diagnosed at 5 or 6 weeks of gestation was consistent with the location on mid-pregnancy ultrasound in 100% of the 111 singleton and twin pregnancies studied, even if in 21.2% of the cases the placenta had moved to an adjacent location (i.e., from fundal, it became anterior or posterior by the second trimester scan). Figure 23.8 shows placental location diagnosis on the two orthogonal planes, and Fig. 23.9 shows 3D renderings of 6 weeks and 3 days and 7 weeks and 5 days pregnancies.

Placental location has a significant impact on pregnancy outcome and on maternal and fetal morbidity and mortality. Early identification of placenta previa allows clinicians to more closely follow the pregnancy, thus reducing risk of low neonatal weight, postpartum hemorrhage, gestational hypertension, and preterm labor and delivery [11, 14, 15]. In the case of cesarean section scar pregnancies, which are on the rise with increasing incidence of cesarean deliveries and which constitute 6.4% of ectopic pregnancies [16], the risk of morbid adherence to the anterior wall of the uterus and the posterior wall of the bladder is considered so high that termination of pregnancy is recommended [17]. Thus, early knowledge of placental location allows the clini-

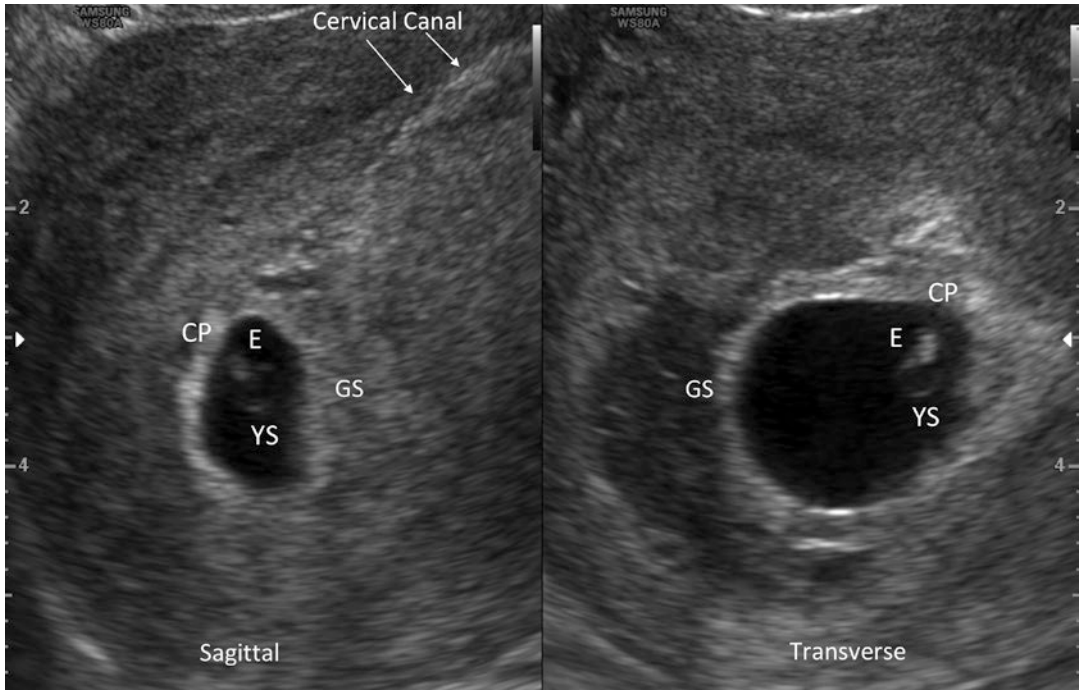

Fig. 23.8 Antero-left placenta at 5 weeks and 1 day pregnancy. CP, chorionic plate

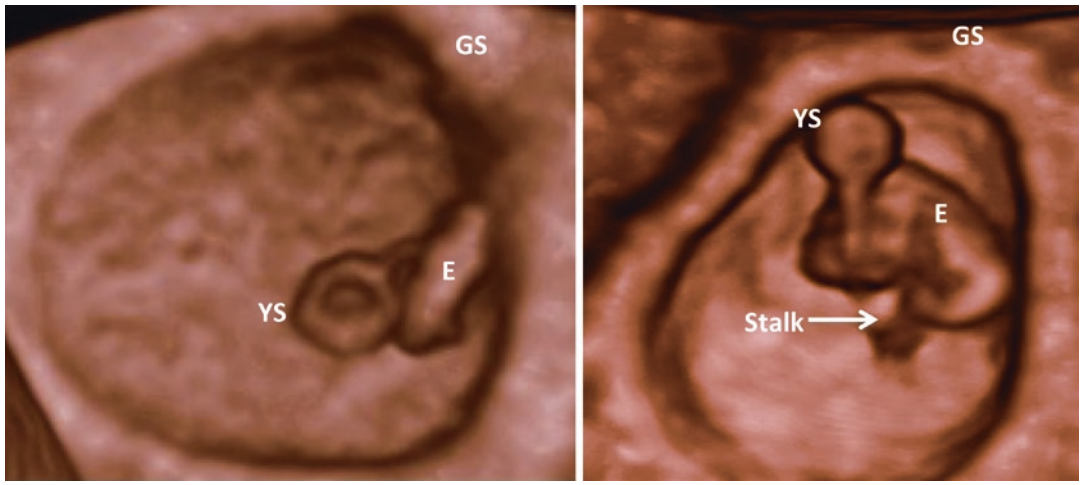

Fig. 23.9 3D renderings of an intrauterine pregnancy at 6 weeks and 3 days' (**a**) and one at 7 weeks and 5 days' gestation (**b**)

cian to identify potential risks and counsel the patient accordingly. Similarly, knowing the site of the placenta in the presence of uterine subseptations can help in counseling the patient about the possible pregnancy outcome. Figure 23.10 shows a subseptate uterus with the GS on the right of the subseptation and the placenta implanted in the right lateral wall.

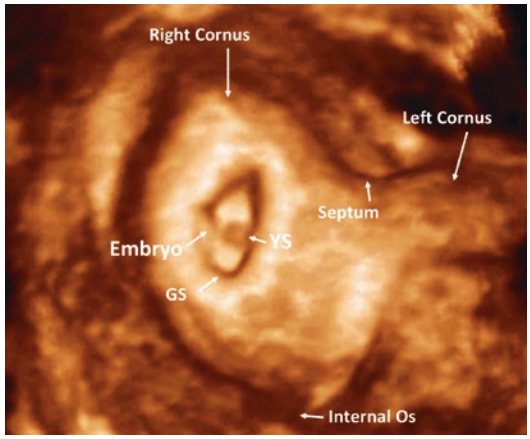

Fig. 23.10 Subseptate uterus with the GS on the right of the subseptation and the placenta implanted in the right lateral wall

Pregnancy Viability

Early pregnancy loss, or failed pregnancy, or miscarriage is defined as a nonviable, intrauterine pregnancy with either an empty gestational sac or a gestational sac containing an embryo or fetus without fetal heart activity within the first 12 complete weeks of gestation [18]. It is the most common complication of early pregnancy, affecting as many as 30% of pregnancies following assisted reproduction technology [19]. In spontaneous pregnancies, the reported incidence of miscarriage is lower, about 10% [20, 21]. The difference is probably due to the fact that spontaneous pregnancy is clinically recognized at a later time than assisted reproduction ones, and an early miscarriage is easily missed. Vaginal bleeding is a common sign of early pregnancy failure; however, it can be confused with a delayed menstruation and remains undiagnosed. Chromosomal abnormalities are the cause of a miscarriage in greater than 50% of the times, and aneuploidy is the most frequently observed abnormality [22, 23]. Changes in the ultrasound features have been alternatively investigated to predict pregnancy outcome and in particular miscarriage. Logistic regression models including large numbers of pregnancies identified maternal age, HR, CRL, and vaginal bleeding as the most significant prognostic variables to predict a miscarriage in both spontaneous [24] and in vitro fertilization pregnancies [25]. However, the models were not specific for a definite gestational age and included parameters, such as maternal age, which, alone, is a well-established risk factor for first trimester miscarriage [26]. A recent systematic review summarized sensitivities and specificities for the ultrasound parameters and found an EHR ≤110 BPM to be the most reliable one to predict a subsequent miscarriage, with a sensitivity of 68.4%, a specificity of 97.8%, a positive likelihood ratio of 31.7 (95% confidence interval 12.8–78.8), and a negative likelihood ratio of 0.32 (95% confidence interval 0.16–0.65) [27]. In women with an HR ≤110 BPM and vaginal bleeding, all the statistics increased, indicating enhanced predictability. It was also reported that, in addition to CRL, GS, and EHR, below the 5th percentile, a YS diameter above the 95th percentile was predictive of early miscarriage (odds ratio 1.04); however, a normal YS did not decrease the risk of miscarriage, if the other parameters were abnormal [28]. Other studies have indicated an enlarged YS to be associated with miscarriage, while an abnormal YS shape was not predictive [5, 29, 30].

All the markers established as predictors of adverse pregnancy outcomes, however, have always been evaluated cross-sectionally with only one ultrasound per patient [5, 24, 25, 27–30]. Our group performed a longitudinal study of all the early pregnancy landmarks. In this study multiple ultrasounds were performed to accurately represent all gestational ages in each patient. This allowed us to obtain longitudinal data in the same patient, further strengthening our study. We previously described a nomogram of YS development during the first 10 weeks of pregnancy with serial ultrasounds (Fig. 23.11a) [6]. After 5 weeks' gestation, the YS reliably detects pregnancies that will end in miscarriage. In these pregnancies, the YS was either smaller or larger than in ongoing pregnancies. While all pregnancies with large YS miscarried within 10 weeks, some pregnancies with smaller YS miscarried beyond the first 10 weeks of pregnancy. In a subsequent study which combined all first trimester parameters, the same group established that YS and GS are the earliest parameters that can be reliably used as a prognostic factor for poor pregnancy outcome later in the first trimester, as they become abnormal as early as 6 weeks of gestation, even if the actual loss occurs after 8 weeks [4]. Figure 23.11 shows the changes of the early pregnancy land-

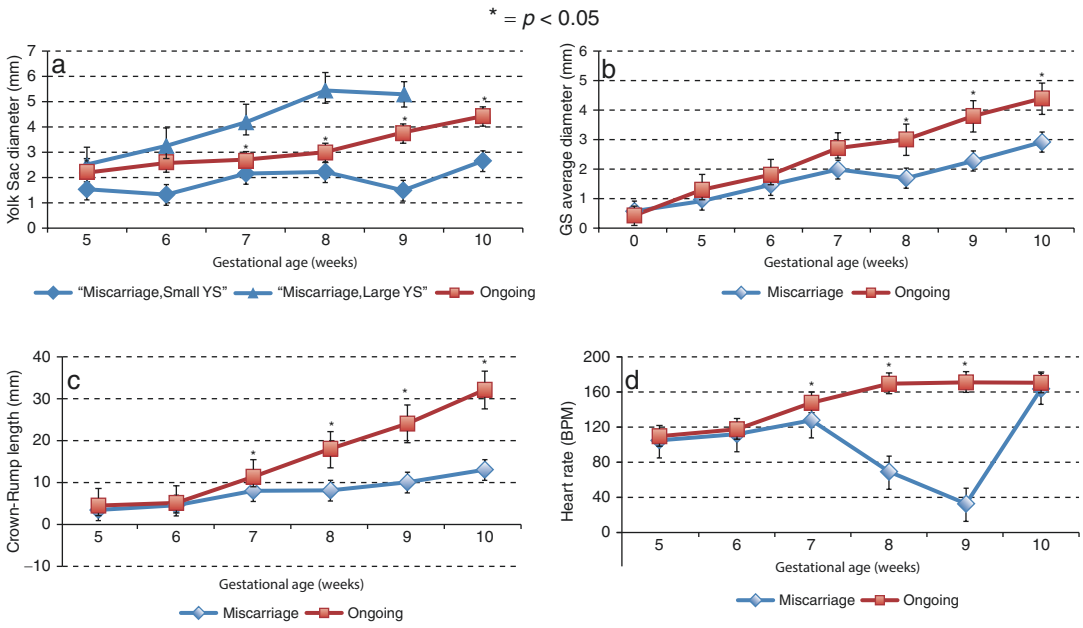

Fig. 23.11 Ultrasonographic measurement changes of the early pregnancy landmarks in ongoing and in failed pregnancies: (**a**) Yolk Sac diameter; (**b**) Gestational Sac; (**c**) Crown-Rump length; (**d**) Embryonic heart rate

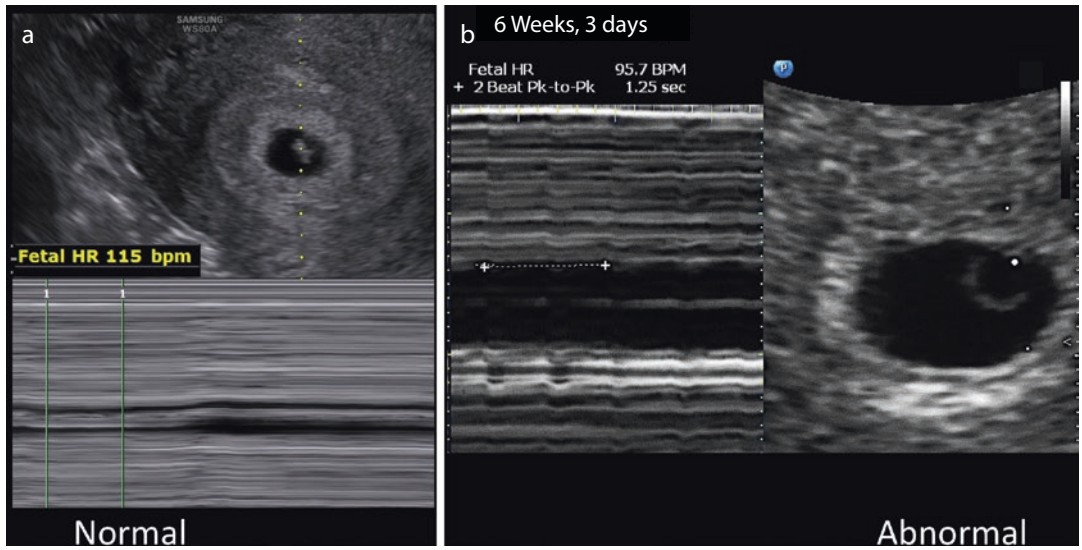

Fig. 23.12 Normal (**a**) and abnormal (**b**) embryonal heart rates

marks in pregnancies with live birth and in early loss. CRL was a very reliable indicator of adverse first trimester outcome; however, it became abnormal at a later gestational age and closer to the event, thus providing little warning of an impending miscarriage. In addition, CRL is difficult to measure between 6 and 7 weeks of gestation, being subject to greater interobserver variability. Given the rather important variation in BPM per second, HR is not a reliable tool to predict the occurrence of a miscarriage unless it is below 100 BPM at a gestational age greater than 6 weeks' gestation [4, 31]. Another shortcoming of HR is that it becomes abnormal close to the event, thus providing little warning of an impending pregnancy failure. Figure 23.12 shows normal and abnormal heart rates in two pregnancies at 6 weeks and 3 days' gestation. The pregnancy

with abnormal EHR ceased to grow and failed 2 days after that TUS.

Chorionicity and Amnionicity in Twin Pregnancies

The rate of twin births has been steadily rising from 18.9 per 1000 births in 1980 to 33.9 per 1000 births in 2014 primarily due to the widespread use of assisted reproductive technologies, and the pace of increase has slowed to a nonsignificantly different rate of 33.4 per 1000 births in 2016 [32]. Twins can be divided into monochorionic (monozygotic, or identical twins, only one placenta for both babies) and dichorionic (dizygotic, or fraternal twins, one placenta for each baby). The monochorionic twins are further subdivided into monoamniotic (both embryos are seen in the same AS) and diamniotic (one AS in each GS, one for each baby).

The most common complication of twin pregnancies is preterm delivery, which carries the risk of prematurity of the babies (acute respiratory distress syndrome, cerebral hemorrhage, necrotizing enterocolitis, long-term chronic respiratory, and intestinal problems) and, ultimately, lower survival rates. However, other complications of twin pregnancies, such as twin-to-twin transfusion syndrome (TTTS) and cord entanglement, are specifically correlated to their chorionicity and amnionicity, and knowing their status in the first trimester could help in tailoring their follow-up and timing intervention.

Determination of chorionicity can be easily performed any time in the first trimester, by the presence of two GSs within the uterus. However, as previously mentioned, amnionicity can be determined only after the seventh week of pregnancy, when the embryo gradually assumes a C-shaped conformation and the AS becomes visible as a translucent membrane projecting from the embryo's stalk within the GS [9]. Amnionicity is very important in monochorionic twins because, if monoamniotic, cord entanglement could occur toward the late phases of pregnancy. If diamniotic, TTTS could develop as early as the second trimester of pregnancy and cause major complications for both fetuses. Figure 23.13 shows a monochorionic diamniotic and a dichorionic diamniotic twin pregnancy.

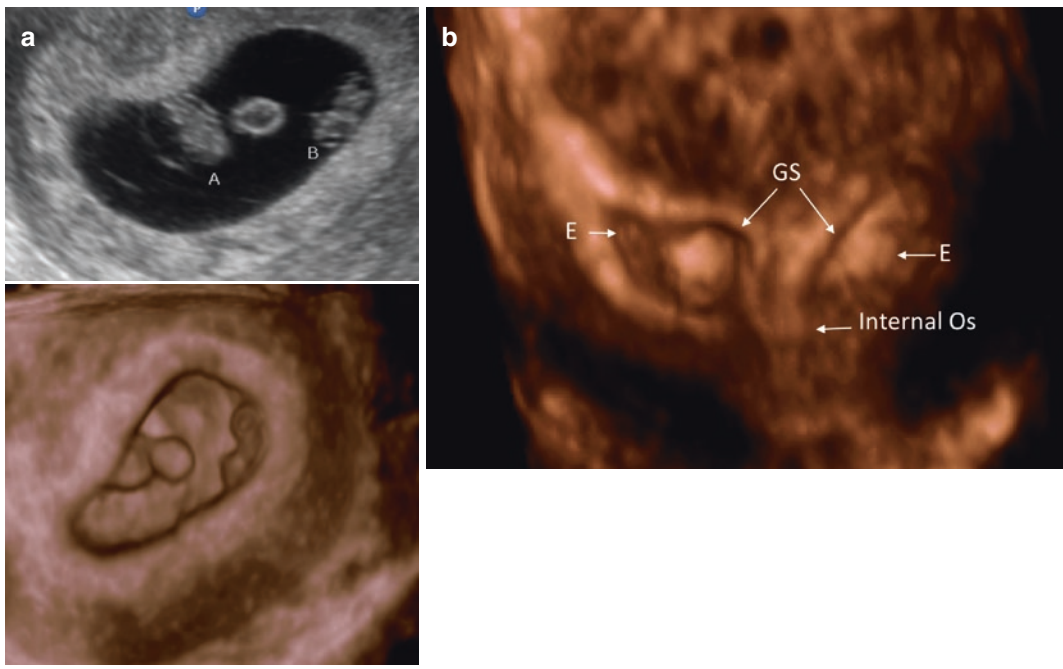

Fig. 23.13 (**a**) Monochorionic-diamniotic twins at 7 weeks and 2 days' gestation (**a**, **b**) and (**b**) dichorionic diamniotic twins at 6 weeks and 2 days' gestation

Conclusion

First trimester ultrasound is extremely important to determine the viability of the pregnancy and to tailor intervention, counseling, and follow-up. The following are important learning points from this chapter:

- The presence of a YS within a GS confirms a pregnancy.
- CRL is the only reliable method to estimate the gestational age.
- A small GS can be associated with impending pregnancy loss, and prediction becomes more accurate in the presence of YS abnormalities.
- A large YS is highly predictive of failing pregnancy.
- EHR = 50 BPM could be normal at 5 weeks' gestation; however, an EHR <100 BPM after 6 weeks' gestation predicts a failing pregnancy in >40% of the times.
- Placental location can be assessed as early as the yolk sac is visible (about 5 weeks' gestation).
- Knowing the placental position early in pregnancy could be of help in predicting the outcome of pregnancies complicated by uterine subseptations, cornual GS, or cesarean section scar GS.

References

1. Dubilet PM, Benson CB, Bourne T, Blaivas M, Barnhart KT, Benacerraf BR, et al. Diagnostic criteria for nonviable pregnancy early in the first trimester. N Engl J Med. 2013;369:1443–51.
2. American College of Obstetricians and Gynecologists. Practice Bulletin No. 193: Tubal Ectopic Pregnancy. Obstet Gynecol. 2018;131:e91–e103. https://doi.org/10.1097/AOG.0000000000002560.
3. Bagratee JS, Ragan L, Khullar V, Connolly C, Moodley J. Reference intervals of gestational sac, yolk sac and embryo volumes using three-dimensional ultrasound. Ultrasound Obstet Gynecol. 2009;34:503–9.
4. Detti L, Francillon L, Christiansen ME, Peregrin-Alvarez I, Goedecke P, Boursac Z, Roman RA. Serial early pregnancy ultrasound measurements and prediction of pregnancy outcome: A logistic model. Under Revision, 2019.
5. Tan S, Pektas MK, Arslan H. Sonographic evaluation of the Yolk sac. J Ultrasound Med. 2012;31:87–95.
6. Detti L, Christiansen ME, Roman RA, Peregrin-Alvarez I, Gini Ikwuezunma, Francillon L. Nomogram of yolk sac growth during the first trimester of pregnancy. Under revision, 2019.
7. Rauch ER, Schattman GL, Christos PJ, Chicketano T, Rosenwaks Z. Embryonic heart rate as a predictor of first-trimester pregnancy loss in infertility patients after in vitro fertilization. Fertil Steril. 2009;91:2451–4.
8. AIUM statement on the safe use of Doppler ultrasound during 11–14 week scans (or earlier in pregnancy). http://www.aium.org/officialStatements/42. Retrieved 2 May 2018.
9. Jirasek JE. An atlas of human prenatal developmental mechanics: anatomy and staging. Philadelphia: Taylor & Francis; 2004.
10. Olive EC, Roberts CL, Nassar N, Algert CS. Test characteristics of placental location screening by transabdominal ultrasound at 18–20 weeks. Ultrasound Obstet Gynecol. 2006;28(7):944–9.
11. Taipale P, Hiilesmaa V, Ylostalo P. Diagnosis of placenta previa by transvaginal sonographic screening at 12–16 weeks in a nonselected population. Obstet Gynecol. 1997;89(3):364–7.
12. Applebaum M. Predicting placental location – the pattern of decidual blood flow in early pregnancy using the gray-scale technique. Ultrasound Obstet Gynecol. 1995;6(4):299–300.
13. Detti L, Gordon J, Christiansen ME, Van de Velde NA, Francillon L, Peregrin-Alvarez I, Roman RA, Rogers AJ. Diagnosis of placental position by early first trimester ultrasound. Reprod Sci 2018;25:1218–23.
14. Magann EF, Doherty DA, Turner K, Lanneau GS Jr, Morrison JC, Newnham JP. Second trimester placental location as a predictor of an adverse pregnancy outcome. J Perinatol. 2007;27(1):9–14.
15. Gizzo S, Noventa M, Vitagliano A, et al. Sonographic assessment of placental location: a mere notional description or an important key to improve both pregnancy and perinatal obstetrical care? A large cohort study. Int J Clin Exp Med. 2015;8(8):13056–66.
16. Seow KM, Huang LW, Lin YH, Lin MY, Tsai YL, Hwang JL. Cesarean scar pregnancy: issues in management. Ultrasound Obstet Gynecol. 2004;23(3):247–53.
17. Timor-Tritsch IE, Monteagudo A, Cali G, El Refaey H, Kaelin Agten A, Arslan AA. Easy sonographic differential diagnosis between intrauterine pregnancy and cesarean delivery scar pregnancy in the early first trimester. Am J Obstet Gynecol. 2016;215(2):225 e221–7.
18. American College of Obstetricians and Gynecologists. Practice Bulletin No. 150: early pregnancy loss. Obstet Gynecol. 2015;125:1258–67.
19. Orvieto R, Ben-Rafael Z, Ashkenazi J, Yoeli R, Messing B, Perri T, Shalev Y, Bar-Hava I. Outcome

of pregnancies derived from assisted reproductive technologies: IVF versus ICSI. J Assist Reprod Genet. 2000;17:385–7.
20. Wang X, Chen C, Wang L, Chen D, Guang W, French J. Conception, early pregnancy loss, and time to clinical pregnancy: a population-based prospective study. Fertil Steril. 2003;79:577–84.
21. Zinaman MJ, Clegg ED, Brown CC, O'Connor J, Selevan SG. Estimates of human fertility and pregnancy loss. Fertil Steril. 1996;65:503–9.
22. Lathi RB, Milki AA. Tissue sampling technique affects accuracy of karyotype from missed abortions. J Assist Reprod Genet. 2002;19:536–8.
23. Liu Y, Liu Y, Chen H, Li Q, Meng L, Chen L, Du T, Zhang J. Relationship of karyotype to embryo crown-rump length and maternal serum human chorionic gonadotropin level in early Miscarriage. Am J Perinatol. 2015;32(1):15–22.
24. Stamatopoulos N, Lu C, Casikar I, Reid S, Mongelli M, Hardy N, Condous G. Prediction of subsequent miscarriage risk in women who present with a viable pregnancy at the first early pregnancy scan. Aust N Z J Obstet Gynaecol. 2015;55(5):464–72.
25. Yi Y, Lu G, Ouyang Y, lin G, Gong F, Li X. A logistic model to predict early pregnancy loss following in vitro fertilization based on 2601 infertility patients. Reprod Biol Endocrinol. 2016;14:15. https://doi.org/10.1186/s12958-016-0147-z.
26. Khalil A, Syngelaki A, Maiz N, Zinevich Y, Nicolaides KH. Maternal age and adverse pregnancy outcome: a cohort study. Ultrasound Obstet Gynecol. 2013;42(6):634–43.
27. Pillai RN, Konje JC, Richardson M, Tincello DG, Potdar N. Prediction of miscarriage in women with viable intrauterine pregnancy-A systematic review and diagnostic accuracy meta-analysis. Eur J Obstet Gynecol Reprod Biol. 2018;220:122–31.
28. Datta MR, Raut A. Efficacy of first-trimester ultrasound parameters for prediction of early spontaneous abortion. Int J Gynaecol Obstet. 2017;138:325–30. https://doi.org/10.1002/ijgo.12231.
29. Berdhal DM, Blaine J, Van Voorhis B, Dokras A. Detection of enlarged yolk sac on early ultrasound is associated with adverse pregnancy outcomes. Fertil Steril. 2010;94:1535–7.
30. Ashoush S, Abuelghar W, Tamara T, Aljobboury D. Relation between types of yolk sac abnormalities and early embryonic morphology in first-trimester missed miscarriage. J Obstet Gynaecol Res. 2016;42(1):21–8. https://doi.org/10.1111/jog.12837.
31. Dubilet PM, Benson CB, Chow JS. Long-term prognosis of pregnancies complicated by slow embryonic heart rates in the early first trimester. J Ultrasound Med. 1999;18:537–41.
32. Martin JA, Hamilton BE, Osterman MJK, Driscoll AK, Drake P. Births: final data for 2016. Natl Vital Stat Rep. 2018;67(1):1–55.

Ectopic Pregnancy

24

Donald L. Fylstra

Ectopic pregnancy, the implantation of a fertilized ovum outside the uterine cavity, has been increasing in number at a staggering pace and now accounts for 2% of all pregnancies in the United States [1]. Since many ectopic pregnancies are now treated in an outpatient setting, true current numbers are hard to obtain. Nearly all ectopic pregnancies (97%) are implanted within the fallopian tube, and a common factor for the development of such ectopics is the presence of a pathological fallopian tube. Causes of such pathology include genital tract infection caused by gonorrhea and chlamydia, tubal surgery including tubal sterilization, previous ectopic pregnancy, and in utero exposure to diethylstilbestrol [2, 3]. Other risk factors for tubal ectopic pregnancy include conception with an intrauterine contraceptive device in place and conception while using a progesterone-only contraceptive method [4, 5].

Ectopic implantation can also occur outside of the fallopian tube: within the cervix, ovary, abdomen, uterine cornua, cesarean scars, and anywhere within the peritoneal cavity. These extratubal implantations may not be associated with tubal pathology or the expected preexisting risk factors for tubal ectopic implantation.

D. L. Fylstra (✉)
Department of Obstetrics and Gynecology, Medical University of South Carolina, Charleston, SC, USA
e-mail: fylstrad@musc.edu

The imaging modality of choice for the diagnosis of early pregnancy, regardless of implantation site, is transvaginal ultrasound.

The discriminatory zone of human chorionic gonadotrophin (hCG) is that level of hCG, which, when reached, an intrauterine pregnancy should be identified within the endometrial cavity with transvaginal ultrasound, when the pregnancy is *normal and singleton*. The discriminatory zone of hCG is usually 1500 mIU/ml. Normal and singleton is important because of the frequent misinterpretation of the hCG discriminatory zone. Waiting until the discriminatory zone of hCG is reached before performing a transvaginal ultrasound could miss early gestational pathology such as an extrauterine implantation (abnormal pregnancies may have hormone levels that are lower at any given gestation age). Likewise, failure to identify an intrauterine gestation with transvaginal ultrasound when the hCG level is greater than the discriminatory zone, may miss an early multiple gestation, particularly those pregnancies that are the result of assisted reproductive technologies.

The confirmation of an intrauterine pregnancy with transvaginal ultrasound relies upon recognition, initially of a true gestational sac, followed soon thereafter by recognition of structures within the sac consistent with a developing embryo. The term "gestational sac" is a sonographic term and not an anatomical structure. A true gestational sac has a thick echogenic rim, a

L. A. Stadtmauer, I. Tur-Kaspa (eds.), *Ultrasound Imaging in Reproductive Medicine*,
https://doi.org/10.1007/978-3-030-16699-1_24

trophoblastic decidual reaction, surrounding a sonolucent center, the chorionic sac. The intradecidual sign is the presence of such a sac buried *beneath* the surface of the endometrium, appearing eccentrically positioned within the endometrium (Fig. 24.1). A "pseudosac" is a collection of fluid *within* the endometrial cavity itself, created by bleeding from the decidualized endometrium associated with an extrauterine pregnancy implantation (Fig. 24.2). The precise location of such an early sonolucent uterine fluid collection should distinguish between a true gestational sac and a pseudosac. However, in order not to miss a potential very early intrauterine gestation, any intrauterine *localized* fluid collection should be considered a possible intrauterine gestational sac until proven otherwise, embarking prematurely upon a treatment for a presumed pseudosac and an ectopic pregnancy.

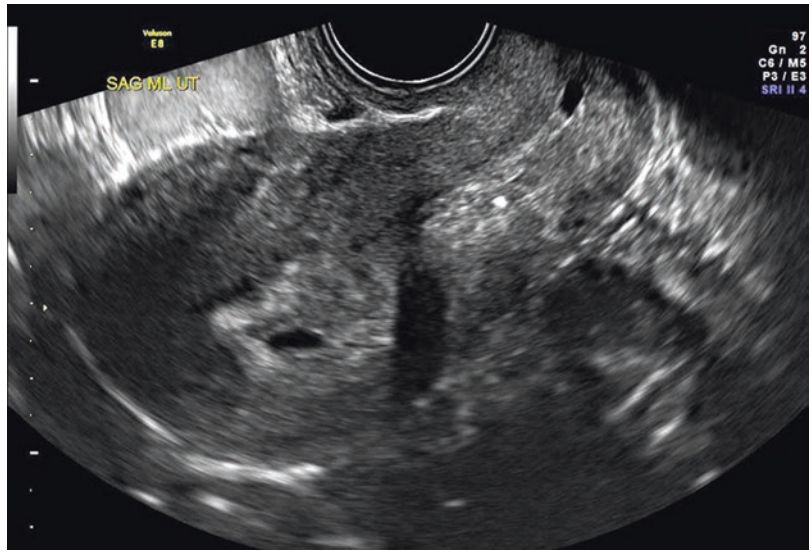

Fig. 24.1 Transvaginal ultrasound: early intrauterine gestational sac, "the intradecidual sign"

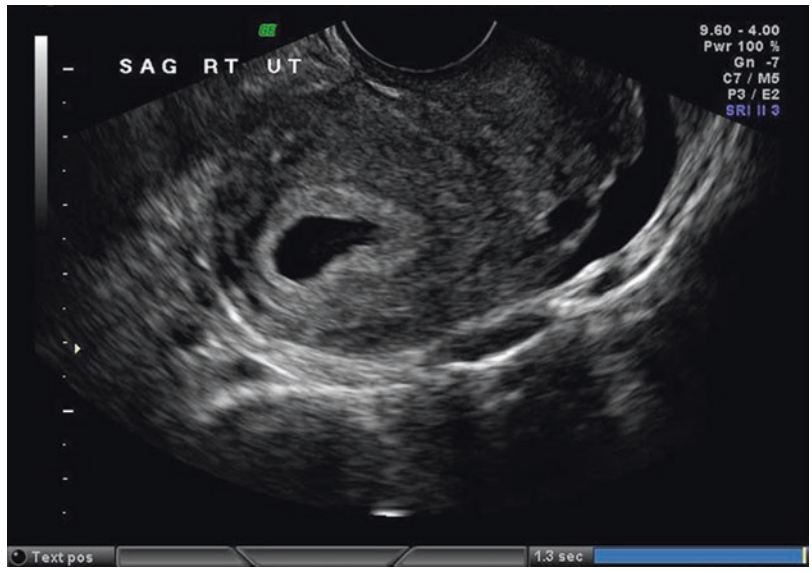

Fig. 24.2 Transvaginal ultrasound: intrauterine pseudosac associated with an ectopic pregnancy

The yoke sac is the first visible structure within the gestational sac, and is a distinct circular structure with a bright echogenic rim and sonolucent center (Fig. 24.3), and is recognized 3 weeks post-conception (5 weeks after the last menstrual period). The embryo is first recognized as a thickening along an edge of the yoke sac (Fig. 24.4), and embryonic cardiac motion can be first observed 3 1/2–4 weeks post-conception (5 1/2–6 weeks after last menstrual period). When exact pregnancy dating is available, an intrauterine pregnancy, regardless of embryonic number, should be identified within the endometrial cavity with transvaginal ultrasonography by 24 embryonic days, or 38 menstrual days (exact 28 day menstrual cycle). This exact pregnancy dating does not rely on human chorionic gonadotropin, hCG, levels. Without such exact pregnancy dating, and with no intrauterine pregnancy identified with transvaginal sonography, the "nondiagnostic ultrasound," a serum level of hCG, is needed for ultrasound interpretation [6]. A word of caution: because of the variation in vaginal ultrasound, technical and interpretive

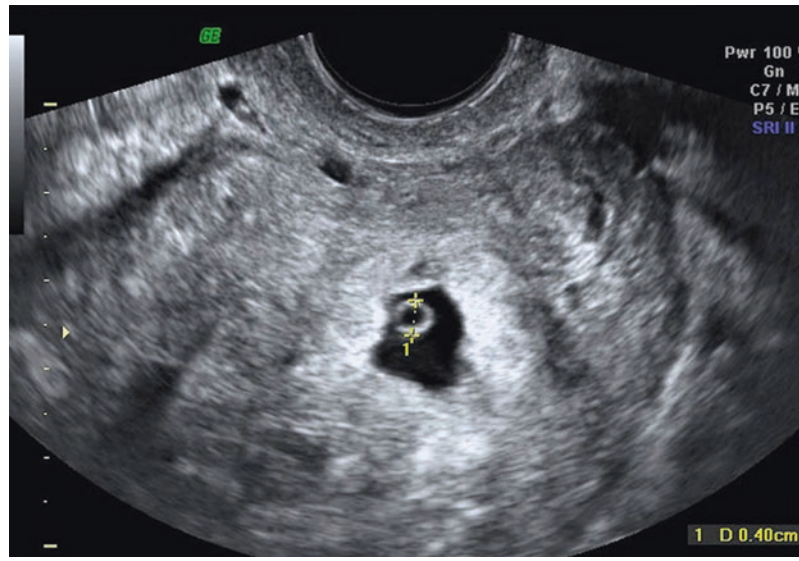

Fig. 24.3 Transvaginal ultrasound: intrauterine gestational sac containing a yolk sac

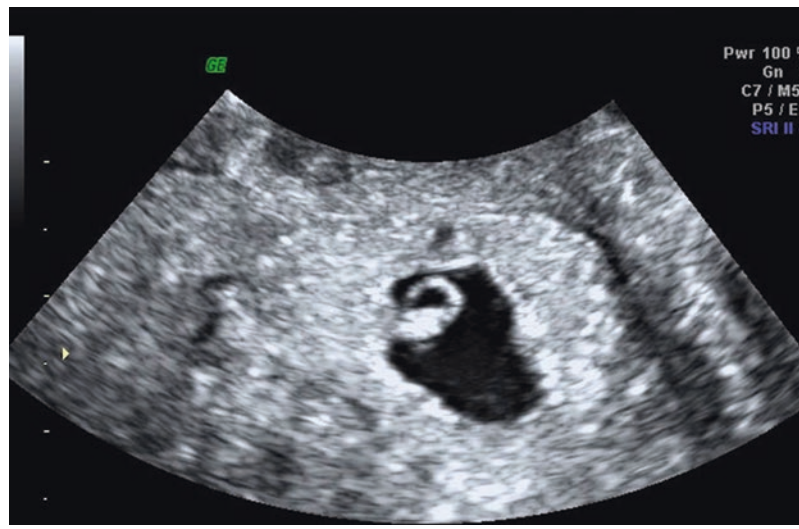

Fig. 24.4 Transvaginal ultrasound: thickened edge of a yolk sac representing an early developing embryo (embryonic cardiac activity may be present)

abilities and lab hCG levels, before embarking on treatment for a presumed ectopic pregnancy, especially with methotrexate, give every pregnancy the "benefit of the doubt." Be certain of the diagnosis or use diagnostic laparoscopy for confirmation.

Additional information can be gained from transvaginal ultrasound measurement of the endometrial echo in early gestation, before the recognition of a gestational sac. Spandorfer and Barnhart reported statistically different endometrial echo thicknesses between patients with normal intrauterine, failed intrauterine, and ectopic gestations [7]. Patients with normal pregnancies had endometrial echo thicknesses of 13.42 ± 0.68 mm. In contrast, those with failed intrauterine and ectopic gestations measured 9.28 ± 0.88 mm and 5.95 ± 0.35 mm, respectively ($P < 0.01$). In this report, 97% of patients with an echo no greater than 8 mm had abnormal pregnancies, and 71% of these abnormal pregnancies were ectopic in location. Only 41% of those patients with an echo thickness greater than 8 mm were abnormal, and only 14.7% were ectopic in location. No patient with an endometrial echo thickness greater than 13 mm had an ectopic pregnancy, and no patients with an echo thickness less than 6 mm had a normal pregnancy. These are well-stratified differences, but other authors have seen much more overlap with endometrial echo measurements.

Usually, the transvaginal ultrasound identification of an intrauterine pregnancy reliably excludes an extrauterine implantation, except in the case of heterotopic pregnancy: the coexistence of an extrauterine implantation with an intrauterine pregnancy. The natural occurrence of heterotopic pregnancy is 1 in 4000 pregnancies, but the frequency is much greater with pregnancies conceived with assisted reproductive technologies. Should a clinical presentation or abnormal pelvic ultrasound appearance suggest an ectopic pregnancy, despite visualization of an intrauterine gestation, the diagnosis of heterotopic pregnancy should be considered, with the probable need for diagnostic laparoscopy confirmation and treatment.

The possibility of ectopic pregnancy is frequently considered before hCG has reached the discriminatory zone and before ultrasound recognition [8]. Human chorionic gonadotropin rises exponentially in early normal pregnancy and should rise at least by 53% in 48 hours [9]. This exponential rise is less reliable after 10,000 mIU/ml, and at this level, pregnancy is better evaluated with ultrasound. Fifteen percent of normal intrauterine pregnancies can demonstrate an abnormal early rise of hCG, but for the majority of gestations, when the hCG rise is abnormal, at a plateau, or falling, an abnormal pregnancy is confirmed, but not its location [10].

Cervical Pregnancy

Less than 1%, and the rarest, of ectopics are implanted within the cervical canal below the level of the internal cervical os [11, 12]. The etiology of such implantations is unknown, but predisposing factors include prior uterine curettage, induced abortion, Asherman's syndrome, leiomyomata, presence of an intrauterine device, in vitro fertilization, and prior in utero exposure to diethylstilbestrol [13–16].

Before the now common use of early pregnancy transvaginal ultrasound, cervical pregnancies were frequently diagnosed at the time of spontaneous abortion or reached the second trimester, both associated with life-threatening hemorrhage frequently requiring hysterectomy as treatment. Usually, the first complaint is painless vaginal bleeding, and speculum examination may reveal an open external cervical os with a fleshy-type endocervical mass presenting. With early transvaginal sagittal ultrasound through with lower uterine segment and cervix, these implantations are easily identified (Fig. 24.5) and can, thus, be treated with conservative fertility-sparing options, such as a modified suction curettage technique described by Fylstra [17].

Rankin suggested that the diagnosis by ultrasound examination of cervical pregnancy required four criteria: enlargement of the cervix, uterine enlargement, diffuse amorphous

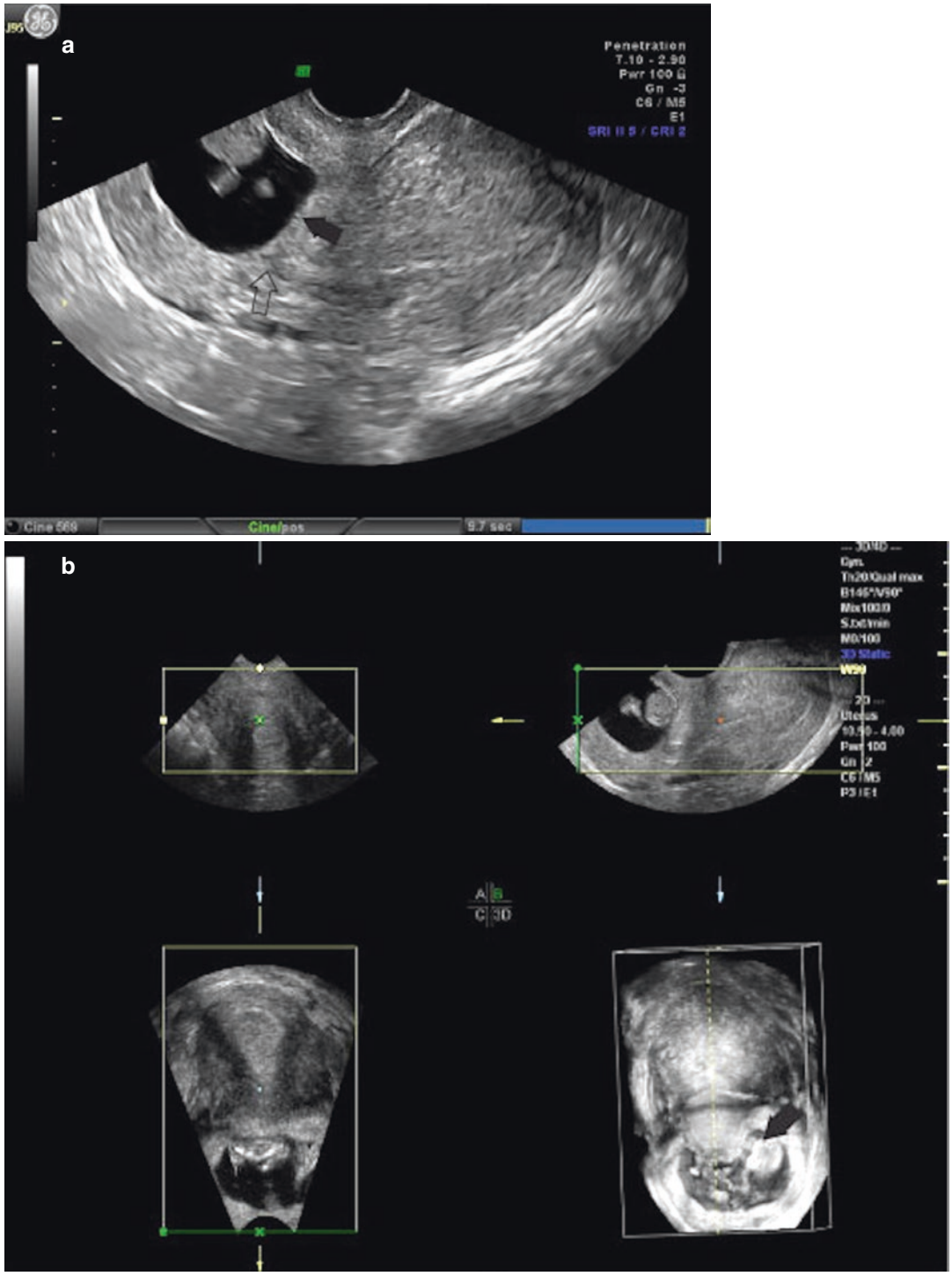

Fig. 24.5 (**a**) Transvaginal ultrasound, midline sagittal image: cervical pregnancy, (*closed arrow*) points to the cervical pregnancy within the cervical canal (*open arrow*). (**b**) Transvaginal ultrasound: 3D rendering of a cervical pregnancy; *closed arrow* points to the internal cervical os

intrauterine echoes, and absence of an intrauterine pregnancy [18]. Timor-Tritsch et al. refined the criteria to include the placenta and entire chorionic sac containing the pregnancy must be below the internal cervical os and the cervical canal must be dilated and barrel shape [19].

If necessary to exclude the diagnosis of a spontaneous abortion in progress, the presence of embryonic cardiac activity and/or Doppler ultrasound indicating vascular attachment confirms a living pregnancy.

Ovarian Pregnancy

One-half of 1% to almost 3% of ectopics are implanted within the ovary [11, 20]. Ovarian pregnancy, like other non-tubal ectopic pregnancies, may occur without the usual expected antecedent risk factors for ectopic pregnancy but does seem to have a strong association with conceptions with an intrauterine contraceptive device in place [21, 22]. The presenting signs and symptoms are similar to other ectopic pregnancies: positive pregnancy test, abdominal pain, and vaginal bleeding.

It is difficult to preoperatively make the diagnosis of ovarian pregnancy. An ultrasound finding suggesting ovarian implantation is a walled cystic mass within or adjacent to an ovary, but this does not exclude a corpus luteum and a tubal implantation. Doppler cannot distinguish between a corpus luteum and an ovarian pregnancy implantation (Fig. 24.6). This diagnosis is usually a pathological diagnosis made by microscopic examination of a surgically removed adnexal mass, via laparotomy or laparoscopy, based on Spiegelberg's criteria: the tube must be intact and distinctly separate from the ovary, the gestational sac must occupy the normal anatomical location of the ovary, the gestational sac must be connected to the uterus by the utero-ovarian ligament, and unquestioned ovarian tissue must be demonstrated in the wall of the gestational sac [23].

It is important for the laparoscopic surgeon to understand that an ovarian pregnancy can look like a corpus luteum ovarian cyst upon direct inspection, and cystectomy and pathology only will reveal the true diagnosis. However, when an adnexal ectopic is diagnosed with a nonsurgical algorithm, conservative medical therapy can be successful without a true diagnosis of location.

Abdominal Pregnancy

Less than 1% of ectopic pregnancies are implanted within the abdominal cavity [11, 24, 25]. The pathogenesis of abdominal implantation is controversial. Many are the results of secondary nidation within the peritoneal cavity after tubal abortion, tubal rupture, or uterine rupture [26]. True primary abdominal implantation must satisfy the criteria of Studdiford. Studdiford, reporting a primary peritoneal implantation in 1942, established three criteria for such a primary abdominal pregnancy: normal fallopian tubes with no evidence of recent or remote trauma, the absence of any uteroperitoneal fistula, and the presence of a pregnancy related exclusively to the peritoneal surface and early enough to eliminate the possibility of secondary implantation following a primary nidation within the tube [26].

The most common abdominal implantation site is the posterior cul-de-sac, followed by the mesosalpinx, the omentum, the bowel and its mesentery, and the peritoneum of the pelvic and abdominal walls, including the anterior cul-de-sac [26]. Other reported locations include the retroperitoneal space, including over the major retroperitoneal vessels, the appendix, the liver, and the spleen [27–32].

With the universal use of early pregnancy imaging, the diagnosis can be confirmed at an early gestational age, but this requires imaging demonstrating a continuity of the cervix and uterus without pregnancy contents, like other ectopic implantations. The presence of an adnexal mass suggestive of ectopic pregnancy, when no intrauterine gestation is identified, could be an ectopic pregnancy of any location, including an abdominal implantation. Failure to follow basic ultrasound principles can miss the diagnosis.

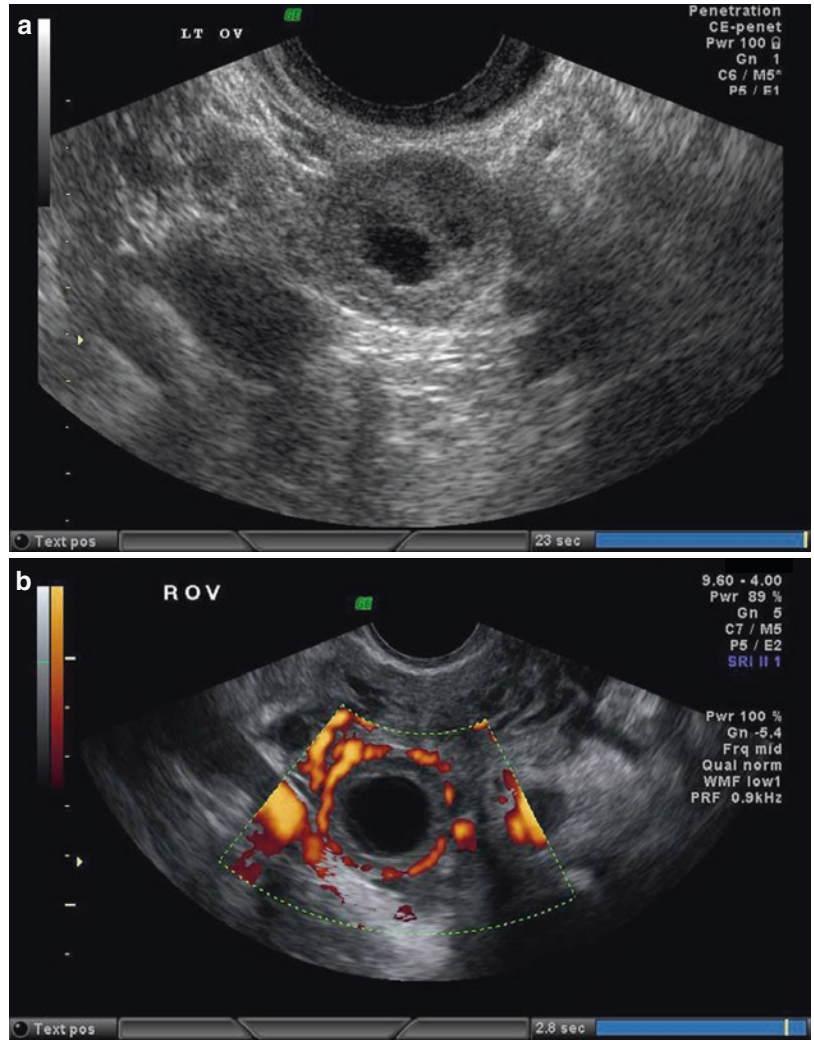

Fig. 24.6 (**a**) Transvaginal ultrasound of an ovarian corpus luteum cyst. (**b**) Transvaginal ultrasound: color Doppler imaging of an ovarian corpus luteum cyst

Such early diagnosis can spare maternal mortality at the expense of fetal mortality, with a perinatal mortality rate of 40–95% [33].

Cesarean Scar Ectopic Pregnancy

Although previously rare, the incidence of pregnancy implantation within the scar of a prior cesarean is increasing due to the increasing number of cesarean deliveries. The natural history of such a condition is unknown, but uterine scar rupture and hemorrhage, even in the first trimester, seem likely if the pregnancy is allowed to continue, with possible serious maternal morbidity and the possible need for hysterectomy and loss of subsequent fertility. Early diagnosis of such implantation is made only with a high level of suspicion: early ultrasound in a woman with a prior cesarean delivery (Fig. 24.7).

Endometrial and myometrial disruption or scarring can predispose to abnormal pregnancy implantation. Trophoblast adherence or invasion is enhanced when the scant decidualization of the lower uterine segment is impaired further by previous myometrial disruption. Implantation of a

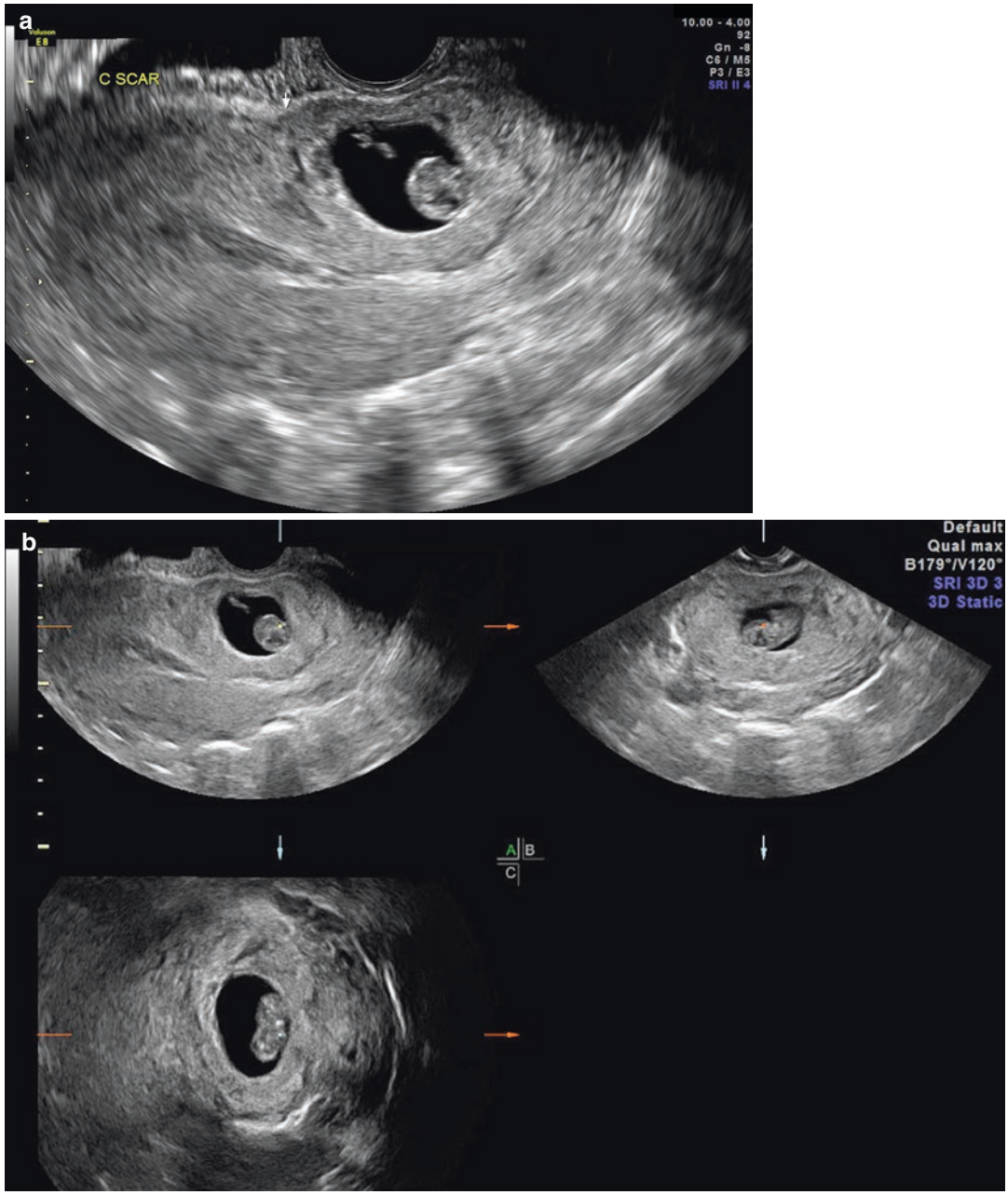

Fig. 24.7 (**a**) Transvaginal ultrasound: midline sagittal image with gestation in the anatomical location of a prior cesarean scar. (**b**) Transvaginal ultrasound: 3D rendering of cesarean scar ectopic

pregnancy within the uterine scar of a prior cesarean delivery is different from an intrauterine pregnancy with placenta accreta. Cesarean scar implantation is a gestation completely surrounded by the myometrium and the fibrous tissue of the scar and separated from the endometrial cavity or fallopian tube (see Fig. 24.7). The mechanism that most probably explains scar implantation, like intramural implantation, is invasion of the myometrium through a micro-

scopic tract. Like intramural pregnancy, such a tract is believed to develop from the trauma of previous uterine surgery, such as curettage, cesarean delivery, myomectomy, metroplasty, hysteroscopy, and even manual removal of the placenta [34–36]. The time interval between such trauma and a subsequent pregnancy may impact upon implantation events. Some of the reported cases were diagnosed and treated within a few months of a prior cesarean delivery suggesting that incomplete healing of the uterine scar may contribute to scar implantation [37, 38].

Early diagnosis with ultrasound can offer treatment options capable of avoiding uterine rupture and hemorrhage and, thereby, preserve the uterus. The differential diagnosis between spontaneous abortion in progress, cervico-isthmic pregnancy, and implantation within a cesarean scar can be difficult. Strict ultrasound imaging criteria must be used to assess the diagnosis of cesarean scar pregnancy. Sagittal midline transvaginal ultrasound should reveal an empty uterine cavity, an empty cervical canal, development of the gestational sac in the anterior part of the uterine isthmus, and an absence of healthy myometrium between the bladder and the gestational sac, this last criterion allowing differentiation from cervico-isthmic implantation [39].

Although cesarean scar pregnancy is an uncommon occurrence, only with a high index of suspicion and the use of early endovaginal sonography can the diagnosis be made early enough to prevent rupture leading to significant maternal morbidity and loss of future fertility. Clinical history and endovaginal ultrasound can aid in differentiating cesarean scar pregnancy from incomplete abortion and cervico-isthmic pregnancy. Precise localization of the early pregnancy by transvaginal ultrasound should be encouraged in all patients with threatening gestational pathology. A sagittal ultrasound view along the long axis of the uterus, through the gestational sac, can localize precisely a cesarean scar implantation (see Fig. 24.7).

There are two types of cesarean scar ectopic implantations: one extending toward the serosal uterine surface and bladder (exophytic) and one extending toward the endometrial cavity (endophytic). Such locations dictate treatment options [40].

Interstitial Ectopic Pregnancy

Two to 3% of ectopics are implanted within the interstitial portion of the fallopian tube, that portion of the tube that transitions from the endometrial cavity to the tubal isthmus through a wall of the myometrium [11]. The interstitial, or cornual, portion of the fallopian tube is tortuous, 0.7 mm in diameter, and 1–2 cm in length [41]. This is a relatively thick segment of fallopian tube with a greater capability to expand before rupture than more distal portions of the fallopian tube [42]. Since implantation within this portion of the fallopian is still "within the tube," it is associated with the same commonly recognized risk factors for tubal ectopic pregnancy. No single factor clearly differentiates women with an interstitial pregnancy from those with isthmic or ampullary ectopic pregnancies.

Transvaginal ultrasound is the primary method for diagnosing interstitial implantation (Fig. 24.8). However, many early ultrasounds show that these pregnancies are surrounded by the myometrium and can be mistaken for normally implanted pregnancies. Three-dimensional ultrasound findings that are highly suggestive of interstitial implantation are the identification on a coronal view of an echogenic line between the gestational sac and the endometrial cavity, "the interstitial line sign," an empty uterine cavity with a gestational sac eccentrically located outside the endometrial cavity with a thin mantle of surrounding myometrium less than 5 mm in thickness [43]. Collectively, these ultrasound findings are 88–93% specific but with a sensitivity of only 40% [44, 45]. Coronal images generated by 3D sonography are helpful in identifying these features (see Fig. 24.8) [46].

Interstitial ectopic pregnancies are frequently mislabeled as "cornual ectopics." Cornual pregnancy refers to a pregnancy within the horn of a bicornuate uterus, communicating or noncommunicating, and the clinical outcome of this implantation varies greatly and depends upon

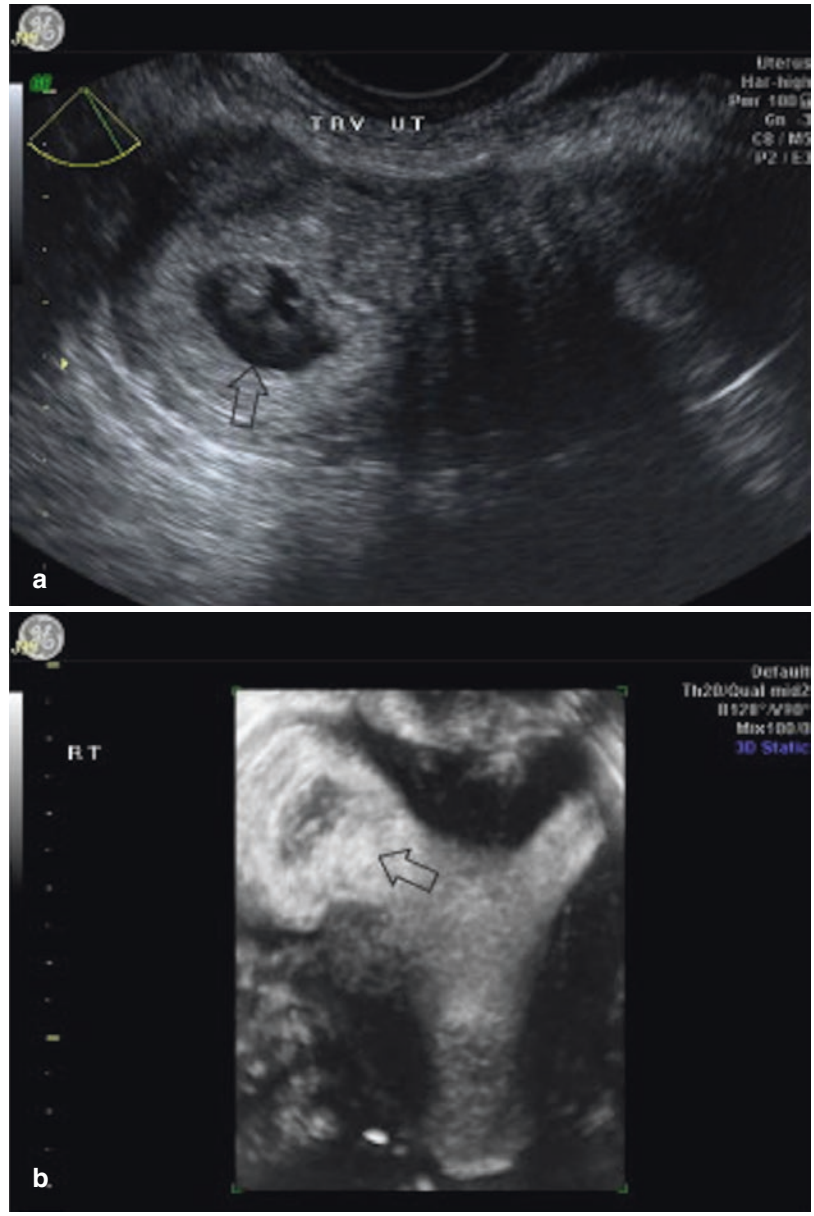

Fig. 24.8 (**a**) Transvaginal ultrasound: transverse view across uterine fundus demonstrating an asymmetrically implanted gestation, concern for interstitial ectopic. (**b**) Transvaginal ultrasound: 3D rendering confirming interstitial pregnancy implantation. *Open arrows* point to gestational sac

the size and expansile capacity of the affected horn [46].

Angular pregnancies are implanted in one of the lateral angles of the uterine cavity, medial to the uterotubal junction, and must be distinguished from interstitial implantations. Angular pregnancies lead to an asymmetric enlargement of the uterus (Fig. 24.9). What distinguishes an interstitial ectopic pregnancy from an angular pregnancy is that the laparoscopic appearance of the bulge of an interstitial pregnancy is lateral to the round ligament, whereas the bulge of an angular pregnancy is medial to the round ligament, displacing the round ligament laterally. Over one third of angular pregnancies end in early abortion, but for those that continue pelvic pain, persistent vaginal bleeding, placental retention during the third stage of labor, and rarely uterine rupture can be expected complications.

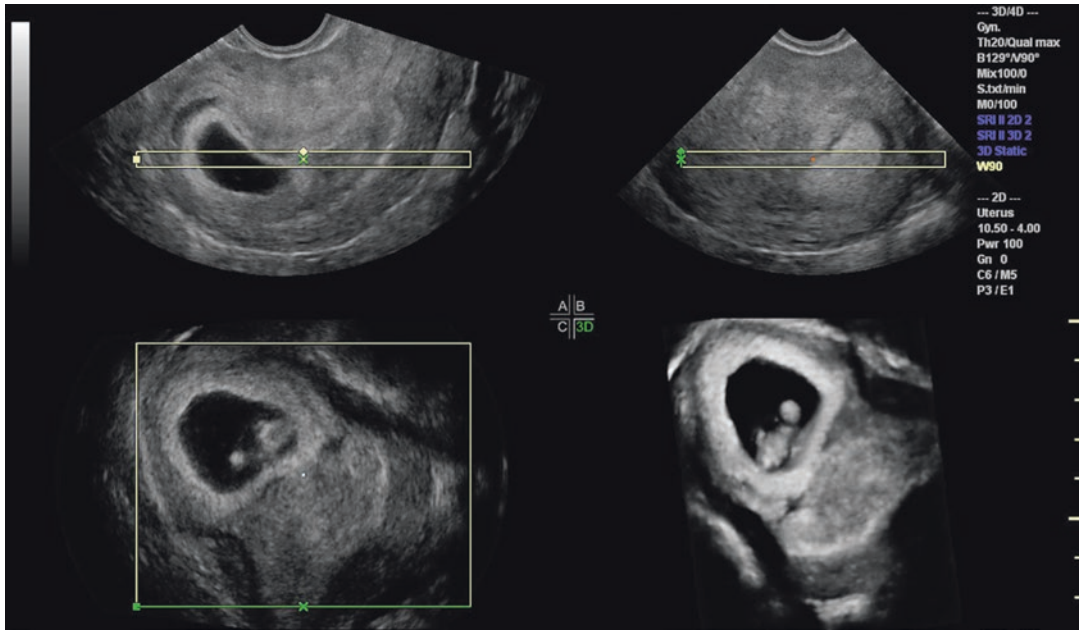

Fig. 24.9 Transvaginal ultrasound: angular pregnancy

Ectopic After Hysterectomy

Seventy-two cases of ectopic pregnancy after hysterectomy have been reported in the world's literature and are rarely suspected before surgical intervention [47]. Over half of such pregnancies have been "early presentations," this occurring because an unrecognized, preclinical pregnancy existed at the time of hysterectomy: a preimplanted fertilized ovum was in transit and confined to the fallopian tube, or sperm was present within the fallopian when the hysterectomy was performed during a peri-ovulatory period, allowing postoperative fertilization and tubal implantation. An immediate pre-hysterectomy pregnancy test would not be expected to be positive under such circumstances. "Late presentation" ectopics have occurred after all types of hysterectomy and as remote as 12 years after the hysterectomy. These post-hysterectomy ectopic pregnancies occur with retention of one or both ovaries with the presence of a vaginal-tubal or vaginal-peritoneal fistula allowing vaginally implanted sperm access to ovulated ova.

Because the symptoms of ectopic pregnancy can be mimicked by common immediate complications after hysterectomy, such as protracted abdominal pain, pelvic hematoma formation, vaginal cuff infection, and vaginal bleeding, ectopic pregnancy is rarely expected in most post-hysterectomy cases until additional imaging or repeat operation confirms the diagnosis.

Summary

Ectopic pregnancy occurs in one out of every 50 pregnancies. Early transvaginal ultrasound can locate most, if not all, early pregnancies and should be performed on every early pregnancy with symptoms of gestational pathology or a high likelihood of ectopic pregnancy based on gynecologic history. With suspected gestational pathology, early vaginal sonography should be performed regardless of hCG level. The late diagnosis of an ectopic pregnancy increases the risk for loss of fertility and for maternal morbidity and mortality. Many non-tubal ectopic locations

can be diagnosed with early transvaginal sonography and then with successful medical management. The pregnancy of unknown location, when diagnosed early and confirmed to be extrauterine, can, likewise, be managed conservatively and successfully. Medical management fails more commonly with more advanced, living ectopic pregnancies, which may occur with non-tubal ectopic pregnancies, requiring surgical intervention [48]. Therefore, it is extremely prudent to diagnose gestational pathology early with transvaginal sonography.

References

1. Centers for Disease Control and Prevention (CDC). Ectopic pregnancy – United States, 1990–1992. MMWR Morb Mortal Wkly Rep. 1995;44:46–8.
2. Ankum WM, Mol BWJ, Van der Veen F, Bodduyt PM. Risk factors for ectopic pregnancy: a meta-analysis. Fertil Steril. 1996;65:1093–9.
3. Peterson HB, Xia Z, Hughes JM, Wilcox LS, Tylor LR, Trussell J. The risk of ectopic pregnancy after tubal sterilization: US Collaborative Review of Sterilization Working Group. N Engl J Med. 1997;336:762–7.
4. Borgatta L, Murphy M, Chuangb C, Beardsley L, Burnhill MS. Pregnancies diagnosed during depo-provera use. Contraception. 2002;66:169–72.
5. Furlong LA. Ectopic pregnancy risk when conception fails: a review. J Reprod Med. 2002;47:881–5.
6. Kadar N, Bohrer M, Kemmann E, Shelden R. The discriminatory human chorionic gonadotropin zone for endovaginal sonography: a prospective, randomized study. Fertil Steril. 1994;61:1016–20.
7. Spandorfer SD, Barnhart KT. Endometrial stripe thickness as a predictor of ectopic pregnancy. Fertil Steril. 1996;66:474–7.
8. Ankum WM, Van der Veen F, Hamerlynck JVTH, Lammes FB. What to do when human chorionic gonadotropin levels are below the discriminatory zone. J Reprod Med. 1995;40:525–8.
9. Barnhart KT, Sammel MD, Rinaudo PF, Zhou L, Hummel AC, Guo W. Symptomatic patients with an early viable intrauterine pregnancy: HCG curves redefined. Obstet Gynecol. 2004;104:50–5.
10. Kadar N, Caldwell BV, Romero R. A method of screening for ectopic pregnancy and its indications. Obstet Gynecol. 1981;52:162–6.
11. Bouyer J, Coste J, Fernandez H, Pouly JL, Job-Spira N. Site of ectopic pregnancy: a 10 year population-based study of 1800 cases. Hum Reprod. 2002;17:3224–30.
12. Ushakov FB, Elchalal U, Aceman PJ, Schenker JG. Cervical pregnancy: past and future. Obstet Gynecol Surv. 1997;52:45–59.
13. Dicker D, Feldberg D, Samuel N, Goldman JA. Etiology of cervical pregnancy: association with abortion, pelvic pathology, IUDs, and Asherman's syndrome. J Reprod Med. 1985;30:25–7.
14. Ginsburg ES, Frates MC, Rein MS, Fox JH, Hornstein MD, Friedman AJ. Early diagnosis and treatment of cervical pregnancy in an in vitro fertilization program. Fertil Steril. 1994;61:966–9.
15. Shinagawa S, Nagayama M. Cervical pregnancy as a possible sequela of induced abortion. Am J Obstet Gynecol. 1969;105:282–4.
16. Thomas RL, Gingold BR, Gallagher MW. Cervical pregnancy: a report of two cases. J Reprod Med. 1991;36:459–62.
17. Fylstra DL. Cervical pregnancy: 13 cases treated with suction curettage and balloon tamponade. Am J Obstet Gynecol. 2014;210:581.e1–5.
18. Raskin MM. Diagnosis of cervical pregnancy by ultrasound: a case report. Am J Obstet Gynecol. 1978;130:234–5.
19. Timor-Tritsch IE, Monteagurdo A, Mandeville EO, Peisner DB, Anaya GP, Pirronw EC. Successful management of a viable cervical pregnancy by local injection of methotrexate guided by transvaginal ultrasonography. Am J Obstet Gynecol. 1994;170:737–9.
20. Grimes HG, Nosal RA, Gallagher JC. Ovarian pregnancy: a series of 24 cases. Obstet Gynecol. 1983;61:174–80.
21. Kraemer B, Kraemer E, Guengoer E, Juhasz-Boess I, Solomayer EF, Wallwiener D, et al. Ovarian ectopic pregnancy: diagnosis, treatment, correlation to Carnegie stage 16 and review based on a clinical case. Fertil Steril. 2009;92:392.e13–5.
22. Sandvei R, Ulstein M. History and finding of ectopic pregnancies in women with and without an IUD. Contracept Deliv Syst. 1980;1:131–8.
23. Spiegelberg O. Zur Casuistik der Ovariaschwangerschaft. Arch Gynekol. 1873;13:73.
24. Shaw SW, Hsu JJ, Chueh HY, Han CM, Chen FC, Chang YL, et al. Management of primary abdominal pregnancy: twelve years of experience in a medical centre. Acta Obstet Gynecol. 2007;86:1058–62.
25. Clark JFJ, Guy RS. Abdominal pregnancy. Am J Obstet Gynecol. 1996;96:511–20.
26. Studdiford WE. Primary peritoneal pregnancy. Am J Obstet Gynecol. 1942;44:487–91.
27. Anderson PM, Opfer EK, Busch JM, Megann EF. An early abdominal wall ectopic pregnancy successfully treated with ultrasound guided intralesional methotrexate: a care report. Obstet Gynecol Int. 2009;2009:247252.
28. Chui AK, Lo KW, Choi PC, Sung MC, Lau JW. Primary hepatic pregnancy. Aust N Z J Surg. 2001;71:260–1.
29. Nama V, Gyampoh B, Karoski M, McRea R, Opemuyi I. Secondary abdominal appendicular ectopic pregnancy. J Minim Invasive Gynecol. 2007;14:516–7.
30. Shippey SH, Bhoola SM, Royek AB, Long ME. Diagnosis and management of hepatic ectopic pregnancy. Obstet Gynecol. 2007;109:544–6.

31. Thompson RJ, Hawe MJ. A rare pathological trinity: an appendiceal ectopic pregnancy, acute appendicitis, and a carcinoid tumor. Ir J Med Sci. 2011;180:579–80. Epub 2009 Feb 6 (epub ahead of print).
32. Yagil Y, Beck-Razi N, Amit A, Kerner H, Gaitini D. Splenic pregnancy: the role of abdominal imaging. J Ultrasound Med. 2007;26:1629–32.
33. Martin JN, Sessums JK, Martin RW, Proyer JA, Morrison JC. Abdominal pregnancy: current concepts of management. Obstet Gynecol. 1988;71:549–62.
34. Fait G, Goyert G, Sundareson A, Pickens A Jr. Intramural pregnancy with fetal survival: case history and discussion of etiologic factors. Obstet Gynecol. 1987;70:472–4.
35. McGowan L. Intramural pregnancy. JAMA. 1965;192:637–8.
36. Miller DA, Chollet JA, Goodwin TM. Clinical risk factors for placenta previa-placenta accreta. Am J Obstet Gynecol. 1997;177:210–4.
37. Huang KH, Lee CL, Wang CJ, Soong YK, Lee KF. Pregnancy in a previous cesarean section scar: case report. Changgeng Yi Xue Za Zhi. 1998;21:323–7.
38. Marcus S, Cheng E, Goff B. Extrauterine pregnancy resulting from early uterine rupture. Obstet Gynecol. 1999;94:804–5.
39. Godin PA, Bassil S, Donnez J. An ectopic pregnancy developing in a previous cesarean section scar. Fertil Steril. 1997;67:398–400.
40. Gonzalez N, Tulandi T. Cesarean scar pregnancy: a systemic review. J Minim Invasive Gynecol. 2017;24(5):731–8.
41. Tulandi T, Al-Jaroudi D. Interstitial pregnancy: results generated from the 92. Society of Reproductive Surgeons Registry. Obstet Gynecol. 2004;103:47–50.
42. Lau S, Tulandi T. Conservative medical and surgical management of interstitial ectopic pregnancy. Fertil Steril. 1999;72:207–15.
43. Moawad NS, Mahajan ST, Moniz MH, Taylor SE, Hurd WW. Current diagnosis and treatment of interstitial pregnancy. Am J Obstet Gynecol. 2010;202:15–29.
44. Ackerman TE, Levi CS, Dashefsky SM, Holt SC, Lindsay DJ. Interstitial line: sonographic finding in interstitial (cornual) ectopic pregnancy. Radiology. 1993;189:83–7.
45. Timor-Tritsch IE, Monteagudo A, Matera C, Veit CR. Sonographic evolution of cornual pregnancy treated without surgery. Obstet Gynecol. 1992;79:1044–9.
46. Rastogi R, Meena GL, Rastogi N, Rastogi V. Interstitial ectopic pregnancy: A rare and difficult clinicosonographic diagnosis. J Hum Reprod Sci. 2008;1:81–2.
47. Fylstra DL. Ectopic pregnancy after hysterectomy: a review and insight into etiology and prevention. Fertil Steril. 2010;94:431–5.
48. American College of Obstetricians and Gynecologists. ACOG Practice Bulletin. Number 94. Medical management of ectopic pregnancy. Obstet Gynecol. 2009;111:1479–85.

Index

L. A. Stadtmauer, I. Tur-Kaspa (eds.), *Ultrasound Imaging in Reproductive Medicine*,
https://doi.org/10.1007/978-3-030-16699-1